

Title	Novel insights into the expression and function of p38 δ MAPK in oesophageal squamous cell carcinoma
Authors	O'Callaghan, Carol
Publication date	2015
Original Citation	O'Callaghan, C. 2015. Novel insights into the expression and function of p38 δ MAPK in oesophageal squamous cell carcinoma. PhD Thesis, University College Cork.
Type of publication	Doctoral thesis
Rights	© 2015, Carol O'Callaghan. - http://creativecommons.org/licenses/by-nc-nd/3.0/
Download date	2024-04-20 14:31:01
Item downloaded from	https://hdl.handle.net/10468/2082

Novel insights into the expression and function of p38 δ MAPK in oesophageal squamous cell carcinoma



Presented to the National University of Ireland, Cork
in fulfilment of the requirements for the degree of
Doctorate of Philosophy

by

Carol O'Callaghan, BSc.

Departments of Pharmacology & Therapeutics and Medicine
National University of Ireland, Cork

2015

Supervisors: Dr. Orla Patricia Barry
Dr. Liam J. Fanning

Head of Department of Pharmacology & Therapeutics: Professor Thomas Walther
Head of Department of Medicine: Professor Fergus Shanahan

Table of Contents

Declaration	viii
Acknowledgements	ix
List of publications	x
Courses attended	xiv
Projects supervised.....	xv
List of figures	xvii
List of tables	xxii
Abbreviations	xxiv
Hypothesis and aims of thesis	xxix
Abstract	xxxiii
1.Introduction	1
1.1 Hallmarks of cancer	2
1.2 Oesophageal cancer	4
1.2.1 Incidence.....	4
1.2.2 Etiology	5
1.2.3 Staging, prognosis and treatment	7
1.2.4 Targeted therapy for oesophageal cancer	8
1.3 p38 δ MAPK: emerging roles of a neglected isoform	9
1.3.1 p38 isoform evolution	9
1.3.2 p38 δ MAPK expression and activation	12
1.3.3 Novel p38 δ MAPK substrates	17
1.3.4 p38 δ MAPK function and new roles in human disease	21
1.3.5 p38 δ MAPK and cancer	27
1.4 Summary	30
1.5 References	31

2. Materials and general methods	40
2.1 Materials	41
2.1.1 Reagents	41
2.1.2 Cell lines	44
2.1.3 Plasmids	48
2.2 General methods	49
2.2.1 Cell culture	51
2.2.2 3-(4,5-Dimethylthiazol-2-yl)-2,5-diphenyltetrazolium bromide (MTT) staining	52
2.2.3 Cell migration	53
2.2.4 Protein preparation and immunoblot analysis	54
2.2.5 Nucleic acid isolation and cDNA synthesis	58
2.2.6 PCR and rt-PCR	60
2.2.7 Restriction digest	62
2.2.8 Agarose gel electrophoresis	64
2.2.9 DNA purification	65
2.2.10 DNA sequencing	65
2.2.11 Ethics	66
2.2.12 Statistical analysis	66
2.3 References	68
3. Generation and expression of three different plasmids	69
3.1 Abstract	70
3.2 Hypothesis and aims	71
3.3 Introduction	72
3.4 Materials and methods	75
3.4.1 Cloning strategy for pcDNA3-MKK6b(E)-(Gly-Glu) ₅ -FLAG-p38 δ fusion plasmid	75

3.4.2 Site-directed mutagenesis	78
3.4.3 PCR generation of (Gly-Glu) ₅ -FLAG-p38 δ fragment	81
3.4.4 Ligation	83
3.4.5 Transformation	83
3.4.6 Miniprep	84
3.4.7 Maxiprep	85
3.4.8 Cell Culture	85
3.4.9 Transient transfection	86
3.4.10 Immunoblot analysis	86
3.5 Results	87
3.5.1 A vector for the fusion construct was created from pcDNA3-MKK6b(E)	87
3.5.2 A (Gly-Glu) ₅ -FLAG-p38 δ insert was successfully amplified from pcDNA3-FLAG-p38 δ	90
3.5.3 Troubleshooting	92
3.5.4 pcDNA3-MKK6b(E)-(Gly-Glu) ₅ -FLAG-p38 δ was successfully generated	98
3.5.5 Expression and activity of MKK6b(E)-(Gly-Glu) ₅ -FLAG-p38 δ fusion protein	102
3.5.6 Generation of pcDNA3-MKK6b-(Gly-Glu) ₅ -FLAG-p38 δ plasmid	104
3.5.7 Generation of control plasmid pcDNA3-MKK6b(E)-(Gly-Glu) ₅ -FLAG- p38 δ _{DN}	106
3.5.8 Expression and activity of pcDNA3-MKK6b-(Gly-Glu) ₅ -FLAG-p38 δ and pcDNA3-MKK6b(E)-(Gly-Glu) ₅ -FLAG-p38 δ _{DN} plasmids	108
3.6 Discussion	110
3.7 References	113

4. Loss of p38delta mitogen-activated protein kinase expression promotes oesophageal squamous cell carcinoma proliferation, migration and anchorage-independent growth	116
4.1 Abstract	117
4.2 Hypothesis and aims	118
4.3 Introduction	119
4.4 Materials and methods	121
4.4.1 Specimens	121
4.4.2 Cell culture	123
4.4.3 Proliferation assay	123
4.4.4 Nuclear and cytosolic extraction	125
4.4.5 Stable transfection	125
4.4.6 Immunoblot analysis	126
4.4.7 Immunohistochemistry	126
4.4.8 ELISA	128
4.4.9 Cell migration	130
4.4.10 Colony forming assay	130
4.4.11 siRNA	130
4.4.12 rt-PCR	131
4.4.13 Proteome Profiler TM antibody array	132
4.5 Results	133
4.5.1 p38 α , - β , - γ and - δ isoforms and MKK3, -4, -6 and 7 are differentially expressed in oesophageal cancer	133
4.5.2 OESCC cell lines lacking endogenous p38 δ MAPK expression proliferate faster than those which express this isoform	140
4.5.3 Generation of stable cell lines expressing p38 δ , phosphorylated p38 δ (p-p38 δ) and p-p38 δ_{DN} MAPK	142

4.5.4 KE-3 cells transfected with p38 δ and p-p38 δ MAPK show reduced proliferation	150
4.5.5 p38 δ and p-p38 δ MAPK play a role in migration and anchorage independent growth of KE-3 cells	155
4.6 Discussion	159
4.7 References	164
5. p38δ MAPK phenotype: An indicator of chemotherapeutic response in oesophageal squamous cell carcinoma	167
5.1 Abstract	168
5.2 Hypothesis and aims	170
5.3 Introduction	171
5.4 Materials and methods	173
5.4.1 Cell culture	173
5.4.2 Drug treatment	173
5.4.3 Cell viability	174
5.4.4 Cell migration	174
5.4.5 Mitochondrial membrane potential ($\Delta\Psi_m$) assay	174
5.4.6 Immunoblot analysis	175
5.4.7 Clonogenic assay	175
5.5 Results	176
5.5.1 p38 δ MAPK negative OESCC demonstrate decreased sensitivity to chemotherapeutic drugs	176
5.5.2 Introduction of p38 δ or p-p38 δ MAPK does not increase OESCC sensitivity to CF treatment	180
5.5.3 ACF treatment significantly delays wound healing and migration compared to CF treatment	182
5.5.4 Triple ACF treatment decreases mitochondrial membrane potential and activates extrinsic pathways in p38 δ negative OESCC	185

5.5.5 Triple ACF treatment induces p38 and ERK1/2 but not JNK1/2 MAPK activation in p38 δ negative OESCC	189
5.5.6 Recovery of KE-3 and KE-8 cells following drug treatments	193
5.6 Discussion	195
5.7 References	199

6. Differential MAPK13 promoter methylation in oesophageal squamous cell carcinoma	202
6.1 Abstract	203
6.2 Hypothesis and aims	204
6.3 Introduction	205
6.4 Materials and methods	208
6.4.1 Cell culture	208
6.4.2 PCR/rt-PCR	208
6.4.3 Quantitative rt-PCR	209
6.4.4 Sodium bisulfite conversion	210
6.4.5 Methylation specific PCR (MSP)	213
6.4.6 Bisulfite sequencing PCR (BSP)	214
6.4.7 5'aza-2'-deoxycytidine treatment	216
6.5 Results	217
6.5.1 p38 δ MAPK mRNA is present in all OESCC cell lines	217
6.5.2 p38 δ MAPK translation start site sequence is intact in OESCC cell lines	219
6.5.3 p38 δ MAPK mRNA expression is downregulated in OESCC cell lines which lack p38 δ MAPK protein expression	221
6.5.4 MAPK13 promoter is differentially methylated in OESCC	223
6.5.5 Treatment with 5'aza-2'deoxycytidine does not induce p38 δ MAPK mRNA expression in KE-3 OESCC cells	226

6.6 Discussion	228
6.7 References	232
7. Investigation into the contribution of p38δ (and p-p38δ) to the cell cycle in OESCC	234
7.1 Abstract	235
7.2 Hypothesis and aims	236
7.3 Introduction	237
7.4 Materials and methods	244
7.4.1 Cell culture	244
7.4.2 Cell cycle gene expression analysis	244
7.5 Results	249
7.5.1 Relative cell cycle gene expression in p38 δ MAPK -positive (KE-6) versus p38 δ MAPK-negative (KE-3) OESCC	249
7.5.2 Relative cell cycle gene expression in p-p38 δ MAPK -positive versus p38 δ MAPK-negative KE-3 OESCC	252
7.6 Discussion	254
7.7 References	257
8. General Discussion	259
8.1 Discussion.....	260
8.2 Future directions	269
8.3 References	271
Appendix I: Plasmid sequences	274
Appendix II: Publications	292

Declaration

I hereby declare that all work presented in this thesis is original and entirely my own. This thesis has not been submitted in whole or in part for a higher degree to this or any other university. Any assistance and contribution by others to this work is acknowledged within the text.

Carol O'Callaghan, BSc.

Acknowledgements

Firstly I would like to thank Dr. Orla Patricia Barry for being the perfect supervisor. I really appreciate all of the support and guidance you have given me over the past 4 and a bit years. Thank you for all of your help both in and out of the lab and for making me believe I could actually finish this! I would not have achieved this without you. Thanks also to my co-supervisor Dr. Liam Fanning for pitching in whenever he was allowed! Your knowledge and advice has been invaluable. Thank you to all the staff and students of the Departments of Pharmacology and Medicine. Those in CUH deserve a particular mention, although I'm not sure if the endless tea and cakes was a hindrance or a help! To my parents, thank you for always telling me how proud you are of me. I am so grateful for everything you have done and continue to do for me. This thesis is dedicated to you both as it took more hard work and sacrifices on your part than it did on mine to achieve. I'm finished, I promise. Finally, to John, thank you for putting up with me, particularly in the last few months – it can't have been easy! Thank you for not pushing when I didn't want to talk about it and for listening when I did. Hopefully you now know almost as much about 'p39 protein' as I do.

List of Publications

This work has previously been published in the following formats:

Journal article/ original research article:

O'Callaghan, C., Fanning, L.J., Houston, A., Barry, O.P.

Loss of p38 δ mitogen-activated protein kinase expression promotes oesophageal squamous cell carcinoma proliferation, migration and anchorage-independent growth. *Int J Oncol* 2013; **43**:405-415.

Citations to date: 4

O'Callaghan, C., Fanning, L.J., Barry, O.P.

p38 δ MAPK phenotype: An indicator of chemotherapeutic response in oesophageal squamous cell carcinoma. *Anti Cancer Drugs* 2014 (Epub ahead of print).

Citations to date: 1

Journal article/ review article:

O'Callaghan, C., Fanning, L.J., Barry, O.P.

p38 δ MAPK: emerging roles of a neglected isoform. *Int J Cell Biol* 2014 (In press).

Citations to date: 3

Poster presentations:

American Association of Cancer Research Annual Meeting

(Washington D.C., April 2013)

O'Callaghan, C., Fanning, L.J., Houston, A., Barry, O.P.

New paradigms for the modulatory actions of p38 δ MAPK restorative expression in esophageal squamous cancer cell growth, migration and response to chemotherapy:

A possible future therapeutic target? *Cancer Research*. Vol. 73. No. 8. 615: Amer Assoc Cancer Research, 2013.

British Pharmacological Society Winter Meeting

(London, December 2012)

O'Callaghan, C., Fanning, L.J., Houston, A., O'Sullivan, G.C., Barry, O.P.

Targeting p38 δ MAPK in oesophageal cancer: A possible future therapeutic goal?

EORTC-NCI-AACR Symposium 'Molecular Targets and Cancer Therapeutics'

(Dublin, November 2012)

O'Callaghan, C., Fanning, L.J., Houston, A., O'Sullivan, G.C., Barry, O.P.

Targeting p38 δ MAPK in oesophageal cancer: A possible future therapeutic goal?

European Journal of Cancer 48 (2012): 173-174.

EACR-IACR Joint Conference 'The Tumour Microenvironment'

(Dublin, September 2012)

O'Callaghan, C., Fanning, L.J., Houston, A., O'Sullivan, G.C., Barry, O.P.

Targeting p38 δ MAPK in oesophageal cancer: A possible future therapeutic goal?

Oral presentation:

Lung Cancer Focus Research Group Meeting

(Cork Cancer Research Centre, April 2014)

O'Callaghan, C. and Barry, O.P.

The value of p38 δ MAPK phenotyping of tumours in deciding on an optimal therapeutic strategy?

Department of Pharmacology & Therapeutics Graduate Studies Committee 2012

O'Callaghan, C., Fanning, L.J., Barry, O.P.

Investigating an anti-tumourigenic role for p38 δ MAPK in oesophageal squamous carcinoma.

Department of Pharmacology & Therapeutics Graduate Studies Committee 2011

O'Callaghan, C., Fanning, L.J., Barry, O.P.

Generation of an MKK6b(E)-p38 δ MAPK fusion protein to enhance the anti-tumourigenic effect of p38 δ MAPK in oesophageal squamous cell carcinoma.

Department of Medicine Graduate Studies Committee 2011

O'Callaghan, C., Fanning, L.J., Barry, O.P.

Targeting p38 δ MAPK in oesophageal cancer: a possible future therapeutic goal?

Other publications:

O'Callaghan, C. and Barry, O.P.

Exploitation of Aberrant Signalling Pathways as Useful Targets for Renal Clear Cell Carcinoma Therapy, Renal Cell Carcinoma (2011), Dr. Hendrik Van Poppel (Ed.), ISBN: 978-953-307-844-1, InTech, DOI: 10.5772/26349.



Courses attended

- **Introduction to intermediate SPSS**

Graduate School

College of Medicine and Health, UCC

- **Laboratory Animal Science & Training (LAST-Ireland)**

National Training Course (Rodent)

Accredited with UK Universities Accreditation Group

- **Teaching and learning for graduate studies**

Teaching & Learning Centre, UCC

Projects supervised

Undergraduate B.Sc. Chemistry of Pharmaceutical Compounds projects

AY10/11

1. Investigation of angiotensin II as a possible future therapeutic target for the treatment of oesophageal cancer.
2. Analysis of p38MAPK isoform subcellular localization in oesophageal cancer cells.

AY11/12

1. Characterization of p38 MAPK and MAPKK expression in pancreatic adenocarcinoma and squamous carcinoma cell lines
2. Analysis of a fusion plasmid pcDNA3-FLAG-MKK6b(E)-(Gly-Glu)₅-p38 δ MAPK in oesophageal squamous cell carcinoma.

AY12/13

1. Does the presence or absence of p38 δ MAPK affect the sensitivity of OESCC to cytotoxic drugs?

AY13/14

1. An investigation of the anti-cancer effect(s) of docosahexaenoic acid derivatives Resolvin D1 and D2 in oesophageal cancer.

2. Development of a methyl 2-(3,6-Diamino-9H-Xanthen-9-yl) benzoate (Dihydrorhodamine 123) assay to measure the production of reactive oxygen species following cytotoxic anti-cancer drug treatment.

Postgraduate Cancer PhD Scholar program projects

AY10/11

Generation of a constitutively active fusion construct to investigate the role of p-p38 δ MAPK on the tumourigenicity of primary and metastatic oesophageal squamous carcinoma (OESCC).

AY11/12

Analysis of p-p38 δ MAPK (phosphorylated-p38 delta mitogen activated protein kinase) activation, expression and subcellular localisation in OESCC (oesophageal squamous cell carcinoma).

List of figures

Figure A.1: p38 MAPK isoform expression analysis in cancer primary and metastatic cell lines	xxx
Chapter 1	
Figure 1.1: Schematic representation of the current understanding of p38 δ MAPK signalling and activation	15
Chapter 2	
Figure 2.1: Standard curve for determination of protein concentration of unknown samples	55
Chapter 3	
Figure 3.1: Schematic of MKK6b(E)-(Gly-Glu) ₅ -FLAG-p38 δ fusion protein	76
Figure 3.2: Steps involved in generating the pcDNA3-MKK6b(E)-(Gly-Glu) ₅ -FLAG-p38 δ fusion construct	77
Figure 3.3: Confirmation of site-directed mutagenesis	89
Figure 3.4: PCR amplification of (Gly-Glu) ₅ -FLAG-p38 δ	91
Figure 3.5: Restriction digest analysis of plasmids generated from ligation of pcDNA3-MKK6b(E) and (Gly-Glu) ₅ -FLAG-p38 δ	93
Figure 3.6: Restriction digest analysis to determine the orientation of the (Gly-Glu) ₅ -FLAG-p38 δ insert	95

Figure 3.7: Control reactions to assess shrimp alkaline phosphatase and T4 DNA ligase activity	97
Figure 3.8: Restriction digest analysis of plasmids generated from ligation of pcDNA3-MKK6b(E) and Gly-Glu ₅ -FLAG-p38 δ	99
Figure 3.9: Restriction digest analysis to determine the orientation of the (Gly-Glu) ₅ -FLAG-p38 δ insert	101
Figure 3.10: Western blot analysis of KE-3 cells transiently transfected with pcDNA3-MKK6b(E)-FLAG-p38 δ fusion plasmids	103
Figure 3.11: Confirmation of successful site-directed mutagenesis of pcDNA3-MKK6b(E)-(Gly-Glu) ₅ -FLAG-p38 δ to generate pcDNA3-MKK6b-(Gly-Glu) ₅ -FLAG-p38 δ plasmid	105
Figure 3.12: Confirmation of successful site-directed mutagenesis of pcDNA3-MKK6b(E)-(Gly-Glu) ₅ -FLAG-p38 δ to generate pcDNA3-MKK6b(E)-(Gly-Glu) ₅ -FLAG-p38 δ _{DN} control plasmid	107
Figure 3.13: Western blot analysis of KE-3 cells transiently transfected with pcDNA3-MKK6b-(Gly-Glu) ₅ -FLAG-p38 δ and pcDNA3- MKK6b(E)-(Gly-Glu) ₅ -FLAG-p38 δ _{DN} control plasmids	109
 Chapter 4	
Figure 4.1: Cell counting with a haemocytometer	124
Figure 4.2: Expression of p38 MAPK isoforms, MKK3, -4, -6 and -7 in oesophageal cancer	135
Figure 4.3: Expression of p38 α , - β , - γ and - δ MAPK isoforms in oesophageal human tissue	138

Figure 4.4: Oesophageal squamous cell carcinoma cell lines lacking endogenous expression of p38 δ MAPK have a higher proliferation rate	141
Figure 4.5: Generation of cell lines stably expressing p38 δ , p-p38 δ and p-p38 δ_{DN}	143
Figure 4.6: Analysis of specific p38 δ MAPK phosphorylation	145
Figure 4.7: Effect of p-p38 δ expression on other MAPKs	147
Figure 4.8: Subcellular localization of transfected and endogenous p38 δ MAPK	149
Figure 4.9: Effect of p38 δ and p-p38 δ MAPK expression on cell proliferation	151
Figure 4.10: Effect of p38 δ MAPK knockdown on proliferation in a cell line which expresses it endogenously	153
Figure 4.11: Effect of p38 δ and p-p38 δ MAPK on KE-3 cell migration	156
Figure 4.12: Effect of p38 δ and p-p38 δ MAPK on KE-3 anchorage independent growth	158

Chapter 5

Figure 5.1: Sensitivity of OESCC to cancer chemotherapeutic drugs is correlated to the presence or absence of p38 δ MAPK	172
Figure 5.2: Effect of p38 δ and p-p38 δ MAPK expression on KE-3 sensitivity to CF treatment	181
Figure 5.3: Effect of chemotherapeutic cytotoxic drugs on wound healing and migration of KE p38 δ MAPK positive and negative cell lines	183
Figure 5.4: Effect of chemotherapeutic drug treatment on the mitochondrial	

membrane potential ($\Delta\Psi_m$) of p38 δ negative OESCCs	186
Figure 5.5: Effect of chemotherapeutic drug treatment on intrinsic and extrinsic mitochondrial pathways in KE-3 and KE-8 cells	188
Figure 5.6: MAPK activation in KE-3 and KE-8 cells following chemotherapeutic drug treatment	190
Figure 5.7: Involvement of MAPKs in CF and ACF induced cell death	192
Figure 5.8: Recovery of KE-3 and KE-8 cells following chemotherapeutic drug withdrawal	194

Chapter 6

Figure 6.1: Overview of bisulfite conversion	211
Figure 6.2: Representative diagram of MAPK13 promoter region CpG sites	215
Figure 6.3: p38 δ MAPK mRNA expression in oesophageal cancer	218
Figure 6.4: MAPK13 translation start site is intact in OESCC cell lines	220
Figure 6.5: Relative p38 δ MAPK mRNA expression in OESCC	222
Figure 6.6: MAPK13 promoter methylation analysis	225
Figure 6.7: Relative p38 δ MAPK mRNA expression in KE-3 cells following 5'-aza-2'-deoxycytidine treatment	227

Chapter 7

Figure 7.1: Schematic diagram of p38 MAPK pathway regulation of the cell cycle	238
Figure 7.2: RT ² Profiler PCR array layout	246
Figure 7.3: Relative expression comparison for 84 cell cycle associated genes between p38 δ MAPK-negative (KE-3) and p38 δ MAPK-	

positive (KE-6) OESCC 250

Figure 7.4: Relative expression comparison for 84 cell cycle associated

genes between KE-3 p-p38 δ MAPK and KE-3 cells 253

List of tables

Chapter 1

Table 1.1: Therapeutic targeting of the acquired capabilities necessary for cancer	3
Table 1.2: Risk factors for oesophageal cancer	7
Table 1.3: Known p38 δ MAPK substrates and their biochemical functions	20

Chapter 2

Table 2.1: Primary antibodies used for detection of proteins by Western blot	42
Table 2.2: KE (OESCC) cell line features	43
Table 2.3: Relevant chapters for experimental techniques	49
Table 2.4: Solutions for preparing gels for SDS-PAGE	56
Table 2.5: Primers for PCR and rt-PCR	60
Table 2.6: PCR/rt-PCR reaction components	61
Table 2.7: PCR/rt-PCR reaction conditions	62
Table 2.8: Incubation temperatures and recognition specificities for restriction enzymes	63
Table 2.9: Restriction digest reaction components and conditions	64
Table 2.10: DNA ladder molecular weight markers	65
Table 2.11: Additional primers for DNA sequence analysis	66

Chapter 3

Table 3.1: Primers for site-directed mutagenesis	79
--	----

Table 3.2: Site-directed mutagenesis reaction components	80
Table 3.3: Mutant strand synthesis reaction conditions	80
Table 3.4: PCR conditions for amplification of (Gly-Glu) ₅ -FLAG-p38δ	82
 Chapter 4	
Table 4.1: OESCC patient features	122
Table 4.2: Primary antibodies for immunohistochemistry/ immunocytochemistry	127
Table 4.3: p38δ MAPK expression in patient specimens	139
 Chapter 6	
Table 6.1: One-step qrt-PCR reaction conditions	209
Table 6.2: Bisulfite conversion reaction conditions	212
Table 6.3: Primers for MSP	213
 Chapter 7	
Table 7.1: RT ² Profiler Human Cell Cycle PCR array gene table	241
Table 7.2: RT ² Profiler PCR array reaction conditions	247
Table 7.3: Changes in fold regulation for cell cycle associated genes between p38δ MAPK-negative (KE-3) and p38δ MAPK-positive (KE-6) OESCC	251

Abbreviations

ACF	doxorubicin, cisplatin and 5-fluorouracil
ALI	acute lung injury
AP1	activator protein 1
ARDS	acute respiratory distress syndrome
ASK1	apoptosis signal regulated kinase 1
ATF2	activating transcription factor 2
ATP	adenosine triphosphate
BCA	bicinchoninic acid
BE	Barrett's Esophagus
BSP	bisulfite sequencing PCR
bp	base pair
BSA	bovine serum albumin
CC	cholangiocarcinoma
cDNA	complementary DNA
CDK	cyclin-dependent kinase
CDKI	cyclin-dependent kinase inhibitor
C/EBP	CCAAT (cytosine-cytosine-adenosine-adenosine-thymidine)- enhancer-binding protein
CF	cisplatin and 5-fluorouracil
COPD	chronic obstructive pulmonary disease
CpG	C-phosphate-G
CTCF	corrected total cell fluorescence
DAB	3,3'-diaminobenzidine
DCF	docetaxel, cisplatin and 5-fluorouracil
ddH₂O	double-distilled water
DLK	dual leucine zipper bearing kinase
DMEM	dulbecco's modified eagle's medium
DMSO	dimethyl-sulfoxide
DN	dominant negative
DNA	deoxyribonucleic acid

dNTP	deoxyribonucleotide triphosphate
dox	doxorubicin
EDTA	Ethylenediaminetetraacetic acid
eEF2	eukaryotic elongation factor 2
eEF2K	eukaryotic elongation factor 2 kinase
eIF4E	eukaryotic translation initiation factor 4E
ELISA	enzyme-linked immunosorbent assay
ERK	extracellular-regulated kinase
FACS	fluorescence activated cell sorting
FBS	foetal bovine serum
FFPE	formalin-fixed paraffin-embedded
FL	FLAG
GAPDH	Glyceraldehyde 3-phosphate dehydrogenase
GDC	genomic DNA control
gDNA	genomic DNA
GOI	gene of interest
GTP	guanosine-5'-triphosphate
GPCR	G-protein coupled receptor
HDAC	histone deacetylase
HKG	housekeeping gene
HNSCC	head and neck squamous cell carcinoma
HPV	human papilloma virus
hr	hour
HRP	horseradish peroxidase
IFN	interferon
IL	interleukin
JC-1	5,5',6,6'-tetrachloro-1,1',3,3'-tetraethylbenzimidazole carbocyanide iodide
JNK	c-jun NH ₂ -terminal kinase
kb	kilobase
kDa	kilo Dalton
KE-3 p38δ	KE-3 cell line stably transfected with pcDNA3-FLAG-p38δ
KE-3 pcDNA3	KE-3 cell line stably transfected with pcDNA3

KE-3 p-p38δ	KE-3 cell line stably transfected with pcDNA3-MKK6b(E)-(Gly-Glu) ₅ -FLAG-p38δ
KE-3 p-p38δ_{DN}	KE-3 cell line stably transfected with pcDNA3-MKK6b(E)-(Gly-Glu) ₅ -FLAG-p38δ _{DN}
KO	knock out
LB	luria broth
LPS	lipopolysaccharide
M	methylated
MAP3K	mitogen-activated protein kinase kinase kinase
MAPK	mitogen-activated protein kinase
MAPKAPK	mitogen-activated protein kinase activated protein kinase
MEF	mouse embryonic fibroblast
MEK	mitogen-activated protein kinase kinase
MEKK	mitogen-activated protein kinase kinase kinase
MGPs	magnetic glass particles
miRNA	micro RNA
min	minute
MKK	mitogen-activated protein kinase kinase
MKKK	mitogen-activated protein kinase kinase kinase
MLK	mixed-lineage kinase
mRNA	messenger RNA
MSP	methylation-specific PCR
MTT	3-(4,5-Dimethylthiazol-2-yl)-2,5-diphenyl tetrazolium bromide
myb	myeloblastosis
NAT	non-tumour adjacent tissue
NC	negative control
NES	nuclear export signal
NGS	normal goat serum
NLS	nuclear localisation signal
NTC	no template control
OA	okadaic acid
OEAC	oesophageal adenocarcinoma
OESCC	oesophageal squamous cell carcinoma

p	probability
PAGE	polyacrylamide gel electrophoresis
PARP	poly ADP ribose polymerase
PBS	phosphate buffered saline
PCR	polymerase chain reaction
PHAS-1	phosphorylated heat- and acid-stable protein 1
PKC	protein kinase C
PKD	protein kinase D
p-p38	phosphorylated p38
PPC	positive PCR control
PTEN	phosphatase and tensin homolog
Rb	retinoblastoma protein
RNA	ribonucleic acid
RNase	ribonuclease
rpm	revolutions per minute
RPMI	Roswell Park Memorial Institute medium
RT	room temperature
RTC	reverse transcription control
rt-PCR	reverse transcription polymerase chain reaction
s	second
SAP	serum response factor accessory protein
SAP	shrimp alkaline phosphatase
SAPK	stress-activated protein kinase
S.E.	standard error
SDM	site-directed mutagenesis
SDS	sodium dodecyl sulphate
siRNA	small-interfering RNA
STAT3	signal transducer and activator of transcription 3
TAB-1	TAK1-binding protein 1
TAK1	transforming growth factor β activated kinase 1
TAO	thousand-and-one amino acid
TB	terrific broth
TBS	tris buffered saline

TBS-T	tris buffered saline – TWEEN
TCGA	The Cancer Genome Atlas
TGF	transforming growth factor
TGY	threonine - glycine - tyrosine
TNBC	triple-negative breast cancer
TNF	tumour necrosis factor
TNM	tumour-node-metastases
TPA	12-O-tetradecanolyphorbol-13-acetate
TS/SAP	tris saline/saponin
TUNEL	terminal deoxynucleotidyl transferase dUTP nick end labeling
U	unmethylated
Unt	untreated
UV	ultra violet
V	voltage
VEGF	vascular endothelial growth factor
WHO	World Health Organisation
WT	wild-type
ZAK	leucine zipper and sterile- α motif kinase
$\Delta\Psi_m$	mitochondrial membrane potential

Hypothesis and aims of thesis

The overall hypothesis of this thesis is that p38 δ MAPK plays a role in the tumourigenicity of oesophageal cancer and may serve as a potential future therapeutic target.

Since their discovery, the p38 mitogen-activated protein kinase (MAPK) family of kinases have been increasingly associated with processes involved in cellular transformation such as proliferation, migration and apoptosis [1]. However these observations relate only to the effects of the p38 MAPK family as a whole or to p38 α MAPK. While p38 α MAPK has been characterised as both a tumour promoter and a tumour suppressor [2, 3], information regarding the role(s) p38 δ MAPK plays in tumourigenicity are seriously lacking. Subsequent to reporting a role for p38 δ in inhibition of cell growth in renal clear cell carcinoma (RCC) [4], our group examined p38 MAPK isoform expression in a panel of cancer cell lines. Preliminary data indicates that p38 δ MAPK, as opposed to $-\alpha$, $-\beta$ and $-\gamma$ isoforms is differentially expressed in a variety of human malignancies. Approximately 75% of cancer cell lines examined fail to express p38 δ MAPK yet consistently express the other p38 MAPK family members. A lack of p38 δ MAPK expression was detected in renal, prostate, lung, liver and oesophageal cancer cell lines (Figure A.1). This thesis focuses on providing novel insights into specific roles for p38 δ MAPK in several aspects of cancer progression, particularly in oesophageal carcinoma. However it is important to note that our findings may be translatable to other cancers which lack p38 δ MAPK expression.

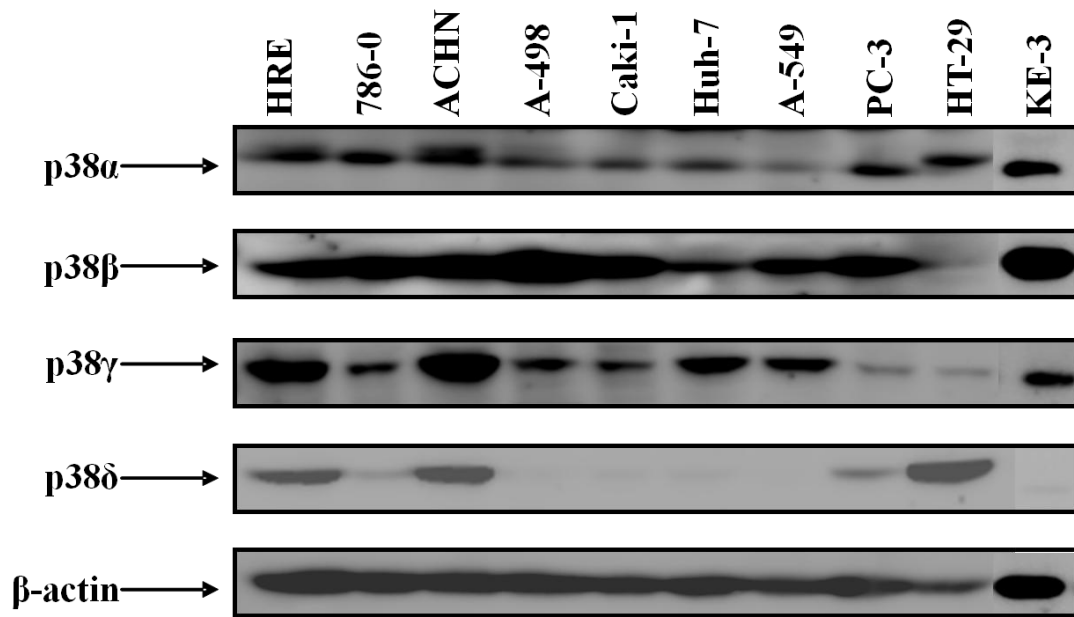


Figure A.1 p38 MAPK isoform expression analysis in cancer primary and metastatic cell lines. Western blot analysis of p38 α , - β , - γ and - δ expression in HRE (normal human renal epithelium); 786-0, ACHN, A-498 and Caki-1 (Renal cell carcinoma); Huh-7 (liver carcinoma); A-549 (lung carcinoma); PC-3 (prostate carcinoma), HT-29 (colon carcinoma) and KE-3 (oesophageal squamous cell carcinoma). Aliquots of 30 μ g protein lysate for each cell line were loaded on a 10% SDS-PAGE gel and analysed by immunoblot using antibodies specific for p38 α , - β , - γ , or - δ . β -actin analysis served as a loading control. The results shown are representative of four independent experiments.

To achieve this overall goal of identifying how p38 δ MAPK contributes to the tumourigenicity of oesophageal squamous cell carcinoma (OESCC), the project was divided into a number of specific aims:

- (1) The first specific aim of this thesis is to develop a method of examining not only the effects of p38 δ MAPK expression in OESCC but also the consequences of expressing constitutively active p-p38 δ MAPK. In Chapter 3, an approach of enzyme-substrate fusion is utilised to generate a constitutively active form of p38 δ MAPK for use in subsequent experiments.
- (2) The second specific aim is to evaluate the roles for p38 δ MAPK in processes essential for OESCC progression such as proliferation, migration and anchorage independent growth. This will be addressed in Chapter 4 using stably transfected OESCC cell lines expressing p38 δ and p-p38 δ MAPK.
- (3) Chapter 5 will aim to outline the effect p38 δ MAPK has on OESCC response to conventional and novel chemotherapeutic drug combinations and also to delineate the specific apoptotic pathways involved.
- (4) As discussed above, p38 δ MAPK is differentially expressed in various cancer cell lines. Chapter 6 aims to uncover how p38 δ MAPK expression is lost in these cells. Here genetic and epigenetic mechanisms of gene silencing are examined.

(5) Finally, as p38 α MAPK is a known regulator of the cell cycle, Chapter 7 aims to elucidate a specific contribution for p38 δ MAPK to cell cycle progression in OESCC using a human cell cycle PCR array.

In summary, this thesis aims to uncover and explain new roles for p38 δ MAPK, particularly in OESCC progression and chemosensitivity and in doing so, evaluate its potential as a therapeutic target for OESCC.

References

1. Ono, K. and J. Han, *The p38 signal transduction pathway: activation and function*. Cell Signal, 2000. **12**(1): p. 1-13.
2. del Barco Barrantes, I. and A.R. Nebreda, *Roles of p38 MAPKs in invasion and metastasis*. Biochem Soc Trans, 2012. **40**(1): p. 79-84.
3. Bulavin, D.V. and A.J. Fornace, Jr., *p38 MAP kinase's emerging role as a tumor suppressor*. Adv Cancer Res, 2004. **92**: p. 95-118.
4. Ambrose, M., et al., *Induction of apoptosis in renal cell carcinoma by reactive oxygen species: involvement of extracellular signal-regulated kinase 1/2, p38delta/gamma, cyclooxygenase-2 down-regulation, and translocation of apoptosis-inducing factor*. Mol Pharmacol, 2006. **69**(6): p. 1879-90.

Abstract

Oesophageal cancer is an aggressive malignancy which is resistant to conventional therapy and has a poor prognosis. A greater understanding of the underlying molecular biology of oesophageal cancer and the identification of novel targets is necessary for the future treatment of this disease. This thesis focuses specifically on the ill-defined and understudied p38 δ mitogen-activated protein kinase (MAPK) and its function(s) in oesophageal squamous cell carcinoma (OESCC). In contrast to the three other p38 isoforms (p38 α , - β and - γ which have to-date been relatively well-studied), p38 δ MAPK signalling is poorly understood. Thus, this research elucidates some of the role(s) played by p38 δ MAPK in cancer progression. This work outlines how loss of p38 δ MAPK expression confers greater tumourigenicity in oesophageal cancer. Restoration of p38 δ MAPK expression, however, has anti-proliferative and anti-migratory effects and decreases OESCC capacity for anchorage-independent growth. Using a novel application of an enzyme-substrate fusion approach, the effect of phosphorylated p38 δ (p-p38 δ) MAPK expression is also considered. The work goes onto describe the effect(s) of p38 δ MAPK status on the chemosensitivity of OESCC to conventional cisplatin and 5-fluorouracil (CF) versus the effectiveness of doxorubicin, cisplatin and 5-fluorouracil (ACF). ACF treatment of p38 δ MAPK-negative OESCC results in decreased proliferation, migration and recovery, and increased apoptosis when compared with CF treatment. This thesis examines the potential mechanisms by which p38 δ MAPK expression is lost in OESCC and identifies epigenetic regulation as the probable cause of differential p38 δ MAPK expression. Also analysed is the role p38 δ MAPK and p-p38 δ MAPK play in the cell

cycle. In summary, this research identifies p38 δ MAPK as a possible molecular target and a potential predictor of response to chemotherapy in OESCC patients.

Chapter 1

Introduction

O'Callaghan, C., Fanning, L.J., Barry, O.P.
p38 δ MAPK: emerging roles of a neglected isoform
Int J Cell Biol 2014; 2014:272689. (Epub).
(Appendix II)

1.1 Hallmarks of cancer

The World Health Organisation (WHO) defines cancer as a group of diseases that can affect any part of the body and are characterised by the rapid creation of abnormal cells that grow beyond their usual boundaries [1]. This definition however lacks the complexity required to fully explain this intricate and multifaceted disease. The seminal article ‘The Hallmarks of Cancer’ identified six capabilities which normal cells acquire as they evolve progressively to invasive cancer cells. These are self-sufficiency in growth signals, evasion of growth suppressors, invasion and metastasis, unlimited replicative potential, angiogenesis, and evasion of cell death. [2] These hallmarks are essential for most forms of cancer, enabling cells to become tumourigenic and malignant. However tumours are now known to consist of more than just cancer cells. The contribution of the ‘tumour microenvironment’ to tumourigenesis must also be considered. As a result, two further acquired characteristics are now being considered as emerging hallmarks of cancer cells [3]. The ability of cancer cells to evade destruction by immune cells and the modification of cellular energetics in order to effectively support cancer cell proliferation may also be crucial to the pathogenesis of some if not most cancers [3]. Underlying the acquisition of these hallmark characteristics are genome instability and mutation of DNA monitoring and repair systems as well as tumour promoting inflammation. These enabling characteristics represent the means by which pre-malignant cells reach the hallmark capabilities detailed above [3]. To date targeted therapies for the treatment of human cancers have focused on molecular targets which are involved in enabling specific hallmark capabilities, some examples of which are outlined in Table 1.1. However this has often led to adaptation of cancer cells to alternative

pathways and/or increased dependence on another hallmark capability. It is possible however that co-targeting of multiple hallmarks and enabling characteristics may in the future provide more effective therapeutics for cancer.

Table 1.1 Therapeutic targeting of the acquired capabilities necessary for cancer [3].

Hallmark/enabling characteristic	Targeted therapy
Self-sufficiency in growth signals	Receptor tyrosine kinase inhibitors
Evasion of growth suppressors	Cyclin-dependent kinase inhibitors
Invasion and metastasis	HGF/c-Met inhibitors
Unlimited replicative potential	Telomerase inhibitors
Angiogenesis	Inhibitors of VEGF signalling
Evasion of cell death	Proapoptotic BH3 mimetics
Avoidance of immune destruction	Anti-CTLA4 mAb
Deregulation of cellular energetic	Aerobic glycolysis inhibitors
Genome instability and mutation	PARP inhibitors
Tumour promoting inflammation	Anti-inflammatory drugs

1.2 Oesophageal cancer

Oesophageal cancer is an aggressive disease which responds poorly to both chemotherapy and radiation therapy and has a poor prognosis – the five-year survival rate in Ireland is ~15% [4]. Worldwide, it is the eighth most common cancer and the sixth leading cause of death from cancer [5]. Despite recent advances in surgical techniques, the lack of adequate preventative strategies, screening techniques, and most significantly, effective therapeutic agents all contribute to the poor outcome. The molecular mechanisms underlying oesophageal carcinoma are not well understood and as a result novel therapeutic targets are lacking. Thus, a greater understanding of the biology of oesophageal cancer is needed in order to identify new effective targeted therapies.

1.2.1 Incidence

In Ireland, oesophageal cancer is the fourteenth most common cancer diagnosed and the sixth leading cause of invasive cancer related death with an average of 372 new cases each year and 333 deaths in 2010 [4]. The lifetime risk (to age 75 years) of oesophageal cancer diagnosis is 0.4% for women and 1.0% for men. Risk increases with age, with a median age at diagnosis of 69 years [4]. Universally, oesophageal cancer is more common in men than women. Approximately 80% of cases worldwide occur in less developed regions. The highest incidence rates are found in Eastern Asia and Southern and Eastern Africa, followed by Northern Europe [5]. There are two main histologic forms of oesophageal cancer: squamous carcinoma (OESCC) which is most commonly found in the middle-third of the oesophagus and

adenocarcinoma (OEAC) which usually occurs in the distal oesophagus [6]. OESCC is dominant in most parts of the world, particularly in high-risk areas such as China; however OESCC incidence rates are declining in most Western countries. In contrast, incidence trends for OEAC are increasing in developed countries [7].

1.2.2 Etiology

Oesophageal cancer is a multifactorial disease. Increased risk of both OESCC and OEAC is most closely associated with smoking. Occurrence of oesophageal cancer correlates directly with both the quantity of cigarettes smoked per day and the duration of smoking [8, 9]. Smoking cessation can cause a considerable decrease in the risk of developing OESCC but does not appear to impact on the risk of OEAC [10, 11]. Risk factors for both OESCC and OEAC are discussed below and summarised in Table 1.1

OESCC

Factors which cause irritation and inflammation of the oesophageal mucosa appear to contribute greatly to the occurrence of OESCC. These include substantial alcohol intake (particularly in combination with smoking), achalasia, and frequent consumption of hot beverages [9, 12-14]. The autosomal dominant disorder nonepidermolytic palmoplantar keratoderma (tylosis) confers up to a 95% risk of OESCC by the age of 70 years in affected families [15, 16]. Incidence of OESCC is also associated with a low socioeconomic status. The reasons for this are not well understood but are thought to include poor nutrition and low intake of fruit and vegetables [9]. Human papilloma virus (HPV) infection is thought to be associated

with the development of OESCC. A recent meta-analysis identified an increased risk of OESCC in patients with HPV infection while the prevalence of HPV in OESCC was found to be 24.8% [17]

OEAC

Chronic gastrointestinal reflux is a major risk factor for OEAC. Patients with recurring reflux have an eight-fold increase in risk of developing OEAC [18]. Barrett's Esophagus (BE), which develops in 5-8% of patients with gastrointestinal reflux disease but can also occur in patients without symptoms of reflux, appears to be a significant risk factor for OEAC [19, 20]. BE is characterised by a change of the oesophageal epithelium from squamous to columnar mucosa and the risk of transformation to adenocarcinoma is estimated to be 0.5% per patient, per year [21]. Obesity, especially visceral obesity, is also a risk factor for OEAC [22]. It has been estimated that obesity accounts for 23% of OEAC cases [23]. The worldwide increase in obesity rates in recent years is thought to be the major contributor to the increasing incidence of OEAC.

Table 1.2 Risk factors for oesophageal cancer

Risk Factor	OESCC	OEAC
Smoking/Tobacco	X	X
Alcohol	X	
Obesity		X
Reflux		X
Barrett's Oesophagus (BE)		X
Poverty	X	
Hot beverages	X	
Nonepidermolytic palmoplantar keratoderma	X	
HPV	X	

1.2.3 Staging, prognosis and treatment

Oesophageal cancer is classified according to the tumour-node-metastases (TNM) system which describes the primary tumour, regional node metastases and distant metastases [24]. At the time of presentation more than 50% of patients have unresectable disease or distant metastases [25]. The five-year survival rate has improved over time from 4% to 14% and improves further following complete surgical removal of the tumour [26]. In terms of survival benefit for patients there is currently no clear optimal adjuvant or neoadjuvant treatment regimen [27]. Preoperative chemotherapy or chemoradiotherapy is the standard treatment for locally advanced disease. For management of advanced (stage IV) disease, chemotherapy is palliative and improves quality of life and dysphagia [25]. Chemotherapy may be given as a single agent or in combination, generally in a fluoropyrimidine/platinum regimen. Combination chemotherapy tends to achieve greater tumour reduction than single-drug treatments, however the median survival time remains unchanged and the potential for toxicity is increased [25].

1.2.4 Targeted therapy for oesophageal cancer

In this era of targeted therapy, the identification of molecular markers and therapeutic targets for oesophageal cancer lags significantly behind that of other malignancies. Although a small number of novel targets have been discovered, the underlying molecular mechanisms governing oesophageal carcinoma remain unclear. Promising molecular targets are generally considered to be genes mutated at a high frequency, regulators of key cancer phenotypes, or receptors overexpressed in cancer cells [25]. Several molecular targets which are commonly found in other cancers have been evaluated for efficacy in oesophageal cancer. These include epidermal growth factor receptors EGFR and HER-2/Neu as well as regulators of angiogenesis (vascular epithelial growth factor, VEGF), inflammation (Cox-2), apoptosis (p53, Bcl-2) and cell cycle control (p16, p21) [25]. Although therapies targeting these molecules in oesophageal cancer continue to undergo phase I/II clinical trials, they have shown limited effectiveness to date [25, 28]. As such the development of novel diagnostic markers and molecular targeted therapies is urgently required.

1.3 p38 δ MAPK – emerging roles of a neglected isoform

p38 δ MAPK is a unique stress responsive protein kinase. While the p38 MAPK family as a whole has been implicated in a wide variety of biological processes, a specific role for p38 δ MAPK in cellular signalling and its contribution to both physiological and pathological conditions are presently lacking. Recent emerging evidence, however, provides some insights into specific p38 δ MAPK signalling. Importantly, these studies have helped to highlight functional similarities as well as differences between p38 δ MAPK and the other members of the p38 MAPK family of kinases. Here we discuss the current understanding of the molecular mechanisms underlying p38 δ MAPK activity. We outline a role for p38 δ MAPK in important cellular processes such as differentiation and apoptosis as well as pathological conditions such as neurodegenerative disorders, diabetes, and inflammatory disease. Interestingly, disparate roles for p38 δ MAPK in tumour development have also recently been reported. Thus, we consider evidence which characterises p38 δ MAPK as both a tumour promoter and a tumour suppressor. In summary, while our knowledge of p38 δ MAPK has progressed somewhat since its identification in 1997, our understanding of this particular isoform in many cellular processes still strikingly lags behind that of its counterparts.

1.3.1 p38 MAPK isoform evolution

The first and now archetypal member of the p38 MAPK family, p38 α MAPK, was identified by four independent groups in 1994. It was isolated as a 38 kDa protein rapidly tyrosine phosphorylated in response to lipopolysaccharide (LPS) stimulation

[29], as a molecule that binds pyridinyl-imidazole drugs which inhibit the synthesis of proinflammatory cytokines [30] and as an activator of MAPK activated protein kinase 2 (MAPKAP-K2/MK2) and small heat shock proteins in cells stimulated with heat shock or interleukin- (IL-) 1 [31, 32]. This was followed by the subsequent identification of p38 β MAPK in the same year, p38 γ MAPK in 1996, and lastly p38 δ MAPK in 1997 [33-37]. The product of the *S. cerevisiae* HOG1 gene, an important component of osmoregulation and the cell cycle, was found to be a homologue of p38 MAPK [38]. This conservation from yeast to mammals is significant as it indicates that the p38 family is responsible for critical cellular processes. A study of the evolutionary history of MAPKs suggests that each p38 MAPK family member evolved from a single ancestor. In fact it appears that MAPK12 (p38 γ) arose from a tandem duplication of MAPK11 (p38 β) on chromosome 22 while MAPK14 (p38 α) and MAPK13 (p38 δ) subsequently resulted from a single segmental duplication of the MAPK11-MAPK12 gene unit on chromosome 6 [39]. These gene duplications appear to have occurred before the species separation of nematodes but after the species separation of arthropods. Interestingly, unlike the other p38 isoforms, MAPK13 has not been identified in teleosts [39]. This indicates that a MAPK13 gene deletion event may have occurred subsequent to gene duplication in the evolution of these species. Duplicated genes are generally assumed to be functionally redundant at the time of origin and are eventually silenced. The evolutionary preservation of the four p38 MAPK isoforms therefore suggests functional differentiation of the individual family members. Thus, while the majority of research to date has focused on p38 α and p38 β MAPKs, each isoform is an important kinase in its own right with distinct cellular functions. This chapter aims to highlight components of the previously neglected p38 δ MAPK signalling pathway

and emphasises recent progress in our understanding of p38 δ MAPK involvement in diverse physiological as well as pathological processes.

The use of pyridinyl-imidazole inhibitors has largely driven the advancement in our understanding of p38 α and p38 β MAPK signalling, functions, and substrates. Both p38 α and p38 β MAPK are highly sensitive to inhibition by SB203580, SB202190, and newer compounds such as L-167307 [30, 33, 40]. In contrast, the observation that p38 δ MAPK is insensitive to inhibition by pyridinyl-imidazole compounds has hindered its study in cellular events [35, 37]. The differential sensitivity to these drugs can be attributed to amino acid sequence variability at the ATP binding pocket where these compounds bind competitively, facilitated by interactions with nearby amino acids. Thr106 of p38 α and p38 β MAPK has been identified as the major determinant for imidazole inhibitor specificity as it orientates the drug to interact with His107 and Leu108 thereby preventing ATP binding [41]. The equivalent residue in p38 δ MAPK is a methionine (Met), the large side chain of which prevents binding of these inhibitors. In fact, substitution of Met106 in p38 δ MAPK with Thr was found to confer some sensitivity to inhibition by SB203580 [42]. Conversely, p38 α MAPK mutants in which Thr106 is replaced with Met displayed reduced sensitivity to inhibition by SB203580 [43]. It is unfortunate that no potent p38 δ MAPK specific inhibitor has been identified to date. Although the diaryl urea compound BIRB796 allosterically inhibits p38 δ MAPK at high concentrations, it is also a powerful inhibitor of p38 α , - β , and - γ MAPK [44]. While varying the concentration of BIRB796 and combining it with SB203580 may be of some use in identifying p38 δ MAPK specific signalling pathways, the possible influence of the

other p38 MAPK isoforms, in particular p38 γ MAPK, must be considered when interpreting any results.

1.3.2 p38 δ MAPK expression and activation

Unsurprisingly, p38 δ MAPK shares highly similar protein sequences with the other p38 MAPK isoforms. It displays 61%, 59%, and 65% amino acid identity to p38 α , - β , and - γ MAPKs, respectively [35]. Differences in sequence between p38 δ MAPK and the other p38 MAPK family members can be observed in the ATP binding pocket. This has consequences for inhibitor sensitivity and contributes to substrate specificity. On the other hand, the greatest sequence similarities lie in the highly conserved kinase domains, where the four isoforms share >90% amino acid identity [45]. Within kinase subdomain VIII (of XI), p38 δ MAPK possesses a Thr-Gly-Tyr (TGY) dual phosphorylation motif which is the hallmark of p38 MAPKs and is conserved among all known mammalian p38 isoforms [35-37, 46]. p38 δ MAPK has a distinct distribution profile in human tissue that is relatively limited compared to that of p38 α and p38 β MAPK isoforms which are largely ubiquitously expressed [36]. High levels of p38 δ messenger RNA (mRNA) have been detected in endocrine tissues such as salivary, pituitary, prostate, and adrenal glands, while more modest levels are expressed in the stomach, colon, trachea, pancreas, skin, kidney, and lung [36]. This differential expression in different cell and tissue types is indicative of a specific biological effect of p38 δ MAPK activation in these cell types, distinct from that of the other p38 family members.

The murine p38 δ MAPK amino acid sequence is 92% identical to the human sequence and the adult mouse displays a broadly similar pattern of p38 δ MAPK expression to that seen in human tissue, that is, lung, testis, kidney, and gut epithelium [46]. Murine p38 δ MAPK expression varies at different stages in the developing mouse embryo. At 9.5 days it is primarily expressed in the developing gut and septum transversum, while by 15.5 days its expression expands to most developing epithelia [46]. This suggests that p38 δ MAPK has a role in embryonic development. However, knock-out of p38 δ MAPK results in mice which are both viable and fertile and exhibit a normal phenotype [47]. Moreover, while p38 β - and p38 γ -null mice as well as p38 γ /p38 δ double knockout (KO) mice are also phenotypically normal [47, 48], genetic ablation of p38 α MAPK is embryonic lethal at day 10.5–11.5 [49]. Functional redundancy among the p38 isoforms is a likely explanation with p38 α , - β , or - γ compensating for the loss of p38 δ MAPK activity during development. However, it appears that p38 α MAPK plays a critical role in early development where its loss cannot be overcome.

p38 α , - β , and - γ MAPK isoforms are activated by alterations in the physical and chemical properties of the extracellular environment with diverse triggers including environmental stress signals, inflammatory cytokines, and mitogenic stimuli [29, 33, 34, 50]. Using transiently expressed epitope-tagged p38 δ MAPK, a similar activation profile has been defined for p38 δ MAPK [35-37]. It is strongly activated by environmental alterations in osmolarity, ultraviolet (UV) irradiation, and oxidation. It is also moderately activated by chemical stressors and proinflammatory cytokines including arsenite, anisomycin, tumour necrosis factor- (TNF-) α , and IL-1. Despite their similar activation profiles, differences in the levels of activation of p38 δ MAPK

and the other p38 MAPK isoforms have been reported. For example, while hyperosmolarity appears to stimulate both p38 α and p38 δ MAPK to a similar degree, under hypoosmotic conditions, p38 α MAPK is more strongly activated than p38 δ MAPK [35]. A range of mitogen-activated protein kinase kinases (MAP3Ks) have been implicated in the activation of the p38 MAPK pathway, including mixed-lineage kinases (MLKs), transforming growth factor β activated kinase 1 (TAK1), apoptosis signal-regulating kinase 1 (ASK1), thousand-and one amino acid (TAO), dual-leucine-zipper-bearing kinase 1 (DLK1), MAPK/ERK kinase kinases (MEKKs), and leucine zipper and sterile- α motif kinase 1 (ZAK1) (Figure 1.1). To date their individual contribution to p38 δ MAPK signalling in particular is not yet understood [51-56]. Further upstream of the MAP3Ks is a complex network involving members of the Ras/Rho family of small GTP-binding proteins and heterotrimeric G-protein coupled receptors (GPCR) [57, 58]. This adds to the diversity of signalling from various stimuli contributing to the crosstalk between p38 MAPKs and other signalling pathways.

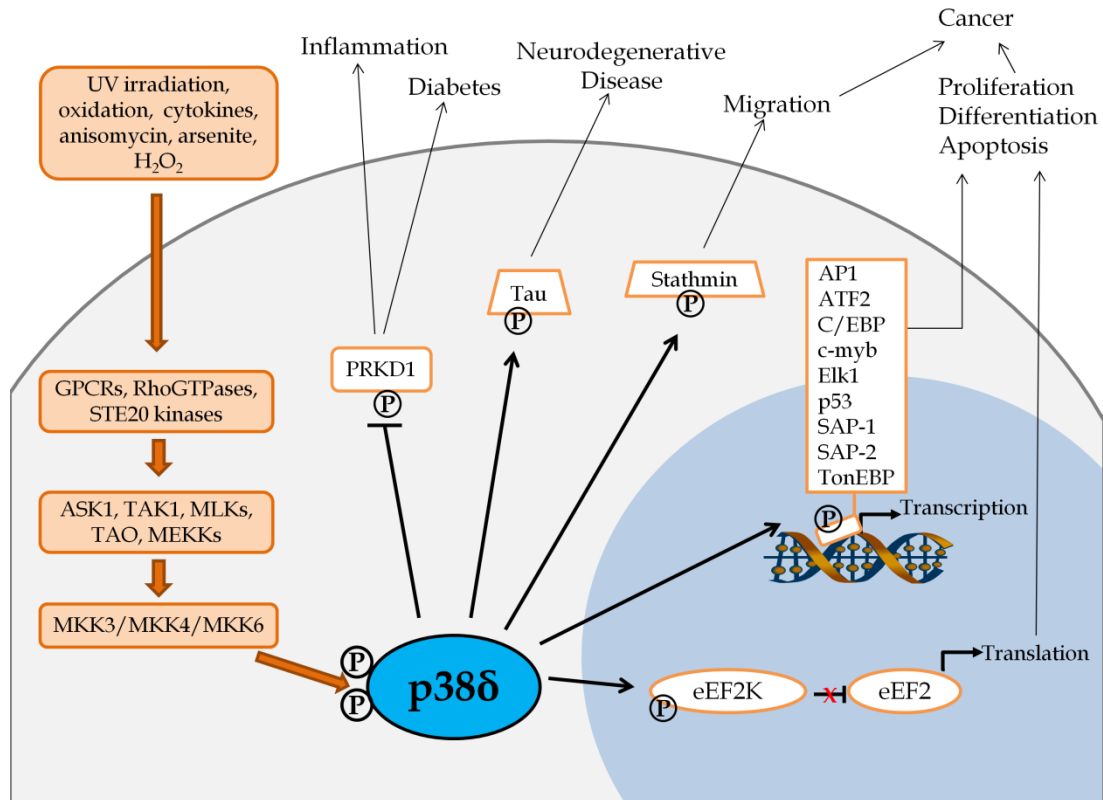


Figure 1.1 Schematic representation of the current understanding of p38 δ MAPK signalling and activation. A variety of extracellular stimuli can activate the MAPK signalling pathway resulting in dual phosphorylation of p38 δ MAPK. Known substrates of active p38 δ MAPK include transcription factors, structural proteins, kinases, and translation repressors. Phosphorylated substrates affect several cellular processes and contribute to the pathogenesis of diseases such as cancer, diabetes, and neurodegenerative and inflammatory conditions.

The upstream direct activators responsible for dual phosphorylation of the p38 MAPK TGY motif are the MAPK kinases (MKKs). p38 δ MAPK is unique as it can be activated by four separate MKKs: the p38 MAPK specific MKK3 and MKK6 and also the JNK MKKs-4 and -7 [35-37, 46]. However, information regarding the specific contributions of these individual MKKs to p38 δ MAPK activation in different cell types and under diverse conditions is lacking. Current evidence suggests that activation of p38 δ MAPK is significantly influenced by both the nature and the strength of the stimulus as well as the cell type involved. This may be the result of varying levels of expression of upstream components of the MAPK signalling cascade in different cell types. For example, MKK3 is the major direct activator of p38 δ MAPK phosphorylation in response to UV radiation, hyperosmotic shock, and TNF α in mouse embryonic fibroblast (MEF) cells [59]. It also appears to be the primary kinase responsible for p38 δ MAPK activation in response to transforming growth factor- β 1 (TGF- β 1) as MKK3 deficiency impairs endogenous p38 δ activation by TGF- β 1 in murine glomerular mesangial cells [60]. On the other hand, MKK6 was identified as the major activator of p38 δ MAPK in KB (HeLa) cells subjected to IL-1, anisomycin, or osmotic stress [37]. Furthermore, MKK7 is reported to be responsible for the activation of p38 δ MAPK in 293T cells under peroxide stress, mediated by the scaffolding action of islet brain-2 [61]. Further complicating the current understanding of p38 δ MAPK activation is the likelihood that, in some cases, the cooperation of two MKKs may be necessary. While MKK4 preferentially phosphorylates JNK on Tyr, MKK7 preferentially phosphorylates JNK on Thr [62-64]. Therefore it must be considered possible that the combined activity of these two MKKs may be required to fully phosphorylate p38 δ MAPK on both the Tyr and the Thr residues. Interestingly, two reports outline a MKK independent

mechanism of activation for p38 α MAPK via autophosphorylation [65, 66]. While autophosphorylation activity is detected in intrinsically active p38 δ mutants [67, 68], no such pathway has been observed which activates the endogenous p38 δ MAPK isoform.

An important factor in determining the biological consequences of p38 δ MAPK phosphorylation is the strength and duration of the activation signal. p38 δ MAPK activation is largely transient with activation and downregulation occurring within minutes of stimulation [45]. This is due to the regulatory action of protein phosphatases which again appears to be cell-type specific. While MAPK phosphatase 1 inactivates p38 δ MAPK in HEK293FT cells, it does not interact with p38 δ MAPK in the NIH3T3 cell line [69, 70]. The protein serine/threonine phosphatases PP1 and PP2A have also been shown to be involved in p38 δ MAPK phosphorylation as okadaic acid (OA), a PP1/PP2A inhibitor, causes increased p38 δ MAPK activity in human epidermal keratinocytes [71].

1.3.3 Novel p38 δ MAPK substrates

While p38 MAPKs are proline-directed kinases, substrate specificity is also determined by docking domains both in the MAPK itself and in the target protein [72]. Therefore, although p38 δ MAPK substrate specificity overlaps to some extent with that of p38 α , - β , and - γ MAPKs, there are a number of notable differences. Common substrates of p38 MAPKs include MBP, PHAS-1, and transcription factors ATF2, SAP1, Elk-1, and p53 (Figure 1.1). In contrast, however, substrates such as MAPK activated protein kinase 2 (MAPKAP-K2) and MAPKAP-K3 which are the

major downstream kinases of p38 α and p38 β MAPK are not phosphorylated by p38 δ MAPK [35-37, 73] (Table 1.2).

Tau

At the time p38 δ MAPK was first described the microtubule-associated protein tau was identified as a strong in vitro substrate for p38 δ MAPK [74]. Tau is a component of the cytoskeleton network and under normal conditions it stabilises microtubule assembly by binding to β -tubulin. Phosphorylation of tau at T50 by p38 δ MAPK causes it to be functionally modified and enhances its capacity to promote microtubule assembly. This effect is seen in neuroblastoma in response to osmotic shock where tau T50 phosphorylation occurs soon after p38 δ MAPK activation, aiding the adaptive response of neurons to changes in osmolarity [74]. It appears, however, that subsequent hyperphosphorylation of tau at additional sites causes it to dissociate from the cytoskeleton, thereby promoting its self-assembly [75]. This aggregation destabilises the microtubule network and contributes to the development of neurofibrillary tangles [76]. Notably, Alzheimer's disease and other neurodegenerative disorders known as tauopathies are characterised by the aggregation in the brain of these neurofilament structures [77]. There is therefore a clearly defined role for p38 δ MAPK in the pathogenesis of neurodegenerative disease, making it a good potential therapeutic target for these disorders.

Stathmin

There is further evidence of a role for p38 δ MAPK in cytoskeleton regulation as the microtubule associated protein stathmin has also been characterised as a good p38 δ MAPK substrate in vitro and in transfected cells exposed to osmotic shock [78]. The

normal physiological role of stathmin is to sequester free tubulin and increase depolymerisation of microtubules [79, 80]. It is possible that phosphorylation of stathmin by p38 δ MAPK blocks its ability to destabilise microtubules and as a result promotes microtubule polymerisation and enhances cell survival under stress conditions.

eEF2K

In response to anisomycin stimulation, p38 δ MAPK has been shown to be the main p38 MAPK isoform which phosphorylates eukaryotic elongation factor 2 kinase (eEF2K) [81]. Phosphorylation of eEF2K on Ser359 inactivates the kinase and as a result removes its inhibitory phosphorylation of eukaryotic elongation factor 2 (eEF2). eEF2 in turn promotes the movement of the ribosome along mRNA during translation [82]. This suggests that, by inhibiting eEF2K and consequently activating eEF2, p38 δ MAPK is responsible for driving the translation of proteins associated with stress responses. Consistent with this hypothesis is the observation that the MKK3/6-p38 δ MAPK/eEF2K pathway in myeloid cells is implicated in the production of the proinflammatory cytokine TNF α in bacterial LPS induced acute liver disease [83]. These differences in substrate specificity in combination with its unique tissue distribution profile demonstrate that despite similarities in stimuli the consequences of p38 δ MAPK can potentially be significantly different to those of the other p38 MAPK isoforms.

Table 1.3 Known p38 δ MAPK substrates and their biochemical functions

Substrate	Function	Consequences of phosphorylation
AP1	Transcription factor	Activation of transcription, involucrin expression, keratinocyte differentiation [84]
ATF2	Transcription factor	Activation of transcription [35, 37]
C/EBP	Transcription factor	Keratinocyte differentiation [85]
c-myb	Transcription factor	c-myb degradation [86]
eEF2K	Inhibitory kinase	eEF2 activation, protein synthesis [81]
Elk1	Transcription factor	Activation of transcription [35, 37]
p53	Transcription factor	p21 expression, G ₁ phase arrest [37, 87]
PHAS-1	Translation repressor	Dissociation from eIF4E, activation of translation [35]
PKD1	Serine-threonine kinase	Inhibition of PRKD1 activity [88]
SAP-1	Transcription factor	Activation of transcription [37]
SAP-2	Transcription factor	Activation of transcription [37]
Stathmin	Microtubule protein	Cytoskeleton reorganisation [78]
Tau	Microtubule protein	Microtubule assembly, tau self-aggregation [74]
TonEBP/OREBP	Transcription factor	Impaired TonEBP/OREBP transcriptional activity [69]

AP1: activator protein 1; ATF2: activating transcription factor 2; C/EBP: CCAAT (cytosine-cytosine-adenosine-adenosine-thymidine)-enhancer-binding protein; myb: myeloblastosis; eEF2K: eukaryotic elongation factor 2 kinase; eEF2: eukaryotic elongation factor 2; PHAS-1: Phosphorylated heat- and acid-stable protein 1; PKD1: protein kinase D 1; SAP: Serum Response Factor Accessory Protein; eIF4E: eukaryotic translation initiation factor 4E

1.3.4 p38 δ MAPK function and new roles in human disease

Since the discovery of p38 δ MAPK in 1997 it has been implicated in a range of diverse physiological events, namely, differentiation, apoptosis, and cytokine production (Figure 1.1). The greatest understanding of its involvement in these cellular processes has been achieved from work using keratinocytes and the majority of these studies have previously been reviewed [89, 90]. Research is now emerging which establishes p38 δ MAPK as a regulator of these processes in other cell types. As a result in the past five years p38 δ MAPK has also been implicated in the pathogenesis of diabetes, inflammatory diseases, and cancer. This progress has been achieved with the development of p38 δ MAPK KO mouse models which are proving to be a useful tool in elucidating novel roles for p38 δ MAPK in vivo.

Differentiation and psoriasis

A number of different studies have identified a role for p38 δ MAPK in keratinocyte differentiation, a process critical for the precise control of normal epidermal homeostasis. p38 δ MAPK induces keratinocyte differentiation by regulating the expression of involucrin, a marker of keratinocyte terminal differentiation [84, 85, 91]. p38 δ MAPK activation by 12-otetradecanoylphorbol-13-acetate (TPA), calcium, OA, or green tea polyphenol corresponds with increased involucrin promoter activity, mRNA, and protein expression, as well as increased levels and activity of AP1 and C/EBP transcription factors [84, 85, 92]. Importantly, these responses are observed in the presence of a p38 α/β MAPK inhibitor. In addition p38 γ MAPK is poorly expressed in keratinocytes [91] confirming a specific role for p38 δ MAPK. Involucrin expression can also be further upregulated in keratinocytes coexpressing p38 δ MAPK and protein kinase C (PKC) η , δ or ϵ isoforms [85]. Of note

cholesterol depleting agents and overexpression of MKK6/MKK7 have previously been shown to induce involucrin expression via activation of p38 α MAPK [91, 93, 94]. This highlights the significance of the stimulus type in determining p38 MAPK isoform activation. A further role for p38 δ MAPK in keratinocyte differentiation was recently identified. p38 δ MAPK can regulate expression of ZO-1, an epidermal tight junction membrane protein associated with keratinocyte differentiation [95]. Inhibition of p38 δ MAPK results in depletion of ZO-1 protein in calcium induced differentiating keratinocytes while other junction proteins remain unaffected [95]. Psoriasis is a benign, chronic inflammatory skin condition that is characterised by hyperproliferation and differentiation of keratinocytes as well as increased expression of inflammatory cytokines. Given the significant role p38 δ MAPK plays in keratinocyte differentiation, it is no surprise that aberrant p38 δ MAPK signalling has been implicated in the pathogenesis of psoriasis. Expression of the MAPK13 gene is commonly upregulated in psoriasis [96]. Furthermore, an increase in p38 δ (as well as - α and - β) MAPK activity has been detected in psoriatic lesions compared to nonlesional psoriatic skin. After treatment for psoriasis, phosphorylated p38 MAPK levels return to those of uninvolved skin [97].

Further to its role in keratinocyte differentiation p38 δ MAPK is also implicated in hematopoiesis. In human primary erythroid cells, p38 δ MAPK mRNA is only expressed in late-stage differentiation where along with p38 α MAPK it is increasingly activated [98]. This may suggest a functional role for p38 δ MAPK in erythrocyte membrane remodelling and enucleation. Interestingly, an increase in p38 δ MAPK mRNA and protein expression is observed as blood monocytes differentiate to macrophages [99]. This suggests a role for p38 δ MAPK in functions

gained by mature macrophages. A possible candidate is phagocytosis given that the microtubule associated protein stathmin is such a strong p38 δ MAPK substrate.

Most recently, p38 δ MAPK has been identified as a component of differentiation in bone repair [100]. In bone cell differentiation during wound healing, wild type (WT) monocytes differentiate to calcifying/bone-forming monoosteophils upon treatment with the peptide LL-37. p38 δ MAPK protein and mRNA is highly expressed in monoosteophils compared to undifferentiated monocytes. Monocytes from p38 δ MAPK KO mice are incapable of this differentiation, suggesting a critical role for p38 δ MAPK in this process [100].

Apoptosis and diabetes

As well as its significant role in keratinocyte differentiation, p38 δ MAPK has also been identified as a regulator of keratinocyte apoptosis. This dual functional role may be attributed to the overlap of differentiation and apoptosis signalling pathways [101]. As well as inducing involucrin expression [92], OA simultaneously causes disruption of mitochondrial membrane potential and caspase-dependent apoptosis [71]. Overexpression of p38 δ MAPK enhances this OA driven apoptotic morphology. This response is specific to p38 δ MAPK activation as it occurred in the presence of the p38 α/β MAPK inhibitor SB203580 [71]. Furthermore, p38 δ MAPK coexpressed with either MEK6 or PKC δ , both upstream p38 MAPK activators, elicited an apoptotic response similar to that induced by OA but in the absence of an external stimulus. This was also independent of SB203580, again ruling out a contribution from other p38 MAPK isoforms [102]. Interestingly, concurrent p38 δ MAPK activation and inactivation of the proliferative MAPK extracellular-

regulated kinase (ERK) 1/2 were observed with OA stimulation and PKC δ /p38 δ MAPK coexpression [71, 92, 102]. In fact a reduction in ERK1/2 activation appears to be critical for apoptosis as its constitutive activation inhibited PKC δ /p38 δ MAPK mediated apoptosis [102]. Therefore, it is likely that a specific balance between prosurvival ERK1/2 and proapoptotic p38 δ MAPK is essential in determining keratinocyte fate. In regulating this balance, p38 δ MAPK and ERK1/2 form a complex that is translocated to the nucleus upon stimulation by PKC δ . This nuclear localisation facilitates ERK1/2 inactivation by nuclear phosphatases, while maintaining p38 δ MAPK activation [102].

A role for p38 δ MAPK in apoptosis has recently been demonstrated in vivo using p38 δ MAPK KO mice. Mice deficient in p38 δ MAPK displayed a fivefold lower rate of pancreatic β cell death in response to oxidative stress than WT mice and are afforded protection against insulin resistance induced by a high-fat diet [88]. This would appear to link p38 δ MAPK to the pathogenesis of diabetes mellitus, a disease characterised by reduced insulin sensitivity and a decrease in insulin-producing pancreatic β cells [88]. Increased p38 MAPK pathway activity has indeed been observed in both type 1 and type 2 diabetes and is correlated with late complications of hyperglycaemia, including neuropathy and nephropathy [103, 104]. p38 δ MAPK specifically has also been implicated in the regulation of insulin secretion. Phosphorylation by p38 δ MAPK negatively regulates the activity of protein kinaseD1 (PKD1), a known positive regulator of neuroendocrine cell secretion [88]. Thus, pronounced activation of PKD1 has been observed in pancreatic β cells lacking p38 δ MAPK. As p38 δ MAPK is normally quite highly expressed in the pancreas this can contribute to heightened insulin secretion and improved glucose

tolerance in p38 δ MAPK-null mice [88]. The pivotal role p38 δ MAPK plays in integrating insulin secretion and survival of pancreatic β cells makes it an attractive potential therapeutic target for the treatment of human diabetes.

Cytokine production and inflammatory diseases

One of the pathways by which p38 α MAPK was discovered was via its identification as a regulator of proinflammatory cytokine biosynthesis [30]. Thus, its role in cytokine signalling and cytokine-dependent inflammatory diseases is well characterised. Consequently, some recent research using p38 δ MAPK KO mouse models has focused on identifying specific roles for p38 δ MAPK in inflammation. A study of p38 δ MAPK KO mice as well as myeloid-restricted deletion of p38 δ MAPK in mice has shown that p38 δ MAPK is required for the recruitment of neutrophils to sites of inflammation [105]. p38 δ MAPK and its downstream target protein kinase D (PKD) 1 conversely regulate phosphatase and tensin homolog (PTEN) activity to control neutrophil extravasation and chemotaxis. The accumulation of neutrophils at inflammatory sites is known to trigger inflammation-induced acute lung injury (ALI) which can cause acute respiratory distress syndrome (ARDS), a condition with a high mortality rate [106]. Therefore, abnormal p38 δ -PKD1 signalling may play an important role in both ALI and ARDS in humans.

Rheumatoid arthritis is a typical example of an inflammatory disease involving chronic synthesis of proinflammatory cytokines which result in synovial hyperplasia and joint destruction [107]. While p38 δ MAPK (along with - α , - β , and - γ) is expressed in the synovium of rheumatoid arthritis patients its level of activation is lower than that of the four other p38 MAPK isoforms [108]. Despite this low level of

activation new research has identified p38 δ MAPK as an essential component of joint damage in a collagen-induced model of arthritis. p38 $\gamma/\delta^{-/-}$ mice displayed reduced arthritis severity compared to WT mice [109]. The decrease in joint destruction was associated with lower expression of IL-1 β and TNF α as well as a reduction in T cell proliferation, interferon (IFN) - γ , and IL-17 production. Lack of either p38 γ or p38 δ MAPK alone yielded intermediate effects, suggesting significant roles for both isoforms in arthritis pathogenesis.

Proinflammatory cytokines also play a significant role in the pathogenesis of inflammatory airway diseases, including asthma, chronic obstructive pulmonary disease (COPD), and cystic fibrosis. While increased mucus production is linked to the morbidity and mortality of such diseases the underlying molecular mechanisms remain somewhat unclear [110]. The critical driver of mucus production is thought to be IL-13 production by immune cells which results in mucin gene expression [111, 112]. In the last few years p38 δ MAPK has been implicated in the signalling pathway responsible for controlling IL-13 driven excess mucus production. Increased MAPK13 gene expression is evident in the lungs of patients with severe COPD [113]. Novel inhibitors with increased activity against p38 δ MAPK blocked mucus production by IL-13 in human airway epithelial cells [113]. Thus, in patients with hypersensitivity airway diseases there exists a potential opportunity for therapeutic intervention should specific p38 δ MAPK inhibitors become clinically available.

1.3.5 p38 δ MAPK and cancer

In recent years, the function of the p38 MAPK signalling pathway in malignant transformation has been intensively studied. As a result, the best characterised isoform, p38 α MAPK, has been identified as both a tumour promoter [114-116] and a tumour suppressor [117-119]. Recent studies have now also implicated p38 δ MAPK in cancer development and progression. Like p38 α MAPK, p38 δ MAPK would also appear to have both pro- and anti-oncogenic roles, depending on the cell type studied.

Interest in p38 δ MAPK as a potential tumour promoter is based on the evidence that p38 δ MAPK expression and activation are significantly increased in a variety of carcinoma cell lines such as human primary cutaneous squamous carcinoma cells [96], head and neck squamous carcinoma cells and tumours [115], cholangiocarcinoma (CC), and liver cancer cell lines [120]. p38 δ MAPK was first shown to promote a malignant phenotype (over eight years ago) in head and neck squamous cell carcinoma (HNSCC) [115]. It was shown to regulate HNSCC invasion and proliferation through controlling expression of matrixmetalloproteinase-1 and -13 [115, 121]. Moreover the expression of dominant-negative (DN) p38 δ MAPK impaired the ability of cutaneous HNSCC cells to implant in the skin of immunodeficiency mice as well as inhibiting the growth of xenografts [115].

p38 δ MAPK-null mice have been utilised to demonstrate that p38 δ MAPK is required for the development of multistage chemical skin carcinogenesis in vivo. When compared with WT mice, p38 δ MAPK-deficient mice displayed reduced

susceptibility to 7, 12-dimethylbenz(a)anthracene/12-O-tetradecanoylphorbol-13-acetate induced skin carcinoma with a significant delay in tumour development [122]. Furthermore, both tumour numbers and size were significantly decreased compared with WT mice [122]. This decreased carcinogenesis was associated with reduced levels of proliferative ERK1/2-AP1 signalling and decreased activation of signal transducer and activator of transcription 3 (Stat3) [122]. The ERK1/2-AP1 pathway is a key cancer promoting cascade previously implicated in skin carcinogenesis [123, 124]. Stat3 meanwhile is an oncogenic transcription factor involved in chemical and UVB-induced transformation [125]. It is also proliferative and plays a role in angiogenesis and invasion [126, 127]. Therefore p38 δ MAPK promotion of proliferation via Stat3 may be a significant mechanism in the promotion of carcinogenesis by p38 δ MAPK. Similarly, p38 δ MAPK KO mice have reduced susceptibility to development of K-ras driven lung tumourigenesis. Compared with WT mice, p38 $\delta^{-/-}$ /KRasG12D $^{+/-}$ mice displayed significantly decreased tumour numbers, average tumour volume, and total tumour volume per lung [122]. This is in contrast to p38 α MAPK-deficient mice which display hyperproliferation of lung epithelium and increased K-Ras-induced lung tumour development [118]. This highlights once again the distinct and often opposing functions of the individual p38 MAPK isoforms.

In contrast to the relatively well characterised role of p38 δ MAPK as a tumour promoter an increasing number of reports since 2011 outline its activity as a tumour suppressor. The first indication of a tumour suppressive role for p38 δ MAPK was observed in MEFs. p38 $\delta^{-/-}$ (and p38 $\gamma^{-/-}$) MEFs displayed increased cell motility compared to WT cells [128]. Furthermore, while WT fibroblasts ceased to proliferate

after reaching 100% confluency, p38 δ ^{-/-} MEFs continued to grow, forming foci rather than a monolayer [128]. This deregulation of contact inhibition is significant as it is a hallmark of malignant transformation [3]. Further supporting the hypothesis that loss of p38 δ MAPK confers a survival advantage, p38 δ MAPK expression was found to be downregulated in brain metastases of triple-negative breast cancer (TNBC). Abolition of p38 δ MAPK expression in TNBC induced cell growth, while overexpression of p38 δ MAPK in brain metastases reduced growth rates [129].

Cancer genomes are increasingly associated with epigenetic alterations whereby tumour suppressor genes exhibit promoter hypermethylation. Interestingly, hypermethylation of the MAPK13 gene promoter region has recently been characterised in both malignant pleural mesothelioma [130] and primary cutaneous melanoma [131]. This methylation was associated with downregulation of p38 δ MAPK mRNA and protein expression. Melanoma cell lines displaying MAPK13 gene promoter methylation do not express significant levels of p38 δ MAPK when compared to fibroblasts, melanocytes, and melanoma cell lines with unmethylated MAPK13 promoters. Furthermore, treatment of melanoma cells with the demethylating agent 5-aza-2'-deoxycytidine significantly increases the expression of the MAPK13 gene [131, 132]. Importantly, reestablishment of p38 δ MAPK expression in melanoma cells with MAPK13 hypermethylation suppressed cell proliferation. The effect was further enhanced upon expression of a constitutively active form of p38 δ MAPK. Interestingly, however, overexpression of p38 δ MAPK or its constitutively active form in cells in which MAPK13 was not epigenetically silenced only marginally affected proliferation [131].

1.4 Summary

Oesophageal cancer is one of the deadliest cancers worldwide with a five-year survival rate of less than 15 % [26]. It is an aggressive disease and is highly insensitive to conventional chemotherapy [133]. Despite this, it remains one of the least studied of all cancer types and the underlying molecular mechanisms which govern oesophageal cancer development and progression are poorly understood. This contributes to the poor prognosis and high-mortality rate of oesophageal cancer as specific tumour markers and effective molecular therapeutic targets are seriously lacking. The p38 MAPK family of kinases has in recent years emerged as important regulators of cellular processes which are critical for tumourigenesis such cell proliferation, migration and apoptosis [134]. As such, these kinases have been characterised as both tumour promoters and tumour suppressors and therefore represent important potential therapeutic targets for a host of cancers. However, much of the research to date has focused p38 α MAPK, or examines the p38 MAPK family as a whole. It is now becoming increasingly clear that conclusions drawn from p38 α MAPK (and to an extent p38 β MAPK) studies cannot be automatically applied to the most recently discovered isoform, p38 δ MAPK, due to their different expression patterns, substrate specificities, and sensitivity to chemical inhibitors. As a result, the p38 δ MAPK isoform remains under-studied and its cellular functions are ill-defined. The limited information available regarding p38 δ MAPK suggests however that it may also play opposing roles in tumourigenesis, depending on cell type. Therefore the aims of this thesis are to provide insights into how this unique isoform contributes to tumourigenicity in OESCC and to evaluate its potential as a much needed therapeutic target for this disease.

1.5 References

1. <http://www.who.int/cancer>.
2. Hanahan, D. and R.A. Weinberg, *The hallmarks of cancer*. Cell, 2000. **100**(1): p. 57-70.
3. Hanahan, D. and R.A. Weinberg, *Hallmarks of cancer: the next generation*. Cell, 2011. **144**(5): p. 646-74.
4. National Cancer Registry, I., *Cancer in Ireland 2013: Annual report of the National Cancer Registry*. 2013.
5. Ferlay J, S.I., Ervik M, Dikshit R, Eser S, Mathers C, Rebelo M, Parkin DM, Forman D, Bray, F., *GLOBOCAN 2012 v1.0, Cancer Incidence and Mortality Worldwide: IARC CancerBase No. 11 [Internet]*. 2013, Lyon, France: International Agency for Research on Cancer.
6. Siewert, J.R. and K. Ott, *Are Squamous and Adenocarcinomas of the Esophagus the Same Disease?* Seminars in Radiation Oncology, 2007. **17**(1): p. 38-44.
7. Jemal, A., et al., *Global Patterns of Cancer Incidence and Mortality Rates and Trends*. Cancer Epidemiology Biomarkers & Prevention, 2010. **19**(8): p. 1893-1907.
8. Wu, A.H., P. Wan, and L. Bernstein, *A multiethnic population-based study of smoking, alcohol and body size and risk of adenocarcinomas of the stomach and esophagus (United States)*. Cancer Causes Control, 2001. **12**(8): p. 721-32.
9. Brown, L.M., et al., *Excess incidence of squamous cell esophageal cancer among US Black men: role of social class and other risk factors*. Am J Epidemiol, 2001. **153**(2): p. 114-22.
10. Blot, W.J. and J.K. McLaughlin, *The changing epidemiology of esophageal cancer*. Semin Oncol, 1999. **26**(5 Suppl 15): p. 2-8.
11. Gammon, M.D., et al., *Tobacco, alcohol, and socioeconomic status and adenocarcinomas of the esophagus and gastric cardia*. J Natl Cancer Inst, 1997. **89**(17): p. 1277-84.
12. Sandler, R.S., et al., *The risk of esophageal cancer in patients with achalasia. A population-based study*. JAMA, 1995. **274**(17): p. 1359-62.
13. Garidou, A., et al., *Life-style factors and medical conditions in relation to esophageal cancer by histologic type in a low-risk population*. Int J Cancer, 1996. **68**(3): p. 295-9.
14. Ghavamzadeh, A., et al., *Esophageal cancer in Iran*. Semin Oncol, 2001. **28**(2): p. 153-7.
15. Risk, J.M., et al., *The tylosis esophageal cancer (TOC) locus: more than just a familial cancer gene*. Dis Esophagus, 1999. **12**(3): p. 173-6.

16. Ellis, A., et al., *Tylosis associated with carcinoma of the oesophagus and oral leukoplakia in a large Liverpool family--a review of six generations*. Eur J Cancer B Oral Oncol, 1994. **30B**(2): p. 102-12.
17. Hardefeldt, H.A., M.R. Cox, and G.D. Eslick, *Association between human papillomavirus (HPV) and oesophageal squamous cell carcinoma: a meta-analysis*. Epidemiol Infect, 2014. **142**(6): p. 1119-37.
18. Lagergren, J., et al., *Symptomatic gastroesophageal reflux as a risk factor for esophageal adenocarcinoma*. N Engl J Med, 1999. **340**(11): p. 825-31.
19. Romero, Y., et al., *Barrett's esophagus: prevalence in symptomatic relatives*. Am J Gastroenterol, 2002. **97**(5): p. 1127-32.
20. Gerson, L.B., K. Shetler, and G. Triadafilopoulos, *Prevalence of Barrett's esophagus in asymptomatic individuals*. Gastroenterology, 2002. **123**(2): p. 461-7.
21. Shaheen, N. and D.F. Ransohoff, *Gastroesophageal reflux, barrett esophagus, and esophageal cancer: Scientific review*. JAMA, 2002. **287**(15): p. 1972-1981.
22. Long, E. and I.L. Beales, *The role of obesity in oesophageal cancer development*. Therap Adv Gastroenterol, 2014. **7**(6): p. 247-68.
23. Olsen, C.M., et al., *Population attributable fractions of adenocarcinoma of the esophagus and gastroesophageal junction*. Am J Epidemiol, 2011. **174**(5): p. 582-90.
24. Sobin, L.H., M.K. Gospodarowicz, and C. Wittekind, *TNM Classification of Malignant Tumours*. 2009: Wiley.
25. Tew, W.P., D.P. Kelsen, and D.H. Ilson, *Targeted therapies for esophageal cancer*. Oncologist, 2005. **10**(8): p. 590-601.
26. Enzinger, P.C. and R.J. Mayer, *Esophageal cancer*. N Engl J Med, 2003. **349**(23): p. 2241-52.
27. Daigo, Y. and Y. Nakamura, *From cancer genomics to thoracic oncology: discovery of new biomarkers and therapeutic targets for lung and esophageal carcinoma*. General Thoracic and Cardiovascular Surgery, 2008. **56**(2): p. 43-53.
28. Macarulla, T., et al., *Emerging strategies in the treatment of advanced esophageal, gastroesophageal junction, and gastric cancer: the introduction of targeted therapies*. Targeted Oncology, 2006. **1**(1): p. 23-33.
29. Han, J., et al., *A MAP kinase targeted by endotoxin and hyperosmolarity in mammalian cells*. Science, 1994. **265**(5173): p. 808-11.
30. Lee, J.C., et al., *A protein kinase involved in the regulation of inflammatory cytokine biosynthesis*. Nature, 1994. **372**(6508): p. 739-746.
31. Rouse, J., et al., *A novel kinase cascade triggered by stress and heat shock that stimulates MAPKAP kinase-2 and phosphorylation of the small heat shock proteins*. Cell, 1994. **78**(6): p. 1027-1037.
32. Freshney, N.W., et al., *Interleukin-1 activates a novel protein kinase cascade that results in the phosphorylation of Hsp27*. Cell, 1994. **78**(6): p. 1039-49.

33. Jiang, Y., et al., *Characterization of the structure and function of a new mitogen-activated protein kinase (p38beta)*. J Biol Chem, 1996. **271**(30): p. 17920-6.
34. Li, Z., et al., *The primary structure of p38 gamma: a new member of p38 group of MAP kinases*. Biochem Biophys Res Commun, 1996. **228**(2): p. 334-40.
35. Jiang, Y., et al., *Characterization of the structure and function of the fourth member of p38 group mitogen-activated protein kinases, p38delta*. J Biol Chem, 1997. **272**(48): p. 30122-8.
36. Wang, X.S., et al., *Molecular cloning and characterization of a novel p38 mitogen-activated protein kinase*. J Biol Chem, 1997. **272**(38): p. 23668-74.
37. Goedert, M., et al., *Activation of the novel stress-activated protein kinase SAPK4 by cytokines and cellular stresses is mediated by SKK3 (MKK6); comparison of its substrate specificity with that of other SAP kinases*. EMBO J, 1997. **16**(12): p. 3563-71.
38. Brewster, J.L., et al., *An osmosensing signal transduction pathway in yeast*. Science, 1993. **259**(5102): p. 1760-3.
39. Li, M., J. Liu, and C. Zhang, *Evolutionary history of the vertebrate mitogen activated protein kinases family*. PLoS One, 2011. **6**(10): p. e26999.
40. Cuenda, A., et al., *SB 203580 is a specific inhibitor of a MAP kinase homologue which is stimulated by cellular stresses and interleukin-1*. FEBS Lett, 1995. **364**(2): p. 229-33.
41. Tong, L., et al., *A highly specific inhibitor of human p38 MAP kinase binds in the ATP pocket*. Nat Struct Biol, 1997. **4**(4): p. 311-6.
42. Evers, P.A., et al., *Conversion of SB 203580-insensitive MAP kinase family members to drug-sensitive forms by a single amino-acid substitution*. Chem Biol, 1998. **5**(6): p. 321-8.
43. Gum, R.J., et al., *Acquisition of sensitivity of stress-activated protein kinases to the p38 inhibitor, SB 203580, by alteration of one or more amino acids within the ATP binding pocket*. J Biol Chem, 1998. **273**(25): p. 15605-10.
44. Kuma, Y., et al., *BIRB796 inhibits all p38 MAPK isoforms in vitro and in vivo*. J Biol Chem, 2005. **280**(20): p. 19472-9.
45. Coulthard, L.R., et al., *p38 MAPK: stress responses from molecular mechanisms to therapeutics*. Trends Mol Med, 2009. **15**(8): p. 369-79.
46. Hu, M.C.-T., et al., *Murine p38- δ Mitogen-activated Protein Kinase, a Developmentally Regulated Protein Kinase That Is Activated by Stress and Proinflammatory Cytokines*. Journal of Biological Chemistry, 1999. **274**(11): p. 7095-7102.
47. Sabio, G., et al., *p38gamma regulates the localisation of SAP97 in the cytoskeleton by modulating its interaction with GKAP*. EMBO J, 2005. **24**(6): p. 1134-45.
48. Beardmore, V.A., et al., *Generation and characterization of p38 β (MAPK11) gene-targeted mice*. Mol Cell Biol, 2005. **25**(23): p. 10454-64.

49. Allen, M., et al., *Deficiency of the stress kinase p38 α results in embryonic lethality: characterization of the kinase dependence of stress responses of enzyme-deficient embryonic stem cells.* J Exp Med, 2000. **191**(5): p. 859-70.
50. Raingeaud, J., et al., *Pro-inflammatory cytokines and environmental stress cause p38 mitogen-activated protein kinase activation by dual phosphorylation on tyrosine and threonine.* J Biol Chem, 1995. **270**(13): p. 7420-6.
51. Kyriakis, J.M. and J. Avruch, *Mammalian MAPK signal transduction pathways activated by stress and inflammation: a 10-year update.* Physiol Rev, 2012. **92**(2): p. 689-737.
52. Cheung, P.C., et al., *Feedback control of the protein kinase TAK1 by SAPK2a/p38 α .* EMBO J, 2003. **22**(21): p. 5793-805.
53. Gallo, K.A. and G.L. Johnson, *Mixed-lineage kinase control of JNK and p38 MAPK pathways.* Nat Rev Mol Cell Biol, 2002. **3**(9): p. 663-72.
54. Ichijo, H., et al., *Induction of apoptosis by ASK1, a mammalian MAPKKK that activates SAPK/JNK and p38 signaling pathways.* Science, 1997. **275**(5296): p. 90-4.
55. Yamaguchi, K., et al., *Identification of a member of the MAPKKK family as a potential mediator of TGF-beta signal transduction.* Science, 1995. **270**(5244): p. 2008-11.
56. Cuevas, B.D., A.N. Abell, and G.L. Johnson, *Role of mitogen-activated protein kinase kinase kinases in signal integration.* Oncogene, 2007. **26**(22): p. 3159-71.
57. Zhang, S., et al., *Rho family GTPases regulate p38 mitogen-activated protein kinase through the downstream mediator Pak1.* J Biol Chem, 1995. **270**(41): p. 23934-6.
58. Marinissen, M.J., et al., *A network of mitogen-activated protein kinases links G protein-coupled receptors to the c-jun promoter: a role for c-Jun NH2-terminal kinase, p38s, and extracellular signal-regulated kinase 5.* Mol Cell Biol, 1999. **19**(6): p. 4289-301.
59. Remy, G., et al., *Differential activation of p38MAPK isoforms by MKK6 and MKK3.* Cell Signal, 2010. **22**(4): p. 660-7.
60. Wang, L., et al., *Requirement of mitogen-activated protein kinase kinase 3 (MKK3) for activation of p38 α and p38 δ MAPK isoforms by TGF-beta 1 in murine mesangial cells.* J Biol Chem, 2002. **277**(49): p. 47257-62.
61. Schoorlemmer, J. and M. Goldfarb, *Fibroblast growth factor homologous factors and the islet brain-2 scaffold protein regulate activation of a stress-activated protein kinase.* J Biol Chem, 2002. **277**(51): p. 49111-9.
62. Lawler, S., et al., *Synergistic activation of SAPK1/JNK1 by two MAP kinase kinases in vitro.* Current Biology, 1998. **8**(25): p. 1387-1391.
63. Tournier, C., et al., *MKK7 is an essential component of the JNK signal transduction pathway activated by proinflammatory cytokines.* Genes Dev, 2001. **15**(11): p. 1419-26.

64. Wada, T., et al., *Impaired synergistic activation of stress-activated protein kinase SAPK/JNK in mouse embryonic stem cells lacking SEK1/MKK4: different contribution of SEK2/MKK7 isoforms to the synergistic activation.* J Biol Chem, 2001. **276**(33): p. 30892-7.
65. Ge, B., et al., *MAPKK-independent activation of p38alpha mediated by TAB1-dependent autophosphorylation of p38alpha.* Science, 2002. **295**(5558): p. 1291-4.
66. Salvador, J.M., et al., *Alternative p38 activation pathway mediated by T cell receptor-proximal tyrosine kinases.* Nat Immunol, 2005. **6**(4): p. 390-5.
67. Avitzour, M., et al., *Intrinsically active variants of all human p38 isoforms.* FEBS J, 2007. **274**(4): p. 963-75.
68. Askari, N., et al., *Hyperactive variants of p38alpha induce, whereas hyperactive variants of p38gamma suppress, activating protein 1-mediated transcription.* J Biol Chem, 2007. **282**(1): p. 91-9.
69. Zhou, X., et al., *MKP-1 inhibits high NaCl-induced activation of p38 but does not inhibit the activation of TonEBP/OREBP: opposite roles of p38alpha and p38delta.* Proc Natl Acad Sci U S A, 2008. **105**(14): p. 5620-5.
70. Tanoue, T., et al., *A Novel MAPK phosphatase MKP-7 acts preferentially on JNK/SAPK and p38 alpha and beta MAPKs.* J Biol Chem, 2001. **276**(28): p. 26629-39.
71. Kraft, C.A., T. Efimova, and R.L. Eckert, *Activation of PKCdelta and p38delta MAPK during okadaic acid dependent keratinocyte apoptosis.* Arch Dermatol Res, 2007. **299**(2): p. 71-83.
72. Cuenda, A. and S. Rousseau, *p38 MAP-Kinases pathway regulation, function and role in human diseases.* Biochimica et Biophysica Acta (BBA) - Molecular Cell Research, 2007. **1773**(8): p. 1358-1375.
73. Kumar, S., et al., *Novel Homologues of CSBP/p38 MAP Kinase: Activation, Substrate Specificity and Sensitivity to Inhibition by Pyridinyl Imidazoles.* Biochemical and Biophysical Research Communications, 1997. **235**(3): p. 533-538.
74. Goedert, M., et al., *Phosphorylation of microtubule-associated protein tau by stress-activated protein kinases.* FEBS Lett, 1997. **409**(1): p. 57-62.
75. Bramblett, G.T., et al., *Abnormal tau phosphorylation at Ser396 in Alzheimer's disease recapitulates development and contributes to reduced microtubule binding.* Neuron, 1993. **10**(6): p. 1089-99.
76. Goedert, M., *The significance of tau and alpha-synuclein inclusions in neurodegenerative diseases.* Curr Opin Genet Dev, 2001. **11**(3): p. 343-51.
77. Lee, V.M., M. Goedert, and J.Q. Trojanowski, *Neurodegenerative tauopathies.* Annu Rev Neurosci, 2001. **24**: p. 1121-59.
78. Parker, C.G., et al., *Identification of Stathmin as a Novel Substrate for p38 Delta.* Biochemical and Biophysical Research Communications, 1998. **249**(3): p. 791-796.

79. Jourdain, L., et al., *Stathmin: a tubulin-sequestering protein which forms a ternary T2S complex with two tubulin molecules*. *Biochemistry*, 1997. **36**(36): p. 10817-21.
80. Curmi, P.A., et al., *The stathmin/tubulin interaction in vitro*. *J Biol Chem*, 1997. **272**(40): p. 25029-36.
81. Knebel, A., N. Morrice, and P. Cohen, *A novel method to identify protein kinase substrates: eEF2 kinase is phosphorylated and inhibited by SAPK4/p38delta*. *EMBO J*, 2001. **20**(16): p. 4360-9.
82. Jorgensen, R., A.R. Merrill, and G.R. Andersen, *The life and death of translation elongation factor 2*. *Biochem Soc Trans*, 2006. **34**(Pt 1): p. 1-6.
83. Gonzalez-Teran, B., et al., *Eukaryotic elongation factor 2 controls TNF-alpha translation in LPS-induced hepatitis*. *J Clin Invest*, 2013. **123**(1): p. 164-78.
84. Balasubramanian, S., T. Efimova, and R.L. Eckert, *Green tea polyphenol stimulates a Ras, MEKK1, MEK3, and p38 cascade to increase activator protein 1 factor-dependent involucrin gene expression in normal human keratinocytes*. *J Biol Chem*, 2002. **277**(3): p. 1828-36.
85. Efimova, T., et al., *Novel protein kinase C isoforms regulate human keratinocyte differentiation by activating a p38 delta mitogen-activated protein kinase cascade that targets CCAAT/enhancer-binding protein alpha*. *J Biol Chem*, 2002. **277**(35): p. 31753-60.
86. Pani, E. and S. Ferrari, *p38MAPK delta controls c-Myb degradation in response to stress*. *Blood Cells Mol Dis*, 2008. **40**(3): p. 388-94.
87. Hawkes, W.C. and Z. Alkan, *Delayed cell cycle progression in selenoprotein W-depleted cells is regulated by a mitogen-activated protein kinase kinase 4-p38/c-Jun NH2-terminal kinase-p53 pathway*. *J Biol Chem*, 2012. **287**(33): p. 27371-9.
88. Sumara, G., et al., *Regulation of PKD by the MAPK p38delta in insulin secretion and glucose homeostasis*. *Cell*, 2009. **136**(2): p. 235-48.
89. Efimova, T., *p38delta mitogen-activated protein kinase regulates skin homeostasis and tumorigenesis*. *Cell Cycle*, 2010. **9**(3): p. 498-05.
90. Eckert, R.L., et al., *p38 Mitogen-activated protein kinases on the body surface--a function for p38 delta*. *J Invest Dermatol*, 2003. **120**(5): p. 823-8.
91. Dashti, S.R., T. Efimova, and R.L. Eckert, *MEK6 regulates human involucrin gene expression via a p38alpha - and p38delta -dependent mechanism*. *J Biol Chem*, 2001. **276**(29): p. 27214-20.
92. Efimova, T., A.M. Broome, and R.L. Eckert, *A regulatory role for p38 delta MAPK in keratinocyte differentiation. Evidence for p38 delta-ERK1/2 complex formation*. *J Biol Chem*, 2003. **278**(36): p. 34277-85.
93. Jans, R., et al., *Cholesterol depletion upregulates involucrin expression in epidermal keratinocytes through activation of p38*. *J Invest Dermatol*, 2004. **123**(3): p. 564-73.
94. Dashti, S.R., T. Efimova, and R.L. Eckert, *MEK7-dependent activation of p38 MAP kinase in keratinocytes*. *J Biol Chem*, 2001. **276**(11): p. 8059-63.

95. Siljamaki, E., et al., *p38delta mitogen-activated protein kinase regulates the expression of tight junction protein ZO-1 in differentiating human epidermal keratinocytes*. Arch Dermatol Res, 2014. **306**(2): p. 131-41.
96. Haider, A.S., et al., *Genomic analysis defines a cancer-specific gene expression signature for human squamous cell carcinoma and distinguishes malignant hyperproliferation from benign hyperplasia*. J Invest Dermatol, 2006. **126**(4): p. 869-81.
97. Johansen, C., et al., *The mitogen-activated protein kinases p38 and ERK1/2 are increased in lesional psoriatic skin*. Br J Dermatol, 2005. **152**(1): p. 37-42.
98. Uddin, S., et al., *Differentiation stage-specific activation of p38 mitogen-activated protein kinase isoforms in primary human erythroid cells*. Proc Natl Acad Sci U S A, 2004. **101**(1): p. 147-52.
99. Hale, K.K., et al., *Differential expression and activation of p38 mitogen-activated protein kinase alpha, beta, gamma, and delta in inflammatory cell lineages*. J Immunol, 1999. **162**(7): p. 4246-52.
100. Zhang, Z. and J.E. Shively, *Acceleration of bone repair in NOD/SCID mice by human monoosteophils, novel LL-37-activated monocytes*. PLoS One, 2013. **8**(7): p. e67649.
101. Gandarillas, A., *Epidermal differentiation, apoptosis, and senescence: common pathways?* Exp Gerontol, 2000. **35**(1): p. 53-62.
102. Efimova, T., A.M. Broome, and R.L. Eckert, *Protein kinase Cdelta regulates keratinocyte death and survival by regulating activity and subcellular localization of a p38delta-extracellular signal-regulated kinase 1/2 complex*. Mol Cell Biol, 2004. **24**(18): p. 8167-83.
103. Price, S.A., et al., *Mitogen-activated protein kinase p38 mediates reduced nerve conduction velocity in experimental diabetic neuropathy: interactions with aldose reductase*. Diabetes, 2004. **53**(7): p. 1851-6.
104. Komers, R., et al., *Renal p38 MAP kinase activity in experimental diabetes*. Lab Invest, 2007. **87**(6): p. 548-58.
105. Ittner, A., et al., *Regulation of PTEN activity by p38delta-PKDI signaling in neutrophils confers inflammatory responses in the lung*. J Exp Med, 2012. **209**(12): p. 2229-46.
106. Ware, L.B. and M.A. Matthay, *The acute respiratory distress syndrome*. N Engl J Med, 2000. **342**(18): p. 1334-49.
107. Brennan, F.M. and I.B. McInnes, *Evidence that cytokines play a role in rheumatoid arthritis*. J Clin Invest, 2008. **118**(11): p. 3537-45.
108. Korb, A., et al., *Differential tissue expression and activation of p38 MAPK alpha, beta, gamma, and delta isoforms in rheumatoid arthritis*. Arthritis Rheum, 2006. **54**(9): p. 2745-56.
109. Criado, G., et al., *Alternative p38 mitogen-activated protein kinases are essential for collagen-induced arthritis*. Arthritis Rheum, 2013.
110. Kuyper, L.M., et al., *Characterization of airway plugging in fatal asthma*. Am J Med, 2003. **115**(1): p. 6-11.

111. Kim, E.Y., et al., *Persistent activation of an innate immune response translates respiratory viral infection into chronic lung disease*. Nat Med, 2008. **14**(6): p. 633-40.
112. Wills-Karp, M., et al., *Interleukin-13: central mediator of allergic asthma*. Science, 1998. **282**(5397): p. 2258-61.
113. Alevy, Y.G., et al., *IL-13-induced airway mucus production is attenuated by MAPK13 inhibition*. J Clin Invest, 2012. **122**(12): p. 4555-68.
114. del Barco Barrantes, I. and A.R. Nebreda, *Roles of p38 MAPKs in invasion and metastasis*. Biochem Soc Trans, 2012. **40**(1): p. 79-84.
115. Junttila, M.R., et al., *p38alpha and p38delta mitogen-activated protein kinase isoforms regulate invasion and growth of head and neck squamous carcinoma cells*. Oncogene, 2007. **26**(36): p. 5267-79.
116. Rousseau, S., et al., *CXCL12 and C5a trigger cell migration via a PAK1/2-p38alpha MAPK-MAPKAP-K2-HSP27 pathway*. Cell Signal, 2006. **18**(11): p. 1897-905.
117. Bulavin, D.V. and A.J. Fornace, Jr., *p38 MAP kinase's emerging role as a tumor suppressor*. Adv Cancer Res, 2004. **92**: p. 95-118.
118. Ventura, J.J., et al., *p38alpha MAP kinase is essential in lung stem and progenitor cell proliferation and differentiation*. Nat Genet, 2007. **39**(6): p. 750-8.
119. Hui, L., et al., *p38alpha: a suppressor of cell proliferation and tumorigenesis*. Cell Cycle, 2007. **6**(20): p. 2429-33.
120. Tan, F.L., et al., *p38delta/MAPK13 as a diagnostic marker for cholangiocarcinoma and its involvement in cell motility and invasion*. Int J Cancer, 2010. **126**(10): p. 2353-61.
121. Egeblad, M. and Z. Werb, *New functions for the matrix metalloproteinases in cancer progression*. Nat Rev Cancer, 2002. **2**(3): p. 161-74.
122. Schindler, E.M., et al., *p38delta Mitogen-activated protein kinase is essential for skin tumor development in mice*. Cancer Res, 2009. **69**(11): p. 4648-55.
123. Bourcier, C., et al., *p44 mitogen-activated protein kinase (extracellular signal-regulated kinase 1)-dependent signaling contributes to epithelial skin carcinogenesis*. Cancer Res, 2006. **66**(5): p. 2700-7.
124. Young, M.R., et al., *Transgenic mice demonstrate AP-1 (activator protein-1) transactivation is required for tumor promotion*. Proc Natl Acad Sci U S A, 1999. **96**(17): p. 9827-32.
125. Kim, D.J., et al., *Signal transducer and activator of transcription 3 (Stat3) in epithelial carcinogenesis*. Mol Carcinog, 2007. **46**(8): p. 725-31.
126. Chan, K.S., et al., *Forced expression of a constitutively active form of Stat3 in mouse epidermis enhances malignant progression of skin tumors induced by two-stage carcinogenesis*. Oncogene, 2008. **27**(8): p. 1087-94.
127. Chan, K.S., et al., *Disruption of Stat3 reveals a critical role in both the initiation and the promotion stages of epithelial carcinogenesis*. J Clin Invest, 2004. **114**(5): p. 720-8.

128. Cerezo-Guisado, M.I., et al., *Evidence of p38 γ and p38 δ involvement in cell transformation processes*. Carcinogenesis, 2011. **32**(7): p. 1093-1099.
129. Choi, Y.K., et al., *Brain-metastatic triple-negative breast cancer cells regain growth ability by altering gene expression patterns*. Cancer Genomics Proteomics, 2013. **10**(6): p. 265-75.
130. Goto, Y., et al., *Epigenetic profiles distinguish malignant pleural mesothelioma from lung adenocarcinoma*. Cancer Res, 2009. **69**(23): p. 9073-82.
131. Gao, L., et al., *Genome-wide promoter methylation analysis identifies epigenetic silencing of MAPK13 in primary cutaneous melanoma*. Pigment Cell Melanoma Res, 2013. **26**(4): p. 542-54.
132. Koga, Y., et al., *Genome-wide screen of promoter methylation identifies novel markers in melanoma*. Genome Res, 2009. **19**(8): p. 1462-70.
133. Klein, C.A. and N.H. Stoecklein, *Lessons from an aggressive cancer: evolutionary dynamics in esophageal carcinoma*. Cancer Res, 2009. **69**(13): p. 5285-8.
134. Ono, K. and J. Han, *The p38 signal transduction pathway: activation and function*. Cell Signal, 2000. **12**(1): p. 1-13.

Chapter 2

Materials and general methods

2.1 Materials

2.1.1 Reagents

All chemicals, reagents and solvents were obtained from Sigma Aldrich Ireland Ltd (Arklow, Ireland) unless otherwise stated. All reagents were stored and prepared according to manufacturer's directions.

Cell culture reagents

Media (RPMI-1640, Dulbecco's modified eagle's medium (DMEM), F12 (Ham) nutrient mixture) and supplements (heat inactivated foetal bovine serum (FBS), penicillin/streptomycin solution), as well as trypsin-EDTA and Dulbecco's phosphate buffered saline were purchased from Sigma Aldrich Ireland Ltd (Arklow, Ireland). Geneticin was supplied by Gibco® (Life Technologies, Grand Island, NY, USA).

Immunoblotting reagents

Primary antibodies for immunoblotting were as outlined in Table 2.1. Secondary antibodies for Western blotting were horseradish peroxidase (HRP)-conjugated polyclonal goat anti-rabbit or rabbit anti-mouse immunoglobulins from Dako Diagnostics Ireland Ltd. (Dublin, Ireland) and anti-biotin HRP linked antibody from Cell Signaling Technologies (Hertfordshire, UK).

Table 2.1 Primary antibodies used for detection of proteins by Western blot

Target antigen (human)	Molecular Weight (kDa)	Supplier	Source	Optimal Dilution	Incubation
β-Actin	42	Sigma Aldrich	Mouse	1:5000	1 hr @ RT
Bad	23	Cell Signaling	Rabbit	1:1000	Overnight @ 4°C
Bak	25	Cell Signaling	Rabbit	1:1000	Overnight @ 4°C
Bax	20	Cell Signaling	Rabbit	1:1000	Overnight @ 4°C
BID	15, 22	Cell Signaling	Rabbit	1:1000	Overnight @ 4°C
Bik	20	Cell Signaling	Rabbit	1:1000	Overnight @ 4°C
Bim	12, 15, 23	Cell Signaling	Rabbit	1:1000	Overnight @ 4°C
Caspase-3 (8G10)	17, 19, 35	Cell Signaling	Rabbit	1:1000	Overnight @ 4°C
Caspase-6	15, 35	Cell Signaling	Rabbit	1:1000	Overnight @ 4°C
Caspase-7 (D2Q3L)	20, 35	Cell Signaling	Rabbit	1:1000	Overnight @ 4°C
Caspase-8 (1C12)	18, 43, 57	Cell Signaling	Mouse	1:1000	Overnight @ 4°C
Caspase-9 (C9)	47, 37, 35	Cell Signaling	Mouse	1:1000	Overnight @ 4°C
COX-2	72	Cayman Chemical	Mouse	1:1000	Overnight @ 4°C
eEF2	95	Cell Signaling	Rabbit	1:1000	Overnight @ 4°C
Fas (C-20)	48	Santa Cruz	Rabbit	1:1000	1 hr @ RT
Fas-L	26, 40	Santa Cruz	Rabbit	1:1000	1 hr @ RT
FLAG®	<10	Sigma Aldrich	Mouse	1:1000	30 min @ RT
MKK3b	40	Cell Signaling	Rabbit	1:1000	Overnight @ 4°C
MKK6	38	Cell Signaling	Rabbit	1:1000	Overnight @ 4°C
MKK7	48	Cell Signaling	Rabbit	1:1000	Overnight @ 4°C
p38α MAPK	43	Cell Signaling	Rabbit	1:1000	Overnight @ 4°C
p38β MAPK	40	Cell Signaling	Rabbit	1:1000	Overnight @ 4°C
p38γ MAPK	46	Cell Signaling	Rabbit	1:1000	Overnight @ 4°C
p38δ MAPK	43	Cell Signaling	Rabbit	1:1000	Overnight @ 4°C

p44/42 MAPK (Erk1/2)	42, 44	Cell Signaling	Rabbit	1:1000	Overnight @ 4°C
p53 (7F5)	53	Cell Signaling	Rabbit	1:1000	Overnight @ 4°C
PARP	89, 116	Cell Signaling	Rabbit	1:1000	Overnight @ 4°C
PARP	85, 116	BD Biosciences	Mouse	1:2000	Overnight @ 4°C
Paxillin	68	Chemicon	Rabbit	1:1000	Overnight @ 4°C
p-eEF2K	105	Santa Cruz	Rabbit	1:1000	1 hr @ RT
Phospho-eEF2	95	Cell Signaling	Rabbit	1:1000	Overnight @ 4°C
Phospho-Bad (Ser112)(40A9)	23	Cell Signaling	Rabbit	1:1000	Overnight @ 4°C
Phospho-MKK3/MKK6	40, 41	Cell Signaling	Rabbit	1:1000	Overnight @ 4°C
Phospho-p38MAPK (Thr180/Tyr182)	43	Cell Signaling	Rabbit	1:1000	Overnight @ 4°C
Phospho-p44/42 MAPK (Erk1/2) (Thr202/Tyr204)	42, 44	Cell Signaling	Rabbit	1:1000	Overnight @ 4°C
Phospho-SAPK/JNK (Thr183/Tyr185)	46, 54	Cell Signaling	Rabbit	1:1000	Overnight @ 4°C
Puma	23	Cell Signaling	Rabbit	1:1000	Overnight @ 4°C
SAPK4 (H-60)	43	Santa Cruz	Rabbit	1:1000	
SEK1/MKK4	44	Cell Signaling	Rabbit	1:1000	Overnight @ 4°C
TRAIL	34, 20	Santa Cruz	Rabbit	1:1000	1 hr @ RT
Wip-1	67	Santa Cruz	Rabbit	1:1000	1 hr @ RT

(Cayman Chemical, Ann Arbor, MI, USA; Santa Cruz Biotechnology, Santa Cruz, CA, USA; BD BioSciences, San Diego, CA, USA).

Molecular biology reagents

All restriction enzymes were purchased from New England BioLabs (Hertfordshire, UK). DNA polymerases Phusion®, DreamTaq™ and Platinum® Taq were purchased from New England BioLabs (Hertfordshire, UK), Fermentas (Thermo Fisher Scientific, Waltham, MA, USA) and Life Technologies, Grand Island, NY, USA) respectively.

2.1.2 Cell lines

KE cell lines

The following KE cell lines were kind gifts from Professor T. Fujii, Kurume University School of Medicine, Japan [1-3]. All KE cell lines were established prior to chemotherapy or radiation treatment. KE cell line features are summarised in Table 2.2.

- KE-3 human oesophageal squamous cell carcinoma cell line was established from a moderately differentiated oesophageal squamous cell carcinoma resected from the lower thoracic oesophagus of a 62 year old male.
- KE-4 human oesophageal squamous cell carcinoma cell line was established from a poorly differentiated oesophageal squamous cell carcinoma resected from the middle and upper thoracic oesophagus of a 50 year old male.
- KE-5 human oesophageal squamous cell carcinoma cell line was established from a well differentiated oesophageal squamous cell carcinoma resected from the middle thoracic oesophagus of a 69 year old male.

- KE-6 human oesophageal squamous cell carcinoma cell line was established from a well differentiated oesophageal squamous cell carcinoma resected from the lower thoracic oesophagus of a 61 year old male.
- KE-8 human oesophageal squamous cell carcinoma cell line was established from a poorly differentiated oesophageal squamous cell carcinoma resected from the middle thoracic oesophagus of a 71 year old female.
- KE-10 human oesophageal squamous cell carcinoma cell line was established from a moderately differentiated oesophageal squamous cell carcinoma resected from a (skip) metastatic site in the stomach of a 58 year old female.

Table 2.2 KE (OESCC) cell line features

KE Features	
Sex	
Male	KE-3, -4, -5, -6
Female	KE-8, -10
Age	Median 67 (50 to 71) years
TNM7 stage	
T stage	
T1	KE-10
T3	KE-3, -5, -6, -8
T4	KE-4
N stage	
N0	KE-5
N1	KE-3, -4, -6, -8, -10
Histological grade	
Well differentiated	KE-5, -6
Moderately differentiated	KE-3, -10
Poorly differentiated	KE-4, -8

KE features are summarised based on gender, age, TNM7 stage and histological stage. Based on the TNM7 categorization for oesophageal cancer.

OC cell lines

The following OC cell lines were kind gifts from the Cork Cancer Research Centre, Biosciences Institute, National University of Ireland, Cork, Ireland. They have been previously used by us [4] and characterised [5].

- OC-1 oesophageal squamous cell carcinoma cell line was established from malignant ascites of a patient with oesophageal cancer.
- OC-3 oesophageal adenocarcinoma cell line was established from a metastatic lymph node of a Barrett's oesophageal lesion.

Commercially available cell lines

- KYSE-70 is a human oesophageal squamous cell carcinoma and is available from the European Collection of Cell Cultures (ECACC). The KYSE-70 cell line was established from a poorly differentiated invasive oesophageal squamous cell carcinoma resected from the middle intra-thoracic oesophagus of a 77 year old Japanese man prior to treatment.
- KYSE-450 human oesophageal squamous cell carcinoma is available from Deutsche Sammlung von Mikroorganismen und Zellkulturen (DSMZ) GmbH (German Collection of Microorganisms and Cell Cultures). The KYSE-450 cell line was established from a well differentiated invasive oesophageal squamous cell carcinoma resected from the middle intra-thoracic oesophagus of a 59 year old Japanese man prior to treatment (depth of invasion was not beyond the submucosa).
- OE-19 human oesophageal adenocarcinoma cell line is available from ECACC. The OE-19 cell line, also known as JROECL19, was established from a moderately differentiated adenocarcinoma of the gastric cardia/oesophageal gastric junction of a 72 year old Caucasian male.
- OE-21 human oesophageal squamous cell carcinoma is available from ECACC. The OE-21 cell line, also known as JROECL21, was established from a moderately differentiated squamous carcinoma of the mid oesophagus of a 74 year old Caucasian male.
- OE-33 human oesophageal carcinoma is available from ECACC. The OE-33 cell line, also known as JROECL33, was established from a poorly differentiated adenocarcinoma of the lower oesophagus (Barrett's metaplasia) of a 73 year old Caucasian female.

2.1.3 Plasmids

Two different plasmids pcDNA3-MKK6b(E) and pcDNA3-FLAG-p38 δ were a kind gift from Professor J. Han, Scripps Research Institute, La Jolla, CA, USA and have previously been described [6]. pcDNA3 vector was obtained from Invitrogen (Life Technologies, Grand Island, NY, USA). Nucleotide sequence of each plasmid is detailed in Appendix I. All other plasmids used for this research project were generated by us and are detailed in Chapter 3.

2.2 General methods

General methods used in multiple chapters are discussed here. Supplementary techniques used in individual chapters are outlined in the relevant chapter as per Table 2.3

Table 2.3 Relevant chapters for experimental techniques

Experimental technique	Outlined in
Agarose gel electrophoresis	Chapter 2
Antibody array	Chapter 4
Bisulfite sequencing PCR	Chapter 6
Boyden chamber cell migration assay	Chapter 2
cDNA synthesis	Chapter 2
Cell culture	Chapter 2
Cloning	Chapter 3
Clonogenic assay	Chapter 5
Colony forming assay	Chapter 4
DNA purification	Chapter 2
DNA sequencing	Chapter 2
Drug treatment	Chapter 5
ELISA	Chapter 4
Ethics	Chapter 2
Immunoblotting	Chapter 2
Immunohistochemistry	Chapter 4

Ligation	Chapter 3
Methylation specific PCR	Chapter 6
Mitochondrial membrane potential assay	Chapter 5
MTT staining	Chapter 2
Nuclear and cytosolic protein extraction	Chapter 4
Nucleic acid isolation	Chapter 2
PCR/rt-PCR	Chapter 2
Plasmid prep	Chapter 3
Preparation of whole cell lysates	Chapter 2
Quantitation of total protein concentration	Chapter 2
Quantitative rt-PCR	Chapter 6
Restriction digest	Chapter 2
SDS-PAGE	Chapter 2
siRNA transfection	Chapter 4
Site-directed mutagenesis	Chapter 3
Sodium bisulfite conversion	Chapter 6
Stable transfection	Chapter 4
Statistical analysis	Chapter 2
Transformation	Chapter 3
Transient transfection	Chapter 3
Trypan blue proliferation assay	Chapter 4
Western blotting	Chapter 2
Wound-healing assay	Chapter 2

2.2.1 Cell culture

Media and supplements

All cell culture procedures were performed using aseptic technique in a Holten LaminAir (Thermo Fisher Scientific, Waltham, MA, USA) laminar flow tissue culture hood. All cell cultures were incubated at 37°C in a 5% CO₂ atmosphere in a Forma Scientific Infrared CO₂ incubator (Thermo Fisher Scientific, Waltham, MA, USA). KE, OE and KYSE-70 cells were maintained in RPMI-1640 medium supplemented with 10% FBS, 100 U/ml penicillin and 100 µg/ml streptomycin (1% penicillin/streptomycin). OC-1 and OC-3 cells were routinely grown in Dulbecco's modified eagle's medium (DMEM) containing 10% FBS and 1% penicillin/streptomycin. KYSE-450 cells were maintained in 45% RPMI-1640/45% F-12 Ham, with 10% FBS and 1% penicillin/streptomycin. Generation of stable cell lines is outlined in Chapter 4. Once established stably transfected cell lines were grown in the appropriate media supplemented with 10% FBS and 400 µg/ml Geneticin (Gibco®, Life Technologies, Grand Island, NY, USA).

Reconstitution of frozen cells

25 ml of the appropriate medium was added to a T150 flask and incubated at 37°C, 5% CO₂. Cryovials were removed from liquid nitrogen storage and transferred to a 37°C waterbath until contents were fully thawed (1-2 min). Contents of cryovials were pipetted slowly into the 150 ml flasks containing the pre-warmed medium.

Passaging/maintenance of cells

In general cell lines were maintained at $\leq 70\%$ confluency. Medium was removed from flasks and cells were washed with 20 ml Dulbecco's phosphate buffered saline (PBS). Cells were incubated with 10 ml Trypsin-EDTA solution per T150 flask, at 37°C , $5\% \text{CO}_2$ for 5-7 min. Flasks were periodically examined under a microscope to determine if cells were detached from the surface. Once cells were observed to be detached from the surface, the contents of the flask were transferred to a 15 ml centrifuge tube. Cells were centrifuged at a speed of 1100 rpm for 5 min. Supernatant was removed from the pelleted cells. Cells were resuspended in 5 ml of the appropriate medium. 1 ml cell suspension was added to 25 ml medium in a fresh flask.

Preparation of liquid N_2 stocks

Cells were pelleted by centrifugation at 1100 rpm for 5 min and supernatant was discarded. Cell pellet was resuspended in the appropriate volume of freezing medium (90% FBS, 10% dimethyl-sulfoxide (DMSO)) to yield a suspension of $1-2 \times 10^6$ cells/ml. Cell suspension was divided into 1 ml aliquots in cryovials and frozen at -80°C overnight in a Nalgene® Cryo 1°C Freezing Container (Thermo Fisher Scientific, Waltham, MA, USA) before being transferred to liquid N_2 storage.

2.2.2 3-(4,5-Dimethylthiazol-2-yl)-2,5-diphenyltetrazolium bromide (MTT) staining

The MTT assay depends on the ability of viable cells to reduce the MTT to a coloured formazan product as previously described [7]. MTT was dissolved at a final

concentration of 0.25 mg/ml in complete culture medium. 2ml MTT solution was added per well of a 6-well plate. Cells were incubated at 37°C, 5% CO₂ for 30 min. Medium was aspirated and the MTT-formazan precipitate was dissolved with 1 ml DMSO per well. Absorbance was measured at 540 nm using a SunriseTM spectrophotometric plate reader and analysed using the XRead software program (Tecan Group Ltd., Männedorf, Switzerland).

2.2.3 Cell migration

Boyden chamber cell migration assay

Migration of untransfected and transfected KE-3 (KE-3 pcDNA3, KE-3 p38δ, KE-3 p-p38δ, KE-3 p-p38δ_{DN}) cells was assessed using a Boyden Chamber assay. Cells were plated in starvation medium at a density of 3×10^4 cells/well into a 96-well plate of the upper chamber. The bottom chamber contained 10% FBS as the chemoattractant. Cells were left migrate for 24 hr through the matrigel filter (8 μm). Migrated cells were treated with MTT as described above to calculate viable cell numbers.

Wound-healing assay

Cell migration was assessed by *in vitro* wound-healing assay as previously described [8]. A linear wound track was made by use of a sterile tip through confluent cells. Cells migrating into the wound were photographed under a phase-contrast microscope 24 hr and 48 hr after wounding. Migration was determined using the ImageJ (National Institutes of Health, Bethesda, Maryland, USA) program as an

average closed area of the wound relative to the initial wound area at 24 hr and 48 hr after wounding.

2.2.4 Protein preparation and immunoblot analysis

Preparation of whole cell lysates

Cells cultured in 6-well plates were washed twice with cold PBS and plates frozen at -80°C. Plates were thawed on ice for 10 min. Lysis buffer consisted of 1X Protease Inhibitor Cocktail (2mM AEBSF, 0.3µM Aprotinin, 130µM Bestatin, 14mM E-64, 1mM Leupeptin, 1mM EDTA) supplemented with 10 mM Sodium Fluoride (NaF) and 25mM Sodium Pyrophosphate (Na₄P₂O₇). 100 µl lysis buffer was added to each well and incubated on ice for 45 min. Cells were scraped into the lysis buffer and collected. Lysates were sonicated twice for 10 pulses on ice at 50% duty cycle for 0.5 s with a 30 s rest period (Ultrasonic Homogenizer 4710 series; Cole-Parmer Instrument Co., Chicago, IL, USA). Following centrifugation at 12 000 rpm for 5 min, ≤ 4°C, supernatants were removed and stored at -20°C.

Quantitation of total protein concentration of samples

Total protein concentration of lysates was quantitated using a Micro BCA™ Protein Assay Kit (Pierce Biotechnology, Rockford, IL, USA). A set of diluted BSA standards ranging from 0.5-40 µg/ml and a blank of ddH₂O only were prepared. Cell lysates were diluted 1:50 and 1:100. 500 µl of each standard, blank and lysate dilution was added to 500 µl Micro BCA Working Reagent (25 parts reagent MA + 24 parts reagent MB + 1 part reagent MC) and incubated in a 60°C water bath for 1 hr. 200 µl of each sample was transferred in triplicate to a 96-well plate and

absorbance at 562 nm was measured using a Sunrise™ spectrophotometric plate reader and analysed using the XRead software program. A standard curve (Figure 2.1) was generated by plotting the Blank-corrected average absorbance reading for each of the standards versus their concentrations in µg/ml. The protein concentration of each unknown sample was determined using this standard curve according to the following equation:

$$y = mx + b$$

where y = blank-corrected absorbance reading at 562 nm, m = the slope of the standard curve and x = concentration in µg/ml.

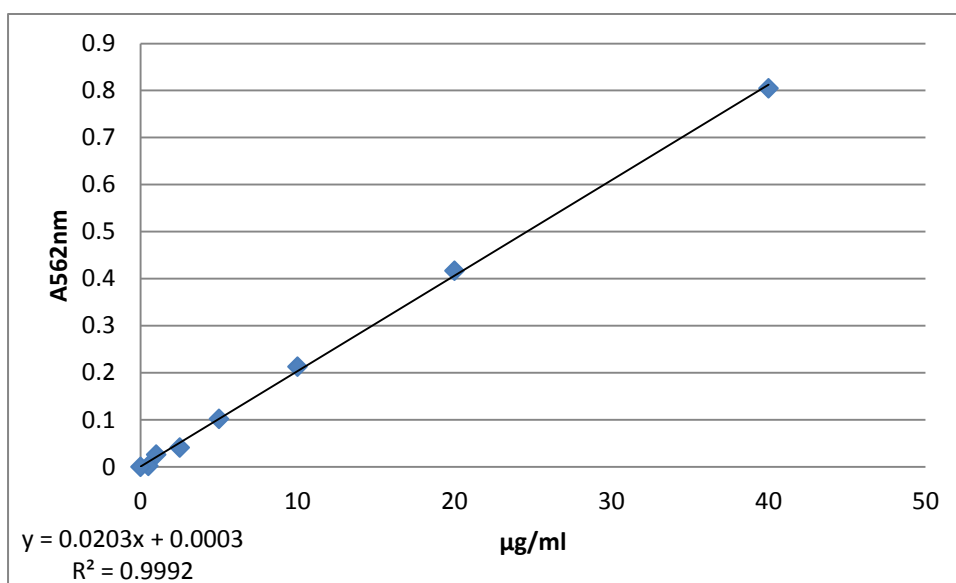


Figure 2.1 Standard curve for determination of protein concentration of unknown samples. Standard curve generated by plotting the absorbance of a series of standards (40-0.5 µg/ml) at 562 nm versus their concentration. Results shown are from a single experiment and are representative of all experiments.

SDS-polyacrylamide gel electrophoresis (SDS-PAGE)

1X Laemmli loading buffer (2% w/v SDS, 10% v/v glycerol, 60 mM Tris-HCL (pH 6.8), 0.002% w/v Bromophenol Blue, 0.64 M β -mercaptoethanol) was added to 15-35 μ g of each protein lysate and samples were incubated at 95°C for 5 min. Proteins were separated by SDS-Polyacrylamide Gel Electrophoresis (SDS PAGE) using a Mini-PROTEAN® system (Bio-Rad, Hercules, CA, USA). Gels consisted of a resolving gel of 10%, to give a linear range of separation of 16-68 kD, overlaid by a 5% stacking gel with components outlined in Table 2.4 [9].

Table 2.4 Solutions for preparing gels for SDS-PAGE [9]

Component	5% Stacking Gel	10% Resolving Gel
H₂O	2.7 ml	4.0 ml
30% acrylamide/bis mix 29:1	670 μ l	3.3 ml
Tris HCl	500 μ l 1.0 M, pH 6.8	2.5 ml 1.5 M, pH 8.8
10% SDS	40 μ l	100 μ l
10% ammonium persulphate	40 μ l	100 μ l
TEMED	4 μ l	4 μ l

Electrophoresis was carried out at 80 V in running buffer (25 mM Tris base, 192 mM Glycine, 0.01% w/v SDS) until the dye front entered the resolving gel, then performed at 120 V until 30 min after the dye front had reached the bottom of the gel, generally taking a total of 3.5-4 hr. A biotinylated protein ladder (Cell Signaling Technologies, Hertfordshire, UK) was used as a molecular weight marker. 1X Laemmli loading buffer was loaded into any unused wells.

Western blotting

Resolved proteins were electrophoretically transferred onto nitrocellulose membrane (GE Healthcare, Buckinghamshire, UK) using a SemiPhor semi-dry transfer unit (Hoefer, Holliston, MA, USA) for 1 hr at 200 mA or a Trans-Blot® Turbo™ Semi Dry Transfer System (Bio-Rad, Hercules, CA, USA) for 30 min @ 25 V, 1.0 A. Blotting paper, cellophane, nitrocellulose and SDS-PAGE resolving gels were initially equilibrated in transfer buffer (25 mM Tris base, 192 mM Glycine, 0.01% w/v SDS, 20% v/v MeOH). Protein transfer was confirmed with Ponceau S staining.

Protein detection/probing

Non-specific binding to the nitrocellulose was blocked by incubation in 1X Tris buffered saline (50 mM Tris Base, 0.25 M NaCl, pH adjusted to 7.6 with 5 N HCl), 0.1% v/v TWEEN (TBS-T) containing 5% w/v marvel milk powder (Premier Foods, Hertfordshire, UK) for 1 hr at RT. Membranes were then washed three times with TBS-T over 15 min. Incubation with primary antibodies (Table 2.1) was performed as per manufacturer's instructions/optimised conditions for each individual antibody.

Secondary antibodies were diluted 1:1000 in TBS-T. After washing three times with TBS-T over 15 min, membranes were incubated with appropriate secondary antibodies for 1 hr at RT, followed by another three 5 min washes with TBS-T. Luminol/Enhancer solution and Peroxidase Buffer (SuperSignal West Dura Extended Duration Substrate, Pierce Biotechnology, Rockford, IL, USA) were mixed at a 1:1 ratio and incubated on membranes for 3 min. After removing excess reagent and covering with plastic, membranes were exposed using an LAS-3000 Lite Intelligent Dark Box (Fujifilm, Dublin, Ireland) or G:Box ChemiXR5 Gel

Documentation System (Syngene Europe, Cambridge, UK). Images were quantified using ImageJ software. Occasionally membranes were stripped by incubation with RestoreTM Western Blot Stripping Buffer (Thermo Fisher Scientific, Waltham, MA, USA) at 37°C for 45 min before being blocked and re-probed as above.

2.2.5 Nucleic acid isolation and cDNA synthesis

DNA isolation

Genomic DNA (gDNA) was isolated from cultured cells using magnetic bead technology with a Magna Pure LC Total Nucleic Acid Isolation Kit (Roche Diagnostics Ltd., West Sussex, UK) according to manufacturer's instructions. 1×10^6 cells were resuspended in PBS and incubated with a chaotropic salt lysis/binding buffer to release nucleic acids and denature nucleases. The automated Magna Pure LC instrument performs the remainder of steps. Proteinase K is added to digest proteins. Magnetic Glass Particles (MGPs) are added and nucleic acids in the sample bind to their silica surface. MGPs with bound nucleic acids are magnetically separated from the residual sample and washed repeatedly with wash buffer to remove unbound substances. Purified nucleic acids are eluted in a low-salt buffer. DNA concentration and quality was determined spectrophotometrically with a BioPhotometer (Eppendorf AG, Hamburg, Germany).

RNA isolation

RNA was isolated from cultured cells with a RNeasy Mini Kit (Qiagen, Manchester, UK) using a silica membrane based purification protocol. 1×10^6 cells per sample were washed with PBS and pelleted by centrifugation at 1200 rpm for 5 min. Cell

pellets were resuspended in 350 μ l Buffer RLT and homogenized by vortexing for 1 min. Cell lysates were stored at -80°C . For RNA isolation, frozen lysates were thawed in a 37°C water bath and RNA was extracted as follows according to the Spin Technology protocol. One volume (350 μ l) of 70% ethanol was added to the lysate and mixed by pipetting. The sample (700 μ l) was loaded into an RNeasy spin column in a 2 ml collection tube and centrifuged at $\geq 10\ 000$ rpm for 15 s. 350 μ l Buffer RW1 was added to the RNeasy spin column and centrifuged for 15 s at $\geq 10\ 000$ rpm. DNaseI was incubated on the column membrane at RT for 15 min. 350 μ l Buffer RW1 was added to the RNeasy spin column and centrifuged for 15 s at $\geq 10\ 000$ rpm. Spin column membrane was washed twice with Buffer RPE, with centrifugations at $\geq 10\ 000$ rpm for 15 s and 2 min. The spin column was placed in a new 2 ml collection tube and centrifuged for 1 min at $\geq 10\ 000$ rpm to eliminate any possible carryover of ethanol. RNA was eluted in RNase-free water by centrifugation for 1 min at $\geq 10\ 000$ rpm. Eluted RNA was stored at -80°C . RNA concentration and quality was determined spectrophotometrically with a BioPhotometer.

cDNA synthesis

First-strand complementary DNA (cDNA) was synthesised using SuperScript® VILO™ cDNA Synthesis Kit (Life Technologies, NY, USA). For a single reaction, SuperScript® Enzyme Mix (including SuperScript® III reverse transcriptase an engineered version of M-MLV reverse transcriptase, RNaseOUT™ Recombinant Ribonuclease Inhibitor, and a helper protein), VILO™ Reaction Mix (including random primers, MgCl_2 , and dNTPs) and up to 2.5 μg RNA were combined in a total volume of 20 μ l. Samples were incubated at 25°C for 10 min, 42°C for 60 min, and 85°C for 5 min. cDNA was stored at -20°C .

2.2.6 PCR and rt-PCR

Primers for PCR and reverse transcription PCR (rt-PCR) (Table 2.5) were designed with the aid of online primer design tools, including Primer3Plus [10] and Integrated DNA Technologies online OligoAnalyzer <http://eu.idtdna.com/analyzer/Applications/OligoAnalyzer/>. Specificity of primers was determined by BLAST analysis of the primer sequences against the RefSeq *Homo sapiens* mRNA database [11]. Primers were synthesised by Sigma Aldrich or Eurofins Genomics (Ebersberg, Germany).

Table 2.5 Primers for PCR and rt-PCR

Primer	Sequence (5'→3')	T _m ^o
P001F	CCACGTTAAACTGCCCATCT	66.0
P001R	CCGCCACAAGCTAAAAAGAG	64.0
P002F	CCGGAAAAAGGGCTTCTACAA	63.8
P002R	GACGTTCTCATGCTGCATGT	63.6
P003F	CCGCGCTTTAAAGGCGAGGGCGAGGGCGAGGGCGAGG GCGAGATGGACTACAAGGACGACGAT	97.1
P003R	TTGATCTTTAAATTATTACAGCTTCATGCCACTTCGT	72.8
P009F	CGAGATCGGGTGCCCGGGAT	65.5
P017R	TCAGCTTCTTGATGGCCACCTTCTC	64.6
SP6	CATTTAGGTGACACTATAG	50.2
T7	TAATACGACTCACTATAGGG	53.2

T_m^o = value provided by manufacturer.

PCR and rt-PCR reactions were carried out in a 50 μ l final volume and included components listed in Table 2.6. For each PCR/rt-PCR reaction a negative control was included in which the template was replaced with the equivalent volume of H₂O in order to identify any non-specific DNA amplification.

Table 2.6 PCR/rt-PCR reaction components

Reaction Component	Final Concentration
PCR Reaction Buffer	1X
Deoxynucleotide (dNTP) Mix	0.2 mM
MgCl₂	1.5 mM
Forward Primer	0.2 μ M
Reverse Primer	0.2 μ M
Template	variable
DNA Polymerase	1-2 units
H₂O	to total reaction volume of 50 μ l

Template: cDNA = 1 μ l; gDNA \leq 100 ng; plasmid DNA \leq 10 ng.

PCR and rt-PCR reactions were performed in a GeneAmp PCR System 2700 (Applied Biosystems, Life Technologies, NY, USA) under the conditions described in Table 2.7.

Table 2.7 PCR/rt-PCR reaction conditions

Step	Temperature °C	Time	Number of cycles
Initial denaturation	95	5 min	1
Denaturation	95	50 s	35
Annealing	lowest primer T _m ° -5	50 s	
Extension	72	1 min/kb	
Final Extension	72	10 min	1

2.2.7 Restriction digest

All restriction enzymes were purchased from New England Biolabs (Hertfordshire, UK). Restriction enzymes used as well as their recognition sequences and incubation temperatures are listed in Table 2.8.

Table 2.8 Incubation temperatures and recognition specificities for restriction enzymes

Restriction Enzyme	Recognition Sequence	Incubation Temperature
BamHI	G [^] GATCC	37°C
BsaAI	YAC [^] GTR	37°C
BstXI	CCANNNNN [^] NTGG	37°C
DraI	TTT [^] AAA	37°C
HindIII	A [^] AGCTT	37°C
MfeI	C [^] AATTG	37°C
SwaI	ATTT [^] AAAT	25°C
XbaI	T [^] CTAGA	37°C
XhoI	C [^] TCGAG	37°C

Y = C or T, R = A or G, N = A or G or C or T. [^] denotes point of cleavage.

Typical restriction digest reaction conditions are outlined in Table 2.9 as advised by New England BioLabs (Hertfordshire, UK) to overcome variability in DNA source, quantity, and purity.

Table 2.9 Restriction digest reaction components and conditions

Component	Condition
Restriction enzyme	10 units
DNA	1 µg
10X buffer	5 µl
Total reaction volume	50 µl
Incubation time	16 hr
Incubation temperature	Enzyme dependent

2.2.8 Agarose gel electrophoresis

0.8 – 1.0% gels were prepared with agarose and 1X TBE (89 mM Trizma base, 89 mM boric acid, 2 mM EDTA) or TAE (40 mM Trizma base, 20 mM glacial acetic acid, 1 mM EDTA) Buffer. SafeView nucleic acid stain (NBS Biologicals, Cambridgeshire, UK) was used for the detection of DNA and RNA. Samples were loaded using 1X DNA loading dye (New England BioLabs, Hertfordshire, UK). Various DNA Ladder molecular weight markers were used depending on the expected size of the product according to Table 2.10.

Table 2.10 DNA ladder molecular weight markers

Sizing range	DNA Ladder	Supplier
50-1000 bp	GeneRuler™ 50bp DNA ladder	Fermentas, Thermo Fisher Scientific, Waltham, MA, USA
250-10 000 bp	GeneRuler™ 1kb DNA ladder	Fermentas, Thermo Fisher Scientific, Waltham, MA, USA
500-10 000 bp	1 kb DNA ladder	New England BioLabs, Hertfordshire, UK

2.2.9 DNA purification

Products were purified from PCR and restriction digest reactions using an Illustra GFX PCR DNA & Gel Band Purification Kit (GE Healthcare, Buckinghamshire, UK) according to manufacturer's instructions. Briefly, the PCR/enzyme reaction was combined with capture buffer and transferred to a GFX MicroSpin column in a collection tube and centrifuged at 16 000 x g for 30 s. Following two wash steps, DNA was eluted in nuclease-free H₂O by centrifugation at 16 000 x g for 1 min.

2.2.10 DNA sequencing

Plasmids and purified PCR products were routinely sent for DNA sequence analysis. All DNA sequencing was performed by Eurofins Genomics using their 'Value Read' modified dideoxychain termination sequencing service. The relevant PCR primers were generally used for sequencing of PCR products. Additional primers for DNA

Sequencing (Table 2.11) were synthesised by Eurofins Genomics (Ebersberg, Germany) and designed using their ‘Design A Primer’ tool.

Table 2.11 Additional primers for DNA sequence analysis

Primer	Sequence (5’-3’)
T7	TAATACGACTCACTATAGGG
SP6	CATTAGGTGACACTATAG
SeqP1	CTCTCGGTCAAGTGAAGATGTG
SeqP2	AGCTGGATGCACTACAACCAGAC
SeqP3	AGACATCCAGGAGCCCAATG
SeqP4	GGATATTTCCATGAGGACGGTG
SeqP5	CTGCTGAAGCACATGCAGCATGAG
SeqP6	TTGGATATTTCCATGAGGACGG

2.2.11 Ethics

This research was approved by the Clinical Research Ethics Committee of the Cork Teaching Hospitals.

2.2.12 Statistical analysis

Results are expressed as mean \pm SE. Statistical comparisons were made by analysis of variance with subsequent application of Student’s *t*-test, as appropriate. The non-parametric Mann-Whitney *U*-test pairwise comparisons were also performed. As the results obtained using both methods were in agreement, only results for the Student’s

t-test are shown. GraphPad InStat 3 software (GraphPad Software, Inc., La Jolla, CA, USA) was used for statistical analysis also.

2.3 References

1. Yamana, H., et al., [*Experimental studies on immunotargeting therapy for esophageal carcinoma*]. *Gan To Kagaku Ryoho*, 1994. **21**(6): p. 755-60.
2. Tsukahara, T., et al., *Identification of human autologous cytotoxic T-lymphocyte-defined osteosarcoma gene that encodes a transcriptional regulator, papillomavirus binding factor*. *Cancer Res*, 2004. **64**(15): p. 5442-8.
3. Nakao, M., et al., *HLA A2601-restricted CTLs recognize a peptide antigen expressed on squamous cell carcinoma*. *Cancer Res*, 1995. **55**(19): p. 4248-52.
4. Barry, O.P., et al., *Constitutive ERK1/2 activation in esophagogastric rib bone marrow micrometastatic cells is MEK-independent*. *J Biol Chem*, 2001. **276**(18): p. 15537-46.
5. O'Sullivan G, C., et al., *Micrometastases in esophagogastric cancer: high detection rate in resected rib segments*. *Gastroenterology*, 1999. **116**(3): p. 543-8.
6. Pramanik, R., et al., *p38 isoforms have opposite effects on AP-1-dependent transcription through regulation of c-Jun. The determinant roles of the isoforms in the p38 MAPK signal specificity*. *J Biol Chem*, 2003. **278**(7): p. 4831-9.
7. O'Sullivan, G.C., et al., *Modulation of p21-activated kinase 1 alters the behavior of renal cell carcinoma*. *Int J Cancer*, 2007. **121**(9): p. 1930-40.
8. Chen, L., J.J. Zhang, and X.Y. Huang, *cAMP inhibits cell migration by interfering with Rac-induced lamellipodium formation*. *J Biol Chem*, 2008. **283**(20): p. 13799-805.
9. Sambrook, J., Fritsch, E.F., Maniatis, T., *Molecular cloning : a laboratory manual*. 2nd ed. ed. 1989: Cold Spring Harbour Laboratory Press.
10. Untergasser, A., et al., *Primer3--new capabilities and interfaces*. *Nucleic Acids Res*, 2012. **40**(15): p. e115.
11. Altschul, S.F., et al., *Gapped BLAST and PSI-BLAST: a new generation of protein database search programs*. *Nucleic Acids Res*, 1997. **25**(17): p. 3389-402.

Chapter 3

Generation and expression of three different plasmids:

(i) pcDNA3-MKK6b(E)-(Gly-Glu)₅-FLAG-p38 δ

(ii) pcDNA3-MKK6b-(Gly-Glu)₅-FLAG-p38 δ

(iii) pcDNA3-MKK6b(E) -(Gly-Glu)₅-FLAG-p38_{DN}

3.1 Abstract

p38 MAPK isoforms are emerging as important regulators of a host of cellular processes and as a result may be considered as possible therapeutic targets for a variety of diseases. The functions of p38 α and - β MAPK in cell differentiation, cell growth and cell death have to-date been well characterised. Recently, additional functions have been ascribed to these isoforms as both pro- and anti-tumourigenic in depending on the cell type. In contrast, the most recently identified isoform, p38 δ MAPK, has been poorly studied to-date. Investigation of the role p38 δ MAPK plays in tumourigenesis has been hindered by the lack of specific chemical activators and constitutively active mutants. To create a constitutively active form of p38 δ MAPK we fused it to an active mutant of its upstream regulator MKK6 in a single vector. Expression of this fusion plasmid in an OESCC cell line resulted in the expression of a single polypeptide and constitutive specific phosphorylation of p38 δ MAPK. We also generated control fusion plasmids expressing either inactive MKK6 or a dominant-negative p38 δ MAPK mutant. These results indicate that the MKK6-p38 δ MAPK fusion protein is a constitutively active kinase and will facilitate future study on the specific effects of p38 δ MAPK phosphorylation in OESCC.

3.2 Hypothesis and aims

The hypothesis for this chapter is that physical linking of p38 δ MAPK to MKK6 in a single peptide will result in specific and constitutive phosphorylation of p38 δ MAPK.

To examine this hypothesis the aims for this chapter are as follows:

- To generate plasmids expressing MKK6b(E) or MKK6 joined to p38 δ via a peptide linker.
- To generate a control plasmid expressing MKK6b(E) joined to a non-phosphorylatable p38 δ MAPK mutant, p38 δ_{DN} .
- To evaluate p-p38 δ MAPK expression in oesophageal squamous carcinoma cells transiently transfected with the plasmids detailed above.

3.3 Introduction

Conventional chemo- and radiotherapy for oesophageal cancer is largely ineffective – its 5 year survival rate is as low as 15% [1]. Therefore, the identification of novel molecular targets is likely to be crucial to the future of oesophageal cancer treatment. The p38 family of mitogen-activated protein kinases is one such potential molecular target. p38 MAPK isoforms $-\alpha$, $-\beta$, $-\gamma$ and $-\delta$ are signalling kinases which incorporate extracellular signals into a variety of cellular processes including proliferation, differentiation, transformation and apoptosis [2]. Roles for p38 α MAPK in tumorigenesis are now well established and it has been characterised as both a tumour promoter [3, 4] and a tumour suppressor [5, 6]. The limited knowledge which exists in relation to p38 δ MAPK also suggests pro- and anti-tumourigenic functions, depending on cell type [3, 7, 8]. Our group has previously reported a role for p38 δ MAPK in the inhibition of cell growth in renal clear cell carcinoma. Introduction of p38 δ MAPK into the RCC 786-0 cell line which does not express it abrogated apoptosis [9]. This prompted an examination of p38 MAPK isoform expression in various other cancer cell lines (see Aims of thesis). In 75% of cell lines examined i.e. renal, liver and lung cells, as well as OESCC cell lines, p38 δ MAPK is differentially expressed.

As the main aim of this thesis is to investigate any potential role for p38 δ MAPK in the tumorigenesis of OESCC, it will therefore be necessary to examine not only the effect of p38 δ MAPK expression but also the consequences of its activation (phosphorylation). Of note, p38 δ MAPK is inactive in the non-phosphorylated state. While transfection with FLAG-tagged p38 δ MAPK in a pcDNA3 vector [10] will

facilitate stable expression of p38 δ MAPK, expression of active p38 δ MAPK presents a greater challenge. Activation of p38 δ MAPK requires dual-phosphorylation of Thr and Tyr residues within a conserved regulatory loop [11]. To date, no external artificial stimulus, such as a pharmacological agent, has been identified which will specifically phosphorylate p38 δ MAPK and not simultaneously affect p38 α , - β or - γ MAPK activation. p38 δ MAPK is directly activated by members of the dual-specificity MAP kinase kinases family, predominately MKK3 and MKK6, although p38 δ MAPK phosphorylation by MKK4 and MKK7 has also been reported [12-14]. Overexpression of an MKK however, as a means of specifically activating p38 δ MAPK would have multiple downstream effectors, possibly resulting in non-specific MAPK activation: MKK3 also phosphorylates p38 α and - γ MAPK, MKK4 can phosphorylate p38 α MAPK and JNK, MKK6 phosphorylates all 4 p38 MAPK isoforms and MKK7 phosphorylates JNKs [13, 15-17].

Attempts have previously been made to generate constitutively active p38 δ MAPK kinase mutants [18, 19]. Mutants were designed on the basis of information obtained from biochemical and structural analysis of naturally occurring activating mutations in the yeast MAPK HOG1 gene and previously synthesised p38 α MAPK mutants [19-21]. While the majority of p38 δ MAPK mutants generated were inactive, a p38 δ ^{F324S} mutant reached an activity level of 13.5% in comparison to that of dually phosphorylated active p38 δ ^{WT} [18]. However, dual phosphorylation cannot be mimicked with intrinsically active kinase variants and no p38 δ MAPK mutant has been identified which reaches the level of phosphorylation obtained by co-expression of p38 δ MAPK with active MKK6 [18, 19]. Therefore the approach of enzyme-

substrate fusion as previously described for p38 α , p38 γ , ERK2 and JNK1 MAPKs would appear to be a more useful tool for investigating the function of p-p38 δ MAPK in oesophageal carcinoma as it more closely represents endogenous MAPK signalling [22-24].

The rate of an enzymatic reaction is greatly influenced by the proximity between the enzyme and its substrate. In eukaryotic cells, the specificity and efficiency of signal transduction is often enhanced by the activity of scaffold proteins. These adaptor proteins organise several components of a signalling pathway to aid the formation of signalling complexes. In fact, p38 δ MAPK has been shown to interact with such a scaffold protein, JNK-interacting protein (JIP) 2 [25]. The technique of enzyme-substrate fusion was chosen under the assumption that p38 δ MAPK may become specifically and constitutively active if physically linked to its upstream activator MKK6. To achieve this, polypeptides were designed which comprised of MKK6b or constitutively active MKK6 (MKK6b(E)) and p38 δ MAPK combined in the same vector. In summary, this chapter outlines that expression of these MKK6b-p38 δ and MKK6b(E)-p38 δ fusion proteins facilitate specific and constitutive *in vitro* phosphorylation of p38 δ MAPK in the absence of an external stimulus. These fusion proteins will be valuable tools in elucidating the roles of p38 δ MAPK activation in OESCC tumourigenesis as outlined in Chapters 4 and 7.

3.4 Materials and methods

3.4.1 Cloning strategy for pcDNA3-MKK6b(E)(Gly-Glu)₅FLAG--p38 δ fusion plasmid

A constitutively active mutant form of MKK6 i.e. MKK6b(E) in a pcDNA3 vector [10] was chosen as the backbone of the fusion construct. To maintain the open-reading frame and allow translation proceed from MKK6b(E) through to the carboxy terminus of p38 δ MAPK it was necessary to replace the TAA stop codon of MKK6b(E) with another amino acid. Site-directed mutagenesis to replace TAA with Phe (TTT) facilitated the introduction of a unique *Swa*I recognition sequence. This new site allowed for a blunt-end cloning strategy.

The gift of the plasmid pcDNA3-FLAG-p38 δ [10] provided a template from which to amplify FLAG-tagged p38 δ MAPK by PCR. To allow the principal components of the fusion protein to interact, a protein linker was needed to provide a flexible region and facilitate protein folding. A decapeptide linker composed of alternating glycine and glutamate (Gly-Glu)₅ was designed to be included 5' of the amplified FLAG-p38 δ sequence (Figure 3.1) [23].

Finally, *Dra*I restriction sites were designed 5' and 3' of the (Gly-Glu)₅-FLAG-p38 δ product to allow the blunt-ended product resulting from digestion to be ligated in-frame to the *Swa*I linearised pcDNA3-MKK6b(E) vector. Figure 3.2 provides a detailed overview of the processes involved in the generation of the fusion construct.

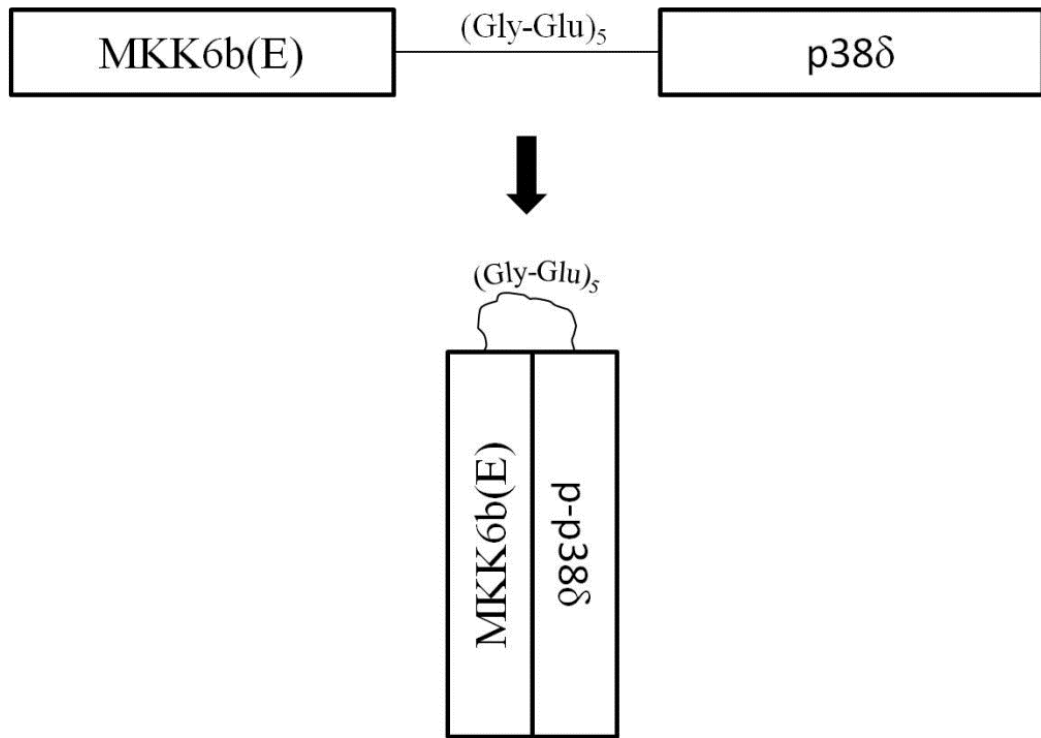


Figure 3.1 Schematic of the MKK6b(E)-(Gly-Glu)₅-FLAG-p38 δ fusion protein. The (Gly-Glu)₅ linker allows for protein folding, facilitating the interaction between MKK6b(E) and p38 δ MAPK (adapted from [23]).

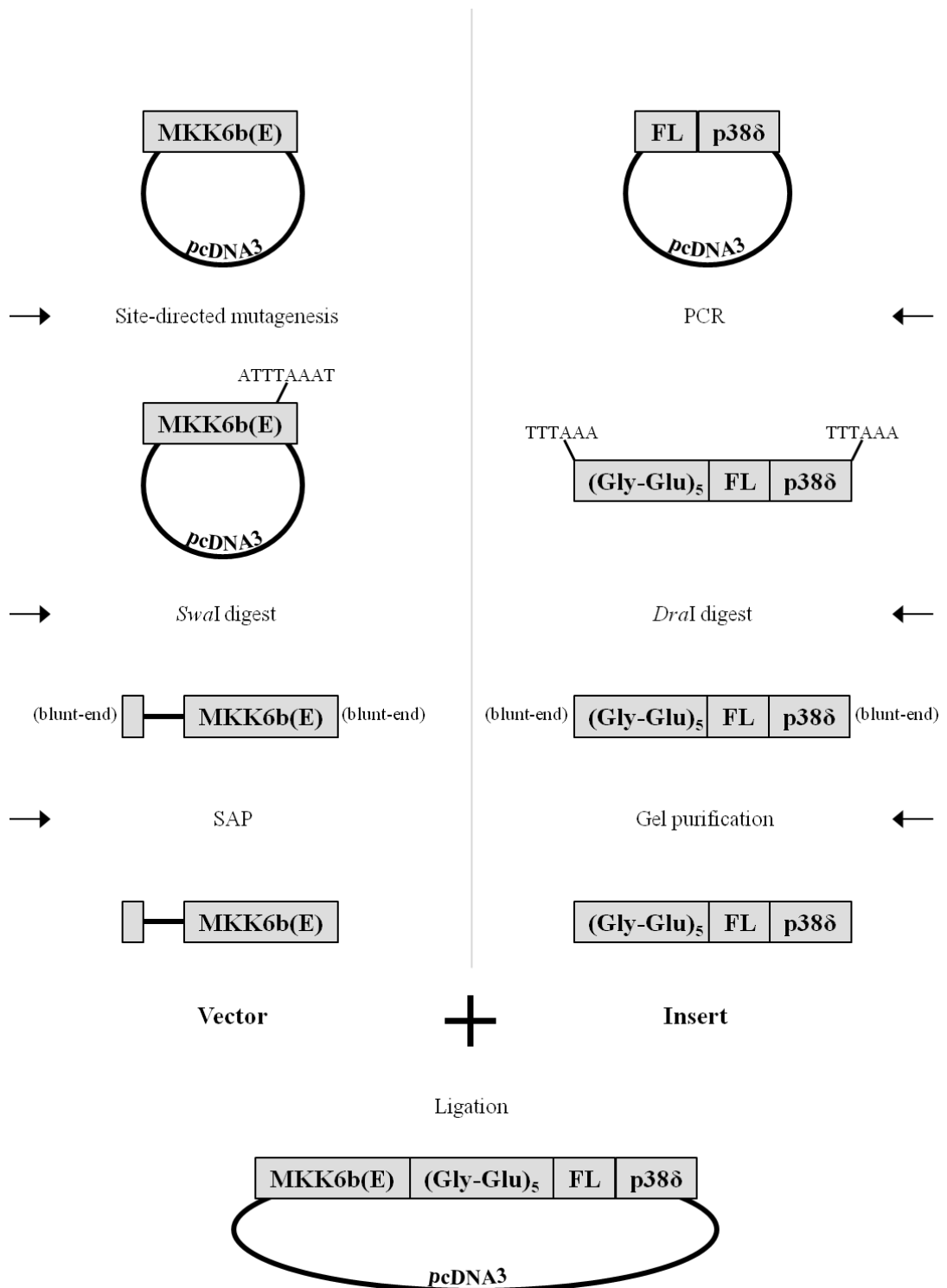


Figure 3.2 Steps involved in generating pcDNA3-MKK6b(E)-(Gly-Glu)₅-FLAG-p38δ fusion construct. Abbreviations; FL: FLAG; SAP: shrimp alkaline phosphatase.

The second plasmid to be designed, pcDNA3-MKK6b-FLAG-p38 δ , lacks constitutive MKK6b activation as it consists of wild-type MKK6b fused to FLAG-p38 δ MAPK in a pcDNA3 vector. To achieve this, the MKK6b(E) activating mutations Glu¹⁵¹ and Glu¹⁵⁵ were replaced with the endogenous MKK6b amino acids in these positions, Ser¹⁵¹ and Thr¹⁵⁵. A control plasmid was also designed. In this pcDNA3-MKK6b(E)-FLAG-p38 δ _{DN} plasmid, wild-type p38 δ MAPK was replaced with a kinase-inactive mutant form.

3.4.2 Site-directed mutagenesis

Site-Directed Mutagenesis was performed using QuikChange Lightning Site-Directed Mutagenesis Kit (Agilent Technologies UK Limited, Cheshire, UK). Primers for Site-Directed Mutagenesis (Table 3.1) were designed using the Agilent Technologies web-based QuikChange Primer Design program, www.agilent.com/genomics/qcpd; and were synthesised by Eurofins Genomics (Ebersberg, Germany).

Table 3.1 Primers for site-directed mutagenesis

Primer	Orientation	Sequence (5'→3')	T_m[°]
SDM1	sense	CATCTTTTGTAAACTGATTCTTGGAGAA TTTAAATCAGTGGACTTAATCGGTTGACC CTACTG	73.9
SDM1	antisense	CAGTAGGGTCAACCGATTAAGTCCACTG ATTTAAATTCTCCAAGAATCAGTTTTACA AAAGATG	73.9
SDM2	sense	TGGAATCAGTGGCTATTTGGTGGACTCTG TTGCTAAAACAATTGATGCAGGTTGCAA ACCATAC	79.2
SDM2	antisense	GTATGGTTTGCAACCTGCATCAATTGTTT TAGCAACAGAGTCCACCAAATAGCCACT GATTCCA	79.2
SDM3	sense	GACGCCGAGATGGCTGGCTTCGTGGTGA CCCG	81.1
SDM3	antisense	CGGGTCACCACGAAGCCAGCCATCTCGG CGTC	81.1

T_m[°] = value provided by Eurofins Genomics

Components of a single mutant strand synthesis (thermal cycling) reaction were as outlined in Table 3.2.

Table 3.2 Site-directed mutagenesis reaction components

Reaction Component	Final Concentration in 50µl reaction
10X Reaction Buffer	1X
Plasmid DNA	1 ng/µl
Sense primer	125 ng
Antisense primer	125 ng
dNTP Mix	1 µl
QuikSolution Reagent	1.5 µl
QuikChange Lightning Enzyme	1 µl

Picomol concentration of 125 ng of each primer was calculated using the formula provided in the QuikChange Lightning Site-Directed Mutagenesis Kit protocol, i.e.

$$x \text{ pmoles of primer} = \frac{\text{ng of primer}}{330 \times \# \text{ of bases in primer}} \times 1000$$

The mutant strand synthesis reaction was cycled in a GeneAmp PCR System 2700 according to the conditions outlined in Table 3.3.

Table 3.3 Mutant strand synthesis reaction conditions

Temperature °C	Time	Number of cycles
95	2 min	1
95	20 s	30
55	10 s	
68	30 s/kb of plasmid length	
65	5 min	1

Following temperature cycling, newly synthesized mutation-containing DNA was selected for by digestion of methylated and hemimethylated parental (template) DNA with DpnI endonuclease. DpnI treated DNA was transformed into SURE 2 Supercompetent cells (Agilent Technologies UK Limited, Cheshire, UK) and plasmid DNA was extracted as outlined below. Presence of mutations was confirmed by restriction digest and DNA sequencing as described in Chapter 2.

3.4.3 PCR generation of (Gly-Glu)₅-FLAG-p38δ fragment

The (Gly-Glu)₅-FLAG-p38δ insert for the fusion plasmid was amplified from pcDNA3-FLAG-p38δ by PCR using Phusion® DNA polymerase (New England BioLabs, Hertfordshire, UK). Other reaction components were as listed in Table 2.6. 5' oligonucleotide (P003F) for PCR included DraI recognition sequence as well as the (Gly-Glu)₅ sequence (5'-CCGCGCTTTAAAGGCGAGGGCGAGGGCGAGGGCGAGGGCGAGATGGATAACAAGGACGACGAT-3'). 3' primer (P003R) also included a *DraI* restriction site (5'-TTGATCTTTAAATTATTACAGCTTCATGC CACTTCGT-3'). PCR was performed in a GeneAmp PCR System 2700 under the conditions described in Table 3.4.

Table 3.4 PCR reaction conditions for amplification of (Gly-Glu)₅-FLAG-p38 δ .

Step	Temperature °C	Time	Number of cycles
Initial denaturation	95	5 min	1
Denaturation	95	30 s	5
Annealing	65.3	30 s	
Extension	72	30 s	
Denaturation	95	30 s	30
Extension	72	30 s	
Final Extension	72	10 min	1

The PCR reaction was analysed by agarose gel electrophoresis before being column purified with an Illustra GFX PCR DNA & Gel Band Purification Kit (as described in Chapter 2). The purified product was analysed by DNA sequencing as described in Chapter 2.

The purified PCR product was then digested with *Dra*I (as described in Chapter 2). The (Gly-Glu)₅-FLAG-p38 δ insert was gel-purified from the restriction enzyme reaction using an Illustra GFX PCR DNA & Gel Band Purification Kit according to manufacturer's instructions. The restriction digest products were separated by agarose gel electrophoresis as described in Chapter 2. Under long wavelength UV light and with minimal exposure time, the band of interest was excised from the gel using a sterile scalpel. The excised band was placed in a 1.5 ml microcentrifuge tube containing Capture buffer type 3 and incubated at 60°C for 15-30 min until the agarose was completely dissolved. The sample mix was transferred to a GFX

MicroSpin column in a collection tube and centrifuged at 16 000 x g for 30 s. Following two wash steps, DNA was eluted in 10 mM Tris-HCl, pH 8.0 by centrifugation at 16 000 x g for 1 min.

3.4.4 Ligation

The pcDNA3-MKK6b(E) vector (linearised by digestion with *Swa*I as described in Chapter 2) and (Gly-Glu)₅-FLAG-p38 δ insert were ligated with insert:vector ratios of 3:1, 6:1 and 10:1 by incubation with T4 DNA Ligase (New England BioLabs, Hertfordshire, UK) at 16°C overnight. Insert:vector ratios were calculated using the following formula:

$$ng\ insert = \frac{ng\ vector\ x\ kb\ size\ of\ insert}{kb\ size\ of\ vector} \times molar\ ratio\ of\ \frac{insert}{vector}$$

Ligation products were transformed into SURE2 Supercompetent Cells as described below. Plasmids prepared by miniprep (outlined below) were analysed by restriction enzyme digestion followed by agarose gel electrophoresis as described in Chapter 2 to confirm ligation and determine the orientation of the insert. Plasmids positive for ligation with the insert in a sense orientation were analysed by DNA sequencing with custom SeqP4 primer (5'-GGATATTTCCATGAGGACGGTG-3').

3.4.5 Transformation

Transformations were performed with SURE 2 Supercompetent cells according to manufacturer's protocols. Cells were thawed on ice and 100 μ l was aliquoted to a

pre-chilled tube with 2 μ l β -mercaptoethanol. After a 10 min incubation on ice, 2 μ l ligation reaction was added to cells and tubes were incubated on ice for 30 min. Cells were heat-pulsed in a 42°C water bath for 30 s then incubated on ice for 2 min. 900 μ l pre-heated (42°C) NZY⁺ broth (Lab M, Lancashire, UK) was added and tubes were incubated at 37°C for 1 hr with shaking at 225 rpm. 50 μ l transformation mixture was plated on luria broth (LB) agar (InvivoGen, Toulouse, France) plates and incubated overnight at 37°C. Controls performed included transformation with 0.01 ng pUC18 and with no DNA added.

3.4.6 Miniprep

A QIAprep Miniprep Kit (Qiagen, Manchester, UK) was used to purify up to 20 μ g molecular biology grade plasmid DNA from bacterial cultures. A single bacterial colony was picked from a freshly streaked agar plate and inoculated in terrific broth (TB) medium (InvivoGen, Toulouse, France) containing the appropriate antibiotic. Cultures were incubated overnight at 37°C with shaking. Bacterial cells were harvested by centrifugation \geq 8000 rpm for 3 min. Using the QIAprep Miniprep Kit, bacteria were lysed under alkaline conditions [26]. Lysate was then neutralised and adjusted to high salt binding conditions. DNA was adsorbed onto the QIAprep silica membrane and purified by a series of wash steps. Plasmid DNA was then eluted from the QIAprep column in Tris buffer. Plasmid DNA concentration and quality was determined spectrophotometrically with a BioPhotometer.

3.4.7 Maxiprep

Transfection-grade plasmid DNA was prepared using an Endofree® Plasmid Maxi Kit (Qiagen, Manchester, UK). A single colony was picked from a freshly streaked selective plate and inoculated in a starter culture of 5 ml TB medium containing the appropriate selective antibiotic. Culture was incubated for 8 hr at 37°C with shaking at 220 rpm. The starter culture was diluted 1/500 into 100 ml selective TB medium and incubated overnight (16 hr) at 37°C with shaking at 220 rpm. Bacterial cells were harvested by centrifugation at 6000 x g for 15 min at 4°C. The bacterial pellet was resuspended in a buffer containing RNaseA. Cells were lysed by addition of an alkaline lysis buffer and incubation at RT for 5 min. Genomic DNA, proteins, cell debris and potassium dodecyl sulphate were precipitated by addition of a neutralisation buffer. Lysate was separated from precipitate by passing through a QIAfilter Maxi cartridge. Endotoxin removal buffer was added to the filtered lysate and incubated on ice for 30 min. Filtered lysate was then applied to the Qiagen-Tip and allowed to enter the Qiagen resin by gravity-flow to facilitate DNA binding. Contaminants were removed by two medium salt washes. DNA was eluted in a high-salt buffer before being concentrated and desalted by isopropanol precipitation. DNA was redissolved in Buffer TE.

3.4.8 Cell culture

The KE-3 and KE-6 oesophageal cancer cell lines were cultured as described in Chapter 2.

3.4.9 Transient transfection

24 hr before transfection, cells were seeded at a density of 2×10^5 cells/well in a 6-well tissue culture plate in the appropriate growth medium without antibiotics. Cells were transfected at 80-90% confluency. For each well, 10 μ l LipofectamineTM 2000 transfection reagent (Life Technologies, NY, USA) and 4 μ g plasmid DNA were each diluted in 250 μ l serum-free media and incubated for 5 min at RT. Diluted LipofectamineTM 2000 and diluted DNA were combined, mixed gently and incubated for 20 min at RT. The DNA and LipofectamineTM 2000 complex was added to each well containing cells and 2 ml antibiotic-free medium. 24 hr following transfection, cells were harvested to prepare protein lysates as described in Chapter 2.

3.4.10 Immunoblot analysis

Supernatants were used for immunoblotting with specific antibodies, p38 δ MAPK, phospho-p38 MAPK and MKK6, as detailed in Chapter 2 and as previously described by us [27, 28].

3.5 Results

3.5.1 A vector for the fusion construct was created from pcDNA3-MKK6b(E)

A pcDNA3-MKK6b(E) vector was created by substituting the MKK6b(E) TAA stop codon in pcDNA3-MKK6b(E) with Phe (TTT) by site directed mutagenesis. Oligonucleotide primers used were P004F: 5'-CATCTTTTGTAAAACTGATTCTTGGAGAATTTAAATCAGTGGACTTAATCGGTTGACCCTACTG-3' (sense) and P004R: 5'-CAGTAGGGTCAACCGATTAAGTCCACTGATTTAAATTCTCCAAGAATCAGTTTTACAAAAGATG-3' (antisense) (mismatches underlined). Three plasmids were amplified from bacterial colonies generated from the transformation reaction following site directed mutagenesis. Plasmids were tested for the presence of the mutation by restriction digest with *Swa*I (successful site directed mutagenesis should have introduced a unique *Swa*I restriction site (ATTTAAAT)). As a positive control for linearization, plasmids were also digested with *Hind*III of which there is a single recognition site in pcDNA3-MKK6b(E). Agarose gel electrophoresis of restriction digest products identified a linear plasmid product following digestion of Plasmid 1 with *Swa*I (Figure 3.3A), indicating the presence of a unique *Swa*I restriction site and successful site directed mutagenesis. Plasmids 2 and 3 were undigested following incubation with *Swa*I (Figure 3.3A), suggesting site directed mutagenesis was unsuccessful in these plasmids.

To confirm the restriction digest results all three plasmids were sent for DNA sequence analysis by Eurofins MWG Operon with custom primer SeqP1 (5'-CTCTCGGTCAAGTGAAGATGTG-3'). Sequence reads were aligned to the original pcDNA3-MKK6b(E) nucleotide sequence using Multalin [29]. The

sequences generated for plasmids 2 and 3 correspond to the sequence of the original pcDNA3-MKK6b(E) plasmid and therefore do not contain the desired mutation (Figure 3.3B). The sequence generated for plasmid 1 contains the expected mutation and indicates successful site directed mutagenesis (Figure 3.3B). A further mutation after the site-directed mutagenesis site was deemed to be silent. Plasmid 1 was therefore used as the vector in all further experiments.

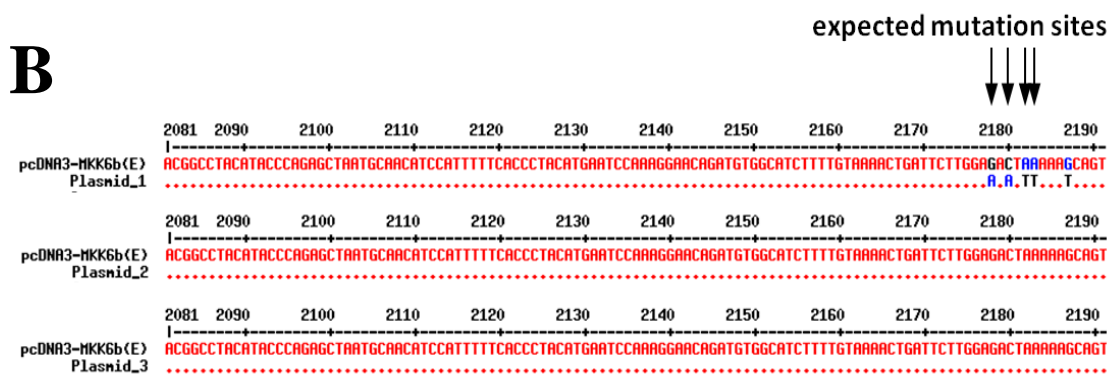
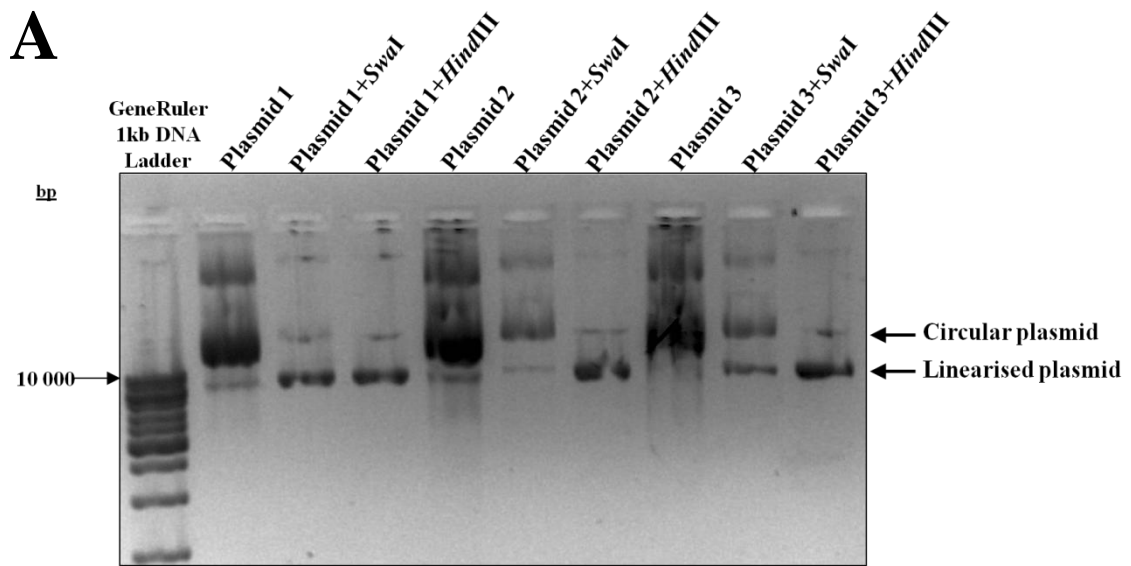


Figure 3.3 Confirmation of site-directed mutagenesis. (A) Agarose gel electrophoresis of SwaI digestion products to confirm site directed mutagenesis of pcDNA3-MKK6b(E). (B) DNA sequence analysis to confirm site directed mutagenesis of pcDNA3-MKK6b(E). Residues identical to the reference sequence (pcDNA3-MKK6b(E)) residue at the same position are represented by a point (•), residues which differ are in uppercase. Expected mutation sites following successful site-directed mutagenesis are highlighted.

3.5.2 A (Gly-Glu)₅-FLAG-p38 δ insert was successfully amplified from pcDNA3-FLAG-p38 δ

PCR of pcDNA3-FLAG-p38 δ with P003F and P003R primers yielded a product between 1000 and 1500 bp (Figure 3.4A). The expected size of a product amplified from pcDNA3-FLAG-p38 δ with P003F and P003R primers is 1182 bp, including FLAG-p38 δ , 5' (Gly-Glu)₅ linker, 5' and 3' DraI restriction sites and 6 extra 5' and 3' nucleotides to facilitate restriction digest.

Purified PCR product was sent for DNA sequence analysis by Eurofins MWG Operon. P003F and P003R, as well as custom sequencing primers, SeqP2 (5'-AGCTGGATGCACTACAACCAGAC-3') and SeqP3 (5'-AGACATCCAGGAGCCCAATG-3'), were used to sequence the entire product. Combined sequence reads were aligned to NM_002754.4 and FLAG nucleotide sequence using Multalin [29]. The sequence generated consists of flanking nucleotides to facilitate restriction enzyme binding, 5' DraI recognition sequence, (Gly-Glu)₅, FLAG, p38 δ MAPK, 3' DraI recognition sequence and flanking nucleotides (Figure 3.4B).

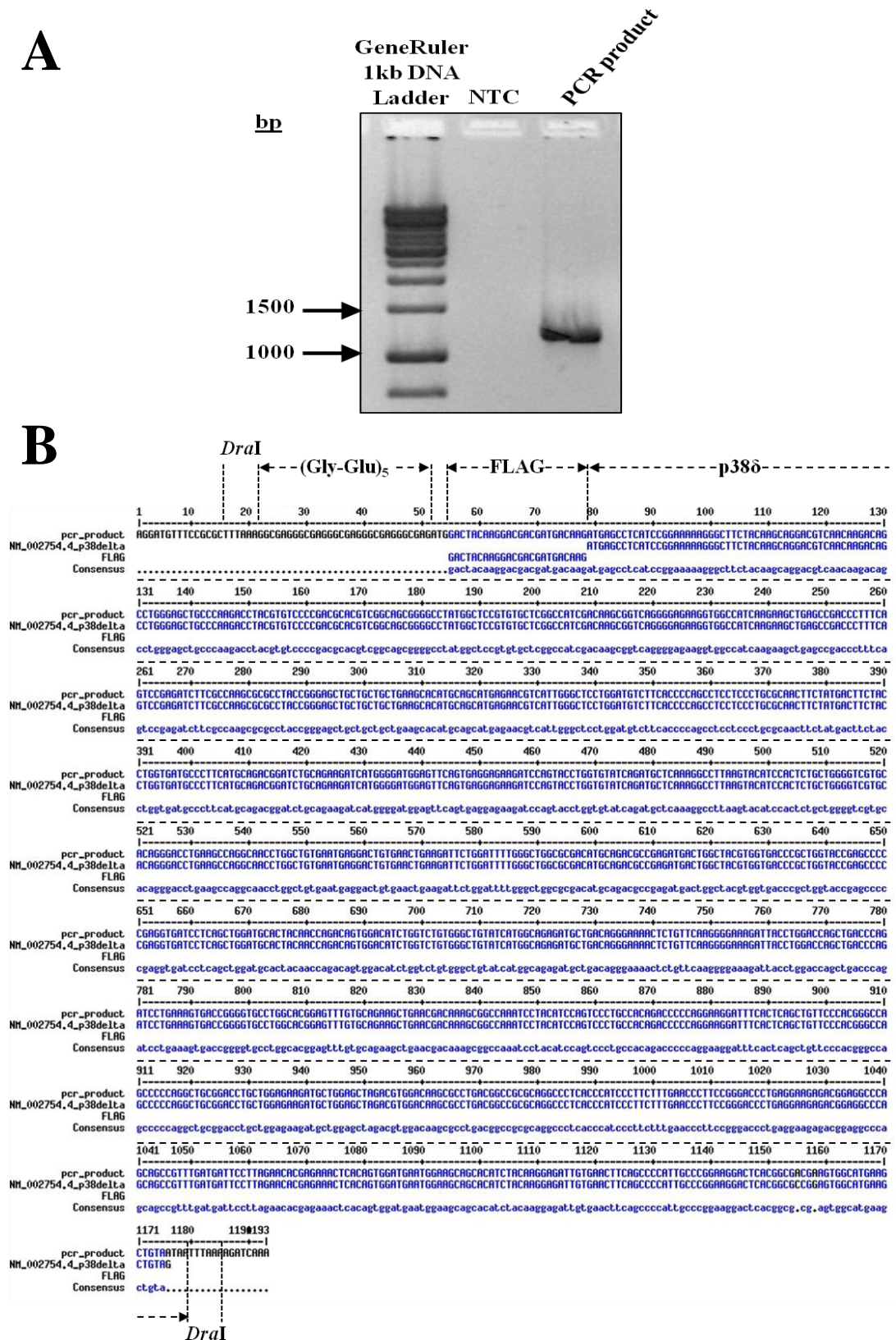


Figure 3.4 PCR amplification of (Gly-Glu)₅-FLAG-p38δ. (A) Agarose gel electrophoresis analysis of PCR product. Expected product size: 1182 bp. (B) DNA sequence analysis of fragment produced by PCR amplification. Alignment with NM002754.4 and FLAG nucleotide sequences. NTC: no template control.

3.5.3 Troubleshooting

Eight plasmids were prepared by miniprep from *E. coli* cells transformed with pcDNA3-MKK6b(E) vector and (Gly-Glu)₅-FLAG-p38 δ insert ligation reactions. Plasmids were digested with HindIII and XbaI restriction endonucleases to determine if they contained the (Gly-Glu)₅-FLAG-p38 δ insert. The expected products from digestion of a plasmid containing the insert are 2650 bp and 5352 bp versus 1486 bp and 5352 bp for plasmids negative for ligation. Restriction digest products were analysed by agarose gel electrophoresis (Figure 3.5). A fragment between 2000 and 3000 bp (highlighted) indicates that this plasmid contains an insert of the size expected following successful pcDNA3-MKK6b(E) vector and (Gly-Glu)₅-FLAG-p38 δ insert ligation.

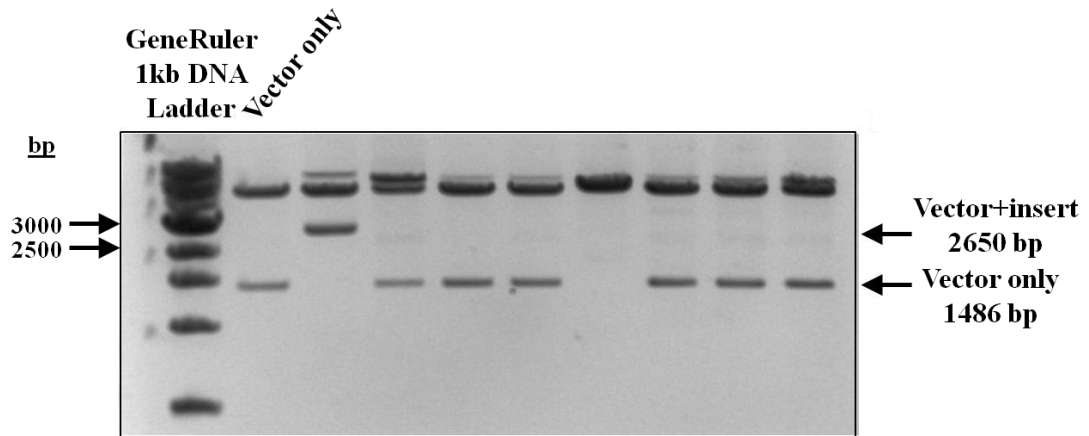


Figure 3.5. Restriction digest analysis of plasmids generated from ligation of pcDNA3-MKK6b(E) and (Gly-Glu)₅-FLAG-p38δ. Agarose gel electrophoresis analysis of products of HindIII and XbaI digestion of plasmids resulting from ligation of pcDNA3-MKK6b(E) and (Gly-Glu)₅-FLAG-p38δ. Highlighted is a fragment of the size expected following successful ligation. pcDNA3-MKK6b(E) linear plasmid (vector) served as a negative control.

The single plasmid determined to be positive for pcDNA3-MKK6b(E) vector and (Gly-Glu)₅-FLAG-p38 δ insert ligation (Figure 3.5) was further analysed to determine the orientation of the insert by digestion with SmaI and XbaI restriction enzymes whose recognition sites are located such that digestion of the plasmids will yield different sized products depending on whether the insert is present in a sense or anti-sense orientation. Agarose gel electrophoresis analysis of restriction digest products identified fragments of 6642 bp and 1360 bp indicating that the insert is present in a reverse orientation (Figure 3.6).

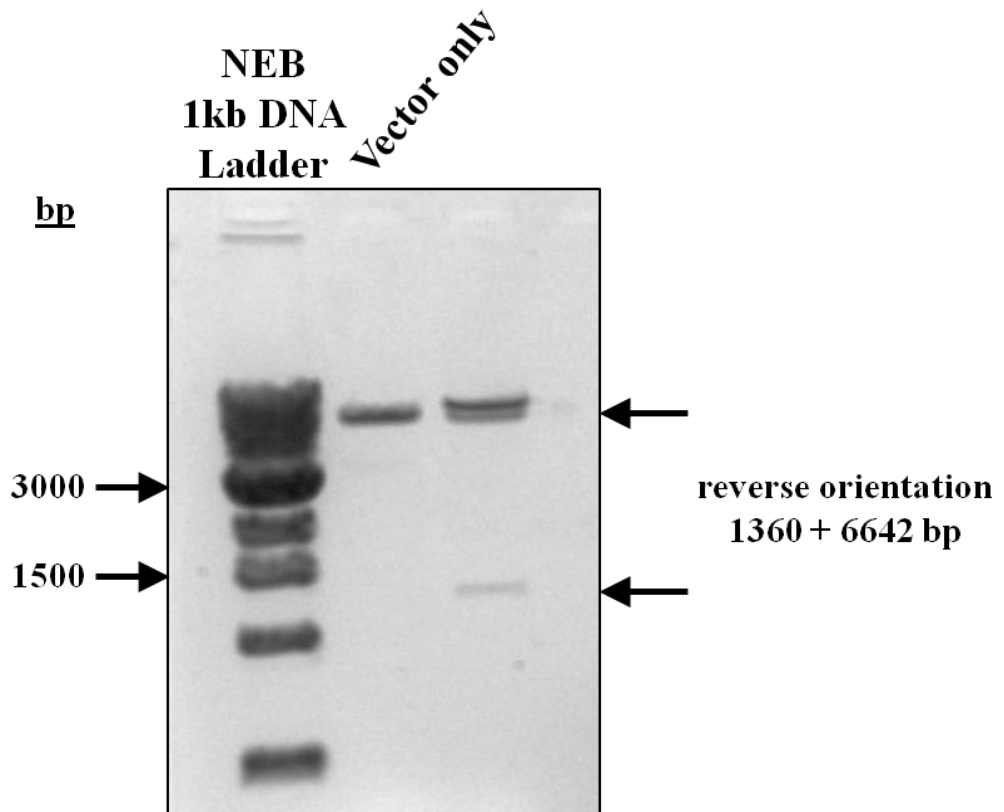


Figure 3.6. Restriction digest analysis to determine the orientation of the (Gly-Glu)₅-FLAG-p38 δ insert. Agarose gel electrophoresis analysis of products of SwaI and XbaI digestion of plasmids positive for (Gly-Glu)₅-FLAG-p38 δ insert. Highlighted are fragments of the size expected if the (Gly-Glu)₅-FLAG-p38 δ insert is present in the reverse orientation (6642 bp, 1360 bp).

In an attempt to reduce the occurrence of anti-sense orientation ligations the pcDNA3-MKK6b(E) vector was treated with 1 U/ μ l DNA shrimp alkaline phosphatase (SAP) (GE Healthcare, Buckinghamshire, UK) at 37°C for 1 hr to remove 5' phosphates. SAP was inactivated by incubation at 65°C for 15 min. To address the poor level of ligation, the insert:vector ratio was increased from 3:1 and 6:1 to 10:1 for all subsequent ligation reactions. Activity of SAP and T4 DNA Ligase was assessed with a number of control reactions. To examine T4 DNA Ligase activity, control reaction I and control reaction IV consisted of SmaI linearised pcDNA3-MKK6b(E) and (Gly-Glu)₅-FLAG-p38 δ respectively, each incubated at 16°C overnight with T4 DNA Ligase. This resulted in re-ligation (circularisation) of pcDNA3-MKK6b(E) as well as self-ligation of (Gly-Glu)₅-FLAG-p38 δ (Figure 3.7). Activity of SAP was assessed using control reactions II and III. For both reactions SmaI linearised pcDNA3-MKK6b(E) was treated with SAP. For control reaction III, SmaI linearised, SAP treated pcDNA3-MKK6b(E) was then incubated as above with T4 DNA Ligase. Treatment with SAP prevented re-ligation of linear pcDNA3-MKK6b(E) by T4 DNA Ligase (Figure 3.7).

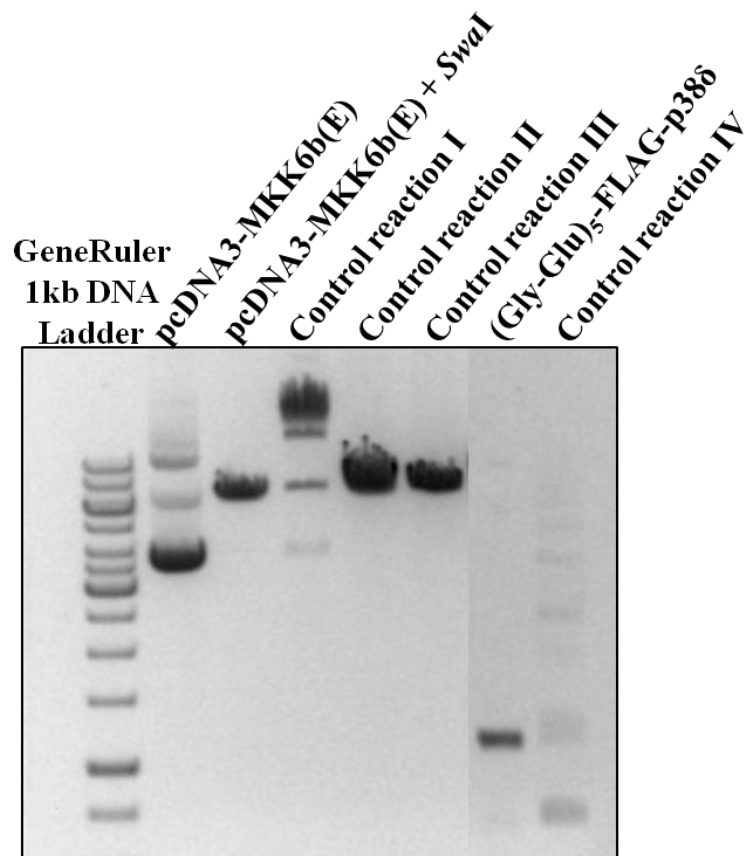


Figure 3.7. Control reactions to assess shrimp alkaline phosphatase and T4 DNA ligase activity. Agarose gel electrophoresis analysis of control ligation reactions. Control reaction I: *Swa*I linearised pcDNA3-MKK6b(E) + T4 DNA Ligase. Control reaction II: *Swa*I linearised pcDNA3-MKK6b(E) + SAP. Control Reaction III: *Swa*I linearised pcDNA3-MKK6b(E) + SAP + T4 DNA Ligase. Control reaction IV: (Gly-Glu)₅-FLAG-p38 δ + T4 DNA Ligase.

3.5.4 pcDNA3-MKK6b(E)-(Gly-Glu)₅-FLAG-p38δ was successfully generated

Twenty-one plasmids prepared by miniprep from *E. coli* cells transformed with SAP treated pcDNA3-MKK6b(E) vector and (Gly-Glu)₅-FLAG-p38δ insert ligation reactions were digested with HindIII and XbaI to determine if they contained the (Gly-Glu)₅-FLAG-p38δ insert. A fragment between 2000 and 3000 bp (highlighted) indicates that these plasmids contain an insert of the size expected following successful pcDNA3-MKK6b(E) vector and (Gly-Glu)₅-FLAG-p38δ insert ligation (Figure 3.8).

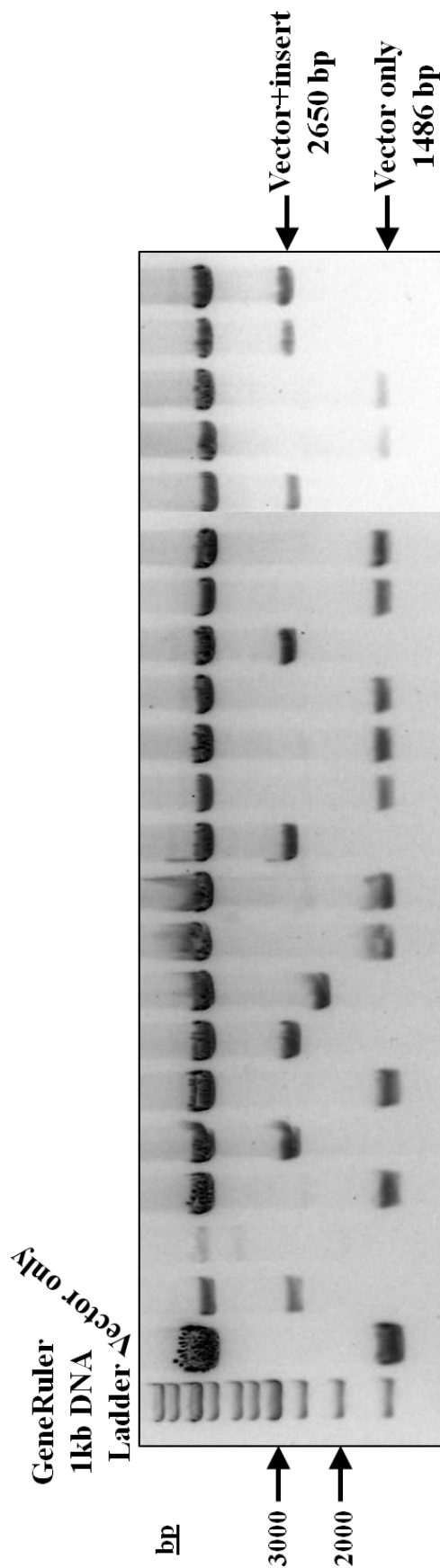


Figure 3.8. Restriction digest analysis of plasmids generated from ligation of pcDNA3-MKK6b(E) and (Gly-Glu)₅-FLAG-p38δ. Agarose gel electrophoresis analysis of products of *Hind*III and *Xba*I digestion of plasmids resulting from ligation of pcDNA3-MKK6b(E) and (Gly-Glu)₅-FLAG-p38δ. Highlighted are fragments of the size expected following successful ligation. pcDNA3-MKK6b(E) linear plasmid (vector) served as a negative control.

The plasmids determined to be positive for pcDNA3-MKK6b(E) vector and (Gly-Glu)₅-FLAG-p38 δ insert ligation were further analysed to identify the orientation of the insert by digestion with three pairs of restriction enzymes (SwaI and XbaI; BstXI and XhoI; BstXI and BamHI) whose recognition sites are located such that digestion of the plasmids will yield different sized products depending on whether the insert is present in a sense or anti-sense orientation (Figure 3.9). Following SwaI and XbaI digestion, four plasmids yielded products of 7806 bp and 196 bp (not visible on gel) suggesting they contain the insert in the correct orientation whereas five generated products of 6642 bp and 1360 bp indicating that the insert is present in a reverse orientation (Figure 3.9A) The four plasmids identified as containing the insert in the sense orientation were also digested by BstXI and XhoI. All four plasmids yielded products of the size expected if the insert is orientated in the correct manner i.e. 6603 bp and 1399 bp (Figure 3.9B). A plasmid which was believed to contain the insert in the reverse orientation was used as a control and resulted in products of 6415 bp and 1587 bp (Figure 3.9B*). Similarly, digestion of the four pcDNA3-MKK6b(E)-FLAG-p38 δ candidate plasmids with BstXI and BamHI generated products of the size expected for plasmids with the insert in the correct orientation (6762 bp and 1240 bp) compared to the suspected negative orientation plasmid (6574 bp and 1428 bp) (Figure 3.9C*).

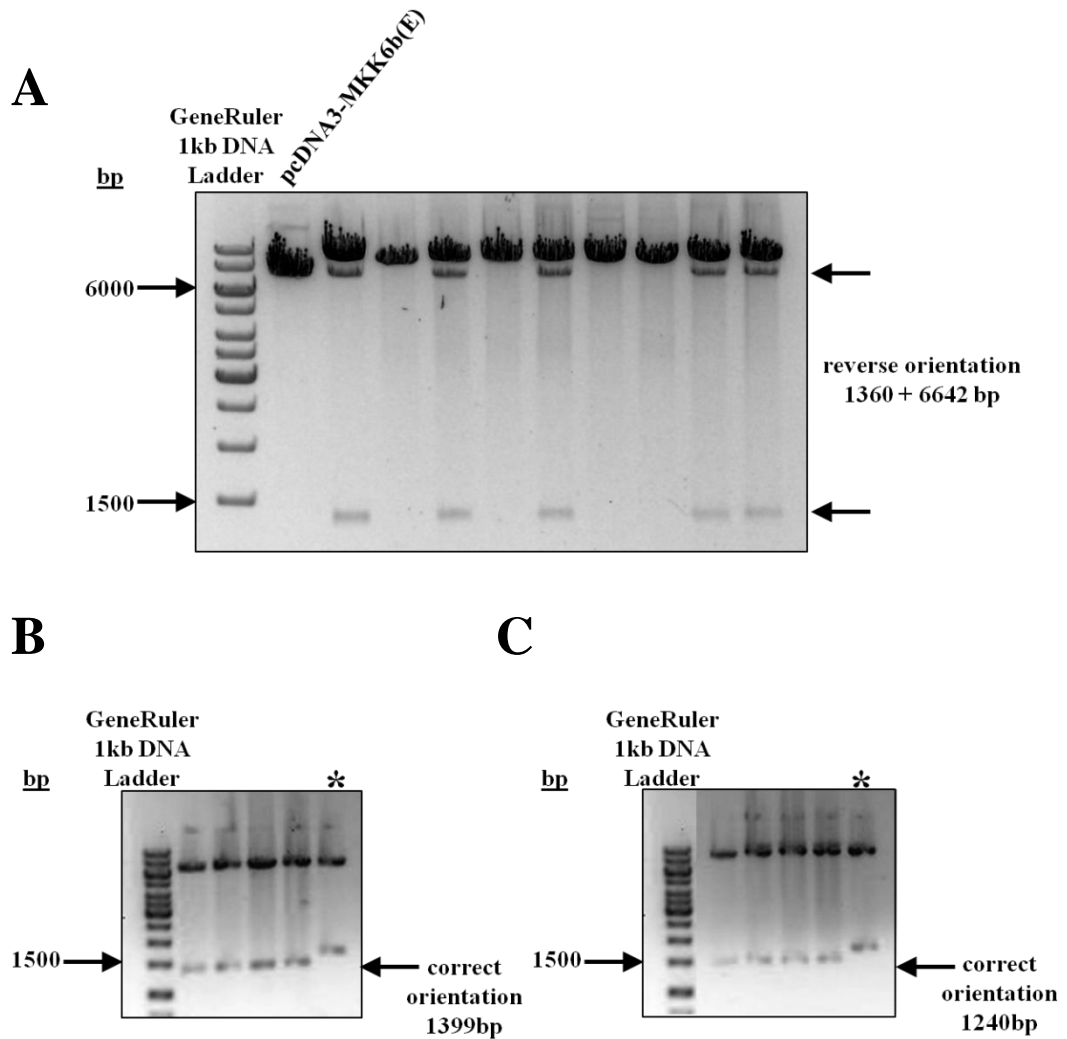


Figure 3.9 Restriction digest analysis to determine the orientation of the (Gly-Glu)₅-FLAG-p38 δ insert. Agarose gel electrophoresis analysis of products of (A) SwaI and XbaI, (B) BstXI and XhoI, and (C) BstXI and BamHI digestion of plasmids positive for (Gly-Glu)₅-FLAG-p38 δ insert. (A) Highlighted are fragments of the size expected if the (Gly-Glu)₅-FLAG-p38 δ insert is present in the reverse orientation (6642 bp, 1360 bp). (B) and (C) Highlighted are fragments of the size expected if the (Gly-Glu)₅-FLAG-p38 δ insert is present in the correct orientation (B 1399 bp; C 1240 bp).

The four plasmids positive for the (Gly-Glu)₅-FLAG-p38 δ insert in a sense orientation were analysed by DNA sequencing. Alignment of DNA sequence reads returned with the expected sequence of pcDNA3-MKK6b(E)-(Gly-Glu)₅-FLAG-p38 δ (Appendix I) confirmed successful ligation of pcDNA3-MKK6b(E) vector and (Gly-Glu)₅-FLAG-p38 δ insert.

3.5.5 Expression and activity of MKK6b(E)-(Gly-Glu)₅-FLAG-p38 δ fusion protein

Western blot analysis of transient transfections of KE-3 cells with the four candidate pcDNA3-MKK6b(E)-FLAG-p38 δ plasmids demonstrated that MKK6b(E)-FLAG-p38 δ is expressed as a single, full-length polypeptide. As expected, MKK6 (38 kDa), p38 δ MAPK (43 kDa) and FLAG (~1 kDa) are each detected at 82 kDa (Figure 3.10 A, B and C respectively). p-p38 MAPK is also detected at 82 kDa indicating that the (Gly-Glu)₅ linker facilitates protein folding and allows MKK6b(E) to constitutively phosphorylate its p38 δ MAPK partner (Figure 3.10D). p-p38 MAPK is not detected at 43 kDa. Thus MKK6(E) expressed in the fusion protein specifically phosphorylates its p38 δ MAPK fusion partner and does not interact with endogenous KE-3 p38 α , - β or - γ MAPK isoforms (Figure 3.10D).

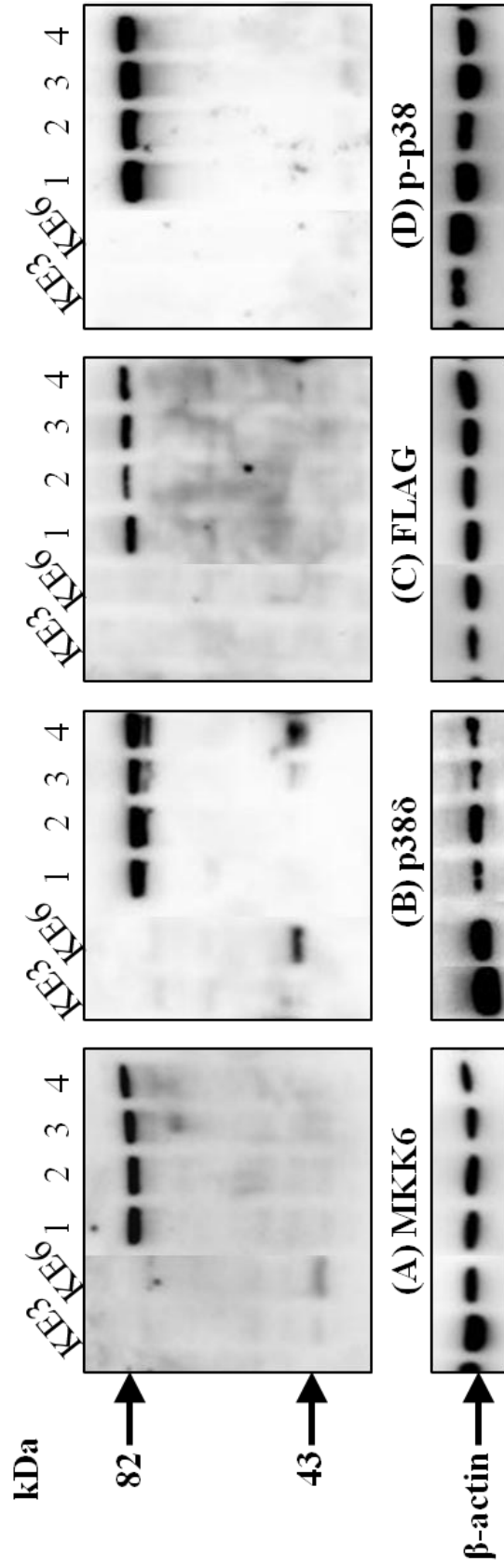


Figure 3.10 Western blot analysis of KE-3 cells transiently transfected with pcDNA3-MKK6b(E)-FLAG-p38 δ fusion plasmids. Transfected and untransfected cells were analysed by immunoblot using antibodies specific for (A) MKK6, (B) p38 δ , (C) FLAG, and (D) p-p38. 30 μ g protein lysate for each sample was loaded on a 10% SDS-PAGE gel. Membranes were probed with an anti- β -actin antibody as a loading control.

3.5.6 Generation of *pcDNA3-MKK6b-(Gly-Glu)₅-FLAG-p38 δ* plasmid

A *pcDNA3-MKK6b-(Gly-Glu)₅-FLAG-p38 δ* plasmid (inactive MKK6) was created from *pcDNA3-MKK6b(E)-FLAG-p38 δ* by substituting Glu¹⁵¹ and Glu¹⁵⁵ with Ser and Thr respectively by site-directed mutagenesis using P010F: 5'-TGGAATCAGTGGCTATTTGGTGGACTCTGTTGCTAAAACAATTGATGCAGGTTGCAAACCATAC-3' (sense) and P010R: 5'-GTATGGTTTGCAACCTGCATCAATTGTTTTAGCAACAGAGTCCACCAAATAGCCACTGATTCCA-3' (antisense) (mismatches underlined) oligonucleotides. This site-directed mutagenesis also introduced a second MfeI recognition site (CAATTG) within the plasmid sequence. Four plasmids which arose from transformation of the site-directed mutagenesis reaction were analysed for the presence of the mutations by restriction digest with MfeI. The expected products of *MfeI* digestion of plasmids containing the Ser¹⁵¹ and Thr¹⁵⁵ mutations are 6354 bp and 1648 bp compared to a single 8002 bp product for plasmids containing Glu¹⁵¹ and Glu¹⁵⁵. Agarose gel electrophoresis of the restriction digest products indicated that three of the four plasmids were positive for the substitution of Glu¹⁵¹ and Glu¹⁵⁵ with Ser and Thr respectively (Figure 3.11A). Plasmids were also analysed for the presence of the desired mutations by DNA sequencing with SeqP6 (5'-TTGGATATTTCCATGAGGACGG-3') sequencing primer. Sequence reads returned identified the Ser and Thr mutations in plasmids 1, 3 and 4, in agreement with the restriction digest results (Figure 3.11B). Plasmid 1 was used for all further experiments.

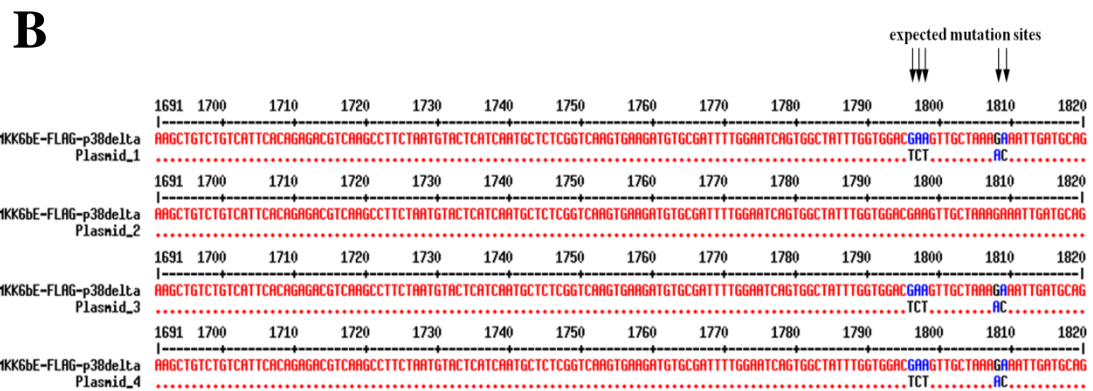
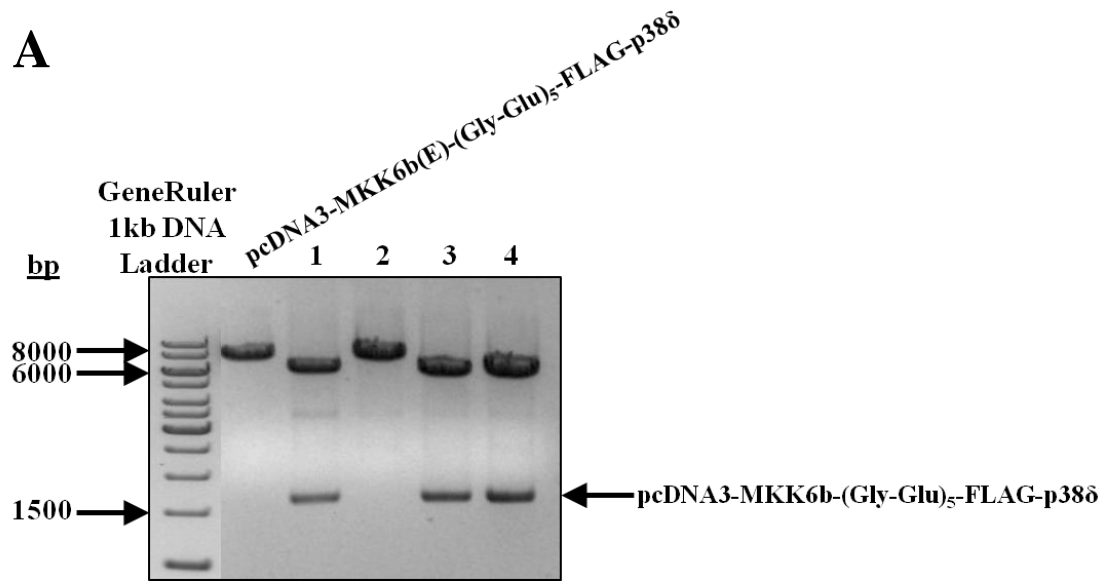


Figure 3.11 Confirmation of successful site-directed mutagenesis of pcDNA3-MKK6b(E)-(Gly-Glu)₅-FLAG-p38 δ to generate pcDNA3-MKK6b-(Gly-Glu)₅-FLAG-p38 δ . (A) Agarose gel electrophoresis analysis of products of MfeI digestion of plasmids following site-directed mutagenesis. Highlighted are fragments of the size expected following successful site-directed mutagenesis (1648 bp). MfeI digestion of untreated pcDNA3-MKK6b(E)-(Gly-Glu)₅-FLAG-p38 δ plasmid was used as a negative control. (B) DNA sequence analysis to confirm site-directed mutagenesis. Alignment of newly synthesised plasmids with original pcDNA3-MKK6b(E)-(Gly-Glu)₅-FLAG-p38 δ plasmid. Residues identical to the reference sequence (pcDNA3-MKK6b(E)-(Gly-Glu)₅-FLAG-p38 δ) residue at the same position are represented by a point (\bullet), residues which differ are in uppercase. Expected mutation sites following successful site-directed mutagenesis are highlighted.

3.5.7 Generation of control plasmid pcDNA3-MKK6b(E)-(Gly-Glu)₅-FLAG-p38δ_{DN}

A pcDNA3-MKK6b(E)-(Gly-Glu)₅-FLAG-p38δ_{DN} control plasmid (non-phosphorylatable p38δ MAPK mutant) was generated from pcDNA3-MKK6b(E)-(Gly-Glu)₅-FLAG-p38δ by changing the conservative phosphorylation motif TGY to AGF using P011F: 5'-GACGCCGAGATGGCTGGCTTCGTGGTGACCCG-3' (sense) and P011R: 5'-CGGGTCACCACGAAGCCAGCCATCTCGGCGTC-3' (antisense) (mismatches underlined) oligonucleotides. This site-directed mutagenesis also altered the BsaAI digestion profile of the plasmids. Four plasmids obtained from transformation of the site-directed mutagenesis reactions were analysed for the presence of the mutations by restriction digest with BsaAI. The expected products of BsaAI digestion of plasmids containing the AGF mutations are 3453, 1781, 1041, 924 and 803 bp compared to a 3453, 1310, 1041, 924, 803 and 471 bp products for plasmids containing the original TGY motif. Agarose gel electrophoresis of the restriction digest products indicated that all four plasmids analysed were positive for the TGY to AGF mutation (Figure 3.12A). This was confirmed by DNA sequence analysis with Seq5 (5'-CTGCTGAAGCACATGCAGCATGAG-3') sequencing primer. Sequence reads returned identified the AGF mutation in all four plasmids. Of note an extra base change was detected in one of the plasmids (Figure 3.12B). This plasmid was not further utilised. Plasmid 1 was used for all further experiments.

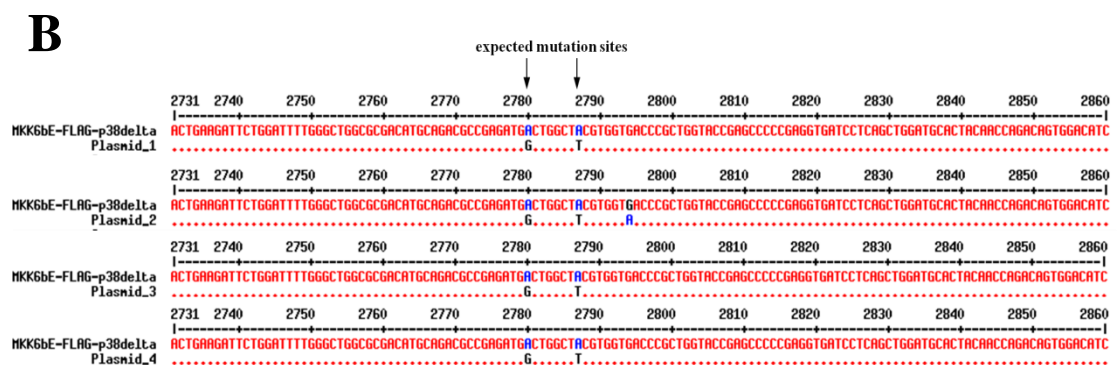
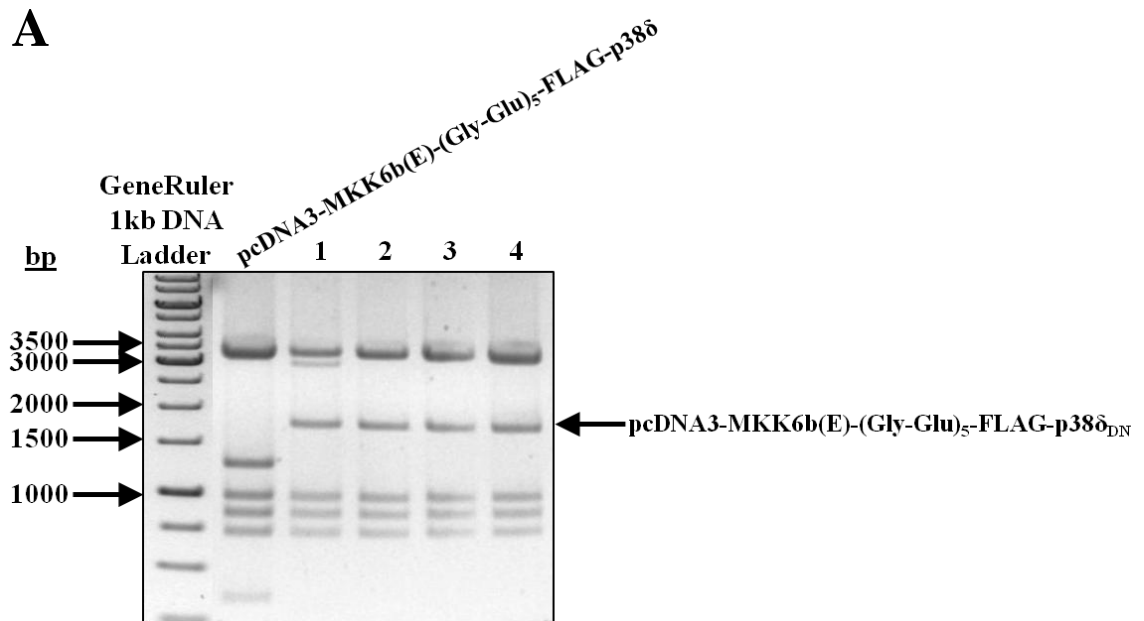


Figure 3.12 Confirmation of successful site-directed mutagenesis of pcDNA3-MKK6b(E)-(Gly-Glu)₅-FLAG-p38δ to generate pcDNA3-MKK6b(E)-(Gly-Glu)₅-FLAG-p38δ_{DN} control plasmid. (A) Agarose gel electrophoresis analysis of products of BsaAI digestion of plasmids following site-directed mutagenesis. Highlighted are unique fragments of the size expected following successful site-directed mutagenesis (1781 bp). BsaAI digestion of untreated pcDNA3-MKK6b(E)-(Gly-Glu)₅-FLAG-p38δ plasmid was used as a negative control. (B) DNA sequence analysis to confirm site-directed mutagenesis. Alignment of newly synthesised plasmids with original pcDNA3-MKK6b(E)-(Gly-Glu)₅-FLAG-p38δ plasmid. Residues identical to the reference sequence (pcDNA3-MKK6b(E)-(Gly-Glu)₅-FLAG-p38δ) residue at the same position are represented by a point (•), residues which differ are in uppercase. Expected mutation sites following successful site-directed mutagenesis are highlighted.

3.5.8 Expression and activity of pcDNA3-MKK6b-(Gly-Glu)₅-FLAG-p38 δ and pcDNA3-MKK6b(E)-(Gly-Glu)₅FLAG-p38 δ _{DN} plasmids

Western blot analysis of transient transfections of KE-3 cells demonstrated that both pcDNA3-MKK6b-FLAG-p38 δ and pcDNA3-MKK6b(E)-p38 δ _{DN} plasmids produced a single polypeptide with a molecular mass of 82 kDa as expected when using a p38 δ MAPK antibody (Figure 3.13). However, expression of pcDNA3-MKK6b(E)-FLAG-p38 δ _{DN} did not result in any detectable phosphorylation of p38 MAPK. In agreement with results previously reported for p38 α/γ and MKK6, following transient transfection of KE-3 cells with pcDNA3-MKK6b-FLAG-p38 δ , expression of phosphorylated p38 MAPK was detected at 82 kDa, similar to that observed for pcDNA3-MKK6b(E)-FLAG-p38 δ (Figure 3.10 and Figure 3.13). As both MKK6b and MKK6b(E) fused to p38 δ MAPK produced the same desired result, only one plasmid, pcDNA3-MKK6b(E)-FLAG-p38 δ , was used for future experiments.

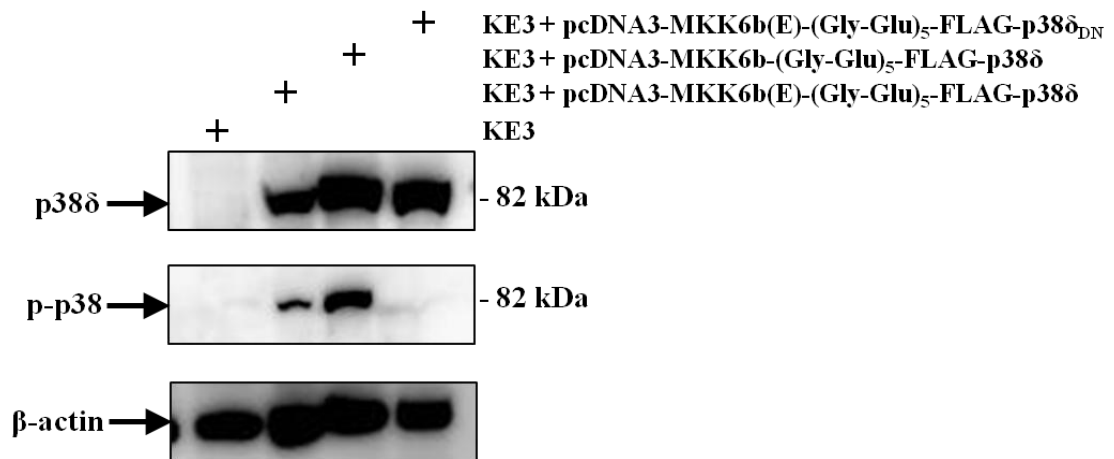


Figure 3.13 Western blot analysis of KE-3 cells transiently transfected with pcDNA3-MKK6b-(Gly-Glu)₅-FLAG-p38 δ and pcDNA3-MKK6b(E)-(Gly-Glu)₅-FLAG-p38 δ _{DN} control plasmids. Transfected and untransfected cells were analysed by immunoblot using antibodies specific for p38 δ and p-p38 MAPK. 30 μ g protein lysate for each sample was loaded on a 10% SDS-PAGE gel. Membranes were probed with an anti- β -actin antibody as a loading control.

3.6 Discussion

To date, functional characterisation of p38 MAPK pathways has relied heavily on the use of constitutively active upstream MKKs as well as pyridinyl-imidazole inhibitors such as SB203580 and SB202190 which specifically inhibit p38 α and β MAPK but have no effect on p38 γ and δ MAPKs. However, this has led to the development of an incomplete and somewhat inaccurate understanding of p38 MAPK signalling particularly in relation to p38 γ and p38 δ MAPK isoforms. The use of constitutively active MKKs and MKKKs does not take in to consideration the possibility of non-specific p38 MAPK isoform activation. To-date there are no specific p38 δ MAPK inhibitors or direct chemical activators commercially available.

Efforts by other groups to generate constitutively active p38 δ MAPK mutants used site-directed mutagenesis of p38 δ MAPK to generate mutations based on known activating mutations in HOG1, p38 α and p38 γ MAPKs [18, 19]. When expressed in *E. coli* cells, the intrinsically active p38 δ ^{F324S} variant reached an activity level of 13.5% that of MKK6 activated p38 δ ^{WT}. Significantly, this p38 δ ^{F324S} active mutant displayed 20% phosphorylation relative to MKK6 activated p38 δ ^{WT} [18]. It appears therefore that there exists a correlation between p38 isoform activation and phosphorylation as the p38 β ^{D176A} isoform also displayed correlated levels of phosphorylation (60%) and activation (60%) [18]. As *E. coli* cells do not express any MKKs the spontaneous activation of p38 δ ^{F324S} has been attributed to autophosphorylation. p38 δ ^{F324S} exhibited a high level of autophosphorylation which correlated with its level of activity while p38 δ ^{WT}, which exhibits no basal activity, displayed negligible levels of autophosphorylation [18]. Autophosphorylation

capabilities have also been attributed to p38 α MAPK mutants [20, 21]. However, while p38 α MAPK is known to autophosphorylate in response to ZAP-70 phosphorylation of Tyr323 in T cells or via interaction with TAB1 (TAK1 – binding protein 1) no evidence exists to-date which suggests that autophosphorylation is a natural mechanism of p38 δ MAPK activation *in vivo* [30, 31]. Although *in vivo* expression of p38 δ MAPK active mutants generated activation levels higher than that of MKK6 activated p38 δ^{WT} , this has been attributed to a positive feedback loop involving autophosphorylation in combination with MKK activation as well as resistance to downregulation by phosphatases [19]. These processes also do not reflect endogenous p38 δ MAPK signalling and highlight the unsuitability of p38 δ active mutants for studying p38 δ MAPK function.

A number of groups have previously demonstrated the efficacy of an enzyme-substrate fusion approach in studying the activation of MAPKs, including ERK, JNK, p38 α MAPK and p38 γ MAPK [22-24]. We show here, for the first time, that fusion of p38 δ MAPK to its upstream kinase activator MKK6, in either the inactive (MKK6b) or active (MKK6b(E)) form specifically and constitutively phosphorylates p38 δ MAPK. This fusion of two kinase partners via a peptide linker to generate a constitutively active form of the downstream kinase may now be considered as a viable alternative to the hit-and-miss approach of identifying activating mutation sites in individual kinases.

The specific mechanisms governing the activation of p38 δ MAPK by MKK6 within the fusion protein were outside the scope of this study and remain unclear. While functional components appear to be required – the MKK6-p38 δ_{DN} protein in which

p38 δ MAPK is non-phosphorylatable is inactive (Figure 3.13) – constitutive activation of MKK6 (MKK6b(E)) is not necessary (Figure 3.13). This result was not unexpected as in previous studies using MKK-MAPK fusion constructs, expression of wild-type kinases in the fusion protein were sufficient to induce phosphorylation [22-24]. Certainly, p38 δ MAPK phosphorylation is not a result of cleavage of the fusion protein and subsequent activity of the released MKK6 module. The MKK6-p38 δ fusion protein is expressed as a single polypeptide with a molecular mass of 82 kDa – equivalent to the combined masses of MKK6 (38 kDa), FLAG (1 kDa) and p38 δ MAPK (43 kDa) – as demonstrated by immunoblot analysis (Figure 3.10). Furthermore it can be assumed that cleaved MKK6 would also phosphorylate p38 α , - β and - γ MAPK isoforms [15]. However no evidence of this was observed as p-p38 was not detected at 38-43 kDa (Figure 3.10).

Thus, the MKK6-p38 δ fusion protein provides, for the first time, an opportunity to evaluate the function of p38 δ MAPK signalling in the absence of involvement of other p38 MAPK isoforms

3.7 References

1. Enzinger, P.C. and R.J. Mayer, *Esophageal cancer*. N Engl J Med, 2003. **349**(23): p. 2241-52.
2. Ono, K. and J. Han, *The p38 signal transduction pathway: activation and function*. Cell Signal, 2000. **12**(1): p. 1-13.
3. Junttila, M.R., et al., *p38alpha and p38delta mitogen-activated protein kinase isoforms regulate invasion and growth of head and neck squamous carcinoma cells*. Oncogene, 2007. **26**(36): p. 5267-79.
4. del Barco Barrantes, I. and A.R. Nebreda, *Roles of p38 MAPKs in invasion and metastasis*. Biochem Soc Trans, 2012. **40**(1): p. 79-84.
5. Bulavin, D.V. and A.J. Fornace, Jr., *p38 MAP kinase's emerging role as a tumor suppressor*. Adv Cancer Res, 2004. **92**: p. 95-118.
6. Hui, L., et al., *p38alpha: a suppressor of cell proliferation and tumorigenesis*. Cell Cycle, 2007. **6**(20): p. 2429-33.
7. Schindler, E.M., et al., *p38delta Mitogen-activated protein kinase is essential for skin tumor development in mice*. Cancer Res, 2009. **69**(11): p. 4648-55.
8. Cerezo-Guisado, M.I., et al., *Evidence of p38 γ and p38 δ involvement in cell transformation processes*. Carcinogenesis, 2011. **32**(7): p. 1093-1099.
9. Ambrose, M., et al., *Induction of apoptosis in renal cell carcinoma by reactive oxygen species: involvement of extracellular signal-regulated kinase 1/2, p38delta/gamma, cyclooxygenase-2 down-regulation, and translocation of apoptosis-inducing factor*. Mol Pharmacol, 2006. **69**(6): p. 1879-90.
10. Pramanik, R., et al., *p38 isoforms have opposite effects on AP-1-dependent transcription through regulation of c-Jun. The determinant roles of the isoforms in the p38 MAPK signal specificity*. J Biol Chem, 2003. **278**(7): p. 4831-9.
11. Jiang, Y., et al., *Characterization of the structure and function of the fourth member of p38 group mitogen-activated protein kinases, p38delta*. J Biol Chem, 1997. **272**(48): p. 30122-8.
12. Goedert, M., et al., *Activation of the novel stress-activated protein kinase SAPK4 by cytokines and cellular stresses is mediated by SKK3 (MKK6); comparison of its substrate specificity with that of other SAP kinases*. EMBO J, 1997. **16**(12): p. 3563-71.
13. Brancho, D., et al., *Mechanism of p38 MAP kinase activation in vivo*. Genes Dev, 2003. **17**(16): p. 1969-78.
14. Hu, M.C.-T., et al., *Murine p38- δ Mitogen-activated Protein Kinase, a Developmentally Regulated Protein Kinase That Is Activated by Stress and Proinflammatory Cytokines*. Journal of Biological Chemistry, 1999. **274**(11): p. 7095-7102.

15. Enslen, H., J. Raingeaud, and R.J. Davis, *Selective activation of p38 mitogen-activated protein (MAP) kinase isoforms by the MAP kinase kinases MKK3 and MKK6*. J Biol Chem, 1998. **273**(3): p. 1741-8.
16. Yao, Z., et al., *Activation of stress-activated protein kinases/c-Jun N-terminal protein kinases (SAPKs/JNKs) by a novel mitogen-activated protein kinase kinase*. J Biol Chem, 1997. **272**(51): p. 32378-83.
17. Lin, A., et al., *Identification of a dual specificity kinase that activates the Jun kinases and p38-Mpk2*. Science, 1995. **268**(5208): p. 286-90.
18. Avitzour, M., et al., *Intrinsically active variants of all human p38 isoforms*. FEBS J, 2007. **274**(4): p. 963-75.
19. Askari, N., et al., *Hyperactive variants of p38 α induce, whereas hyperactive variants of p38 γ suppress, activating protein 1-mediated transcription*. J Biol Chem, 2007. **282**(1): p. 91-9.
20. Bell, M., et al., *Isolation of hyperactive mutants of the MAPK p38/Hog1 that are independent of MAPK kinase activation*. J Biol Chem, 2001. **276**(27): p. 25351-8.
21. Diskin, R., et al., *Active Mutants of the Human p38 α Mitogen-activated Protein Kinase*. Journal of Biological Chemistry, 2004. **279**(45): p. 47040-47049.
22. Qi, X., et al., *p38 α antagonizes p38 γ activity through c-Jun-dependent ubiquitin-proteasome pathways in regulating Ras transformation and stress response*. J Biol Chem, 2007. **282**(43): p. 31398-408.
23. Robinson, M.J., et al., *A constitutively active and nuclear form of the MAP kinase ERK2 is sufficient for neurite outgrowth and cell transformation*. Current Biology, 1998. **8**(21): p. 1141-1152.
24. Zheng, C., et al., *The JNKK2-JNK1 Fusion Protein Acts As a Constitutively Active c-Jun Kinase That Stimulates c-Jun Transcription Activity*. Journal of Biological Chemistry, 1999. **274**(41): p. 28966-28971.
25. Buchsbaum, R.J., B.A. Connolly, and L.A. Feig, *Interaction of Rac exchange factors Tiam1 and Ras-GRF1 with a scaffold for the p38 mitogen-activated protein kinase cascade*. Mol Cell Biol, 2002. **22**(12): p. 4073-85.
26. Birnboim, H.C. and J. Doly, *A rapid alkaline extraction procedure for screening recombinant plasmid DNA*. Nucleic Acids Res, 1979. **7**(6): p. 1513-23.
27. Barry, O.P., et al., *Constitutive ERK1/2 activation in esophagogastric rib bone marrow micrometastatic cells is MEK-independent*. J Biol Chem, 2001. **276**(18): p. 15537-46.
28. O'Sullivan, G.C., et al., *Modulation of p21-activated kinase 1 alters the behavior of renal cell carcinoma*. Int J Cancer, 2007. **121**(9): p. 1930-40.
29. Corpet, F., *Multiple sequence alignment with hierarchical clustering*. Nucleic Acids Res, 1988. **16**(22): p. 10881-90.
30. Salvador, J.M., et al., *Alternative p38 activation pathway mediated by T cell receptor-proximal tyrosine kinases*. Nat Immunol, 2005. **6**(4): p. 390-5.

31. Ge, B., et al., *MAPKK-independent activation of p38alpha mediated by TAB1-dependent autophosphorylation of p38alpha*. *Science*, 2002. **295**(5558): p. 1291-4.

Chapter 4

Loss of p38 δ mitogen-activated protein kinase expression promotes oesophageal squamous cell carcinoma proliferation, migration and anchorage-independent growth

O'Callaghan, C., Fanning, L.J., Houston, A., Barry, O.P.

Loss of p38 δ mitogen-activated protein kinase expression promotes oesophageal squamous cell carcinoma proliferation, migration and anchorage-independent growth

Int J Oncol 2013; **43**:405-415.

(Appendix II)

4.1 Abstract

Oesophageal cancer is an aggressive tumour which responds poorly to both chemotherapy and radiation therapy and has a poor prognosis. Thus, a greater understanding of the biology of oesophageal cancer is needed in order to identify novel therapeutic targets. Among these targets p38 MAPK isoforms are becoming increasingly important for a variety of cellular functions. The physiological functions of p38 α and β MAPKs are now well documented in contrast to γ and δ MAPKs which are comparatively under-studied and ill-defined. A major obstacle to deciphering the role(s) of the latter two p38 MAPK isoforms is the lack of specific chemical activators and inhibitors. In this chapter we analysed p38 MAPK isoform expression in oesophageal cancer cell lines as well as human normal and tumour tissue. We observed specifically differential p38 δ MAPK expression. The role(s) of p38 δ and active (phosphorylated) p38 δ (p-p38 δ) MAPK in oesophageal squamous cell carcinoma (OESCC) was delineated using wild type p38 δ MAPK as well as active p-p38 δ MAPK, generated by fusing p38 δ MAPK to its upstream activator MKK6b(E) via a decapeptide (Gly-Glu)₅ linker. OESCC cell lines which are p38 δ MAPK negative (KE-3 and -8) grew more quickly than cell lines (KE-6 and -10) which express endogenous p38 δ MAPK. Re-introduction of p38 δ MAPK resulted in a time-dependent decrease in OESCC cell proliferation which was exacerbated with p-p38 δ MAPK. In addition we observed that p38 δ and p-p38 δ MAPK negatively regulated OESCC cell migration *in vitro*. Finally both p38 δ and p-p38 δ MAPK altered OESCC anchorage-independent growth. Our results suggest that p38 δ and p-p38 δ MAPK have a role in the suppression of OESCC. Our research may provide a new potential target for the treatment of oesophageal cancer.

4.2 Hypothesis and aims

The hypothesis for this chapter is that p38 δ MAPK has a role in the proliferation, migration and anchorage-independent growth of oesophageal squamous cell carcinoma (OESCC).

To examine this hypothesis the aims for this chapter are as follows:

- To examine p38 δ MAPK expression in OESCC cell lines and human tissue.
- To generate stable OESCC cell lines expressing p38 δ and p-p38 δ MAPK.
- To evaluate the consequences of p38 δ and p-p38 δ MAPK expression on OESCC proliferation, migration, invasion and anchorage-independent growth.

4.3 Introduction

Oesophageal cancer is the seventh most common cancer worldwide [1] with its five year survival rate being dismally low at no more than 15% [2]. Oesophageal squamous cell carcinoma (OESCC) is an exceptionally drug-resistant tumour. Despite recent advances in the detection of OESCC and the development of multimodal therapy [3, 4], its incidence is on the rise and outcome for patients remains poor [5, 6]. Thus, a greater understanding of the initiation and progression of OESCC is required in order to be able to identify predictive and prognostic factors that may in the future lead to novel therapeutic strategies.

The mitogen-activated protein kinases (MAPKs) are serine/threonine kinases and include the extracellular-regulated kinase (ERK), c-jun NH₂-terminal kinase (JNK) and p38 MAPK families. The p38 MAPK family consists of four members; p38 α (MAPK14) of which there are two splice variants [7], p38 β (MAPK11), p38 γ (MAPK12), and p38 δ (MAPK13) [8]. Although these isoforms are 60-70% identical in amino acid sequence they differ greatly in their tissue distribution [9], substrate specificity [10] and sensitivity to chemical inhibitors [11]. In recent years, we have gained an increased appreciation of the importance of p38 MAPK isoforms for a variety of cellular functions including proliferation, differentiation, transformation, and programmed cell death [12]. Their roles, however, are more complex than previously thought, with distinct members appearing to have different functions. In addition, the roles of p38 MAPK in various pathologic conditions remain to be elucidated [13].

To-date most of the published literature refers to the p38 MAPK family as a whole or indeed have focused on the first discovered isoform p38 α MAPK [10, 13]. There is an obvious dearth of research pertaining to the latter two isoforms, p38 γ and - δ MAPK, due partly to the lack of commercially available specific chemical activators or inhibitors for each of these isoforms [14]. In this chapter we have overcome this obstacle using an enzyme-substrate fusion approach for the generation of constitutively active p38 δ MAPK. We now provide new information regarding the role(s) of p38 δ and active (phosphorylated) p38 δ (p-p38 δ) MAPK in OESCC. We identified differential p38 δ MAPK expression in OESCC. Lack of p38 δ MAPK expression in OESCC allows for a more aggressive phenotype including increased proliferation, increased migration and increased capacity for anchorage independent growth. Restoration of p38 δ MAPK expression, however, reverses these effects. Together, our results provide evidence for a novel role for p38 δ MAPK-induced suppressive effects in OESCC. With survival rates being poor for patients with OESCC, there is an urgent need to find novel strategies to improve current therapy. Our work suggests isoform specific activation of p38 δ MAPK as a possible potential approach for treatment of patients with OESCC.

4.4 Materials and Methods

4.4.1 Specimens

The patient cohort consisted of ten patients with OESCC of both genders ranging in age from 44 to 81 years. Formalin-fixed, paraffin-embedded (FFPE) oesophagectomy specimens from ten patients consisted of ten paired samples of primary tumour and metastatic lymph nodes with 10 samples of non-tumour adjacent tissues (NAT). All patient tumour biopsies were staged and group staged (in a blinded manner) histopathologically in accordance with TNM7 and performed by a pathologist at the Mercy University Hospital. Patient features are summarized in Table 4.1.

Table 4.1 OESCC patient features

Patient Features	No. of patients
Sex	
Male	4
Female	6
Age	Median 63 (44 to 81) years
TNM7 stage	
T stage	
T3	10
N stage	
N1	3
N2	7
Histological grade	
Well differentiated	1
Moderately differentiated	6
Poorly differentiated	3

Patient features are summarised based on gender, age, TNM7 stage and histological stage. Based on the TNM7 categorization for oesophageal cancer N1 = 1-2 lymph nodes and N2= 3-6 lymph nodes.

4.4.2 Cell culture

The KE oesophageal cancer cell lines as well as KYSE-70, KYSE-450, OE-19, OE-21, OE-33, OC-3 cells and stably transfected KE-3 cell lines were cultured as described in Chapter 2. KE cell line features are summarized in Table 2.2.

4.4.3 Proliferation assay

Cell viability was assessed by trypan blue (0.4% w/v) exclusion assay as previously described [15]. KE cells were seeded at a density of 3×10^4 cells/well in a 6-well tissue culture plate and incubated for the times indicated. Wells were washed with PBS and cells were harvested with Trypsin-EDTA as in Chapter 2 and resuspended in the appropriate medium. A cover-slip was affixed to the haemocytometer. Equal volume trypan blue solution was mixed with cell suspension. 20 μ l trypan blue/cell suspension mixture was pipetted onto the haemocytometer under the cover-slip. Viable cells were counted in all 4 large corner squares according to Figure 4.1, using a Diaphot phase contrast microscope (Nikon, Tokyo, Japan). Cell concentration per ml was calculated as follows:

$$\text{Average number of cells in one large square} \times \text{dilution factor} (2) \times 10^4$$

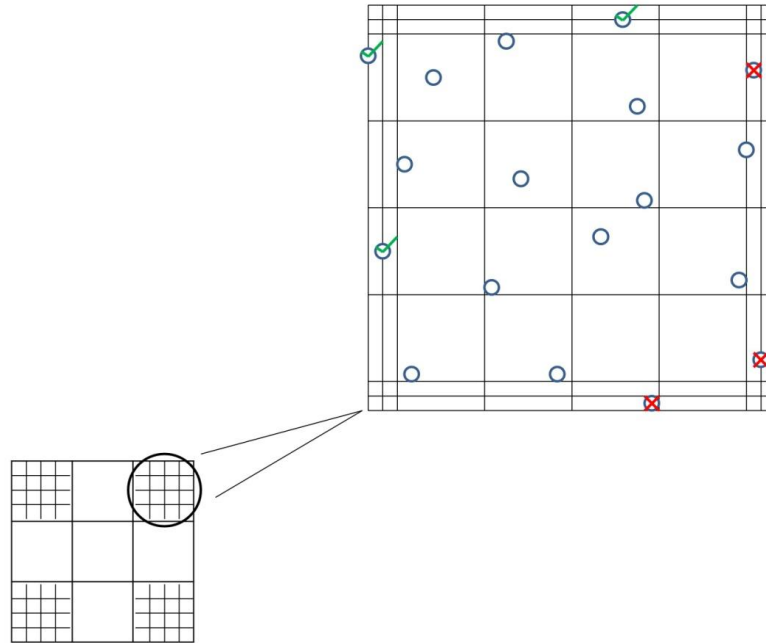


Figure 4.1 Cell counting with a haemocytometer. Cells were counted in each of the four corner squares according to the following rule – count cells on top and left touching middle line of the perimeter of each square (✓). Do not count cells touching the middle line at bottom and right sides (X).

4.4.4 Nuclear and cytosolic extraction

Nuclear and cytoplasmic fractions were prepared using NE-PER® Nuclear and Cytoplasmic Extraction Reagents (Thermo Fisher Scientific) according to manufacturer's instructions. 2×10^6 cells were transferred to a 15ml tube and centrifuged at 1100 rpm for 5 min. Supernatant was discarded and cells were washed by resuspending in 1ml PBS. Cell suspension was transferred to a 1.5ml microcentrifuge tube and cells were pelleted by centrifugation at $500 \times g$ for 3 min. Supernatant was discarded, leaving the cell pellet as dry as possible. Ice-cold CERI (supplemented with Protease Inhibitor Cocktail) was added, and the tube was vortexed vigorously for 15 s to fully resuspend the pellet. Following a 10 min incubation on ice, ice-cold CERII was added and vortexed for 5 s. Samples were centrifuged at a speed of 10 000 rpm for 5 min. Supernatants (cytoplasmic extract) were transferred to pre-chilled microcentrifuge tubes and stored at -20°C . Remaining insoluble fractions were resuspended in ice-cold NER by vortexing for 15 s every 10 min, for a total of 40 min. Samples were centrifuged at 10 000 rpm for 10 min. Supernatants (nuclear extract) were collected in pre-chilled microcentrifuge tubes and stored at -20°C . Samples were stored on ice throughout the extraction procedure and all centrifugation steps were performed at $\leq 4^{\circ}\text{C}$.

4.4.5 Stable transfection

KE-3 cells were stably transfected with pcDNA3, pcDNA3-FLAG-p38 δ , pcDNA3-MKK6b(E)-(Gly-Glu)₅-FLAG-p38 δ , or pcDNA3-MKK6b(E)-(Gly-Glu)₅-FLAG-p38 δ_{DN} . Transfection procedure was as described in Chapter 3 for transient transfection. Twenty-four hours following transfection cells were transferred to 100

mm diameter dishes. Transfected cells were selected for by incubation in normal growth medium supplemented with 800 µg/ml geneticin. After 4-8 weeks, individual cell colonies were transferred to culture flasks for clone expansion. Stably transfected cell lines were maintained in the appropriate media supplemented 400 µg/ml geneticin.

4.4.6 Immunoblot analysis

Supernatants used for immunoblotting with specific antibodies, p38 α , - β , - γ and - δ , phospho-p38 MAPK and MKK3, MKK4, MKK6 and MKK7 antibodies were prepared as detailed in Chapter 2 and have previously been described by us [15, 16].

4.4.7 Immunohistochemistry

p38 MAPK isoform expression in FFPE OESCC and NAT sections, as well as expression of p38 δ and p-p38 MAPK in control and stably transfected KE-3 cells was examined using immunohistochemistry as previously described [16]. FFPE OESCC and NAT sections were de-paraffinized in xylene and re-hydrated prior to analysis. Antigen retrieval was performed by microwave irradiation on 0.01 M citrate buffer, pH 6.0 (citrate acid, H₂O).

Endogenous peroxidase activity was quenched by incubation in 3% v/v H₂O₂ for 10 min. To block non-specific binding of antibody, samples were incubated with 5% v/v Normal Goat Serum in 0.05M Tris Saline pH 7.6 (0.04M Trizma HCl, 0.01M Trizma Base, 0.15M NaCl, 0.005M KCl, pH adjusted to 7.6 with 5N HCl), 0.001%

w/v Saponin (NGS TS/SAP) for 1 hr at RT. Washes were performed between each incubation with 1% NGS TS/SAP. Primary antibodies (Table 4.2) were diluted in 1% NGS, 0.05M Tris Buffer (0.04M Trizma HCl, 0.01M Trizma Base) – at concentrations specified by the manufacturer. Primary antibodies were incubated on coverslips overnight at 4°C in a humidified environment. A negative control was performed for each experiment by eliminating the primary antibody.

Table 4.2 Primary antibodies for immunohistochemistry/immunocytochemistry.

Target antigen (human)	Molecular weight	Supplier	Source
p38α MAPK	43 kDa	Cell Signaling Technology	Rabbit
p38β MAPK	40 kDa	Zymed Laboratories, CA, USA	Mouse
p38γ MAPK	46 kDa	Upstate, Lake Placid, NY, USA	Rabbit
p38δ MAPK	43 kDa	R&D Systems	Rabbit
phospho-p38 MAPK	43 kDa	Cell Signaling Technology	Rabbit

Biotinylated anti-rabbit and anti-mouse secondary antibodies (Vector Laboratories, Burlingame, CA, USA) were diluted 1:200 in 1% NGS TS/SAP and incubated on samples for 45 min at RT. A preformed avidin and biotinylated horseradish peroxidase macromolecular complex (Vectastain® Elite® ABC Kit, Vector Laboratories) was applied to the samples and incubated for 45 min RT. Cells were stained by incubation with 3,3'-diaminobenzidine (DAB Substrate Kit for Peroxidase, Vector Laboratories) for 5 min in the dark. Cells were counterstained

with Mayer's haematoxylin for 3 min. Coverslips were mounted to glass slides with aqueous mounting medium and allowed to dry overnight.

Slides were examined using the brightfield view of an Olympus BX61 microscope. Images were captured by an Olympus DP71 camera and analysed using Olympus cell[^]F analysis image processing software (Olympus, Essex, UK).

4.4.8 Immunocytochemistry

p38 and p-p38 MAPK expression in control and stably transfected KE-4 cells was examined using immunocytochemistry. Cells were seeded at a density of 50 000 or 80 000 cells per well of a 6-well plate with each well containing a 22mm x 22mm coverglass. On reaching the appropriate confluency, media was removed and cells were washed 3 times with PBS. Cells were fixed to coverslips by incubation in 2ml 4% w/v paraformaldehyde for 15 min followed by three washes with PBS. Cells were permeabilized by incubation with 0.5% v/v Triton-X-100 in PBS for 5 min, followed by three washes with PBS. Antibody binding and detection was performed as described above for immunohistochemistry.

4.4.9 ELISA

A DuoSet® IC Human Phospho-p38δ (T180/Y182) sandwich enzyme-linked immunosorbent assay (ELISA) (R&D Systems Europe Ltd., Abingdon, UK) was used according to manufacturer's instructions to measure p38δ MAPK phosphorylated at T180/Y182 in cell lysates. To prepare lysates, cells were

resuspended at 1×10^7 cells/ml in Lysis Buffer #6 (1 mM EDTA, 0.5% v/v Triton-X-100, 5 mM NaF, 6 M urea, 10 µg/ml leupeptin, 10 µg/ml pepstatin, 100 µM PMSF, 3 µg/ml aprotinin, 2.5 mM $\text{Na}_4\text{P}_2\text{O}_7$, 1 mM sodium orthovanadate (Na_3VO_4)) and incubated on ice for 15 min. Lysates were stored at -80°C . Before use lysates were diluted 6-fold with IC Diluent #8 (1 mM EDTA, 0.5% v/v Triton-X-100, 5 mM NaF) and further serial dilutions were prepared in IC Diluent #3 (1 mM EDTA, 0.5% v/v Triton-X-100, 5 mM NaF, 1 M urea).

Phospho-p38δ MAPK (T180/Y182) Standard was reconstituted with IC Diluent #7 (1 mM EDTA, 0.5% v/v Triton-X-100, 5 mM NaF, 6 M urea). It was then initially diluted 6-fold with IC Diluent #8 before additional dilutions were prepared in IC Diluent #3. These dilutions generated a six point standard curve using 2-fold dilutions and a high standard of 10 000 pg/ml. Phospho-38δ (T180/Y182) Capture Antibody was reconstituted in PBS. Phospho-38δ (T180/Y182) Detection Antibody was reconstituted in IC Diluent #1 (1% BSA).

A 96 well microplate was coated with 100 µl per well of 1.0 µg/ml Capture Antibody in PBS, sealed and incubated overnight at RT. Capture Antibody was aspirated and wells washed three times with Wash Buffer (0.05% v/v TWEEN®20 in PBS). Plates were blocked by incubating with 300 µl Block Buffer (1% BSA, 0.05% NaN_3 , PBS) per well for 1 – 2 hr at RT. Aspiration/washing was repeated. 100 µl of diluted sample or standards was added per well, sealed and incubated for 2 hr at RT. Aspiration/washing was repeated. 100 µl 1.0 µg/ml Detection Antibody in IC Diluent #1 was added per well, sealed and incubated for 2 hr at RT. Aspiration/washing was repeated. 100 µl Streptavidin-HRP in IC Diluent #1 was added to each well and

incubated in the dark for 20 min at RT. Aspiration/washing was repeated. 100 μ l Substrate Solution was added per well and incubated in the dark for 20 min at RT. 50 μ l Stop Solution was added per well. The absorbance of each well at 450 nm (with a wavelength correction of 540 nm) was measured immediately on a SunriseTM spectrophotometric plate reader and analysed using the XRead software program.

A standard curve was generated by plotting the Blank-corrected average absorbance reading for each of the standards versus their concentrations in pg/ml. The concentration of phospho-p38 δ MAPK (T180/Y182) in each unknown sample was determined using this standard curve according to the following equation:

$$y = mx + b$$

where y = blank-corrected absorbance reading, m = the slope of the standard curve and x = concentration in pg/ml.

4.4.10 Cell migration

Migration of untransfected and transfected KE-3 cells was assessed using both a Boyden Chamber assay and a wound-healing assay as described in Chapter 2.

4.4.11 Colony forming assay

The role of p38 δ MAPK in anchorage-independent growth was assayed using a soft agar colony-forming assay as previously described [16]. Cells were plated at a density of 3×10^5 cells/100-mm dish in medium containing 0.4% (w/v) agar on an

underlay of 0.8% (w/v) agar. After 21 days incubation colonies were stained with MTT as outlined in Chapter 2.

4.4.12 siRNA

KE-6 cells at 75% confluency were transfected with p38 δ MAPK small interfering RNA (siRNA) (Santa Cruz Biotechnology) or control siRNA-A (Santa Cruz Biotechnology) as recently described [17]. 24 hr before transfection, 2×10^5 cells were seeded per well of a 6-well tissue culture plate in antibiotic-free growth medium. Cells were incubated with 100 nM p38 δ MAPK siRNA or control siRNA-A and 6 μ l siRNA Transfection Reagent (Santa Cruz Biotechnology) in 800 μ l serum-free, antibiotic-free medium/well for 7 hr. 1 ml normal growth medium containing two times the normal serum and antibiotics concentration was added per well and incubated for an additional 24 hr before being replaced with 2 ml normal growth medium. Cells were assayed (proliferation and whole cell lysates) 24, 48, 72 and 96 hr after the addition of normal growth medium.

4.4.13 rt-PCR

p38 δ MAPK mRNA was amplified from cellular cDNA (synthesised as described in Chapter 2) using DreamTaqTM DNA polymerase (Fermentas, Thermo Fisher Scientific) and oligonucleotide primers P001F 5'- CCACGTTAAACTGCCCATCT-3' and P001R 5'- CCGCCACAAGCTAAAAAGAG-3'. Other reaction components were as listed in Table 2.6. rt-PCR was performed in a GeneAmp PCR System 2700

under the conditions described in Table 2.7. rt-PCR products were analysed by agarose gel electrophoresis as described in Chapter 2.

4.4.14 Proteome ProfilerTM antibody array

The relative levels of phosphorylation of 26 kinases was examined in cell lysates using a Proteome ProfilerTM Human Phospho-MAPK Array (R&D Systems Europe Ltd.) according to manufacturer's instructions. Cells rinsed with PBS were resuspended at 1×10^7 cells/ml in Lysis Buffer 6. Lysates were rocked at 4°C for 30 min then centrifuged at $14\,000 \times g$ for 5 min. Supernatants were stored at -80°C. Total protein concentration of samples was quantitated as described in Chapter 2. All incubations were performed on a platform rocker. Arrays were blocked for 1 hr at RT in Array Buffer 5 (a buffered protein base with preservatives). 200 µg cell lysate was combined with 20 µl Detection Antibody Cocktail and incubated for 1 hr at RT before being incubated overnight at 4°C on arrays. Three 10 min washes were performed between each of the remaining steps with 1X Wash Buffer. Streptavidin-HRP, diluted 1:2000 in Array Buffer 5, was incubated on arrays for 30 min at RT. Chemi Reagent Mix (equal volumes Chemi Reagent 1 and 2) was pipetted evenly onto each membrane and incubated for 1 min before excess reagent was drained away. Positive signals were detected using a SYNGene G:Box Chemi XR5 Gel Documentation System. Pixel density of each spot was analysed using Scion Image software (Scion Corp., Frederick MD, USA).

4.5 Results

4.5.1 p38 α , - β , - γ and - δ MAPK isoforms and MKK3, -4, -6 and 7 are differentially expressed in oesophageal cancer

The expression of p38 MAPK as a family has previously been outlined in oesophageal cancer as well as other cancer types [10, 13, 18, 19]. While these reports refer to the p38 MAPK family, analysis of individual p38 MAPK isoform expression in oesophageal cancer has to date never been reported. A previous study by us outlining differential p38 MAPK isoform expression in renal cancer prompted us to investigate further the effects of individual p38 MAPK family members in cancer in general [20]. Using Western blot analysis we examined p38 MAPK isoform expression in nine OESCC cell lines (KE-3, -4, -5, -6, -8, -10, KYSE-70, KYSE-450 and OE-21) and three oesophageal adenocarcinoma cell lines (OC-3, OE-19 and OE-33). We used antibodies specific for each isoform p38 α , - β , - γ and - δ MAPKs as previously described by us [20]. All twelve oesophageal cancer cell lines (squamous and adenocarcinoma) expressed p38 α , - β and - γ MAPKs (albeit at different levels) (Figure 4.2A). In contrast p38 δ MAPK expression was present in the three adenocarcinoma cell lines but absent in four of the OESCC cell lines KE-3, -8, KYSE-70 and OE-21 (Figure 4.2A). The specific loss of p38 δ MAPK isoform expression only has previously been reported by us in renal carcinoma (786-0) [20] and also observed by us in liver (Huh-7), lung (A-549) prostate (PC-3 and DU-145) and skin (MeWo) cancer cell lines (Figure A.1). Upstream MKK3 and -6 are thought to be the major protein kinases responsible for p38 MAPK activation [18] but the selectivity of p38 MAPK isoform activation is stimulus type and strength dependent [21]. We observed strong MKK3 and -4 expression for all cell lines except KE-3 and

-8 OESCC which were MKK3 negative. In contrast levels of MKK6 and -7 expression were considerably lower (Figure 4.2B).

Finally, analysis of p38 δ MAPK at the mRNA level surprisingly proved positive for all cell lines examined including the four OESCC cell lines that were negative for p38 δ MAPK protein expression (Figure 4.2C). Primers specific for a 292bp fragment of the 3' untranslated region of p38 δ MAPK mRNA amplified cDNA from all twelve cell lines. Other primer sets within the coding sequence yielded similar results. In addition DNA sequence analysis of PCR products did not identify any mutations such as a stop codon or a missense mutation which could possibly explain loss of p38 δ MAPK protein expression and is outlined in Chapter 6.

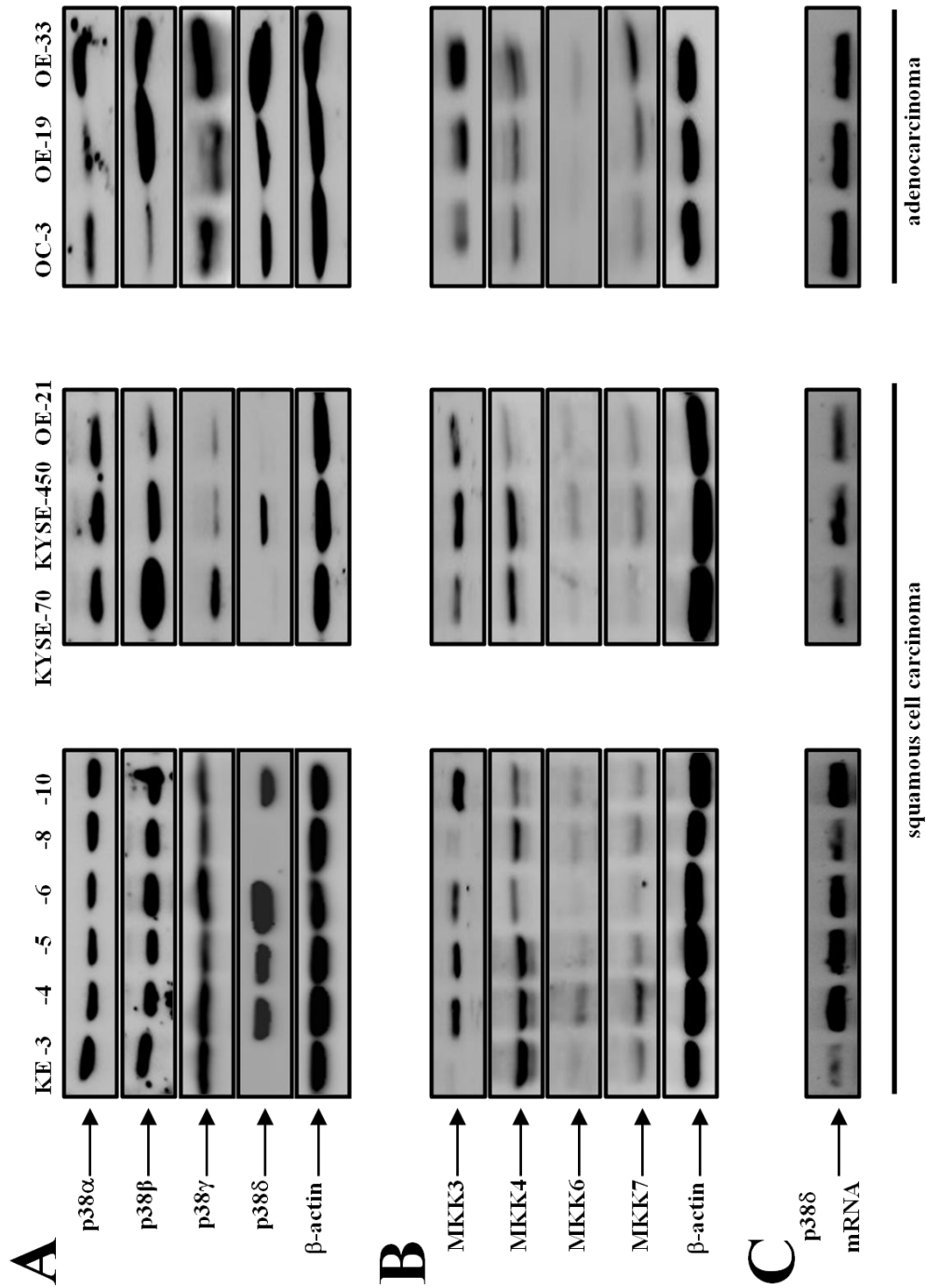


Figure 4.2 Expression of p38 MAPK isoforms, MKK3, -4, -6 and -7 in oesophageal cancer.
(Figure legend- next page)

Figure 4.2 Expression of p38 MAPK isoforms, MKK3, -4, -6 and -7 in oesophageal cancer. (A) Western blot analysis of p38 MAPK isoform expression in KE-3, -4, -5, -6, -8 and -10, KYSE-70, -450, and OE-21 (oesophageal squamous cell carcinoma cell lines) as well as OC-3, OE-19 and OE-33 (oesophageal adenocarcinoma cell lines). (B) Western blot analysis of MKK3, -4, -6 and -7 in the same twelve cell lines. Aliquots of 30 μ g of protein lysate were loaded on a 10 % SDS-PAGE gel and analyzed by immunoblot using antibodies specific for p38 α , - β , - γ and - δ MAPKs. β -actin analysis served as a loading control. The results shown are representative of four independent experiments. (C) Agarose gel electrophoresis analysis of DNA fragments produced by PCR amplification of p38 δ MAPK mRNA from oesophageal squamous (KE3, -4, -5, -6, -8, 10, KYSE70, -450 and OE21) and adenocarcinoma (OC3, OE19 and -33) cell lines.

To investigate whether the p38 MAPK isoform expression pattern we observed *in vitro* with the OESCC cell lines could be translatable to the *in vivo* situation we analyzed the expression profile and localization of all four p38 MAPK isoforms (α , β , γ and δ) in FFPE oesophagectomy specimens from ten patients with squamous cell carcinoma. Samples consisted of ten paired primary tumour and metastatic (lymph nodes) as well as corresponding NAT as outlined in Table 4.1. Samples were staged according to the new TNM7 categorization for oesophageal cancer (Table 4.1) [22]. Consistent levels of p38 α and β MAPK expression was evident in all ten normal, primary and metastatic OESCC samples (Figure 4.3). Similarly, we did not observe a change in p38 γ MAPK expression between normal, primary tumour and metastatic samples albeit the intensity of brown staining was less than that observed for p38 α and β MAPK (Figure 4.3). p38 δ MAPK expression, however, was considerably different in normal versus primary tumour versus metastatic disease (Figure 4.3 and Table 4.3). p38 δ MAPK expression was observed in both the nuclei and cytoplasm of nine of the ten oesophageal NAT tissue samples. However, a significant decrease in expression was observed in both the nuclei and cytoplasm in the ten primary tumour specimens as evidenced from the lighter brown staining compared to NAT samples in six patient samples and complete loss of expression in four of the samples (Figure 4.3, Table 4.3). Furthermore, eight out of the ten metastatic tissue specimens demonstrated complete loss of p38 δ MAPK expression with both the nuclei and cytoplasm appearing blue in colour (Figure 4.3). This is an important finding considering identification of lymph node metastasis is the single most important prognostic factor in oesophageal cancer [1].

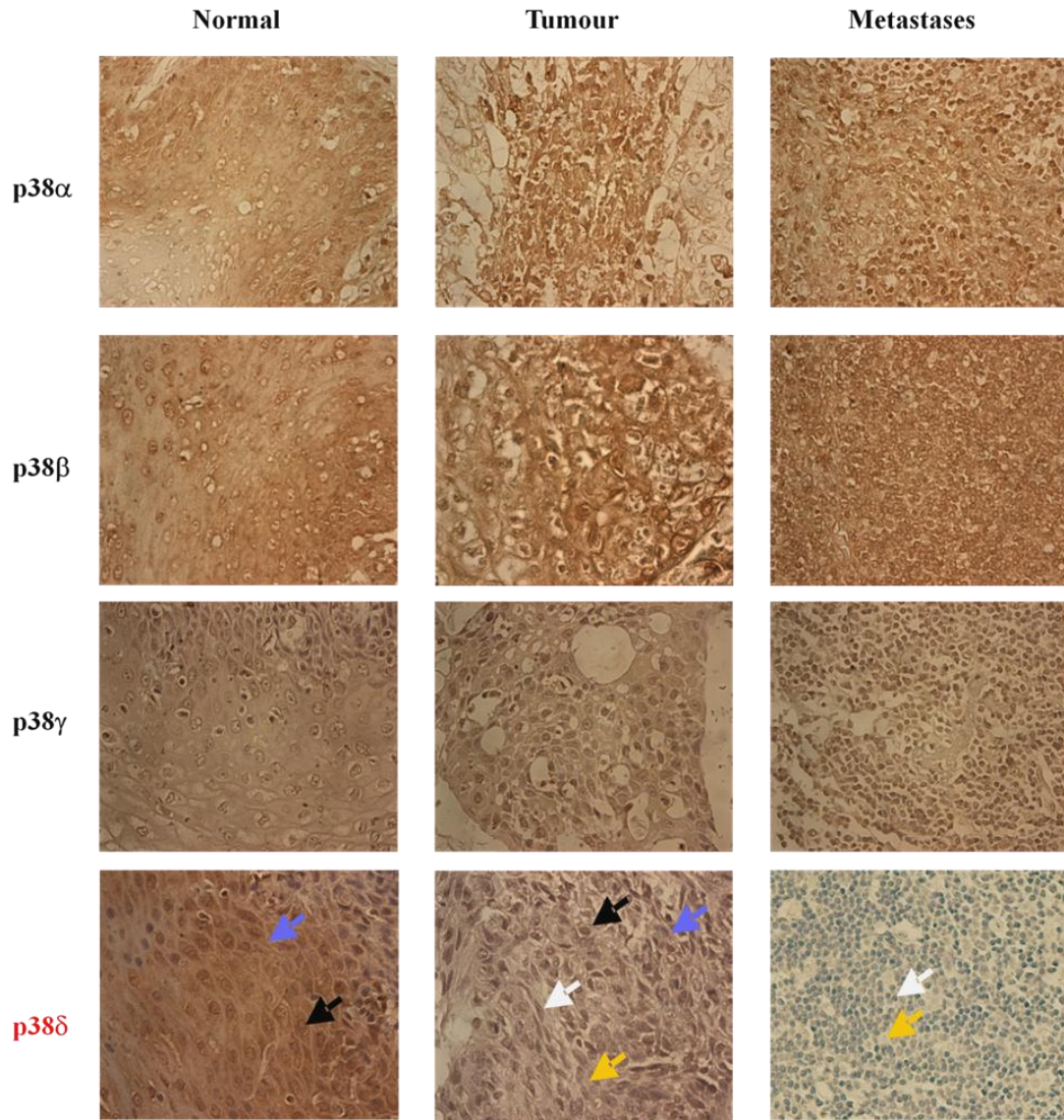


Figure 4.3 Expression of p38 α , - β , - γ and - δ MAPK isoforms in oesophageal human tissue. Immunohistochemical staining of p38 α , - β , - γ and - δ MAPK isoforms in normal, tumourigenic and metastatic (lymph node) oesophageal human tissue. Immunohistochemical staining was performed as outlined in Materials and methods. Blue arrow indicates cytoplasmic staining; black arrow indicates nuclear staining; white arrow indicates blue unstained nuclei and yellow arrow indicates blue unstained cytoplasm. Magnification is 400 \times . The results shown are representative of ten patients.

Table 4.3 p38 δ MAPK expression in patient specimens

Diagnosis	p38δ MAPK expression	
	Positive	Negative
NAT (n=10)	9	1
OESCC Primary (n=10)	6*	4
OESCC Nodes (n=10)	2	8

Samples obtained from ten patients consisted of ten paired primary tumour and metastatic lymph nodes as well as corresponding non-tumour adjacent tissues for analysis of p38 δ MAPK expression. *Denotes that p38 δ MAPK expression was considerably lower than in the corresponding NAT.

4.5.2 OESCC cell lines lacking endogenous p38 δ MAPK expression proliferate faster than those which express this isoform

The results obtained for differential p38 δ MAPK expression in both the oesophageal cell lines and the human samples prompted us to investigate further the effect(s) if any this particular isoform may have on the tumourigenicity of OESCC. Firstly, we examined whether the presence or absence of endogenous p38 δ MAPK expression could have an effect on the proliferation rate of our OESCC cell lines. Using the trypan blue exclusion assay we compared the proliferation rate of KE-3, and -8 cell lines (which do not express p38 δ MAPK) versus KE-6 and -10 (which express p38 δ MAPK). We observed that at all time points studied (24-120 hr) both cell lines KE-3 and -8 proliferated faster than KE-6 and -10 cells (Figure 4.4).

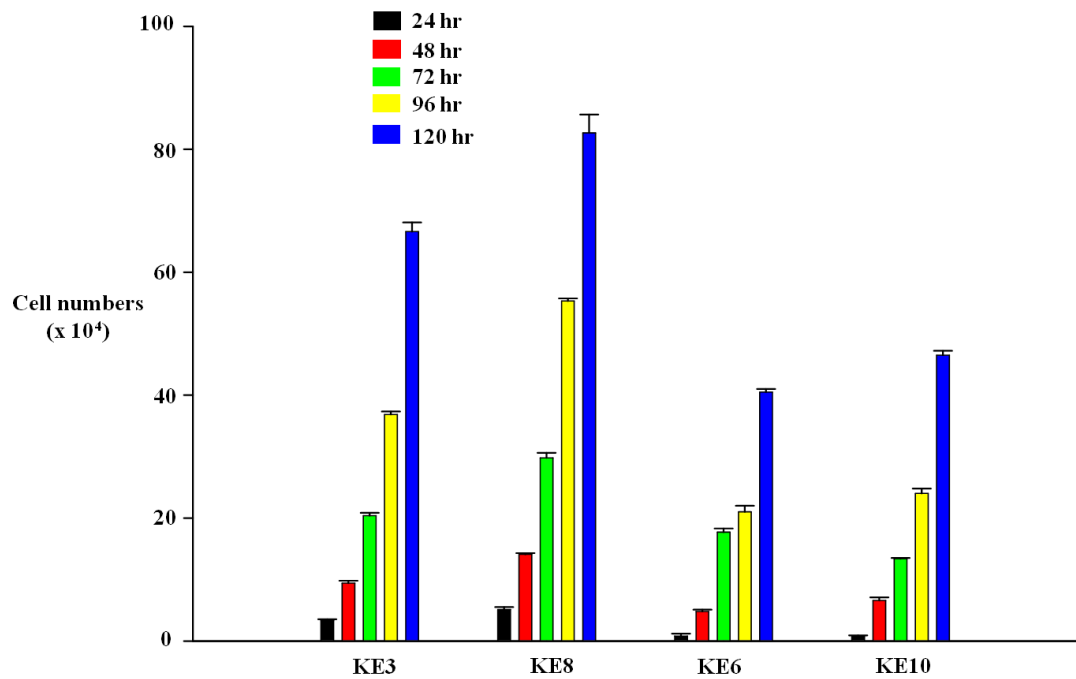


Figure 4.4 Oesophageal squamous cell carcinoma cell lines lacking endogenous expression of p38 δ MAPK have a higher proliferation rate. KE-3, and -8 cell lines (lacking endogenous p38 δ MAPK expression) and KE-6 and -10 cell lines (expressing endogenous p38 δ MAPK) were seeded (3×10^4) and counted for 24-120 hr. The results shown are mean \pm S.E. of three independent experiments.

4.5.3 Generation of stable cell lines expressing p38 δ , phosphorylated p38 δ (p-p38 δ) and p-p38 δ_{DN} MAPK

To investigate whether p38 δ or active (phosphorylated) p38 δ (p-p38 δ) MAPK drives the observed anti-proliferative phenotype (Figure 4.4) we re-introduced wild type p38 δ MAPK into KE-3 cells which have lost its expression. In the absence of a specific commercially available p38 δ MAPK activator (and to investigate the effect(s) of active p-p38 δ MAPK) we generated a constitutively active p38 δ MAPK through enzyme substrate fusion as discussed in Chapter 3. As both MKK6b and MKK6b(E) fused in frame to p38 δ MAPK produced the same desired result (transient transfections Chapter 3) only one plasmid (MKK6b(E)-p38 δ) was used for subsequent experiments. Western blot analysis of stable transfections of KE-3 cells demonstrated that pcDNA3-MKK6b(E)-(Gly-Glu)₅-FLAG-p38 δ produced a single polypeptide with a molecular mass of 82 kDa as expected when using p38 δ MAPK, p-p38 MAPK and MKK6 antibodies respectively (Figure 4.5A(i), (ii), (iii)). Western blot analysis of KE-3 cells stably transfected with pcDNA3-MKK6b(E)-(Gly-Glu)₅-FLAG-p38 δ_{DN} also produced a single polypeptide with a molecular mass of 82 kDa upon incubation with p38 δ MAPK and MKK6 antibodies (Figure 4.5A(i), (iii)) but did not demonstrate p38 MAPK activation (phosphorylation) (Figure 4.5A(ii)). Stable transfection of KE3 cells with pcDNA3-MKK6b(E)-(Gly-Glu)₅-FLAG-p38 δ was also confirmed by PCR. T7 and SP6 primers specific for pcDNA3 amplified a 2723bp fragment from genomic DNA of KE3 cells transfected with pcDNA3-MKK6b(E)-(Gly-Glu)₅-FLAG-p38 δ and maintained in geneticin (400 μ g/ml) supplemented medium (Figure 4.5B).

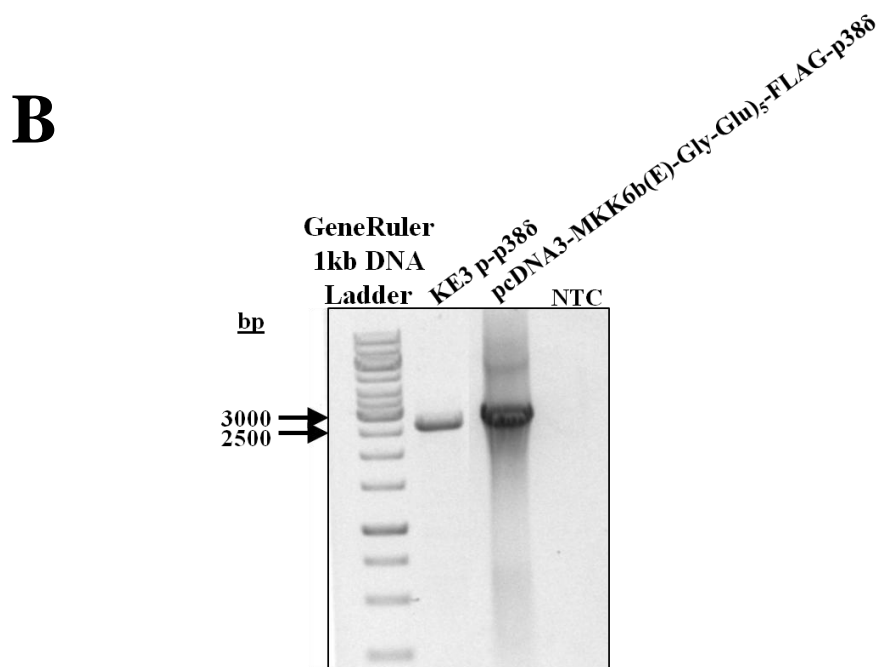
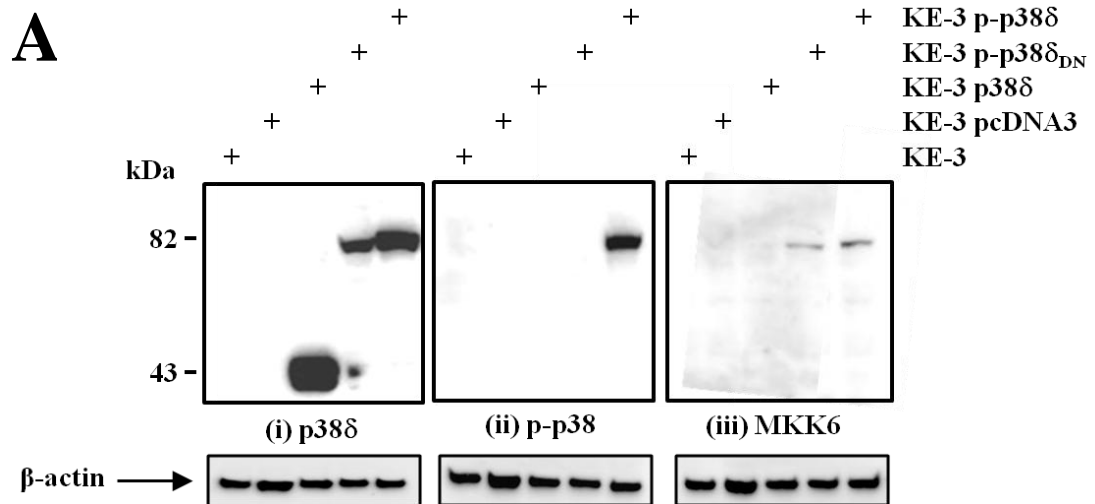


Figure 4.5 Generation of cell lines stably expressing p38 δ , p-p38 δ and p-p38 δ_{DN} MAPK. (A) Western blot analysis of 30 μ g protein lysate of KE-3 cells stably transfected with empty vector (pcDNA3), wild type p38 δ MAPK, p-p38 δ MAPK and p-p38 δ_{DN} MAPK using antibodies specific for p38 δ MAPK (i), p-p38 MAPK (ii) and MKK6 (iii). The results shown are representative of four independent experiments. (B) Agarose gel electrophoresis analysis of products of PCR of genomic DNA from KE3 cells stably transfected with pcDNA2-MKK6b(E)-(Gly-Glu)₅-FLAG-p38 δ using pcDNA3 specific T7 and SP6 primers. pcDNA3-MKK6b(E)-(Gly-Glu)₅-FLAG-p38 δ plasmid DNA was used as a positive control. NTC: no template control.

Of note the antibody used in Figure 4.5A(ii) is a pan phospho-p38 MAPK antibody. To our knowledge there is no commercially available antibody to test for active (phosphorylated) p-p38 δ MAPK specifically by Western blot analysis. Therefore, to confirm p38 δ MAPK activation we performed a sandwich ELISA which measures p38 δ MAPK isoform phosphorylation specifically. Transfection of KE-3 cells with wild type p38 δ MAPK alone revealed activation (Figure 4.6). This is in strong agreement with previous reports where adenovirally expressed wild type p38 δ MAPK was activated in head and neck squamous cell carcinoma [23] and human keratinocytes [24]. A fourfold ($p < 0.001$) increase in activation of p38 δ MAPK was observed following stable transfection of KE-3 cells with p-p38 δ (Figure 4.6). This level of activation is similar to p38 δ MAPK co-expressed with MKK3/MKK6 in HEK293 cells [25]. As expected we did not observe phosphorylation of p38 δ MAPK in cells transfected with p-p38 δ_{DN} (Figure 4.6). We also analysed KE-6 and KE-10 cell lines (which express endogenous p38 δ MAPK expression) but did not observe p38 δ MAPK phosphorylation in either cell line (Figure 4.6).

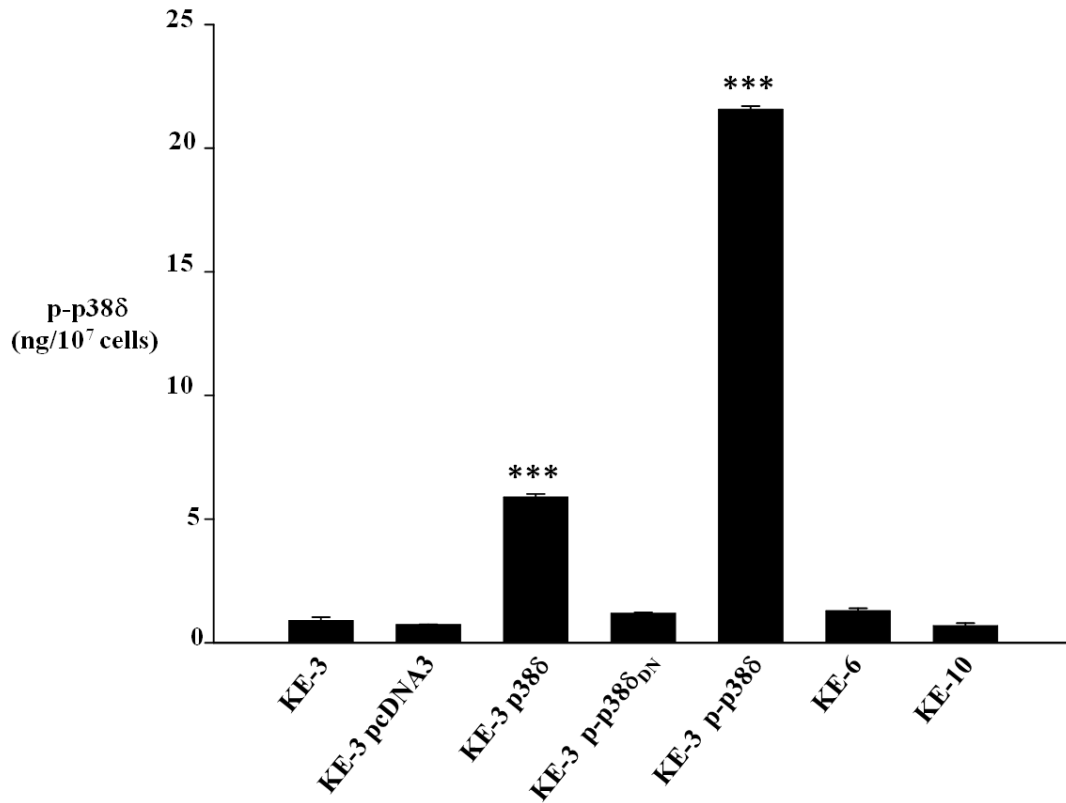


Figure 4.6 Analysis of specific p38δ MAPK phosphorylation. Transfected and non-transfected KE-3, KE-6 and KE-10 cells were analysed to determine the amount of activated i.e. phosphorylated p38δ MAPK expression using the human phospho-p38δ (T180/Y182) ELISA commercial kit. The ELISA assay was carried out according to manufacturer's protocol. The results shown are mean \pm S.E. of three independent experiments. Significant (***, $p < 0.001$) changes from control non-transfected KE-3 cells were determined by application of Student's t-test.

To ensure specific phosphorylation of p38 δ MAPK only and not the other three p38 MAPK isoforms (α , $-\beta$ and $-\gamma$) we performed a human phospho-MAPK antibody array. We did not observe phosphorylation of p38 α , $-\beta$ or $-\gamma$ MAPK in non-transfected KE-3 cells or cells stably transfected with p38 δ MAPK or p-p38 δ MAPK (Figure 4.7A and B). We did, however, observe an increase ($p < 0.001$) in phosphorylation in KE-3 p38 δ MAPK wild type transfected cells which was amplified in KE-3 p-p38 δ MAPK transfected cells (Figure 4.7A and B) in agreement with our ELISA results (Figure 4.6). These results confirm phosphorylation of p38 δ MAPK only in our studies. We also observed MKK6 phosphorylation in KE-3 p-p38 δ MAPK as expected (Figure 4.7A and B). A previous report outlined p38 δ MAPK induced inactivation of ERK1/2 [26] however, we did not find any change in ERK1/2 or indeed JNK1/2/3 (Figure 4.7A and B).

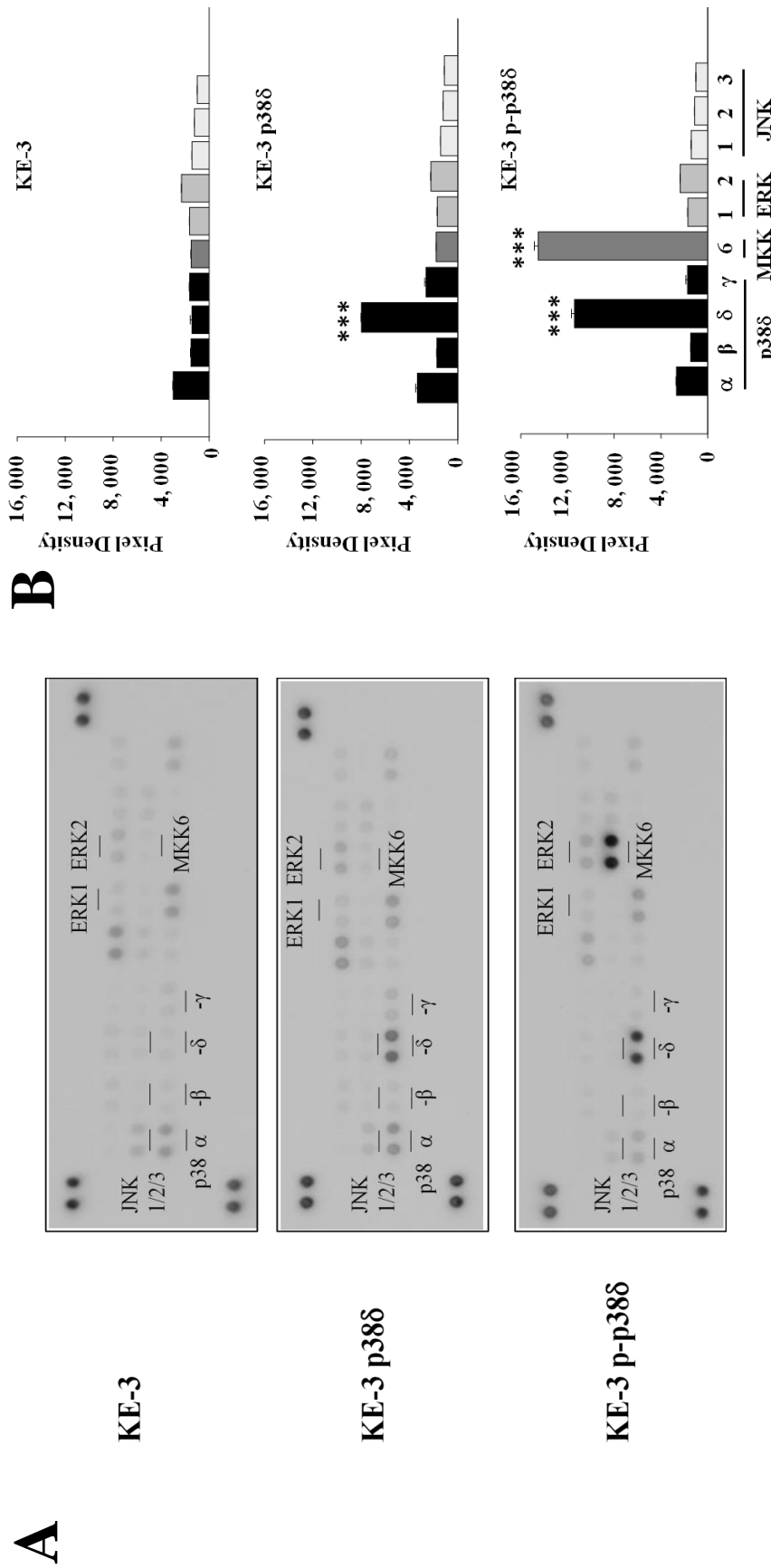


Figure 4.7 Effect of p-p38 δ MAPK expression on other MAPKs. (A) The human phospho-MAPK array shows the effects of stably transfecting KE-3 cells with p38 δ and p-p38 δ MAPK. Arrays were incubated with 200 μ g of cell lysate. (B) Corresponding pixel density for p38 α , - β , - δ and - γ MAPK, MKK-6, ERK1/2 and JNK1/2/3 phosphorylation in non-transfected and transfected KE-3 cells. Significant (***) changes from control non-transfected KE-3 cells were determined by application of Student's t-test.

Finally, the physical location of a protein either in the nucleus or the cytoplasm directly influences its biological function. Members of the p38 MAPK family do not contain either a nuclear localisation signal or a nuclear export signal but their subcellular localisation can be regulated in part by their interacting proteins [27]. We compared the subcellular localization of p38 δ and p-p38 MAPK in KE-3 transfected cells with endogenous p38 δ MAPK expression in KE-6 cells. As expected p38 δ and p-p38 MAPK were absent from both compartments in non-transfected KE-3 cells (Figure 4.8A). p38 δ and p-p38 MAPK were detected in both the cytoplasm and the nucleus of KE-3 stably transfected cells (Figure 4.8A). This pattern of expression correlated with the subcellular localization of p38 δ and p-p38 MAPK in KE-6 cells in the presence and absence of anisomycin (30 μ M). To confirm our immunohistochemical findings cytosolic and nuclear extracts were prepared from transfected and non-transfected KE-3 and KE-6 cells and examined by Western blot analysis. The use of poly ADP ribose polymerase (PARP) as a nuclear-restricted marker and paxillin as a cytosolic marker ensured that there was no cross contamination between the subcellular fractions [16]. Similar results were observed demonstrating the presence of p38 δ and p-p38 MAPK in both the cytoplasm and nucleus of KE-3 and -6 cells (Figure 4.8B).

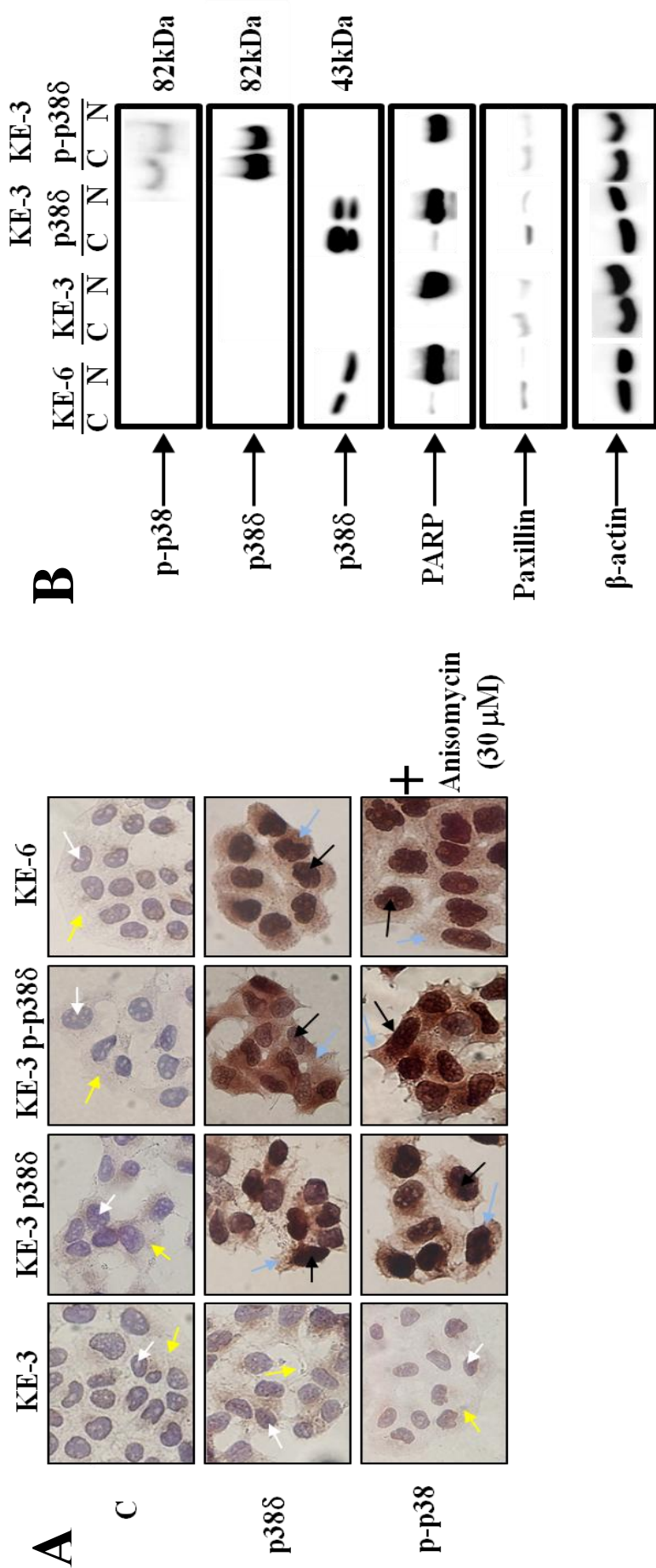


Figure 4.8 Subcellular localization of transfected and endogenous p38δ MAPK. (A) Immunohistochemical subcellular localization of p38δ and p-p38 MAPK in KE-3 non-transfected cells and cells transfected with p38δ and p-p38δ MAPK. KE-6 cells were or were not treated with anisomycin (30 μM). Blue arrow indicates cytoplasmic staining; black arrow indicates nuclear staining; white arrow indicates blue unstained nuclei and yellow arrow indicates blue unstained cytoplasm. (B) Nuclear and cytoplasmic localization of p38δ and p-p38 MAPK in KE-3 and KE-6 cells. The results shown are representative of four independent experiments (A and B).

4.5.4 KE-3 cells transfected with p38 δ and p-p38 δ MAPK show reduced proliferation

Uncontrolled cellular proliferation is a hallmark of cancer. To investigate if loss of p38 δ MAPK expression specifically drives the higher growth kinetics observed in Figure 4.4 we compared the growth rates of KE-3 non-transfected and transfected cells. We observed a significant ($p < 0.001$) time dependent decrease in the proliferation rate of KE-3 cells when transfected with wild type p38 δ MAPK compared with non-transfected cells and cells transfected with empty pcDNA3 vector (Figure 4.9). This anti-proliferative effect was amplified further in KE-3 cells transfected with active p-p38 δ MAPK (Figure 4.9). KE-3 cells transfected with p-p38 δ_{DN} MAPK demonstrated the same proliferation rate as non-transfected cells or cells transfected with pcDNA3 only (Figure 4.5A).

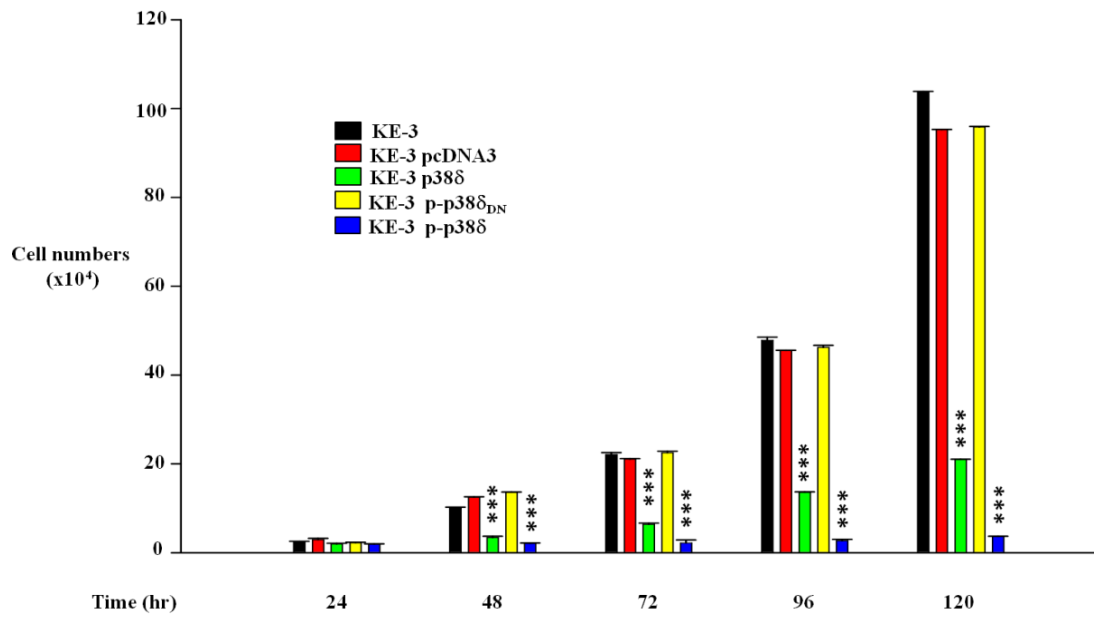


Figure 4.9 Effect of p38 δ and p-p38 δ MAPK expression on cell proliferation. KE-3, KE-3 pcDNA3, KE-3 p38 δ , KE-3 p-p38 δ and KE-3 p-p38 δ _{DN} cells were seeded (3×10^4) and counted for 24-120 hr. The results shown are mean \pm S.E. of three independent experiments. Significant (***, $p < 0.001$) changes from control non-transfected KE-3 cells were determined by application of Student's t-test.

To further examine the hypothesis that p38 δ MAPK is anti-proliferative in OESCC we employed a siRNA approach using the KE-6 cell line which expresses endogenous p38 δ MAPK (Figures. 4.2, 4.8A and B). KE-6 cells were transiently transfected with p38 δ MAPK siRNA or control siRNA as previously described [17]. We observed a 51.9% \pm 6.5% reduction in KE-6 p38 δ MAPK expression at 24 hr following p38 δ MAPK siRNA transfection which increased to 72.6% \pm 2.6% by 96 hr when compared to control siRNA transfected KE-6 cells (Figure 4.10A and B). No change in p38 δ MAPK expression was observed when KE-6 cells were transfected with control siRNA for all time points studied (24-96 hr) (only 24 hr is shown in Figure 4.10A). A significant ($p < 0.001$) increase in cell proliferation was observed for KE-6 cells transfected with p38 δ MAPK siRNA compared to cells transfected with control siRNA for all time points studied (Figure 4.10C). The anti-proliferative effect was observed even in the absence of active p38 δ MAPK in KE-6 cells (Figure 4.6). This effect on proliferation may be independent of its kinase activity as has previously been reported for p38 α MAPK in regulating HeLa cell proliferation [28] and p38 γ MAPK in rat intestinal epithelial cells [29].

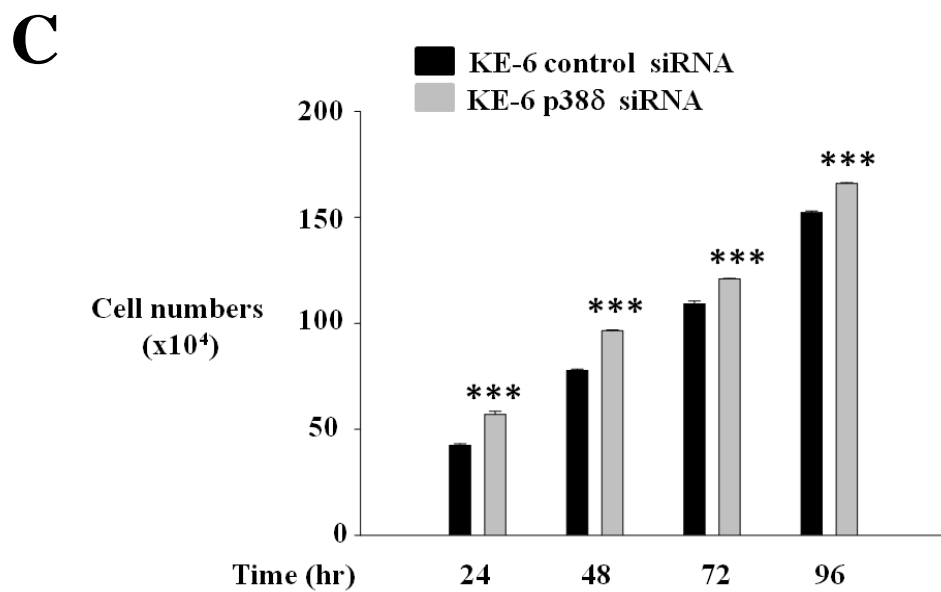
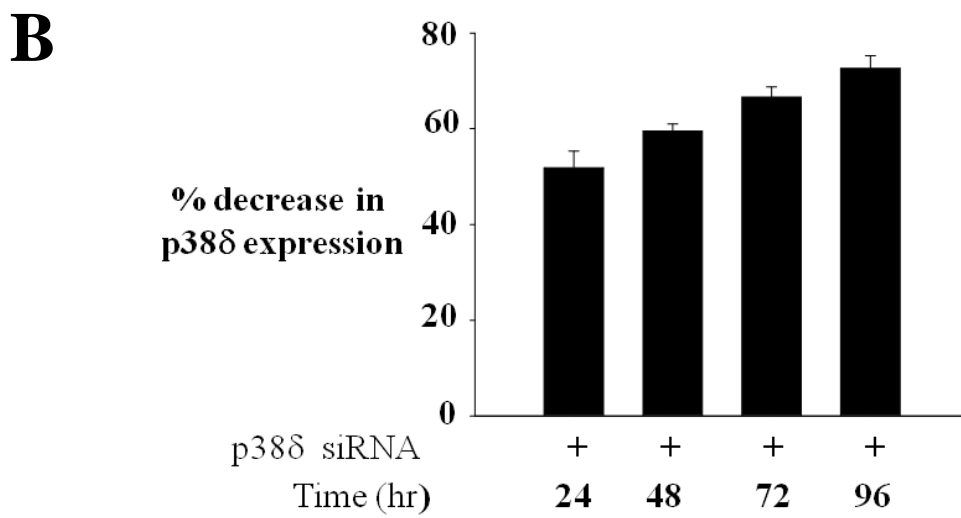
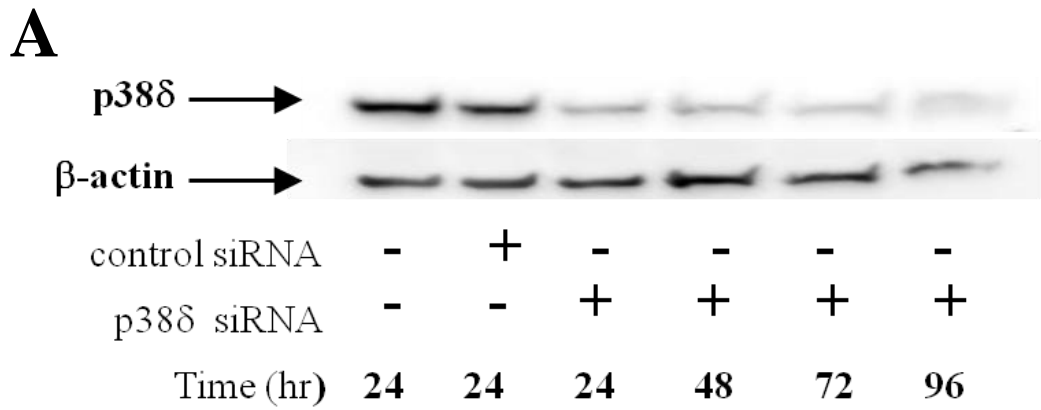


Figure 4.10 Effect of p38δ MAPK knockdown on proliferation in a cell line which expresses it endogenously (Figure legend – next page).

Figure 4.10 Effect of p38 δ MAPK knockdown on proliferation in a cell line which expresses it endogenously. (A) Western blot analysis of KE-6 cells transiently transfected or not transfected with p38 δ MAPK siRNA or control siRNA for 24-96 hr. Cells were analysed by immunoblot using a p38 δ MAPK antibody. Aliquots of 30 μ g protein lysate were loaded on a 10% SDS-PAGE gel. The results shown are representative of three independent experiments. (B) Densitometric analysis was performed to analyse % knockdown of KE-6 p38 δ MAPK protein. (C) KE-6 cells (3×10^4) transfected with p38 δ MAPK siRNA or control siRNA were seeded and counted for 24-96 hr. The results shown are mean \pm S.E. of three independent experiments each done in triplicate. Significant (***, $p < 0.001$) changes from control siRNA transfected KE-6 cells were determined by application of Student's t-test.

4.5.5 p38 δ and p-p38 δ MAPK play a role in migration and anchorage independent growth of KE-3 cells

A key characteristic of cancer cells is their ability to migrate and progress from primary tumors to metastases in distant organs. A recent report summarizes the roles of p38 MAPKs in cancer invasion and metastasis [30]. This review however, as in previous reports documents the roles of p38 MAPK family as a whole or p38 α MAPK [10, 13]. We examined the role of p38 δ MAPK in OESCC cell migration using both a Boyden chamber assay and a wound healing assay. We observed a 66% \pm 7.5% and 88.7% \pm 1.9% decrease in migration after 24 hr for KE-3 p38 δ and p-p38 δ cells respectively compared to non-transfected cells (Figure 4.11A). In addition p38 δ and p-p38 δ MAPK induced a significant decrease in KE-3 migration at 24 hr (55.65% \pm 1.5% and 75.65% \pm 0.3% ($p < 0.001$), respectively) and 48 hr (37.9% \pm 0.8%, ($p < 0.01$) and 82.7% \pm 1.4%, ($p < 0.001$) respectively) compared with non-transfected KE-3 cells using a wound healing assay (Figure 4.11B and C).

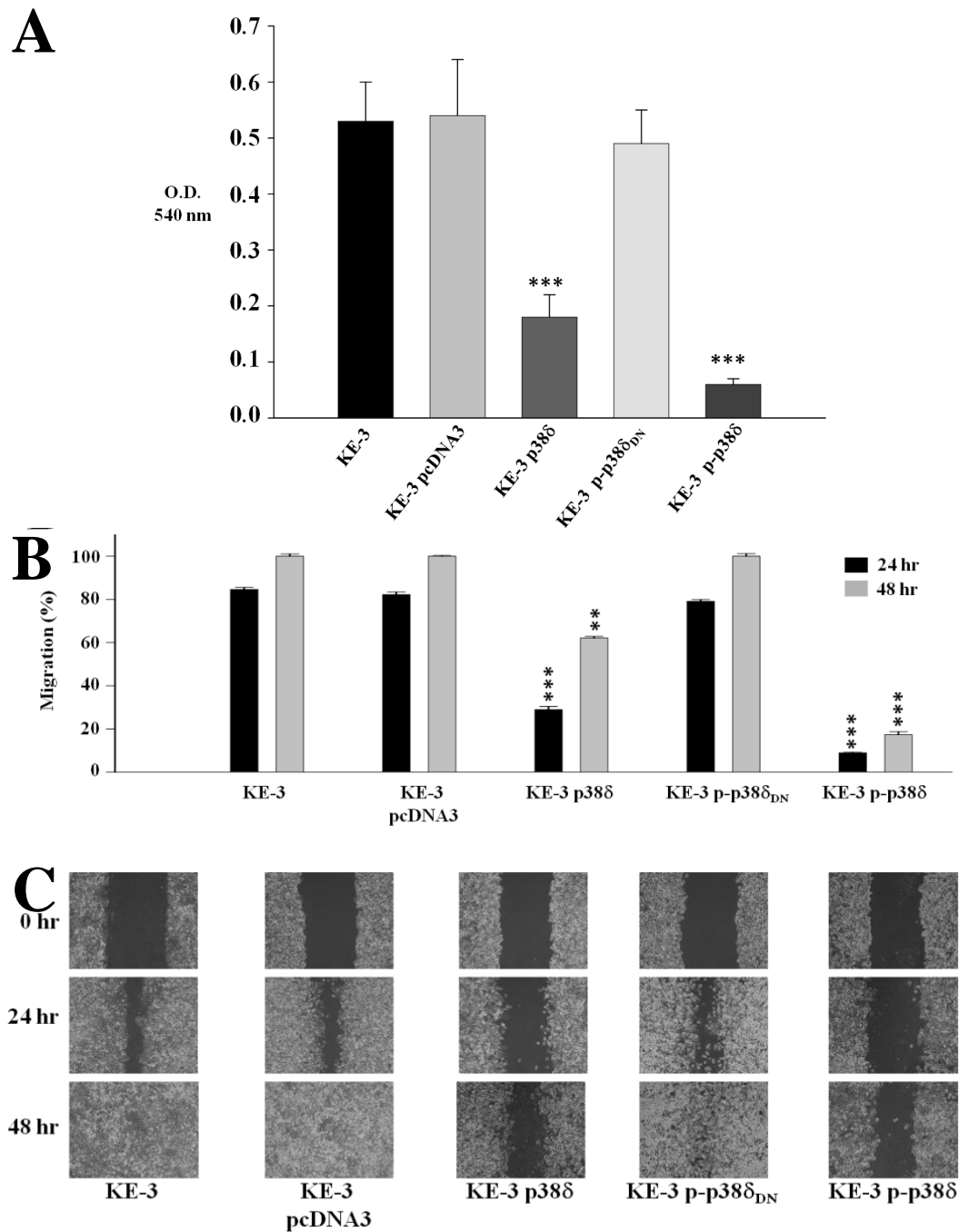


Figure 4.11 Effect of p38 δ and p-p38 δ MAPK on KE-3 cell migration. KE-3, KE-3 pcDNA3, KE-3 p38 δ , KE-3 p-p38 δ and KE-3 p-p38 δ _{DN} cells were analysed for cell migration. (A and B) p38 δ and p-p38 δ MAPK inhibit KE-3 migration at 24hr (A, Boyden Chamber) and 24 and 48 hr (B, wound healing). (C) Representative wound healing images at 0, 24, and 48 hr. Wound healing rates decrease in p38 δ and p-p38 δ MAPK transfected KE-3 cells. The results shown are representative of three independent experiments. Significant (**, $p < 0.01$; ***, $p < 0.001$) changes from control non-transfected KE-3 cells were determined by application of Student's t-test.

Finally, to further examine the influence of p38 δ and p-p38 δ MAPK on the growth characteristics of KE-3 cells, we measured their ability to grow in an anchorage-independent manner. Non-transfected KE-3 cells growing in soft agar for 21 days gave rise to 175 ± 18 colonies/plate (Figure 4.12). This was similar to the number of colonies/plate that grew for cells transfected with empty vector (160 ± 20) or p-p38 δ_{DN} (177 ± 21) (Figure 4.12). In contrast, however, p38 δ and p-p38 δ MAPK transfected cells produced a significant ($p < 0.001$) decrease in colony numbers in p38 δ transfected cells (13 ± 3) with no colonies observable for p-p38 δ MAPK transfected cells (Figure 4.12).

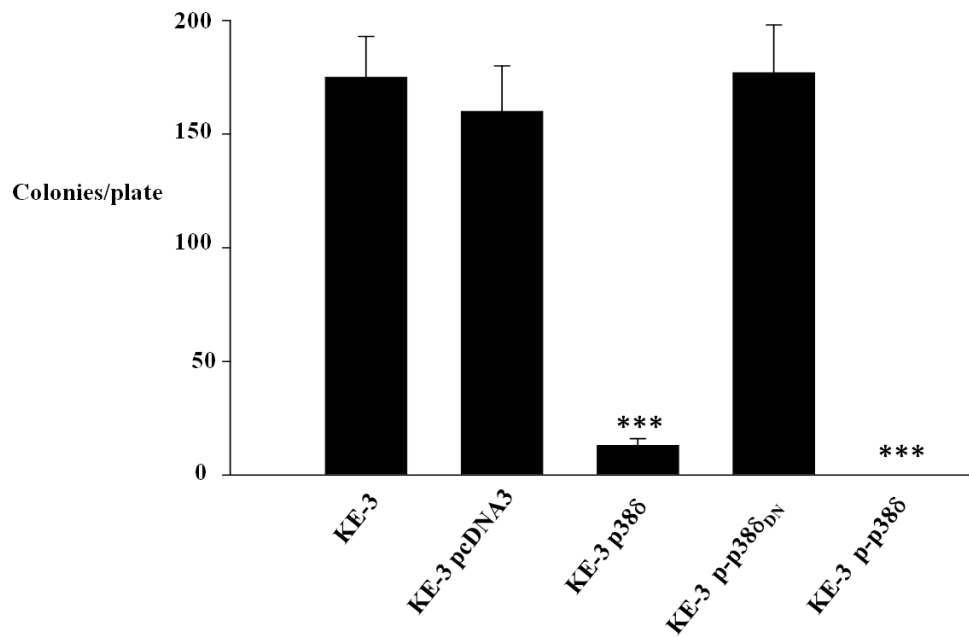


Figure 4.12 Effect of p38 δ and p-p38 δ MAPK on KE-3 anchorage independent growth. Anchorage-independent growth potential of KE-3 non-transfected and transfected cells were measured by their ability to form colonies on soft agar. Plates were stained with 3-(4, 5-dimethylthiazol-2-yl)-2, 5-diphenyl tetrazolium bromide to visualize colonies. The number of colonies per plate is shown. The results shown are mean \pm S.E. of four independent experiments. Significant (**, $p < 0.01$; ***, $p < 0.001$) changes from control non-transfected KE-3 cells were determined by application of Student's t-test.

4.6 Discussion

Oesophageal cancer is a highly aggressive treatment-refractory disease with a high mortality rate [2, 5, 6]. As conventional therapy is ineffective, targeting specific potential molecular tumor markers may prove to be the future of oesophageal cancer treatment. Despite current studies of molecular targets in oesophageal cancer [31], we are still somewhat hindered by limited knowledge of the genes and pathways involved in the tumourigenesis of the oesophagus when it comes to treatment.

Emerging role(s) for p38 MAPKs in different aspects of cancer has recently been outlined. To-date the best studied and reviewed isoform in cancer is p38 α MAPK. It has been characterized as both a potential tumour suppressor [19, 32-34] and tumour promoter [23, 30]. In comparison the role(s) of p38 δ MAPK in cancer is largely uncharacterised. The limited current knowledge pertaining to p38 δ MAPK, however, also alludes to disparate role(s) for this kinase in tumour development. An oncogenic role for p38 δ MAPK has been suggested in p38 δ -deficient mice that have reduced susceptibility to skin carcinogenesis [35] as well as promoting head and neck squamous carcinoma cell growth [23]. In contrast a very recent study outlined a role for p38 δ MAPK as a tumour suppressor in mouse fibroblasts [36]. In our study outlined here we show for the first time the differential expression of p38 δ MAPK in OESCC cell lines and *in vivo*. The loss of p38 δ MAPK expression provides a survival advantage for OESCC which demonstrates increased cell proliferation, migration and contact inhibition. Re-introduction of p38 δ MAPK, however, leads to reversal of these tumourigenic effects. Thus, recent evidence [36] as well as our present study suggests that targeting p38 δ MAPK may offer a powerful protection

against carcinogenesis. Targeting p38 MAPK isoforms or pathways for therapeutic purposes, however, should perhaps be strictly dependent on cell context, tumour cell type and tumour stage.

The fusion of p38 δ MAPK to its upstream kinase MKK6b or active MKK6b (MKK6b(E)) generated a constitutively active p38 δ MAPK which was used as a tool to study its specific effect(s) in OESCC. Re-introduction of p38 δ MAPK (with subsequent activation) or active p-p38 δ MAPK into KE-3 OESCC attenuated cell proliferation, migration and anchorage-independent growth. The strength and duration of p38 MAPK activation has been shown to play a crucial role in determining cell fate. Strong activation has been shown to induce apoptosis whereas lower levels results in cell survival [21, 34]. In our study we observed strong anti-proliferative, anti-migratory effects as well as effects on anchorage-independent growth upon re-introduction of p38 δ MAPK into KE-3 cells which subsequently became active. These anti-tumourigenic effects were amplified further in KE-3 cells transfected with constitutively active p-p38 δ MAPK. It is possible that owing to the localization of both p38 δ and p-p38 δ MAPK in the nucleus and the cytoplasm of OESCC that this kinase may modify its target(s) either structurally or subcellularly [18]. Furthermore p38 δ and p-p38 δ MAPK induced anti-tumourigenic effects in OESCC may arise by a combination of both phosphorylation-dependent and independent effects as previously described [28, 29].

Although the trypan blue exclusion assay is the most commonly used procedure for measurement of cell viability, we recognize that it has some limitations in the depth of information that it can provide. Alternative cell proliferation assays such as a

BrDU incorporation assay which measures the rate of DNA synthesis may provide further insight into the effect(s) of p38 δ and p-p38 δ MAPK expression on OESCC cell proliferation. Flow cytometry using propidium iodide to measure cellular DNA content and thereby discriminate between cells in G₁, S, G₂ or M phases of the cell cycle could help to delineate the stage(s) at which p38 δ MAPK exerts its effect(s).

The Boyden chamber cell migration assay was performed without consideration of the effect of cell proliferation. The time allowed for cells to migrate through the membrane (24 hr) was much shorter than the doubling time for KE-3 cells (~48 hr) therefore the impact of reduced cell proliferation on migration was deemed not to be a factor. Further reducing the assay time or introduction of mitomycin c treatment to inhibit proliferation would minimize any potential cell proliferation effects.

There are many paradigms in the literature of cross-talk between different MAPK pathways. In this instance, however, when KE-3 cells were stably transfected with p38 δ or p-p38 δ MAPK we did not observe changes in either p38 MAPK isoform (α , β and γ), ERK1/2 or JNK1/2/3 activation levels. This is in agreement with a recent bio-informatics analysis of MAPK pathways which specifically identified that persistent activation of p38 δ MAPK is resistant to interaction with other MAPKs [37]. This lack of interference from other MAPKs will permit us to specifically study the effects of p38 δ MAPK on cell cycle control, pathway components and regulatory mechanisms in OESCC (Chapter 7). In addition negative feedback mechanisms have been shown to contribute to fine-tuning p38 MAPK activity levels. One such report outlines an increase in MKK6 expression and stability in p38 $\alpha^{-/-}$ cardiomyocytes from transgenic mice [38]. We did not observe a correlation between the presence or

absence of p38 δ MAPK expression in OESCC cells and MKK expression. Of notable exception is MKK3 whose expression is absent from KE-3 and -8 cells (both negative for p38 δ MAPK) but present in KE-4, 5, -6 and -10 cells (all positive for p38 δ MAPK). However, this pattern of expression does not hold for KYSE-70 and OE-21 OESCC cell lines which express MKK3 but are also negative for p38 δ MAPK protein expression.

Reports of the involvement of p38 MAPKs in a variety of different pathological conditions is continuing to increase fuelling interest in the development of potent and specific drugs for modulating the activity of these kinases. Presently there are a number of p38 MAPK inhibitors undergoing clinical trials for the treatment of inflammatory diseases [39, 40]. Results arising from our study demonstrate that loss of p38 δ MAPK expression in OESCC provides a more sinister phenotype with increased proliferation, migration and anchorage independent growth. Thus, it is possible that isoform specific activation (rather than inhibition) of p38 δ MAPK may provide a therapeutic benefit for patients with OESCC which express this isoform. In addition how p38 δ MAPK activators may interact and enhance the effectiveness of traditional therapeutics in combination therapy warrants attention.

In summary, our results reveal previously undocumented p38 δ MAPK differential expression and function in OESCC. We identified a subset of OESCC cell lines as well as human primary and metastatic tumour samples that exhibit p38 δ MAPK protein expression downregulation. We now provide evidence that loss of expression of this particular isoform may be a mechanism by which OESCC cells promote carcinogenesis. Re-introduction of p38 δ MAPK into OESCC negative cell lines

suppressed different aspects of tumorigenesis. Our data warrant further investigation to understand the important physiological and pathophysiological effects of p38 δ MAPK in OESCC and is currently in progress. This knowledge should identify which pathways, substrates or regulators are affected specifically by p38 δ MAPK in providing an anti-tumorigenic effect in OESCC. Armed with this information uncovering novel targets and the development of new therapeutics may be possible for this common cancer that continues to demonstrate a generally poor clinical outcome.

4.7 References

1. Kayani, B., et al., *Lymph node metastases and prognosis in oesophageal carcinoma--a systematic review*. Eur J Surg Oncol, 2011. **37**(9): p. 747-53.
2. Enzinger, P.C. and R.J. Mayer, *Esophageal cancer*. N Engl J Med, 2003. **349**(23): p. 2241-52.
3. Almhanna, K. and J.R. Strosberg, *Multimodality approach for locally advanced esophageal cancer*. World J Gastroenterol, 2012. **18**(40): p. 5679-87.
4. Thallinger, C.M., et al., *Pre- and postoperative treatment modalities for esophageal squamous cell carcinoma*. Anticancer Res, 2012. **32**(11): p. 4609-27.
5. Klein, C.A. and N.H. Stoecklein, *Lessons from an aggressive cancer: evolutionary dynamics in esophageal carcinoma*. Cancer Res, 2009. **69**(13): p. 5285-8.
6. Bird-Lieberman, E.L. and R.C. Fitzgerald, *Early diagnosis of oesophageal cancer*. Br J Cancer, 2009. **101**(1): p. 1-6.
7. Sanz, V., I. Arozarena, and P. Crespo, *Distinct carboxy-termini confer divergent characteristics to the mitogen-activated protein kinase p38alpha and its splice isoform Mxi2*. FEBS Lett, 2000. **474**(2-3): p. 169-74.
8. Raman, M., W. Chen, and M.H. Cobb, *Differential regulation and properties of MAPKs*. Oncogene, 2007. **26**(22): p. 3100-12.
9. Hui, L., et al., *p38alpha suppresses normal and cancer cell proliferation by antagonizing the JNK-c-Jun pathway*. Nat Genet, 2007. **39**(6): p. 741-9.
10. Ono, K. and J. Han, *The p38 signal transduction pathway: activation and function*. Cell Signal, 2000. **12**(1): p. 1-13.
11. Zarubin, T. and J. Han, *Activation and signaling of the p38 MAP kinase pathway*. Cell Res, 2005. **15**(1): p. 11-8.
12. Kyriakis, J.M. and J. Avruch, *Mammalian MAPK signal transduction pathways activated by stress and inflammation: a 10-year update*. Physiol Rev, 2012. **92**(2): p. 689-737.
13. Cuenda, A. and S. Rousseau, *p38 MAP-Kinases pathway regulation, function and role in human diseases*. Biochimica et Biophysica Acta (BBA) - Molecular Cell Research, 2007. **1773**(8): p. 1358-1375.
14. Evers, P.A., et al., *Conversion of SB 203580-insensitive MAP kinase family members to drug-sensitive forms by a single amino-acid substitution*. Chem Biol, 1998. **5**(6): p. 321-8.
15. Barry, O.P., et al., *Constitutive ERK1/2 activation in esophagogastric rib bone marrow micrometastatic cells is MEK-independent*. J Biol Chem, 2001. **276**(18): p. 15537-46.
16. O'Sullivan, G.C., et al., *Modulation of p21-activated kinase 1 alters the behavior of renal cell carcinoma*. Int J Cancer, 2007. **121**(9): p. 1930-40.

17. Adhikary, G., et al., *PKC-delta and -eta, MEKK-1, MEK-6, MEK-3, and p38-delta are essential mediators of the response of normal human epidermal keratinocytes to differentiating agents*. *J Invest Dermatol*, 2010. **130**(8): p. 2017-30.
18. Cargnello, M. and P.P. Roux, *Activation and function of the MAPKs and their substrates, the MAPK-activated protein kinases*. *Microbiol Mol Biol Rev*, 2011. **75**(1): p. 50-83.
19. Wagner, E.F. and A.R. Nebreda, *Signal integration by JNK and p38 MAPK pathways in cancer development*. *Nat Rev Cancer*, 2009. **9**(8): p. 537-49.
20. Ambrose, M., et al., *Induction of apoptosis in renal cell carcinoma by reactive oxygen species: involvement of extracellular signal-regulated kinase 1/2, p38delta/gamma, cyclooxygenase-2 down-regulation, and translocation of apoptosis-inducing factor*. *Mol Pharmacol*, 2006. **69**(6): p. 1879-90.
21. Remy, G., et al., *Differential activation of p38MAPK isoforms by MKK6 and MKK3*. *Cell Signal*, 2010. **22**(4): p. 660-7.
22. Reid, T.D., et al., *Relative prognostic value of TNM7 vs TNM6 in staging oesophageal cancer*. *Br J Cancer*, 2011. **105**(6): p. 842-6.
23. Junttila, M.R., et al., *p38alpha and p38delta mitogen-activated protein kinase isoforms regulate invasion and growth of head and neck squamous carcinoma cells*. *Oncogene*, 2007. **26**(36): p. 5267-79.
24. Efimova, T., A.M. Broome, and R.L. Eckert, *Protein kinase Cdelta regulates keratinocyte death and survival by regulating activity and subcellular localization of a p38delta-extracellular signal-regulated kinase 1/2 complex*. *Mol Cell Biol*, 2004. **24**(18): p. 8167-83.
25. Jiang, Y., et al., *Characterization of the structure and function of the fourth member of p38 group mitogen-activated protein kinases, p38delta*. *J Biol Chem*, 1997. **272**(48): p. 30122-8.
26. Efimova, T., A.M. Broome, and R.L. Eckert, *A regulatory role for p38 delta MAPK in keratinocyte differentiation. Evidence for p38 delta-ERK1/2 complex formation*. *J Biol Chem*, 2003. **278**(36): p. 34277-85.
27. Li, Q., et al., *Determinants that control the distinct subcellular localization of p38alpha-PRAK and p38beta-PRAK complexes*. *J Biol Chem*, 2008. **283**(16): p. 11014-23.
28. Fan, L., et al., *A novel role of p38 alpha MAPK in mitotic progression independent of its kinase activity*. *Cell Cycle*, 2005. **4**(11): p. 1616-24.
29. Tang, J., et al., *Essential role of p38gamma in K-Ras transformation independent of phosphorylation*. *J Biol Chem*, 2005. **280**(25): p. 23910-7.
30. del Barco Barrantes, I. and A.R. Nebreda, *Roles of p38 MAPKs in invasion and metastasis*. *Biochem Soc Trans*, 2012. **40**(1): p. 79-84.
31. Izzo, J.G., et al., *Emerging molecular targets in esophageal cancers*. *Gastrointest Cancer Res*, 2007. **1**(4 Suppl 2): p. S3-6.
32. Bulavin, D.V. and A.J. Fornace, Jr., *p38 MAP kinase's emerging role as a tumor suppressor*. *Adv Cancer Res*, 2004. **92**: p. 95-118.

33. Hui, L., et al., *p38alpha: a suppressor of cell proliferation and tumorigenesis*. Cell Cycle, 2007. **6**(20): p. 2429-33.
34. Ventura, J.J., et al., *p38alpha MAP kinase is essential in lung stem and progenitor cell proliferation and differentiation*. Nat Genet, 2007. **39**(6): p. 750-8.
35. Schindler, E.M., et al., *p38delta Mitogen-activated protein kinase is essential for skin tumor development in mice*. Cancer Res, 2009. **69**(11): p. 4648-55.
36. Cerezo-Guisado, M.I., et al., *Evidence of p38 γ and p38 δ involvement in cell transformation processes*. Carcinogenesis, 2011. **32**(7): p. 1093-1099.
37. Sundaramurthy, P., S. Gakkhar, and R. Sowdhamini, *Analysis of the impact of ERK5, JNK, and P38 kinase cascades on each other: a systems approach*. Bioinformatics, 2009. **3**(6): p. 244-9.
38. Ambrosino, C., et al., *Negative feedback regulation of MKK6 mRNA stability by p38alpha mitogen-activated protein kinase*. Mol Cell Biol, 2003. **23**(1): p. 370-81.
39. Coulthard, L.R., et al., *p38(MAPK): stress responses from molecular mechanisms to therapeutics*. Trends Mol Med, 2009. **15**(8): p. 369-79.
40. Gaestel, M. and M. Kracht, *Peptides as signaling inhibitors for mammalian MAP kinase cascades*. Curr Pharm Des, 2009. **15**(21): p. 2471-80.

Chapter 5

p38 δ MAPK phenotype: an indicator of chemotherapeutic response in oesophageal squamous cell carcinoma

O'Callaghan, C., Fanning, L.J., Barry, O.P.

p38 δ MAPK phenotype: an indicator of chemotherapeutic response in oesophageal
squamous cell carcinoma

Anti Cancer Drugs 2015; 26(1):4655.

(Appendix II)

5.1 Abstract

The previous chapter documented p38 δ MAPK differential expression and function in OESCC. This study expands upon these findings and investigates whether p38 δ MAPK status in OESCC can influence response(s) to cytotoxic drugs. The antiproliferative effect of conventional cisplatin and 5-fluorouracil (CF) treatment was compared with the recently reviewed triple regime of cisplatin, 5-fluorouracil and doxorubicin (ACF). p38 δ MAPK positive and p38 δ MAPK negative cell lines were employed using cell-growth and clonogenic assays. Key regulators of intrinsic and extrinsic apoptotic pathways were measured. Wound-healing assays and a Boyden chamber were used to investigate the effect of drug treatments on cell migration. Functional networks were analysed in terms of changes in MAPK expression. p38 δ MAPK negative OESCC is less sensitive to standard CF chemotherapy compared with p38 δ MAPK positive cells. However, following ACF treatment p38 δ MAPK negative cells showed markedly decreased proliferation and cell migration, and increased apoptosis. ACF induced apoptosis through the extrinsic pathway involving Fas activation, caspase-8 and caspase-3 cleavage and degradation of PARP. Loss of mitochondrial membrane potential ($\Delta\Psi_m$) was observed but downregulation of multidomain proapoptotic proteins, as well as BH3-only proteins, suggests involvement of pathways other than the mitochondrial pathway. Interestingly, induction of p38 MAPK and ERK1/2, but not JNK1/2, was observed following ACF treatment. p38 δ MAPK negative OESCC is more resistant to traditional CF treatment compared with p38 δ MAPK positive OESCC. In light of these results, p38 δ MAPK phenotyping of tumour tissue may be of considerable

value in deciding on an optimal therapeutic strategy for patients with p38 δ MAPK negative OESCC.

5.2 Hypothesis and aims

The hypothesis for this chapter is that p38 δ MAPK status influences OESCC response to chemotherapeutic drugs.

To examine this hypothesis the aims for this chapter are as follows:

- To compare the sensitivity of p38 δ MAPK positive and p38 δ MAPK negative OESCC cell lines to common chemotherapeutic drug combinations.
- To compare the effect(s) of different chemotherapeutic drug combinations on OESCC migration, invasion and recovery.
- To examine the apoptotic cell death and MAPK pathways activated in p38 δ MAPK negative OESCC by chemotherapeutic drugs.

5.3 Introduction

Oesophageal cancer is a highly aggressive and fatal malignancy and is the seventh most common cancer worldwide [1]. Oesophageal squamous cell carcinoma (OESCC) is an exceptionally drug-resistant tumour. Although surgery is the best modality in terms of local control [2], outcomes following resection for OESCC remain unsatisfactory because of locoregional and distant failure [3]. Preoperative chemotherapy or chemoradiotherapy with a fluoropyrimidine/platinum combination – that is, a cisplatin and 5-fluorouracil (CF) regimen – has been the standard treatment for locally advanced disease since the 1980s. At present, multimodal therapy is being investigated for different stages of OESCC, even if the tumour is operable [4]. Preoperative chemotherapy with docetaxel plus CF (DCF) has recently been investigated (with or without radiotherapy) with good local control and pathological remission rate being recorded [4, 5]. More recently doxorubicin, cisplatin and 5-fluorouracil (ACF) have undergone a revival, demonstrating higher response rates than CF treatment, a good safety profile and promising long-term outcomes for patients with highly advanced oesophageal carcinoma [6-8].

The involvement of p38 MAPKs in a variety of pathological conditions is continuing to fuel interest in this particular family of kinases. The expression of p38 MAPKs as a family has previously been outlined in oesophageal cancer, as well as in other cancer types [9-12]. We have previously outlined for the first time the differential expression of individual p38 MAPK isoforms in cancer and in particular OESCC [13, 14]. We now know that loss of p38 δ MAPK expression in OESCC affords a more sinister phenotype, with increased proliferation, migration and anchorage-

independent growth, thus identifying p38 δ MAPK as a possible molecular target in OESCC [14].

Advancing these studies a step further, this chapter evaluates whether p38 δ MAPK status could influence cytotoxic responses to drug treatments in OESCC. Both negative and positive p38 δ MAPK cell lines were used, isolated from patients with OESCC with no prior treatment, as outlined in Chapter 4. Cell viability, wound healing, migration and apoptosis were evaluated following standard CF treatment and ACF treatment. To carry out functional networks expression analysis, we also analysed changes in ERK1/2, JNK1/2 and p38 MAPK expression. In conclusion, this study indicates that p38 δ MAPK status may be a predictor of response to chemotherapy in OESCC patients.

5.4 Materials and methods

5.4.1 Cell culture

The KE oesophageal squamous cancer cell lines were cultured as described in Chapter 2. KE cell line features are summarized in Table 2.1.

5.4.2 Drug Treatment

Chemotherapeutic drugs used were: 5-fluorouracil (Calbiochem, Merck KGaA, Darmstadt, Germany), cis-platinum (II) diammine dichloride, docetaxel, doxorubicin hydrochloride, hydroxyurea, methotrexate and paclitaxel, all from Sigma Aldrich. MAPK inhibitors were BIRB 796 (Doramapimod) (Cayman Chemical, Ann Arbor, MI, USA), SB203590 and U0126, both purchased from Cell Signalling Technologies (Hertfordshire, UK). Cells were seeded at 2×10^5 cells/well of a 6-well tissue culture plate 24 hr before treatment. Immediately prior to treatment, growth media in all wells was replaced with 2 ml of fresh media. All drugs were resuspended in DMSO according to their product information data sheets and diluted to concentrations 2000-fold higher than the final concentrations indicated. 1 μ l of each concentrated drug was added to the relevant well to give the desired final concentrations. Controls included untreated cells and cells treated with equivalent amounts of DMSO. Cells were incubated with chemotherapeutic drugs for 24 or 48 hr.

5.4.3 Cell viability

Cell viability was assessed using the MTT assay, which depends on the ability of viable cells to reduce MTT to a coloured formazan product, as described in Chapter 2.

5.4.4 Cell migration

Cell migration was assessed using Boyden chamber and in-vitro wound-healing assays as described in Chapter 2.

5.4.5 Mitochondrial membrane potential ($\Delta\Psi_m$) assay

The decline of mitochondrial membrane potential ($\Delta\Psi_m$) was assessed using a mitochondrial voltage-sensitive dye, 5,5',6,6'-tetrachloro-1,1',3,3'-tetraethylbenzimidazole carbocyanide iodide (JC-1), according to the manufacturer's instructions [15]. The dye underwent a reversible change in fluorescence emission from red (i.e. aggregate forms of JC-1) to green (i.e. monomer forms of JC-1) as the mitochondrial membrane potential decreased. KE cells were or were not treated with drugs for 24 hr. Cells were then washed twice with PBS and loaded with JC-1 for 30 min at 37°C. Images were obtained using an inverted fluorescence microscope (Olympus, Essex, UK). The ratio of red to green fluorescence intensity, which was indicative of a change in $\Delta\Psi_m$, was calculated using the ImageJ software. To measure fluorescence intensities using Image J a region was drawn around each cell to be measured. The same size region was drawn in an area without fluorescent objects to be used for background subtraction. For accuracy three selections were

used from around the cell. These steps were repeated for the other cells in the field of view that were to be measured. The data in the results window of Image J were copied and pasted into an excel worksheet. To calculate the corrected total cell fluorescence (CTCF) the following calculation was performed – Integrated Density – (Area of selected cell x Mean fluorescence of background readings).

5.4.6 Immunoblot analysis

Supernatants used for immunoblotting with specific antibodies, PARP, caspases-3, -6, -7, -8 and 9, Puma, Bak, Bik, Bim, Bid, Bax, p38 MAPK, phospho-p38 MAPK, JNK1/2, phospho-JNK1/2, ERK1/2, phospho-ERK1/2, Fas and FasL were prepared as described in Chapter 2 and as previously described by us [13, 14].

5.4.7 Clonogenic assay

A clonogenic assay determines whether cells can recover from treatment. Following treatment, 1000 viable cells were reseeded in fresh media (without drug) in a six-well plate (in triplicate) and allowed to grow for 14 days. Colonies were stained with MTT and subsequently counted using ImageJ software.

5.5 Results

5.5.1 p38 δ MAPK negative OESCC shows decreased sensitivity to chemotherapeutic drugs

Monotherapy is not beneficial in the treatment of patients with oesophageal cancer [16]. Thus, we evaluated the cell viability of KE p38 δ MAPK positive and p38 δ MAPK negative OESCC cell lines (outlined in Chapter 4 [14]) following double versus triple drug treatments using a range of concentrations of cytotoxic drugs. Interestingly, KE-3 and KE-8 (p38 δ MAPK negative cell lines) are significantly less sensitive to CF treatment compared with KE-4, KE-5, KE-6 and KE-10 (p38 δ MAPK positive cell lines; Fig. 1A–C). As docetaxel has recently been added to the CF regime [4, 5], we investigated the effect of DCF on cell viability. There was a further decrease in KE-3 and KE-8 cell viability (Figure 5.1A and B). However, no further reduction in cell viability was observed in the KE p38 δ MAPK positive cell lines upon DCF treatment using physiologically relevant drug concentrations (30 μ M; Figure 5.1C) [17-19]. As doxorubicin (together with CF) has recently re-emerged as a promising drug treatment strategy for patients with oesophageal cancer [6-8], we also investigated its effects. Interestingly, the greatest loss in KE-3 and KE-8 cell viability was after triple CF plus doxorubicin (ACF) treatment (Figure 5.1A and B). Of note, these results are comparable with the loss in cell viability seen in the p38 δ MAPK positive cells upon CF treatment at physiological concentrations (Figure 5.1C). Taking the results obtained with physiological drug concentrations of CF (30 μ M each) a step further, we investigated the appropriate triple ACF drug treatment concentrations for KE-3 and KE-8 cell lines. Using a range of doxorubicin drug concentrations, we ascertained that the best triple ACF concentration using

physiological concentrations of all three drugs is 30 μ M each of CF and 1 μ M doxorubicin (Figure 5.1D). No significant further decrease in cell viability was observed at a higher doxorubicin drug concentration of 3 μ M (Figure 5.1D).

As other chemotherapeutic drug combinations have also been tested for their efficacy in patients with OESCC, namely CF plus methotrexate [20], CF plus paclitaxel [20, 21] and CF plus hydroxyurea [22], we also investigated these three additional drug combinations again using a range of different drug concentrations. Interestingly, KE-3 and KE-8 showed less sensitivity to all three triple-drug combinations compared with ACF treatment (Figure 5.1E and F). Thus, as the greatest loss in KE-3 and KE-8 cell viability was observed with triple ACF treatment (Figure 5.1A, B and D), all subsequent experiments compared traditional CF treatment with ACF treatment.

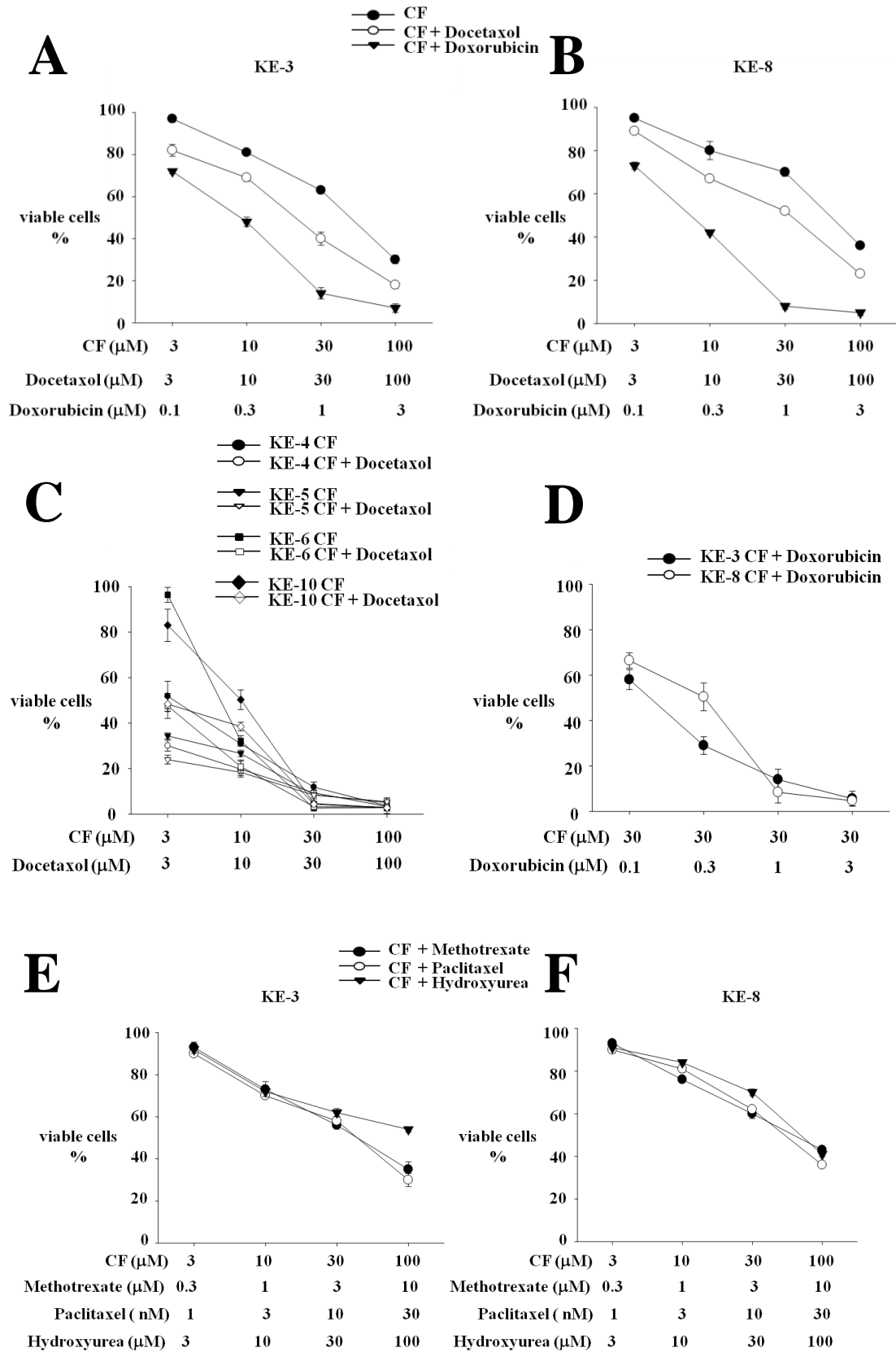


Figure 5.1 Sensitivity of OESCC to cancer chemotherapeutic drugs is correlated to the presence or absence of p38 δ MAPK. (Figure legend – next page)

Figure 5.1 Sensitivity of OESCC to cancer chemotherapeutic drugs is correlated to the presence or absence of p38 δ MAPK. (A–F) KE cell lines (KE-3 and KE-8, p38 δ -negative; KE-4, KE-5, KE-6 and KE-10, p38 δ -positive) were seeded (2×10^5) in six-well plates, and cell viability was assessed using the MTT assay at 48 hr to determine the sensitivity of each cell line to different drug combinations. (A, B) KE-3 and KE-8 cells were subjected to double treatment with cisplatin (3–100 μ M) and 5-fluorouracil (3–100 μ M; CF), or triple treatment with cisplatin (3–100 μ M), 5-fluorouracil (3–100 μ M; CF) and either docetaxel (3–100 μ M) or doxorubicin (0.1–3 μ M). (C) KE-4, KE-5, KE-6 and KE-10 cells were treated either with cisplatin (3–100 μ M) and 5-fluorouracil (3–100 μ M; CF), or with cisplatin (3–100 μ M), 5-fluorouracil (3–100 μ M; CF) and docetaxel (3–100 μ M). (D) KE-3 and KE-8 cells were subjected to triple treatment with constant drug concentrations of cisplatin (30 μ M) and 5-fluorouracil (30 μ M; CF) plus varying drug concentrations of doxorubicin (0.1–3 μ M). (E, F) KE-3 and KE-8 cells were subjected to triple treatment with cisplatin (3–100 μ M), 5-fluorouracil (3–100 μ M; CF) and either methotrexate (0.3–10 μ M), paclitaxel (1–30 nM) or hydroxyurea (3–100 μ M). Results shown in (A–F) are mean \pm SE of three independent experiments.

5.5.2 Introduction of p38 δ or p-p38 δ MAPK expression does not increase OESCC sensitivity to CF treatment

As p38 δ MAPK positive cell lines KE-4, KE-5, KE-6 and KE-10 were observed to be significantly more sensitive to CF treatment than p38 δ MAPK negative KE-3 and KE-8 cell lines (Figure 5.1 A-C), we examined the effects of stably transfected p38 δ and p-p38 δ MAPK expression on KE-3 cell sensitivity to CF treatment. We found that the stable expression of p38 δ or p-p38 δ MAPK did not increase KE-3 sensitivity to CF treatment (Figure 5.2). In fact, a statistically significant ($p < 0.01$) increase in cell viability was observed in KE-3 cells expressing p38 δ and p-p38 δ MAPK compared with non-transfected p38 δ MAPK negative cells (Figure 5.2). However, we also observed a statistically significant ($p < 0.01$) increase in cell viability in KE-3 cells transfected with an empty vector (pcDNA3) following CF treatment.

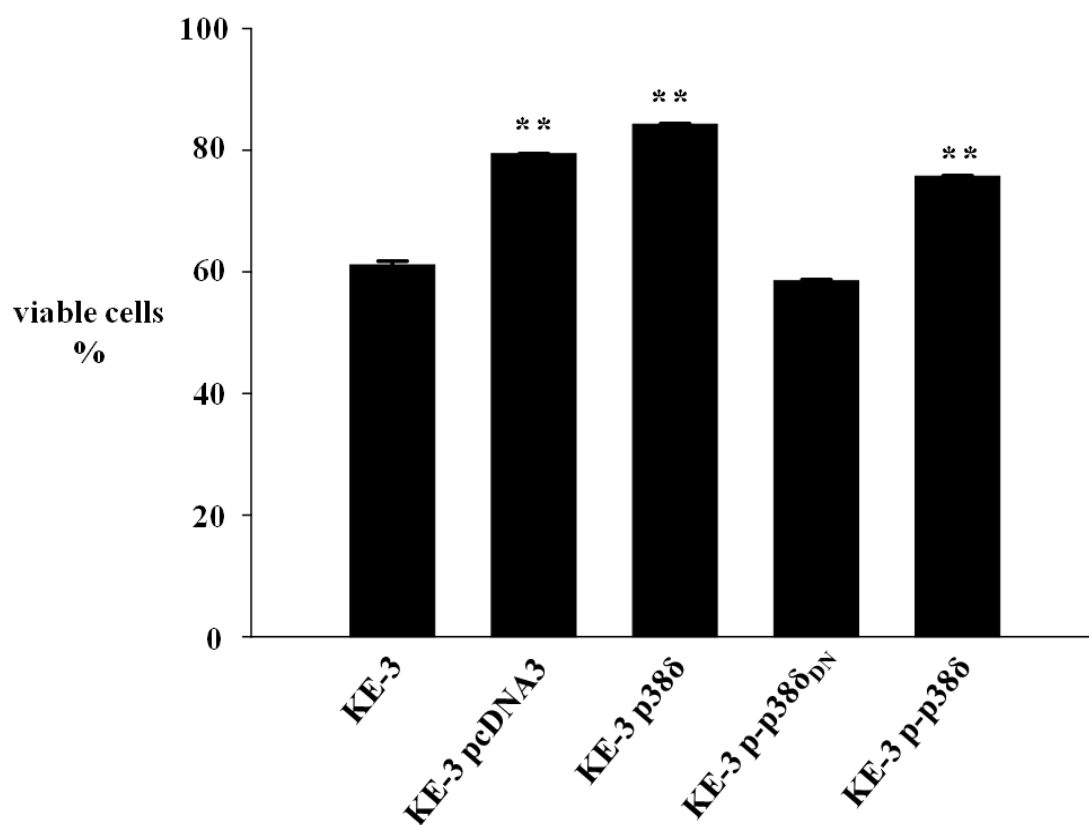


Figure 5.2 Effect of p38 δ and p-p38 δ MAPK expression on KE-3 sensitivity to CF treatment. KE-3, KE-3 pcDNA3, KE-3 p38 δ , KE-3 p-p38 δ _{DN} and KE-3 p-p38 δ cells were seeded (2×10^5) in six-well plates, and cell viability was assessed using the MTT assay at 48 hr to determine the sensitivity of each cell line to double treatment with cisplatin (30 μ M) and 5-fluoruracil (30 μ M; CF). The results shown are the mean \pm S.E. of two independent experiments. ** $p < 0.01$, significant changes from control non-transfected KE-3 cells were determined by application of Student's t-test.

5.5.3 ACF treatment significantly delays wound healing and migration compared with CF treatment

A key characteristic of cancer cells is their ability to migrate and progress from primary tumours to metastases in distant organs [14]. We examined whether the p38 δ MAPK status of OESCCs could influence their wound healing and cell migration following drug treatment. Double CF treatment of KE-6 and KE-10 (p38 δ MAPK positive cells) for 48 hr brought about a significant delay in wound healing, with a 60.0 ± 7 and $66.0 \pm 1.2\%$ loss in wound healing, respectively, compared with untreated cells (Figure 5.3A and B). In contrast, CF treatment did not impair the ability of KE-3 and KE-8 cells to migrate into the wound (Figure 5.3A and B). Triple ACF treatment, however, significantly delayed the wound-healing ability of KE-3 and KE-8 cell lines, with a 72.8 ± 2.5 and $84.0 \pm 3.9\%$ loss in wound healing at 48 hr, respectively. There was a further $15 \pm 5.8\%$ loss in wound healing upon ACF treatment, compared with CF treatment alone, of KE-6 cells but no significant change in KE-10 cells (Figure 5.3A and B). Doxorubicin (300 nM) alone did not have any significant effect on the wound-healing ability of either p38 δ MAPK positive or p38 δ MAPK negative cells (Figure 5.3A and B). Further, we compared the migration of p38 δ MAPK positive and p38 δ MAPK negative cells following CF versus ACF treatment using a Boyden chamber assay. Double CF treatment induced a significant (78.7 ± 5.2 and $78.7 \pm 7.8\%$, respectively) decrease in cell migration of KE-6 and KE-10 cells at 24 hr; however, no significant change in cell migration was observed upon CF treatment of KE-3 and KE-8 cells (Figure 5.3C). In contrast, triple ACF treatment of KE-3 and KE-8 significantly decreased their cell migration by 75.9 ± 2.4 and $81.3 \pm 6.9\%$, respectively (Figure 5.3C).

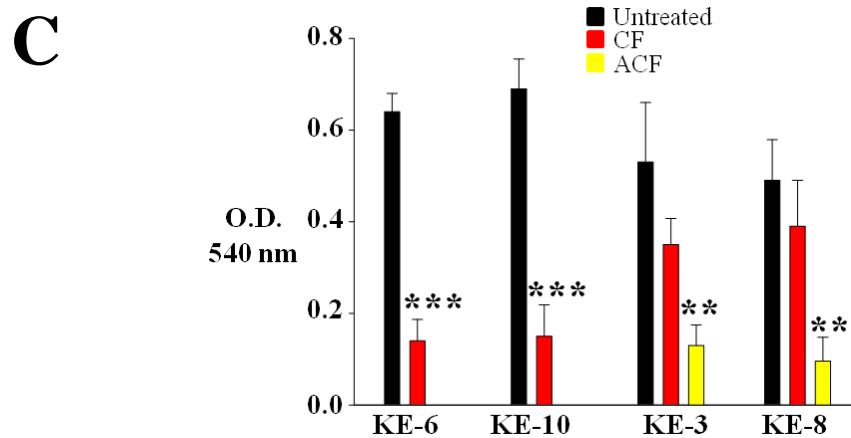
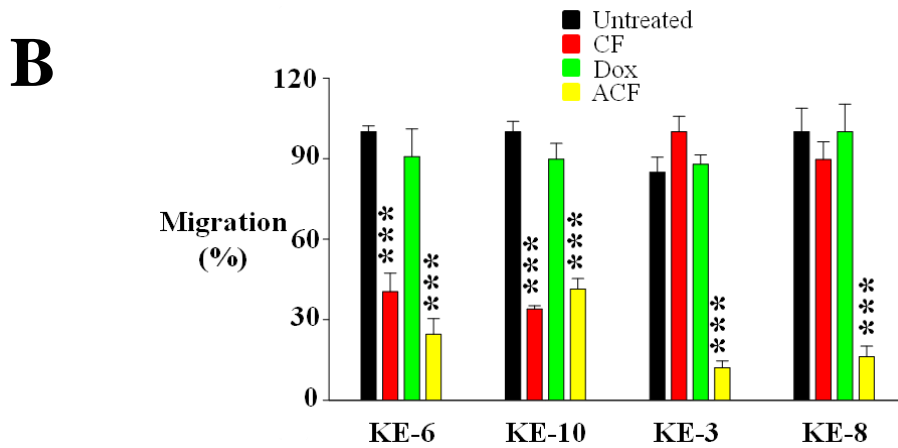
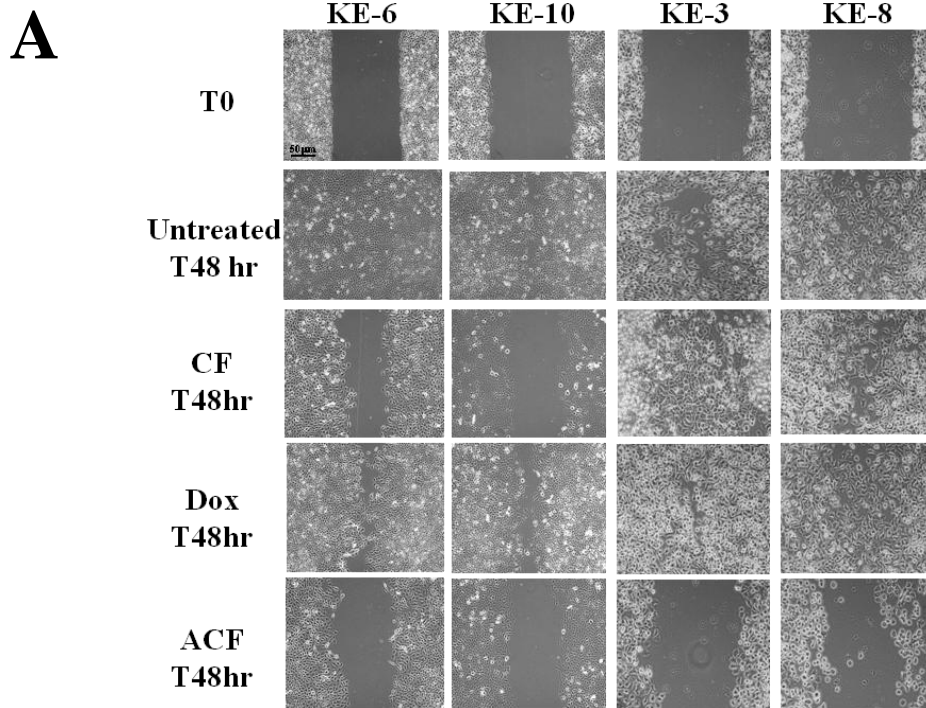


Figure 5.3 Effect of chemotherapeutic cytotoxic drugs on wound healing and migration of KE p38δ MAPK positive and negative cell lines. (Figure legend – next page)

Figure 5.3 Effect of chemotherapeutic cytotoxic drugs on wound healing and migration of KE p38 δ MAPK positive and negative cell lines. KE-6 and KE-10 cells (p38 δ MAPK positive), as well as KE-3 and KE-8 cells (p38 δ MAPK negative), were analysed for (A, B) wound healing and (C) cell migration following treatment with cisplatin (3 μ M) and 5-fluorouracil (3 μ M; CF), doxorubicin (Dox; 300 nM) alone or cisplatin (3 μ M), 5-fluorouracil (3 μ M) and doxorubicin (300 nM; triple treatment; ACF). (A) Representative wound-healing images at 0 and 48 hr with or without drug treatment. The results shown in (A) are representative of three independent experiments, whereas the results shown in (B) and (C) are the mean \pm SE of three independent experiments. *** p <0.001, ** p <0.01, significant changes from control untreated cells were determined by application of Student's t-test.

5.5.4 Triple ACF treatment decreases mitochondrial membrane potential and activates extrinsic pathways in p38 δ MAPK negative OESCCs

Initially, we investigated the involvement of the mitochondria in OESCC apoptosis using the JC-1 cationic dye. It selectively enters the mitochondria and reversibly changes in colour from red to green as the membrane potential decreases [15]. KE-6 and KE-10 cells show a marked decrease in $\Delta\Psi_m$ following CF and ACF treatment (Figure 5.4A and B). Similar losses in $\Delta\Psi_m$ in KE-3 and KE-8 cells were observed only upon ACF treatment (Figure 5.4A and B). Doxorubicin alone did not alter the $\Delta\Psi_m$ of KE-6 and KE-10 cells, but it did produce a significant ($p < 0.01$) decrease in the $\Delta\Psi_m$ of KE-3 and KE-8, comparable to CF treatment (Figure 5.4A and B).

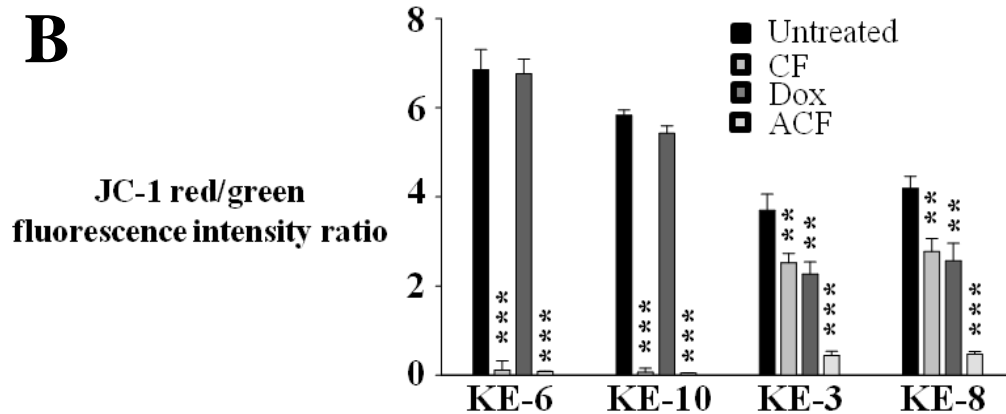
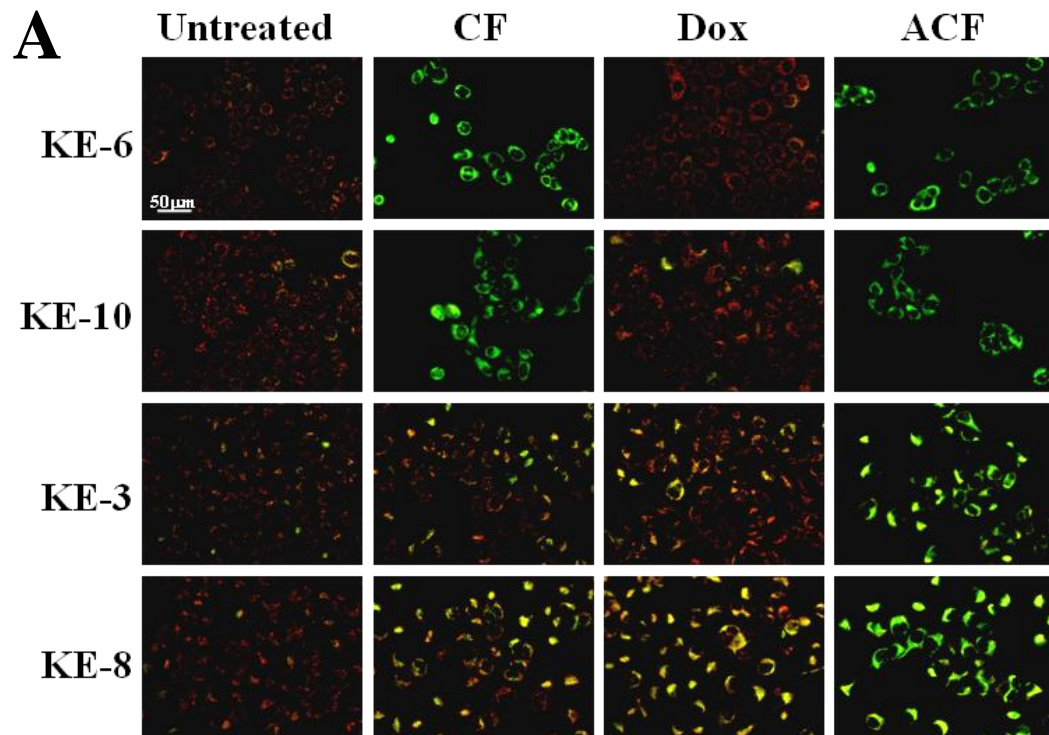


Figure 5.4 Effect of chemotherapeutic drug treatment on the mitochondrial membrane potential ($\Delta\Psi_m$) of p38 δ -negative OESCCs. (A) The mitochondrial membrane potential ($\Delta\Psi_m$) of KE cells before and after treatment with cisplatin (30 μ M) and 5-fluorouracil (30 μ M; CF) and doxorubicin (1 μ M; Dox) or cisplatin (30 μ M), 5-fluorouracil (30 μ M) and doxorubicin (1 μ M; ACF) for 24 hr. Representative images (red/green mixed channels) show the changes in mitochondrial $\Delta\Psi_m$ in KE cells, detected using JC-1 dye. Red fluorescence indicates high membrane potential and functional capacity in mitochondria, whereas green cytoplasmic fluorescence is indicative of inactive mitochondria. (B) Decreased red/green fluorescence ratio suggests a decrease in $\Delta\Psi_m$. The results shown in A are representative of four independent experiments, whereas the results shown in B are the mean \pm S.E. of four independent experiments. *** $p < 0.001$, ** $p < 0.01$, significant changes from control untreated cells were determined by application of Student's t-test.

To further investigate the effects of CF-induced versus ACF-induced apoptosis in KE p38 δ MAPK negative cells, intrinsic (mitochondrial) and extrinsic (Fas) apoptotic pathways were investigated. Expression of the relevant apoptosis-related proteins was examined by Western blot analysis. To investigate the role of the intrinsic mitochondrial pathway we examined the expression levels of Bcl-2 family members including multidomain proapoptotic proteins Bak and Bax, as well as BH3-only proapoptotic proteins Puma, Bik, Bid and Bim. Interestingly CF treatment downregulated all Bcl-2 proapoptotic members examined, with further reductions in expression being observed in the presence of ACF treatment (Figure 5.5A). The mitochondrial apoptotic pathway-related caspase-9 was not cleaved (Figure 5.5A).

To investigate whether CF and ACF activate the extrinsic apoptotic pathway, we examined the expression levels of death receptor signalling-related proteins including Fas, caspase-3 and caspase-8 and PARP. Alterations in the expression of Fas and FasL, members of the tumour necrosis family, have been reported previously in OESCC with Fas-activated apoptosis being shown to limit the growth of OESCCs [23, 24]. We observed an increase in Fas expression when both KE-3 and KE-8 cells were treated with ACF, but not on CF treatment, implicating the involvement of the extrinsic death pathway. The expression level of FasL was very low in both cell lines, and there was no appreciable change after treatment with CF or ACF (Figure 5.5B). We observed that ACF (but not CF) treatment of KE-3 and KE-8 cell lines activated (cleaved) caspase-3 and caspase-8, as well as activated (cleaved) their substrate PARP, producing the 85 kDa proteolytic fragment indicative of caspase activation and apoptosis (Figure 5.5B). The extrinsic apoptotic pathway-related caspases-6 and caspase-7 were not cleaved upon CF or ACF treatment (Figure 5.5B).

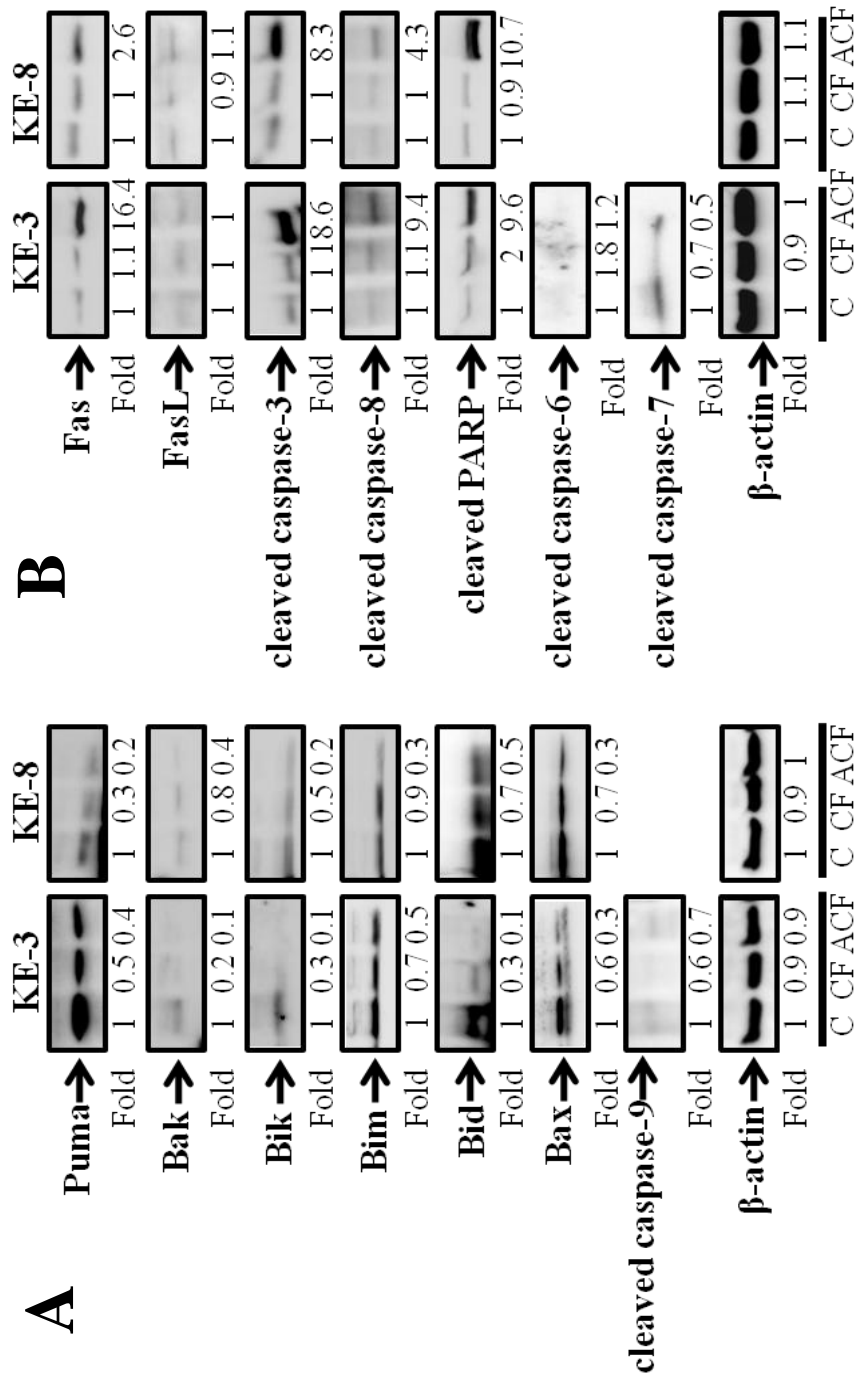


Figure 5.5 Effect of chemotherapeutic drug treatment on intrinsic and extrinsic mitochondrial pathways in KE-3 and KE-8 cells. Western blot analysis of (A) proapoptotic Puma, Bak, Bik, Bim, Bid, Bax and Bid, Fas and FasL, cleaved caspases-3, -6, -7 and -8, and PARP in KE-3 and KE-8 cells following treatment with cisplatin (30 μ M) and 5-fluorouracil (30 μ M; CF), or following triple treatment with cisplatin (30 μ M), 5-fluorouracil (30 μ M) and doxorubicin (1 μ M; ACF) for 24 hr. The results shown in are representative of four independent experiments.

5.5.5 Triple ACF treatment induces p38 and ERK1/2 but not JNK1/2 MAPK activation in p38 δ MAPK negative OESCC

To gain further insight into CF-induced versus ACF-induced cytotoxic effects, we analysed MAPK expression. We observed p38 MAPK phosphorylation upon ACF treatment but not CF treatment (Figure 5.6). CF induced ERK1/2 phosphorylation, which was further enhanced with ACF treatment (Figure 5.6). In contrast, JNK1/2 activation was not observed following either CF or ACF treatment (Figure 5.6).

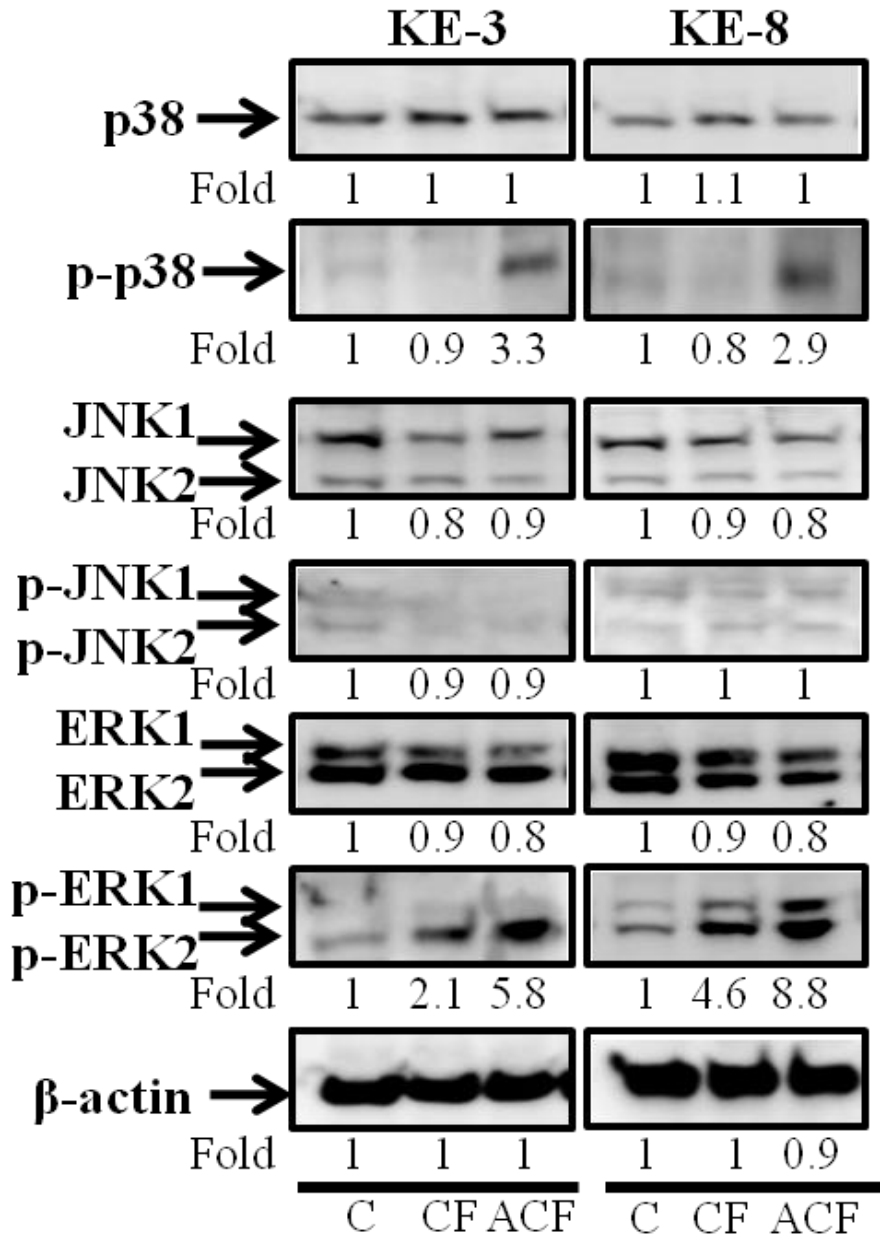


Figure 5.6 MAPK activation in KE-3 and KE-8 cells following chemotherapeutic drug treatment. Western blot analysis of the three different MAPKs (p38 MAPK, JNKs and ERKs) following treatment with cisplatin (30 μ M) and 5-fluorouracil (30 μ M; CF), or following triple treatment with cisplatin (30 μ M), 5-fluorouracil (30 μ M) and doxorubicin (1 μ M; ACF) for 24 hr. The results shown are representative of four independent experiments.

To assess whether p38 and ERK1/2 MAPK activation is causal to the actions of the chemotherapeutics we used specific pharmacological inhibitors of p38 MAPK and MEK. Interestingly, both SB203590 (20 μ M) and BIRB 796 (5 μ M), inhibitors of p38 α and p38 β MAPK (but not p38 γ and p38 δ MAPK) [18, 25] did not prevent the antiproliferative effects of either CF or ACF (Figure 5.7). In fact, in agreement with recent reports (with similar cytotoxic drug combinations), p38 MAPK blockade enhanced the cytotoxic effects of ACF treatment significantly (but not CF treatment) at 24 hr (Figure 5.7) [18, 19]. The enhanced antiproliferative effect of p38 MAPK inhibition observed at 24 hr with ACF was not obvious at 48 hr because of the high level of cell death at this time point (Figure 5.7). The specific MEK inhibitor U0126 (20 μ M) [26] brought about a significant abolition of the effects of both CF and ACF drug treatments in both cell lines, indicating that ERK1/2 may be directly involved in drug-induced cytotoxicity (Figure 5.7).

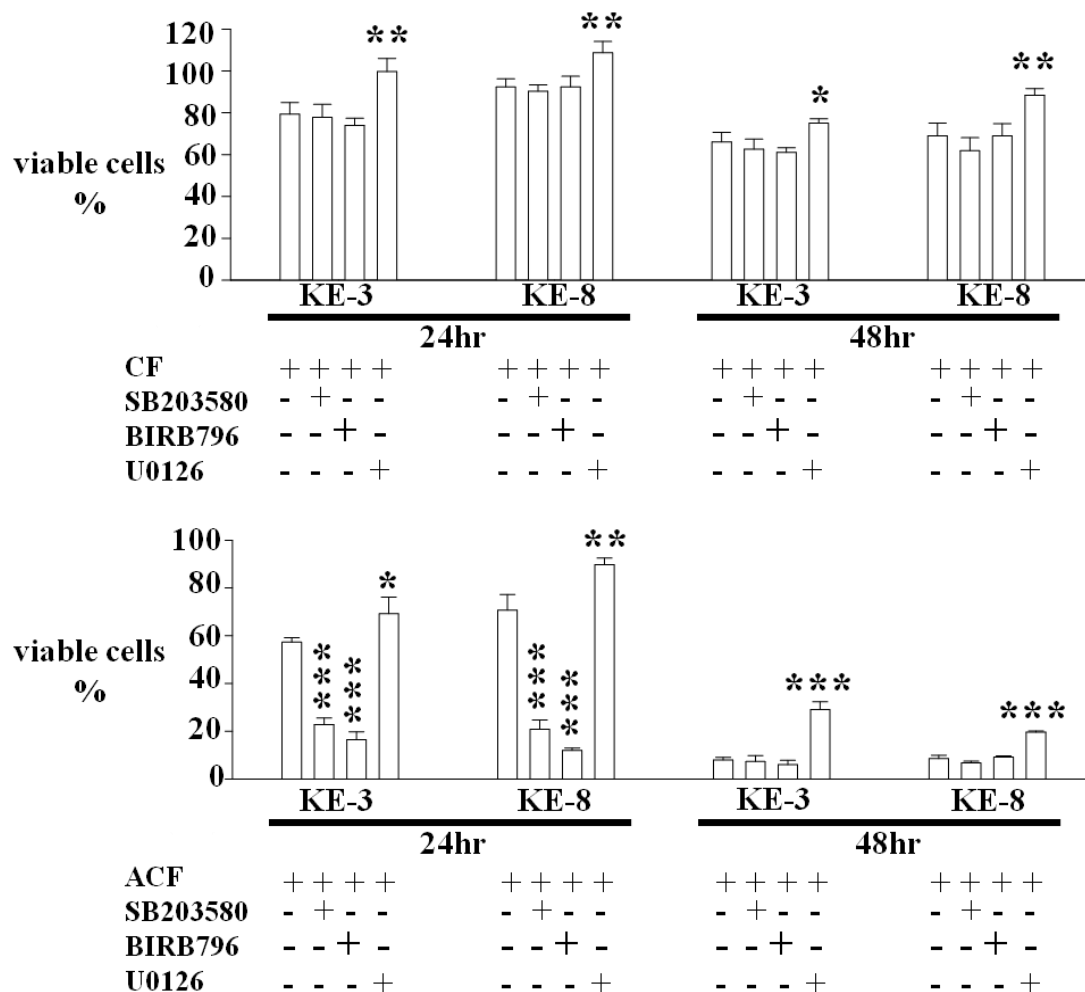


Figure 5.7 Involvement of MAPKs in CF and ACF induced cell death. KE-3 and KE-8 cells were treated with SB203580 (20 μ M), BIRB796 (5 μ M) or U0126 (20 μ M) followed by double treatment with cisplatin (30 μ M) and 5-fluorouracil (30 μ M; CF), or triple treatment with cisplatin (30 μ M), 5-fluorouracil (30 μ M; CF) and doxorubicin (1 μ M; ACF). Cell viability was assessed using the MTT assay as described in Chapter 2. Results shown are the mean \pm S.E. of four independent experiments. *** p < 0.001, ** p <0.01, * p < 0.05, significant changes from CF treated or ACF-treated cells were determined by application of Student's t-test.

5.5.6 Recovery of KE-3 and KE-8 cells following drug treatments

One of the most important parameters for the efficacy of chemotherapeutic drug treatments is the long-term effect on cell viability. Thus, we evaluated the effects of CF, doxorubicin alone and ACF treatment on the capacity of KE-3 and KE-8 cells to recover in assays of clonogenic growth. All three different drug treatments had a significant effect on the recovery of both KE-3 and KE-8 cell lines (Figure 5.8A and B). However, of note, cell recovery following ACF treatment was never observed, whereas colonies – that is, cell recovery – were observed following treatment with CF or doxorubicin alone (Figure 5.8A and B).

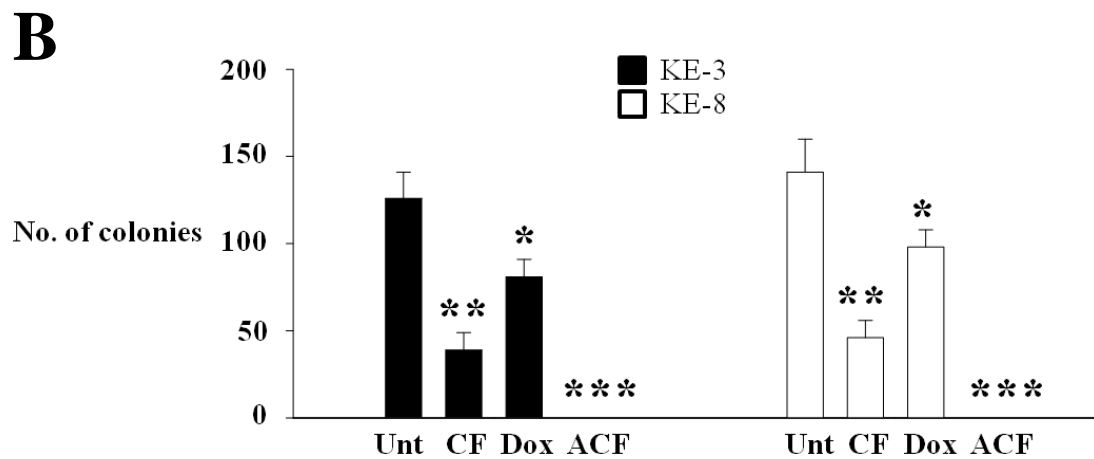
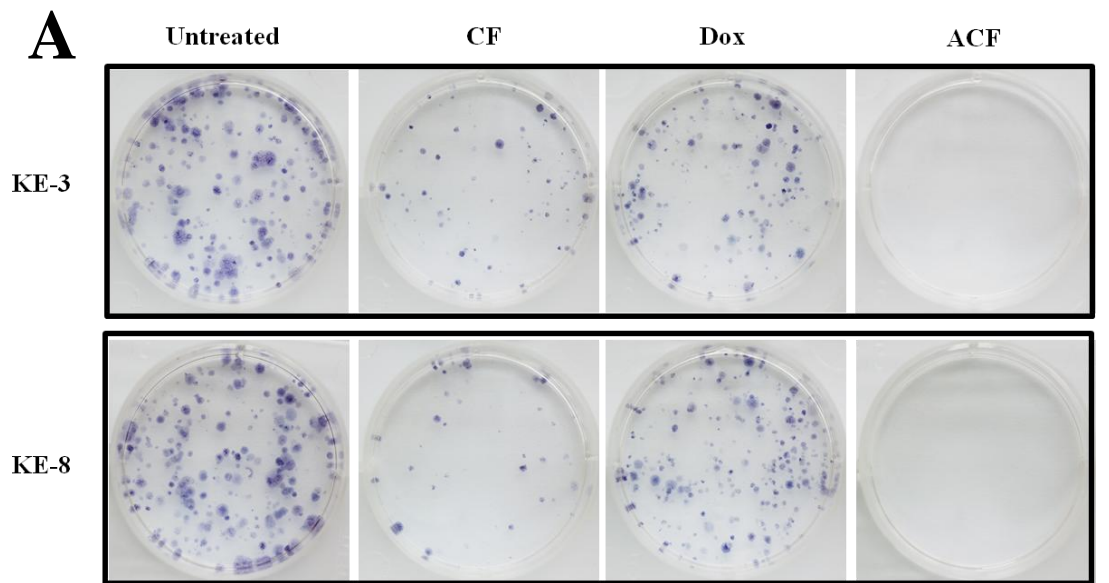


Figure 5.8 Recovery of KE-3 and KE-8 cells following chemotherapeutic drug withdrawal. The ability of p38 δ -negative OESCC cell lines KE-3 and KE-8 to recover after drug withdrawal was assessed with a colony formation assay (clonogenic assay). KE-3 and KE-8 cells were or were not treated (Unt) with cisplatin (30 μ M) and 5-fluorouracil (30 μ M; CF), doxorubicin (1 μ M; Dox) alone or the combination of all three drugs (ACF) for 48 hr. Viable, adherent cells were counted and reseeded (1000 cell/well) in a six-well plate (in triplicate) in the absence of drug. (A) Fourteen days later, colonies were stained with MTT. Each well shown is a representative image of nine similar wells (three independent experiments). (B) Colonies were counted using ImageJ software. *** $p < 0.001$, ** $p < 0.01$, * $p < 0.05$, significant changes from untreated cells were determined by application of Student's t-test.

5.6 Discussion

The purpose of this chapter was to determine whether differences in the OESCC p38 δ MAPK phenotype could influence the chemosensitivity of OESCC to conventional CF versus ACF drug combinations.

Single-agent response rates of 10–25% remain poor for oesophageal cancer [16]. Further, the use of double CF is of limited effectiveness in the treatment of patients with OESCC, with respect to improving overall survival time and patient quality of life [3, 8]. Triple ACF combination therapy was first reported as far back as 1983 [27], but of late it has sparked renewed interest [4, 8]. Doxorubicin is an effective, widely used chemotherapeutic agent in the treatment of a variety of solid tumours and malignant haematologic diseases [28]. There are now reports documenting the usefulness and, importantly, the safety of ACF therapy for the treatment of advanced oesophageal carcinoma [7, 8, 29]. Despite the absence of phase III clinical trials, ACF is currently used in the clinical setting for treatment of patients with OESCC [8].

All three drugs in this study, cisplatin, 5-fluorouracil and doxorubicin, used as monotherapy or double therapy have been reported to induce intrinsic apoptosis in oesophageal cancer [17, 30]. We examined typical markers of both intrinsic and extrinsic apoptotic cell death in p38 δ MAPK negative cell lines. Although we observed mitochondrial depolarization following ACF treatment, there was no subsequent caspase-9 activation. Interestingly, we also observed downregulation of Bcl-2 multidomain, as well as BH-3 proapoptotic proteins. However, decreased

expression of these intrinsic pathway proteins is in agreement with a recent report on oxaliplatin-induced apoptosis in squamous oesophageal cancer cell lines [31]. Potentially, the presence of Bcl-2 multidomain and BH3-only proapoptotic molecules may be an important predictor of p38 δ MAPK negative OESCC response to combination therapy without being directly involved. Our findings suggest that ACF suppresses cell growth in p38 δ MAPK negative OESCC through extrinsic apoptotic pathway activation of the Fas death receptor, with caspase-8 and caspase-3 cleavage and subsequent degradation of PARP. Further analysis of cell death following ACF treatment could have been performed by assessing DNA fragmentation using TUNEL or by measuring cytochrome c release. The identification of cells in the various stages of apoptosis could have been achieved using propidium iodide/Annexin V staining to further discriminate between healthy, early apoptotic, necrotic and dead cells.

Although p38 δ MAPK status appears to be a predictor of OESCC response to conventional CF therapy, the expression of p38 δ MAPK alone does not appear to be responsible for the increased sensitivity of p38 δ MAPK positive KE-4, KE-5, KE-6 and KE-10 cells to CF treatment. Introduction of p38 δ and p-p38 δ MAPK in cells which lack endogenous expression of this isoform failed to increase their sensitivity to CF treatment. It is unclear from our studies why KE-3 cells expressing p38 δ or p-p38 δ MAPK did not demonstrate increased sensitivity to CF treatment. A possible explanation is that transfected p38 δ MAPK may not activate the same signalling pathways as endogenous p38 δ MAPK in response to cytotoxic drug treatment. Comparison of the subcellular localisation of transfected and endogenous p38 δ MAPK following CF treatment as well as identification of the signalling pathways

activated downstream of p38 δ MAPK could provide further insight into this differential sensitivity. There are many reports linking MAPK involvement following exposure to mechanistically different chemotherapeutic drugs [32]. However, their suppression and activation and indeed the absence of any role in apoptosis have been attributed to all three MAPKs [32-34]. Thus, the activation of MAPKs by chemotherapeutic drugs and the subsequent consequences of MAPK activation appear to be very much cell-type specific [33]. Although we observed p38 MAPK activation upon ACF treatment, our findings with the p38 MAPK pharmacological inhibitors do not support a direct role for p38 MAPK activity in drug-induced cytotoxicity. In contrast, ERK1/2 activation may play a more direct role as its inhibition by U0126 can partly reverse the antiproliferative effects of both CF and ACF treatments.

The increased antiproliferative and proapoptotic effects of ACF treatment over CF treatment in this study suggest that the former may be considered as mainstay treatment of patients with p38 δ MAPK negative OESCC. It remains to be investigated whether patients with p38 δ MAPK negative OESCC may benefit more from ACF treatment compared with classical CF treatment, and whether or not ACF treatment can influence overall survival. Further investigations into the mechanistic strategies underpinning p38 δ MAPK negativity related loss in drug sensitivity are warranted. The clonogenic assay is a valuable tool in gauging long-term consequences of single, double and triple chemotherapy in p38 δ MAPK negative OESCC. This assay closely mirrors the clinical situation in which patients are treated with chemotherapeutic drugs in a pulsed rather than a continuous manner. Two weeks post-treatment, ACF-treated p38 δ MAPK negative OESCC cells never

recovered. Although we observed a statistically significant reduction in colony formation on CF double or doxorubicin treatment, cell recovery was always observed, clearly demonstrating resistance. In general, the MTT assay demonstrated lower cytotoxic activity than the clonogenic assay with these drugs. Of note, a high degree of correlation between both assays is not always apparent, and it may be influenced by both cell type and anticancer drug type [35-37]. Thus, unlike ACF treatment, the limited efficacy of CF or doxorubicin alone could provide an opportunity for cancer persistence in patients with p38 δ MAPK negative OESCC.

In summary, the present study indicates that p38 δ MAPK may be a significant predictor of treatment response in patients with p38 δ -negative OESCC. p38 δ MAPK phenotyping of pre-treatment biopsy may potentially be a useful predictor of response to chemotherapy and ultimately prognosis in OESCC patients. Our data support the value of known p38 δ MAPK status in the decision process used to inform the optimal treatment of patients with OESCC.

5.7 References

1. Kayani, B., et al., *Lymph node metastases and prognosis in oesophageal carcinoma--a systematic review*. Eur J Surg Oncol, 2011. **37**(9): p. 747-53.
2. Kuwano, H., M. Fukuchi, and H. Kato, *Thoracoscopic surgery for esophageal cancer*. Ann Thorac Cardiovasc Surg, 2006. **12**(5): p. 305-7.
3. Mariette, C., G. Piessen, and J.-P. Triboulet, *Therapeutic strategies in oesophageal carcinoma: role of surgery and other modalities*. The Lancet Oncology, 2007. **8**(6): p. 545-553.
4. Nakajima, M. and H. Kato, *Treatment options for esophageal squamous cell carcinoma*. Expert Opin Pharmacother, 2013. **14**(10): p. 1345-54.
5. Nakamura, K., et al., *Three-arm phase III trial comparing cisplatin plus 5-FU (CF) versus docetaxel, cisplatin plus 5-FU (DCF) versus radiotherapy with CF (CF-RT) as preoperative therapy for locally advanced esophageal cancer (JCOG1109, NExT study)*. Jpn J Clin Oncol, 2013. **43**(7): p. 752-5.
6. Kosugi, S., et al., *Efficacy and toxicity of fluorouracil, doxorubicin, and cisplatin/nedaplatin treatment as neoadjuvant chemotherapy for advanced esophageal carcinoma*. Scand J Gastroenterol, 2005. **40**(8): p. 886-92.
7. Honda, M., et al., *Doxorubicin, cisplatin, and fluorouracil combination therapy for metastatic esophageal squamous cell carcinoma*. Dis Esophagus, 2010. **23**(8): p. 641-5.
8. Yamasaki, M., et al., *p53 genotype predicts response to chemotherapy in patients with squamous cell carcinoma of the esophagus*. Ann Surg Oncol, 2010. **17**(2): p. 634-42.
9. Ono, K. and J. Han, *The p38 signal transduction pathway: activation and function*. Cell Signal, 2000. **12**(1): p. 1-13.
10. Cuenda, A. and S. Rousseau, *p38 MAP-Kinases pathway regulation, function and role in human diseases*. Biochimica et Biophysica Acta (BBA) - Molecular Cell Research, 2007. **1773**(8): p. 1358-1375.
11. Cargnello, M. and P.P. Roux, *Activation and function of the MAPKs and their substrates, the MAPK-activated protein kinases*. Microbiol Mol Biol Rev, 2011. **75**(1): p. 50-83.
12. Wagner, E.F. and A.R. Nebreda, *Signal integration by JNK and p38 MAPK pathways in cancer development*. Nat Rev Cancer, 2009. **9**(8): p. 537-49.
13. Ambrose, M., et al., *Induction of apoptosis in renal cell carcinoma by reactive oxygen species: involvement of extracellular signal-regulated kinase 1/2, p38delta/gamma, cyclooxygenase-2 down-regulation, and translocation of apoptosis-inducing factor*. Mol Pharmacol, 2006. **69**(6): p. 1879-90.
14. O'Callaghan, C., et al., *Loss of p38delta mitogen-activated protein kinase expression promotes oesophageal squamous cell carcinoma proliferation, migration and anchorage-independent growth*. Int J Oncol, 2013. **43**(2): p. 405-15.

15. Bernardi, P., et al., *Mitochondria and cell death. Mechanistic aspects and methodological issues*. Eur J Biochem, 1999. **264**(3): p. 687-701.
16. Ku, G.Y. and D.H. Ilson, *Chemotherapeutic options for gastroesophageal junction tumors*. Semin Radiat Oncol, 2013. **23**(1): p. 24-30.
17. O'Donovan, T.R., G.C. O'Sullivan, and S.L. McKenna, *Induction of autophagy by drug-resistant esophageal cancer cells promotes their survival and recovery following treatment with chemotherapeutics*. Autophagy, 2011. **7**(5): p. 509-24.
18. Pereira, L., et al., *Inhibition of p38 MAPK sensitizes tumour cells to cisplatin-induced apoptosis mediated by reactive oxygen species and JNK*. EMBO Mol Med, 2013. **5**(11): p. 1759-74.
19. Elsea, C.R., et al., *Inhibition of p38 MAPK suppresses inflammatory cytokine induction by etoposide, 5-fluorouracil, and doxorubicin without affecting tumoricidal activity*. PLoS One, 2008. **3**(6): p. e2355.
20. Chen, W.W., et al., *Prognostic factors of metastatic or recurrent esophageal squamous cell carcinoma in patients receiving three-drug combination chemotherapy*. Anticancer Res, 2013. **33**(9): p. 4123-8.
21. Chen, J., et al., *Postoperative radiation therapy with or without concurrent chemotherapy for node-positive thoracic esophageal squamous cell carcinoma*. Int J Radiat Oncol Biol Phys, 2013. **86**(4): p. 671-7.
22. Taieb, J., et al., *Optimisation of 5-fluorouracil (5-FU)/cisplatin combination chemotherapy with a new schedule of hydroxyurea, leucovorin, 5-FU and cisplatin (HLFP regimen) for metastatic oesophageal cancer*. Eur J Cancer, 2002. **38**(5): p. 661-6.
23. Chan, K.W., et al., *Clinical relevance of Fas expression in oesophageal squamous cell carcinoma*. J Clin Pathol, 2006. **59**(1): p. 101-4.
24. Matsuzaki, I., et al., *Cisplatin induces fas expression in esophageal cancer cell lines and enhanced cytotoxicity in combination with LAK cells*. Oncology, 2000. **59**(4): p. 336-43.
25. He, D., et al., *BIRB796, the inhibitor of p38 mitogen-activated protein kinase, enhances the efficacy of chemotherapeutic agents in ABCB1 overexpression cells*. PLoS One, 2013. **8**(1): p. e54181.
26. Alessi, D.R., et al., *PD 098059 is a specific inhibitor of the activation of mitogen-activated protein kinase kinase in vitro and in vivo*. J Biol Chem, 1995. **270**(46): p. 27489-94.
27. Gisselbrecht, C., et al., *Fluorouracil (F), Adriamycin (A), and cisplatin (P) (FAP): combination chemotherapy of advanced esophageal carcinoma*. Cancer, 1983. **52**(6): p. 974-7.
28. Weiss, R.B., *The anthracyclines: will we ever find a better doxorubicin?* Semin Oncol, 1992. **19**(6): p. 670-86.
29. Shimakawa, T., et al., *Neoadjuvant chemotherapy (FAP) for advanced esophageal cancer*. Anticancer Res, 2008. **28**(4C): p. 2321-6.

30. Juan, H.C., et al., *Insulin-like growth factor 1 mediates 5-fluorouracil chemoresistance in esophageal carcinoma cells through increasing survivin stability*. *Apoptosis*, 2011. **16**(2): p. 174-83.
31. Ngan, C.Y., et al., *Oxaliplatin induces mitotic catastrophe and apoptosis in esophageal cancer cells*. *Cancer Sci*, 2008. **99**(1): p. 129-39.
32. Boldt, S., U.H. Weidle, and W. Kolch, *The role of MAPK pathways in the action of chemotherapeutic drugs*. *Carcinogenesis*, 2002. **23**(11): p. 1831-8.
33. Brozovic, A. and M. Osmak, *Activation of mitogen-activated protein kinases by cisplatin and their role in cisplatin-resistance*. *Cancer Lett*, 2007. **251**(1): p. 1-16.
34. de la Cruz-Morcillo, M.A., et al., *P38MAPK is a major determinant of the balance between apoptosis and autophagy triggered by 5-fluorouracil: implication in resistance*. *Oncogene*, 2012. **31**(9): p. 1073-1085.
35. Buch, K., et al., *Determination of cell survival after irradiation via clonogenic assay versus multiple MTT Assay--a comparative study*. *Radiat Oncol*, 2012. **7**: p. 1.
36. Sumantran, V.N., *Cellular chemosensitivity assays: an overview*. *Methods Mol Biol*, 2011. **731**: p. 219-36.
37. Kawada, K., et al., *Comparison of chemosensitivity tests: clonogenic assay versus MTT assay*. *Acta Med Okayama*, 2002. **56**(3): p. 129-34.

Chapter 6

Differential MAPK13 promoter methylation in oesophageal squamous cell carcinoma

Note: This chapter does not represent a complete body of work. Due to both time and financial constraints, the research presented here is unfinished. The experiments required to complete this study will be discussed further in Chapter 8.

6.1 Abstract

Previous chapters have characterised p38 δ MAPK function as a tumour suppressor in OESCC and outlined the effects its lack of expression has on OESCC response(s) to chemotherapeutic drugs. The differential expression of p38 δ MAPK in OESCC has important consequences for chemosensitivity as p38 δ MAPK negative OESCC is more resistant to traditional CF treatment compared with p38 δ MAPK positive OESCC. Loss of p38 δ MAPK expression is also a mechanism by which OESCC proliferation, migration and anchorage-independent growth is increased. This new study investigated how loss of p38 δ MAPK expression is achieved in OESCC. p38 δ mRNA expression was detected in all cell lines regardless of p38 δ MAPK protein status. gDNA sequence analysis did not identify any loss of function causing genomic mutations. Differential epigenetic control of p38 δ MAPK expression was also investigated. We outline here for the first time differential MAPK13 promoter methylation in OESCC. Our results suggest that epigenetic regulation may be responsible for suppression of p38 δ MAPK expression and promotion of tumourigenesis in OESCC.

6.2 Hypothesis and aims

The hypothesis for this chapter is that the differential expression of p38 δ in OESCC is caused by genetic mutation or differential epigenetic regulation of p38 δ MAPK expression.

To examine this hypothesis the aims for this chapter are as follows:

- To examine p38 δ MAPK mRNA expression in OESCC cell lines.
- To examine p38 δ MAPK DNA sequence in p38 δ MAPK negative OESCC for a mutation which would explain loss of p38 δ MAPK expression.
- To examine the methylation status of CpG sites in the p38 δ promoter in OESCC cell lines.

6.3 Introduction

Previous chapters have documented the differential expression of p38 δ MAPK in OESCC and the consequences of p38 δ MAPK expression on OESCC tumourigenicity and response to cytotoxic drugs. Loss of p38 δ MAPK expression contributes to a pro-oncogenic phenotype in OESCC and affords a level of resistance to conventional cisplatin and 5-fluorouracil treatment [1, 2]. Re-introduction of p38 δ and p-p38 δ MAPK expression resulted in a decrease in OESCC cell proliferation, migration and anchorage-independent growth [1]. These results demonstrated significant tumour suppressive functions for p38 δ MAPK in OESCC. Loss of p38 δ MAPK expression can therefore be considered as a significant pro-survival mechanism in OESCC. In general, loss or inactivation of tumour suppressor genes occurs via genetic changes such as point mutations and deletions or by epigenetic regulation [3]. This chapter sheds light on some mechanism(s) by which the loss of p38 δ MAPK expression may occur in OESCC.

At the genomic level, point mutations, insertions and deletions of genetic material are common mechanisms by which expression of tumour suppressor genes are inactivated. The somatic mutation rate for OESCC is higher than in breast carcinoma, with C.G \rightarrow T.A transitions the most common, followed by C.G \rightarrow G.C transversions [4, 5]. Point mutations can be responsible for converting a codon into a premature stop codon or replacing an essential amino acid thereby abolishing or reducing the production of a functioning gene product. Point mutations can also cause aberrant RNA splicing, again abolishing the function of the gene [6]. The tumour suppressor p53 is frequently mutated in OESCC and p53 mutated

oesophageal cancer is recognised as being resistant to conventional chemotherapy [7, 8]. Insertion or deletion of even a single nucleotide can cause a frameshift in the coding sequence which could explain the loss of p38 δ MAPK protein expression.

As well as mutations and chromosomal abnormalities, cancer genomes are also characterised by epigenetic changes such as aberrant DNA methylation. DNA methylation occurs in cytosines which precede guanines i.e. CpG dinucleotides and is essential for normal maintenance of tissue-specific gene expression [9]. In comparison with normal cells, cancer cells display global DNA hypomethylation, particularly in repetitive DNA sequences and introns which mediates genome instability [10]. This is coupled with specific hypermethylation of tumour suppressor genes which is responsible for gene silencing as DNA methylation inhibits transcription factor binding to promoter regions [11]. Hypermethylation of CpG-rich regions in gene promoters (known as CpG islands) is in fact one of the most common epigenetic changes to occur in tumours. Interestingly, it is found in almost all types of human neoplasms and gene inactivation by epigenetic silencing is at least as common as the classic coding-region mutation based disruption of tumour suppressor genes [12, 13]. This form of epigenetic regulation is increasingly implicated in the development and progression of many cancers, including oesophageal carcinomas where tumour suppressor genes involved in the cell cycle such as p16^{INK4b} and p14^{ARF} are frequently hypermethylated [3, 11]. Notably, promoter hypermethylation has previously been implicated in the epigenetic silencing of p38 δ MAPK in different cancer types. In malignant pleural mesothelioma and primary cutaneous melanoma MAPK13 promoter methylation is associated with decreased p38 δ MAPK mRNA and protein expression [14, 15].

Restoration of p38 δ MAPK expression in melanoma cells decreases proliferation [14].

In this study mRNA and gDNA sequences from p38 δ MAPK protein positive and negative cell lines were compared in order to identify any of the genetic abnormalities discussed above which may explain the differential loss of p38 δ MAPK expression. Possible epigenetic regulation of p38 δ MAPK expression was investigated using methylation-specific PCR (MSP) and bisulfite sequencing PCR (BSP) analysis of CpG islands in the MAPK13 promoter region.

6.4 Materials and methods

6.4.1 Cell culture

KE cell lines as well as KYSE-70, KYSE-450, OE21 and OC-1 were cultured as described in Chapter 2. KE cell line features are summarized in Table 2.2.

6.4.2 PCR/rt-PCR

p38 δ MAPK mRNA was amplified from cellular cDNA (synthesised as described in Chapter 2) using DreamTaqTM DNA polymerase (Fermentas, Thermo Fisher Scientific, Waltham, MA, USA) and oligonucleotide primers P009F (5'-CGAGATCGGGTGCCCGGGAT-3') or P002F (5'-CCGGAAAAAGGGCTTCTACAA) and P001R (5'-CCGCCACAAGCTAAAAAGAG-3'). A 748bp fragment of MAPK13, corresponding to positions 2189-2936 (GenBank accession no. NC_000006.12), was amplified from gDNA (isolated as described in Chapter 2) using Platinum[®] Taq DNA Polymerase (Life Technologies, Grand Island, NY, USA) and oligonucleotide primers P009F (5'-CGAGATCGGGTGCCCGGGAT-3') and P017R (5'-TCAGCTTCTTGATGGCCACCTTCTC-3'). All other reaction components were as listed in Table 2.6. PCR and rt-PCR were performed in a GeneAmp PCR System 2700 under the conditions described in Table 2.7. PCR and rt-PCR products were analysed by agarose gel electrophoresis as described in Chapter 2.

6.4.3 Quantitative rt-PCR

Nucleic acid isolation

Total cellular RNA was isolated from KE-3, KE-6, KE-8, KYSE-70, KYSE-450, OE-21 and OC-1 cells as outlined in Chapter 2.

QuantiFast® Probe Assay

p38 δ MAPK mRNA expression was quantitated using a Qiagen QuantiFast® Probe Assay with one-step rt-PCR and simultaneous detection of GAPDH. 100 ng RNA was added to genomic DNA removal reaction mix (QuantiFast Master Mix 1) in a 96-well PCR plate and incubated for 5 min at RT. rt-PCR reaction mix (QuantiFast Master Mix 2, MAPK13 QuantiFast Probe Assay, GAPDH QuantiFast Probe Assay, ROX dye solution, QuantiFast RT Mix) was added to PCR plate and reactions underwent thermal cycling according to the conditions outlined in Table 6.1 in an ABI 7500 Real-Time PCR System (Applied Biosystems, Life Technologies, Grand Island, NY, USA). All quantification experiments included a no template control (NTC), for detection of contamination and a no reverse transcriptase control to test for contaminating gDNA.

Table 6.1 One-step qrt-PCR reaction conditions

Step	Temperature °C	Time	Cycles
Reverse Transcription	50	20 min	
PCR initial activation	95	5 min	
Denaturation	95	15 s	45
Annealing/extension*	60	30 s	

*Fluorescence data collection

Data analysis

Data analysis was performed using the $\Delta\Delta C_T$ method according to the formula below [16] and aided by the SABiosciences data analysis website www.SABiosciences.com/pcrarraydataanalysis.php. Baseline was set automatically. Cycle threshold value was set in the linear exponential phase of the amplification plot and kept the same across all experiments.

$$\Delta\Delta C_T = \Delta C_T \text{ Sample}(C_T^{\text{MAPK13}} - C_T^{\text{GAPDH}}) - \Delta C_T \text{ Control}(C_T^{\text{MAPK13}} - C_T^{\text{GAPDH}})$$

6.4.4 Sodium bisulfite conversion

The methylation status of DNA was determined using sodium bisulfite conversion with an EpiMark® Bisulfite Conversion Kit (New England BioLabs, Hertfordshire, UK) according to manufacturer's instructions. Incubation of the target DNA with sodium bisulfite results in the conversion of all unmethylated cytosines to uracils, leaving the methylated bases intact (Figure 6.1).

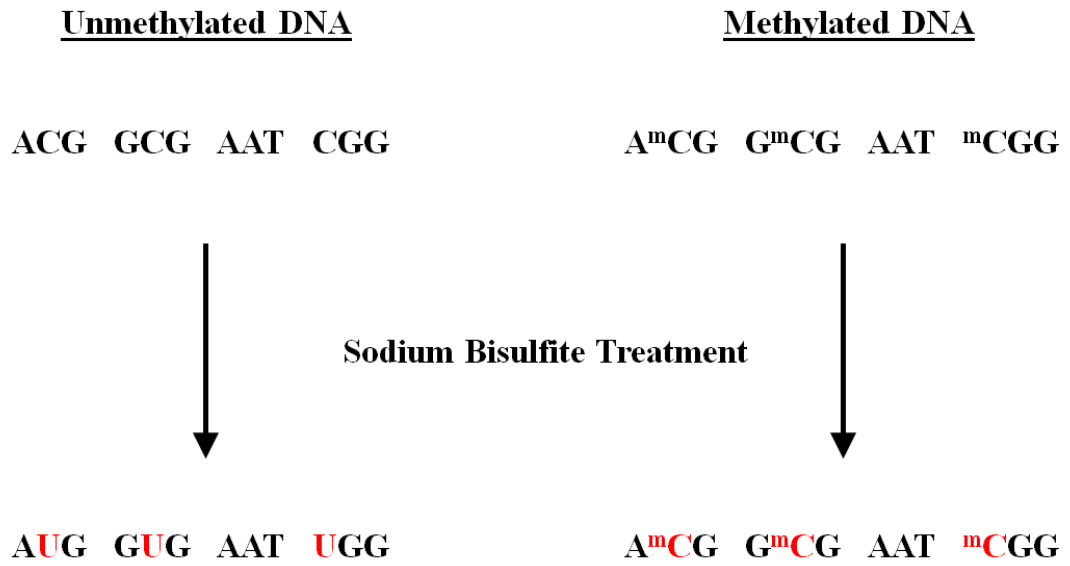


Figure 6.1 Overview of bisulfite conversion. 5-methylcytosines remain unchanged while unmethylated cytosines are deaminated to uracil as a result of treatment with sodium bisulfite.

1 µg gDNA was combined with a sodium metabisulfite mixture and mixed gently by pipetting. The bisulfite conversion reaction was performed in a GeneAmp PCR System 2700 under the conditions outlined in Table 6.2.

Table 6.2 Bisulfite conversion reaction conditions

Step	Temperature °C	Time
Denaturation	95	5 min
Incubation	65	30 min
Denaturation	95	5 min
Incubation	65	60 min
Denaturation	95	5 min
Incubation	65	90 min
Hold	18-20	up to 12 hr

On completion of the conversion reaction, DNA Binding Buffer was added to the mixture and mixed briefly. Samples were loaded on to an EpiMark spin column and centrifuged at 15 000 x g for 1 min. Following a wash step, Desulphonation Reaction Buffer was added to each column and incubated at RT for 15 min. Columns were centrifuged at 15 000 x g for 1 min before two further wash steps. Bisulfite converted DNA was eluted in 40 µl Elution Buffer.

6.4.5 Methylation specific PCR (MSP)

MSP is a method of assessing the methylation status of a group of CpG sites using individual pairs of primers specific for methylated (M) versus unmethylated (U) DNA [17]. MSP primers (Table 6.3) were designed within a CpG island in the MAPK13 promoter region (Figure 6.2) with the aid of MethPrimer, an online program for designing bisulfite-conversion-based primers (<http://www.urogene.org/methprimer/>) [18]. Specificity of the assay was ensured by the presence of two CpG pairs in each primer.

Table 6.3 Primers for MSP

Specificity	Primer	Sequence (5'→3')	T _m ^o
M	M01F	TTTGTTTGGATTTATTAGTTTCGTC	54.8
	M01R	GAACCTATCCAACCCTACGCT	59.8
U	U01F	GTTTGGATTTATTAGTTTTGTTGT	52.5
	U01R	CAAACCTATCCAACCCTACACT	58.4

MSP amplicons were analysed by agarose gel electrophoresis and subsequently confirmed by sequencing analysis as described in Chapter 2.

6.4.6 Bisulfite sequencing PCR (BSP)

Primer sequences were designed using MethPrimer [18] to amplify a fragment of a CpG island in the MAPK13 promoter region of bisulfite converted DNA regardless of methylation status (Figure 6.2). Oligonucleotide primers BSP01F (5'-TTGGGAGTTGGTTAGAAATGTA-3') and BSP01R (5'-AACAATACTTCCCAA TTCCCT-3') were used to amplify a 270 bp fragment, from bisulfite converted DNA with Platinum® Taq DNA Polymerase. Other reaction components were as listed in Table 2.6. BSP was performed in a GeneAmp PCR System 2700 under the conditions described in Table 2.7. PCR products were analysed by agarose gel electrophoresis as per Chapter 2 and subsequently sequenced to determine the average methylation status for each of the four CpG dinucleotides present in the amplicon.

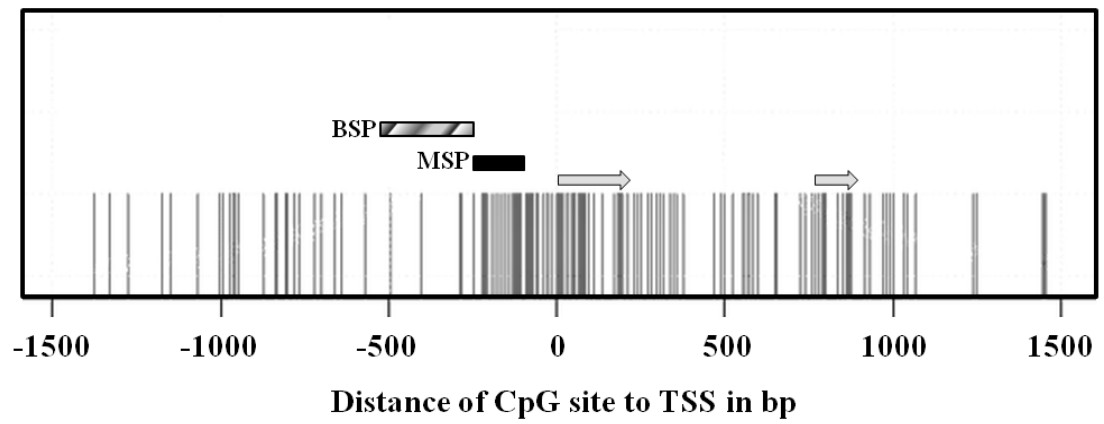


Figure 6.2 Representative diagram of MAPK13 promoter region CpG sites. Each vertical line represents a single CpG site. Transcription start site (0), exons (grey arrows), location of methylation specific PCR assay (black bar, MSP) and location of bisulfite sequencing PCR (striped bar, BSP) are indicated. Adapted from RefGene [19].

6.4.7 5'-aza-2'-deoxycytidine treatment

5'-aza-2'-deoxycytidine was dissolved at 50 mg/ml in DMSO. KE-3 cells were treated with 2 μ M 5'-aza-2'-deoxycytidine (Decitabine, Sigma Aldrich Ireland Ltd, Arklow, Ireland) or DMSO (control) for 96 hr. Culture medium was replaced with medium containing fresh 5'-aza-2'-deoxycytidine or DMSO every 24 hr.

6.5 Results

6.5.1 p38 δ MAPK mRNA is present in all OESCC cell lines

As discussed in Chapter 4, primers specific for a fragment within the 3' untranslated region of p38 δ MAPK mRNA amplified cDNA from all oesophageal squamous and adenocarcinoma cell lines examined regardless of their p38 δ MAPK protein status (Figure 4.1C). However, the region amplified by this primer pair (P001F and P001R) does not span an exon-exon boundary and gDNA contamination of the template is possible. Intron-spanning primer sets within the p38 δ MAPK coding region consistently strongly amplified cDNA from p38 δ MAPK protein positive cell lines KE-4, -5, -6, 10, KYSE-450, OC-3, OE-19 and -33, as well as from p38 δ MAPK protein negative cell lines OE21 and OC1 (Figure 6.3A and B). Varying levels of amplicon were observed from KE-3, KE-8 and KYSE-70 (p38 δ MAPK protein negative) cells, depending on the primer pair used. Primers specific for a 1575 bp portion of p38 δ mRNA (P002F and P001R) weakly amplified cDNA from KE-8 and KYSE-70 cells but not from KE-3 cells (Figure 6.3A). PCR with a primer pair specific for a 1605 bp region of p38 δ mRNA (P009F and P001R) did not yield any detectable product from KYSE-70 cDNA but did weakly amplify cDNA from KE-3 and KE-8 cells (Figure 6.3B).

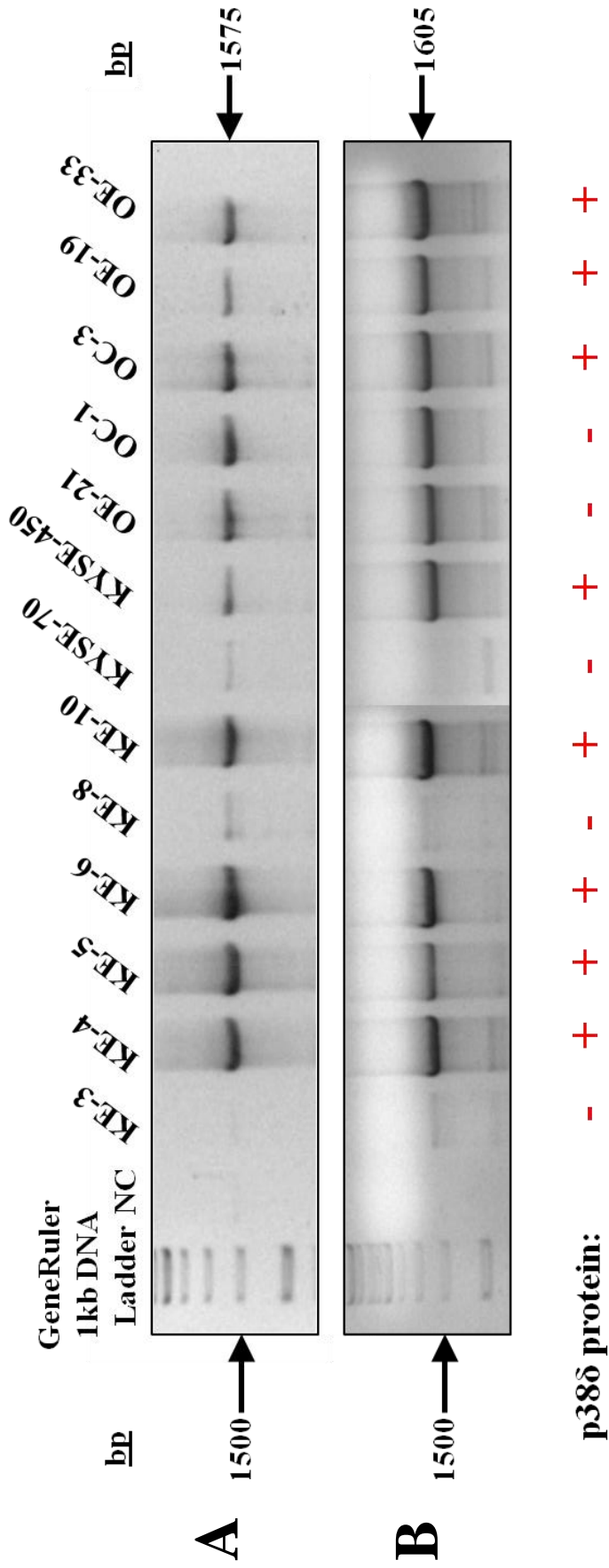


Figure 6.3 p38δ MAPK mRNA expression in oesophageal cancer. Agarose gel electrophoresis analysis of DNA fragments produced by PCR amplification of p38δ MAPK mRNA from p38δ MAPK protein positive (KE-4, KE-5, KE-6, KE-10, KYSE-450, OC-3, OE-19, OE-33) and p38δ MAPK protein negative (KE-3, KE-8, KYSE-70, OE-21, OC-1) oesophageal carcinoma cells with (A) P002F, P001R and (B) P009F, P001R primers.

6.5.2 p38 δ MAPK translation start site sequence is intact in OESCC cell lines

As p38 δ MAPK mRNA was detected in all cell lines examined (Figure 6.3), the possibility of a genetic abnormality at the transcriptional level was discounted. Therefore, the p38 δ MAPK translation start site was amplified and sequenced in order to identify any potential mutations such as the presence of a premature stop codon or a mutated start codon which could possibly explain the absence of p38 δ MAPK protein expression in KE-3, KE-8 and KYSE-70 cells. The translation start site of p38 δ MAPK was amplified from gDNA with specific primers P009F and P017R. All cell lines examined were positive for the 748 bp fragment, including KE-3, KE-8 and KYSE-70 cell lines which were negative for p38 δ MAPK protein expression (Figure 6.4A). PCR products were analysed by DNA sequencing and the returned sequence reads were compared with the MAPK13 reference sequence (NC_000006.12). Differences in the first ~10 bases of the sequence read were ignored as these peaks tend to be poorly resolved in the electropherogram. The p38 δ MAPK ATG start codon was found to be intact in all cell lines examined i.e. KE-3, KE-8, KYSE-70, OE-21, OC-1 (p38 δ MAPK negative) and KYSE-450 (p38 δ MAPK positive) (Figure 6.4B(i)). Any mutations identified were deemed to be silent or located within a non-coding (intron) region (Figure 6.4B(ii) and (iii) respectively).

6.5.3 p38δ MAPK mRNA expression is downregulated in OESCC cell lines which lack p38δ protein expression

In the absence of any detectable mutations at the genomic level, differential p38δ MAPK mRNA expression remained the most likely cause of p38δ MAPK protein loss. Therefore p38δ MAPK mRNA expression was further analysed. Quantitative real-time PCR was used to determine the relative levels of p38δ MAPK mRNA expression in each of the OESCC cell lines being studied. p38δ MAPK mRNA expression was found to be highest in p38δ MAPK protein positive cells KE-6 and KYSE-450, although there was a significant ($p<0.01$) difference between the two cell lines (Figure 6.5). p38δ MAPK mRNA expression was similarly and significantly ($p<0.001$) downregulated in p38δ MAPK protein negative cell lines KE-3, KE-8 and KYSE-70 when compared with both KE-6 and KYSE-450 p38δ MAPK protein positive cells (Figure 6.5). OE-21 and OC-1 (both p38δ MAPK protein negative) demonstrated intermediate levels of p38δ MAPK mRNA expression yet still with significant ($p<0.001$ and $p<0.01$) decreases from KE-6 and KYSE-450 expression (Figure 6.5).

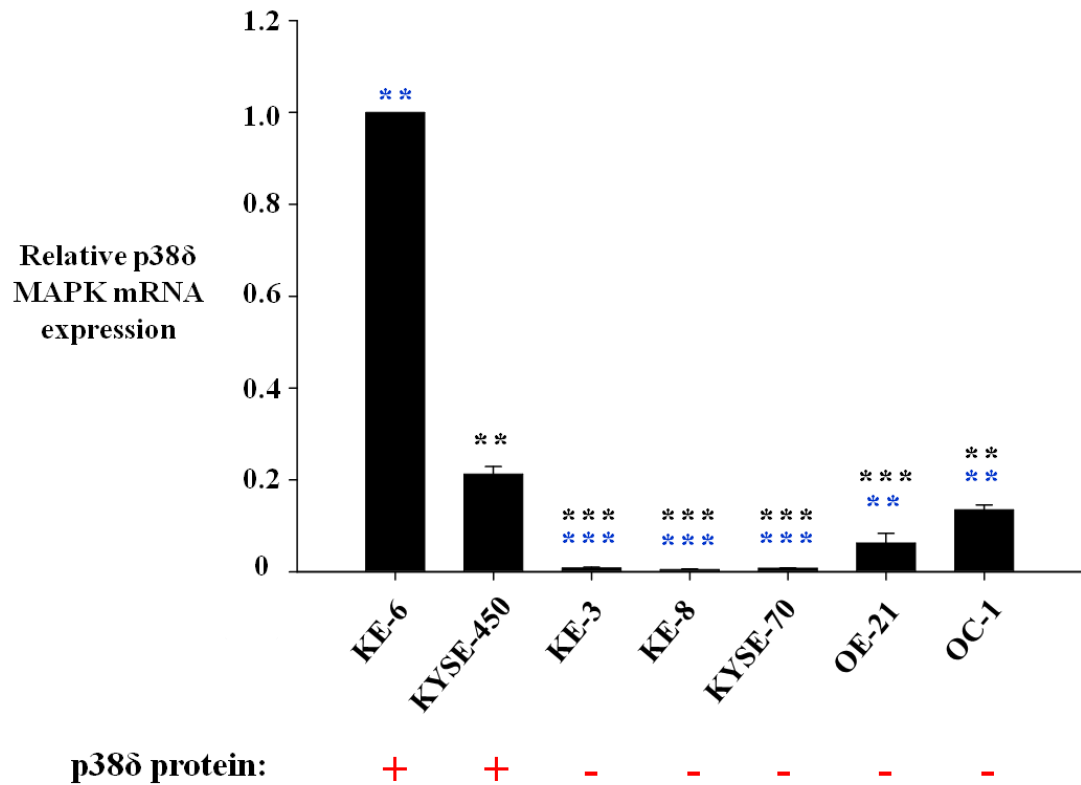


Figure 6.5 Relative p38δ MAPK mRNA expression in OESCC. p38δ MAPK mRNA levels in p38δ MAPK protein negative OESCC cell lines KE-3, KE-8, KYSE-70, OE-21 and OC-1 were compared with p38δ MAPK protein positive KE-6 and KYSE-450 cells. GAPDH was measured as an internal control. Relative values were calculated by normalizing $2^{-\Delta\Delta CT}$. Results shown are the mean \pm S.E. of three independent qrt-PCR experiments. ***p<0.001, **p<0.01, significant changes in p38δ MAPK expression from (black) KE-6 and (blue) KYSE-450 cells were determined by application of Student's t-test.

6.5.4 MAPK13 promoter is differentially methylated in OESCC

As a genetic mutation had been ruled out as an explanation for the differential loss of p38 δ MAPK in OESCC, epigenetic regulation of p38 δ MAPK expression was considered. DNA methylation was detected by MSP in KE-3, KE-8, KYSE-70 and OC-1 OESCC (Figure 6.6A (M)). In contrast, no substantial DNA methylation was identified in KE-6, KYSE-450 and OE-21 cells (Figure 6.6A (M)). Furthermore, unmethylated DNA was poorly amplified in KE-3, KE-8 and KYSE-70 cells (Figure 6.6A (U)). This is indicative of the presence of MAPK13 promoter hypermethylation in p38 δ MAPK protein negative OESCC, with the exception of the OE-21 cell line.

BSP was used for further validation and analysis of MAPK13 promoter methylation density in OESCC. The methylation status of four individual CpG sites within a MAPK13 promoter region CpG island was analysed. Comparison of DNA sequence reads of PCR products with in silico bisulfite-converted MAPK13 reference sequence (NC_000006.12) identified differential CpG methylation in OESCC (Figure 6.5B). Unmethylated CpG cytosines (C) in the MAPK13 reference sequence are converted to uracil (T). Identical residues at the equivalent positions in the PCR products indicates the CpG residue is not methylated in that particular cell line while the presence of unconverted C residues is indicative of DNA methylation at that individual CpG site (Figure 6.6B).

Of the four MAPK13 promoter region CpG sites analysed by BSP, only one was found to be methylated in KE-6 and KYSE-450 p38 δ MAPK protein positive OESCCs (Figure 6.6B and C). Conversely, DNA methylation was detected at all four CpG sites in KE-3, KE-8 and KYSE-70 p38 δ MAPK protein negative OESCCs

(Figure 6.6B and C). In p38 δ MAPK protein negative OE-21 and OC-1, DNA methylation was identified at one and two CpG sites respectively (Figure 6.6B and C)

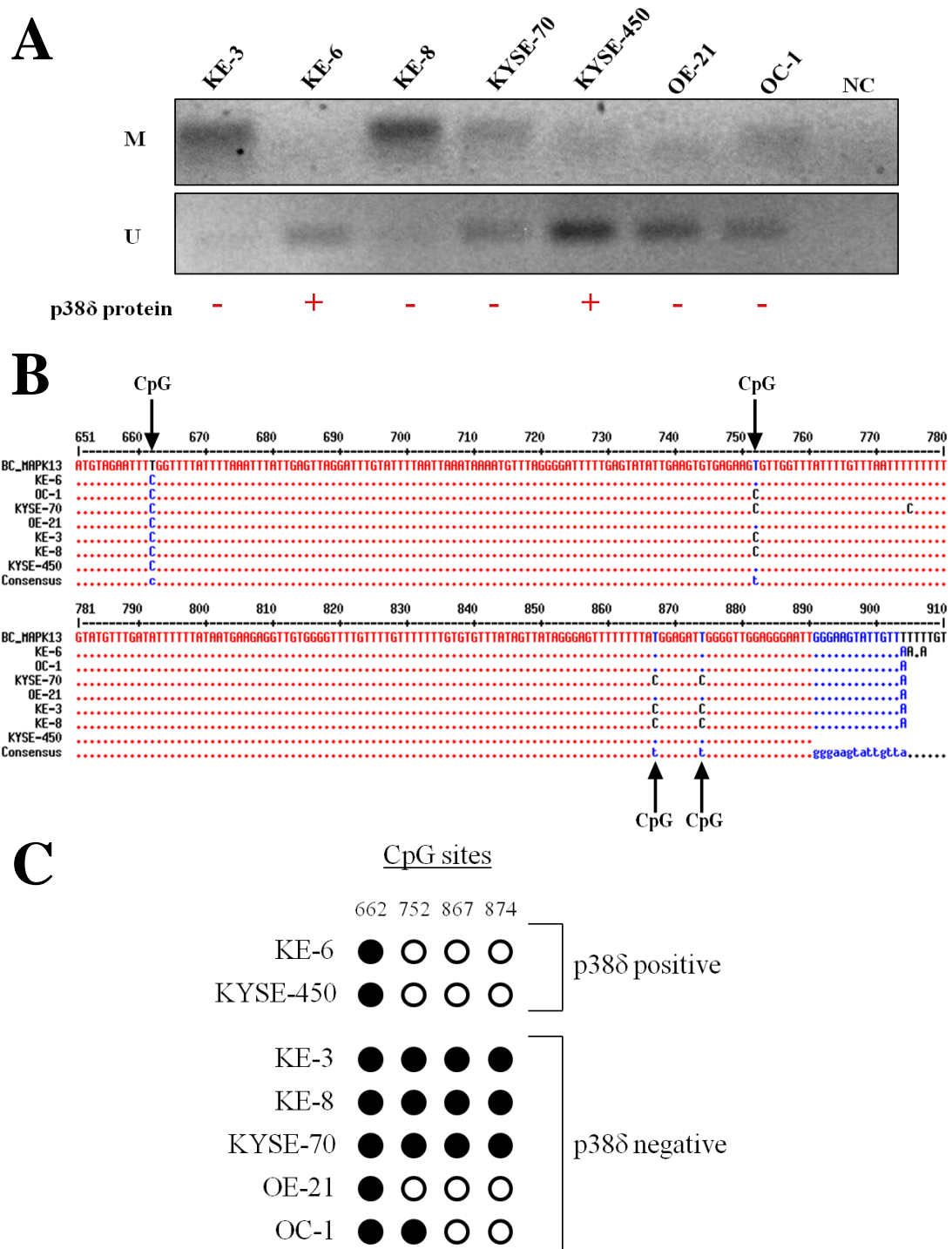


Figure 6.6 MAPK13 promoter methylation analysis. (A) Agarose gel electrophoresis analysis of MAPK13 MSP products. (B) DNA sequence analysis of MAPK13 CpG island BSP products. Residues identical to the reference sequence (MAPK13 NC_000006.12) residue at the same position are represented by a point (•), residues which differ are in uppercase. (C) Representative BSP analysis of CpG methylation. An unmethylated cytosine is depicted as a white circle, a methylated cytosine as a black circle.

6.5.5 Treatment with 5'-aza-2'-deoxycytidine does not induce p38 δ MAPK mRNA expression in KE-3 OESCC cells

5'-aza-2'-deoxycytidine is an epigenetic modifier. It demethylates or hemi-demethylates DNA by inhibiting DNA methyltransferase activity. KE-3 cells were treated with 5'-aza-2'-deoxycytidine and the effect on p38 δ MAPK expression was analysed by qrt-PCR. No significant change in p38 δ MAPK mRNA expression was detected between 5'-aza-2'-deoxycytidine and DMSO (control) treated cells (Figure 6.7). Of note, these results were obtained from a single preliminary experiment – no replicates were performed.

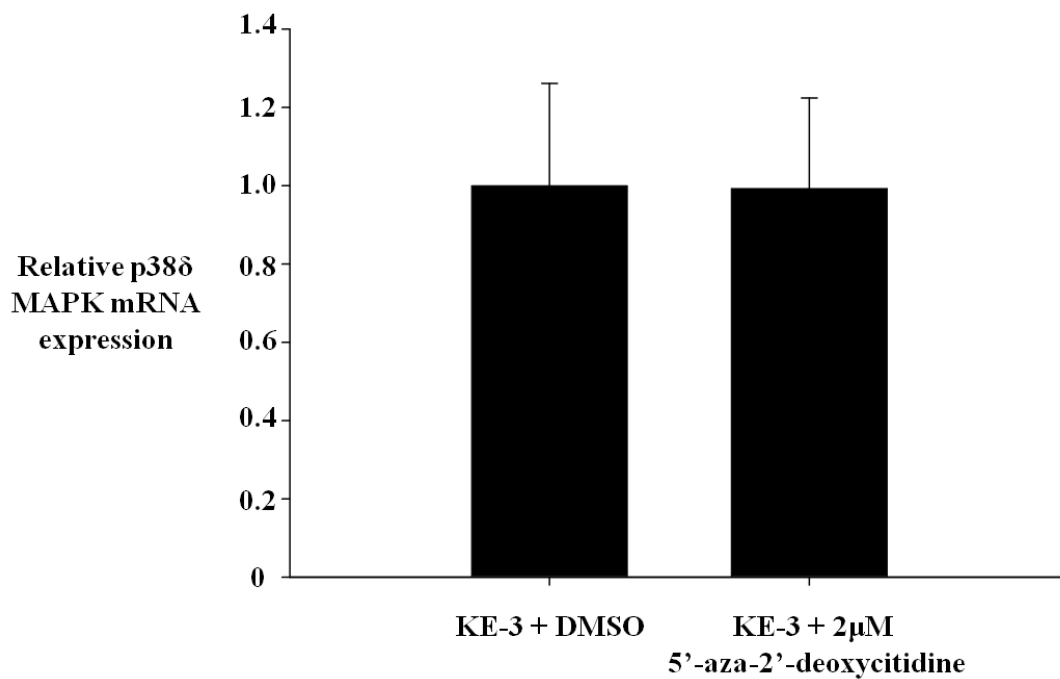


Figure 6.7 Relative p38δ MAPK mRNA expression in KE-3 cells following 5'-aza-2'-deoxycytidine treatment. p38δ MAPK mRNA level in KE-3 cells following treatment for 96 hr with 2μM 5'-aza-2'-deoxycytidine was compared with DMSO treated KE-3 cells. GAPDH expression was measured as an internal control. Relative values were calculated by normalizing to KE-3 + DMSO $2^{-\Delta\Delta CT}$. Results shown are the mean \pm S.E of 3 replicate wells in a single qrt-PCR experiment.

6.6 Discussion

Tumour suppressor gene function can be lost in a variety of ways in order for cancer cells to gain the capacity for uncontrolled proliferation, migration and escape from apoptosis. These include somatic mutations, including insertions, deletions or point mutations, and/or epigenetic changes such as DNA methylation or histone deacetylation. p38 δ MAPK displays tumour suppressor functions in OESCC – its loss promotes proliferation, migration, anchorage-independent growth and resistance to conventional chemotherapy [1, 2]. p38 δ MAPK expression is absent at the protein level in OESCC cell lines KE-3, KE-8, KYSE-70, OE-21 and OC-1. In this study we outline how this inactivation of p38 δ MAPK expression may occur in OESCC.

The results presented here indicate that this loss of protein expression cannot be attributed to a genetic mutation or deletion. p38 δ MAPK mRNA is expressed in all OESCC cell lines, regardless of p38 δ MAPK protein status. Furthermore, no mutations were identified in exon 1 of the coding region which would prevent or disrupt translation from mRNA to protein. However, differential mRNA expression levels were observed between p38 δ MAPK protein positive and protein negative cell lines. The highest levels of p38 δ MAPK mRNA expression were observed in p38 δ protein positive cell lines KE-6 and KYSE-450. Significantly lower levels of p38 δ MAPK mRNA were detected in p38 δ MAPK protein negative cell lines. This suggests that the absence of p38 δ MAPK protein expression in these cells may be attributed to p38 δ MAPK mRNA expression failing to reach the threshold required to achieve a detectable level of protein synthesis.

Our results show that the downregulation of p38 δ MAPK mRNA expression in KE-3, KE-8, KYSE-70, OE-21 and OC-1 cells is most likely caused by MAPK13 promoter hypermethylation. The MAPK13 promoter regions of the OESCC cell lines with the lowest levels of p38 δ MAPK mRNA expression (KE-3, KE-8 and KYSE-70 p38 δ protein negative cells) are highly methylated, as demonstrated by both MSP and BSP analysis. Conversely, in p38 δ MAPK protein positive cell lines KE-6 and KYSE-450, in which p38 δ MAPK mRNA expression was significantly higher ($p < 0.001$), a decreased incidence of DNA methylation was detected by both MSP and BSP. OC-1 cells also expressed significantly higher ($p < 0.001$) levels of p38 δ MAPK mRNA than KE-3, KE-8 and KYSE-70 cells despite the fact that they are also p38 δ MAPK protein negative. Interestingly however, the MAPK13 promoter was also found to be hypermethylated in this cell line when compared with p38 δ MAPK protein positive cells (two CpG sites methylated versus one CpG site methylated). There appears to be an inverse correlation therefore between MAPK13 promoter methylation and p38 δ MAPK mRNA expression in OESCC. Of note, methylation of the specific CpG sites examined here may not be the critical determinants of MAPK13 expression but rather these results reflect a general pattern of MAPK13 promoter methylation. This would explain why the OE21 cell line does not appear to fit this model of p38 δ MAPK epigenetic regulation – the loss of p38 δ MAPK expression in the OE21 cell line may be caused by MAPK13 promoter methylation at a critical CpG site not included in this analysis.

Confirmation of epigenetic silencing of p38 δ MAPK in OESCC could be achieved with further experimentation. The DNA methyltransferase inhibitor 5'-aza-2'-deoxycytidine causes passive demethylation and has been shown to reactivate

epigenetically silenced genes [14, 20]. Although the preliminary experiment outlined here did not detect activation of p38 δ MAPK expression following 5'-aza-2'-deoxycytidine treatment, it is possible that conditions used (2 μ M 5'-aza-2'-deoxycytidine for 96 hr) were not sufficient to induce DNA demethylation. Examples in the literature use concentrations of 5'-aza-2'-deoxycytidine as high as 10 μ M as well as numerous time-points to achieve DNA demethylation [21, 22]. CpG island demethylation following 5'-aza-2'-deoxycytidine treatment was not assessed in this study but could be confirmed using BSP before proceeding with analysis of p38 δ MAPK mRNA expression. Increased p38 δ MAPK mRNA expression in KE-3, KE-8, KYSE-70, OE-21 and OC-1 cells following 5'-aza-2'-deoxycytidine treatment would confirm that p38 δ MAPK is epigenetically regulated in OESCC and that the MAPK13 promoter methylation identified above is associated with loss of p38 δ MAPK expression. This was found to be the case in melanoma cells where a nearly undetectable level of MAPK13 expression was increased significantly upon treatment with 5'-aza-2'-deoxycytidine [14]. Importantly, introduction of p38 δ MAPK expression in melanoma cell lines exhibiting MAPK13 promoter hypermethylation resulted in decreased proliferation, particularly when a constitutively active form of p38 δ MAPK was used [14]. This is consistent with our results outlined in Chapter 4 and further strengthens the argument for the tumour suppressive functions of this gene [1].

The implication of MAPK13 promoter methylation in promoting tumourigenesis in OESCC could have therapeutic implications. Epigenetic alterations, as opposed to genetic mutations can be pharmacologically reversed. 5'-aza-2'-deoxycytidine (as decitabine) is in fact used as a treatment for myelodysplastic syndromes and

leukaemia [23, 24]. 5'-aza-2'-deoxycytidine acts as a cytidine analog during DNA replication but cannot be methylated by DNMT1 and instead causes degradation of DNMT1 and reduces methylation in rapidly dividing cancer cells [25]. Histone deacetylation is another mechanism by which gene expression can be repressed. Methyl domain binding proteins bound to methylated CpG sites recruit histone deacetylases (HDAC) to the histone, further inhibiting transcription [26]. HDAC inhibitors have also demonstrated antitumour effects in various cancers. Suberanilohydroxamic acid (Vorinostat) is used in the treatment of T cell lymphomas. It causes hyperacetylation of not only histones but also p53 and hsp90, thereby inducing apoptosis [27]. The HDAC inhibitor Trichostatin A has recently been shown to suppress proliferation and promote apoptosis in OESCC [28]. HDAC inhibitors can also induce the expression of cancer-testis antigens (CTAs), thereby increasing the immunogenicity of cancer cells [29]. Furthermore, HDAC inhibitors can promote demethylation by downregulation of DNMT1. The combination of a HDAC inhibitor and a demethylating agent has been found to have synergistic effects [30]. Potential lies in the combination of epigenetic and non-epigenetic therapies. The re-expression of tumour suppressor genes by epigenetic drugs weakens the ability of cancer cells to withstand cytotoxic treatment, thereby lowering the dose of chemotherapeutic drug required to induce cell death [30]. Another potential clinical use of the findings presented here is as a prognostic tool. DNA methylation analysis techniques would facilitate the sensitive and quantitative detection of a hypermethylated MAPK13 promoter in biopsy specimens. As we have seen in Chapter 5, pre-treatment identification of p38 δ MAPK status may be useful in determining the optimal treatment and predicting response in OESCC patients.

6.7 References

1. O'Callaghan, C., et al., *Loss of p38delta mitogen-activated protein kinase expression promotes oesophageal squamous cell carcinoma proliferation, migration and anchorage-independent growth*. *Int J Oncol*, 2013. **43**(2): p. 405-15.
2. O'Callaghan, C., L.J. Fanning, and O.P. Barry, *p38δ MAPK phenotype: an indicator of chemotherapeutic response in oesophageal squamous cell carcinoma*. *Anti-Cancer Drugs*, 2014. **Publish Ahead of Print**: p. 10.1097/CAD.000000000000156.
3. McCabe, M.L. and Z. Dlamini, *The molecular mechanisms of oesophageal cancer*. *International Immunopharmacology*, 2005. **5**(7-8): p. 1113-1130.
4. Song, Y., et al., *Identification of genomic alterations in oesophageal squamous cell cancer*. *Nature*, 2014. **509**(7498): p. 91-5.
5. Agrawal, N., et al., *Comparative genomic analysis of esophageal adenocarcinoma and squamous cell carcinoma*. *Cancer Discov*, 2012. **2**(10): p. 899-905.
6. Strachan, T. and A.P. Read, *Human Molecular Genetics 3*. 2004: Garland Science.
7. Kihara, C., et al., *Mutations in zinc-binding domains of p53 as a prognostic marker of esophageal-cancer patients*. *Jpn J Cancer Res*, 2000. **91**(2): p. 190-8.
8. Petitjean, A., et al., *Impact of mutant p53 functional properties on TP53 mutation patterns and tumor phenotype: lessons from recent developments in the IARC TP53 database*. *Hum Mutat*, 2007. **28**(6): p. 622-9.
9. Delcuve, G.P., M. Rastegar, and J.R. Davie, *Epigenetic control*. *J Cell Physiol*, 2009. **219**(2): p. 243-50.
10. Feinberg, A.P. and B. Vogelstein, *Hypomethylation distinguishes genes of some human cancers from their normal counterparts*. *Nature*, 1983. **301**(5895): p. 89-92.
11. Esteller, M., *Epigenetics in cancer*. *N Engl J Med*, 2008. **358**(11): p. 1148-59.
12. Baylin, S.B. and J.G. Herman, *DNA hypermethylation in tumorigenesis: epigenetics joins genetics*. *Trends Genet*, 2000. **16**(4): p. 168-74.
13. Jones, P.A. and S.B. Baylin, *The fundamental role of epigenetic events in cancer*. *Nat Rev Genet*, 2002. **3**(6): p. 415-28.
14. Gao, L., et al., *Genome-wide promoter methylation analysis identifies epigenetic silencing of MAPK13 in primary cutaneous melanoma*. *Pigment Cell Melanoma Res*, 2013. **26**(4): p. 542-54.
15. Goto, Y., et al., *Epigenetic profiles distinguish malignant pleural mesothelioma from lung adenocarcinoma*. *Cancer Res*, 2009. **69**(23): p. 9073-82.

16. Livak, K.J. and T.D. Schmittgen, *Analysis of relative gene expression data using real-time quantitative PCR and the 2(-Delta Delta C(T)) Method*. *Methods*, 2001. **25**(4): p. 402-8.
17. Herman, J.G., et al., *Methylation-specific PCR: a novel PCR assay for methylation status of CpG islands*. *Proceedings of the National Academy of Sciences*, 1996. **93**(18): p. 9821-9826.
18. Li, L.C. and R. Dahiya, *MethPrimer: designing primers for methylation PCRs*. *Bioinformatics*, 2002. **18**(11): p. 1427-31.
19. <http://refgene.com/gene/5603>.
20. Michalowsky, L.A. and P.A. Jones, *Differential nuclear protein binding to 5-azacytosine-containing DNA as a potential mechanism for 5-aza-2'-deoxycytidine resistance*. *Mol Cell Biol*, 1987. **7**(9): p. 3076-83.
21. Jowaed, A., et al., *Methylation Regulates Alpha-Synuclein Expression and Is Decreased in Parkinson's Disease Patients' Brains*. *The Journal of Neuroscience*, 2010. **30**(18): p. 6355-6359.
22. Chiurazzi, P., et al., *Synergistic Effect of Histone Hyperacetylation and DNA Demethylation in the Reactivation of the FMR1 Gene*. *Human Molecular Genetics*, 1999. **8**(12): p. 2317-2323.
23. Oki, Y., E. Aoki, and J.P. Issa, *Decitabine--bedside to bench*. *Crit Rev Oncol Hematol*, 2007. **61**(2): p. 140-52.
24. Mack, G.S., *Epigenetic cancer therapy makes headway*. *J Natl Cancer Inst*, 2006. **98**(20): p. 1443-4.
25. Momparler, R.L., *Pharmacology of 5-Aza-2'-deoxycytidine (decitabine)*. *Semin Hematol*, 2005. **42**(3 Suppl 2): p. S9-16.
26. Ng, H.H., et al., *MBD2 is a transcriptional repressor belonging to the MeCP1 histone deacetylase complex*. *Nat Genet*, 1999. **23**(1): p. 58-61.
27. Heerboth, S., et al., *Use of Epigenetic Drugs in Disease: An Overview*. *Genetics & Epigenetics*, 2014. **6**: p. 9-19.
28. Ma, J., et al., *Trichostatin A, a histone deacetylase inhibitor, suppresses proliferation and promotes apoptosis of esophageal squamous cell lines*. *Mol Med Rep*, 2015.
29. Weiser, T.S., et al., *Induction of MAGE-3 expression in lung and esophageal cancer cells*. *Ann Thorac Surg*, 2001. **71**(1): p. 295-301; discussion 301-2.
30. Sarkar, S., et al., *Demethylation and re-expression of epigenetically silenced tumor suppressor genes: sensitization of cancer cells by combination therapy*. *Epigenomics*, 2013. **5**(1): p. 87-94.

Chapter 7

Investigation into the contribution of p38 δ (and p-p38 δ) MAPK to the cell cycle in OESCC

Note: This chapter does not represent a complete body of work. Due to both time and financial constraints, the research presented here is unfinished. The experiments required to complete this study will be discussed further in Chapter 8.

7.1 Abstract

We have previously shown that p38 δ MAPK negative OESCC cells proliferate more quickly than cells which endogenously express p38 δ MAPK. Introduction, however, of p38 δ MAPK expression in p38 δ MAPK negative OESCC cells caused a significant decrease in the rate of cell proliferation. This effect was further enhanced by constitutive expression of phosphorylated p38 δ MAPK (Chapter 4). Cell proliferation arises from a particular balance between cell division and cell death which is tightly controlled by the cell cycle. While the p38 MAPK pathway can both positively and negatively regulate cell division (depending on cell type and stimulus) the specific contribution of the individual p38 MAPK isoforms has not been elucidated. This chapter aims to uncover how the cell cycle is influenced by the introduction of p38 δ MAPK and p-p38 δ MAPK in reducing OESCC proliferation. The effects of p38 δ MAPK and p-p38 δ MAPK on the expression of 84 cell cycle regulated genes was examined using an RT² Profiler human cell cycle PCR array.

7.2 Hypothesis and aims

The hypothesis for this chapter is that p38 δ (and p-p38 δ) MAPK negatively regulates cell cycle progression by influencing the expression of a cell cycle associated gene(s).

To examine this hypothesis the aims for this chapter are as follows:

- To compare the expression of cell cycle associated genes in p38 δ MAPK negative and p38 δ MAPK positive OESCC cell lines.
- To compare the expression of cell cycle associated genes in p38 δ MAPK negative and p-p38 δ MAPK positive OESCC cell lines.

7.3 Introduction

The p38 MAPK family has long been recognised as a regulator of cell growth since overexpression of mammalian p38 α MAPK in yeast was found to significantly slow proliferation [1]. In recent years p38 α MAPK has been shown to regulate cell cycle progression and checkpoint controls by a number of mechanisms in both G₁/S and G₂/M phases of the cell cycle (Figure 7.1). Depending on cell-type and the activating signal, p38 α can either activate G₁/S phase arrest or promote progression through the checkpoint [2]. p38 α MAPK activation promotes proliferation and progression through the cell cycle in a variety of mammalian cells by regulating the activity of transcription factors such as NF- κ B, ATF-1, ATF-2, CREB and C/EBP family members [3]. On the other hand, arrest of NIH3T3 cells at G₁/S phase of the cell cycle by Cdc42 has been shown to be dependent on p38 α MAPK activation [4]. Interestingly, expression of Cdc42 in MEFs is associated with downregulation of p38 δ MAPK activity and progression of MEFs through G₁/S, highlighting the significance of the cell type in determining the specific role of p38 MAPK signalling [5]. Osmotic shock also induces G₁/S phase arrest in Mori human fibroblast via p38 activation [6].

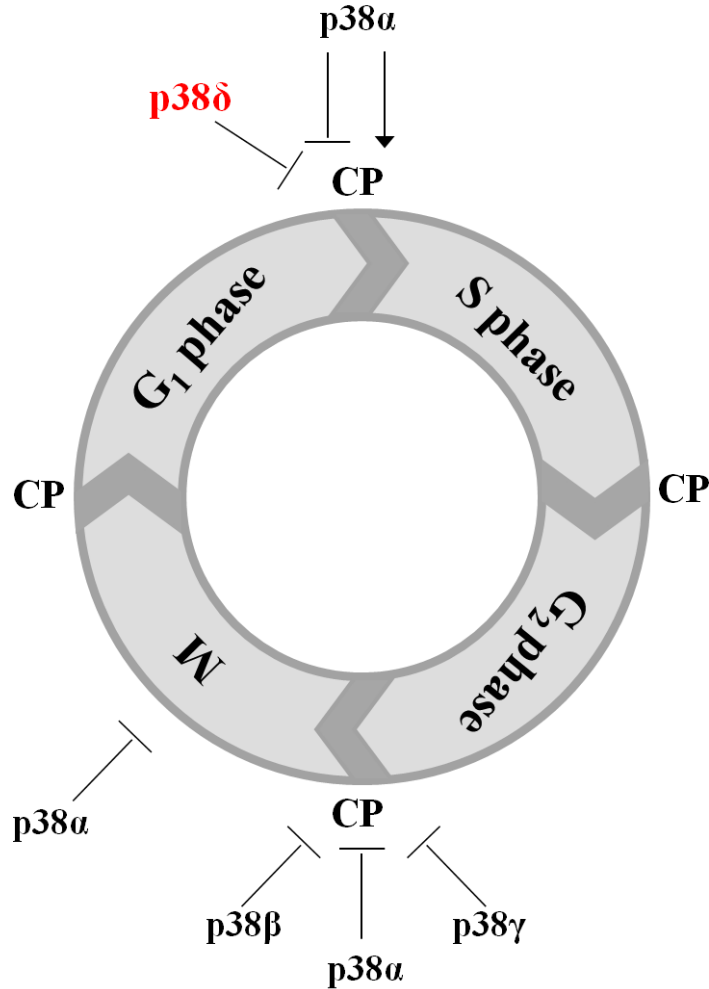


Figure 7.1 Schematic diagram of p38 MAPK pathway regulation of the cell cycle. The four phases of the eukaryotic cell cycle are the Gap-1 phase (G₁), DNA synthesis (S phase), Gap-2 phase (G₂) and the mitotic phase (M). p38α MAPK is known to both inhibit and promote progression through the G₁/S phase checkpoint (CP), depending on the cell type and/or stimulus. Several reports identify p38α MAPK as an inhibitor of G₂/M transition and progression through M-phase. p38β MAPK prevents entry into M phase when DNA replication is incomplete. p38γ induces G₂ arrest in response to γ-irradiation. p38δ MAPK induces G₁ phase arrest through p53 and p21 in keratinocytes.

Several mechanisms have been proposed for p38 α MAPK mediated G₁/S arrest. These involve well characterised p38 α MAPK substrates such as p53, p21 and HMG-box transcription factor 1 [6-8] or downregulation of cyclin D expression and protein stability [9-11]. p38 α MAPK has also been identified as a mediator of G₂ arrest induced by environmental stimuli such as UV irradiation. p38 α MAPK is responsible for the phosphorylation of Cdc25B which increases its affinity for 14-3-3 proteins and ultimately its inactivation. Inhibition of p38 α MAPK abolishes the G₂ delay induced by UV irradiation [12]. p38 α MAPK is also activated in M phase arrest by disruption of the spindle with nocodazole [13]. In contrast, Fas receptor stimulation results in p38 MAPK mediated phosphorylation of the G₁/S transition regulator retinoblastoma protein (Rb). Phosphorylation of Rb reverts Rb-regulated growth suppression by causing it to dissociate from E2F, thereby increasing E2F transcriptional activity.

Specific roles for p38 β and - γ MAPKs in cell cycle control have also been described. p38 β MAPK (in combination with p38 α MAPK) is responsible for inhibiting entry into M phase when DNA replication is ongoing or has stalled by keeping cyclin B1/cyclin dependent kinase (CDK) -1 complexes inactive [14]. p38 γ MAPK plays a critical role in γ -irradiation induced G₂ arrest. Activation of p38 γ in response to γ -irradiation is mediated by ATM and leads to regulation of the G₂ checkpoint via activation of Chk2 and Cdc25C [15]

Despite the significant roles p38 α , - β , and - γ MAPK signalling play in the cell cycle, a clear function for p38 δ MAPK in cell cycle control has yet to be defined. There is increasing evidence however which suggests that p38 δ MAPK negatively regulates

cell cycle progression. p38 δ MAPK has been shown to be involved in the induction of G₁ phase arrest in response to selenoprotein W depletion [16]. MKK-4 activated p38 δ MAPK phosphorylates p53 on Ser-33. Phosphorylated p53 is protected from proteosomal degradation and accumulates in the nucleus where it activates expression of the cyclin-dependent kinase inhibitor (CDKI) p21. p21 expression is then responsible for inducing G₁ phase arrest [16]. p38 δ MAPK has also recently been implicated in the suppression of keratinocyte proliferation. PKC δ -induced p38 δ MAPK activation was shown to be responsible for the upregulation of p53 expression (rather than phosphorylation) which in turn induced p21 expression [17].

To elucidate the specific contribution of p38 δ to cell cycle progression in OESCC we compared the expression of 84 cell cycle regulated genes in p38 δ positive (KE-6), p38 δ negative (KE-3) and p-p38 δ positive (KE-3 pcDNA3-MKK6b(E)-(Gly-Glu)₅-FLAG-p38 δ) oesophageal squamous carcinoma cell lines using an RT² Profiler human cell cycle PCR array (Qiagen, Manchester, UK). Genes analysed by the array include positive and negative regulators of the cell cycle, phase transitions, checkpoints, and DNA replication. The complete list of genes and their functional categories are outlined in Table 7.1.

Table 7.1 RT² Profiler Human Cell Cycle PCR array gene table

Gene	Description	Category
ABL1	c-abl oncogene 1, non-receptor tyrosine kinase	2/6
ANAPC2	Anaphase promoting complex subunit 2	1/3/6
ATM	Ataxia telangiectasia mutated	5/7
ATR	Ataxia telangiectasia and Rad3 related	5/6
AURKA	Aurora kinase A	6
AURKB	Aurora kinase B	4
BCCIP	BRCA2 and CDKN1A interacting protein	3/6
BCL2	B-cell CLL/lymphoma 2	6
BIRC5	Baculoviral IAP repeat containing 5	3
BRCA1	Breast cancer 1, early onset	5/7
BRCA2	Breast cancer 2, early onset	5/6
CASP3	Caspase 3, apoptosis-related cysteine peptidase	5/7
CCNA2	Cyclin A2	3/5
CCNB1	Cyclin B1	3/6
CCNB2	Cyclin B2	4/6
CCNC	Cyclin C	6
CCND1	Cyclin D1	1/6
CCND2	Cyclin D2	6
CCND3	Cyclin D3	6
CCNE1	Cyclin E1	1/6
CCNF	Cyclin F	4/6
CCNG1	Cyclin G1	3
CCNG2	Cyclin G2	5
CCNH	Cyclin H	3/6
CCNT1	Cyclin T1	3/6
CDC16	Cell division cycle 16 homolog (<i>S. cerevisiae</i>)	4/6
CDC20	Cell division cycle 20 homolog (<i>S. cerevisiae</i>)	4/6
CDC25A	Cell division cycle 25 homolog A (<i>S. pombe</i>)	1/3/5
CDC25C	Cell division cycle 25 homolog C (<i>S. pombe</i>)	4/5/6
CDC34	Cell division cycle 34 homolog (<i>S. cerevisiae</i>)	1/5
CDC6	Cell division cycle 6 homolog (<i>S. cerevisiae</i>)	2/4/6

CDK1	Cyclin-dependent kinase 1	4/5/6
CDK2	Cyclin-dependent kinase 2	5/6
CDK4	Cyclin-dependent kinase 4	1/6
CDK5R1	Cyclin-dependent kinase 5, regulatory subunit 1 (p35)	3/6
CDK5RAP1	CDK5 regulatory subunit associated protein 1	3
CDK6	Cyclin-dependent kinase 6	1/6
CDK7	Cyclin-dependent kinase 7	3/6
CDK8	Cyclin-dependent kinase 8	6
CDKN1A	Cyclin-dependent kinase inhibitor 1B (p21, Cip1)	5/6
CDKN1B	Cyclin-dependent kinase inhibitor 1B (p27, Kip1)	1/5/6
CDKN2A	Cyclin-dependent kinase inhibitor 2A (melanoma, p16, inhibits CDK4)	5
CDKN2B	Cyclin-dependent kinase inhibitor 2B (p15, inhibits CDK4)	5/7
CDKN3	Cyclin-dependent kinase inhibitor 3	1/3/5
CHEK1	CHK1 checkpoint homolog (<i>S. pombe</i>)	5
CHEK2	CHK2 checkpoint homolog (<i>S. pombe</i>)	5
CKS1B	CDC28 protein kinase regulatory subunit 1B	3/6
CKS2	CDC28 protein kinase regulatory subunit 2	3
CUL1	Cullin 1	1/5
CUL2	Cullin 2	1/5
CUL3	Cullin 3	1/5
E2F1	E2F transcription factor 1	1/6
E2F4	E2F transcription factor 4, p107/p130-binding	6
GADD45A	Growth arrest and DNA-damage-inducible, alpha	5/6
GTSE1	G-2 and S-phase expressed 1	3
HUS1	HUS checkpoint homolog (<i>S. pombe</i>)	5
KNTC1	Kinetochores associated 1	5/6
KPNA2	Karyopherin alpha 2 (RAG cohort 1, importin alpha 1)	3
MAD2L1	MAD2 mitotic arrest deficient-like 1 (yeast)	5
MAD2L2	MAD2 mitotic arrest deficient-like 2 (yeast)	5
MCM2	Minichromosome maintenance complex component 2	2
MCM3	Minichromosome maintenance complex component 3	2

MCM4	Minichromosome maintenance complex component 4	2
MCM5	Minichromosome maintenance complex component 5	2
MDM2	Mdm2 p53 binding protein homolog (mouse)	5
MKI67	Antigen identified by monoclonal antibody Ki-67	6
MNAT1	Menage a trois homolog 1, cyclin H assembly factor (<i>Xenopus laevis</i>)	3
MRE11A	MRE11 meiotic recombination 11 homolog A (<i>S. cerevisiae</i>)	4
NBN	Nibrin	5
RAD1	RAD1 homolog (<i>S. pombe</i>)	5
RAD17	RAD17 homolog (<i>S. pombe</i>)	5
RAD51	RAD51 homolog (<i>S. cerevisiae</i>)	4
RAD9A	RAD9 homolog A (<i>S. pombe</i>)	5/6
RB1	Retinoblastoma 1	5/6
RBBP8	Retinoblastoma binding protein 8	5
RBL1	Retinoblastoma-like 1 (p107)	7
RBL2	Retinoblastoma-like 2 (p130)	7
SERTAD1	SERTA domain containing 1	3
SKP2	S-phase kinase-associated protein 2 (p45)	1/6
STMN1	Stathmin 1	4
TFDP1	Transcription factor Dp-1	6
TFDP2	Transcription factor Dp-2 (E2F dimerization partner 2)	6
TP53	Tumour protein p53	5/7
WEE1	WEE1 homolog (<i>S. pombe</i>)	2/5/6

Categories of function gene grouping: 1, G₁ phase and G₁/S transition; 2, S phase and DNA replication; 3, G₂ phase and G₂/M transition; 4, M phase; 5, cell cycle checkpoint and cell cycle arrest; 6, regulation of cell cycle; 7, negative regulation of cell cycle (www.sabiosciences.com)

7.4 Materials and methods

7.4.1 Cell culture

KE-3 and KE-6 cell lines as well as stably transfected KE-3 pcDNA3-MKK6b(E)-(Gly-Glu)₅-FLAG-p38 δ (KE-3 p-p38 δ) cells were cultured as described in Chapter 2.

7.4.2 Cell cycle gene expression analysis

Nucleic acid isolation

Total cellular RNA was isolated from KE-3, KE-6 and KE-3 p-p38 δ cells using an RNeasy Mini Kit (Qiagen, Manchester, UK) as outlined in Chapter 2.

cDNA synthesis

500ng high quality RNA (A_{260}/A_{280} 1.8 to 2.0, $A_{260}/A_{230} > 1.7$) was converted into cDNA using an RT² First Strand cDNA kit according to manufacturer's instructions (Qiagen, Manchester, UK). Each RNA sample was combined with genomic DNA elimination mix (Buffer GE) and incubated for 5 min at 42°C before being placed on ice for ≥ 1 min. Reverse transcription mix (Buffer BC3, Control P2, RE3 Reverse Transcriptase Mix) was added to each genomic DNA elimination reaction and incubated at 42°C for 15 min. The reaction was stopped by incubating at 95°C for 5 min. RNase-free H₂O was added to each reaction and reactions were placed on ice before proceeding immediately with the RT² Profiler PCR array assay.

RT² Profiler PCR array

Cell cycle gene expression in KE-3, KE-6 and KE-3 p-p38 δ cells was determined using the Cell Cycle RT² Profiler PCR array (PAHS-020Z) according to the manufacturer's instructions (Qiagen, Manchester, UK). RT² SYBR Green Mastermix was centrifuged for 15 s to bring contents to the bottom of the tube. The cDNA synthesis reaction was combined with RT² SYBR Green Mastermix and RNase-free H₂O in a loading reservoir before being dispensed into each well of the RT² Profiler PCR array.

RT² Profiler PCR array layout is outlined in Figure 7.2. As well as the 84 cell cycle focused genes, arrays included five housekeeping genes to enable normalization of data. In addition, one well in each array contained a gDNA control (GDC) to specifically detect nontranscribed genomic DNA contamination. Reverse transcription controls (RTC; 3 replicate wells per array) tested the efficiency of the RT² First Strand Kit reverse-transcription reaction by detecting template synthesised from the kits built-in external RNA control. Finally, the efficiency of the PCR reaction itself was tested in 3 replicate wells containing a predisposed artificial DNA sequence and the assay which detects it (positive PCR control, PPC).

ABL1 A01	ANAPC2 A02	ANAPC4 A03	DIRAS3 A04	ATM A05	ATR A06	BAX A07	BCCIP A08	BCL2 A09	BIRC5 A10	BRCA1 A11	BRCA2 A12
CCNB1 B01	CCNB2 B02	CCNC B03	CCND1 B04	CCND2 B05	CCNE1 B06	CCNF B07	CCNG1 B08	CCNG2 B09	CCNH B10	CCNT1 B11	CCNT2 B12
CDC16 C01	CDK1 C02	CDC20 C03	CDC34 C04	CDK2 C05	CDK4 C06	CDK5R1 C07	CDK5RAP1 C08	CDK6 C09	CDK7 C10	CDK8 C11	CDKN1A C12
CDKN1B D01	CDKN2A D02	CDKN2B D03	CDKN3 D04	CHEK1 D05	CHEK2 D06	CKS1B D07	CKS2 D08	CUL1 D09	CUL2 D10	CUL3 D11	DDX11 D12
DNM2 E01	E2F4 E02	GADD45A E03	GTF2H1 E04	GTSE1 E05	HERC5 E06	HUS1 E07	KNTC1 E08	KPNA2 E09	MAD2L1 E10	MAD2L2 E11	MCM2 E12
MCM3 F01	MCM4 F02	MCM5 F03	MIK167 F04	MINAT1 F05	MRE11A F06	NBN F07	PCNA F08	RAD1 F09	RAD17 F10	RAD51 F11	RAD9A F12
RB1 G01	RBBP8 G02	RBL1 G03	RBL2 G04	RPA3 G05	SERTAD1 G06	SKP2 G07	SUMO1 G08	TFDP1 G09	TFDP2 G10	TP53 G11	UBA1 G12
B2M H01	HPRT1 H02	RPL13A H03	GAPDH H04	ACTB H05	HGDC H06	RTC H07	RTC H08	RTC H09	PPC H10	PPC H11	PPC H12

Figure 7.2 RT² Profiler PCR array layout. Wells A1 to G12 each contain a real-time PCR assay for a cell cycle related gene. Wells H1 to H5 (yellow) contain a housekeeping gene panel to normalize array data. Well H6 (red) contains a g DNA control (GDC). Wells H7 to H9 (green) contain replicate reverse-transcription controls (RTC). Wells H10 to H12 (blue) contain replicate positive PCR controls (PPC).

RT² Profiler PCR array plates were sealed with optical adhesive film (Applied Biosystems, Life Technologies, Grand Island, NY, USA). Arrays underwent thermal cycling according to the conditions outlined in Table 7.2 in an ABI 7500 Real-Time PCR System (Applied Biosystems, Life Technologies, Grand Island, NY, USA).

Table 7.2 RT² Profiler PCR array reaction conditions

Step	Temperature °C	Time	Cycles
Activation of HotStart DNA Taq Polymerase	95	10 min	1
	95	15 s	40
Fluorescence data collection	60	1 min	

Data analysis

Data analysis was performed using the $\Delta\Delta C_T$ method according to the formula below [18] and aided by the SABiosciences data analysis website www.SABiosciences.com/pcrarraydataanalysis.php. Baseline was set automatically. Cycle threshold value was set in the linear exponential phase of the amplification plot and kept the same across all arrays.

$$\Delta\Delta C_T = \Delta C_T \text{ Sample}(C_T^{\text{GOI}} - C_T^{\text{HKG}}) - \Delta C_T \text{ Control}(C_T^{\text{GOI}} - C_T^{\text{HKG}})$$

where GOI is the gene of interest and HKG is the housekeeping genes used for normalization.

C_T values >35 for the gDNA control wells were considered acceptable as the level of gDNA contamination was too low to affect gene expression profiling results. RTC values were analysed by calculating

$$\Delta C_T = \text{AVG } C_T^{\text{RTC}} - \text{AVG } C_T^{\text{PPC}}$$

A value <5 was considered acceptable as an indication that no inhibition of the reverse transcription reaction had occurred. For PPC wells an average C_T^{PPC} value of 20 ± 2 on each array and variation ≤ 2 cycles between arrays was accepted.

7.5 Results

7.5.1 Relative cell cycle gene expression in p38 δ MAPK negative (KE-3) versus p38 δ MAPK positive (KE-6) OESCC

p38 δ MAPK negative cells proliferate at a significantly faster rate than p38 δ MAPK positive cells (Chapter 4) [19]. In order to identify the pathway(s) responsible for differential regulation of proliferation in p38 δ MAPK negative and p38 δ MAPK positive OESCC, this study compared the relative expression of 84 cell cycle associated genes (Table 7.1) between KE-3 (p38 δ MAPK negative) and KE-6 (p38 δ MAPK positive) OESCC cells. Two criteria were used to define a meaningful difference in gene expression between the KE-3 and KE-6 groups: the average relative expression in three independent experiments must be (1) increased or decreased by ≥ 2 -fold and (2) must be statistically significant following application of Student's *t*-test ($p < 0.05$). Figure 7.3 displays a scatter plot analysis of the results obtained from the RT² Profiler PCR array. Thirty cell cycle associated genes demonstrated at least a 2-fold difference in gene expression between the p38 δ MAPK negative and p38 δ MAPK positive cells. Downregulation was observed in nine genes, while twenty-one genes appeared to be upregulated in the p38 δ MAPK negative KE-3 cells (Figure 7.3). Fold regulation of the 21 genes which satisfied the dual criteria outlined above are listed in Table 7.3.

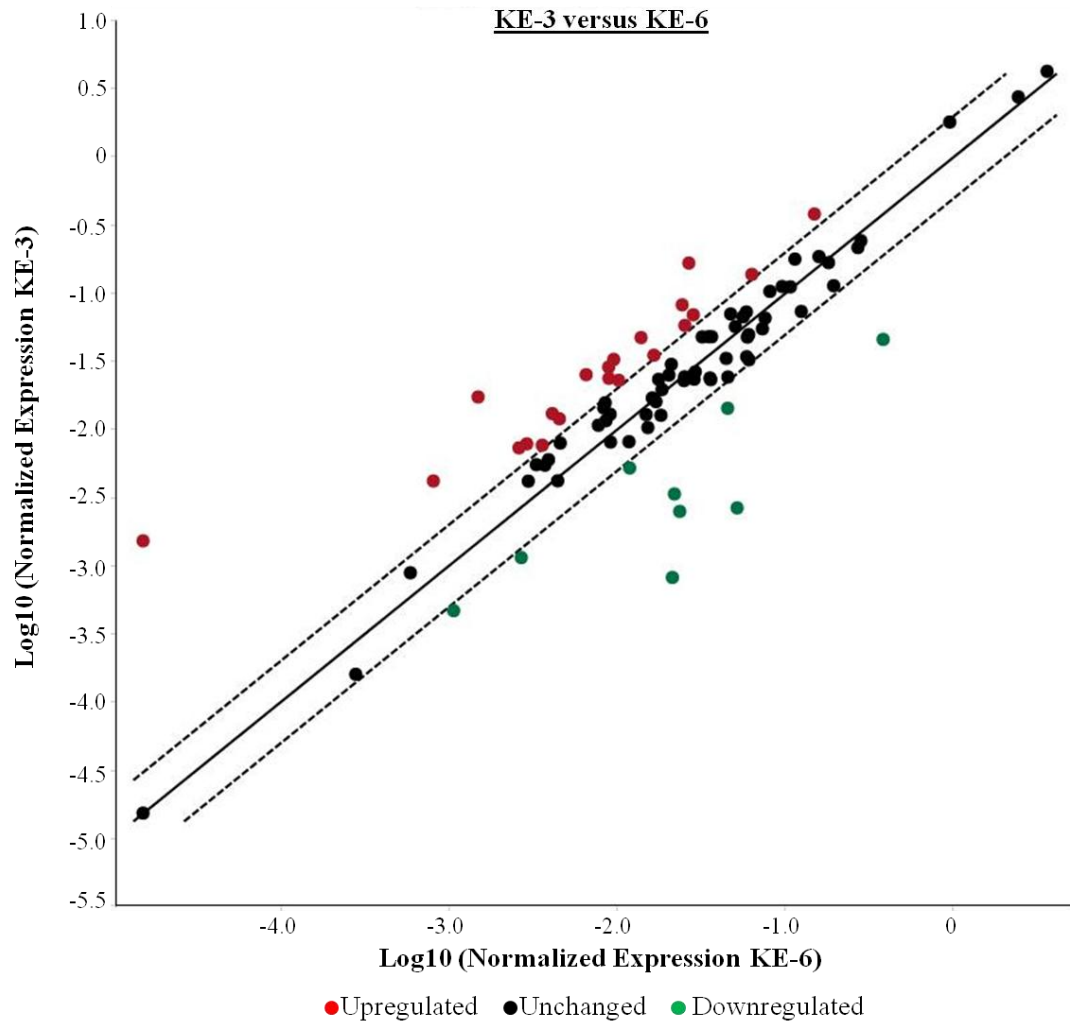


Figure 7.3 Relative expression comparison for 84 cell cycle associated genes between p38 δ MAPK negative (KE-3) and p38 δ MAPK positive (KE-6) OESCC. Depicted is a log₁₀ transformation plot of the normalized relative expression level of each gene between KE-3 (y-axis) and KE-6 (x-axis) cells. Dotted lines indicate a 2-fold change in gene expression threshold. Results shown are mean fold change of mRNA expression from three independent experiments.

Table 7.3 Changes in fold regulation for cell cycle associated genes between p38 δ MAPK negative (KE-3) and p38 δ MAPK positive (KE-6) OESCC

Gene	Fold Regulation KE-3/KE-6	p value
CCND2	101.42	0.038890
CCNG1	6.22	0.015122
ATM	5.21	0.003923
MRE11A	3.86	0.043477
CUL1	3.40	0.034541
CCNE1	3.23	0.047776
BIRC5	2.72	0.000828
CHEK1	2.66	0.036834
KPNA2	2.54	0.028599
WEE1	2.44	0.045845
CUL2	2.29	0.020438
BCCIP	2.16	0.045158
CDC16	2.12	0.020739
BCL2	-2.27	0.003914
ATR	-2.28	0.000936
RB1	-3.18	0.002726
CDKN1A	-6.52	0.000011
CCND1	-8.36	0.000138
CDKN1B	-9.41	0.000597
CDK6	-19.48	0.000204
CCNC	-25.95	0.000229

7.5.2 Relative cell cycle gene expression in p-p38 δ MAPK positive versus p38 δ MAPK negative KE-3 OESCC

Introduction of p-p38 δ MAPK expression in KE-3 cells significantly decreases the rate of proliferation (Chapter 4) [19]. The second RT² Profiler PCR experiment was designed to identify any changes in cell cycle gene expression induced by expression of p-p38 δ MAPK in KE-3 cells. The relative expression of 84 cell cycle associated genes (Table 7.1) was compared between stably transfected KE-3 p-p38 δ cells and p38 δ MAPK negative KE-3 cells. The dual criteria for meaningful changes in gene expression outlined above were also applied here. Of the 84 genes examined in the array, seven demonstrated at least a 2-fold difference in gene expression between KE-3 p-p38 δ and WT KE-3 cells. Of these seven differentially expressed genes one (CDK6) appeared to be upregulated in p-p38 δ expressing cells while six were downregulated (ANAPC2, CCNT1, CDKN2B, MCM3, MREIIA, WEE1) (Figure 7.4). All genes analysed by the RT² Profiler PCR array failed to satisfy the dual criteria as none of the alterations in gene expression observed were found to be statistically significant.

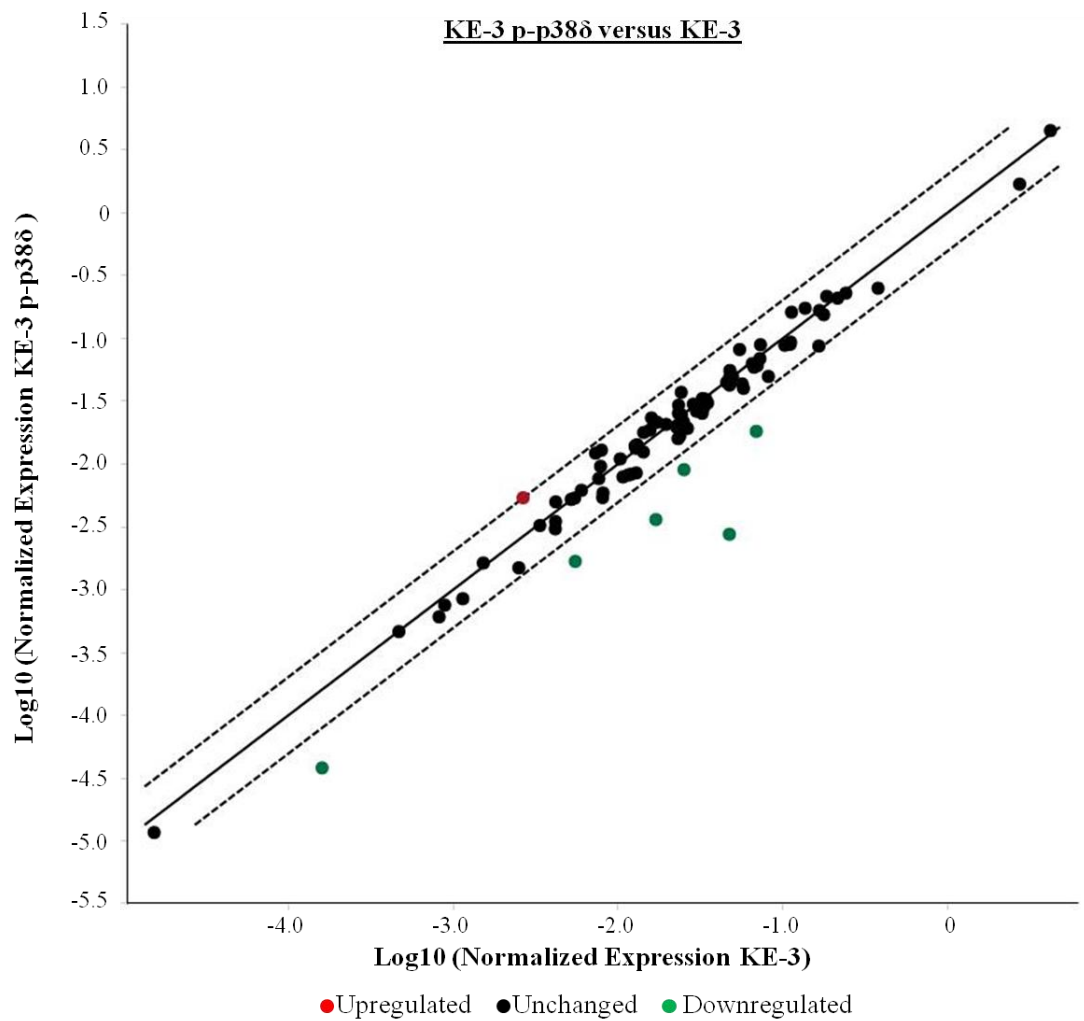


Figure 7.4 Relative expression comparison for 84 cell cycle associated genes between KE-3 p-p38 δ MAPK and KE-3 cells. Depicted is a log10 transformation plot of the normalized relative expression level of each gene between KE-3 (x-axis) and KE-3 p-p38 δ (y-axis) cells. Dotted lines indicate a 2-fold change in gene expression threshold. Results shown are mean fold change of mRNA expression from three independent experiments.

7.6 Discussion

A key mechanism by which p38 α MAPK is thought to control cell cycle progression is through the D-type cyclins [9-11]. Induction of cyclin D1, -2 and -3 expression is an early event during G₁ to S phase transition. Co-expression of MKK3 and p38 α MAPK in CCL39 cells significantly inhibited cyclin D1 expression while inhibition of p38 α MAPK activity with SB203580 enhanced cyclin D1 mRNA and protein levels [10]. In this study we did not observe any increase in cyclin D1 expression between in p38 δ MAPK negative cells compared with p38 δ MAPK positive cells. In fact, there was a significant ($p < 0.001$) 8-fold decrease in cyclin D1 expression detected between p38 δ MAPK positive KE-6 cells and p38 δ MAPK negative KE-3 cells. On the other hand, cyclin D2 expression was significantly ($p < 0.05$) upregulated by >100-fold in p38 δ MAPK negative KE-3 cells. This suggests that while p38 α MAPK may regulate the cell cycle through inhibition of cyclin D1, p38 δ MAPK may act preferentially on cyclin D2. The lack of p38 δ MAPK expression in KE-3 cells therefore removes inhibition of cyclin D2 expression. Cyclins E1 and G1 are also significantly upregulated in KE-3 cells compared to KE-6 cells (3-fold and 6-fold respectively, $p < 0.05$). These cyclins may also play a role in driving the increased proliferation observed in KE-3 cells.

The decreased expression of CDKIs, negative regulators of G₁ to S phase transition, is another mechanism by which p38 δ MAPK may exert its effects on cell proliferation in KE-3 cells. The expression of both CDKN1B (p27) and CDKN1A (p21), is significantly downregulated (>9-fold and >6-fold respectively, $p < 0.001$) in p38 δ MAPK negative KE-3 cells compared with p38 δ MAPK positive KE-6 cells.

Induction of p21 expression in keratinocytes has previously been shown to be mediated by p38 δ MAPK activation of p53 expression [17]. However we did not observe any changes in p53 expression between KE-6 and KE-3 cells. It is possible that reduced phosphorylation of p53 protein in the absence of p38 δ MAPK rather than decreased mRNA is responsible for the decrease in p21 expression in KE-3 cells, as has been previously described [16]. The significant differences in the rates of proliferation of KE-3 and KE-6 cells observed in Chapter 4 may therefore be the result of decreased p53 and p21-mediated G₁ phase arrest in the p38 δ MAPK-negative KE-3 cells.

It is important to note that not all differences in gene expression between KE-3 and KE-6 cells can be attributed to differential p38 δ MAPK expression. As KE-3 and KE-6 cells are separate cell lines arising from distinct individuals, the differing gene expression profiles could be caused by other factors such as different karyotypes and gene copy numbers.

The absence of statistically significant changes in cell cycle gene expression between KE-3 p-p38 δ and WT KE-3 cells was somewhat surprising as the differences in proliferation between these cells is so striking (Figure 4.8). The 84 genes analysed by the array represent a subset of human genes which are involved in the cell cycle. Changes in expression of cell cycle associated genes which are not included in the array may be responsible for the effect of p38 δ and p-p38 δ MAPK on KE-3 proliferation. Furthermore it is possible that the effect of (p-)p38 δ MAPK expression on proliferation may not be occurring at a transcriptional level but rather is a result of altered kinase activity. Further research into the role of p38 δ MAPK signalling in

OESCC would benefit from the use of kinase profiling analysis. By using arrays which measure differences in kinase phosphorylation levels rather than expression, the signalling pathway responsible for the differences in proliferation between p38 δ MAPK negative and p38 δ /p-p38 δ MAPK positive cells could be delineated.

In this study, differentially expressed genes were defined as those with a fold change in expression between two groups of ≥ 2 and a p value of < 0.05 . The advantage of this approach is that it integrates the concepts of statistically significant differences in gene expression (based on p value) and a biologically meaningful difference in expression (fold change). However, depending on the choice of fold change threshold and statistical significance cut-off, alternative interpretations of the array data set are possible. Quantitative rt-PCR analysis of individual differentially expressed genes would be beneficial to validate the RT² Profiler PCR array gene expression results. Western blots or ELISA may also be performed to determine whether the observed differences in gene expression represent changes at the protein level.

7.7 References

1. Han, J., et al., *A MAP kinase targeted by endotoxin and hyperosmolarity in mammalian cells*. *Science*, 1994. **265**(5173): p. 808-11.
2. Ambrosino, C. and A.R. Nebreda, *Cell cycle regulation by p38 MAP kinases*. *Biol Cell*, 2001. **93**(1-2): p. 47-51.
3. Ono, K. and J. Han, *The p38 signal transduction pathway: activation and function*. *Cell Signal*, 2000. **12**(1): p. 1-13.
4. Molnar, A., et al., *Cdc42Hs, but not Rac1, inhibits serum-stimulated cell cycle progression at G1/S through a mechanism requiring p38/RK*. *J Biol Chem*, 1997. **272**(20): p. 13229-35.
5. Philips, A., et al., *Differential effect of Rac and Cdc42 on p38 kinase activity and cell cycle progression of nonadherent primary mouse fibroblasts*. *J Biol Chem*, 2000. **275**(8): p. 5911-7.
6. Kishi, H., et al., *Osmotic shock induces G1 arrest through p53 phosphorylation at Ser33 by activated p38MAPK without phosphorylation at Ser15 and Ser20*. *J Biol Chem*, 2001. **276**(42): p. 39115-22.
7. Kim, G.Y., et al., *The stress-activated protein kinases p38 alpha and JNK1 stabilize p21(Cip1) by phosphorylation*. *J Biol Chem*, 2002. **277**(33): p. 29792-802.
8. Xiu, M., et al., *The transcriptional repressor HBPI is a target of the p38 mitogen-activated protein kinase pathway in cell cycle regulation*. *Mol Cell Biol*, 2003. **23**(23): p. 8890-901.
9. Casanovas, O., et al., *Osmotic stress regulates the stability of cyclin D1 in a p38SAPK2-dependent manner*. *J Biol Chem*, 2000. **275**(45): p. 35091-7.
10. Lavoie, J.N., et al., *Cyclin D1 expression is regulated positively by the p42/p44MAPK and negatively by the p38/HOGMAPK pathway*. *J Biol Chem*, 1996. **271**(34): p. 20608-16.
11. Kida, A., et al., *Glycogen synthase kinase-3beta and p38 phosphorylate cyclin D2 on Thr280 to trigger its ubiquitin/proteasome-dependent degradation in hematopoietic cells*. *Oncogene*, 2007. **26**(46): p. 6630-40.
12. Bulavin, D.V., et al., *Initiation of a G2/M checkpoint after ultraviolet radiation requires p38 kinase*. *Nature*, 2001. **411**(6833): p. 102-7.
13. Takenaka, K., T. Moriguchi, and E. Nishida, *Activation of the protein kinase p38 in the spindle assembly checkpoint and mitotic arrest*. *Science*, 1998. **280**(5363): p. 599-602.
14. Llopis, A., et al., *The stress-activated protein kinases p38alpha/beta and JNK1/2 cooperate with Chk1 to inhibit mitotic entry upon DNA replication arrest*. *Cell Cycle*, 2012. **11**(19): p. 3627-37.
15. Wang, X., et al., *Involvement of the MKK6-p38gamma cascade in gamma-radiation-induced cell cycle arrest*. *Mol Cell Biol*, 2000. **20**(13): p. 4543-52.

16. Hawkes, W.C. and Z. Alkan, *Delayed cell cycle progression in selenoprotein W-depleted cells is regulated by a mitogen-activated protein kinase kinase 4-p38/c-Jun NH2-terminal kinase-p53 pathway*. J Biol Chem, 2012. **287**(33): p. 27371-9.
17. Saha, K., et al., *p38 δ Regulates p53 to Control p21Cip1 Expression in Human Epidermal Keratinocytes*. Journal of Biological Chemistry, 2014.
18. Livak, K.J. and T.D. Schmittgen, *Analysis of relative gene expression data using real-time quantitative PCR and the 2(-Delta Delta C(T)) Method*. Methods, 2001. **25**(4): p. 402-8.
19. O'Callaghan, C., et al., *Loss of p38delta mitogen-activated protein kinase expression promotes oesophageal squamous cell carcinoma proliferation, migration and anchorage-independent growth*. Int J Oncol, 2013. **43**(2): p. 405-15.

Chapter 8

General Discussion

8.1 Discussion

Interestingly, the p38 family of kinases can both positively and negatively regulate a host of cellular processes such as proliferation, migration and apoptosis [1]. The dysregulation of these normal cell functions is critical for malignant transformation and as a result significant roles for the p38 MAPK signalling pathway in cancer have previously been outlined [2]. However, these roles are generally attributed to the best characterised isoform, p38 α MAPK. The individual contributions by the other isoforms, particularly p38 δ MAPK, remain unclear. Depending on cell type, p38 α MAPK can act as either a tumour promoter or a tumour suppressor [3, 4]. The limited information available pertaining to p38 δ MAPK would appear to suggest similar dual roles. p38 δ MAPK has been shown to promote proliferation and invasion in HNSCC [5]. Furthermore, it is required for the development of skin carcinoma and lung tumourigenesis in mice, clearly demonstrating a pro-oncogenic role for this isoform [6]. On the other hand, p38 δ MAPK has been characterised as a tumour suppressor in MEFs where p38 δ ^{-/-} MEFs displayed increased migration and impaired contact inhibition compared to WT MEFs [7]. Similarly, in melanoma cells and brain metastases of TNBC, introduction of p38 δ MAPK expression significantly reduces cell proliferation [8, 9].

The findings we present in this thesis support some of the studies which suggest an anti-tumourigenic role for p38 δ MAPK. We have established that p38 δ MAPK functions as a tumour suppressor in OESCC. The loss of p38 δ MAPK expression which we observed in 50% of OESCC cell lines and *in vivo* appears to be a significant event which contributes to the tumourigenicity of OESCC. Importantly,

we have demonstrated in our studies that re-introduction of p38 δ MAPK can reverse these oncogenic effects. Expression of p38 δ MAPK reduces not only OESCC proliferation but also impairs cell migration and the capacity for anchorage-independent growth. Of note, these anti-proliferative and anti-migratory effects were further enhanced upon expression of p-p38 δ MAPK. As we observed some phosphorylation of p38 δ MAPK in KE-3 cells transfected with WT p38 δ MAPK (as demonstrated by ELISA analysis of specific p38 δ MAPK phosphorylation), it is possible that activation and/or expression of p38 δ MAPK is driving the anti-tumourigenic effects observed in transfected KE-3 cells.

Recent documented roles for p38 δ MAPK in human diseases ranging from neurodegenerative disorders to diabetes is fuelling increased interest in the development of p38 δ MAPK specific inhibitors [10]. Based on our research findings focusing on the identification of specific p38 δ MAPK activators is also warranted. The PP1 and PP2A serine/threonine protein phosphatase inhibitor OA can specifically activate p38 δ MAPK (without affecting p38 α , - β , or - γ MAPKs) in keratinocytes [11, 12]. Attempts by our group to replicate these results in OESCC have to-date been unsuccessful. Based on our research findings we observed that activated p-p38 δ MAPK (more so than simply expression of p38 δ MAPK) can further decrease proliferation, migration and anchorage-independent growth in OESCC. Thus, future development of specific p38 δ MAPK activators may present a potential future therapeutic strategy in the treatment of p38 δ MAPK positive OESCC. Furthermore, the identification of specific p38 δ MAPK activators, as well as inhibitors, could also afford us the opportunity to delineate novel p38 δ MAPK functions. The lack of such compounds has to date been the main limiting factor in

the future studies of p38 δ MAPK. This may in turn identify further diseases where p38 δ MAPK could be a potential therapeutic target.

Neoadjuvant chemotherapy, alone or in combination with chemoradiotherapy, is now considered the standard approach for locally advanced oesophageal cancer. Unfortunately, OESCC is a particularly drug-resistant disease [13]. Single-drug treatments yield poor response rates of 10-25%. Although the combination of fluoropyrimidine and platinum agents can achieve greater tumour reduction, it has little effect on overall survival time and recurrence is common [14, 15]. Meta-analyses of neoadjuvant therapy trials indicate that patient response to chemotherapy is variable regardless of clinical stage and 60-70% of patients do not respond well to neoadjuvant treatments [16, 17]. Very recently, a number of biomarkers which may predict patient response to neoadjuvant therapy in oesophageal cancer have been identified by examining gene expression patterns, single nucleotide polymorphisms (SNPs) and microRNAs (miRNAs) (reviewed by [13]). Several gene expression microarray studies have highlighted different gene expression patterns which can discriminate between oesophageal cancer patients which respond to treatment and those which are resistant with a high degree of sensitivity and specificity [18-20]. However, while gene expression profiling for breast cancer has now translated to use in the clinical setting, further research is required to develop such a clinically useful predictive test for oesophageal cancer [21]. The association between SNPs in genes involved in DNA base excision repair and oesophageal cancer patient response to chemo- and radiotherapy has also been investigated. Particular SNPs in the XRCC1 and ERCC1 genes have been found to be predictive of therapy response [22, 23]. As above, further validation studies for the predictive potential of SNPs in oesophageal

cancer are required. Abnormal expression patterns for microRNAs (miRNAs), short non-coding RNA sequences which inhibit mRNA translation, have been detected in oesophageal cancers [24]. Several miRNAs have been identified as having prognostic value in oesophageal cancer. miR-296 is of particular interest as it is significantly differentially expressed between treatment responsive and non-responsive patient groups and its inhibition increases oesophageal cancer cell sensitivity to chemotherapy [25]. However, while clinical trials evaluating miRNA biomarkers in breast and ovarian carcinomas are ongoing [26], the clinical application of miRNAs as predictive markers in oesophageal cancer remains to be examined.

Interestingly our research adds to the list of biomarkers making p38 δ MAPK a new possible predictive marker for patient response to chemotherapy in OESCC. As well as the conventional combination of cisplatin and 5-fluorouracil (CF), we have outlined a greater response of OESCC to the triple combination of doxorubicin, cisplatin and 5-fluorouracil (ACF). Although such triple therapy is not considered as standard treatment, it is presently used for patients with OESCC in Japan and its efficacy and safety is well reported [27-29]. Thus, further investigation is warranted on a more global scale to determine whether ACF treatment can provide greater benefits for p38 δ MAPK negative OESCC patients compared with CF treatment, particularly in terms of overall survival. Based on our results p38 δ MAPK phenotyping of tumour tissue may prove useful in determining the optimal treatment strategy in individual OESCC patients.

Aberrant DNA methylation has previously been reported in oesophageal cancer and is associated with the silencing of tumour suppressors and cell cycle regulatory genes [30]. We detected hypermethylation of the MAPK13 promoter in three of the four p38 δ MAPK negative cell lines examined when compared with p38 δ MAPK positive cell lines. For the fourth cell line we examined only a portion of the CpG sites present in the MAPK13 promoter. Thus, it is possible that these cells are also epigenetically regulated by hypermethylation but at a different location in the MAPK13 promoter. Redesigning of primers used for BSP to amplify an alternative region of the MAPK13 promoter could identify differential methylation of CpG sites in these cells. Alternatively, other methods of detecting DNA methylation are available, such as bisulfite melting curve analysis which would assess DNA methylation across the promoter region rather than at individual CpG sites [31]. Aberrant methylation of the MAPK13 promoter region has previously been reported in mesothelioma and melanoma therefore epigenetic control of p38 δ MAPK is a likely explanation for its differential expression in OESCC [8, 32].

Presently, we are unable to definitively confirm epigenetic regulation of p38 δ MAPK in OESCC. Epigenetic silencing of p38 δ MAPK has been outlined in melanoma cells where 5'-aza-2'-deoxycytidine treatment induced a significant increase in p38 δ MAPK expression [8]. Our attempts to induce p38 δ MAPK expression in hypermethylated cells with 5'-aza-2'-deoxycytidine treatment were not successful mainly due to inadequate optimisation. We could not determine the methylation status of MAPK13 promoter sites following 5'-aza-2'-deoxycytidine treatment. As a result, we cannot comment on whether p38 δ MAPK expression remained unchanged because 5'-aza-2'-deoxycytidine treatment was not effective in

demethylating DNA or because the observed DNA methylation is not causing epigenetic regulation. At this juncture further experimentation is warranted to confirm differential epigenetic control of p38 δ MAPK expression in OESCC. Importantly, research of this nature this could have significant consequences in the clinical setting. DNA methylation biomarkers are increasingly considered as viable tools for the early detection, diagnosis and prognosis of cancer [33]. Comparison of MAPK13 promoter methylation in normal oesophageal, primary tumour and metastatic tissue could provide interesting insights into the potential usefulness of aberrant MAPK13 promoter methylation analysis as a biomarker for OESCC. Presently, 5'-aza'2-deoxycytidine has proven effective in the treatment of leukaemia and myelodysplastic syndromes. Therefore, induction of p38 δ MAPK expression using demethylating agents should be evaluated as a potential treatment strategy in p38 δ MAPK negative OESCC.

As the yeast p38 MAPK homolog HOG1 is an important regulator of the cell cycle, a role for p38 MAPK signalling in cell cycle control has been extensively studied [34]. p38 α MAPK and to an extent p38 β and γ MAPKs, have clearly defined roles in regulating cell cycle progression. However, a role(s) for p38 δ MAPK is clearly lacking. Given the significant pro-proliferative effect that loss of p38 δ MAPK has in OESCC it may be assumed that p38 δ MAPK is a negative regulator of the cell cycle [35-37]. The difference in human cell cycle gene expression that we observed between p38 δ MAPK negative and positive cell lines provides a number of potential mechanisms by which loss of p38 δ promotes cell cycle progression and proliferation. Interestingly, increased expression of cyclins, namely cyclin D2, E1 and G1 was detected in p38 δ MAPK negative cells when compared with OESCC cells which

endogenously express p38 δ MAPK. As p38 α MAPK is a known negative regulator of cyclin D1 expression, in a similar fashion, expression of p38 δ MAPK may decrease the expression of cyclin D2, E1 and/or G1 [38]. Therefore lack of this regulation in p38 δ MAPK negative cells may be responsible for driving the increased proliferation of these cells. Another possible explanation for increased OESCC proliferation in the absence of p38 δ MAPK expression is the downregulation of cyclin-dependent kinase inhibitors. Previous reports have identified specific roles for p38 δ MAPK in controlling p21 expression by upregulating either p53 expression or activation [36, 37]. We observed a significant decrease in p21 expression in p38 δ MAPK negative cells and although no corresponding reduction in p53 expression was detected, decreased p53 phosphorylation in the absence of p38 δ MAPK could be responsible. Although further experimentation is clearly needed to define the mechanisms involved in a role for p38 δ MAPK in OESCC cell cycle control, our research findings have alluded to some potential pathways.

Interestingly, and somewhat surprisingly, we found no differences in cell cycle gene expression between p38 δ MAPK negative and transfected p-p38 δ MAPK positive cells, despite the significant differences in their rates of proliferation. Thus, it may be possible that p-p38 δ MAPK is exerting its effects on OESCC cells at a kinase rather than a transcriptional level. This assumption is also based on our ELISA evidence (in Chapter 4) which demonstrates that WT p38 δ MAPK is phosphorylated when transfected into KE-3 cells. Future research would benefit from examining the signal transduction pathways activated by introduction of p38 δ and p-p38 δ MAPK expression using peptide microarrays (Pamgene, Hertogenbosch, The Netherlands).

These arrays facilitate kinome analysis in cell lysates by immobilizing 144 peptides derived from known human kinase phosphorylation sites on a microarray. Peptide phosphorylation by cell lysates is measured in real-time by a fluorescently labelled anti-phosphotyrosine antibody [39]. Using these arrays to compare the kinomes of p38 δ MAPK negative, p38 δ MAPK positive and p-p38 δ MAPK positive cells may prove worthwhile in contributing to our current understanding of p38 δ MAPK signalling and further advance our knowledge of its specific roles in OESCC.

While our findings to date pertain to the role(s) of p38 δ MAPK in OESCC, it is important to note that they may be also translatable to other cancer types. We have previously reported that renal carcinoma cells fail to express p38 δ MAPK [40] and we have also observed loss of p38 δ MAPK expression in liver, prostate and lung carcinomas (Figure A.1). Thus, it is possible that loss of p38 δ MAPK is also promoting tumourigenicity in these cancers. However, of note p38 α MAPK has been characterised as both a tumour promoter and a tumour suppressor, depending on the cell type [3-5, 41]. Experimental evidence to date provided by us and others suggests that p38 δ MAPK function appears to be similarly context-dependent. Thus, whether p38 δ MAPK plays a pro- or anti-oncogenic role may be cancer type specific.

In final summation of our work, loss of p38 δ MAPK expression, possibly due to MAPK13 promoter methylation, confers a selective advantage in OESCC progression. This may possibly be related to increased cyclin expression and/or downregulation of cyclin-dependent kinase inhibitors. The increased tumourigenicity observed in p38 δ MAPK negative OESCC, combined with reduced sensitivity to conventional chemotherapy (CF), results in a highly aggressive, treatment resistant

disease. Interestingly, the absence of p38 δ MAPK may potentially be an important predictor of increased sensitivity to the triple chemotherapeutic combination of ACF. Introduction of p38 δ MAPK, and especially p-p38 δ MAPK in OESCC cells (which lack endogenous expression) has significant anti-tumourigenic effects. It is unfortunate that to date there are no pharmacological agents currently available which specifically activate p38 δ MAPK. Future development of such activators could potentially be an important therapeutic strategy in the treatment of p38 δ positive OESCC. Importantly, our research findings presented in this thesis may also be translatable to other cancer types which are also p38 δ MAPK negative. Thus, p38 δ MAPK may therefore in the near future be considered as a new potential therapeutic target not only for OESCC but also for a host of other malignancies.

8.2 Future directions

The role of p38 δ MAPK in the cell cycle remains unclear. It would be beneficial to delineate the point in the cell cycle at which p38 δ and p-p38 δ MAPK is exerting an effect. This may provide additional potential targets for the treatment of OESCC. Future studies exploring the function of p38 δ MAPK in the cell cycle should focus on validating the data presented in this thesis but also examine cell cycle components and pathways not included in our analysis. Assessment of the signal transduction pathways activated by p38 δ and p-p38 δ MAPK expression using peptide microarrays should also be considered.

This thesis presents opportunities for further research in the continuation of the studies outlined in Chapters 6 and 7. Future experimentation arising from this thesis should focus initially on generating further knowledge in these areas. Additional research is warranted to create a greater understanding of the epigenetic mechanisms controlling p38 δ MAPK expression in OESCC. Analysis of p38 δ MAPK methylation in OESCC tumour tissue as well as re-establishment of p38 δ MAPK expression in OESCC cell lines through treatment with epigenetic drugs would provide valuable information regarding the epigenetic regulation of this isoform in OESCC. Subsequent analysis of the effects on cell proliferation and chemotherapeutic drug sensitivity could provide a basis for the consideration of epigenetic drugs as a treatment option for p38 δ MAPK negative OESCC.

Opportunities for translational research also arise from the findings presented in this thesis. The potential for p38 δ MAPK to act as a predictive biomarker for treatment response in OESCC should be explored further. The comparison of p38 δ MAPK expression in OESCC patient tumour samples with treatment response and outcome data would be advantageous for the continuation of this research. The Cancer Genome Atlas (TCGA) currently contains exome, SNP, methylation, mRNA, miRNA and clinical data for 185 oesophageal carcinoma samples [42, 43]. Analysis of the data available on TCGA could provide useful information relating to p38 δ MAPK methylation and expression in OESCC as well as providing further insights into the prospective use of p38 δ MAPK as a predictor of patient response.

8.2 References

1. Ono, K. and J. Han, *The p38 signal transduction pathway: activation and function*. Cell Signal, 2000. **12**(1): p. 1-13.
2. Koul, H.K., M. Pal, and S. Koul, *Role of p38 MAP Kinase Signal Transduction in Solid Tumors*. Genes Cancer, 2013. **4**(9-10): p. 342-59.
3. del Barco Barrantes, I. and A.R. Nebreda, *Roles of p38 MAPKs in invasion and metastasis*. Biochem Soc Trans, 2012. **40**(1): p. 79-84.
4. Bulavin, D.V. and A.J. Fornace, Jr., *p38 MAP kinase's emerging role as a tumor suppressor*. Adv Cancer Res, 2004. **92**: p. 95-118.
5. Junttila, M.R., et al., *p38alpha and p38delta mitogen-activated protein kinase isoforms regulate invasion and growth of head and neck squamous carcinoma cells*. Oncogene, 2007. **26**(36): p. 5267-79.
6. Schindler, E.M., et al., *p38delta Mitogen-activated protein kinase is essential for skin tumor development in mice*. Cancer Res, 2009. **69**(11): p. 4648-55.
7. Cerezo-Guisado, M.I., et al., *Evidence of p38 γ and p38 δ involvement in cell transformation processes*. Carcinogenesis, 2011. **32**(7): p. 1093-1099.
8. Gao, L., et al., *Genome-wide promoter methylation analysis identifies epigenetic silencing of MAPK13 in primary cutaneous melanoma*. Pigment Cell Melanoma Res, 2013. **26**(4): p. 542-54.
9. Choi, Y.K., et al., *Brain-metastatic triple-negative breast cancer cells regain growth ability by altering gene expression patterns*. Cancer Genomics Proteomics, 2013. **10**(6): p. 265-75.
10. Alevy, Y.G., et al., *IL-13-induced airway mucus production is attenuated by MAPK13 inhibition*. J Clin Invest, 2012. **122**(12): p. 4555-68.
11. Efimova, T., et al., *Novel protein kinase C isoforms regulate human keratinocyte differentiation by activating a p38 delta mitogen-activated protein kinase cascade that targets CCAAT/enhancer-binding protein alpha*. J Biol Chem, 2002. **277**(35): p. 31753-60.
12. Kraft, C.A., T. Efimova, and R.L. Eckert, *Activation of PKCdelta and p38delta MAPK during okadaic acid dependent keratinocyte apoptosis*. Arch Dermatol Res, 2007. **299**(2): p. 71-83.
13. Uemura, N. and T. Kondo, *Current status of predictive biomarkers for neoadjuvant therapy in esophageal cancer*. World J Gastrointest Pathophysiol, 2014. **5**(3): p. 322-34.
14. Tew, W.P., D.P. Kelsen, and D.H. Ilson, *Targeted therapies for esophageal cancer*. Oncologist, 2005. **10**(8): p. 590-601.
15. Mariette, C., G. Piessen, and J.-P. Triboulet, *Therapeutic strategies in oesophageal carcinoma: role of surgery and other modalities*. The Lancet Oncology, 2007. **8**(6): p. 545-553.

16. GebSKI, V., et al., *Survival benefits from neoadjuvant chemoradiotherapy or chemotherapy in oesophageal carcinoma: a meta-analysis*. *Lancet Oncol*, 2007. **8**(3): p. 226-34.
17. Xu, X.H., et al., *Neoadjuvant chemotherapy for resectable esophageal carcinoma: a meta-analysis of randomized clinical trials*. *Asian Pac J Cancer Prev*, 2012. **13**(1): p. 103-10.
18. Maher, S.G., et al., *Gene expression analysis of diagnostic biopsies predicts pathological response to neoadjuvant chemoradiotherapy of esophageal cancer*. *Ann Surg*, 2009. **250**(5): p. 729-37.
19. Motoori, M., et al., *Prediction of the response to chemotherapy in advanced esophageal cancer by gene expression profiling of biopsy samples*. *Int J Oncol*, 2010. **37**(5): p. 1113-20.
20. Duong, C., et al., *Pretreatment gene expression profiles can be used to predict response to neoadjuvant chemoradiotherapy in esophageal cancer*. *Ann Surg Oncol*, 2007. **14**(12): p. 3602-9.
21. van 't Veer, L.J., et al., *Gene expression profiling predicts clinical outcome of breast cancer*. *Nature*, 2002. **415**(6871): p. 530-6.
22. Wu, X., et al., *Genetic variations in radiation and chemotherapy drug action pathways predict clinical outcomes in esophageal cancer*. *J Clin Oncol*, 2006. **24**(23): p. 3789-98.
23. Warnecke-Eberz, U., et al., *ERCC1 and XRCC1 gene polymorphisms predict response to neoadjuvant radiochemotherapy in esophageal cancer*. *J Gastrointest Surg*, 2009. **13**(8): p. 1411-21.
24. Hu, Y., et al., *Prognostic significance of differentially expressed miRNAs in esophageal cancer*. *Int J Cancer*, 2011. **128**(1): p. 132-43.
25. Hong, L., et al., *The prognostic and chemotherapeutic value of miR-296 in esophageal squamous cell carcinoma*. *Ann Surg*, 2010. **251**(6): p. 1056-63.
26. Zhang, J., et al., *Secretory miRNAs as novel cancer biomarkers*. *Biochim Biophys Acta*, 2012. **1826**(1): p. 32-43.
27. Honda, M., et al., *Doxorubicin, cisplatin, and fluorouracil combination therapy for metastatic esophageal squamous cell carcinoma*. *Dis Esophagus*, 2010. **23**(8): p. 641-5.
28. Yamasaki, M., et al., *p53 genotype predicts response to chemotherapy in patients with squamous cell carcinoma of the esophagus*. *Ann Surg Oncol*, 2010. **17**(2): p. 634-42.
29. Shimakawa, T., et al., *Neoadjuvant chemotherapy (FAP) for advanced esophageal cancer*. *Anticancer Res*, 2008. **28**(4C): p. 2321-6.
30. Baba, Y., M. Watanabe, and H. Baba, *Review of the alterations in DNA methylation in esophageal squamous cell carcinoma*. *Surg Today*, 2013. **43**(12): p. 1355-64.
31. Wojdacz, T.K. and A. Dobrovic, *Melting curve assays for DNA methylation analysis*. *Methods Mol Biol*, 2009. **507**: p. 229-40.

32. Goto, Y., et al., *Epigenetic profiles distinguish malignant pleural mesothelioma from lung adenocarcinoma*. *Cancer Res*, 2009. **69**(23): p. 9073-82.
33. Mikeska, T., et al., *DNA methylation biomarkers in cancer: progress towards clinical implementation*. *Expert Rev Mol Diagn*, 2012. **12**(5): p. 473-87.
34. Duch, A., E. de Nadal, and F. Posas, *The p38 and Hog1 SAPKs control cell cycle progression in response to environmental stresses*. *FEBS Letters*, 2012. **586**(18): p. 2925-2931.
35. O'Callaghan, C., et al., *Loss of p38delta mitogen-activated protein kinase expression promotes oesophageal squamous cell carcinoma proliferation, migration and anchorage-independent growth*. *Int J Oncol*, 2013. **43**(2): p. 405-15.
36. Saha, K., et al., *p38 δ Regulates p53 to Control p21Cip1 Expression in Human Epidermal Keratinocytes*. *Journal of Biological Chemistry*, 2014.
37. Hawkes, W.C. and Z. Alkan, *Delayed cell cycle progression in selenoprotein W-depleted cells is regulated by a mitogen-activated protein kinase kinase 4-p38/c-Jun NH2-terminal kinase-p53 pathway*. *J Biol Chem*, 2012. **287**(33): p. 27371-9.
38. Lavoie, J.N., et al., *Cyclin D1 expression is regulated positively by the p42/p44MAPK and negatively by the p38/HOGMAPK pathway*. *J Biol Chem*, 1996. **271**(34): p. 20608-16.
39. Hilhorst, R., et al., *Peptide microarrays for profiling of serine/threonine kinase activity of recombinant kinases and lysates of cells and tissue samples*. *Methods Mol Biol*, 2013. **977**: p. 259-71.
40. Ambrose, M., et al., *Induction of apoptosis in renal cell carcinoma by reactive oxygen species: involvement of extracellular signal-regulated kinase 1/2, p38delta/gamma, cyclooxygenase-2 down-regulation, and translocation of apoptosis-inducing factor*. *Mol Pharmacol*, 2006. **69**(6): p. 1879-90.
41. Hui, L., et al., *p38alpha: a suppressor of cell proliferation and tumorigenesis*. *Cell Cycle*, 2007. **6**(20): p. 2429-33.
42. The Cancer Genome Atlas Research, N., et al., *The Cancer Genome Atlas Pan-Cancer analysis project*. *Nat Genet*, 2013. **45**(10): p. 1113-1120.
43. The Cancer Genome Atlas Research, N., <https://tcga-data.nci.nih.gov/tcga/tcgaCancerDetails.jsp?diseaseType=ESCA&diseaseName=Esophageal%20carcinoma>.

Appendix I

Plasmid sequences

3481 TCCCGGGAGCTTGTATATCCATTTTCGGATCTGATCAAGAGACAGGATGAGGATCGTTTC
3541 GCATGATTGAACAAGATGGATTGCACGCAGGTTCTCCGGCCGCTTGGGTGGAGAGGCTAT
3601 TCGGCTATGACTGGGCACAACAGACAATCGGCTGCTCTGATGCCGCCGTGTTCCGGCTGT
3661 CAGCGCAGGGGCGCCCGTTCTTTTTGTCAAGACCGACCTGTCCGGTGCCCTGAATGAAC
3721 TGCAGGACGAGGCAGCGCGGCTATCGTGGCTGGCCACGACGGGCGTTCCTTGCGCAGCTG
3781 TGCTCGACGTTGTCACTGAAGCGGAAGGGACTGGCTGCTATTGGGCGAAGTGCCGGGGC
3841 AGGATCTCCTGTCATCTCACCTTGCTCCTGCCGAGAAAGTATCCATCATGGCTGATGCAA
3901 TCGGCGGCTGCATACGCTTGATCCGGCTACCTGCCATTGACCACCAAGCGAAACATC
3961 GCATCGAGCGAGCACGTACTIONCGGATGGAAGCCGGTCTTGTCGATCAGGATGATCTGGACG
4021 AAGAGCATCAGGGGCTCGCGCCAGCCGAACTGTTCCGCCAGGCTCAAGGCGCGCATGCCCG
4081 ACGGCGAGGATCTCGTCGTGACCCATGGCGATGCCTGCTTGCCGAATATCATGGTGGAAA
4141 ATGGCCGCTTTTCTGGATTCATCGACTGTGGCCGGCTGGGTGTGGCGGACCGCTATCAGG
4201 ACATAGCGTTGGCTACCCGTGATATTGCTGAAGAGCTTGGCGGCGAATGGGCTGACCGCT
4261 TCCTCGTGCTTTACGGTATCGCCGCTCCCGATTGCGAGCGCATCGCCTTCTATCGCCTTC
4321 TTGACGAGTTCTTCTGAGCGGGACTCTGGGGTTCGAAATGACCGACCAAGCGACGCCAA
4381 CCTGCCATCACGAGATTTGATTCCACCGCCGCCTTCTATGAAAGGTTGGGCTTCGGAAT
4441 CGTTTTCCGGGACGCCGGCTGGATGATCCTCCAGCGCGGGGATCTCATGCTGGAGTTCTT
4501 CGCCACCCCAACTTGTTTATTGCAGCTTATAATGGTTACAAATAAAGCAATAGCATCAC
4561 AAATTTACAAATAAAGCATTTTTTTTCACTGCATTCTAGTTGTGGTTTTGTCCAAACTCAT
4621 CAATGTATCTTATCATGTCTGTATAACCGTCGACCTCTAGCTAGAGCTTGGCGTAATCATG
4681 GTCATAGCTGTTTCCTGTGTGAAATTGTTATCCGCTCACAATTCCACACAACATACGAGC
4741 CGGAAGCATAAAGTGTAAGCCTGGGGTGCCTAATGAGTGAGCTAACTCACATTAATTGC
4801 GTTGCCTCACTGCCCGCTTTCCAGTCGGGAAACCTGTCGTGCCAGCTGCATTAATGAAT
4861 CGGCCAACGCGCGGGGAGAGGCGGTTTTCGTATTGGGCGCTCTTCCGCTTCTCGCTCAC
4921 TGACTIONGCTCGCTCGGTCGTTCCGGCTGCGGCGAGCGGTATCAGCTCACTCAAAGGCGGT
4981 AATACGGTTATCCACAGAATCAGGGGATAACGCAGGAAAGAACATGTGAGCAAAAGGCCA
5041 GCAAAAGGCCAGGAACCGTAAAAAGGCCGCGTTGCTGGCGTTTTTCCATAGGCTCCGCC
5101 CCCTGACGAGCATCACAAAAATCGACGCTCAAGTCAGAGGTGGCGAAACCCGACAGGACT

5161 ATAAAGATACCAGGCGTTTCCCCCTGGAAGCTCCCTCGTGCCTCTCCTGTTCCGACCCT
5221 GCCGCTTACCGGATACCTGTCCGCCTTTCTCCCTTCGGGAAGCGTGGCGCTTTCTCAATG
5281 CTCACGCTGTAGGTATCTCAGTTCGGTGTAGGTCGTTTCGCTCCAAGCTGGGCTGTGTGCA
5341 CGAACCCCCCGTTCAGCCCGACCGCTGCGCCTTATCCGGTAACTATCGTCTTGAGTCCAA
5401 CCCGGTAAGACACGACTTATCGCCACTGGCAGCAGCCACTGGTAACAGGATTAGCAGAGC
5461 GAGGTATGTAGGCGGTGCTACAGAGTTCCTGAAGTGGTGGCCTAACTACGGCTACACTAG
5521 AAGGACAGTATTTGGTATCTGCGCTCTGCTGAAGCCAGTTACCTTCGAAAAAGAGTTGG
5581 TAGCTCTTGATCCGGCAAACAAACCACCGCTGGTAGCGGTGGTTTTTTTTGTTTGCAAGCA
5641 GCAGATTACGCGCAGAAAAAAGGATCTCAAGAAGATCCTTTGATCTTTTCTACGGGGTC
5701 TGACGCTCAGTGGAACGAAAACCTCACGTTAAGGGATTTTGGTCATGAGATTATCAAAAAG
5761 GATCTTCACCTAGATCCTTTTAAATTAATAAATGAAGTTTTAAATCAATCTAAAGTATATA
5821 TGAGTAAACTTGGTCTGACAGTTACCAATGCTTAATCAGTGAGGCACCTATCTCAGCGAT
5881 CTGTCTATTTTCGTTTCATCCATAGTTGCCTGACTCCCCGTCGTGTAGATAACTACGATACG
5941 GGAGGGCTTACCATCTGGCCCCAGTGCTGCAATGATACCGCGAGACCCACGCTCACCGGC
6001 TCCAGATTTATCAGCAATAAACCAGCCAGCCGGAAGGGCCGAGCGCAGAAGTGGTCCTGC
6061 AACTTTATCCGCCTCCATCCAGTCTATTAATTGTTGCCGGGAAGCTAGAGTAAGTAGTTC
6121 GCCAGTTAATAGTTTGCGCAACGTTGTTGCCATTGCTACAGGCATCGTGGTGTACGCTC
6181 GTCGTTTGGTATGGCTTCATTCAGCTCCGGTTCCCAACGATCAAGGCGAGTTACATGATC
6241 CCCCATGTTGTGCAAAAAAGCGGTTAGCTCCTTCGGTCCCTCCGATCGTTGTCAGAAGTAA
6301 GTTGGCCGAGTGTATCACTCATGGTTATGGCAGCACTGCATAAATTCTTACTGTCAT
6361 GCCATCCGTAAGATGCTTTTCTGTGACTGGTGAAGTACTCAACCAAGTATTCTGAGAATA
6421 GTGTATGCGGCGACCGAGTTGCTCTTGCCCGGTCAATACGGGATAATACCGCGCCACA
6481 TAGCAGAACTTTAAAAGTGCTCATCATTGGAAAACGTTCTTCGGGGCGAAAACCTCTCAAG
6541 GATCTTACCGCTGTTGAGATCCAGTTCGATGTAACCCACTCGTGCACCCAAGTATCTTC
6601 AGCATCTTTTACTTTACCAGCGTTTCTGGGTGAGCAAAAACAGGAAGGCAAAATGCCGC
6661 AAAAAAGGGAATAAGGGCGACACGGAAATGTTGAATACTCATACTCTTCCTTTTTCAATA
6721 TTATTGAAGCATTATCAGGGTTATTGTCTCATGAGCGGATACATATTTGAATGTATTTA
6781 GAAAAATAACAAATAGGGGTTCCGCGCACATTTCCCCGAAAAGTGCCACCTGACGTC

2101 GGC GGCCGCTCGAGTCTAGAGGGCCCGTTTAAACCCGCTGATCAGCCTCGACTGTGCCTT
2161 CTAGTTGCCAGCCATCTGTTGTTTGCCCTCCCCGTGCCTTCCTTGACCCTGGAAGGTG
2221 CCACTCCCCTGTCTTTTCTAATAAAATGAGGAAATTGCATCGCATTGTCTGAGTAGGT
2281 GTCATTCTATTCTGGGGGGTGGGGTGGGGCAGGACAGCAAGGGGGAGGATTGGGAAGACA
2341 ATAGCAGGCATGCTGGGGATGCGGTGGGCTCTATGGCTTCTGAGGCGGAAAGAACCAGCT
2401 GGGGCTCTAGGGGGTATCCCCACGCGCCCTGTAGCGGCGCATTAAAGCGCGGCGGGTGTGG
2461 TGGTTACGCGCAGCGTGACCGCTACACTTGCCAGCGCCCTAGCGCCCGCTCCTTTTCGCTT
2521 TCTTCCCTTCCTTTCTCGCCACGTTCCGCCGGCTTCCCCGTCAAGCTCTAAATCGGGGCA
2581 TCCCTTTAGGGTTCCGATTTAGTGCTTTACGGCACCTCGACCCAAAAAACTTGATTAGG
2641 GTGATGGTTCACGTAGTGGGCCATCGCCCTGATAGACGGTTTTTCGCCCTTTGACGTTGG
2701 AGTCCACGTTCTTTAATAGTGGACTCTTGTTCCAACTGGAACAACACTCAACCCTATCT
2761 CGGTCTATTCTTTTGATTTATAAGGGATTTTGGGGATTTTCGGCCTATTGGTTAAAAAATG
2821 AGCTGATTTAACAAAAATTTAACGCGAATTAATTCTGTGGAATGTGTGTCAGTTAGGGTG
2881 TGGAAAGTCCCCAGGCTCCCCAGGCAGGCAGAAGTATGCAAAGCATGCATCTCAATTAGT
2941 CAGCAACCAGGTGTGGAAAGTCCCCAGGCTCCCCAGCAGGCAGAAGTATGCAAAGCATGC
3001 ATCTCAATTAGTCAGCAACCATAGTCCCGCCCTAACTCCGCCCATCCCGCCCTAACTC
3061 CGCCAGTTCGCCCATTTCTCCGCCCATGGCTGACTAATTTTTTTTTATTTATGCAGAGG
3121 CCGAGGCCGCTCTGCCTCTGAGCTATTCCAGAAGTAGTGAGGAGGCTTTTTTTGGAGGCC
3181 TAGGCTTTTGAAAAAGCTCCCGGGAGCTTGATATCCATTTTCGGATCTGATCAAGAGA
3241 CAGGATGAGGATCGTTTCGCATGATTGAACAAGATGGATTGCACGCAGGTTCTCCGGCCG
3301 CTTGGGTGGAGAGGCTATTCGGCTATGACTGGGCACAACAGACAATCGGCTGCTCTGATG
3361 CCGCCGTGTTCCGGCTGTCAGCGCAGGGGCGCCCGTTCTTTTTGTCAAGACCGACCTGT
3421 CCGGTGCCCTGAATGAACTGCAGGACGAGGCAGCGCGGCTATCGTGCTGGCCACGACGG
3481 GCGTTCCTTGCGCAGCTGTGCTCGACGTTGTCCTGAAGCGGGAAGGGACTGGCTGCTAT
3541 TGGGCGAAGTGCCGGGGCAGGATCTCCTGTCATCTCACCTTGCTCCTGCCGAGAAAGTAT
3601 CCATCATGGCTGATGCAATGCGGCGGCTGCATACGCTTGATCCGGCTACCTGCCATTTCG
3661 ACCACCAAGCGAAACATCGCATCGAGCGAGCACGTA CTGGATGGAAGCCGGTCTTGTCG
3721 ATCAGGATGATCTGGACGAAGAGCATCAGGGGCTCGCGCCAGCCGAACTGTTCCGCCAGGC

3781 TCAAGGCGCGCATGCCCGACGGCGAGGATCTCGTCGTGACCCATGGCGATGCCTGCTTGC
3841 CGAATATCATGGTGGAAAATGGCCGCTTTTCTGGATTCATCGACTGTGGCCGGCTGGGTG
3901 TGGCGGACCGCTATCAGGACATAGCGTTGGCTACCCGTGATATTGCTGAAGAGCTTGGCG
3961 GCGAATGGGCTGACCGCTTCTCTGTGCTTTACGGTATCGCCGCTCCCGATTTCGAGCGCA
4021 TCGCCTTCTATCGCCTTCTTGACGAGTTCTTCTGAGCGGGACTCTGGGGTTTCGAAATGAC
4081 CGACCAAGCGACGCCAACCTGCCATCACGAGATTTGATTCCACCGCCGCTTCTATGA
4141 AAGGTTGGGCTTCGGAATCGTTTTCCGGGACGCCGGCTGGATGATCCTCCAGCGCGGGGA
4201 TCTCATGCTGGAGTTCTTCGCCCACCCAACTTGTTTATTGCAGCTTATAATGGTTACAA
4261 ATAAAGCAATAGCATCACAAATTTACAAATAAAGCATTTTTTTCTACTGCATTCTAGTTG
4321 TGGTTTGTCCAAACTCATCAATGTATCTTATCATGTCTGTATACCGTCGACCTCTAGCTA
4381 GAGCTTGGCGTAATCATGGTCATAGCTGTTTCTGTGTGAAATTGTTATCCGCTCACAAAT
4441 TCCACACAACATACGAGCCGGAAGCATAAAGTGTAAGCCTGGGGTGCCTAATGAGTGAG
4501 CTAACTCACATTAATTGCGTTGCGCTCACTGCCCGCTTCCAGTCGGGAAACCTGTCGTG
4561 CCAGCTGCATTAATGAATCGGCCAACGCGCGGGGAGAGGCGGTTTGCGTATTGGGCGCTC
4621 TTCCGCTTCTCGCTCACTGACTCGCTGCGCTCGGTGTTCCGGCTGCGGGCAGCGGTATC
4681 AGCTCACTCAAAGGCGGTAATACGGTTATCCACAGAATCAGGGGATAACGCAGGAAAGAA
4741 CATGTGAGCAAAAGGCCAGCAAAAGGCCAGGAACCGTAAAAAGGCCGCTTGTGGCGTT
4801 TTTCCATAGGCTCCGCCCCCTGACGAGCATCACAAAAATCGACGCTCAAGTCAGAGGTG
4861 GCGAAACCCGACAGGACTATAAAGATAACCAGGCGTTTCCCCCTGGAAGCTCCCTCGTGCG
4921 CTCTCTGTTCCGACCCTGCCGCTTACCGGATACCTGTCCGCCTTCTCCCTTCGGGAAG
4981 CGTGGCGCTTTCTCAATGCTCACGCTGTAGGTATCTCAGTTCGGTGTAGGTCGTTGCTC
5041 CAAGCTGGGCTGTGTGCACGAACCCCCGTTCCAGCCGACCGCTGCGCCTTATCCGGTAA
5101 CTATCGTCTTGAGTCCAACCCGGTAAGACACGACTTATCGCCACTGGCAGCAGCCACTGG
5161 TAACAGGATTAGCAGAGCGAGGTATGTAGGCGGTGCTACAGAGTTCTTGAAGTGGTGGCC
5221 TAACTACGGCTACACTAGAAGGACAGTATTTGGTATCTGCGCTCTGCTGAAGCCAGTTAC
5281 CTTCCGAAAAAGAGTTGGTAGCTCTTGATCCGGCAAACAAACCACCGCTGGTAGCGGTGG
5341 TTTTTTTGTTTGAAGCAGCAGATTACGCGCAGAAAAAAGGATCTCAAGAAGATCCTTT
5401 GATCTTTTCTACGGGGTCTGACGCTCAGTGGAACGAAAACCTCACGTTAAGGGATTTTGGT

5461 CATGAGATTATCAAAAAGGATCTTCACCTAGATCCTTTTAAATTA AAAATGAAGTTTTAA
5521 ATCAATCTAAAGTATATATGAGTAAACTTGGTCTGACAGTTACCAATGCTTAATCAGTGA
5581 GGCACCTATCTCAGCGATCTGTCTATTTTCGTTTCATCCATAGTTGCCTGACTCCCCGTCGT
5641 GTAGATAACTACGATACGGGAGGGCTTACCATCTGGCCCCAGTGCTGCAATGATACCGCG
5701 AGACCCACGCTCACCGGCTCCAGATTTATCAGCAATAAACCAGCCAGCCGGAAGGGCCGA
5761 GCGCAGAAGTGGTCTGCAACTTTATCCGCCTCCATCCAGTCTATTAATTGTTGCCGGGA
5821 AGCTAGAGTAAGTAGTTCGCCAGTTAATAGTTTGCGCAACGTTGTTGCCATTGCTACAGG
5881 CATCGTGGTGTACGCTCGTCGTTTTGGTATGGCTTCATTCAGCTCCGGTTCCCAACGATC
5941 AAGGCGAGTTACATGATCCCCATGTTGTGCAAAAAGCGGTTAGCTCCTTCGGTCCTCC
6001 GATCGTTGTCAGAAGTAAGTTGGCCGCAAGTGTATCACTCATGGTTATGGCAGCACTGCA
6061 TAATTCTTACTGTCATGCCATCCGTAAGATGCTTTTCTGTGACTGGTGAGTACTCAAC
6121 CAAGTCATTCTGAGAATAGTGTATGCGGCGACCGAGTTGCTCTTGCCCGGCGTCAATACG
6181 GGATAATACCGCGCCACATAGCAGAACTTTAAAAGTGCTCATCATTGGAAAACGTTCTTC
6241 GGGGCGAAAACCTCTCAAGGATCTTACCGCTGTTGAGATCCAGTTCGATGTAACCCACTCG
6301 TGCACCCAACTGATCTTCAGCATCTTTTACTTTACCAGCGTTTCTGGGTGAGCAAAAAC
6361 AGGAAGGCAAAATGCCGCAAAAAGGGAATAAGGGCGACACGGAAATGTTGAATACTCAT
6421 ACTCTTCCTTTTCAATATTATTGAAGCATTATCAGGGTTATTGTCTCATGAGCGGATA
6481 CATATTTGAATGTATTTAGAAAAATAAACAATAGGGGTTCCGCGCACATTTCCCCGAAA
6541 AGTGCCACCTGACGTC

4081 ATTAGGGTGATGGTTCACGTAGTGGGCCATCGCCCTGATAGACGGTTTTTCGCCCTTTGA
4141 CGTTGGAGTCCACGTTCTTTAATAGTGGACTCTTGTTCCAACTGGAACAACACTCAACC
4201 CTATCTCGGTCTATTCTTTTGATTTATAAGGGATTTTGGGGATTTTCGGCCTATTGGTTAA
4261 AAAATGAGCTGATTTAACAAAAATTTAACGCGAATTAATTCTGTGGAATGTGTGTCAGTT
4321 AGGGTGTGGAAAGTCCCCAGGCTCCCCAGGCAGGCAGAAGTATGCAAAGCATGCATCTCA
4381 ATTAGTCAGCAACCAGGTGTGGAAAGTCCCCAGGCTCCCCAGCAGGCAGAAGTATGCAAA
4441 GCATGCATCTCAATTAGTCAGCAACCATAGTCCCGCCCCTAACTCCGCCCATCCCGCCCC
4501 TAACTCCGCCCAGTTCCGCCCATTTCTCCGCCCATGGCTGACTAATTTTTTTTTATTATG
4561 CAGAGGCCGAGGCCCTCTGCCTCTGAGCTATTCCAGAAGTAGTGAGGAGGCTTTTTTTG
4621 GAGGCCTAGGCTTTTGCAAAAAGCTCCCGGGAGCTTGATATCCATTTTCGGATCTGATC
4681 AAGAGACAGGATGAGGATCGTTTTCGCATGATTGAACAAGATGGATTGCACGCAGGTTCTC
4741 CGGCCGCTTGGGTGGAGAGGCTATTCGGCTATGACTGGGCACAACAGACAATCGGCTGCT
4801 CTGATGCCGCCGTGTTCCGGCTGTCAGCGCAGGGGCGCCCGTTCTTTTTGTCAAGACCG
4861 ACCTGTCCGGTGCCCTGAATGAACTGCAGGACGAGGCAGCGGGCTATCGTGGCTGGCCA
4921 CGACGGGCGTTCCCTTGCGCAGCTGTGCTCGACGTTGTCACTGAAGCGGGAAGGGACTGGC
4981 TGCTATTGGGCGAAGTGCCGGGGCAGGATCTCCTGTCATCTCACCTTGCTCCTGCCGAGA
5041 AAGTATCCATCATGGCTGATGCAATGCGGCGGCTGCATACGCTTGATCCGGCTACCTGCC
5101 CATTGACCACCAAGCGAAACATCGCATCGAGCGAGCACGTACTCGGATGGAAGCCGGTC
5161 TTGTCGATCAGGATGATCTGGACGAAGAGCATCAGGGGCTCGCGCCAGCCGAAGTTCG
5221 CCAGGCTCAAGGCGCGCATGCCCGACGGCGAGGATCTCGTCGTGACCCATGGCGATGCCT
5281 GCTTGCCGAATATCATGGTGGAAAATGGCCGCTTTTCTGGATTCATCGACTGTGGCCGGC
5341 TGGGTGTGGCGGACCGCTATCAGGACATAGCGTTGGCTACCCGTGATATTGCTGAAGAGC
5401 TTGGCGGCGAATGGGCTGACCGCTTCTCGTGCTTTACGGTATCGCCGCTCCCGATTTCG
5461 AGCGCATCGCCTTCTATCGCCTTCTTGACGAGTTCTTCTGAGCGGGACTCTGGGGTTCGA
5521 AATGACCGACCAAGCGACGCCCAACCTGCCATCACGAGATTTTCGATTCCACCGCCGCTT
5581 CTATGAAAGGTTGGGCTTCGGAATCGTTTTCCGGGACGCCGGCTGGATGATCCTCCAGCG
5641 CGGGGATCTCATGCTGGAGTTCTTCGCCACCCCAACTTGTTTTATTGCAGCTTATAATGG
5701 TTACAAATAAAGCAATAGCATCACAAATTTACAAATAAAGCATTTTTTTTCACTGCATTC

5761 TAGTTGTGGTTTGTCCAAACTCATCAATGTATCTTATCATGTCTGTATACCGTCGACCTC
5821 TAGCTAGAGCTTGGCGTAATCATGGTCATAGCTGTTTCCTGTGTGAAATTGTTATCCGCT
5881 CACAATCCACACAACATACGAGCCGGAAGCATAAAGTGTAAGCCTGGGGTGCCTAATG
5941 AGTGAGCTAACTCACATTAATTGCGTTGCGCTCACTGCCCGCTTCCAGTCGGGAAACCT
6001 GTCGTGCCAGCTGCATTAATGAATCGGCCAACGCGCGGGGAGAGGCGGTTTTCGTATTGG
6061 GCGCTCTTCCGCTTCCCTCGCTCACTGACTCGCTGCGCTCGGTCGTTTCGGCTGCGGCGAGC
6121 GGTATCAGCTCACTCAAAGGCGGTAATACGGTTATCCACAGAATCAGGGGATAACGCAGG
6181 AAAGAACATGTGAGCAAAAGGCCAGCAAAAGGCCAGGAACCGTAAAAAGGCCGCGTTGCT
6241 GCGTTTTTCCATAGGCTCCGCCCCCTGACGAGCATCACAAAATCGACGCTCAAGTCA
6301 GAGGTGGCGAAACCCGACAGGACTATAAAGATACCAGGCGTTTCCCCCTGGAAGCTCCCT
6361 CGTGCGCTCTCCTGTTCCGACCCTGCCGTTACCGGATACCTGTCCGCTTTCTCCCTTC
6421 GGGAAAGCGTGGCGCTTTCTCAATGCTCACGCTGTAGGTATCTCAGTTCGGTGTAGGTCGT
6481 TCGCTCCAAGCTGGGCTGTGTGCACGAACCCCCGTTACGCCGACCGCTGCGCCTTATC
6541 CGGTAACTATCGTCTTGAGTCCAACCCGGTAAGACACGACTTATCGCCACTGGCAGCAGC
6601 CACTGGTAACAGGATTAGCAGAGCGAGGTATGTAGGCGGTGCTACAGAGTTCTTGAAGTG
6661 GTGGCCTAACTACGGCTACACTAGAAGGACAGTATTTGGTATCTGCGCTCTGCTGAAGCC
6721 AGTTACCTTCGGAAAAAGAGTTGGTAGCTCTTGATCCGGCAAACAAACCACCGCTGGTAG
6781 CGGTGGTTTTTTTTGTTTGAAGCAGCAGATTACGCGCAGAAAAAAGGATCTCAAGAAGA
6841 TCCTTGATCTTTTCTACGGGGTCTGACGCTCAGTGGAACGAAAACCTCACGTTAAGGGAT
6901 TTTGGTCATGAGATTATCAAAAAGGATCTTACCTAGATCCTTTTAAATTAATAATGAAG
6961 TTTTAAATCAATCTAAAGTATATATGAGTAACTTGGTCTGACAGTTACCAATGCTTAAT
7021 CAGTGAGGCACCTATCTCAGCGATCTGTCTATTTTCGTTCCATAGTTGCCTGACTCCC
7081 CGTCGTGTAGATAACTACGATACGGGAGGGCTTACCATCTGGCCCCAGTGCTGCAATGAT
7141 ACCGCGAGACCCACGCTCACCGGCTCCAGATTTATCAGCAATAAACAGCCAGCCGGAAG
7201 GGCCGAGCGCAGAAGTGGTCCTGCAACTTTATCCGCTCCATCCAGTCTATTAATTGTTG
7261 CCGGGAAGCTAGAGTAAGTAGTTCGCCAGTTAATAGTTTTCGCAACGTTGTTGCCATTGC
7321 TACAGGCATCGTGGTGTACGCTCGTCGTTTGGTATGGCTTCATTACAGCTCCGGTTCCCA
7381 ACGATCAAGGCGAGTTACATGATCCCCATGTTGTGCAAAAAAGCGGTTAGCTCCTTCGG

7441 TCCTCCGATCGTTGTCAGAAGTAAGTTGGCCGAGTGTTATCACTCATGGTTATGGCAGC
7501 ACTGCATAATTCTTACTGTCATGCCATCCGTAAGATGCTTTTCTGTGACTGGTGAGTA
7561 CTCAACCAAGTCATTCTGAGAATAGTGTATGCGGCGACCGAGTTGCTCTTGCCCGGCGTC
7621 AATACGGGATAATACCGCGCCACATAGCAGAACTTTAAAAGTGCTCATCATTGGAAAACG
7681 TTCTTCGGGGCGAAAACCTCAAGGATCTTACCGCTGTTGAGATCCAGTTCGATGTAACC
7741 CACTCGTGCACCCAACTGATCTTCAGCATCTTTTACTTTCACCAGCGTTTCTGGGTGAGC
7801 AAAAACAGGAAGGCAAATGCCGCAAAAAGGAATAAGGGCGACACGGAAATGTTGAAT
7861 ACTCATACTCTTCCTTTTTCAATATTATTGAAGCATTATCAGGGTTATTGTCTCATGAG
7921 CGGATACATATTTGAATGTATTTAGAAAAATAAACAAATAGGGGTTCGCGCACATTTCC
7981 CCGAAAAGTGCCACCTGACGTC

Appendix II

Publications

Review Article

p38 δ MAPK: Emerging Roles of a Neglected Isoform

Carol O'Callaghan,¹ Liam J. Fanning,² and Orla P. Barry¹

¹ Department of Pharmacology and Therapeutics, Western Gateway Building, Western Road, University College Cork, Cork, Ireland

² Molecular Virology Diagnostic & Research Laboratory, Department of Medicine, Clinical Sciences Building, University College Cork and Cork University Hospital, Cork, Ireland

Correspondence should be addressed to Orla P. Barry; o.barry@ucc.ie

Received 23 June 2014; Revised 29 August 2014; Accepted 31 August 2014; Published 17 September 2014

Academic Editor: Rony Seger

Copyright © 2014 Carol O'Callaghan et al. This is an open access article distributed under the Creative Commons Attribution License, which permits unrestricted use, distribution, and reproduction in any medium, provided the original work is properly cited.

p38 δ mitogen activated protein kinase (MAPK) is a unique stress responsive protein kinase. While the p38 MAPK family as a whole has been implicated in a wide variety of biological processes, a specific role for p38 δ MAPK in cellular signalling and its contribution to both physiological and pathological conditions are presently lacking. Recent emerging evidence, however, provides some insights into specific p38 δ MAPK signalling. Importantly, these studies have helped to highlight functional similarities as well as differences between p38 δ MAPK and the other members of the p38 MAPK family of kinases. In this review we discuss the current understanding of the molecular mechanisms underlying p38 δ MAPK activity. We outline a role for p38 δ MAPK in important cellular processes such as differentiation and apoptosis as well as pathological conditions such as neurodegenerative disorders, diabetes, and inflammatory disease. Interestingly, disparate roles for p38 δ MAPK in tumour development have also recently been reported. Thus, we consider evidence which characterises p38 δ MAPK as both a tumour promoter and a tumour suppressor. In summary, while our knowledge of p38 δ MAPK has progressed somewhat since its identification in 1997, our understanding of this particular isoform in many cellular processes still strikingly lags behind that of its counterparts.

1. p38 Isoform Evolution

The first and now archetypal member of the p38 MAPK family, p38 α MAPK, was identified by four independent groups in 1994. It was isolated as a 38 kDa protein rapidly tyrosine phosphorylated in response to lipopolysaccharide stimulation [1], as a molecule that binds pyridinyl-imidazole drugs which inhibit the synthesis of proinflammatory cytokines [2] and as an activator of MAPK activated protein kinase 2 (MAPKAP-K2/MK2) and small heat shock proteins in cells stimulated with heat shock or interleukin- (IL-) 1 [3, 4]. This was followed by the subsequent identification of p38 β MAPK in the same year, p38 γ MAPK in 1996, and lastly p38 δ MAPK in 1997 [5–9]. The product of the *S. cerevisiae* HOG1 gene, an important component of osmoregulation and the cell cycle, was found to be a homologue of p38 MAPK [10]. This conservation from yeast to mammals is significant as it indicates that the p38 family is responsible for critical cellular processes. A study of the evolutionary history of MAPKs suggests that each p38 MAPK family

member evolved from a single ancestor. In fact it appears that MAPK12 (p38 γ) arose from a tandem duplication of MAPK11 (p38 β) on chromosome 22 while MAPK14 (p38 α) and MAPK13 (p38 δ) subsequently resulted from a single segmental duplication of the MAPK11-MAPK12 gene unit on chromosome 6 [11]. These gene duplications appear to have occurred before the species separation of nematodes but after the species separation of arthropods. Interestingly, unlike the other p38 isoforms, MAPK13 has not been identified in teleosts [11]. This indicates that a MAPK13 gene deletion event may have occurred subsequent to gene duplication in the evolution of these species. Duplicated genes are generally assumed to be functionally redundant at the time of origin and are eventually silenced. The evolutionary preservation of the four p38 MAPK isoforms therefore suggests functional differentiation of the individual family members. Thus, while the majority of research to date has focused on p38 α and p38 β MAPKs, each isoform is an important kinase in its own right with distinct cellular functions. This review aims to highlight components of the previously neglected p38 δ

MAPK signalling pathway and emphasises recent progress in our understanding of p38 δ MAPK involvement in diverse physiological as well as pathological processes.

The use of pyridinyl-imidazole inhibitors has largely driven the advancement in our understanding of p38 α and p38 β MAPK signalling, functions, and substrates. Both p38 α and p38 β MAPK are highly sensitive to inhibition by SB203580, SB202190, and newer compounds such as L-167307 [2, 5, 12]. In contrast, the observation that p38 δ MAPK is insensitive to inhibition by pyridinyl-imidazole compounds has hindered its study in cellular events [7, 9]. The differential sensitivity to these drugs can be attributed to amino acid sequence variability at the ATP binding pocket where these compounds bind competitively, facilitated by interactions with nearby amino acids. Thr106 of p38 α and p38 β MAPK has been identified as the major determinant for imidazole inhibitor specificity as it orientates the drug to interact with His107 and Leu108 thereby preventing ATP binding [13]. The equivalent residue in p38 δ MAPK is a methionine (Met), the large side chain of which prevents binding of these inhibitors. In fact, substitution of Met106 in p38 δ MAPK with Thr was found to confer some sensitivity to inhibition by SB203580 [14]. Conversely, p38 α MAPK mutants in which Thr106 is replaced with Met displayed reduced sensitivity to inhibition by SB203580 [15]. It is unfortunate that no potent p38 δ MAPK specific inhibitor has been identified to date. Although the diaryl urea compound BIRB796 allosterically inhibits p38 δ MAPK at high concentrations, it is also a powerful inhibitor of p38 α , - β , and - γ MAPK [16]. While varying the concentration of BIRB796 and combining it with SB203580 may be of some use in identifying p38 δ MAPK specific signalling pathways, the possible influence of the other p38 MAPK isoforms, in particular p38 γ MAPK, must be considered when interpreting any results.

2. p38 δ MAPK Expression and Activation

Unsurprisingly, p38 δ MAPK shares highly similar protein sequences with the other p38 MAPK isoforms. It displays 61%, 59%, and 65% amino acid identity to p38 α , - β , and - γ MAPKs, respectively [7]. Differences in sequence between p38 δ MAPK and the other p38 MAPK family members can be observed in the ATP binding pocket. This has consequences for inhibitor sensitivity and contributes to substrate specificity. On the other hand, the greatest sequence similarities lie in the highly conserved kinase domains, where the four isoforms share >90% amino acid identity [17]. Within kinase subdomain VIII (of XI), p38 δ MAPK possesses a TGY dual phosphorylation motif which is the hallmark of p38 MAPKs and is conserved among all known mammalian p38 isoforms [7–9, 18]. p38 δ MAPK has a distinct distribution profile in human tissue that is relatively limited compared to that of p38 α and p38 β MAPK isoforms which are largely ubiquitously expressed [8]. High levels of p38 δ mRNA have been detected in endocrine tissues such as salivary, pituitary, prostate, and adrenal glands, while more modest levels are expressed in the stomach, colon, trachea, pancreas, skin, kidney, and lung [8]. This differential expression in different

cell and tissue types is indicative of a specific biological effect of p38 δ MAPK activation in these cell types, distinct from that of the other p38 family members.

The murine p38 δ MAPK amino acid sequence is 92% identical to the human sequence and the adult mouse displays a broadly similar pattern of p38 δ MAPK expression to that seen in human tissue, that is, lung, testis, kidney, and gut epithelium [18]. Murine p38 δ MAPK expression varies at different stages in the developing mouse embryo. At 9.5 days it is primarily expressed in the developing gut and septum transversum, while by 15.5 days its expression expands to most developing epithelia [18]. This suggests that p38 δ MAPK has a role in embryonic development. However, knock-out of p38 δ MAPK results in mice which are both viable and fertile and exhibit a normal phenotype [19]. Moreover, while p38 β - and p38 γ -null mice as well as p38 γ /p38 δ double knockout (KO) mice are also phenotypically normal [19, 20], genetic ablation of p38 α MAPK is embryonic lethal at day 10.5–11.5 [21]. Functional redundancy among the p38 isoforms is a likely explanation with p38 α , - β , or - γ compensating for the loss of p38 δ MAPK activity during development. However, it appears that p38 α MAPK plays a critical role in early development where its loss cannot be overcome.

p38 α , - β , and - γ MAPK isoforms are activated by alterations in the physical and chemical properties of the extracellular environment with diverse triggers including environmental stress signals, inflammatory cytokines, and mitogenic stimuli [1, 5, 6, 22]. Using transiently expressed epitope-tagged p38 δ MAPK, a similar activation profile has been defined for p38 δ MAPK [7–9]. It is strongly activated by environmental alterations in osmolarity, ultraviolet (UV) irradiation, and oxidation. It is also moderately activated by chemical stressors and proinflammatory cytokines including arsenite, anisomycin, tumour necrosis factor- (TNF-) α , and IL-1. Despite their similar activation profiles, differences in the levels of activation of p38 δ MAPK and the other p38 MAPK isoforms have been reported. For example, while hyperosmolarity appears to stimulate both p38 α and p38 δ to a similar degree, under hypoosmotic conditions, p38 α MAPK is more strongly activated than p38 δ MAPK [7]. A range of MAP3Ks have been implicated in the activation of the p38 MAPK pathway, including MLKs (mixed-lineage kinases), TAK1 (transforming growth factor β activated kinase 1), ASK1 (apoptosis signal-regulating kinase 1), TAO (thousand-and-one amino acid), DLK1 (dual-leucine-zipper-bearing kinase 1) MEKKs, and ZAK1 (leucine zipper and sterile- α motif kinase 1) (Figure 1). To date their individual contribution to p38 δ MAPK signalling in particular is not yet understood [23–28]. Further upstream of the MAP3Ks is a complex network involving members of the Ras/Rho family of small GTP-binding proteins and heterotrimeric G-protein coupled receptors [29, 30]. This adds to the diversity of signalling from various stimuli contributing to the crosstalk between p38 MAPKs and other signalling pathways.

The upstream direct activators responsible for dual phosphorylation of the p38 MAPK TGY motif are the MAPK kinases (MKKs). p38 δ MAPK is unique as it can be activated by four separate MKKs: the p38 MAPK specific MKK3 and MKK6 and also the JNK MKKs-4 and -7 [7–9, 18].

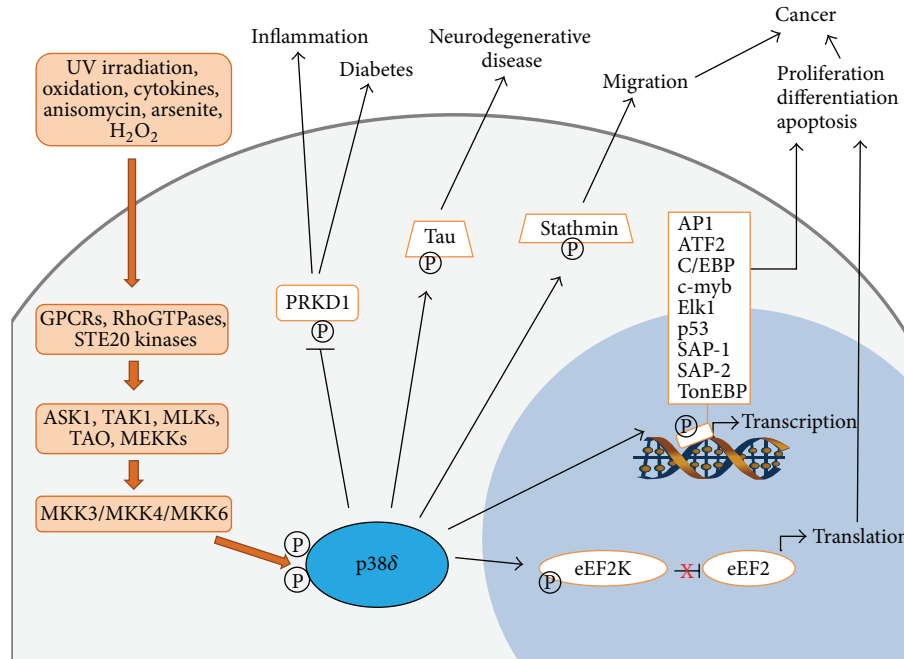


FIGURE 1: Schematic representation of the current understanding of p38 δ MAPK signalling and activation. A variety of extracellular stimuli can activate the MAPK signalling pathway resulting in dual phosphorylation of p38 δ MAPK. Known substrates of active p38 δ MAPK include transcription factors, structural proteins, kinases, and translation repressors. Phosphorylated substrates affect several cellular processes and contribute to the pathogenesis of diseases such as cancer, diabetes, and neurodegenerative and inflammatory conditions.

However, information regarding the specific contributions of these individual MKKs to p38 δ MAPK activation in different cell types and under diverse conditions is lacking. Current evidence suggests that activation of p38 δ MAPK is significantly influenced by both the nature and the strength of the stimulus as well as the cell type involved. This may be the result of varying levels of expression of upstream components of the MAPK signalling cascade in different cell types. For example, MKK3 is the major direct activator of p38 δ MAPK phosphorylation in response to UV radiation, hyperosmotic shock, and TNF α in mouse embryonic fibroblast (MEF) cells [31]. It also appears to be the primary kinase responsible for p38 δ MAPK activation in response to transforming growth factor- β 1 (TGF- β 1) as MKK3 deficiency impairs endogenous p38 δ activation by TGF- β 1 in murine glomerular mesangial cells [32]. On the other hand, MKK6 was identified as the major activator of p38 δ MAPK in KB (HeLa) cells subjected to IL-1, anisomycin, or osmotic stress [9]. Furthermore, MKK7 is reported to be responsible for the activation of p38 δ MAPK in 293T cells under peroxide stress, mediated by the scaffolding action of islet brain-2 [33]. Further complicating the current understanding of p38 δ MAPK activation is the likelihood that, in some cases, the cooperation of two MKKs may be necessary. While MKK4 preferentially phosphorylates JNK on Tyr, MKK7 preferentially phosphorylates JNK on Thr [34–36]. Therefore it must be considered possible that the combined activity of these two MKKs may be required to fully phosphorylate p38 δ MAPK on both the Tyr and the Thr residues. Interestingly, two reports outline a MKK-independent mechanism of activation for p38 α MAPK via

autophosphorylation [37, 38]. While autophosphorylation activity is detected in intrinsically active p38 δ mutants [39, 40], no such pathway has been observed which activates the endogenous p38 δ MAPK isoform.

An important factor in determining the biological consequences of p38 δ MAPK phosphorylation is the strength and duration of the activation signal. p38 δ MAPK activation is largely transient with activation and downregulation occurring within minutes of stimulation [17]. This is due to the regulatory action of protein phosphatases which again appears to be cell-type specific. While MAPK phosphatase 1 inactivates p38 δ MAPK in HEK293FT cells, it does not interact with p38 δ MAPK in the NIH3T3 cell line [41, 42]. The protein serine/threonine phosphatases PP1 and PP2A have also been shown to be involved in p38 δ MAPK phosphorylation as okadaic acid (OA), a PP1/PP2A inhibitor, causes increased p38 δ MAPK activity in human epidermal keratinocytes [43].

3. Novel p38 δ MAPK Substrates

While p38 MAPKs are proline-directed kinases, substrate specificity is also determined by docking domains both in the MAPK itself and in the target protein [44]. Therefore, although p38 δ MAPK substrate specificity overlaps to some extent with that of p38 α , - β , and - γ MAPKs, there are a number of notable differences. Common substrates of p38 MAPKs include MBP, PHAS-1, and transcription factors ATF2, SAP1, Elk-1, and p53 (Figure 1). In contrast, however, substrates

TABLE 1: Known p38 δ MAPK substrates and their biochemical functions.

Substrate	Function	Consequences of phosphorylation
API	Transcription factor	Activation of transcription, involucrin expression, keratinocyte differentiation [58]
ATF2	Transcription factor	Activation of transcription [7, 9]
C/EBP	Transcription factor	Keratinocyte differentiation [59]
c-myb	Transcription factor	c-myb degradation [109]
eEF2K	Inhibitory kinase	eEF2 activation, protein synthesis [53]
Elk1	Transcription factor	Activation of transcription [7, 9]
p53	Transcription factor	p21 expression, G ₁ phase arrest [9, 110]
PHAS-1	Translation repressor	Dissociation from eIF4E, activation of translation [7]
PRKD1	Serine-threonine kinase	Inhibition of PRKD1 activity [72]
SAP-1	Transcription factor	Activation of transcription [9]
SAP-2	Transcription factor	Activation of transcription [9]
Stathmin	Microtubule protein	Cytoskeleton reorganisation [50]
Tau	Microtubule protein	Microtubule assembly, tau self-aggregation [46]
TonEBP/OREBP	Transcription factor	Impaired TonEBP/OREBP transcriptional activity [41]

API: activator protein 1; ATF2: activating transcription factor 2; C/EBP: CCAAT (cytosine-cytosine-adenosine-adenosine-thymidine)-enhancer-binding protein; myb: myeloblastosis; eEF2K: eukaryotic elongation factor 2 kinase; eEF2: eukaryotic elongation factor 2; PHAS-1: phosphorylated heat- and acid-stable protein 1; PRKD1: protein kinase D 1; SAP: serum response factor accessory protein; eIF4E: eukaryotic translation initiation factor 4E.

such as MAPK activated protein kinase 2 (MAPKAP-K2) and MAPKAP-K3 which are the major downstream kinases of p38 α and p38 β MAPK are not phosphorylated by p38 δ MAPK [7–9, 45] (Table 1).

3.1. Tau. At the time p38 δ MAPK was first described the microtubule-associated protein tau was identified as a strong *in vitro* substrate for p38 δ MAPK [46]. Tau is a component of the cytoskeleton network and under normal conditions it stabilises microtubule assembly by binding to β -tubulin. Phosphorylation of tau at T50 by p38 δ MAPK causes it to be functionally modified and enhances its capacity to promote microtubule assembly. This effect is seen in neuroblastoma in response to osmotic shock where tau T50 phosphorylation occurs soon after p38 δ MAPK activation, aiding the adaptive response of neurons to changes in osmolarity [46]. It appears, however, that subsequent hyperphosphorylation of tau at additional sites causes it to dissociate from the cytoskeleton, thereby promoting its self-assembly [47]. This aggregation destabilises the microtubule network and contributes to the development of neurofibrillary tangles [48]. Notably, Alzheimer's disease and other neurodegenerative disorders known as tauopathies are characterised by the aggregation in the brain of these neurofilament structures [49]. There is therefore a clearly defined role for p38 δ MAPK in the pathogenesis of neurodegenerative disease, making it a good potential therapeutic target for these disorders.

3.2. Stathmin. There is further evidence of a role for p38 δ MAPK in cytoskeleton regulation as the microtubule-associated protein stathmin has also been characterised as a good p38 δ MAPK substrate *in vitro* and in transfected cells exposed to osmotic shock [50]. The normal physiological

role of stathmin is to sequester free tubulin and increase depolymerisation of microtubules [51, 52]. It is possible that phosphorylation of stathmin by p38 δ MAPK blocks its ability to destabilise microtubules and as a result promotes microtubule polymerisation and enhances cell survival under stress conditions.

3.3. eEF2K. In response to anisomycin stimulation, p38 δ MAPK has been shown to be the main p38 MAPK isoform which phosphorylates eukaryotic elongation factor 2 kinase (eEF2K) [53]. Phosphorylation of eEF2K on Ser359 inactivates the kinase and as a result removes its inhibitory phosphorylation of eEF2. eEF2 in turn promotes the movement of the ribosome along mRNA during translation [54]. This suggests that, by inhibiting eEF2K and consequently activating eEF2, p38 δ MAPK is responsible for driving the translation of proteins associated with stress responses. Consistent with this hypothesis is the observation that the MKK3/6-p38 δ MAPK-eEF2K pathway in myeloid cells is implicated in the production of the proinflammatory cytokine TNF α in bacterial LPS induced acute liver disease [55]. These differences in substrate specificity in combination with its unique tissue distribution profile demonstrate that despite similarities in stimuli the consequences of p38 δ MAPK can potentially be significantly different to those of the other p38 MAPK isoforms.

4. p38 δ MAPK Function and New Roles in Human Disease

Since the discovery of p38 δ MAPK in 1997 it has been implicated in a range of diverse physiological events, namely, differentiation, apoptosis, and cytokine production (Figure 1). The greatest understanding of its involvement in these

cellular processes has been achieved from work using keratinocytes and the majority of these studies have previously been reviewed [56, 57]. Research is now emerging which establishes p38 δ MAPK as a regulator of these processes in other cell types. As a result in the past five years p38 δ MAPK has also been implicated in the pathogenesis of diabetes, inflammatory diseases, and cancer. This progress has been achieved with the development of p38 δ MAPK KO mouse models which are proving to be a useful tool in elucidating novel roles for p38 δ MAPK *in vivo*.

4.1. Differentiation and Psoriasis. A number of different studies have identified a role for p38 δ MAPK in keratinocyte differentiation, a process critical for the precise control of normal epidermal homeostasis. p38 δ MAPK induces keratinocyte differentiation by regulating the expression of involucrin, a marker of keratinocyte terminal differentiation [58–60]. p38 δ MAPK activation by 12-*O*-tetradecanoylphorbol-13-acetate (TPA), calcium, OA, or green tea polyphenol corresponds with increased involucrin promoter activity, mRNA, and protein expression, as well as increased levels and activity of AP1 and C/EBP transcription factors [58, 59, 61]. Importantly, these responses are observed in the presence of a p38 α/β MAPK inhibitor. In addition p38 γ MAPK is poorly expressed in keratinocytes [60] confirming a specific role for p38 δ MAPK. Involucrin expression can also be further upregulated in keratinocytes coexpressing p38 δ MAPK and PKC η , $-\delta$ or $-\epsilon$ isoforms [59]. Of note cholesterol-depleting agents and overexpression of MKK6/MKK7 have previously been shown to induce involucrin expression via activation of p38 α MAPK [60, 62, 63]. This highlights the significance of the stimulus type in determining p38 MAPK isoform activation. A further role for p38 δ MAPK in keratinocyte differentiation was recently identified. p38 δ MAPK can regulate expression of ZO-1, an epidermal tight junction membrane protein associated with keratinocyte differentiation [64]. Inhibition of p38 δ MAPK results in depletion of ZO-1 protein in calcium induced differentiating keratinocytes while other junction proteins remain unaffected [64]. Psoriasis is a benign, chronic inflammatory skin condition that is characterised by hyperproliferation and differentiation of keratinocytes as well as increased expression of inflammatory cytokines. Given the significant role p38 δ MAPK plays in keratinocyte differentiation, it is no surprise that aberrant p38 δ MAPK signalling has been implicated in the pathogenesis of psoriasis. Expression of the MAPK13 gene is commonly upregulated in psoriasis [65]. Furthermore, an increase in p38 δ (as well as $-\alpha$ and $-\beta$) MAPK activity has been detected in psoriatic lesions compared to nonlesional psoriatic skin. After treatment for psoriasis, phosphorylated p38 MAPK levels return to those of uninvolved skin [66].

Further to its role in keratinocyte differentiation p38 δ MAPK is also implicated in hematopoiesis. In human primary erythroid cells, p38 δ MAPK mRNA is only expressed in late-stage differentiation where along with p38 α MAPK it is increasingly activated [67]. This may suggest a functional role for p38 δ MAPK in erythrocyte membrane remodelling and enucleation. Interestingly, an increase in p38 δ MAPK mRNA

and protein expression is observed as blood monocytes differentiate to macrophages [68]. This suggests a role for p38 δ MAPK in functions gained by mature macrophages. A possible candidate is phagocytosis given that the microtubule associated protein stathmin is such a strong p38 δ MAPK substrate.

Most recently, p38 δ MAPK has been identified as a component of differentiation in bone repair [69]. In bone cell differentiation during wound healing, wild type (WT) monocytes differentiate to calcifying/bone-forming monoosteophils upon treatment with the peptide LL-37. p38 δ MAPK protein and mRNA is highly expressed in monoosteophils compared to undifferentiated monocytes. Monocytes from p38 δ MAPK KO mice are incapable of this differentiation, suggesting a critical role for p38 δ MAPK in this process [69].

4.2. Apoptosis and Diabetes. As well as its significant role in keratinocyte differentiation, p38 δ MAPK has also been identified as a regulator of keratinocyte apoptosis. This dual functional role may be attributed to the overlap of differentiation and apoptosis signalling pathways [70]. As well as inducing involucrin expression [61], OA simultaneously causes disruption of mitochondrial membrane potential and caspase-dependent apoptosis [43]. Overexpression of p38 δ MAPK enhances this OA driven apoptotic morphology. This response is specific to p38 δ MAPK activation as it occurred in the presence of the p38 α/β MAPK inhibitor SB203580 [43]. Furthermore, p38 δ MAPK coexpressed with either MEK6 or PKC δ , both upstream p38 MAPK activators, elicited an apoptotic response similar to that induced by OA but in the absence of an external stimulus. This was also independent of SB203580, again ruling out a contribution from other p38 MAPK isoforms [71]. Interestingly, concurrent p38 δ MAPK activation and inactivation of the proliferative MAPK ERK1/2 were observed with OA stimulation and PKC δ /p38 δ MAPK coexpression [43, 61, 71]. In fact a reduction in ERK1/2 activation appears to be critical for apoptosis as its constitutive activation inhibited PKC δ /p38 δ MAPK mediated apoptosis [71]. Therefore, it is likely that a specific balance between prosurvival ERK1/2 and proapoptotic p38 δ MAPK is essential in determining keratinocyte fate. In regulating this balance, p38 δ MAPK and ERK1/2 form a complex that is translocated to the nucleus upon stimulation by PKC δ . This nuclear localisation facilitates ERK1/2 inactivation by nuclear phosphatases, while maintaining p38 δ MAPK activation [71].

A role for p38 δ MAPK in apoptosis has recently been demonstrated *in vivo* using p38 δ MAPK KO mice. Mice deficient in p38 δ MAPK displayed a fivefold lower rate of pancreatic β cell death in response to oxidative stress than WT mice and are afforded protection against insulin resistance induced by a high-fat diet [72]. This would appear to link p38 δ MAPK to the pathogenesis of diabetes mellitus, a disease characterised by reduced insulin sensitivity and a decrease in insulin-producing pancreatic β cells [72]. Increased p38 MAPK pathway activity has indeed been observed in both type 1 and type 2 diabetes and is correlated with late complications of hyperglycemia, including neuropathy and nephropathy [73, 74]. p38 δ MAPK specifically has

also been implicated in the regulation of insulin secretion. Phosphorylation by p38 δ MAPK negatively regulates the activity of protein kinase D1 (PKD1), a known positive regulator of neuroendocrine cell secretion [72]. Thus, pronounced activation of PKD1 has been observed in pancreatic β cells lacking p38 δ MAPK. As p38 δ MAPK is normally quite highly expressed in the pancreas this can contribute to heightened insulin secretion and improved glucose tolerance in p38 δ MAPK-null mice [72]. The pivotal role p38 δ MAPK plays in integrating insulin secretion and survival of pancreatic β cells makes it an attractive potential therapeutic target for the treatment of human diabetes.

4.3. Cytokine Production and Inflammatory Diseases. One of the pathways by which p38 α MAPK was discovered was via its identification as a regulator of proinflammatory cytokine biosynthesis [2]. Thus, its role in cytokine signalling and cytokine-dependent inflammatory diseases is well characterised. Consequently, some recent research using p38 δ MAPK KO mouse models has focused on identifying specific roles for p38 δ MAPK in inflammation. A study of p38 δ MAPK KO mice as well as myeloid-restricted deletion of p38 δ MAPK in mice has shown that p38 δ MAPK is required for the recruitment of neutrophils to sites of inflammation [75]. p38 δ MAPK and its downstream target PKD1 conversely regulate PTEN activity to control neutrophil extravasation and chemotaxis. The accumulation of neutrophils at inflammatory sites is known to trigger inflammation-induced acute lung injury (ALI) which can cause acute respiratory distress syndrome (ARDS), a condition with a high mortality rate [76]. Therefore, abnormal p38 δ -PKD1 signalling may play an important role in both ALI and ARDS in humans.

Rheumatoid arthritis is a typical example of an inflammatory disease involving chronic synthesis of proinflammatory cytokines which result in synovial hyperplasia and joint destruction [77]. While p38 δ MAPK (along with $-\alpha$, $-\beta$, and $-\gamma$) is expressed in the synovium of rheumatoid arthritis patients its level of activation is lower than that of the four other p38 MAPK isoforms [78]. Despite this low level of activation new research has identified p38 δ MAPK as an essential component of joint damage in a collagen-induced model of arthritis. p38 $\gamma/\delta^{-/-}$ mice displayed reduced arthritis severity compared to WT mice [79]. The decrease in joint destruction was associated with lower expression of IL-1 β and TNF α as well as a reduction in T cell proliferation, IFN γ , and IL-17 production. Lack of either p38 γ or p38 δ MAPK alone yielded intermediate effects, suggesting significant roles for both isoforms in arthritis pathogenesis.

Proinflammatory cytokines also play a significant role in the pathogenesis of inflammatory airway diseases, including asthma, chronic obstructive pulmonary disease (COPD), and cystic fibrosis. While increased mucus production is linked to the morbidity and mortality of such diseases the underlying molecular mechanisms remain somewhat unclear [80]. The critical driver of mucus production is thought to be IL-13 production by immune cells which results in mucin gene expression [81, 82]. In the last few years p38 δ MAPK has been implicated in the signalling pathway responsible for controlling IL-13 driven excess mucus production. Increased

MAPK13 gene expression is evident in the lungs of patients with severe COPD [83]. Novel inhibitors with increased activity against p38 δ MAPK blocked mucus production by IL-13 in human airway epithelial cells [83]. Thus, in patients with hypersensitivity airway diseases there exists a potential opportunity for therapeutic intervention should specific p38 δ MAPK inhibitors become clinically available.

5. p38 δ MAPK and Cancer

In recent years, the function of the p38 MAPK signalling pathway in malignant transformation has been intensively studied. As a result, the best characterised isoform, p38 α MAPK, has been identified as both a tumour promoter [84–86] and a tumour suppressor [87–89]. Recent studies have now also implicated p38 δ MAPK in cancer development and progression. Like p38 α MAPK, p38 δ MAPK would also appear to have both pro- and antioncogenic roles, depending on the cell type studied.

Interest in p38 δ MAPK as a potential tumour promoter is based on the evidence that p38 δ MAPK expression and activation are significantly increased in a variety of carcinoma cell lines such as human primary cutaneous squamous carcinoma cells [65], head and neck squamous carcinoma cells and tumours [85], cholangiocarcinoma, and liver cancer cell lines [90]. p38 δ MAPK was first shown to promote a malignant phenotype (over eight years ago) in head and neck squamous cell carcinoma (HNSCC) [85]. It was shown to regulate HNSCC invasion and proliferation through controlling expression of matrix metalloproteinase-1 and -13 [85, 91]. Moreover the expression of dominant-negative p38 δ MAPK impaired the ability of cutaneous HNSCC cells to implant in the skin of immunodeficiency mice as well as inhibiting the growth of xenografts [85].

p38 δ MAPK-null mice have been utilised to demonstrate that p38 δ MAPK is required for the development of multistage chemical skin carcinogenesis *in vivo*. When compared with WT mice, p38 δ MAPK-deficient mice displayed reduced susceptibility to 7, 12-dimethylbenz(a)anthracene/12-O-tetradecanoylphorbol-13-acetate induced skin carcinoma with a significant delay in tumour development [92]. Furthermore, both tumour numbers and size were significantly decreased compared with WT mice [92]. This decreased carcinogenesis was associated with reduced levels of proliferative ERK1/2-AP1 signalling and decreased activation of signal transducer and activator of transcription 3 (Stat3) [92]. The ERK1/2-AP1 pathway is a key cancer promoting cascade previously implicated in skin carcinogenesis [93, 94]. Stat3 meanwhile is an oncogenic transcription factor involved in chemical and UVB-induced transformation [95]. It is also proliferative and plays a role in angiogenesis and invasion [96, 97]. Therefore p38 δ MAPK promotion of proliferation via Stat3 may be a significant mechanism in the promotion of carcinogenesis by p38 δ MAPK. Similarly, p38 δ MAPK KO mice have reduced susceptibility to development of K-ras driven lung tumorigenesis. Compared with WT mice, p38 $\delta^{-/-}$ /K-RasG12D $^{+/-}$ mice displayed significantly decreased tumour numbers, average tumour volume, and total tumour volume

per lung [92]. This is in contrast to p38 α MAPK-deficient mice which display hyperproliferation of lung epithelium and increased K-Ras-induced lung tumour development [88]. This highlights once again the distinct and often opposing functions of the individual p38 MAPK isoforms.

Further evidence for a specific role of p38 δ MAPK in promoting cancer progression has most recently been demonstrated in cholangiocarcinoma (CC) [90]. p38 δ MAPK expression is upregulated in CC when compared with normal biliary tract tissue. Knockdown, however, of p38 δ MAPK expression by siRNA transfection significantly inhibited motility and invasiveness of CC cells. In contrast, overexpression of p38 δ MAPK in these cells results in enhanced invasive behaviour. Significantly, p38 δ MAPK may prove to be a useful marker for the differential diagnosis of CC over hepatocellular carcinoma where it lacks expression [90].

In contrast to the relatively well characterised role of p38 δ MAPK as a tumour promoter an increasing number of reports since 2011 outline its activity as a tumour suppressor. The first indication of a tumour suppressive role for p38 δ MAPK was observed in mouse embryonic fibroblasts (MEF). p38 $\delta^{-/-}$ (and p38 $\gamma^{-/-}$) MEFs displayed increased cell motility compared to WT cells [98]. Furthermore, while WT fibroblasts ceased to proliferate after reaching 100% confluency, p38 $\delta^{-/-}$ MEFs continued to grow, forming foci rather than a monolayer [98]. This deregulation of contact inhibition is significant as it is a hallmark of malignant transformation [99]. Our own recent studies have also identified a role for p38 δ MAPK in the control of oesophageal squamous cell carcinoma (OESCC) migration, invasion and contact inhibition, processes which are crucial for the progression of primary tumours to distant metastases [100]. Reintroduction of p38 δ MAPK into OESCC cells which lack endogenous expression significantly impaired cell proliferation, migration, and invasion as well as significantly reducing the number of colonies formed on soft agar compared to WT. These effects were further enhanced in cells transfected with a constitutively active form of p38 δ MAPK [100]. Furthermore, p38 δ MAPK expression appears to influence the chemosensitivity of OESCC to apoptosis. Our recent study indicates that OESCC cells expressing p38 δ MAPK are significantly more sensitive to cisplatin and 5-fluorouracil combination therapy than p38 δ MAPK-deficient cells [101]. These findings are significant as they suggest that p38 δ MAPK may be a useful predictor of response to chemotherapy in OESCC patients. Further supporting the hypothesis that loss of p38 δ MAPK confers a survival advantage, p38 δ MAPK expression was found to be downregulated in brain metastases of triple-negative breast cancer (TNBC). Abolition of p38 δ MAPK expression in TNBC induced cell growth, while overexpression of p38 δ MAPK in brain metastases reduced growth rates [102].

Cancer genomes are increasingly associated with epigenetic alterations whereby tumour suppressor genes exhibit promoter hypermethylation. Interestingly, hypermethylation of the MAPK13 gene promoter region has recently been characterised in both malignant pleural mesothelioma [103] and primary cutaneous melanoma [104]. This methylation is associated with downregulation of p38 δ MAPK mRNA and

protein expression. Melanoma cell lines displaying MAPK13 gene promoter methylation do not express significant levels of p38 δ MAPK when compared to fibroblasts, melanocytes, and melanoma cell lines with unmethylated MAPK13 promoters. Furthermore, treatment of melanoma cells with the demethylating agent 5-aza-2'-deoxycytidine significantly increases the expression of the MAPK13 gene [104, 105]. Importantly, reestablishment of p38 δ MAPK expression in melanoma cells with MAPK13 hypermethylation suppresses cell proliferation. The effect was further enhanced upon expression of a constitutively active form of p38 δ MAPK. Interestingly, however, overexpression of p38 δ MAPK or its constitutively active form in cells in which MAPK13 was not epigenetically silenced only marginally affected proliferation [104].

6. Conclusions and Future Directions for p38 δ MAPK Research

p38 δ MAPK is a unique stress-responsive protein kinase. It is mainly activated by environmental stresses, including UV radiation, osmotic shock, and oxidative stress, to illicit an adaptive response within the cell. This is mediated through phosphorylation of substrates involved in cytoskeleton organisation such as tau and stathmin, as well as transcription factors responsible for the expression of stress-responsive genes [106, 107]. Since the discovery of the p38 MAPK family in the mid-nineties they have increasingly been associated with cellular processes such as proliferation, differentiation, development, apoptosis, and migration [108]. Research to date has generally focused on the first two isoforms to be discovered. It is now becoming increasingly clear however that conclusions drawn from p38 α MAPK (and to an extent p38 β MAPK) studies cannot be automatically applied to the p38 γ and p38 δ MAPK isoforms due to their different expression patterns, substrate specificities, and sensitivity to chemical inhibitors. Studies carried out in the last few years have led to some small advances in our knowledge of the regulation of p38 δ MAPK and its physiological roles. In particular, the development of p38 δ MAPK KO mouse models has yielded a greater understanding of the consequences of p38 δ MAPK signalling *in vivo*. Roles for p38 δ MAPK in important cellular processes such as differentiation and apoptosis have been identified [69, 72]. As a result, p38 δ MAPK is now implicated in a variety of pathological conditions including inflammatory diseases, diabetes, and cancer [72, 75, 92, 98]. Most importantly, p38 δ MAPK may now be considered as a potential therapeutic target for the treatment of these disorders.

The implication of p38 δ MAPK in a wide range of human diseases should strengthen future research interest in this isoform. The main limiting factors to the further study of p38 δ MAPK functions, however, are the lack of specific inhibitors and activators. Fuelled by the prospect of therapeutic benefit for patients with diabetes or inflammatory disease, for example, the search for more potent and specific inhibitors of p38 δ MAPK is ongoing [83]. These may not only provide potential treatments for the conditions outlined here but could also afford us the opportunity to delineate specific p38 δ MAPK functions in the absence of involvement from other

p38 MAPK isoforms. This in turn may identify other diseases where p38 δ MAPK could be a potential therapeutic target. In this review we also present important and interesting observations which suggest that focusing on identification of specific p38 δ MAPK activators is also warranted. This may in the future translate to the development of novel therapeutic strategies for patients with OESCC or melanoma. Whether considering the possible therapeutic benefits of p38 δ MAPK inhibitors or activators it is important to heed the diversity and important role(s) of p38 δ MAPK signalling in normal physiological processes. In conclusion, uncovering some of the physiological as well as pathological roles of p38 δ MAPK since its discovery almost twenty years ago has been somewhat successful. However, based on our current knowledge continued focused research on this particular isoform is necessary if p38 δ is to translate into a novel therapeutic target for a range of diverse human diseases.

Abbreviations

UV:	Ultraviolet
GPCR:	G-protein coupled receptor
GTP:	Guanine tyrosine phosphatase
STE20:	Sterile 20
ASK1:	Apoptosis signal-regulating kinase 1
TAK1:	Transforming growth factor β activated kinase 1
MLK:	Mixed-lineage kinase
TAO:	Thousand-and-one amino acid
MEKK:	Mitogen activated protein kinase kinase kinase
MKK:	Mitogen activated protein kinase kinase
PRKD1:	Protein kinase D 1
API:	Activator protein 1
ATF2:	Activating transcription factor 2
C/EBP:	CCAAT (cytosine-cytosine-adenosine-adenosine-thymidine)-enhancer-binding protein
myb:	Myeloblastosis
SAP:	Serum response factor accessory protein
eEF2K:	Eukaryotic elongation factor 2 kinase
eEF2:	Eukaryotic elongation factor 2
PHAS-1:	Phosphorylated heat- and acid-stable protein 1
eIF4E:	Eukaryotic translation initiation factor 4E.

Conflict of Interests

The authors declare that there is no conflict of interests regarding the publication of this paper.

References

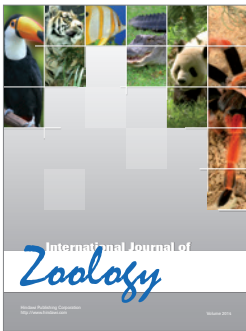
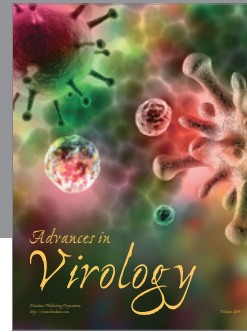
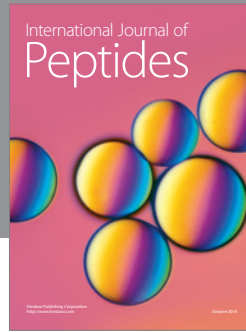
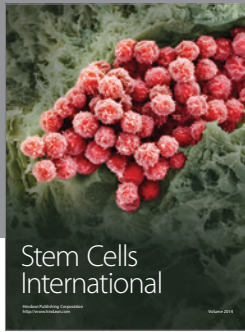
- [1] J. Han, J.-D. Lee, L. Bibbs, and R. J. Ulevitch, "A MAP kinase targeted by endotoxin and hyperosmolarity in mammalian cells," *Science*, vol. 265, no. 5173, pp. 808–811, 1994.
- [2] J. C. Lee, J. T. Laydon, P. C. McDonnell et al., "A protein kinase involved in the regulation of inflammatory cytokine biosynthesis," *Nature*, vol. 372, no. 6508, pp. 739–746, 1994.
- [3] J. Rouse, P. Cohen, S. Trigon et al., "A novel kinase cascade triggered by stress and heat shock that stimulates MAPKAP kinase-2 and phosphorylation of the small heat shock proteins," *Cell*, vol. 78, no. 6, pp. 1027–1037, 1994.
- [4] N. W. Freshney, L. Rawlinson, F. Guesdon et al., "Interleukin-1 activates a novel protein kinase cascade that results in the phosphorylation of Hsp27," *Cell*, vol. 78, no. 6, pp. 1039–1049, 1994.
- [5] Y. Jiang, C. Chen, Z. Li et al., "Characterization of the structure and function of a new mitogen-activated protein kinase (p38 β)," *The Journal of Biological Chemistry*, vol. 271, no. 30, pp. 17920–17926, 1996.
- [6] Z. Li, Y. Jiang, R. J. Ulevitch, and J. Han, "The primary structure of p38 γ : a new member of p38 group of MAP kinases," *Biochemical and Biophysical Research Communications*, vol. 228, no. 2, pp. 334–340, 1996.
- [7] Y. Jiang, H. Gram, M. Zhao et al., "Characterization of the structure and function of the fourth member of p38 group mitogen-activated protein kinases, p38 δ ," *The Journal of Biological Chemistry*, vol. 272, no. 48, pp. 30122–30128, 1997.
- [8] X. S. Wang, K. Diener, C. L. Manthey et al., "Molecular cloning and characterization of a novel p38 mitogen-activated protein kinase," *Journal of Biological Chemistry*, vol. 272, no. 38, pp. 23668–23674, 1997.
- [9] M. Goedert, A. Cuenda, M. Craxton, R. Jakes, and P. Cohen, "Activation of the novel stress-activated protein kinase SAPK4 by cytokines and cellular stresses is mediated by SKK3 (MKK6); comparison of its substrate specificity with that of other SAP kinases," *The EMBO Journal*, vol. 16, no. 12, pp. 3563–3571, 1997.
- [10] J. L. Brewster, T. de Valoir, N. D. Dwyer, E. Winter, and M. C. Gustin, "An osmosensing signal transduction pathway in yeast," *Science*, vol. 259, no. 5102, pp. 1760–1763, 1993.
- [11] M. Li, J. Liu, and C. Zhang, "Evolutionary history of the vertebrate mitogen activated protein kinases family," *PLoS ONE*, vol. 6, no. 10, Article ID e26999, 2011.
- [12] A. Cuenda, J. Rouse, Y. N. Doza et al., "SE 203580 is a specific inhibitor of a MAP kinase homologue which is stimulated by cellular stresses and interleukin-1," *FEBS Letters*, vol. 364, no. 2, pp. 229–233, 1995.
- [13] L. Tong, S. Pav, D. M. White et al., "A highly specific inhibitor of human p38 MAP kinase binds in the ATP pocket," *Nature Structural Biology*, vol. 4, no. 4, pp. 311–316, 1997.
- [14] P. A. Eyers, M. Craxton, N. Morrice, P. Cohen, and M. Goedert, "Conversion of SB 203580-insensitive MAP kinase family members to drug-sensitive forms by a single amino-acid substitution," *Chemistry and Biology*, vol. 5, no. 6, pp. 321–328, 1998.
- [15] R. J. Gum, M. M. McLaughlin, S. Kumar et al., "Acquisition of sensitivity of stress-activated protein kinases to the p38 inhibitor, SB 203580, by alteration of one or more amino acids within the ATP binding pocket," *The Journal of Biological Chemistry*, vol. 273, no. 25, pp. 15605–15610, 1998.
- [16] Y. Kuma, G. Sabio, J. Bain, N. Shpiro, R. Márquez, and A. Cuenda, "BIRB796 inhibits all p38 MAPK isoforms in vitro and in vivo," *Journal of Biological Chemistry*, vol. 280, no. 20, pp. 19472–19479, 2005.
- [17] L. R. Coulthard, D. E. White, D. L. Jones, M. F. McDermott, and S. A. Burchill, "p38MAPK: stress responses from molecular

- mechanisms to therapeutics," *Trends in Molecular Medicine*, vol. 15, no. 8, pp. 369–379, 2009.
- [18] M. C.-T. Hu, Y.-p. Wang, and A. Mikhail, "Murine p38- δ mitogen-activated protein kinase, a developmentally regulated protein kinase that is activated by stress and proinflammatory cytokines," *Journal of Biological Chemistry*, vol. 274, no. 11, pp. 7095–7102, 1999.
- [19] G. Sabio, J. S. C. Arthur, Y. Kuma et al., "p38 γ regulates the localisation of SAP97 in the cytoskeleton by modulating its interaction with GKAP," *EMBO Journal*, vol. 24, no. 6, pp. 1134–1145, 2005.
- [20] V. A. Beardmore, H. J. Hinton, C. Eftychi et al., "Generation and characterization of p38 β (MAPK11) gene-targeted mice," *Molecular and Cellular Biology*, vol. 25, no. 23, pp. 10454–10464, 2005.
- [21] M. Allen, L. Svensson, M. Roach, J. Hambor, J. McNeish, and C. A. Gabel, "Deficiency of the stress kinase p38 α results in embryonic lethality: Characterization of the kinase dependence of stress responses of enzyme-deficient embryonic stem cells," *Journal of Experimental Medicine*, vol. 191, no. 5, pp. 859–870, 2000.
- [22] J. Raingeaud, S. Gupta, J. S. Rogers et al., "Pro-inflammatory cytokines and environmental stress cause p38 mitogen-activated protein kinase activation by dual phosphorylation on tyrosine and threonine," *Journal of Biological Chemistry*, vol. 270, no. 13, pp. 7420–7426, 1995.
- [23] J. M. Kyriakis and J. Avruch, "Mammalian mitogen-activated protein kinase signal transduction pathways activated by stress and inflammation," *Physiological Reviews*, vol. 81, no. 2, pp. 807–869, 2001.
- [24] P. C. F. Cheung, D. G. Campbell, A. R. Nebreda, and P. Cohen, "Feedback control of the protein kinase TAK1 by SAPK2a/p38 α ," *EMBO Journal*, vol. 22, no. 21, pp. 5793–5805, 2003.
- [25] K. A. Gallo and G. L. Johnson, "Mixed-lineage kinase control of JNK and p38 MAPK pathways," *Nature Reviews Molecular Cell Biology*, vol. 3, no. 9, pp. 663–672, 2002.
- [26] H. Ichijo, E. Nishida, K. Irie et al., "Induction of apoptosis by ASK1, a mammalian MAPKKK that activates SAPK/JNK and p38 signaling pathways," *Science*, vol. 275, no. 5296, pp. 90–94, 1997.
- [27] K. Yamaguchi, K. Shirakabe, H. Shibuya et al., "Identification of a member of the MAPKKK family as a potential Mediator of TGF- β signal transduction," *Science*, vol. 270, no. 5244, pp. 2008–2011, 1995.
- [28] B. D. Cuevas, A. N. Abell, and G. L. Johnson, "Role of mitogen-activated protein kinase kinase kinases in signal integration," *Oncogene*, vol. 26, no. 22, pp. 3159–3171, 2007.
- [29] S. Zhang, J. Han, M. A. Sells et al., "Rho family GTPases regulate p38 mitogen-activated protein kinase through the downstream mediator Pak1," *The Journal of Biological Chemistry*, vol. 270, no. 41, pp. 23934–23936, 1995.
- [30] M. J. Marinissen, M. Chiariello, M. Pallante, and J. S. Gutkind, "A network of mitogen-activated protein kinases links G protein-coupled receptors to the c-jun promoter: a role for c-Jun NH2-terminal kinase, p38s, and extracellular signal-regulated kinase 5," *Molecular and Cellular Biology*, vol. 19, no. 6, pp. 4289–4301, 1999.
- [31] G. Remy, A. M. Risco, F. A. Iñesta-Vaquera et al., "Differential activation of p38MAPK isoforms by MKK6 and MKK3," *Cellular Signalling*, vol. 22, no. 4, pp. 660–667, 2010.
- [32] L. Wang, R. Ma, R. A. Flavell, and M. E. Choi, "Requirement of mitogen-activated protein kinase kinase 3 (MKK3) for activation of p38 α and p38 δ MAPK isoforms by TGF- β 1 in murine mesangial cells," *The Journal of Biological Chemistry*, vol. 277, no. 49, pp. 47257–47262, 2002.
- [33] J. Schoorlemmer and M. Goldfarb, "Fibroblast growth factor homologous factors and the islet brain-2 scaffold protein regulate activation of a stress-activated protein kinase," *Journal of Biological Chemistry*, vol. 277, no. 51, pp. 49111–49119, 2002.
- [34] S. Lawler, Y. Fleming, M. Goedert, and P. Cohen, "Synergistic activation of SAPK1/JNK1 by two MAP kinase kinases in vitro," *Current Biology*, vol. 8, no. 25, pp. 1387–1391, 1998.
- [35] C. Tournier, C. Dong, T. K. Turner, S. N. Jones, R. A. Flavell, and R. J. Davis, "MKK7 is an essential component of the JNK signal transduction pathway activated by proinflammatory cytokines," *Genes and Development*, vol. 15, no. 11, pp. 1419–1426, 2001.
- [36] T. Wada, K. Nakagawa, T. Watanabe et al., "Impaired synergistic activation of stress-activated protein kinase SAPK/JNK in mouse embryonic stem cells lacking SEK1/MKK4: different contribution of SEK2/MKK7 isoforms to the synergistic activation," *Journal of Biological Chemistry*, vol. 276, no. 33, pp. 30892–30897, 2001.
- [37] B. Ge, H. Gram, F. di Padova et al., "MAPKK-independent activation of p38alpha mediated by TAB1-dependent autophosphorylation of p38alpha," *Science*, vol. 295, no. 5558, pp. 1291–1294, 2002.
- [38] J. M. Salvador, P. R. Mittelstadt, T. Guszczynski et al., "Alternative p38 activation pathway mediated by T cell receptor-proximal tyrosine kinases," *Nature Immunology*, vol. 6, no. 4, pp. 390–395, 2005.
- [39] M. Avitzour, R. Diskin, B. Raboy, N. Askari, D. Engelberg, and O. Livnah, "Intrinsically active variants of all human p38 isoforms," *FEBS Journal*, vol. 274, no. 4, pp. 963–975, 2007.
- [40] N. Askari, R. Diskin, M. Avitzour, R. Capone, O. Livnah, and D. Engelberg, "Hyperactive variants of p38 α induce, whereas hyperactive variants of p38 γ suppress, activating protein 1-mediated transcription," *Journal of Biological Chemistry*, vol. 282, no. 1, pp. 91–99, 2007.
- [41] X. Zhou, J. D. Ferraris, N. I. Dmitrieva, Y. Liu, and M. B. Burg, "MKP-1 inhibits high NaCl-induced activation of p38 but does not inhibit the activation of TonEBP/OREBP: opposite roles of p38 α and p38 δ ," *Proceedings of the National Academy of Sciences of the United States of America*, vol. 105, no. 14, pp. 5620–5625, 2008.
- [42] T. Tanoue, T. Yamamoto, R. Maeda, and E. Nishida, "A Novel MAPK phosphatase MKP-7 acts preferentially on JNK/SAPK and p38 alpha and beta MAPKs," *The Journal of Biological Chemistry*, vol. 276, no. 28, pp. 26629–26639, 2001.
- [43] C. A. Kraft, T. Efimova, and R. L. Eckert, "Activation of PKC δ and p38 δ MAPK during okadaic acid dependent keratinocyte apoptosis," *Archives of Dermatological Research*, vol. 299, no. 2, pp. 71–83, 2007.
- [44] A. Cuenda and S. Rousseau, "p38 MAP-Kinases pathway regulation, function and role in human diseases," *Biochimica et Biophysica Acta—Molecular Cell Research*, vol. 1773, no. 8, pp. 1358–1375, 2007.
- [45] S. Kumar, P. C. McDonnell, R. J. Gum, A. T. Hand, J. C. Lee, and P. R. Young, "Novel homologues of CSBP/p38 MAP kinase: activation, substrate specificity and sensitivity to inhibition by pyridinyl imidazoles," *Biochemical and Biophysical Research Communications*, vol. 235, no. 3, pp. 533–538, 1997.

- [46] M. Goedert, M. Hasegawa, R. Jakes, S. Lawler, A. Cuenda, and P. Cohen, "Phosphorylation of microtubule-associated protein tau by stress-activated protein kinases," *FEBS Letters*, vol. 409, no. 1, pp. 57–62, 1997.
- [47] G. T. Bramblett, M. Goedert, R. Jakes, S. E. Merrick, J. Q. Trojanowski, and V. M. Y. Lee, "Abnormal tau phosphorylation at Ser396 in Alzheimer's disease recapitulates development and contributes to reduced microtubule binding," *Neuron*, vol. 10, no. 6, pp. 1089–1099, 1993.
- [48] M. Goedert, "The significance of tau and α -synuclein inclusions in neurodegenerative diseases," *Current Opinion in Genetics and Development*, vol. 11, no. 3, pp. 343–351, 2001.
- [49] V. M.-Y. Lee, M. Goedert, and J. Q. Trojanowski, "Neurodegenerative tauopathies," *Annual Review of Neuroscience*, vol. 24, pp. 1121–1159, 2001.
- [50] C. G. Parker, J. Hunt, K. Diener et al., "Identification of stathmin as a novel substrate for p38 delta," *Biochemical and Biophysical Research Communications*, vol. 249, no. 3, pp. 791–796, 1998.
- [51] L. Jourdain, P. Curmi, A. Sobel, D. Pantaloni, and M.-F. Carlier, "Stathmin: a tubulin-sequestering protein which forms a ternary T2S complex with two tubulin molecules," *Biochemistry*, vol. 36, no. 36, pp. 10817–10821, 1997.
- [52] P. A. Curmi, S. S. L. Andersen, S. Lachkar et al., "The stathmin/tubulin interaction in vitro," *Journal of Biological Chemistry*, vol. 272, no. 40, pp. 25029–25036, 1997.
- [53] A. Knebel, N. Morrice, and P. Cohen, "A novel method to identify protein kinase substrates: eEF2 kinase is phosphorylated and inhibited by SAPK4/p38 δ ," *EMBO Journal*, vol. 20, no. 16, pp. 4360–4369, 2001.
- [54] R. Jørgensen, A. R. Merrill, and G. R. Andersen, "The life and death of translation elongation factor 2," *Biochemical Society Transactions*, vol. 34, no. 1, pp. 1–6, 2006.
- [55] B. Gonzalez-Teran, J. R. Cortes, E. Manieri et al., "Eukaryotic elongation factor 2 controls TNF-alpha translation in LPS-induced hepatitis," *The Journal of Clinical Investigation*, vol. 123, no. 1, pp. 164–178, 2013.
- [56] T. Efimova, "p38delta mitogen-activated protein kinase regulates skin homeostasis and tumorigenesis," *Cell Cycle*, vol. 9, no. 3, pp. 498–505, 2010.
- [57] R. L. Eckert, T. Efimova, S. Balasubramanian, J. F. Crish, F. Bone, and S. Dashti, "p38 mitogen-activated protein kinases on the body surface—a function for p38 δ ," *Journal of Investigative Dermatology*, vol. 120, no. 5, pp. 823–828, 2003.
- [58] S. Balasubramanian, T. Efimova, and R. L. Eckert, "Green tea polyphenol stimulates a Ras, MEKK1, MEK3, and p38 cascade to increase activator protein 1 factor-dependent involucrin gene expression in normal human keratinocytes," *The Journal of Biological Chemistry*, vol. 277, no. 3, pp. 1828–1836, 2002.
- [59] T. Efimova, A. Deucher, T. Kuroki, M. Ohba, and R. L. Eckert, "Novel protein kinase C isoforms regulate human keratinocyte differentiation by activating a p38 δ mitogen-activated protein kinase cascade that targets CCAAT/enhancer-binding protein α ," *The Journal of Biological Chemistry*, vol. 277, no. 35, pp. 31753–31760, 2002.
- [60] S. R. Dashti, T. Efimova, and R. L. Eckert, "MEK6 regulates human involucrin gene expression via a p38 α - and p38 δ -dependent mechanism," *Journal of Biological Chemistry*, vol. 276, no. 29, pp. 27214–27220, 2001.
- [61] T. Efimova, A.-M. Broome, and R. L. Eckert, "A regulatory role for p38delta MAPK in keratinocyte differentiation: evidence for p38delta-ERK1/2 complex formation," *The Journal of Biological Chemistry*, vol. 278, no. 36, pp. 34277–34285, 2003.
- [62] R. Jans, G. Atanasova, M. Jadot, and Y. Poumay, "Cholesterol depletion upregulates involucrin expression in epidermal keratinocytes through activation of p38," *Journal of Investigative Dermatology*, vol. 123, no. 3, pp. 564–573, 2004.
- [63] S. R. Dashti, T. Efimova, and R. L. Eckert, "MEK7-dependent activation of p38 MAP kinase in keratinocytes," *The Journal of Biological Chemistry*, vol. 276, no. 11, pp. 8059–8063, 2001.
- [64] E. Siljamäki, L. Raiko, M. Toriseva et al., "p38delta mitogen-activated protein kinase regulates the expression of tight junction protein ZO-1 in differentiating human epidermal keratinocytes," *Archives of Dermatological Research*, vol. 306, no. 2, pp. 131–141, 2014.
- [65] A. S. Haider, S. B. Peters, H. Kaporis et al., "Genomic analysis defines a cancer-specific gene expression signature for human squamous cell carcinoma and distinguishes malignant hyperproliferation from benign hyperplasia," *Journal of Investigative Dermatology*, vol. 126, no. 4, pp. 869–881, 2006.
- [66] C. Johansen, K. Kragballe, M. Westergaard, J. Henningsen, K. Kristiansen, and L. Iversen, "The mitogen-activated protein kinases p38 and ERK1/2 are increased in lesional psoriatic skin," *British Journal of Dermatology*, vol. 152, no. 1, pp. 37–42, 2005.
- [67] S. Uddin, J. Ah-Kang, J. Ulaszek, D. Mahmud, and A. Wickrema, "Differentiation stage-specific activation of p38 mitogen-activated protein kinase isoforms in primary human erythroid cells," *Proceedings of the National Academy of Sciences of the United States of America*, vol. 101, no. 1, pp. 147–152, 2004.
- [68] K. K. Hale, D. Trollinger, M. Rihaneck, and C. L. Manthey, "Differential expression and activation of p38 mitogen-activated protein kinase α , β , γ , and δ in inflammatory cell lineages," *The Journal of Immunology*, vol. 162, no. 7, pp. 4246–4252, 1999.
- [69] Z. Zhang and J. E. Shively, "Acceleration of bone repair in NOD/SCID mice by human Monoosteophils, novel LL-37-activated monocytes," *PLoS ONE*, vol. 8, no. 7, Article ID e67649, 2013.
- [70] A. Gandarillas, "Epidermal differentiation, apoptosis, and senescence: common pathways?" *Experimental Gerontology*, vol. 35, no. 1, pp. 53–62, 2000.
- [71] T. Efimova, A.-M. Broome, and R. L. Eckert, "Protein kinase Cdelta regulates keratinocyte death and survival by regulating activity and subcellular localization of a p38delta-extracellular signal-regulated kinase 1/2 complex," *Molecular and Cellular Biology*, vol. 24, no. 18, pp. 8167–8183, 2004.
- [72] G. Sumara, I. Formentini, S. Collins et al., "Regulation of PKD by the MAPK p38delta in insulin secretion and glucose homeostasis," *Cell*, vol. 136, no. 2, pp. 235–248, 2009.
- [73] S. A. Price, S. Agthong, A. B. Middlemas, and D. R. Tomlinson, "Mitogen-activated protein kinase p38 mediates reduced nerve conduction in experimental diabetic neuropathy: interactions with aldose reductase," *Diabetes*, vol. 53, no. 7, pp. 1851–1856, 2004.
- [74] R. Komers, J. N. Lindsley, T. T. Oyama, D. M. Cohen, and S. Anderson, "Renal p38 MAP kinase activity in experimental diabetes," *Laboratory Investigation*, vol. 87, no. 6, pp. 548–558, 2007.
- [75] A. Ittner, H. Block, C. A. Reichel et al., "Regulation of PTEN activity by p38delta-PKD1 signaling in neutrophils confers inflammatory responses in the lung," *Journal of Experimental Medicine*, vol. 209, no. 12, pp. 2229–2246, 2012.

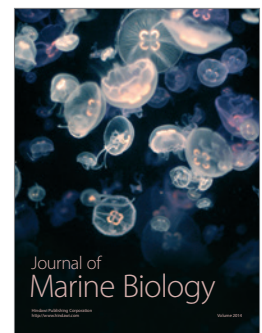
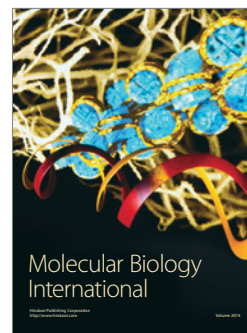
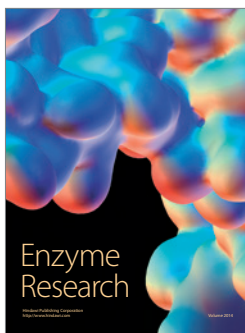
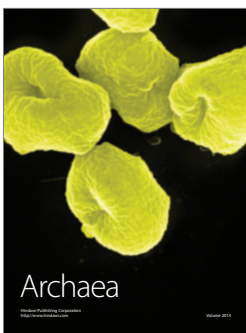
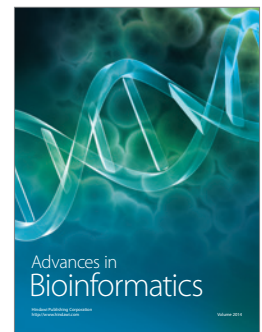
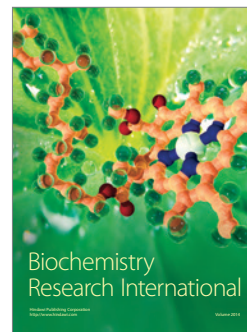
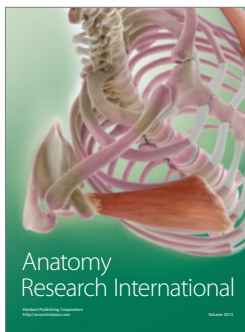
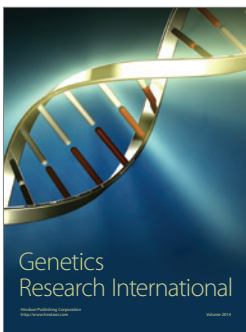
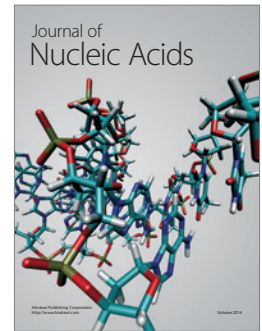
- [76] L. B. Ware and M. A. Matthay, "The acute respiratory distress syndrome," *New England Journal of Medicine*, vol. 342, no. 18, pp. 1334–1349, 2000.
- [77] F. M. Brennan and I. B. McInnes, "Evidence that cytokines play a role in rheumatoid arthritis," *The Journal of Clinical Investigation*, vol. 118, no. 11, pp. 3537–3545, 2008.
- [78] A. Korb, M. Tohidast-Akrad, E. Cetin, R. Axmann, J. Smolen, and G. Schett, "Differential tissue expression and activation of p38 MAPK α , β , γ , and δ isoforms in rheumatoid arthritis," *Arthritis and Rheumatism*, vol. 54, no. 9, pp. 2745–2756, 2006.
- [79] G. Criado, A. Risco, D. Alsina-Beauchamp, M. J. Pérez-Lorenzo, A. Escós, and A. Cuenda, "Alternative p38 MAPKs are essential for collagen-induced arthritis," *Arthritis and Rheumatology*, vol. 66, no. 5, pp. 1208–1217, 2014.
- [80] L. M. Kuyper, P. D. Paré, J. C. Hogg et al., "Characterization of airway plugging in fatal asthma," *American Journal of Medicine*, vol. 115, no. 1, pp. 6–11, 2003.
- [81] E. Y. Kim, J. T. Battaile, A. C. Patel et al., "Persistent activation of an innate immune response translates respiratory viral infection into chronic lung disease," *Nature Medicine*, vol. 14, no. 6, pp. 633–640, 2008.
- [82] M. Wills-Karp, J. Luyimbazi, X. Xu et al., "Interleukin-13: central mediator of allergic asthma," *Science*, vol. 282, no. 5397, pp. 2258–2261, 1998.
- [83] Y. G. Alevy, A. C. Patel, A. G. Romero et al., "IL-13-induced airway mucus production is attenuated by MAPK13 inhibition," *Journal of Clinical Investigation*, vol. 122, no. 12, pp. 4555–4568, 2012.
- [84] I. del Barco Barrantes and A. R. Nebreda, "Roles of p38 MAPKs in invasion and metastasis," *Biochemical Society Transactions*, vol. 40, no. 1, pp. 79–84, 2012.
- [85] M. R. Juntila, R. Ala-Aho, T. Jokilehto et al., "p38 α and p38 δ mitogen-activated protein kinase isoforms regulate invasion and growth of head and neck squamous carcinoma cells," *Oncogene*, vol. 26, no. 36, pp. 5267–5279, 2007.
- [86] S. Rousseau, I. Dolado, V. Beardmore et al., "CXCL12 and C5a trigger cell migration via a PAK1/2-p38 α MAPK-MAPKAP-K2-HSP27 pathway," *Cellular Signalling*, vol. 18, no. 11, pp. 1897–1905, 2006.
- [87] D. V. Bulavin and A. J. Fornace Jr., "p38 MAP kinase's emerging role as a tumor suppressor," *Advances in Cancer Research*, vol. 92, pp. 95–118, 2004.
- [88] J. J. Ventura, S. Tenbaum, E. Perdiguero et al., "p38 α MAP kinase is essential in lung stem and progenitor cell proliferation and differentiation," *Nature Genetics*, vol. 39, no. 6, pp. 750–758, 2007.
- [89] L. Hui, L. Bakiri, E. Stepniak, and E. F. Wagner, "p38 α : a suppressor of cell proliferation and tumorigenesis," *Cell Cycle*, vol. 6, no. 20, pp. 2429–2433, 2007.
- [90] F. L.-S. Tan, A. Ooi, D. Huang et al., "p38 δ /MAPK13 as a diagnostic marker for cholangiocarcinoma and its involvement in cell motility and invasion," *International Journal of Cancer*, vol. 126, no. 10, pp. 2353–2361, 2010.
- [91] M. Egeblad and Z. Werb, "New functions for the matrix metalloproteinases in cancer progression," *Nature Reviews Cancer*, vol. 2, no. 3, pp. 161–174, 2002.
- [92] E. M. Schindler, A. Hindes, E. L. Gribben et al., "p38 δ Mitogen-activated protein kinase is essential for skin tumor development in mice," *Cancer Research*, vol. 69, no. 11, pp. 4648–4655, 2009.
- [93] C. Bourcier, A. Jacquel, J. Hess et al., "p44 mitogen-activated protein kinase (extracellular signal-regulated kinase 1)-dependent signaling contributes to epithelial skin carcinogenesis," *Cancer Research*, vol. 66, no. 5, pp. 2700–2707, 2006.
- [94] M. R. Young, J. J. Li, and M. Rincón, "Transgenic mice demonstrate AP-1 (activator protein-1) transactivation is required for tumor promotion," *Proceedings of the National Academy of Sciences of the United States of America*, vol. 96, no. 17, pp. 9827–9832, 1999.
- [95] J. K. Dae, K. S. Chan, S. Sano, and J. DiGiovanni, "Signal transducer and activator of transcription 3 (Stat3) in epithelial carcinogenesis," *Molecular Carcinogenesis*, vol. 46, no. 8, pp. 725–731, 2007.
- [96] K. S. Chan, S. Sano, K. Kataoka et al., "Forced expression of a constitutively active form of Stat3 in mouse epidermis enhances malignant progression of skin tumors induced by two-stage carcinogenesis," *Oncogene*, vol. 27, no. 8, pp. 1087–1094, 2008.
- [97] K. S. Chan, S. Sano, K. Kiguchi et al., "Disruption of Stat3 reveals a critical role in both the initiation and the promotion stages of epithelial carcinogenesis," *Journal of Clinical Investigation*, vol. 114, no. 5, pp. 720–728, 2004.
- [98] M. I. Cerezo-guisado, P. del Reino, G. Remy et al., "Evidence of p38 γ and p38 δ involvement in cell transformation processes," *Carcinogenesis*, vol. 32, no. 7, pp. 1093–1099, 2011.
- [99] D. Hanahan and R. A. Weinberg, "Hallmarks of cancer: the next generation," *Cell*, vol. 144, no. 5, pp. 646–674, 2011.
- [100] C. O'Callaghan, L. J. Fanning, A. Houston, and O. P. Barry, "Loss of p38 δ expression promotes oesophageal squamous cell carcinoma proliferation, migration and anchorage-independent growth," *International Journal of Oncology*, vol. 43, no. 2, pp. 405–415, 2013.
- [101] C. O'Callaghan, L. J. Fanning, and O. P. Barry, "p38 δ MAPK phenotype: an indicator of chemotherapeutic response in oesophageal squamous cell carcinoma," *Anti-Cancer Drugs*, 2014.
- [102] Y. K. Choi, S.-M. Woo, S.-G. Cho et al., "Brain-metastatic triple-negative breast cancer cells regain growth ability by altering gene expression patterns," *Cancer Genomics and Proteomics*, vol. 10, no. 6, pp. 265–275, 2013.
- [103] Y. Goto, K. Shinjo, Y. Kondo et al., "Epigenetic profiles distinguish malignant pleural mesothelioma from lung adenocarcinoma," *Cancer Research*, vol. 69, no. 23, pp. 9073–9082, 2009.
- [104] L. Gao, M. A. Smit, J. J. van den Oord et al., "Genome-wide promoter methylation analysis identifies epigenetic silencing of MAPK13 in primary cutaneous melanoma," *Pigment Cell and Melanoma Research*, vol. 26, no. 4, pp. 542–554, 2013.
- [105] Y. Koga, M. Pelizzola, E. Cheng et al., "Genome-wide screen of promoter methylation identifies novel markers in melanoma," *Genome Research*, vol. 19, no. 8, pp. 1462–1470, 2009.
- [106] A. Risco and A. Cuenda, "New insights into the p38 γ and p38 δ MAPK pathways," *Journal of Signal Transduction*, vol. 2012, Article ID 520289, 8 pages, 2012.
- [107] A. Cuadrado and A. R. Nebreda, "Mechanisms and functions of p38 MAPK signalling," *Biochemical Journal*, vol. 429, no. 3, pp. 403–417, 2010.
- [108] J. M. Kyriakis and J. Avruch, "Mammalian MAPK signal transduction pathways activated by stress and inflammation: a 10-year update," *Physiological Reviews*, vol. 92, no. 2, pp. 689–737, 2012.

- [109] E. Pani and S. Ferrari, "p38MAPK δ controls c-Myb degradation in response to stress," *Blood Cells, Molecules, and Diseases*, vol. 40, no. 3, pp. 388–394, 2008.
- [110] W. C. Hawkes and Z. Alkan, "Delayed cell cycle progression in selenoprotein w-depleted cells is regulated by a mitogen-activated protein kinase kinase 4-p38/c-Jun NH 2-terminal kinase-p53 pathway," *Journal of Biological Chemistry*, vol. 287, no. 33, pp. 27371–27379, 2012.



Hindawi

Submit your manuscripts at
<http://www.hindawi.com>



Loss of p38 δ mitogen-activated protein kinase expression promotes oesophageal squamous cell carcinoma proliferation, migration and anchorage-independent growth

CAROL O'CALLAGHAN¹, LIAM J. FANNING², AILEEN HOUSTON² and ORLA P. BARRY¹

Departments of ¹Pharmacology and Therapeutics and ²Medicine, University College Cork, Ireland

Received March 21, 2013; Accepted May 3, 2013

DOI: 10.3892/ijo.2013.1968

Abstract. Oesophageal cancer is an aggressive tumour which responds poorly to both chemotherapy and radiation therapy and has a poor prognosis. Thus, a greater understanding of the biology of oesophageal cancer is needed in order to identify novel therapeutic targets. Among these targets p38 MAPK isoforms are becoming increasingly important for a variety of cellular functions. The physiological functions of p38 α and - β are now well documented in contrast to - γ and - δ which are comparatively under-studied and ill-defined. A major obstacle to deciphering the role(s) of the latter two p38 isoforms is the lack of specific chemical activators and inhibitors. In this study, we analysed p38 MAPK isoform expression in oesophageal cancer cell lines as well as human normal and tumour tissue. We observed specifically differential p38 δ expression. The role(s) of p38 δ and active (phosphorylated) p38 δ (p-p38 δ) in oesophageal squamous cell carcinoma (OESCC) was delineated using wild-type p38 δ as well as active p-p38 δ , generated by fusing p38 δ to its upstream activator MKK6b(E) via a decapeptide (Gly-Glu)₅ linker. OESCC cell lines which are p38 δ -negative (KE-3 and -8) grew more quickly than cell lines (KE-6 and -10) which express endogenous p38 δ . Re-introduction of p38 δ resulted in a time-dependent decrease in OESCC cell proliferation which was exacerbated with p-p38 δ . In addition, we observed that p38 δ and p-p38 δ negatively regulated OESCC cell migration *in vitro*. Finally both p38 δ and p-p38 δ altered OESCC anchorage-independent growth. Our results suggest that p38 δ and p-p38 δ have a role in the suppression of OESCC. Our research may provide a new potential target for the treatment of oesophageal cancer.

Introduction

Oesophageal cancer is the seventh most common cancer worldwide (1) with its 5-year survival rate being dismally low at $\leq 15\%$ (2). Oesophageal squamous cell carcinoma

(OESCC) is an exceptionally drug-resistant tumour. Despite recent advances in the detection of OESCC and the development of multimodal therapy (3,4), its incidence is on the rise and outcome for patients remains poor (5,6). Thus, a greater understanding of the initiation and progression of OESCC is required in order to be able to identify predictive and prognostic factors that may in the future lead to novel therapeutic strategies.

The mitogen-activated protein kinases (MAPKs) are serine/threonine kinases and include the extracellular-regulated kinase (ERK), c-jun NH₂-terminal kinase (JNK) and p38 MAPK families. The p38 MAPK family consists of four members; p38 α (MAPK14) of which there are two splice variants (7), p38 β (MAPK11), p38 γ (MAPK12) and p38 δ (MAPK13) (8). Although these isoforms are 60-70% identical in amino acid sequence they differ greatly in their tissue distribution (9), substrate specificity (10) and sensitivity to chemical inhibitors (11). In recent years, we have gained an increased appreciation of the importance of p38 isoforms for a variety of cellular functions including proliferation, differentiation, transformation and programmed cell death (12). Their roles, however, are more complex than previously thought, with distinct members appearing to have different functions. In addition, the roles of p38 in various pathologic conditions remain to be elucidated (13).

To-date most of the published literature refers to the p38 family as a whole or indeed have focused on the first discovered isoform p38 α (10,13). There is an obvious dearth of research pertaining to the latter two isoforms, p38 γ and - δ , due partly to the lack of commercially available specific chemical activators or inhibitors for each of these isoforms (14). In the present study we have overcome this obstacle using an enzyme-substrate fusion approach for the generation of constitutively active p38 δ . We now provide new information regarding the role(s) of p38 δ and active (phosphorylated) p38 δ (p-p38 δ) in OESCC. We identified differential p38 δ expression in OESCC. Lack of p38 δ expression in OESCC allows for a more aggressive phenotype including increased proliferation, increased migration and increased capacity for anchorage-independent growth. Restoration of p38 δ expression, however, reverses these effects. Together, our results provide evidence for a novel role for p38 δ -induced suppressive effects in OESCC. With survival rates being poor for patients with OESCC, there is an urgent need to find novel strategies to

Correspondence to: Dr Orla Patricia Barry, Department of Pharmacology and Therapeutics, Room 3.89, Western Gateway Building, Western Road, University College Cork, Cork, Ireland
E-mail: o.barry@ucc.ie

Key words: oesophageal cancer, p38 δ mitogen-activated protein kinase, proliferation, migration, anchorage-independent growth

improve current therapy. Our study suggests isoform specific activation of p38 δ as a possible potential approach for treatment of patients with OESCC.

Materials and methods

Reagents. All chemicals and cell culture reagents were purchased from Sigma-Aldrich (Wicklow, Ireland), enzymes from New England BioLabs (Hertfordshire, UK) and primary antibodies from Cell Signaling Technologies (Hertfordshire, UK), unless otherwise stated.

Specimens. The patient cohort consisted of ten patients with OESCC of both genders ranging in age from 44 to 81 years. Formalin-fixed, paraffin-embedded (FFPE) oesophagectomy specimens from ten patients consisted of ten paired samples of primary tumour and metastatic lymph nodes with 10 samples of non-tumour adjacent tissues (NAT). Patient features are summarized in Table IA.

Cell culture. The KE oesophageal cancer cell lines (kind gifts from Professor T. Fujii, Kurume University School of Medicine, Japan) (15-17) as well as KYSE-70, OE-19, OE-21 and OE-33 (ATCC, Rockville, MD, USA) were cultured in RPMI-1640 supplemented with 10% FCS, 100 μ g/ml streptomycin and 100 U/ml penicillin. KE cell line features are summarized in Table IB. The metastatic oesophageal cancer cell line, OC-3 [a kind gift from Cork Cancer Research Centre, (Biosciences Institute, National University of Ireland, Cork, Ireland) (18) was cultured in DMEM supplemented with 10% FCS, 100 μ g/ml streptomycin and 100 U/ml penicillin. KYSE-450 cells (ATCC, Rockville, MD, USA) were maintained in 45% RPMI-1640/45% Ham's F-12 nutrient mixture supplemented with 10% FCS, 100 μ g/ml streptomycin and 100 U/ml penicillin.

Proliferation assay. KE cells were plated at a density of 3×10^4 cells/well in a 6-well tissue culture plate. Cell viability was assessed by trypan blue (0.4% w/v) exclusion assay at the indicated times (18).

Nuclear and cytosolic extraction. Nuclear and cytosolic fractions were isolated from 2×10^6 cells using the NE-PER Isolation kit (Pierce Biotechnology, Rockford, IL, USA) according to the manufacturer's instructions.

Generation of MKK6b-p38 δ MAPK, MKK6b(E)-p38 δ MAPK and MKK6b(E)-p38 δ_{DN} MAPK fusion proteins. p38 δ (pcDNA3-FLAG-p38 δ) and constitutively active MKK6b [pcDNA3-MKK6b(E)] plasmids were a kind gift from Professor J. Han (Scripps Research Institute, La Jolla, CA, USA) and have previously been described (19). To construct the pcDNA3-MKK6b(E)-FLAG-p38 δ (p-p38 δ) fusion plasmid the TAA stop codon of MKK6b(E) was replaced with a unique *Swa*I restriction sequence using a QuikChange Lightning Site-Directed Mutagenesis kit (Agilent Technologies) (5'-CAT CTTTGTAAAAGTCTGATTCTTGGAGAATTTAAATCAG TGGACTTAATCGGTTGACCCTACTG-3'; 5'-CAGTAG GGTCAACCGATTAAGTCCACTGATTTAAATTCTCCAA GAATCAGTTTACAAAAGATG-3'). A PCR generated

Table I. Patient characteristics, and cell lines used.

A, OESCC patient features

Patient features	No. of patients
Gender	
Male	4
Female	6
Age, median (years)	63 (44-81)
TNM7 stage	
T stage	
T3	10
N stage	
N1	3
N2	7
Histological grade	
Well differentiated	1
Moderately differentiated	6
Poorly differentiated	3

B, KE (OESCC) cell line features

KE features	
Gender	
Male	KE-3, -4, -5, -6
Female	KE-8, -10
Age, median (years)	67 (50-71)
TNM7 stage	
T stage	
T1	KE-10
T3	KE-3, -5, -6, -8
T4	KE-4
N stage	
N0	KE-5
N1	KE-3, -4, -6, -8, -10
Histological grade	
Well differentiated	KE-5, -6
Moderately differentiated	KE-3, -10
Poorly differentiated	KE-4, -8

C, p38 δ MAPK expression in patient specimens

Diagnosis	p38 δ MAPK expression	
	Positive	Negative
NAT (n=10)	9	1
OESCC primary (n=10)	6 ^a	4
OESCC nodes (n=10)	2	8

A, Patient features and B, KE features are summarised based on gender, age, TNM7 stage and histological stage. Based on the TNM7 categorization for oesophageal cancer N1=1-2 lymph nodes and N2=3-6 lymph nodes. C, Samples obtained from ten patients consisted of ten paired primary tumour and metastatic lymph nodes as well as corresponding non-tumour adjacent tissues for analysis of p38 δ expression. ^ap38 δ expression was considerably lower than in the corresponding NAT.

DraI-DraI fragment encoding FLAG-p38 δ with a 5' (Gly-Glu)₅ linker (5'-CCGCGCTTTAAAGGCGAGGGCGAGGGCGAGGGCGAGGGCGAGATGGACTACAAGGACGACGAT-3'; 5'-TTGATCTTTAAATTATTACAGCTTCATGCCACTTCGT-3') to facilitate folding as previously described (20) was ligated to *SwaI* linearised pcDNA3-MKK6b(E) with T4 DNA ligase. The pcDNA3-MKK6b-FLAG-p38 δ plasmid (inactive MKK6b) was created by the substitution of Glu¹⁵¹ and Glu¹⁵⁵ with Ser and Thr respectively by site-directed mutagenesis (5'-TGGAATCAGTGGCTATTTGGTGGACTCTGTGCTAAACAATTGATGCAGTTGCAAACCATAC-3'; 5'-GTATGGTTTGC AACCTGCATCAATTGTTTTAGCAA CAGAGTCCACCAAATAGCCACTGATTCCA-3'). The pcDNA3-MKK6b(E)-FLAG-p38 δ_{DN} (dominant negative) (p-p38 δ_{DN}) plasmid was created by substituting Thr¹⁸⁰ and Tyr¹⁸² of p38 δ with Ala and Phe respectively by site-directed mutagenesis (5'-GACGCCGAGATGGCTGGCTTCGTGGTGACCCG-3'; 5'-CGGGTCACCACGAAGCCAGCCATCTCGGCGTC-3'). DNA sequence analysis confirmed the integrity of all plasmids.

Stable transfection. KE-3 cells were transfected using Lipofectamine™ 2000 reagent (Life Technologies™) and a total of 4 μ g of plasmid DNA according to the manufacturer's instructions. Twenty-four hours following transfection cells were transferred to 100-mm diameter dishes and transfected cells were selected in growth medium containing 800 μ g/ml Geneticin. After 4-8 weeks, individual cell colonies were transferred for clone expansion.

Immunoblot analysis. Supernatants used for immunoblotting with specific antibodies, p38 α and - δ , phospho-p38 MAPK and MKK6 antibodies (New England Biolabs), p38 γ (Upstate) and p38 β_2 antibody (Zymed Laboratories Inc.) have previously been described by us (18,21). Chemiluminescent detection was performed using SuperSignal® WestDura Extended Duration Substrate (Pierce Biotechnology) and bands were visualized using a Syngene G:Box ChemiXR5 Gel Documentation System.

Immunohistochemistry. This was performed as previously described by us (21). Briefly, FFPE OESCC and NAT sections were de-paraffinized in xylene and re-hydrated prior to analysis. Antigen retrieval was performed by microwave irradiation in 0.01 M citrate buffer, pH 6.0. In addition cultured cells grown on coverslips were fixed in 2-4% paraformaldehyde and permeabilised with 0.5% Triton-X-100. Samples were blocked with 5% NGS in TS/SAP. Slides were incubated with primary antibody overnight at 4°C. Antibody binding was localized using a biotinylated secondary antibody, avidin-conjugated HRP and DAB substrate, contained within the Vectastain ABC detection kit (Vector Laboratories, Burlingame, CA, USA). Slides were counterstained with hematoxylin.

ELISA. Cell lysates were analysed for p38 δ phosphorylation at T180/Y182 using the R&D Systems DuoSet® IC Human phospho-p38 δ (T180/Y182) sandwich ELISA (DYC2124-5) according to the manufacturer's instructions. Absorbance was read at 450 nm on a Tecan Sunrise spectrophotometric plate reader and analysed using the XRead software program.

Boyden chamber cell migration assay. Cells were plated in starvation medium at a density of 3x10⁴ cells/well into a 96-well plate of the upper chamber. The bottom chamber contained 10% FCS as the chemoattractant. Cells were left migrate for 24 h through the matrigel filter (8 mm). Migrated cells were treated with MTT (3-(4,5-dimethylthiazol-2-yl)-2,5-diphenyltetrazolium bromide) (5 mg/ml) and absorbance read at 540 nm to calculate viable cell numbers as previously described (21).

Wound-healing assay. Cell migration was assessed by *in vitro* wound-healing assay as previously described (22). A linear wound track was made by use of a sterile tip through confluent cells. Cells migrating into the wound were captured under a phase-contrast microscope 24 and 48 h after wounding. Migration was determined using the ImageJ program as an average closed area of the wound relative to the initial wound area at 24 and 48 h after wounding.

Colony forming assay. The role of p38 δ in anchorage-independent growth was assayed using a soft agar colony-forming assay as previously described (21). Cells were plated at a density of 3x10⁵ cells/100-mm dish in medium containing 0.4% (w/v) agar on an underlay of 0.8% (w/v) agar. After a 21-day incubation colonies were stained with MTT (5 mg/ml) overnight and counted.

siRNA. KE-6 cells at 75% confluency in antibiotic-free media were transfected with 100 nM p38 δ MAPK siRNA or control siRNA-A (Santa Cruz Biotechnology, Santa Cruz, CA, USA) according to the manufacturer's instructions and as recently described (23).

RT-PCR. First-strand cDNA was synthesised using SuperScript® VILO™ cDNA Synthesis kit (Life Technologies) from total RNA isolated from cells using an Illustra RNASpin Mini kit (GE Healthcare, Buckinghamshire, UK) according to the manufacturer's instructions. p38 δ mRNA was amplified from cellular cDNA under the following conditions: ddH₂O, 1X DreamTaq buffer, 0.2 mM dNTPs, 0.25 μ M p38 δ forward primer: 5'-CCACGTAAACTGCCCATCT-3', 0.25 μ M p38 δ reverse primer: 5'-CCGCCACAAGCTAAAAGAG-3', 1 μ l cDNA and 1 U DreamTaq DNA polymerase (Thermo Fisher Scientific; Waltham, MA, USA). RT-PCR products were analysed by agarose gel electrophoresis.

Proteome Profiler™ antibody array. The relative levels of phosphorylation of 26 kinases was examined in cell lysates using a Proteome Profiler Human Phospho-MAPK array (R&D Systems, Abingdon, UK) according to the manufacturer's instructions. Following chemiluminescent detection, pixel density of each spot was analysed using Scion image software.

Ethics. The research was approved by the Clinical Research Ethics Committee of the Cork Teaching Hospitals.

Statistical analysis. Results are expressed as mean \pm SE. Statistical comparisons were made by using analysis of variance with subsequent application of Student's t-test, as

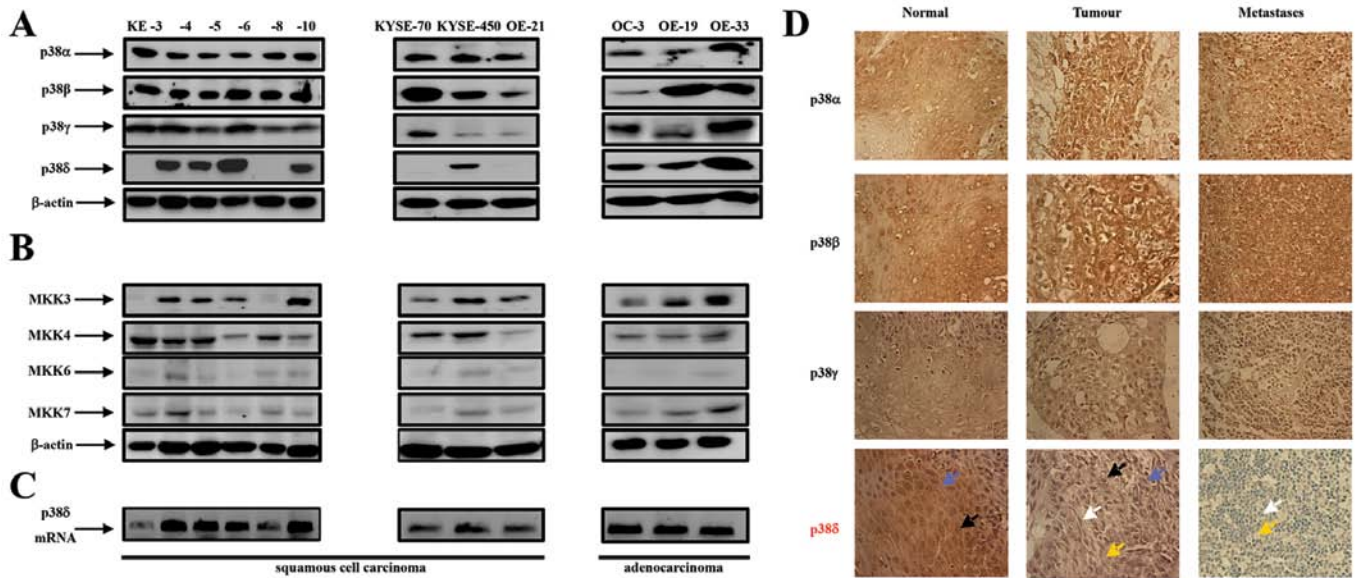


Figure 1. Expression of p38 MAPK isoforms, MKK3, -4, -6 and -7 in oesophageal cancer. (A) Western blot analysis of p38 isoform expression in KE-3, -4, -5, -6, -8 and -10, KYSE-70, -450 and OE-21 (oesophageal squamous cell carcinoma cell lines) as well as OC-3, OE-19 and OE-33 (oesophageal adenocarcinoma cell lines). (B) Western blot analysis of MKK3, -4, -6 and -7 in the same twelve cell lines. Aliquots of 30 μ g of protein lysate were loaded on a 10% SDS-PAGE gel and analyzed by immunoblotting using antibodies specific for p38 α , - β , - γ and - δ . β -actin analysis served as a loading control. The results shown are representative of four independent experiments. (C) Agarose gel electrophoresis analysis of DNA fragments produced by PCR amplification of p38 δ mRNA from oesophageal squamous (KE3, -4, -5, -6, -8, 10, KYSE70, -450 and OE21) and adenocarcinoma (OC3, OE19 and -33) cell lines. (D) Immunohistochemical staining of p38 α , - β , - γ and - δ isoforms in normal, tumourigenic and metastatic (lymph node) oesophageal human tissue. Immunohistochemical staining was performed as outlined in Materials and methods. Blue arrow indicates cytoplasmic staining; black arrow indicates nuclear staining; white arrow indicates blue unstained nuclei and yellow arrow indicates blue unstained cytoplasm. Magnification, x400. The results shown are representative of ten patients.

appropriate. GraphPad InStat 3 software was used also for statistical analysis.

Results

p38 α , - β , - γ and - δ isoforms and MKK3, -4, -6 and 7 are differentially expressed in oesophageal cancer. The expression of p38 as a family has previously been outlined in oesophageal cancer as well as other cancer types (10,13,24,25). While these reports refer to the p38 family, analysis of individual p38 isoform expression in oesophageal cancer has to date never been reported. A previous study by us outlining differential p38 isoform expression in renal cancer prompted us to investigate further the effects of individual p38 family members in cancer in general (26). Using western blot analysis we examined p38 MAPK isoform expression in nine OESCC cell lines (KE-3, -4, -5, -6, -8, -10, KYSE-70, KYSE-450 and OE-21) and three oesophageal adenocarcinoma cell lines (OC-3, OE-19 and OE-33). We used antibodies specific for each isoform p38 α , - β , - γ and - δ as previously described by us (26). All twelve oesophageal cancer cell lines (squamous and adenocarcinoma) expressed p38 α , - β and - γ (albeit at different levels) (Fig. 1A). In contrast p38 δ expression was present in the three adenocarcinoma cell lines but absent in four of the OESCC cell lines KE-3, -8, KYSE-70 and OE-21 (Fig. 1A). The specific loss of p38 δ isoform expression only has previously been reported by us in renal carcinoma (786-0) (26) and also observed by us in liver (Huh-7), lung (A-549) prostate (PC-3 and DU-145) and skin (MeWo) cancer cell lines (Barry *et al*, unpublished data). Upstream MKK3 and -6 are thought to be the major protein kinases responsible for p38 activation

(24) but the selectivity of p38 isoform activation is stimulus type and strength dependent (27). We observed strong MKK3 and -4 expression for all cell lines except KE-3 and -8 OESCC which were MKK3 negative. In contrast levels of MKK6 and -7 expression were considerably lower (Fig. 1B).

Finally, analysis of p38 δ at the mRNA level surprisingly proved positive for all cell lines examined including the four OESCC cell lines that were negative for p38 δ protein expression (Fig. 1C). Primers specific for a 292-bp fragment of the 3'-untranslated region of p38 δ mRNA amplified cDNA from all twelve cell lines. Other primer sets within the coding sequence yielded similar results (data not shown). In addition DNA sequence analysis of PCR products did not identify any mutations such as a stop codon or a missense mutation which could possibly explain loss of p38 δ protein expression (data not shown).

To investigate whether the p38 isoform expression pattern we observed *in vitro* with the OESCC cell lines could be translatable to the *in vivo* situation we analyzed the expression profile and localization of all four p38 isoforms (α , - β , - γ and - δ) in FFPE oesophagectomy specimens from ten patients with squamous cell carcinoma. Samples consisted of ten paired primary tumour and metastatic (lymph nodes) as well as corresponding non-tumour adjacent tissues (NAT) as outlined in Table IA. Samples were staged according to the new TNM7 categorization for oesophageal cancer (Table IA) (28). Consistent levels of p38 α and - β expression was evident in all ten normal, primary and metastatic OESCC samples (Fig. 1D). Similarly, we did not observe a change in p38 γ expression between normal, primary tumour and metastatic samples albeit the intensity of brown staining was less than that

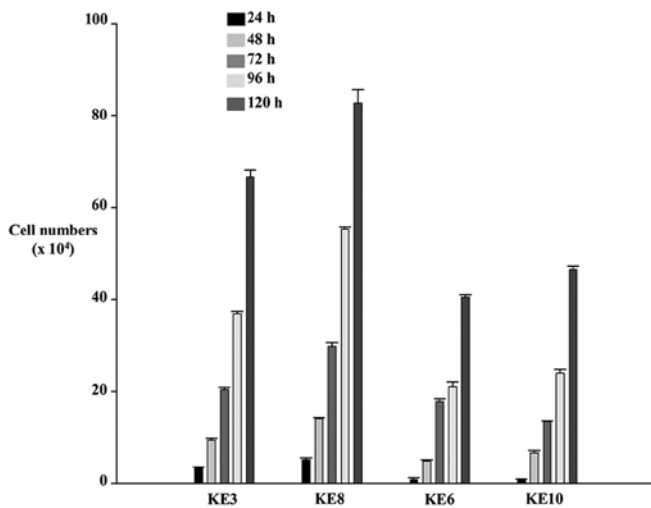


Figure 2. Oesophageal squamous cell carcinoma cell lines lacking endogenous expression of p38 δ MAPK have a higher proliferation rate. KE-3 and -8 cell lines (lacking endogenous p38 δ expression) and KE-6 and -10 cell lines (expressing endogenous p38 δ expression) were seeded (3×10^4) and counted for 24-120 h. The results shown are mean \pm SE of three independent experiments.

observed for p38 α and - β (Fig. 1D). p38 δ expression, however, was considerably different in normal vs primary tumour vs metastatic disease (Fig. 1D and Table IC). p38 δ expression was observed in both the nuclei and cytoplasm of nine of the ten oesophageal NAT tissue samples. However, a significant decrease in expression was observed in both the nuclei and cytoplasm in the ten primary tumour specimens as evidenced from the lighter brown staining compared to NAT samples in six patient samples and complete loss of expression in four of the samples (Fig. 1D and Table IC). Furthermore, eight out of the ten metastatic tissue specimens demonstrated complete loss of p38 δ expression with both the nuclei and cytoplasm appearing blue in colour (Fig. 1D). This is an important finding considering identification of lymph node metastasis is the single most important prognostic factor in oesophageal cancer (1).

OESCC cell lines lacking endogenous p38 δ MAPK expression proliferate faster than those which express this isoform. The results obtained for differential p38 δ expression in both the oesophageal cell lines and the human samples prompted us to investigate further the effect(s) if any this particular isoform may have on the tumourigenicity of OESCC. Firstly, we examined whether the absence or presence of endogenous p38 δ expression could have an effect on the proliferation rate of our OESCC cell lines. Using the trypan blue exclusion assay we compared the proliferation rate of KE-3 and -8 cell lines (which do not express p38 δ) versus KE-6 and -10 (which express p38 δ). We observed that at all time-points studied (24-120 h) both cell lines KE-3 and -8 proliferated faster than KE-6 and -10 cells (Fig. 2).

Generation of active (phosphorylated) p38 δ (p-p38 δ) MAPK fusion proteins. To investigate whether p38 δ or active (phosphorylated) p38 δ (p-p38 δ) drives the observed anti-proliferative phenotype (Fig. 2) we re-introduced wild-type p38 δ into KE-3

cells which have lost its expression. In the absence of a specific commercially available p38 δ activator [and to investigate the effect(s) of active (p-p38 δ)] we generated a constitutively active p38 δ through enzyme substrate fusion as previously described for JNK (Fig. 3A) (20). Western blot analysis of stable transfections of KE-3 cells demonstrated that pcDNA3-MKK6b-(Gly-Glu)₅-FLAG-p38 δ (data not shown) as well as pcDNA3-MKK6b(E)-(Gly-Glu)₅-FLAG-p38 δ both produced a single polypeptide with a molecular mass of 82 kDa as expected when using p38 δ , p-p38 and MKK6 antibodies, respectively (Fig. 3B). As both MKK6b and MKK6b(E) fused in frame to p38 δ produced the same desired result only one plasmid (MKK6b(E)-p38 δ) was used for subsequent experiments. Western blot analysis of KE-3 cells stably transfected with pcDNA3-MKK6b(E)-(Gly-Glu)₅-FLAG-p38 δ _{DN} also produced a single polypeptide with a molecular mass of 82 kDa upon incubation with p38 δ and MKK6 antibodies (Fig. 3Bi and iii) but did not demonstrate p38 activation (phosphorylation) (Fig. 3Bii). Of note the antibody used in Fig. 3Bii is a pan phospho-p38 antibody. To our knowledge there is no commercially available antibody to test for active (phosphorylated) p-p38 δ specifically by western blot analysis. Therefore, to confirm p38 δ activation we performed a sandwich ELISA which measures p38 δ isoform phosphorylation specifically. Transfection of KE-3 cells with wild-type p38 δ alone revealed activation (Fig. 3C). This is in strong agreement with previous reports where adenovirally expressed wild-type p38 δ was activated in head and neck squamous cell carcinoma (29) and human keratinocytes (30). A 4-fold ($p < 0.001$) increase in activation of p38 δ was observed following stable transfection of KE-3 cells with p-p38 δ (Fig. 3C). This level of activation is similar to KE-3 p38 δ transfected cells upon activation with anisomycin (30 μ M) (data not shown). As expected we did not observe phosphorylation of p38 δ in cells transfected with p-p38 δ _{DN} (Fig. 3C). We also analysed KE-6 and KE-10 cell lines (which express endogenous p38 δ expression) but did not observe p38 δ phosphorylation in either cell line (Fig. 3C).

To ensure specific phosphorylation of p38 δ only and not the other three p38 isoforms (α , - β and - γ) we performed a human phospho-MAPK antibody array (R&D Systems). We did not observe phosphorylation of p38 α , - β or - γ in non-transfected KE-3 cells or cells stably transfected with p38 δ or p-p38 δ (Fig. 3D and E). We did, however, observe an increase ($p < 0.001$) in phosphorylation in KE-3 p38 δ wild-type transfected cells which was amplified in KE-3 p-p38 δ transfected cells (Fig. 3D and E) in agreement with our ELISA results (Fig. 3C). These results confirm phosphorylation of p38 δ only in our studies. We also observed MKK6 phosphorylation in KE-3 p-p38 δ as expected (Fig. 3D and E). A previous report outlined p38 δ induced inactivation of ERK1/2 (31) however, we did not find any change in ERK1/2 or indeed JNK1/2/3 (Fig. 3D and E).

Finally, the physical location of a protein either in the nucleus or the cytoplasm directly influences its biological function. Members of the p38 family do not contain either a nuclear localisation signal (NLS) or a nuclear export signal (NES) but their subcellular localisation can be regulated in part by their interacting proteins (32). We compared the subcellular localization of p38 δ and p-p38 in KE-3 transfected cells with endogenous p38 δ expression in KE-6 cells. As expected p38 δ

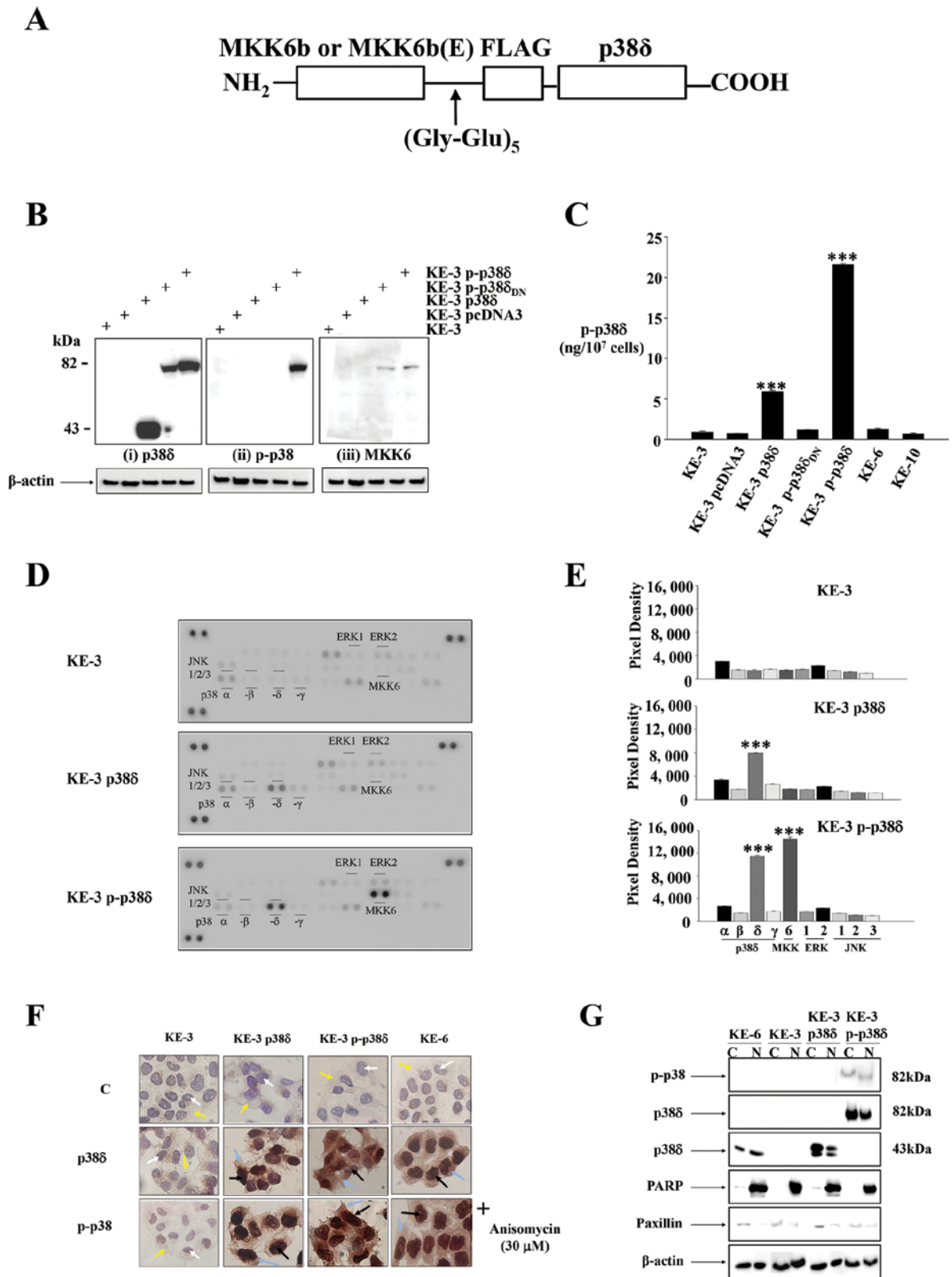


Figure 3. Generation of active p38δ (p-p38δ) MAPK fusion proteins. (A) A schematic representation of MKK6b-p38δ or MKK6b(E)-p38δ MAPK fusion protein. The coding region of p38δ was fused in frame to the 3'-end of the stop codon-less MKK6b or MKK6b(E) through a peptide linker (Gly-Glu)₅. (B) Western blot analysis of KE-3 cells stably transfected with empty vector (pcDNA3), wild-type p38δ, p-p38δ and p-p38δ^{DN}. Cells were analysed by immunoblot using antibodies specific for p38δ (i), p-p38 (ii) and MKK6 (iii). Aliquots of 30 μg protein lysate for each cell line were loaded on a 10% SDS-PAGE gel. The results shown are representative of four independent experiments. (C) Transfected and non-transfected KE-3, KE-6 and KE-10 cells were analysed to determine the amount of activated i.e., phosphorylated p38δ expression using the human phospho-p38δ (T180/Y182) ELISA commercial kit (R&D Systems). The ELISA assay was carried out according to the manufacturer's protocol. The results shown are mean ± SE of three independent experiments. Significant (***) p<0.001 changes from control non-transfected KE-3 cells. (D) The human phospho-MAPK array shows the effects of stably transfecting KE-3 cells with p38δ and p-p38δ. Arrays were incubated with 200 μg of cell lysate. (E) Corresponding pixel density for p38α, -β, -δ and -γ, MKK-6, ERK1/2 and JNK1/2/3 phosphorylation in non-transfected and transfected KE-3 cells. (F) Immunohistochemical subcellular localization of p38δ and p-p38 in KE-3 non-transfected cells and cells transfected with p38δ and p-p38δ. KE-6 cells were or were not treated with anisomycin (30 μM). (G) Nuclear and cytoplasmic localization of p38δ and p-p38 in KE-3 and KE-6 cells. The results shown are representative of four independent experiments (F and G).

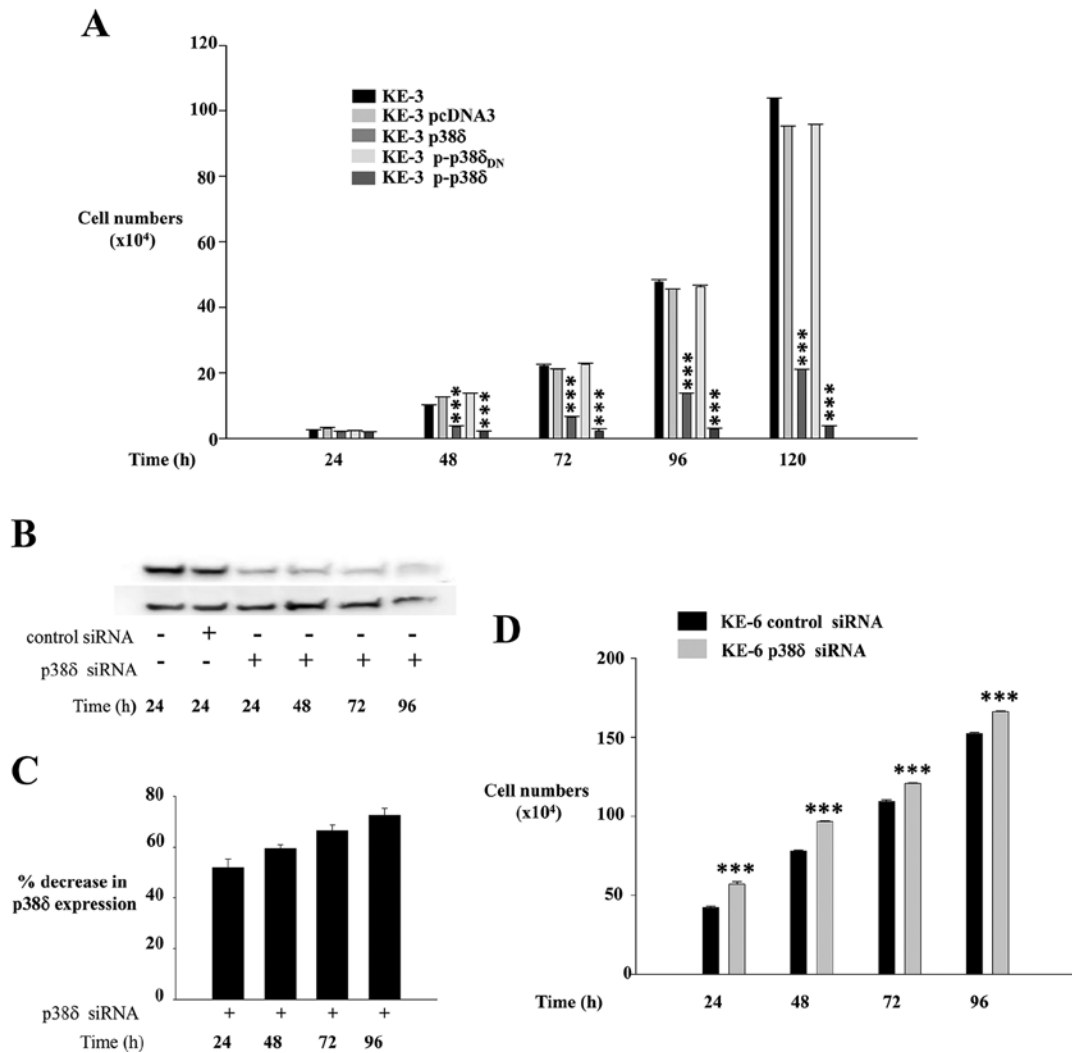


Figure 4. Effect of p38 δ and p-p38 δ MAPK expression on cell proliferation. (A) KE-3, KE-3 pcDNA3, KE-3 p38 δ , KE-3 p-p38 δ and KE-3 p-p38 δ_{DN} cells were seeded (3×10^4) and counted for 24-120 h. The results shown are mean \pm SE of three independent experiments. Significant (** $p < 0.001$) changes from control non-transfected KE-3 cells. (B) Western blot analysis of KE-6 cells transiently transfected or not transfected with p38 δ siRNA or control siRNA for 24-96 h. Cells were analysed by immunoblotting using a p38 δ antibody. Aliquots of 30 μ g protein lysate were loaded on a 10% SDS-PAGE gel. The results shown are representative of three independent experiments. (C) Densitometric analysis was performed to analyse % knockdown of KE-6 p38 δ protein. (D) KE-6 cells (3×10^4) transfected with p38 δ siRNA or control siRNA were seeded and counted for 24-96 h. The results shown are mean \pm SE of three independent experiments each done in triplicate. Significant (** $p < 0.001$) changes from control siRNA transfected KE-6 cells.

and p-p38 were absent from both compartments in non-transfected KE-3 cells (Fig. 3F). p38 δ and p-p38 were detected in both the cytoplasm and the nucleus of KE-3 stably transfected cells (Fig. 3F). This pattern of expression correlated with the subcellular localization of p38 δ and p-p38 in KE-6 cells in the presence and absence of anisomycin (30 μ M). To confirm our immunohistochemical findings cytosolic and nuclear extracts were prepared from transfected and non-transfected KE-3 and KE-6 cells and examined by western blot analysis. The use of PARP as a nuclear-restricted marker and Paxillin as a cytosolic marker ensured that there was no cross contamination between the subcellular fractions (21). Similar results were observed demonstrating the presence of p38 δ and p-p38 in both the cytoplasm and nucleus of KE-3 and -6 cells (Fig. 3G).

KE-3 cells transfected with p38 δ and p-p38 δ MAPK show reduced proliferation. Uncontrolled cellular proliferation is a

hallmark of cancer. To investigate if loss of p38 δ expression specifically drives the higher growth kinetics observed in Fig. 2 we compared the growth rates of KE-3 non-transfected and transfected cells. We observed a significant ($p < 0.001$) time-dependent decrease in the proliferation rate of KE-3 cells when transfected with wild-type p38 δ compared with non-transfected cells and cells transfected with empty pcDNA3 vector (Fig. 4A). This anti-proliferative effect was amplified further in KE-3 cells transfected with active p-p38 δ (Fig. 4A). KE-3 cells transfected with p-p38 δ_{DN} demonstrated the same proliferation rate as non-transfected cells or cells transfected with pcDNA3 only (Fig. 4A).

To further examine the hypothesis that p38 δ is anti-proliferative in OESCC we employed a siRNA approach using the KE-6 cell line which expresses endogenous p38 δ (Figs. 1, 3F and G). KE-6 cells were transiently transfected with p38 δ siRNA or control siRNA as previously described (23). We

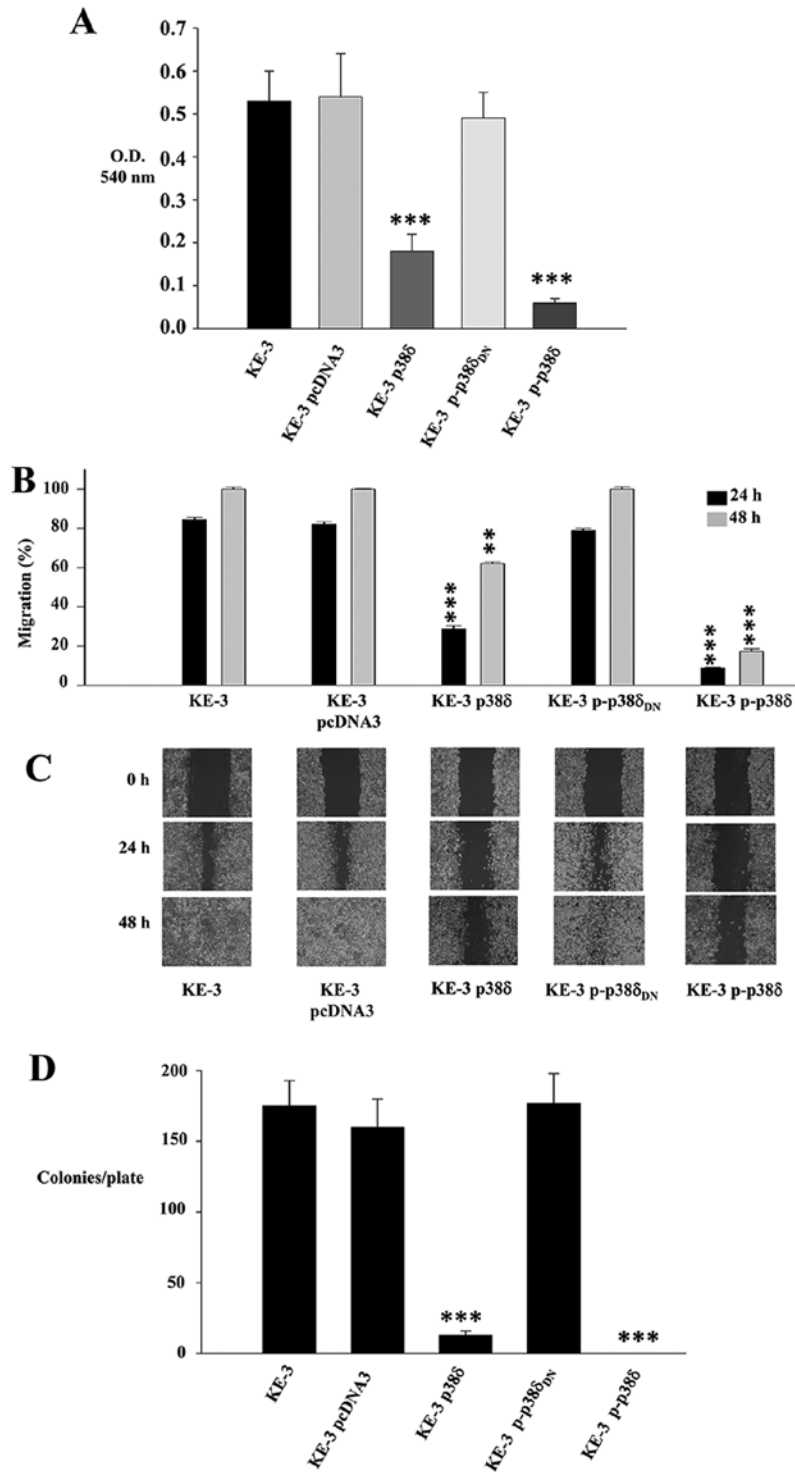


Figure 5. Effect of p38δ and p-p38δ MAPK on KE-3 cell migration and anchorage-independent growth. KE-3, KE-3 pcDNA3, KE-3 p38δ, KE-3 p-p38δ and KE-3 p-p38δ_{DN} cells were analysed for cell migration (A-C) and anchorage-independent growth (D). (A and B) p38δ and p-p38δ inhibit KE-3 migration at 24 h (A, Boyden Chamber) and 24 and 48 h (B, wound healing). (C) Representative wound healing images at 0, 24 and 48 h. Wound healing rates decrease in p38δ and p-p38δ transfected KE-3 cells. The results shown are representative of three independent experiments. (D) Anchorage-independent growth potential of KE-3 non-transfected and transfected cells were measured by their ability to form colonies on soft agar. Plates were stained with 3-(4,5-dimethylthiazol-2-yl)-2, 5-diphenyl tetrazolium bromide to visualize colonies. The number of colonies per plate is shown. The results shown are mean ± SE of four independent experiments (A, B and D). Significant (** p<0.01; *** p<0.001) changes from control non-transfected KE-3 cells.

observed a 51.9±6.5% reduction in KE-6 p38δ expression at 24 h following p38δ siRNA transfection which increased to 72.6±2.6% by 96 h when compared to control siRNA transfected KE-6 cells (Fig. 4B and C). No change in p38δ expression was observed when KE-6 cells were transfected

with control siRNA for all time-points studied (24-96 h) (only 24 h is shown in Fig. 4B). A significant (p<0.001) increase in cell proliferation was observed for KE-6 cells transfected with p38δ siRNA compared to cells transfected with control siRNA for all time-points studied (Fig. 4D). The anti-proliferative

effect was observed even in the absence of active p38 δ in KE-6 cells (Fig. 3C). This effect on proliferation may be independent of its kinase activity as has previously been reported for p38 α in regulating HeLa cell proliferation (33) and p38 γ in rat intestinal epithelial cells (34).

p38 δ and p-p38 δ MAPK play a role in migration and anchorage-independent growth of KE-3 cells. A key characteristic of cancer cells is their ability to migrate and progress from primary tumours to metastases in distant organs. A recent report summarizes the roles of p38 MAPKs in cancer invasion and metastasis (35). This review, however, as in previous reports documents the roles of p38 family as a whole or p38 α (10,13). We examined the role of p38 δ in OESCC cell migration using both a Boyden chamber assay and a wound healing assay. We observed a 66 \pm 7.5 and 88.7 \pm 1.9% decrease in migration after 24 h for KE-3 p38 δ and p-p38 δ cells respectively compared to non-transfected cells (Fig. 5A). In addition p38 δ and p-p38 δ induced a significant decrease in KE-3 migration at 24 h [55.65 \pm 1.5 and 75.65 \pm 0.3% (p <0.001), respectively] and 48 h [37.9 \pm 0.8, (p <0.01) and 82.7 \pm 1.4%, (p <0.001) respectively] compared with non-transfected KE-3 cells using a wound healing assay (Fig. 5B and C). Finally, to further examine the influence of p38 δ and p-p38 δ on the growth characteristics of KE-3 cells, we measured their ability to grow in an anchorage-independent manner. Non-transfected KE-3 cells growing in soft agar for 21 days gave rise to 175 \pm 18 colonies/plate (Fig. 5D). This was similar to the number of colonies/plate that grew for cells transfected with empty vector (160 \pm 20) or p-p38 δ_{DN} (177 \pm 21) (Fig. 5D). In contrast, however, p38 δ and p-p38 δ transfected cells produced a significant (p <0.001) decrease in colony numbers in p38 δ transfected cells (13 \pm 3) with no colonies observable for p-p38 δ transfected cells (Fig. 5D).

Discussion

Oesophageal cancer is a highly aggressive treatment-refractory disease with a high mortality rate (2,5,6). As conventional therapy is ineffective, targeting specific potential molecular tumour markers may prove to be the future of oesophageal cancer treatment. Despite current studies of molecular targets in oesophageal cancer (36), we are still somewhat hindered by limited knowledge of the genes and pathways involved in the tumorigenesis of the oesophagus when it comes to treatment.

Emerging role(s) for p38 MAPKs in different aspects of cancer has recently been outlined. To-date the best studied and reviewed isoform in cancer is p38 α . It has been characterized as both a potential tumour suppressor (25,37-39) and tumour promoter (29,35). In comparison the role(s) of p38 δ in cancer is largely uncharacterised. The limited current knowledge pertaining to p38 δ , however, also alludes to disparate role(s) for this kinase in tumour development. An oncogenic role for p38 δ has been suggested in p38 δ -deficient mice that have reduced susceptibility to skin carcinogenesis (40) as well as promoting head and neck squamous carcinoma cell growth (29). In contrast a very recent study outlined a role for p38 δ as a tumour suppressor in mouse fibroblasts (41). In our study outlined here we show for the first time the differential expression of p38 δ in OESCC cell lines and *in vivo*. The loss

of p38 δ expression provides a survival advantage for OESCC which demonstrates increased cell proliferation, migration and contact inhibition. Re-introduction of p38 δ , however, leads to reversal of these tumourigenic effects. Thus, recent evidence (41) as well as our present study suggests that targeting p38 δ may offer a powerful protection against carcinogenesis. Targeting p38 MAPK isoforms or pathways for therapeutic purposes, however, should perhaps be strictly dependent on cell context, tumour cell type and tumour stage.

The fusion of p38 δ to its upstream kinase MKK6b or active MKK6b [MKK6b(E)] generated a constitutively active p38 δ which was used as a tool to study its specific effect(s) in OESCC. Re-introduction of p38 δ (with subsequent activation) or active p-p38 δ into KE-3 OESCC attenuated cell proliferation, migration and anchorage-independent growth. The strength and duration of p38 activation has been shown to play a crucial role in determining cell fate. Strong activation has been shown to induce apoptosis whereas lower levels results in cell survival (27,39). In our study we observed strong anti-proliferative, anti-migratory effects as well as effects on anchorage-independent growth upon re-introduction of p38 δ into KE-3 cells which subsequently became active. These antitumourigenic effects were amplified further in KE-3 cells transfected with constitutively active p-p38 δ . It is possible that owing to the localization of both p38 δ and p-p38 δ in the nucleus and the cytoplasm of OESCC that this kinase may modify its target(s) either structurally or subcellularly. We are presently researching whether they are in free form or docked with specific cytoplasmic or nuclear partners (24). Furthermore, p38 δ and p-p38 δ induced antitumourigenic effects in OESCC may arise by a combination of both phosphorylation-dependent and independent effects as previously described (33,34).

There are many paradigms in the literature of cross-talk between different MAPK pathways. In this instance, however, when KE-3 cells were stably transfected with p38 δ or p-p38 δ we did not observe changes in either p38 isoform (α , β and γ), ERK1/2 or JNK1/2/3 expression (data not shown) or activation levels. This is in agreement with a recent bio-informatics analysis of MAPK pathways which specifically identified that persistent activation of p38 δ is resistant to interaction with other MAPKs (42). This lack of interference from other MAPKs permits us to specifically study the effects of p38 δ on cell cycle control, pathway components and regulatory mechanisms in OESCC which is currently ongoing in our laboratory. In addition negative feedback mechanisms have been shown to contribute to fine-tuning p38 MAPK activity levels. One such report outlines an increase in MKK6 expression and stability in p38 $\alpha^{-/-}$ cardiomyocytes from transgenic mice (43). We did not observe a correlation between the presence or absence of p38 δ expression in OESCC cells and MKK expression. Of notable exception is MKK3 whose expression is absent from KE-3 and -8 cells (both negative for p38 δ) but present in KE-4, -5, -6 and -10 cells (all positive for p38 δ). However, this pattern of expression does not hold for KYSE-70 and OE-21 OESCC cell lines which express MKK3 but are also negative for p38 δ protein expression.

Reports of the involvement of p38 MAPKs in a variety of different pathological conditions is continuing to increase fuelling interest in the development of potent and specific drugs for modulating the activity of these kinases. Presently

there are a number of p38 inhibitors undergoing clinical trials for the treatment of inflammatory diseases (44,45). Results arising from our study demonstrate that loss of p38 δ expression in OESCC provides a more sinister phenotype with increased proliferation, migration and anchorage-independent growth. Thus, it is possible that isoform specific activation (rather than inhibition) of p38 δ may provide a therapeutic benefit for patients with OESCC which express this isoform. In addition, how p38 δ activators may interact and enhance the effectiveness of traditional therapeutics in combination therapy warrants attention.

In conclusion, our results reveal previously undocumented p38 δ differential expression and function in OESCC. We identified a subset of OESCC cell lines as well as human primary and metastatic tumour samples that exhibit downregulation of p38 δ protein expression. We now provide evidence that loss of expression of this particular isoform may be a mechanism by which OESCC cells promote carcinogenesis. Re-introduction of p38 δ into OESCC negative cell lines suppressed different aspects of tumourigenesis. Our data warrant further investigation to understand the important physiological and pathophysiological effects of p38 δ in OESCC and is currently in progress. This knowledge should identify which pathways, substrates or regulators are affected specifically by p38 δ in providing an antitumourigenic effect in OESCC. Armed with this information uncovering novel targets and the development of new therapeutics may be possible for this common cancer that continues to demonstrate a generally poor clinical outcome.

Acknowledgements

This study was supported by the Health Research Board, Ireland (grant HRA/2009/17).

References

- Kayani B, Zacharakis E, Ahmed K and Hanna GB: Lymph node metastases and prognosis in oesophageal carcinoma - a systematic review. *Eur J Surg Oncol* 37: 747-753, 2011.
- Enzinger PC and Mayer RJ: Esophageal cancer. *N Engl J Med* 349: 2241-2252, 2003.
- Almhanna K and Strosberg JR: Multimodality approach for locally advanced esophageal cancer. *World J Gastroenterol* 18: 5679-5687, 2012.
- Thallinger CM, Kiesewetter B, Raderer M and Hejna M: Pre- and postoperative treatment modalities for esophageal squamous cell carcinoma. *Anticancer Res* 32: 4609-4627, 2012.
- Klein CA and Stoecklein NH: Lessons from an aggressive cancer: evolutionary dynamics in esophageal cancer. *Cancer Res* 69: 5285-5288, 2009.
- Bird-Lieberman EL and Fitzgerald RC: Early diagnosis of oesophageal cancer. *Br J Cancer* 101: 1-6, 2009.
- Sanz V, Arozarena I and Crespo P: Distinct carboxy-termini confer divergent characteristics to the mitogen-activated protein kinase p38 α and its splice isoform Mxi2. *FEBS Lett* 474: 169-174, 2000.
- Raman M, Chen W and Cobb MH: Differential regulation and properties of mapks. *Oncogene* 26: 3100-3112, 2007.
- Hui L, Bakiri L, Mairhorfer A, Schweifer N, Haslinger C, Kenner L, Komnenovic V, Scheuch H, Beug H and Wagner EF: P38alpha suppresses normal and cancer cell proliferation by antagonizing the jnk-c-jun pathway. *Nat Genet* 39: 741-749, 2007.
- Ono K and Han J: The p38 signal transduction pathway: activation and function. *Cell Signal* 12: 1-13, 2000.
- Zarubin T and Han J: Activation and signaling of the p38 MAP kinase pathway. *Cell Res* 15: 11-18, 2005.
- Kyriakis JM and Avruch J: Mammalian MAPK signal transduction pathways activated by stress and inflammation: a 10-year update. *Physiol Rev* 92: 689-737, 2012.
- Cuenda A and Rousseau S: p38 MAP-kinases pathway regulation, function and role in human diseases. *Biochim Biophys Acta* 1773: 1358-1375, 2007.
- Eyers PA, Craxton M, Morrice N, Cohen P and Goedert M: Conversion of SB 203580-insensitive MAP kinase family members to drug-sensitive forms by a single amino-acid substitution. *Chem Biol* 5: 321-328, 1998.
- Yamana H, Kakegawa T, Tanaka T, Higaki K, Fujii T and Tou U: Experimental studies on immunotargeting therapy for esophageal carcinoma. *Gan To Kagaku Ryoho* 21: 755-760, 1994.
- Tsukahara T, Nabeta Y, Kawaguchi S, Ikeda H, Sato Y, Shimozawa K, Ida K, Asanuma H, Hirohashi Y, Torigoe T, Hiraga H, Nagoya S, Wada T, Yamashita T and Sato N: Identification of human autologous cytotoxic T-lymphocyte-defined osteosarcoma gene that encodes a transcriptional regulator, papillomavirus binding factor. *Cancer Res* 64: 5442-5448, 2004.
- Nakao M, Yamann H, Imai Y, Toh Y, Toh U, Kimura A, Yanoma S, Kakegawa T and Hoir K: HLA A2601-restricted CTLs recognize a peptide antigen expressed on squamous cell carcinoma. *Cancer Res* 55: 4248-4252, 1995.
- Barry OP, Mullan B, Sheehan D, Kazanietz MG, Shanahan F, Collins JK and O'Sullivan GC: Constitutive ERK1/2 activation in esophagogastric rib bone marrow micrometastatic cells is MEK-independent. *J Biol Chem* 276: 15537-15546, 2001.
- Pramanik R, Qi X, Borowicz S, Choubey D, Schultz RM, Han J and Chen G: p38 isoforms have opposite effects on AP-1-dependent transcription through regulation of c-Jun. The determinant roles of the isoforms in the p38 MAPK signal specificity. *J Biol Chem* 278: 4831-4839, 2003.
- Zheng C, Xiang J, Hunter T and Lin A: The JNKK2-JNK1 fusion protein acts as a constitutively active c-Jun Kinase that stimulates c-Jun transcription activity. *J Biol Chem* 274: 28966-28971, 1999.
- O'Sullivan GC, Tangney M, Casey G, Ambrose M, Houston A and Barry OP: Modulation of p21-activated kinase 1 alters the behavior of renal cell carcinoma. *Int J Cancer* 121: 1930-1940, 2007.
- Chen L, Zhang JJ and Huang XY: cAMP inhibits cell migration by interfering with Rac-induced lamellipodium formation. *J Biol Chem* 283: 13799-13805, 2008.
- Adhikary G, Chew YC, Reece EA and Eckert RL: PKC-delta and -eta, MEK-1, MEK-6, MEK-3 and p38-delta are essential mediators of the response of normal human epidermal keratinocytes to differentiating agents. *J Invest Dermatol* 130: 2017-2030, 2010.
- Cargnello M and Roux P: Activation and function of the MAPKs and their substrates, the MAPK-activated protein kinases. *Microbiol Mol Biol Rev* 75: 50-83, 2011.
- Wagner EF and Nebreda AR: Signal integration by JNK and p38 MAPK pathways in cancer development. *Nat Rev Cancer* 9: 537-549, 2009.
- Ambrose M, Ryan A, O'Sullivan GC, Dunne C and Barry OP: Induction of apoptosis in renal cell carcinoma by reactive oxygen species: involvement of extracellular signal-regulated kinase 1/2, p38delta/gamma, cyclooxygenase-2 down-regulation and translocation of apoptosis-inducing factor. *Mol Pharmacol* 69: 1879-1890, 2006.
- Remy G, Risco AM, Iñesta-Vaquera FA, González-Terán B, Sabio G, Davis RJ and Cuenda A: Differential activation of p38MAPK isoforms by MKK6 and MKK3. *Cell Signal* 22: 660-667, 2010.
- Reid TD, Sanyaolu LN, Chan D, Williams GT and Lewis WG: Relative prognostic value of TNM7 vs TNM6 in staging oesophageal cancer. *Br J Cancer* 105: 842-846, 2011.
- Junttila MR, Ala-aho R, Jokilehto T, Peltonen J, Kallajoki M, Grenman R, Jaakkola P, Westermarck J and Kähäri V-M: p38 α and p38 δ mitogen-activated protein kinase isoforms regulate invasion and growth of head and neck squamous carcinoma cells. *Oncogene* 26: 5267-5279, 2007.
- Efimova T, Broome A-M and Eckert RL: Protein kinase C δ regulates keratinocyte death and survival by regulating activity and subcellular localization of a p38 δ -extracellular signal-regulated kinase 1/2 complex. *Mol Cell Biol* 24: 8167-8183, 2004.
- Efimova T, Broome AM and Eckert RL: A regulatory role for p38 δ MAPK in keratinocyte differentiation. Evidence for p38 δ -ERK1/2 complex formation. *J Biol Chem* 278: 34277-34285, 2003.

32. Li Q, Zhang N, Zhang D, Wang Y, Lin T, Wang Y, Zhou H, Ye Z, Zhang F, Lin S-C and Han J: Determinants that control the distinct subcellular localization of p38 α -PRAK and p38 β -PRAK complexes. *J Biol Chem* 283: 11014-11023, 2008.
33. Fan L, Yang X, Du J, Marshall M, Blanchard K and Ye X: A novel role of p38 α MAPK in mitotic progression independent of its kinase activity. *Cell Cycle* 4: 1616-1624, 2005.
34. Tang J, Qi X, Mercola D, Han J and Chen G: Essential role of p38 γ in K-Ras transformation independent of phosphorylation. *J Biol Chem* 280: 23910-23917, 2005.
35. Del Barco Barrantes I and Nebreda AR: Roles of p38 MAPKs in invasion and metastasis. *Biochem Soc Trans* 40: 79-84, 2012.
36. Izzo JG, Luthra R, Sims-Mourtada J, Chao KSC, Lee JH, Wu T-T, Correa AM, Luthra M, Aggarwal B, Hung M-C and Ajani JA: Emerging molecular targets in esophageal cancers. *Gastrointest Cancer Res* 1: S3-S6, 2007.
37. Bulavin DV and Fornace AJ: p38 MAP kinases's emerging role as a tumour suppressor. *Adv Cancer Res* 92: 95-118, 2004.
38. Hui L, Bakiri L, Stepniak E and Wagber EF: p38 α a supressor of cell proliferation and tumorigenesis. *Cell Cycle* 6: 2429-2433, 2007.
39. Ventura JJ, Tenbaum S, Perdiguero E, Huth M, Guerra C, Barbacid M, Pasparakis M and Nebreda AR: p38 α MAP kinase is essential in lung stem and progenitor cell proliferation and differentiation. *Nat Genet* 39: 750-758, 2007.
40. Schindler EM, Hinds A, Gribben EL, Burns CJ, Yin Y, Lin M-H, Owen RJ, Longmore GD, Kissling GE, Arthur JSC and Efimova T: p38 δ mitogen-activated protein kinase is essential for skin tumor development in mice. *Cancer Res* 69: 4648-4655, 2009.
41. Cerezo-Guisado MI, Del Reino P, Remy G, Kuma Y, Arthur JSC, Gallego-Ortega D and Cuenda A: Evidence of p38 γ and p38 δ involvement in cell transformation processes. *Carcinogenesis* 32: 1093-1099, 2011.
42. Sundaramurthy P, Gakkhar S and Sowdhamini R: Analysis of the impact of ERK5, JNK and p38 kinase cascades on each other: a systems approach. *Bioinformation* 3: 244-249, 2009.
43. Ambrosino C, Mace G, Galban S, Fritsch C, Vintersten k, Black E, Gorospe M and Nebreda AR: Negative feedback regulation of MKK6 mRNA stability by p38 α mitogen-activated protein kinase. *Mol Cell Biol* 23: 370-381, 2003.
44. Coulthars LR, White DE, Jones DL, McDermott MF and Burchill SA: p38^{MAPK}: stress responses from molecular mechanisms to therapeutics. *Trends Mol Med* 15: 369-379, 2009.
45. Gaestel M and Kracht M: Peptides as signalling inhibitors for mammalian MAP kinase cascades. *Curr Pharm Des* 15: 2471-2480, 2009.

p38 δ MAPK phenotype: an indicator of chemotherapeutic response in oesophageal squamous cell carcinoma

Carol O'Callaghan^a, Liam J. Fanning^b and Orla P. Barry^a

We recently documented p38 δ differential expression and function in oesophageal squamous cell carcinoma (OESCC). This study expands upon these findings and investigates whether p38 δ status in OESCC can influence response(s) to cytotoxic drugs. The antiproliferative effect of conventional cisplatin and 5-fluorouracil (CF) treatment was compared with the recently reviewed triple regime of cisplatin, 5-fluorouracil and doxorubicin (ACF). p38 δ -positive and p38 δ -negative cell lines were employed using cell-growth and clonogenic assays. Key regulators of intrinsic and extrinsic apoptotic pathways were measured. Wound-healing assays and a Boyden chamber were used to investigate the effect of drug treatments on cell migration. Functional networks were analysed in terms of changes in MAPK expression. p38 δ -negative OESCC is less sensitive to standard CF chemotherapy compared with p38 δ -positive cells. However, following ACF treatment p38 δ -negative cells showed markedly decreased proliferation and cell migration, and increased apoptosis. ACF induced apoptosis through the extrinsic pathway involving Fas activation, caspase-8 and caspase-3 cleavage and degradation of PARP. Loss of mitochondrial membrane potential ($\Delta\Psi_m$) was observed but downregulation of multidomain

proapoptotic proteins, as well as BH3-only proteins, suggests involvement of pathways other than the mitochondrial pathway. Interestingly, induction of p38 and ERK1/2, but not JNK1/2, was observed following ACF treatment. p38 δ -negative OESCC is more resistant to traditional CF treatment compared with p38 δ -positive OESCC. In light of these results, p38 δ phenotyping of tumour tissue may be of considerable value in deciding on an optimal therapeutic strategy for patients with p38 δ -negative OESCC. *Anti-Cancer Drugs* 00:000–000 © 2014 Wolters Kluwer Health | Lippincott Williams & Wilkins.

Anti-Cancer Drugs 2014, 00:000–000

Keywords: cisplatin, doxorubicin, 5-fluorouracil, oesophageal squamous cell carcinoma, p38 δ MAPK

Departments of ^aPharmacology and Therapeutics and ^bMedicine, University College Cork, Cork, Ireland

Correspondence to Orla P. Barry, PhD, Department of Pharmacology and Therapeutics, Rm. 3.89, Western Gateway Building, University College Cork, Cork, Ireland
Tel: +353 21 420 5493; e-mail: o.barry@ucc.ie

Received 12 March 2014 Revised form accepted 3 July 2014

Introduction

Oesophageal cancer is a highly aggressive and fatal malignancy and is the seventh most common cancer worldwide [1]. Oesophageal squamous cell carcinoma (OESCC) is an exceptionally drug-resistant tumour. Although surgery is the best modality in terms of local control [2], outcomes following resection for OESCC remain unsatisfactory because of locoregional and distant failure [3]. Preoperative chemotherapy or chemoradiotherapy with a fluoropyrimidine/platinum combination – that is, a cisplatin and 5-fluorouracil (CF) regimen – has been the standard treatment for locally advanced disease since the 1980s. At present, multimodal therapy is being investigated for different stages of OESCC, even if the tumour is operable [4]. Preoperative chemotherapy with docetaxel plus CF (DCF) has recently been investigated (with or without radiotherapy) with good local control and pathological remission rate being recorded [4, 5]. More recently doxorubicin, cisplatin and 5-fluorouracil (ACF) have undergone a revival, demonstrating higher

response rates than CF treatment, a good safety profile and promising long-term outcomes for patients with highly advanced oesophageal carcinoma [6–8].

The involvement of p38 MAPKs in a variety of pathological conditions is continuing to fuel interest in this particular family of kinases. It consists of four isoforms: p38 α (MAPK14), p38 β (MAPK11), p38 γ (MAPK12) and p38 δ (MAPK13), which to date remains the least studied isoform [9]. The expression of p38 as a family has previously been outlined in oesophageal cancer, as well as in other cancer types [10–13]. We recently outlined for the first time the differential expression of individual p38 isoforms in cancer and in particular OESCC [14,15]. We now know that loss of p38 δ expression in OESCC affords a more sinister phenotype, with increased proliferation, migration and anchorage-independent growth, thus identifying p38 δ as a possible molecular target in OESCC [15].

Advancing our studies a step further we evaluated whether p38 δ status could influence cytotoxic responses to drug treatments in OESCC. We used both negative and positive p38 δ cell lines isolated from patients with OESCC with no prior treatment, as previously outlined by us [15]. Cell viability, wound healing, migration and

This is an open access article distributed under the Creative Commons Attribution-NonCommercial-NoDerivatives License 4.0, where it is permissible to download, share and reproduce the work in any medium, provided it is properly cited. The work cannot be changed in any way or used commercially.

apoptosis were evaluated following standard CF treatment and ACF treatment. To carry out functional networks expression analysis, we also analysed changes in ERK1/2, JNK1/2 and p38 MAPK expression. In conclusion, our study indicates that p38 δ status may be a predictor of response to chemotherapy in OESCC patients.

Materials and methods

Reagents

All chemicals and cell culture reagents were purchased from Sigma Aldrich (Wicklow, Ireland) and primary antibodies from Cell Signalling Technologies (Hertfordshire, UK), unless otherwise stated.

Cell culture

The KE oesophageal squamous cancer cell lines were a kind gift from Professor T. Fujii, Kurume University School of Medicine, Japan [15–18]. Cells were cultured in RPMI-1640 supplemented with 10% foetal calf serum, 100 μ g/ml streptomycin and 100 U/ml penicillin. KE cell line features have been summarized previously by us [15].

3-(4,5-Dimethylthiazol-2-yl)-2,5-diphenyl-2H-tetrazolium bromide assay

Cell viability was assessed using the 3-(4,5-dimethylthiazol-2-yl)-2,5-diphenyl-2H-tetrazolium bromide (MTT) assay, which depends on the ability of viable cells to reduce MTT to a coloured formazan product, as described previously [19].

Boyden chamber cell migration in-vitro assay

Cells were plated in starvation medium at a density of 3×10^4 cells/well onto a 96-well plate of the upper chamber. The bottom chamber contained 10% foetal calf serum as the chemoattractant. Cells were left to migrate for 24 h through the matrigel filter (8 μ m) and stained as previously described [19].

Wound-healing assay

Cell migration was assessed using an in-vitro wound-healing assay as previously described [20]. Cells migrating into the wound were photographed under a phase-contrast microscope 48 h after wounding. Migration was determined using the ImageJ (National Institutes of Health, Bethesda, Maryland, USA) program as an average closed area of the wound relative to the initial wound area at 48 h after wounding.

Mitochondrial membrane potential ($\Delta\Psi_m$) assay

The decline of mitochondrial membrane potential ($\Delta\Psi_m$) was assessed using a mitochondrial voltage-sensitive dye, 5,5',6,6'-tetrachloro-1,1',3,3'-tetraethylbenzimidazole carbocyanide iodide (JC-1), according to the manufacturer's instructions [21]. The dye underwent a reversible change in fluorescence emission from red (i.e. aggregate forms of JC-1) to green (i.e. monomer forms of JC-1) as the mitochondrial membrane potential decreased. Briefly, KE cells

were or were not treated with drugs for 24 h. Cells were then washed twice with PBS and loaded with JC-1 for 30 min at 37°C. Images were obtained using an inverted fluorescence microscope (Olympus, Southend-on-Sea, UK). The ratio of red to green fluorescence intensity, which was indicative of a change in $\Delta\Psi_m$, was calculated using the ImageJ software.

Immunoblot analysis

Supernatants used for immunoblotting with specific antibodies, PARP, caspases-3 and 8, Puma, Bak, Bik, Bim, Bid, Bax, p38, phospho-p38, JNK1/2, phospho-JNK1/2, ERK1/2 and phospho-ERK1/2 (New England Biolabs, Hertfordshire, UK), as well as Fas and FasL (Santa Cruz Biotechnology, Santa Cruz, California, USA), have previously been described by us [14,15]. Chemiluminescence detection was performed using SuperSignal WestDura Extended Duration Substrate (Pierce Biotechnology, Rockford, Illinois, USA), and bands were visualized using a Syngene G:Box ChemiXR5 Gel Documentation System (Syngene, Cambridge, UK). Images were quantified using ImageJ software.

Colony formation assay

A colony formation assay determines whether cells can recover from treatment. Following treatment, viable cells were reseeded in fresh media (without drug) in a six-well plate (in triplicate) and allowed to grow for 14 days. Colonies were stained with MTT and subsequently counted using ImageJ software.

Statistical analysis

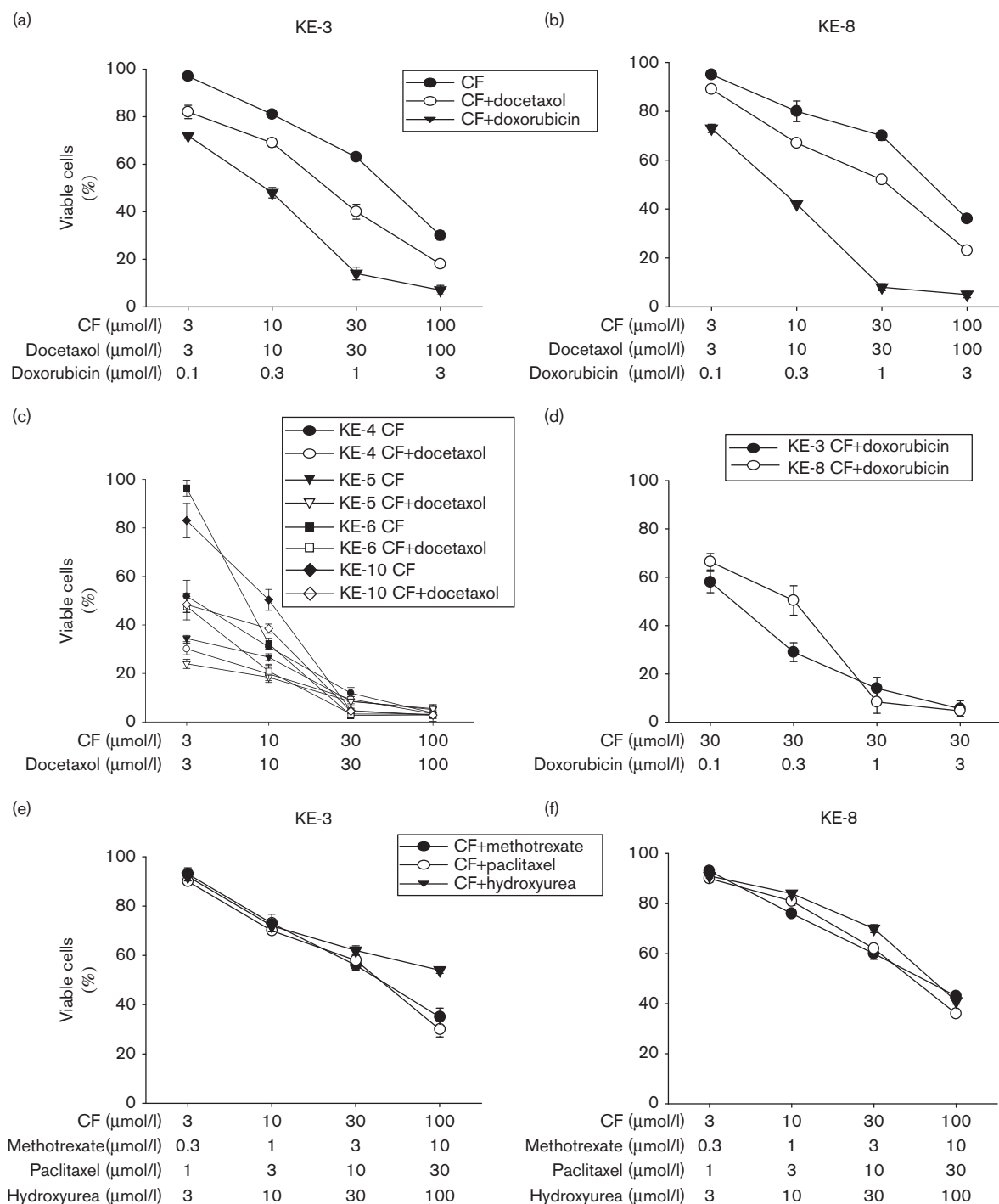
Statistical comparisons were made by analysis of variance with subsequent application of Student's *t*-test, as appropriate. The non-parametric Mann–Whitney *U*-test pairwise comparisons were also performed. As the results obtained using both methods were in agreement, only results for the Student's *t*-test are shown.

Results

p38 δ MAPK-negative OESCC shows decreased sensitivity to chemotherapeutic drugs

Monotherapy is not beneficial in the treatment of patients with oesophageal cancer [22]. Thus, we evaluated the cell viability of KE p38 δ -positive and p38 δ -negative OESCC cell lines (differential p38 δ expression was recently reported by us [15]) following double versus triple drug treatments using a range of concentrations of cytotoxic drugs. Interestingly, KE-3 and KE-8 (p38 δ -negative cell lines) are significantly less sensitive to CF treatment compared with KE-4, KE-5, KE-6 and KE-10 (p38 δ -positive cell lines; Fig. 1a–c). As docetaxel has recently been added to the CF regime [4,5], we investigated the effect of DCF on cell viability. There was a further decrease in KE-3 and KE-8 cell viability (Fig. 1a and b). However, no further reduction in cell viability was observed in the KE p38 δ -positive cell lines upon

Fig. 1



Sensitivity of OESCC to cancer chemotherapeutic drugs is correlated to the presence or absence of p38 δ MAPK. (a–f) KE cell lines (KE-3 and KE-8, p38 δ negative; KE-4, KE-5, KE-6 and KE-10, p38 δ positive) were seeded (2×10^5) in six-well plates, and cell viability was assessed using the MTT assay (as described in the Materials and methods section) at 48 h to determine the sensitivity of each cell line to different drug combinations. (a, b) KE-3 and KE-8 cells were subjected to double treatment with cisplatin (3–100 $\mu\text{mol/l}$) and 5-fluorouracil (3–100 $\mu\text{mol/l}$; CF), or triple treatment with cisplatin (3–100 $\mu\text{mol/l}$), 5-fluorouracil (3–100 $\mu\text{mol/l}$; CF) and either docetaxel (3–100 $\mu\text{mol/l}$) or doxorubicin (0.1–3 $\mu\text{mol/l}$). (c) KE-4, KE-5, KE-6 and KE-10 cells were treated either with cisplatin (3–100 $\mu\text{mol/l}$) and 5-fluorouracil (3–100 $\mu\text{mol/l}$; CF), or with cisplatin (3–100 $\mu\text{mol/l}$), 5-fluorouracil (3–100 $\mu\text{mol/l}$; CF) and docetaxel (3–100 $\mu\text{mol/l}$). (d) KE-3 and KE-8 cells were subjected to triple treatment with constant drug concentrations of cisplatin (30 $\mu\text{mol/l}$) and 5-fluorouracil (30 $\mu\text{mol/l}$; CF) plus varying drug concentrations of doxorubicin (0.1–3 $\mu\text{mol/l}$). (e, f) KE-3 and KE-8 cells were subjected to triple treatment with cisplatin (3–100 $\mu\text{mol/l}$), 5-fluorouracil (3–100 $\mu\text{mol/l}$; CF) and either methotrexate (0.3–10 $\mu\text{mol/l}$), paclitaxel (1–30 nmol/l) or hydroxyurea (3–100 $\mu\text{mol/l}$). Results shown in (a–f) are mean \pm SE of three independent experiments. MTT, 3-(4,5-dimethylthiazol-2-yl)-2,5-diphenyl-2H-tetrazolium bromide; OESCC, oesophageal squamous cell carcinoma.

DCF treatment using physiologically relevant drug concentrations (30 $\mu\text{mol/l}$; Fig. 1c) [23–25]. As doxorubicin (together with CF) has recently re-emerged as a promising drug treatment strategy for patients with oesophageal cancer [6–8], we also investigated its effects. Interestingly, the greatest loss in KE-3 and KE-8 cell viability was after triple CF plus doxorubicin (ACF) treatment (Fig. 1a and b). Of note, these results are comparable with the loss in cell viability seen in the p38 δ -positive cells upon CF treatment at physiological concentrations (Fig. 1c). Taking the results we obtained with physiological drug concentrations of CF (30 $\mu\text{mol/l}$ each) a step further, we investigated the appropriate triple ACF drug treatment concentrations for KE-3 and KE-8 cell lines. Using a range of doxorubicin drug concentrations, we ascertained that the best triple ACF concentration using physiological concentrations of all three drugs is 30 $\mu\text{mol/l}$ each of CF and 1 $\mu\text{mol/l}$ doxorubicin (Fig. 1d). No significant further decrease in cell viability was observed at a higher doxorubicin drug concentration of 3 $\mu\text{mol/l}$ (Fig. 1d).

As other chemotherapeutic drug combinations have also been tested for their efficacy in patients with OESCC, namely CF plus methotrexate [26], CF plus paclitaxel [26,27] and CF plus hydroxyurea [28], we also investigated these three additional drug combinations again using a range of different drug concentrations. Interestingly, KE-3 and KE-8 showed less sensitivity to all three triple-drug combinations compared with ACF treatment (Fig. 1e and f). Thus, as the greatest loss in KE-3 and KE-8 cell viability was observed with triple ACF treatment (Fig. 1a, b and d), all subsequent experiments compared traditional CF treatment with ACF treatment.

ACF treatment significantly delays wound healing and migration compared with CF treatment

A key characteristic of cancer cells is their ability to migrate and progress from primary tumours to metastases in distant organs [15]. We examined whether the p38 δ status of OESCCs could influence their wound healing and cell migration following drug treatment. Initially, we identified the highest concentration of drug(s) that does not lead to loss of cell viability – that is, 3 $\mu\text{mol/l}$ of each drug for CF and 300 nmol/l doxorubicin (data not shown). Double CF treatment of KE-6 and KE-10 (p38 δ -positive cells) for 48 h brought about a significant delay in wound healing, with a 60.0 ± 7 and $66.0 \pm 1.2\%$ loss in wound healing, respectively, compared with untreated cells (Fig. 2a and b). In contrast, CF treatment did not impair the ability of KE-3 and KE-8 cells to migrate into the wound (Fig. 2a and b). Triple ACF treatment, however, significantly delayed the wound-healing ability of KE-3 and KE-8 cell lines, with a 72.8 ± 2.5 and $84.0 \pm 3.9\%$ loss in wound healing at 48 h, respectively. There was a further $15 \pm 5.8\%$ loss in wound healing upon ACF

treatment, compared with CF treatment alone, of KE-6 cells but no significant change in KE-10 cells (Fig. 2a and b). Doxorubicin (300 nmol/l) alone did not have any significant effect on the wound-healing ability of either p38 δ -positive or p38 δ -negative cells (Fig. 2a and b). Further, we compared the migration of p38 δ -positive and p38 δ -negative cells following CF versus ACF treatment using a Boyden chamber assay. Double CF treatment induced a significant (78.7 ± 5.2 and $78.7 \pm 7.8\%$, respectively) decrease in cell migration of KE-6 and KE-10 cells at 24 h; however, no significant change in cell migration was observed upon CF treatment of KE-3 and KE-8 cells (Fig. 2c). In contrast, triple ACF treatment of KE-3 and KE-8 significantly decreased their cell migration by 75.9 ± 2.4 and $81.3 \pm 6.9\%$, respectively (Fig. 2c).

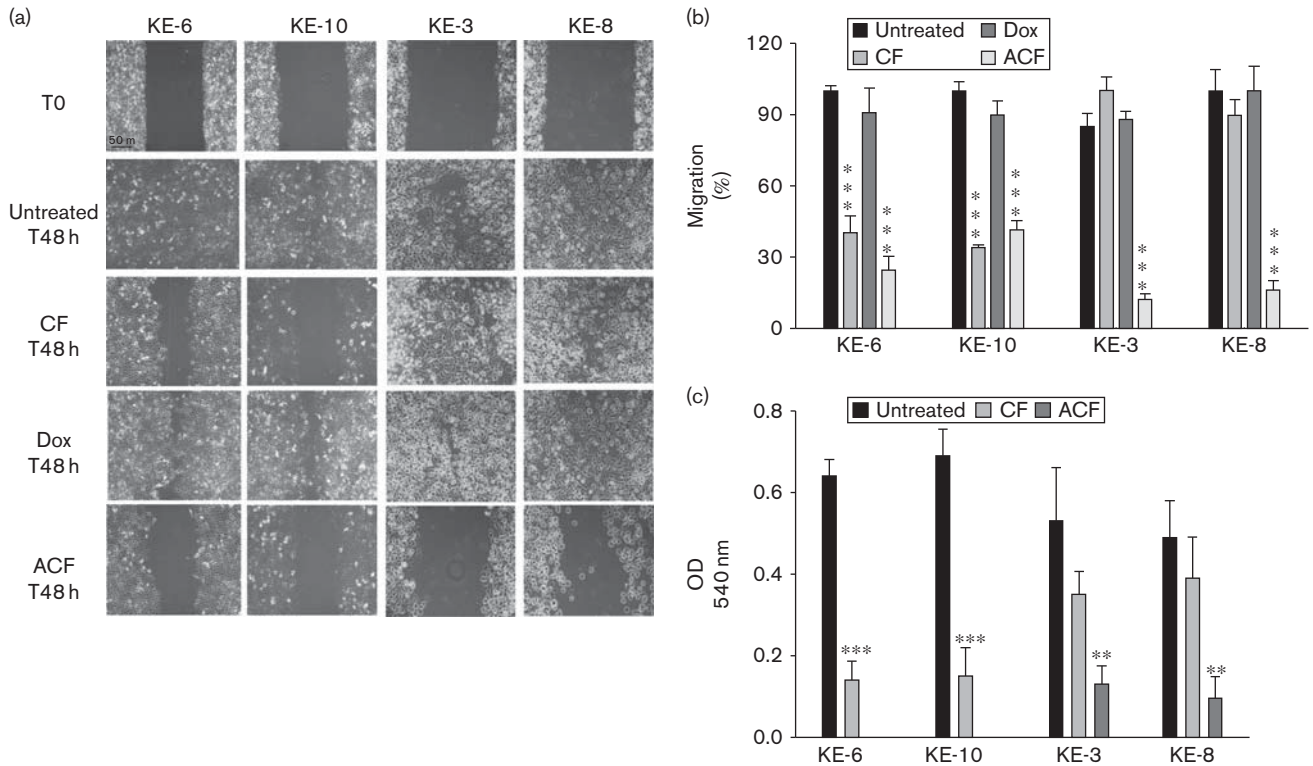
Triple ACF treatment decreases mitochondrial membrane potential and activates extrinsic pathways in p38 δ negative OESCCs

Initially, we investigated the involvement of the mitochondria in OESCC apoptosis using the JC-1 cationic dye. It selectively enters the mitochondria and reversibly changes in colour from red to green as the membrane potential decreases [21]. KE-6 and KE-10 cells show a marked decrease in $\Delta\Psi\text{m}$ following CF and ACF treatment (Fig. 3a and b). Similar losses in $\Delta\Psi\text{m}$ in KE-3 and KE-8 cells were observed only upon ACF treatment (Fig. 3a and b). Doxorubicin alone did not alter the $\Delta\Psi\text{m}$ of KE-6 and KE-10 cells, but it did produce a significant ($P < 0.01$) decrease in the $\Delta\Psi\text{m}$ of KE-3 and KE-8, comparable to that on CF treatment (Fig. 3a and b).

To further investigate the effects of CF-induced versus ACF-induced apoptosis on KE p38 δ -negative cells, intrinsic (mitochondrial) and extrinsic (Fas) apoptotic pathways were investigated. Expression of the relevant apoptosis-related proteins was examined by western blot analysis. To investigate the role of the intrinsic mitochondrial pathway we examined the expression levels of Bcl-2 family members including multidomain proapoptotic proteins Bak and Bax, as well as BH3-only proapoptotic proteins Puma, Bik, Bid and Bim. Interestingly CF treatment downregulated all Bcl-2 proapoptotic members examined, with further reductions in expression being observed in the presence of ACF treatment (Fig. 3c). The mitochondrial apoptotic pathway-related caspase-9 was not cleaved (data not shown).

To investigate whether CF and ACF activate the extrinsic apoptotic pathway, we examined the expression levels of death receptor signalling-related proteins including Fas, caspase-3 and caspase-8 and PARP. Alterations in the expression of Fas and FasL, members of the tumour necrosis family, have been reported previously in OESCC with Fas-activated apoptosis being shown to limit the growth of OESCCs [29,30]. We observed an increase in Fas expression when both KE-3 and KE-8 cells were treated with ACF, but not on CF treatment, implicating the involvement of the extrinsic

Fig. 2



Effect of chemotherapeutic cytotoxic drugs on wound healing and migration of KE p38 δ MAPK positive and negative cell lines. KE-6 and KE-10 cells (p38 δ positive), as well as KE-3 and KE-8 cells (p38 δ negative), were analysed for (a, b) wound healing and (c) cell migration following treatment with cisplatin (3 μ mol/l) and 5-fluorouracil (3 μ mol/l; CF), doxorubicin (Dox; 300 nmol/l) alone or cisplatin (3 μ mol/l), 5-fluorouracil (3 μ mol/l) and doxorubicin (300 nmol/l; triple treatment; ACF). (a) Representative wound-healing images at 0 and 48 h with or without drug treatment. The results shown in (a) are representative of three independent experiments, whereas the results shown in (b) and (c) are the mean \pm SE of three independent experiments. *** $P < 0.001$, ** $P < 0.01$, significant changes from control untreated cells.

death pathway. The expression level of FasL was very low in both cell lines, and there was no appreciable change after treatment with CF or ACF (Fig. 3d). We observed that ACF (but not CF) treatment of KE-3 and KE-8 cell lines activated (cleaved) caspase-3 and caspase-8, as well as activated (cleaved) their substrate PARP, producing the 85 kDa proteolytic fragment indicative of caspase activation and apoptosis (Fig. 3d). The extrinsic apoptotic pathway-related caspases-6 and caspase-7 were not cleaved upon CF or ACF treatment (data not shown).

Triple ACF treatment induces p38 and ERK1/2 but not JNK1/2 MAPK activation in p38 δ -negative OESCC

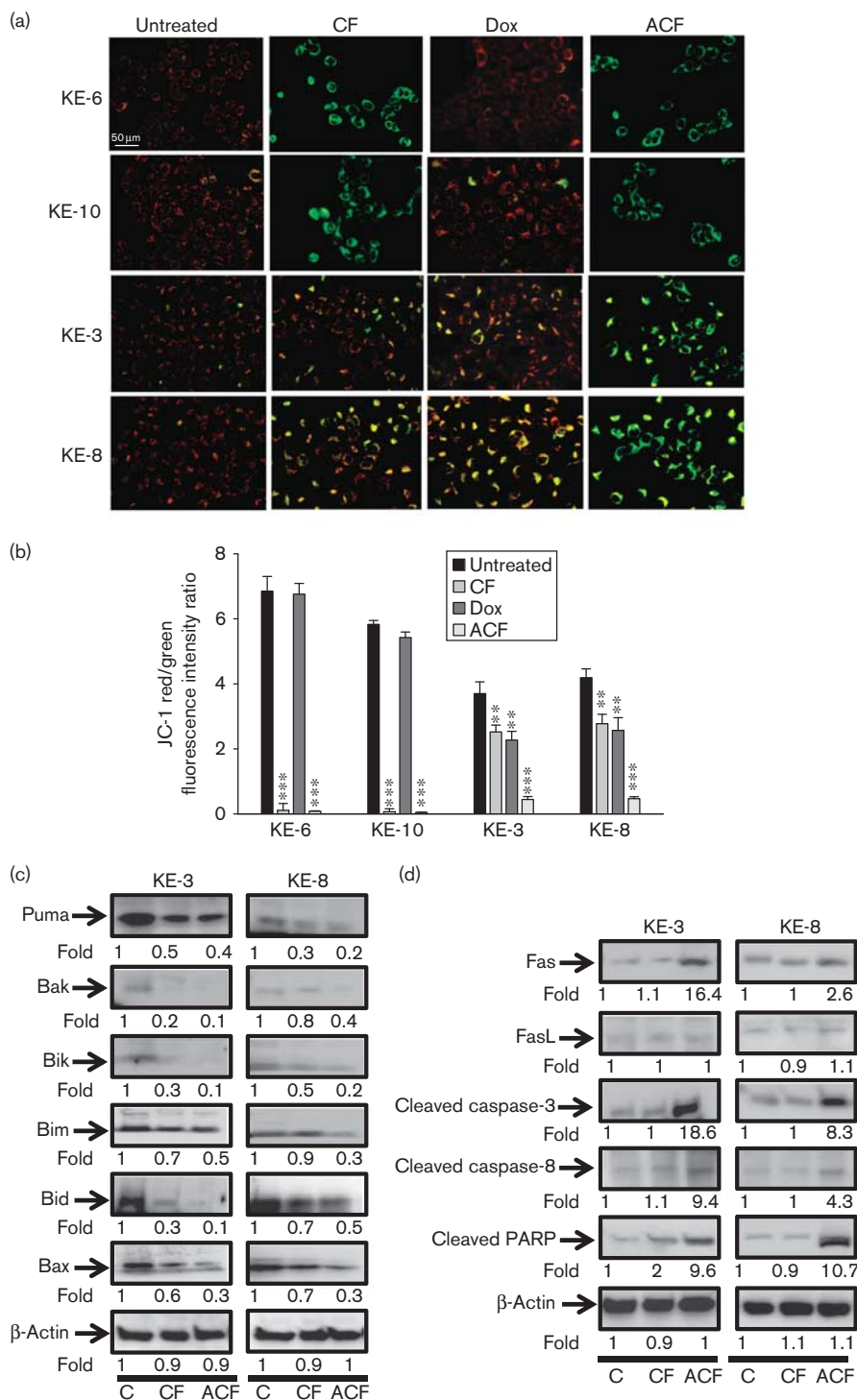
To gain further insight into CF-induced versus ACF-induced cytotoxic effects, we analysed MAPK expression. We observed p38 phosphorylation upon ACF treatment but not CF treatment (Fig. 4a). CF induced ERK1/2 phosphorylation, which was further enhanced with ACF treatment (Fig. 4a). In contrast, JNK1/2 activation was not observed following either CF or ACF treatment (Fig. 4a).

To assess whether p38 and ERK1/2 activation is causal to the actions of our chemotherapeutics we used specific pharmacological inhibitors of p38 and MEK. Interestingly, both SB203590 (20 micromolar) and BIRB 796 (5 micromolar), inhibitors of p38 α and p38 β (but not p38 γ and p38 δ) [24,31] did not prevent the antiproliferative effects of either CF or ACF (Fig. 4b). In fact, in agreement with recent reports (with similar cytotoxic drug combinations), p38 blockade enhanced the cytotoxic effects of ACF treatment significantly (but not CF treatment) at 24 h (Fig. 4b) [24,25]. The enhanced antiproliferative effect of p38 inhibition observed at 24 h with ACF was not obvious at 48 h because of the high level of cell death at this time point (Fig. 4b). The specific MEK inhibitor U0126 (20 micromolar) [32] brought about a significant abolition of the effects of both CF and ACF drug treatments in both cell lines, indicating that ERK1/2 may be directly involved in drug-induced cytotoxicity (Fig. 4b).

Recovery of KE-3 and KE-8 cells following drug treatments

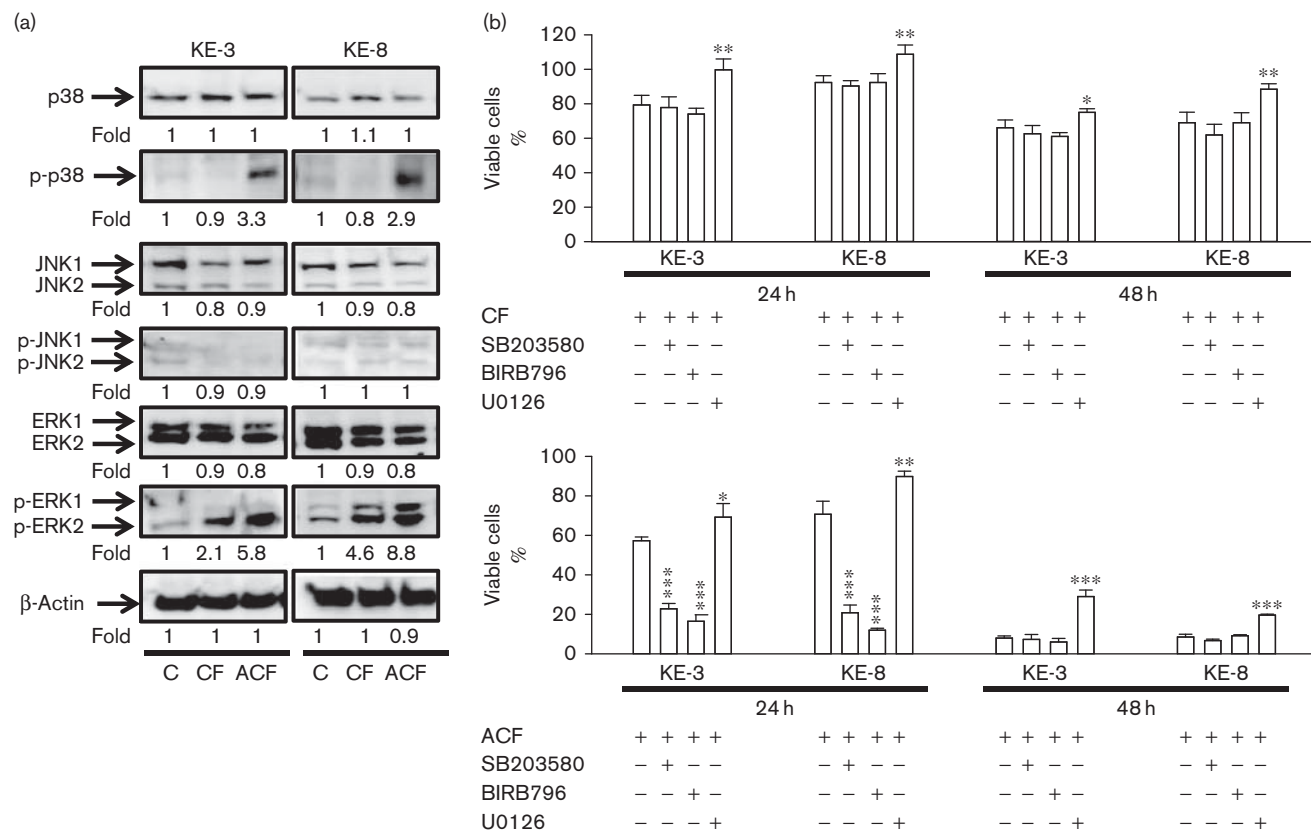
One of the most important parameters for the efficacy of chemotherapeutic drug treatments is the long-term effect

Fig. 3



Effect of chemotherapeutic drug treatment on intrinsic and extrinsic mitochondrial pathways in KE-3 and KE-8 cells. (a) The mitochondrial membrane potential ($\Delta\Psi_m$) of KE cells before and after treatment with chemotherapeutic drugs for 24 h. Representative images (red/green mixed channels) show the changes in mitochondrial membrane potential ($\Delta\Psi_m$) in KE cells, detected using JC-1 dye. Red fluorescence indicates high membrane potential and functional capacity in mitochondria, whereas green cytoplasmic fluorescence is indicative of inactive mitochondria. (b) Decreased red/green fluorescence ratio suggests a decrease in $\Delta\Psi_m$. (c) Whole cell lysates were analysed by western blot analysis of proapoptotic Puma, Bak, Bik, Bim, Bid and Bax, as well as (d) Fas and FasL, cleaved caspase-3 and caspase-8 and PARP in KE-3 and KE-8 cells. The results shown in (a), (c) and (d) are representative of four independent experiments, whereas the results shown in (b) are the mean \pm SE of four independent experiments. *** $P < 0.001$, ** $P < 0.01$, significant changes from control untreated cells.

Fig. 4



MAPK activation in KE-3 and KE-8 cells following chemotherapeutic drug treatment. Western blot analysis of the three different MAPKs (p38 MAPK, JNKs and ERKs) following treatment with cisplatin (30 μ mol/l) and 5-fluorouracil (30 μ mol/l; CF), or following triple treatment with cisplatin (30 μ mol/l), 5-fluorouracil (30 μ mol/l) and doxorubicin (1 μ mol/l; ACF) for 24 h. The results shown in (a) are representative of four independent experiments, whereas the results shown in (b) are the mean \pm SE of four independent experiments. *** P < 0.001, ** P < 0.01, * P < 0.05, significant changes from CF-treated or ACF-treated cells.

on cell viability. Thus, we evaluated the effects of CF, doxorubicin alone and ACF treatment on the capacity of KE-3 and KE-8 cells to recover in assays of clonogenic growth. All three different drug treatments had a significant effect on the recovery of both KE-3 and KE-8 cell lines (Fig. 5a and b). However, of note, cell recovery following ACF treatment was never observed, whereas colonies – that is, cell recovery – were observed following treatment with CF or doxorubicin alone (Fig. 5a and b).

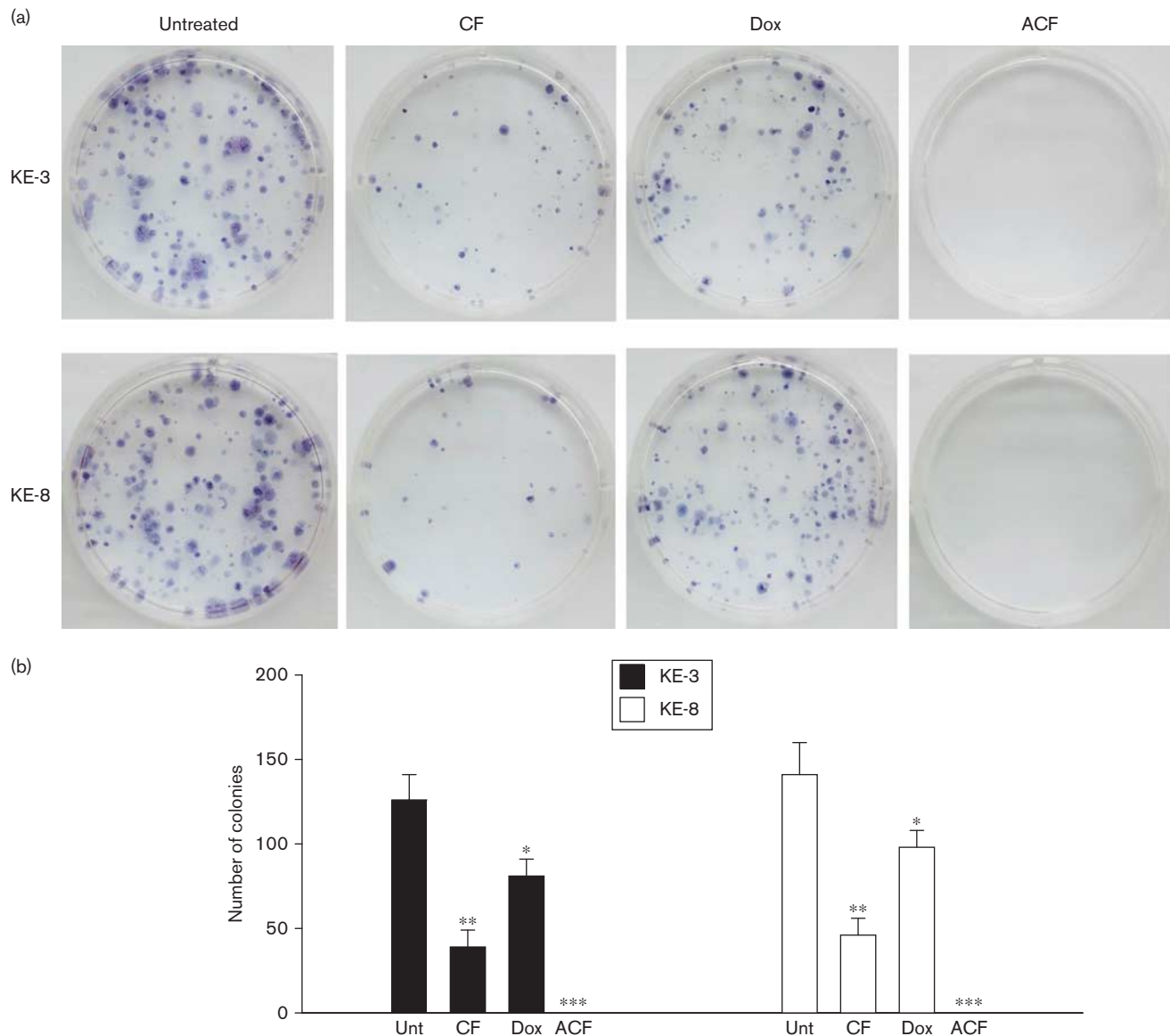
Discussion

In this study, we focused on OESCCs, as this cell phenotype shows differential p38 δ expression [15]. Loss of this important serine/threonine kinase confers greater tumourgenicity and may be a mechanism by which OESCC promotes carcinogenesis [15]. The purpose of this study was to determine whether differences in the OESCC p38 δ phenotype could influence the chemosensitivity of OESCC to conventional CF versus ACF drug combinations.

Single-agent response rates of 10–25% remain poor for oesophageal cancer [22]. Further, the use of double CF is of limited effectiveness in the treatment of patients with OESCC, with respect to improving overall survival time and patient quality of life [3,8]. Triple ACF combination therapy was first reported as far back as 1983 [33], but of late it has sparked renewed interest [4,8]. Doxorubicin is an effective, widely used chemotherapeutic agent in the treatment of a variety of solid tumours and malignant haematologic diseases [34]. There are now reports documenting the usefulness and, importantly, the safety of ACF therapy for the treatment of advanced oesophageal carcinoma [7,8,35]. Despite the absence of phase III clinical trials, ACF is currently used in the clinical setting for treatment of patients with OESCC [8].

All three drugs in this study, cisplatin, 5-fluorouracil and doxorubicin, used as monotherapy or double therapy have been reported to induce intrinsic apoptosis in oesophageal cancer [23,36]. We examined typical markers of both intrinsic and extrinsic apoptotic cell death in our p38 δ -negative cell lines. Although we observed

Fig. 5



Recovery of KE-3 and KE-8 cells following chemotherapeutic drug withdrawal. The ability of p38δ-negative OESCC cell lines KE-3 and KE-8 to recover after drug withdrawal was assessed with a colony formation assay (clonogenic assay). KE-3 and KE-8 cells were or were not treated (Unt) with cisplatin (30 μmol/l) and 5-fluorouracil (30 μmol/l; CF), doxorubicin (1 μmol/l; Dox) alone or the combination of all three drugs (ACF) for 48 h. Viable, adherent cells were counted and reseeded (1000 cell/well) in a six-well plate (in triplicate) in the absence of drug. (a) Fourteen days later, colonies were stained with MTT. Each well shown is a representative image of nine similar wells (three independent experiments). (b) Colonies were counted using ImageJ software. ****P* < 0.001, ***P* < 0.01, **P* < 0.05, significant changes from untreated cells. MTT, 3-(4,5-dimethylthiazol-2-yl)-2,5-diphenyl-2H-tetrazolium bromide; OESCC, oesophageal squamous cell carcinoma.

mitochondrial depolarization following ACF treatment, there was no subsequent caspase-9 activation. Interestingly, we also observed downregulation of Bcl-2 multidomain, as well as BH-3 proapoptotic proteins. However, decreased expression of these intrinsic pathway proteins is in agreement with a recent report on oxaliplatin-induced apoptosis in squamous oesophageal cancer cell lines [37]. Potentially, the presence of Bcl-2 multidomain and BH3-only proapoptotic molecules may be an important predictor of p38δ-negative OESCC

response to combination therapy without being directly involved. Our findings suggest that ACF suppresses cell growth in p38δ-negative OESCC through extrinsic apoptotic pathway activation of the Fas death receptor, with caspase-8 and caspase-3 cleavage and subsequent degradation of PARP.

There are many reports linking MAPK involvement following exposure to mechanistically different chemotherapeutic drugs [38]. However, their suppression

and activation and indeed the absence of any role in apoptosis have been attributed to all three MAPKs [38–40]. Thus, the activation of MAPKs by chemotherapeutic drugs and the subsequent consequences of MAPK activation appear to be very much cell-type specific [39]. Although we observed p38 activation upon ACF treatment, our findings with the p38 pharmacological inhibitors do not support a direct role for p38 MAPK activity in drug-induced cytotoxicity. In contrast, ERK1/2 activation may play a more direct role as its inhibition through MEK can partly reverse the antiproliferative effects of both CF and ACF treatments.

The increased antiproliferative and proapoptotic effects of ACF treatment over CF treatment in our study suggest that the former may be considered as mainstay treatment of patients with p38δ-negative OESCC. It remains to be investigated whether patients with p38δ-negative OESCC may benefit more from ACF treatment compared with classical CF treatment, and whether or not ACF treatment can influence overall survival. Further investigations into the mechanistic strategies underpinning p38δ-negativity related loss in drug sensitivity are warranted. The clonogenic assay is a valuable tool in gauging long-term consequences of single, double and triple chemotherapy in p38δ-negative OESCC. This assay closely mirrors the clinical situation in which patients are treated with chemotherapeutic drugs in a pulsed rather than a continuous manner. After 2 weeks of treatment, our ACF-treated p38δ-negative OESCC cells never recovered. Although we observed a statistically significant reduction in colony formation on CF double or doxorubicin treatment, cell recovery was always observed, clearly demonstrating resistance. In general, the MTT assay demonstrated lower cytotoxic activity than the clonogenic assay with these drugs. Of note, a high degree of correlation between both assays is not always apparent, and it may be influenced by both cell type and anticancer drug type [41–43]. Thus, unlike ACF treatment, the limited efficacy of CF or doxorubicin alone could provide an opportunity for cancer persistence in patients with p38δ-negative OESCC.

In summary, the present study indicates that p38δ may be a significant predictor of treatment response in patients with p38δ-negative OESCC. p38δ genotyping of pretreatment biopsy may potentially be a useful predictor of response to chemotherapy and ultimately prognosis in OESCC patients. Our data support the value of known p38δ status in the decision process used to inform the optimal treatment of patients with OESCC.

Acknowledgements

This work was supported by the Health Research Board, Ireland (Grant HRA/2009/17 to Barry).

Conflicts of interest

There are no conflicts of interest.

References

- Kayani B, Zacharakis E, Ahmed K, Hanna GB. Lymph node metastases and prognosis in oesophageal carcinoma – a systematic review. *Eur J Surg Oncol* 2011; **37**:747–753.
- Kuwano H, Fukuchi M, Kato H. Thoracoscopic surgery for esophageal cancer. *Ann Thorac Cardiovasc Surg* 2006; **12**:305–307.
- Mariette C, Piessen G, Triboulet JP. Therapeutic strategies in oesophageal carcinoma: role of surgery and other modalities. *Lancet Oncol* 2007; **8**:545–553.
- Nakajima M, Kato H. Treatment options for esophageal squamous cell carcinoma. *Expert Opin Pharmacother* 2013; **14**:1345–1354.
- Nakamura K, Kato K, Igaki H, Ito Y, Mizusawa J, Ando N, *et al.* Japan Esophageal Oncology Group/Japan Clinical Oncology Group. Three-arm phase III trial comparing cisplatin plus 5-FU (CF) versus docetaxel, cisplatin plus 5-FU (DCF) versus radiotherapy with CF (CF-RT) as preoperative therapy for locally advanced esophageal cancer (JCOG1109, NEXt study). *Jpn J Clin Oncol* 2013; **43**:752–755.
- Kosugi S, Kanda T, Nakagawa S, Ohashi M, Nishimaki T, Hatakeyama K. Efficacy and toxicity of fluorouracil, doxorubicin and cisplatin/nedaplatin treatment as neoadjuvant chemotherapy for advanced esophageal carcinoma. *Scand J Gastroenterol* 2005; **40**:886–892.
- Honda M, Miura A, Izumi Y, Kato T, Ryotokuji T, Monma K, *et al.* Doxorubicin, cisplatin, and fluorouracil combination therapy for metastatic esophageal squamous cell carcinoma. *Dis Esophagus* 2010; **23**:641–645.
- Yamasaki M, Miyata H, Fujiwara Y, Takiguchi S, Nakajima K, Nishida T, *et al.* p53 genotype predicts response to chemotherapy in patients with squamous cell carcinoma of the esophagus. *Ann Surg Oncol* 2010; **17**:634–642.
- Raman M, Chen W, Cobb MH. Differential regulation and properties of MAPKs. *Oncogene* 2007; **26**:3100–3112.
- Ono K, Han J. The p38 signal transduction pathway: activation and function. *Cell Signal* 2000; **12**:1–13.
- Cuenda A, Rousseau S. p38 MAP-kinases pathway regulation, function and role in human diseases. *Biochim Biophys Acta* 2007; **1773**:1358–1375.
- Cargnello M, Roux PP. Activation and function of the MAPKs and their substrates, the MAPK-activated protein kinases. *Microbiol Mol Biol Rev* 2011; **75**:50–83.
- Wagner EF, Nebreda AR. Signal integration by JNK and p38 MAPK pathways in cancer development. *Nat Rev Cancer* 2009; **9**:537–549.
- Ambrose M, Ryan A, O'Sullivan GC, Dunne C, Barry OP. Induction of apoptosis in renal cell carcinoma by reactive oxygen species: involvement of extracellular signal-regulated kinase 1/2, p38delta/gamma, cyclooxygenase-2 down-regulation, and translocation of apoptosis-inducing factor. *Mol Pharmacol* 2006; **69**:1879–1890.
- O'Callaghan C, Fanning LJ, Houston A, Barry OP. Loss of p38δ mitogen-activated protein kinase expression promotes oesophageal squamous cell carcinoma proliferation, migration and anchorage-independent growth. *Int J Oncol* 2013; **43**:405–415.
- Yamana H, Kakegawa T, Tanaka T, Higaki K, Fujii T, Tou U. Experimental studies on immunotargeting therapy for esophageal carcinoma. *Gan To Kagaku Ryoho* 1994; **21**:755–760.
- Tsukahara T, Nabeta Y, Kawaguchi S, Ikeda H, Sato Y, Shimozaawa K, *et al.* Identification of human autologous cytotoxic T-lymphocyte-defined osteosarcoma gene that encodes a transcriptional regulator, papillomavirus binding factor. *Cancer Res* 2004; **64**:5442–5448.
- Nakao M, Yamana H, Imai Y, Toh Y, Toh U, Kimura A, *et al.* HLA A2601-restricted CTLs recognize a peptide antigen expressed on squamous cell carcinoma. *Cancer Res* 1995; **55**:4248–4252.
- O'Sullivan GC, Tangney M, Casey G, Ambrose M, Houston A, Barry OP. Modulation of p21-activated kinase 1 alters the behavior of renal cell carcinoma. *Int J Cancer* 2007; **121**:1930–1940.
- Chen L, Zhang JJ, Huang XY. cAMP inhibits cell migration by interfering with Rac-induced lamellipodium formation. *J Biol Chem* 2008; **283**:13799–13805.
- Bernardi P, Scorrano L, Colonna R, Petronilli V, Di Lisa F. Mitochondria and cell death. Mechanistic aspects and methodological issues. *Eur J Biochem* 1999; **264**:687–701.
- Ku GY, Ilson DH. Chemotherapeutic options for gastroesophageal junction tumors. *Semin Radiat Oncol* 2013; **23**:24–30.
- O'Donovan TR, O'Sullivan GC, McKenna SL. Induction of autophagy by drug-resistant esophageal cancer cells promotes their survival and recovery following treatment with chemotherapeutics. *Autophagy* 2011; **7**:509–524.

- 24 Pereira L, Igea A, Canovas B, Dolado I, Nebreda AR. Inhibition of p38 MAPK sensitizes tumour cells to cisplatin-induced apoptosis mediated by reactive oxygen species and JNK. *EMBO Mol Med* 2013; **5**:1759–1774.
- 25 Elsea CR, Roberts DA, Druker BJ, Wood LJ. Inhibition of p38 MAPK suppresses inflammatory cytokine induction by etoposide, 5-fluorouracil, and doxorubicin without affecting tumoricidal activity. *PLoS One* 2008; **3**:e2355.
- 26 Chen WW, Lin CC, Huang TC, Cheng AL, Yeh KH, Hsu CH. Prognostic factors of metastatic or recurrent esophageal squamous cell carcinoma in patients receiving three-drug combination chemotherapy. *Anticancer Res* 2013; **33**:4123–4128.
- 27 Chen J, Pan J, Liu J, Li J, Zhu K, Zheng X, *et al*. Postoperative radiation therapy with or without concurrent chemotherapy for node-positive thoracic esophageal squamous cell carcinoma. *Int J Radiat Oncol Biol Phys* 2013; **86**:671–677.
- 28 Taieb J, Artru P, Baujat B, Mabro M, Carola E, Maindrault F, *et al*. Optimisation of 5-fluorouracil (5-FU)/cisplatin combination chemotherapy with a new schedule of hydroxyurea, leucovorin, 5-FU and cisplatin (HLFP regimen) for metastatic oesophageal cancer. *Eur J Cancer* 2002; **38**:661–666.
- 29 Chan KW, Lee PY, Lam AK, Law S, Wong J, Srivastava G. Clinical relevance of Fas expression in oesophageal squamous cell carcinoma. *J Clin Pathol* 2006; **59**:101–104.
- 30 Matsuzaki I, Suzuki H, Kitamura M, Minamiya Y, Kawai H, Ogawa J. Cisplatin induces fas expression in esophageal cancer cell lines and enhanced cytotoxicity in combination with LAK cells. *Oncology* 2000; **59**:336–343.
- 31 He D, Zhao XQ, Chen XG, Fang Y, Singh S, Talele TT, *et al*. BIRB796, the inhibitor of p38 mitogen-activated protein kinase, enhances the efficacy of chemotherapeutic agents in ABCB1 overexpression cells. *PLoS One* 2013; **8**:e54181.
- 32 Alessi DR, Cuenda A, Cohen P, Dudley DT, Saltiel AR. PD 098059 is a specific inhibitor of the activation of mitogen-activated protein kinase kinase in vitro and in vivo. *J Biol Chem* 1995; **270**:27489–27494.
- 33 Gisselbrecht C, Calvo F, Mignot L, Pujade E, Bouvry M, Danne O, *et al*. Fluorouracil (F), adriamycin (A), and cisplatin (P) (FAP): combination chemotherapy of advanced esophageal carcinoma. *Cancer* 1983; **15**:974–977.
- 34 Weiss RB. The anthracyclines: will we ever find a better doxorubicin? *Semin Oncol* 1992; **19**:670–686.
- 35 Shimakawa T, Naritaka Y, Asaka S, Isohata N, Murayama M, Konno S, *et al*. Neoadjuvant chemotherapy (FAP) for advanced esophageal cancer. *Anticancer Res* 2008; **28**:2321–2326.
- 36 Juan HC, Tsai HT, Chang PH, Huang CY, Hu CP, Wong FH. Insulin-like growth factor 1 mediates 5-fluorouracil chemoresistance in esophageal carcinoma cells through increasing survivin stability. *Apoptosis* 2011; **16**:174–183.
- 37 Ngan CY, Yamamoto H, Takagi A, Fujie Y, Takemasa I, Ikeda M, *et al*. Oxaliplatin induces mitotic catastrophe and apoptosis in esophageal cancer cells. *Cancer Sci* 2008; **99**:129–139.
- 38 Boldt S, Weidle UH, Kolch W. The role of MAPK pathways in the action of chemotherapeutic drugs. *Carcinogenesis* 2002; **23**:1831–1838.
- 39 Brozovic A, Osmak M. Activation of mitogen-activated protein kinases by cisplatin and their role in cisplatin-resistance. *Cancer Lett* 2007; **251**:1–16.
- 40 De la Cruz-Morcillo MA, Valero ML, Callejas-Valera JL, Arias-González L, Melgar-Rojas P, Galán-Moya EM, *et al*. p38MAPK is a major determinant of the balance between apoptosis and autophagy triggered by 5-fluorouracil: implication in resistance. *Oncogene* 2012; **31**:1073–1085.
- 41 Buch K, Peters T, Nawroth T, Sängler M, Schmidberger H, Langguth P. Determination of cell survival after irradiation via clonogenic assay versus multiple MTT assay – a comparative study. *Radiat Oncol* 2012; **7**:1.
- 42 Sumantran VN. Cellular chemosensitivity assays: an overview. *Methods Mol Biol* 2011; **731**:219–236.
- 43 Kawada K, Yonei T, Ueoka H, Kiura K, Tabata M, Takigawa N, *et al*. Comparison of chemosensitivity tests: clonogenic assay versus MTT assay. *Acta Med Okayama* 2002; **56**:129–134.

Exploitation of Aberrant Signalling Pathways as Useful Targets for Renal Clear Cell Carcinoma Therapy

Carol O'Callaghan and Orla Patricia Barry
*University College Cork
Ireland*

1. Introduction

Renal cell carcinoma (RCC) is the third leading cause of death among urological tumours, annually afflicts about 150,000 people globally and causes nearly 78,000 deaths (Jemal et al., 2008; Zbar et al., 2003). RCC is an epithelial tumour consisting of several different histological subtypes of which clear cell RCC is the prototypical. Traditionally treatment has been via surgery and immunotherapy. Surgical resection is appropriate for some patient cohorts including those with isolated metastases. However, recurrence is common even when the primary and metastatic sites have been aggressively resected (Couillard & deVere White, 1993). RCC is highly unresponsive to standard chemotherapy and the use of cytokine therapy with interleukin (IL)-2 or interferon (IFN)- α is associated with low rates of response and high rates of toxicity (Oudard et al., 2007). Thus, development of new therapies continues to be crucial to improve outcomes in patients with RCC.

The increased understanding of the molecular structure and aberrant activity of signalling pathways in RCC has led to a flurry of research activity in the arena of targeted therapies namely anti-angiogenic vascular endothelial growth factor (VEGF) and the mammalian target of rapamycin (mTOR), both of which are involved in the pathogenesis of RCC (Mulders, 2009). These advancements in an obvious therapeutic gap have significantly improved the progression free survival (PFS) of patients with RCC. Despite the explosion in drug development during the past five years, however, PFS for patients with metastatic RCC (mRCC) still remains poor as none of the current targeted therapies possess the capacity to induce remission. In addition these drugs provide dose-limiting toxic side effects and so we are still faced with a considerable task in developing newer safer therapeutics for use as either first line agents or in combination with existing ones.

2. Targeted therapy for RCC

As the understanding of the molecular biology underlying RCC has increased, various components of growth and angiogenic signal transduction pathways have been identified as rational targets for therapeutic intervention in the treatment of patients with RCC and mRCC. The VEGF/VEGF receptor (VEGFR) pathway is one such target. VEGF expression is induced under hypoxic conditions triggering several mechanisms that promote

angiogenesis (Ellis & Hicklin, 2008). Members of the VEGF family namely VEGF-A, -B, -C and -D regulate angiogenesis through binding to the related family of receptor tyrosine kinases (RTKs): VEGF receptors (VEGFR)-1, -2 and -3. The VEGFR consists of an extracellular ligand binding site, a transmembrane α -helical domain and an intracellular protein-tyrosine kinase region. Once activated, phosphorylated tyrosine residues on these receptor kinases provide high-affinity binding sites for components of the Raf/MEK/ERK (MAP Kinase) and PI3K/AKT signalling pathways which mediate cell growth and angiogenesis. Inhibition of the pathway involving VEGF-A activation of VEGFR-2 has undergone the most extensive investigation in recent years. This pathway mediates the formation and preservation of the blood vessel network which is vital for tumour cell survival and proliferation (Casanovas et al., 2005). In RCC, VEGF is also a powerful tumour growth factor. RCCs over-express the different VEGFRs and also produce as paracrine and autocrine growth factors, large amounts of VEGF (Qian et al., 2009). In tumours the VEGF isoforms -C and -D have been shown to activate the VEGFR3 receptor and to initiate the development and maintenance of a lymphatic system (He et al., 2005). Targeting this process in cancer treatment is now in the early stages of development. Presently, different therapeutic avenues exist for inhibiting the activation of receptor tyrosine kinases (RTKs). Monoclonal antibodies (mAbs) against growth factor ligands, or antibody fragments against RTK ligand-binding domain, can prevent binding of growth factors, thus attenuating RTK activity. Alternatively, the protein kinase can be targeted. Drugs that bind reversibly to the ATP-binding site within the kinase domain or to a small pocket that is immediately adjacent to the ATP-binding site are used to block the enzymatic activity of the kinase. Due to similarities within the amino acid structure of the kinase domain, ATP-competitive inhibitors can have cross reactivity with other structurally related kinases.

2.1 VEGF- antibody therapy/ligand competitors

2.1.1 Bevacizumab

Bevacizumab is an i.v. administered humanized monoclonal IgG1 antibody that targets and neutralises all major isoforms of circulating VEGF (Presta et al., 1997). By binding with high affinity to VEGF, bevacizumab inhibits its interaction with tyrosine kinase receptors thereby preventing the initiation of an angiogenic signal (Figure 1). This weakens existing microvasculature and production of new vasculature is inhibited. The loss of vascularisation eventually leads to tumour cell death (Jain, 2005).

Bevacizumab is used in the treatment of a wide range of cancer types including RCC, colon, brain and lung cancers. It was approved in 2009 for the first-line treatment of patients with advanced RCC or mRCC in combination with IFN- α . FDA approval came as a result of the phase III AVOREN trial. RCC patients following previous nephrectomy were randomized to receive either bevacizumab plus IFN- α or placebo plus IFN- α (Escudier et al., 2007a). The addition of bevacizumab to IFN- α significantly improved both the overall response rate (ORR) (30.6 vs. 12.4%, $P < 0.0001$) and PFS (10.2 vs. 5.4 months). Subgroup analysis, however, indicated that the advantage in PFS related only to favourable and intermediate risk patients and not to the poor risk group. The final overall survival (OS) results reported no significant difference between the bevacizumab and control groups (23.3 vs. 21.3 months). However, these findings may have been influenced by the fact that 63% of patients in the placebo plus IFN- α group and 55% of patients in the bevacizumab plus IFN- α group received second-line therapy with other agents (Escudier et al., 2010).

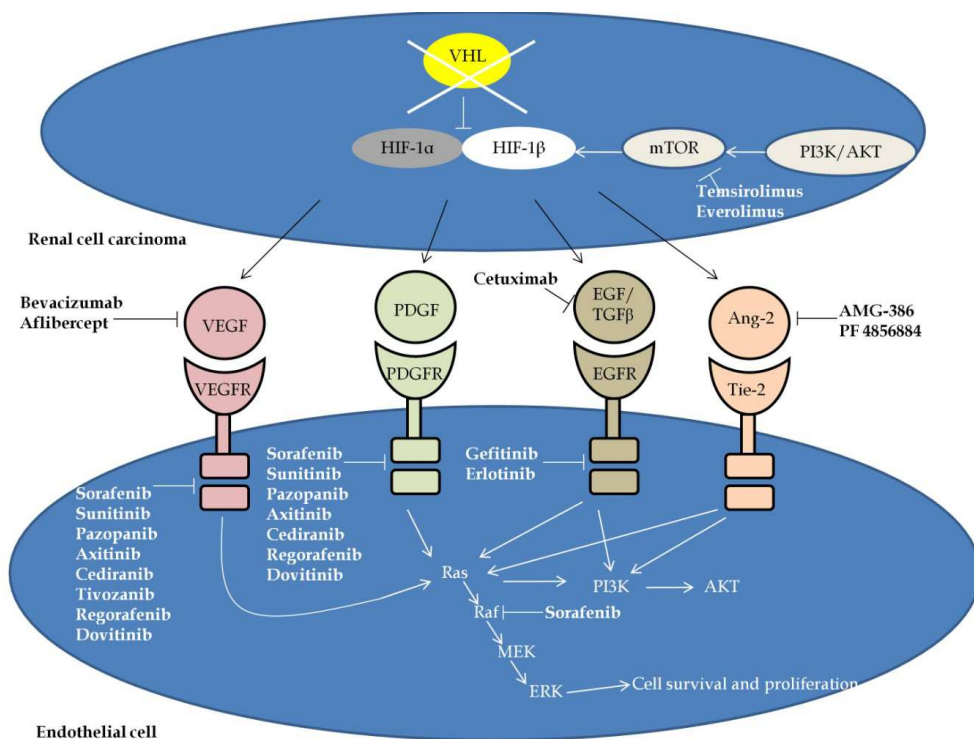


Fig. 1. Schematic representation of the signalling pathways contributing to angiogenesis and cell proliferation in RCC and the targeted agents which inhibit them. HIF activation upregulates the expression of VEGF, PDGF, EGF and Ang-2. Binding of these ligands to their receptors induces downstream activation of MAPK signalling, resulting in angiogenesis. Abbreviations; VHL: Von Hippel Lindau; HIF: hypoxia-inducible factor; mTOR: mammalian target of rapamycin; PI3K: phosphoinositol-3 kinase; VEGF(R): vascular endothelial growth factor (receptor); PDGF(R): platelet-derived growth factor (receptor); EGF(R): epidermal growth factor (receptor); TGF- β : transforming growth factor beta; Ang-2: angiopoietin 2. Inhibitory arrows (\perp) show clinically available or in development therapeutic agents for the treatment of RCC and mRCC.

2.1.2 Aflibercept

Aflibercept is an engineered fusion protein designed to interact with all isoforms of VEGF and to placental growth factor (PLGF), thereby preventing them from binding to VEGFRs. It is composed of the extracellular domain 2 of VEGFR1 and extracellular domain 3 of VEGFR2 fused to an Fc segment of human IgG1 (Wulff et al., 2002). Aflibercept appears to have a greater affinity for VEGF than bevacizumab, resulting in a more complete obstruction of VEGF signalling. This together with the fact that aflibercept binds to PLGF while bevacizumab does not, may explain why preclinical studies have shown aflibercept to be more effective than bevacizumab (Kim et al., 2002).

2.2 Receptor tyrosine kinase inhibitors (RTKIs)

The intracellular kinase activity of growth factor receptors also provides an attractive target for therapeutic intervention. Three receptor tyrosine kinase inhibitors are currently available for the treatment of clear cell RCC and many more are in development (Figure 1). By targeting the intracellular tyrosine kinase domain of multiple growth factor receptors these drugs inhibit not only the VEGF pathway but also the platelet derived growth factor (PDGF) pathway as well as other kinases critical for proliferation and angiogenesis.

2.2.1 Sorafenib

Sorafenib was the first multi-targeted kinase inhibitor approved for the treatment of patients with cytokine-refractory advanced RCC or mRCC. It is a potent small molecule dual-action inhibitor, first identified in *in vitro* assays as an inhibitor of Ras signalling. Sorafenib also inhibits VEGFRs and PDGFRs (Wilhelm et al., 2004). As multiple kinases are inhibited by sorafenib it is difficult to determine the relative contribution of each target to the anti-tumour activity of this drug. Preclinical studies in a variety of cancer models suggest sorafenib acts on both tumour cells and tumour vasculature by inhibiting cellular proliferation and angiogenesis pathways (Wilhelm et al., 2008).

Sorafenib's approval by the FDA in 2005 was as a result of a phase III trial namely; Treatment Approaches in Renal Cell Cancer Global Evaluation Trial (TARGET). All participants had advanced RCC and had experienced disease progression in spite of the then standard cytokine therapy. Patients were randomly assigned to receive sorafenib or placebo (Escudier et al., 2007b). At the first interim analysis the ORR was 10% for sorafenib compared with 2% for placebo. Also, sorafenib treated patients had a significant PFS advantage of 5.5 months versus 2.8 months for the placebo group. At this point those patients initially assigned to receive placebo were allowed to switch to sorafenib, potentially obscuring differences in end point results. In fact the final analysis of all patients registered in the trial did not show a statistically significant difference in the OS of the initial intent-to-treat population (17.8 vs. 15.2 months in sorafenib and placebo treated patients, respectively). However, a secondary analysis was performed in which patients who crossed over to sorafenib after initial treatment with placebo were censored. This demonstrated a significant benefit for sorafenib treatment with a median OS of 17.8 months compared to 14.3 months for placebo (Escudier et al., 2009). In terms of side effect profile sorafenib treated patients reported fewer adverse effects and a better overall quality of life than those receiving IFN- α . Both hypertension and skin toxicity, in general, are common manifestations of toxicity with multiple tyrosine kinase inhibitors, with incidences of 17% and 40% respectively, outlined in the TARGET trial. Other adverse effects associated with sorafenib treatment are diarrhea (Escudier et al., 2007b), and an additive loss of muscle mass above that usually observed in patients with advanced cancer (Antoun et al., 2010).

2.2.2 Sunitinib

Sunitinib is a RTKI designed to prevent cells from responding to the elevated level of pro-angiogenic signals associated with RCC. It is an orally available, small molecule, multi-targeted kinase inhibitor with activity against VEGFRs, PDGFRs, fms-like tyrosine kinase receptor-3 (FLT-3) and stem cell factor receptor (c-KIT). Sunitinib is classified as an ATP competitive inhibitor. It received accelerated approval by the FDA in 2006 based on responses in patients with mRCC who had failed cytokine therapy. Regular approval was obtained in 2007 as a result of a phase III study evaluating sunitinib as a first-line therapy

compared with IFN- α . Results of the trial demonstrated a considerable advantage for sunitinib over IFN- α and both OS rates and PFS were significantly higher for the sunitinib treated group (Motzer et al., 2007a; Motzer et al., 2009). Sunitinib is now the standard of care for initial therapy of good to moderate prognosis mRCC patients. OS of over two years is a marked improvement on the one year OS rates observed before the advent of targeted kinase inhibitor therapy (Motzer et al., 2009).

As sunitinib inhibits multiple kinases and therefore blocks several signalling pathways, numerous side effects are associated with treatment. These, however, are favourable when compared to the significant toxicity profile associated with the previous therapeutic option for RCC i.e. immunotherapy. In the phase III trial which led to the approval of sunitinib, slightly different toxicity profiles were observed between the two treatment groups. Sunitinib treated patients more commonly experienced diarrhea, hypertension, hand-foot syndrome, neutropenia and thrombocytopenia while fatigue occurred more commonly in the IFN- α group. Overall, however, patients who received sunitinib reported a better quality of life compared to patients treated with IFN- α .

2.2.3 Pazopanib

Pazopanib is the latest multiple kinase inhibitor approved for the first-line treatment of patients with advanced RCC. It inhibits signalling by VEGFRs, PDGFRs, and c-KIT by competitively binding to the ATP enzymatic pocket of the RTK. Pazopanib differs from sunitinib and sorafenib as the range of targets it potently inhibits is narrower. FDA approval followed a phase III trial involving clear cell (or predominately clear cell) RCC patients with no previous treatment history (54%), or who had progressed following a single prior cytokine treatment (46%) (Sternberg et al., 2010). Patients were randomized to receive either pazopanib or placebo daily. In the overall population the primary end point of PFS was significantly higher in the pazopanib group compared to placebo (9.2 vs. 4.2 months). The ORR for the pazopanib group was 30%. Although a non-significant improvement in median OS of 22.9 months for the pazopanib group versus 20.5 months for the placebo group was reported, this analysis had been confounded by the early and high level of patient cross-over from placebo to pazopanib upon progression (Sternberg, 2010).

The toxicity profile associated with pazopanib treatment is similar to both sunitinib and sorafenib. The most common effects observed include hypertension, diarrhea, nausea, hair depigmentation and asthenia. Clinical trials cannot easily be compared, however, as evident from a phase III trial of pazopanib which demonstrated lower incidence of hand-foot syndrome, diarrhea and asthenia compared with sunitinib and sorafenib. Conversely, the incidence of hypertension associated with pazopanib treatment in the phase III trial is high (40%) when compared to sunitinib and sorafenib trials (Lang & Harrison, 2010).

2.2.4 In development

The new generation of RTKIs in development for the treatment of RCC display greater potency and selectivity for VEGFRs compared to the established kinase inhibitors discussed above. It is hoped that this increased potency and high specificity will give rise to enhanced anti-tumour activity. Furthermore, the absence of off-target (non-VEGFR) inhibition may result in less toxicity than is normally associated with kinase inhibitors in general.

2.2.5 Axitinib (AG-013736)

Axitinib is an orally available RTKI. Picomolar concentrations are sufficient for axitinib to inhibit VEGFRs, while it inhibits PDGFR- β and c-KIT at low nanomolar concentrations (Hu-Lowe et al., 2008). In this study and others (Inai et al., 2004) axitinib in mouse models has demonstrated anti-tumour, anti-angiogenic and anti-metastatic properties as well as having an ability to induce central necrosis. Axitinib is now being looked at for the second-line treatment of advanced RCC. In a phase II trial of patients with cytokine-refractory mRCC (Rixe et al., 2007), axitinib displayed an ORR of 44.2% and median PFS of 15.7 months, greater than any agent investigated for mRCC treatment to-date. However, this efficacy has not been examined in comparative trials with other targeted agents.

2.2.6 Cediranib (AZD2171)

Cediranib is an ATP-competitive inhibitor of RTKs and like axitinib is a potent inhibitor of VEGFRs and PDGFR- β at subnanomolar concentrations (Gomez-Rivera et al., 2007; Takeda et al., 2007). In a recent placebo controlled phase II trial, a median PFS of 12.1 months was observed in patients treated with cediranib compared to 2.7 months for those who received placebo. Furthermore, the mean change in tumour size in patients receiving cediranib was a 20% decrease versus a mean increase of 19% for patients randomized to placebo (Bhargava & Robinson, 2011).

2.2.7 Tivozanib (AV-951)

Tivozanib is an orally active RTKI and is selective for VEGFRs at picomolar concentrations (Nakamura et al., 2006). In a phase II trial, clear cell RCC patients who had undergone nephrectomy displayed an ORR of 32% to 1.5 mg tivozanib daily. The median PFS for patients was 14.8 months (Bhargava et al., 2010). This potency combined with the selectivity of tivozanib for VEGFRs reduces the inhibition of off-target kinases, resulting in less toxicity. The most common side effects reported in this trial were hypertension and dysphonia while incidences of other toxicities usually associated with RTKIs (fatigue, diarrhea and hand-foot syndrome) were low. The occurrence of fewer toxicities together with the specificity of tivozanib allows it to be safely combined at full dose and scheduled with another targeted agent. For example, preliminary results of a phase I trial combining tivozanib and the mTOR inhibitor temsirolimus in mRCC patients reported no dose limiting toxicities (Fishman et al., 2009).

2.2.8 Regorafenib

Regorafenib is a potentially significant multi-kinase inhibitor in that it inhibits the traditional targets of VEGFRs, PDGF- β and fibroblast growth factor (FGF)-1, as well as the endothelium specific receptor tyrosine kinase Tie-2. The inhibition of targets both within and external to the VEGF axis may offer valuable therapeutic advantages when it comes to avoiding resistance and enhancing the efficacy of targeted therapy. A phase II trial of regorafenib in mRCC patients showed that those receiving regorafenib had a 27% partial response and a 42% stable disease rate (Eisen et al., 2009).

2.2.9 Dovitinib (TKI258)

Dovitinib is also a promising agent targeting VEGFRs, PDGFRs, FLT3 as well as FGF receptors namely FGFR3. This is significant as not only does the FGF angiogenic signalling

pathway provide a potential mechanism of resistance to VEGF therapy, activating mutations or upregulation of FGF/FGFRs have been identified in RCC (Emoto et al., 1994). Members of the FGF family are involved in proliferation, differentiation and migration of a range of cell types. A phase II study of dovitinib in previously treated advanced RCC or mRCC patients has reported results which include a median PFS and OS of 6.1 and 16 months, respectively (Angevin et al., 2011).

3. Targeting EGFR

Disruption of EGF signalling is a popular therapeutic mechanism in a number of cancer types. As the expression of ligands of the EGFR (including EGF and the angiogenesis promoting transforming growth factor (TGF)- β) is upregulated by *VHL* inactivation, the validity of this approach in clear cell RCC was explored in a number of trials. In single-agent EGFR inhibitor trials, gefitinib (a selective EGFR TKI) and cetuximab (a recombinant mouse-human mAb) were administered as monotherapy. Neither agent demonstrated a complete or partial response (Stahler et al., 2005). In a randomized phase II trial, clear cell RCC patients received either bevacizumab or bevacizumab plus the EGFR inhibitor erlotinib. The results showed identical median PFS and ORR between the two groups (Bukowski et al., 2007). EGFR inhibition therefore does not appear to be a viable approach for the treatment of clear cell RCC. A possible reason for this may be the rarity of EGFR mutations in RCC, when compared to other cancers (Dancey, 2004). Furthermore, the activators of EGFR signalling which are upregulated in RCC can also initiate VEGFR signalling, making the inhibition of EGFR alone insufficient to disrupt tumour proliferation and angiogenesis.

4. Targeting PDGF

Members of the PDGF family include PDGF-A, -B, -C and -D and mediate their effects through binding to PDGFR- α and - β leading to the activation of various signalling pathways giving rise to tumour growth (Guo et al., 2003; Pietras et al., 2003). High levels of PDGF-D has been shown to be associated with RCC and its progression has been linked to PDGF-D/PDGFR- β signalling and PDGFR- α expression (Sulzbacher et al., 2003). Although there is not a wealth of data published on PDGF and PDGFR in RCC there are currently many drugs either clinically available or in development that target this RTK as outlined above and in Figure 1.

5. Limitations of currently available targeted agents

Comparison of the relative benefit of each targeted treatment in advanced RCC and mRCC is exceptionally difficult. Trials conducted targeting RTKs involved varied patient populations with differences in prior treatment status, prognosis and histology of RCC. According to Flaherty & Puzanov the easiest comparison is ORR. This comparison identifies two groups: bevacizumab and sorafenib generate a response rate of $\leq 10\%$, while sunitinib and pazopanib induce a response in $\geq 30\%$ of patients. However, this does not reflect any clinical benefit as higher response rates do not appear to be associated with improved PFS or OS (Flaherty & Puzanov, 2010).

Resistance is a major problem with both older and newer therapies as well as mono and poly therapies. Few complete responses are associated with any of the targeted therapies

discussed. All patients will eventually develop resistance and progress, usually within 8 to 16 months (Sosman & Puzanov, 2009). A number of mechanisms have been described outlining how resistance can occur. Sorafenib, sunitinib and pazopanib therapy is associated with a significant increase in VEGF production (Deprimo et al., 2007; Kumar et al., 2007; Veronese et al., 2006). Resistance may occur if the increase in VEGF reaches a threshold that can overcome the inhibition. Another hypothesis has been examined in animal models of tumour angiogenesis. These models outline that the inhibition of VEGF or VEGFR leads to upregulation of PDGF and basic FGF (bFGF) production by tumours activating alternative pathways for angiogenic signalling (Fernando et al., 2008). Despite the overlap of targets and inevitable resistance, however, RCC tumours do not appear to be totally cross-resistant to sequential therapy with different agents. In a phase II study, patients who had progressed on sunitinib underwent treatment with sorafenib. Objective responses resulted in 10% of patients with a median PFS of 16 weeks (Di Lorenzo et al., 2009). A possible explanation is that when the initial inhibitor is removed (once resistance has occurred and the tumour has progressed), cells revert back to VEGF signalling.

Presently, it is hoped that combination therapies for the treatment of patients with RCC will see improvements in PFS, ORR and OS greater than those seen with any single agent. There are two options for the combination of targeted therapies i.e. vertical blockade and horizontal blockade. Vertical blockade involves targeting several steps along a single signalling pathway. This is an attractive option in treatment of RCC combining drugs which inhibit hypoxia-inducible factor (HIF) translation, VEGF or VEGFR. This approach could provide an opportunity to overcome the resistance associated with increased levels of VEGF. A phase I trial evaluated the potential benefit of combining sorafenib with bevacizumab in mRCC patients (Sosman, 2008). Due to toxicity, the dosage of both agents had to be reduced from their usual levels to half the recommended dose of bevacizumab and one-quarter the usual dose of sorafenib. Despite this a 50% response rate was observed, a vast improvement on the 10-15% achieved with full doses of each agent alone. The combination strategy of horizontal blockade entails simultaneously targeting more than one signalling pathway crucial for tumour cell survival and proliferation. Horizontal blockade is an appealing option as combining VEGFR inhibitors with other tyrosine kinase inhibitors may prove useful in preventing resistance by the mechanism of alternative angiogenic pathways.

6. PI3K/AKT/mTOR signalling pathway

The phosphatidylinositol 3-kinase/protein kinase B/mammalian target of rapamycin-pathway (PI3K/AKT/mTOR-pathway) is one of the most common aberrant pathways activated in cancer, regulating many known oncogenic pathways including apoptosis, proliferation and cell migration (Carracedo & Pandolfi, 2008; Klein & Levitzki, 2009; Inoki et al., 2005). Activation of PI3K occurs at the cell membrane in response to several RTKs including the EGFR, the insulin-like growth factor receptor (IGFR) and the PDGFR leading to the production of the second messenger phosphatidylinositol-3,4,5-triphosphate (PIP3). Levels of PIP3 are tightly regulated by the tumour suppressor phosphatase and tensin homolog (PTEN), serving as the negative regulator of the PI3K/AKT/mTOR pathway. AKT is recruited to the cell membrane by PIP3 and phosphorylated to its fully activated form by phosphoinositide dependent protein kinase 1 (PDK1). Activated AKT can directly activate mTOR by phosphorylation or indirectly through inactivation of the tuberous sclerosis complex 2 (TSC2) which normally inhibits mTOR (Figure 2).

mTOR is a 290kDa serine/threonine protein kinase and is highly conserved from fungi to mammals. It forms multimolecular complexes and plays a key role in diverse signalling events such as growth, proliferation, survival, angiogenesis and protein synthesis (Dowling et al., 2010). mTOR responds to a range of diverse stimuli including growth factors, cytokines, and hormones but also acts as an important sensor of cellular stresses imposed by hypoxia, pH or osmotic alterations, heat shock, oxidative stress and DNA damage. Defects in signalling components upstream of mTOR including excessive growth factor receptor activation or mutation correlates with a more aggressive tumour and a worse prognosis (Faivre et al., 2006). mTOR exists as two distinct complexes, mTOR complex 1 (mTORC1) and mTOR complex 2 (mTORC2) (Figure 2). Regulation of mTOR activation is controlled by two components of the tuberous sclerosis complex (TSC) comprising TSC1 (hamartin) and TSC2 (tuberin). When they heterodimerise mTOR is inhibited and can no longer phosphorylate downstream substrates (Dancey, 2005). Phosphorylation of TSC2 by AKT, however, promotes dissociation of the TSC1/TSC2 complex which activates the guanosine triphosphate Rheb. Rheb activity subsequently activates mTORC1. mTORC1 is bound to raptor (regulatory-associated protein of mTOR), mLST8 (mammalian lethal with sec 13 protein 8), also known as G β L and PRAS40 (proline-rich AKT substrate 40kDa) which is phosphorylated by AKT causing its dissociation from raptor and its subsequent activation. mTORC2 complexes with rictor (rapamycin-insensitive companion of mTOR), mSIN1, mLST8 and Protor-1 or Protor-2. Both complexes phosphorylate the hydrophobic motifs of AGC kinase family members. mTORC1 phosphorylates S6K and the inhibitory binding protein 4E-BP1 at Thr37 and Thr 46 which acts as a priming event essential for the phosphorylation of Ser65 and Thr70 leading to the release of eIF4E and subsequent assembly of the eIF4F complex (Gingras et al., 2001). Activation of S6K in turn leads to phosphorylation of inhibitory sites (Ser636 and 639) on the insulin receptor substrate-1 (IRS-1), thereby suppressing IRS-1 mediated activation of the PI3K/AKT pathway. mTORC2 activation leads to phosphorylation of AKT, SGK1 and PKC which control cell survival and cytoskeletal organization (Figure 2).

mTORC1 is frequently dysregulated in cancer (Guertin & Sabatini, 2007). Loss or inactivation of tumour suppressors such as p53, liver kinase B1 (LKB1), PTEN and TSC1/2 which antagonise PI3K-dependent activation of mTORC1 can promote tumorigenesis via increased signalling through mTORC1 (Sabatini, 2006; Shaw et al., 2004). Moreover, increased levels and/or phosphorylation of downstream targets of mTORC1 have been reported in various human malignancies in which they correlate with tumour aggressiveness and poor prognosis (Guertin & Sabatini, 2007; Mamane et al., 2006). Collectively these studies suggest that aberrant mTORC1 signalling is linked to dysregulated control in cancer and for this reason the spotlight has been shone on mTORC1 as a possible therapeutic target for anti-cancer therapy.

6.1 mTOR and RCC

As outlined above the signalling network controlled by the PI3K/AKT/mTOR axis is very often found to be dysregulated in human malignancy. There is a wealth of data to support the notion that signalling through mTOR is dysregulated in RCC. This makes this cancer type in particular an attractive target for mTOR inhibitor therapy. RCC demonstrates increased phosphorylation of AKT, S6K1 and mTOR as well as increased expression of PTEN and disrupted TSC complexes (Pantuck et al., 2007). mTOR activation ultimately leads to increased production of angiogenic factors leading to a highly vascularised tumour which is evident in RCC.

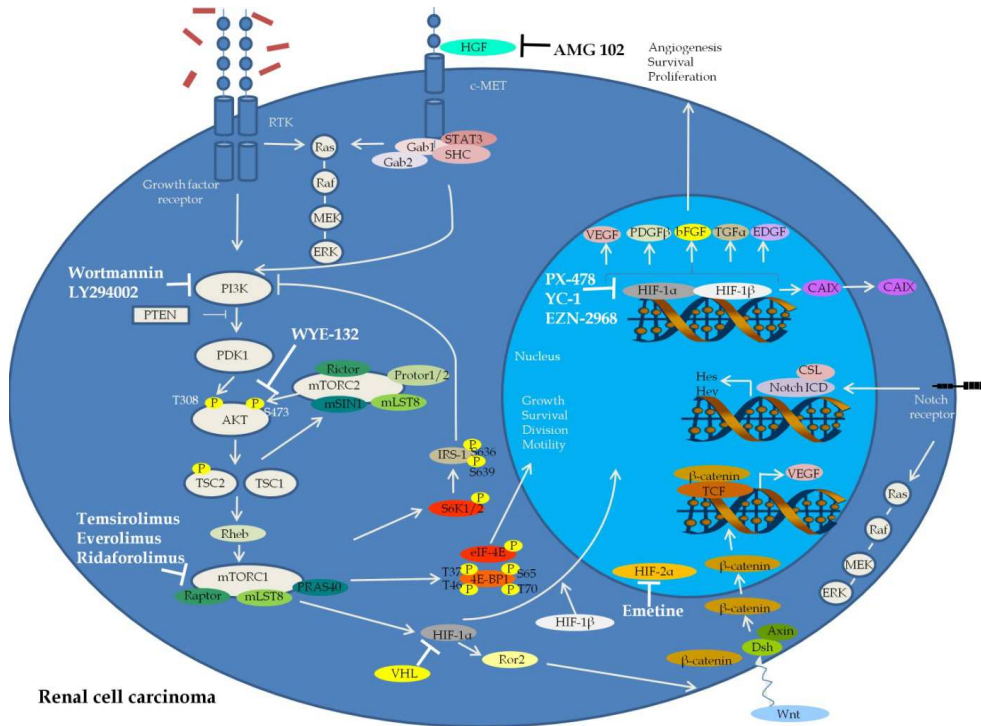


Fig. 2. Schematic representation of mTOR signalling, phosphatidylinositol 3'-OH-kinase/AKT/mTOR signalling, Wnt/ β -catenin signalling, HGF signalling and core NOTCH signalling pathways. In relation to growth factor signalling, PI3K activates downstream mTORC1 giving rise to HIF-1 α activation, which in turn switches on gene expression required for angiogenesis and cell proliferation in endothelial cells. HGF binding to MET leads to its phosphorylation and subsequent recruitment of adapter proteins such as Gab1, Gab2, SHC, STAT3 and PI3K with downstream activation of Ras/MAPK and PI3K/AKT pathways. Wnt pathway activation leads to hypophosphorylated β -catenin where it translocates into the nucleus and forms a complex with TCF. Ligand binding to the Notch receptor leads to release of the intracellular domain (ICD) of Notch. Notch ICD subsequently translocates into the nucleus, where it forms a complex with essential cofactors such as the transcription factor CSL. This complex mediates the transcription of target genes such as HES and HEY. Abbreviations; RTK: receptor tyrosine kinase; PI3K: phosphatidylinositol 3-kinase; PDK1: phosphoinositide dependent protein kinase 1; PTEN: phosphatase and tensin homolog; mTOR: mammalian target of rapamycin; TSC: tuberous sclerosis complex; mLST8: mammalian lethal with sec 13 protein 8; PRAS40: prolin-rich AKT substrate 40 kDa; IRS-1: insulin receptor substrate-1; VHL: von Hippel-Lindau; HIF: hypoxia inducible factor; TCF: T cell factor; HGF: hepatocyte growth factor; CSL: CBF1, Suppressor of hairless, Lag-1; HES: hairy enhancer of split; Hey: hairy enhancer of split related with YRPW. Inhibitory arrows (\dashv) show clinically available or in development therapeutic targets for the treatment of RCC and mRCC.

mTOR inhibitors were originally developed as immunosuppressants for patients undergoing transplantation with rapamycin (also known as sirolimus or Rapamune®) being the first mTOR inhibitor identified. Clinical experience and subsequent trials identified the anti-proliferative (Schmelzle & Hall, 2000) and anti-angiogenic (Del Bufalo et al., 2006) properties of these agents in various cancer types, including RCC. This is of particular clinical importance as RCC demonstrates significant uncontrolled angiogenesis. More specifically mTORC1 activity is inhibited by rapamycin and associated analogs (temsirolimus, everolimus and ridaforolimus) which are collectively termed rapalogs. mTORC2, however, is largely insensitive to rapalogs, although prolonged treatment may be able to reduce mTORC2 activity in some cell types (Sarbasov et al., 2006).

6.1.1 mTOR inhibitors-rapamycin

Rapamycin is a naturally occurring macrolide triene antibiotic that acts as a specific, allosteric inhibitor of mTORC1 (Hay & Sonenberg, 2004). Rapamycin either associates with the immunophilin FKBP12 (FK 506-binding protein of 12 kDa) and the resulting complex interacts with the FRB (FKBP12-rapamycin binding) domain located in the C-terminus of mTOR or directly to FRB. This binding prevents the binding of mTORC1 to raptor which is thought to uncouple it from its substrates 4E-BPs and S6Ks (Oshiro et al., 2004). The ability of rapamycin to suppress both cellular proliferation and growth through its interaction with mTORC1 indicated that it could be used as an anti-cancer agent (Faivre et al., 2006). This led to the development of rapamycin analogs (rapalogs) which display the same pharmacodynamics as the parent drug but have improved pharmacokinetic properties.

6.1.2 Temsirolimus

Temsirolimus (Torisel®), also known as CCI-779, is a macrocyclic lactone and a water-soluble ester prodrug of rapamycin. It is administered by i.v. injection, is rapidly cleared from the plasma and is converted by CYP4503A4/5 into rapamycin. It binds with high affinity to the immunophilin FKBP12 and selectively inhibits mTORC1 with no effect on mTORC2 (Le Tourneau et al., 2008). Inhibition of mTORC1 kinase activity results in decreased phosphorylation of S6K and 4E-BP1. In addition by inhibiting mTORC1 it has been shown to reduce expression of HIF-1 α and -2 α which leads to decreased VEGF and PDGF expression (Thomas et al., 2006). Thus, the clinical efficacy of temsirolimus reflects bimodal pharmacodynamics resulting in null signalling of RTK cascades and inhibition of protein synthesis can result in inhibition of cell cycle and tumourigenesis. Temsirolimus was approved as first-line therapy for patients with mRCC in the US and Europe in May 2007 demonstrating improved efficacy in poor-prognosis patients in comparison with IFN- α (Hudes et al., 2009). The efficacy of temsirolimus in the second-line setting remains unclear. However, recently it has demonstrated disease control rate of 70% and overall median time to progression of four months in intermediate to poor-prognosis patients with VEGF-refractory mRCC (Mackenzie et al., 2011). Side effects of the drug include diarrhoea, asthenia stomatitis, rash, nausea, anorexia, hypertension, dyspnea, hyperglycaemia, hypercholesterolemia and anemia.

6.1.3 Temsirolimus plus immunotherapy combination

Temsirolimus was first investigated as combination therapy with IFN- α in phase I/II study (Motzer et al., 2007b). This study revealed that the combination of the two had an accepted

safety profile and displayed anti-tumour activity in patients with mRCC. A pivotal phase III trial was also carried out comparing temsirolimus or temsirolimus plus IFN- α with IFN- α alone in patients with mRCC. In summary, the median OS time was significantly longer with temsirolimus alone than with IFN- α alone (10.9 months versus 7.3 months, respectively), and combination therapy with temsirolimus and IFN- α did not lead to a significantly longer median OS time than with IFN- α alone (8.4 months versus 7.3 months, respectively) (Hudes et al., 2007).

6.1.4 Temsirolimus plus anti-angiogenics combination

Phase I studies examining the efficacy of temsirolimus with sunitinib have not shown sufficient safety to-date. Trials using temsirolimus in combination with sunitinib and temsirolimus in combination with sorafenib were discontinued owing to significant toxicity (Patel et al., 2009). The efficacy of temsirolimus plus bevacizumab has also been studied but again based on toxicity profiles a phase II trial has indicated that this combination cannot be recommended for patients with mRCC (Negrier et al., 2011). In summary, the combined usage of temsirolimus and anti-angiogenic agents has proved disappointing to date, phase III trials are still continuing whose results may shed light on possible best practice for combination therapy in the near future.

6.2 Everolimus

Everolimus (Afinitor®) is an orally bioavailable hydroxyethyl ester of rapamycin. Like temsirolimus it is an inhibitor of mTORC1 and was approved on March 30th, 2009 for patients suffering from advanced RCC following failure when treated with previous TKI therapy (de Reijke et al., 2009). It has now become the standard second-line agent after the approved first-line drugs sunitinib and/or sorafenib (Soulieres, 2009).

6.2.1 Everolimus plus anti-angiogenics combination

The combination of everolimus and the VEGFR TKIs are showing promise in initial studies. A phase II study of everolimus plus sorafenib has been prompted following successful completion of a phase I trial with the combination of both demonstrating acceptable toxicity and evidence of anti-tumour activity in patients with previously untreated mRCC (Harzstark et al., 2011). Similarly, a phase II trial of everolimus plus sunitinib is warranted following successful maximum-tolerated dose of everolimus plus sunitinib in patients with mRCC (Kroog et al., 2009). In contrast, everolimus plus imatinib is not recommended for future studies following results from a phase II study in previously treated patients with mRCC as the combination did not demonstrate a three month PFS rate of 49%, which did not meet the specified criteria for continuation (Ryan et al., 2011). Finally, in a phase II trial with two different mRCC patient cohorts, one with and one without prior TKI treatment, everolimus plus bevacizumab was active and well tolerated (Hainsworth et al., 2010). This regimen which uses full doses of each agent, is being evaluated as first-line therapy in a phase II study, RECORD (Renal Cell Cancer Treatment With Oral RAD 001 Given Daily)-2.

6.3 Ridaforolimus

The mTOR inhibitor, ridaforolimus (formerly deforolimus), is yet another promising rapamycin analog in RCC treatment but not yet approved. Ridaforolimus (also known as AP23573), a non-prodrug of rapamycin, has demonstrated prominent anti-proliferative

activity against a range of cancers (Hartford et al., 2009). The most common side effects associated with ridaforolimus to-date include stomatitis, fatigue, diarrhoea and thrombocytopenia. Important additional information such as OS and the safety profile of ridaforolimus has yet to be identified.

6.4 Combination therapy

At present there are numerous ongoing and planned studies evaluating the efficacy of both temsirolimus and everolimus with other targeted therapies including VEGF ligand competitors, VEGFR inhibitors, AKT inhibitors, p70S6R inhibitors, tubulin inhibitors, IGF-1R antagonists and Bcr-ABL antagonists (Pal & Figlin, 2011). Information pertaining to the successes associated with these exploratory trials is limited at present.

6.5 New mTOR inhibitors

Presently, temsirolimus and everolimus are approved for the treatment of mRCC. Despite their efficacy there are some drawbacks including resistance but also the fact that they are both specific mTORC1 inhibitors that lack activity against mTORC2. This allows the latter to activate AKT. Indeed, increased activation i.e. phosphorylation of AKT has been documented in tumour biopsies isolated from patients treated with rapalogs (O'Reilly et al., 2006). In addition the crosstalk with other pathways such as MEK/ERK on AKT could limit the efficacy of mTOR inhibitors. There are reports of newer drugs targeting mTORC2 as well as MAPK interacting pathways. New mTOR inhibitors are not rapalogs but are small molecule inhibitors resembling TKIs. They bind competitively and reversibly to the mTOR-ATP binding pocket blocking the enzymatic activity of the kinase. Compounds such as PP242, Torin1, WYE-354, WYE-125132 (WYE-132) and Ku-006379 suppress both mTORC1 and mTORC2 displaying more dramatic effects on cell growth, proliferation and cell cycle than rapamycin. This has been attributed to suppression of mTORC2 mediated AKT phosphorylation at Ser 473 and greater inhibition of 4E-BP1 phosphorylation (Thoreen et al., 2009). Active site mTOR inhibitors have the potential to be potent anti-cancer drugs as they inhibit mTORC2 activity which rapamycin and its analogs do not but also because they counteract the activation of AKT which can occur as a result of rapamycin-mediated disruption of the mTOR/S6K/IRS-1 negative feedback loop. To-date these potentially effective cancer therapeutic agents have yet to be investigated in patients with RCC or mRCC.

7. Targeting mTOR upstream moieties – PI3K

PI3K is a lipid kinase that converts phosphatidylinositol bisphosphate to PIP3. PI3K further recruits PDK1 and AKT to the cell membrane where PDK1 activates AKT. Because of its location upstream of mTOR, it has become another attractive target for treatment of patients with RCC to be used solely or in combination with existing mTOR inhibitors. Recently, activation of the PI3K pathway has been shown to be directly linked to adverse clinical outcomes in patients with RCC (Merseburger et al., 2008). The PI3K inhibitor prototypes wortmannin and LY294002 have been shown to decrease AKT activation and significantly reduce cell growth *in vitro* particularly in PTEN-null or PI3K-overexpressing RCCs with the latter also demonstrating *in vivo* tumour regression (Soubrier et al., 2006). Given that PI3K is highly expressed in RCC metastases, which are themselves radioresistant, newer generation PI3K inhibitors such as PX-866, with better bioavailability and less toxicity, may show utility

as radiosensitizers in RCC metastases. Another chemotherapeutic drug, PI-103, has recently been shown to independently inhibit both PI3K α and mTOR (Fan et al., 2006) thereby overcoming a potential disadvantage of rapamycin in the treatment of AKT-dependent tumors. In fact GDC-0941 which is derived from PI-103 has demonstrated improved bioavailability and partial response in breast and ovarian cancer patients. Ongoing studies using PI3K and dual PI3K/mTOR inhibitors such as SAR245408, SAR245408, NVP-BKM120 and NVP-BE235 modified for clinical use are ongoing (Maira et al., 2008). These have yet to be tested in patients with RCC.

7.1 PDK1

Similar to PI3K, a key mediator of AKT activation, PDK1 is poised to respond to targeted inhibition with blockade of AKT signalling (Figure 2). Both highly specific inhibitors, such as AR-12 (Arno), and inhibitors with dual function on PDK1/PI3K or PDK1/AKT are in development (Najafov et al., 2010). These targets present another potentially robust way to render the AKT pathway completely inhibited, mitigating the confounding issues of inhibition of each of the AKT family members.

7.2 AKT

AKT, also known as protein kinase B (PKB), can be activated by a number of mechanisms including PIP3 activation of PDK1 at Thr308 and at Ser473 by mTORC2 (Figure 2). Decreased expression of the inhibitory PTEN can also activate AKT (Hara et al., 2005). Upon phosphorylation (p-)AKT is known to interact with a large set of substrates, including mTOR and through inactivation of the TSC impacts many key cellular processes such as cell cycle progression and apoptosis, both of which play a vital role in oncogenesis. Recently, p-AKT expression was shown to be correlated with pathologic variables and survival, with higher levels of cytoplasmic p-AKT expression compared with nuclear p-AKT in primary RCC (Pantuck et al., 2007). Recently, a specific p-AKT (S473) inhibitor, WYE-132, has been tested on RCC cell lines and achieved complete regression of A498 large tumours when administered with bevacizumab (Yu et al., 2010).

8. Targeting downstream moieties-HIF-1 α

RCC is closely linked to mutations in the von Hippel-Lindau (*VHL*) gene. A deletion of one allele of *VHL* has been identified in >90% of patients with sporadic clear cell RCC (Gnarra et al., 1994). The remaining *VHL* allele is also commonly inactivated by a deletion event or altered methylation (Nickerson et al., 2008). In normal cell conditions, the VHL protein is a direct inhibitor of the activity of a key regulator of responses to hypoxia i.e. HIF. HIFs are heterodimers and contain an α and a β subunit. VHL targets the HIF- α isoform for proteasomal degradation. This prevents it from translocating to the nucleus and binding to HIF- β which would result in the induction of over 200 target genes that contain hypoxia-response elements in their promoters. The best described of the numerous HIF targets are growth factors which promote angiogenesis and proliferation (Figures 1 and 2). Under hypoxic conditions, VHL itself is degraded. This stabilizes HIF- α within the cell and allows it to accumulate in the nucleus. Here it initiates the expression of genes which promote cell survival and growth. The effects of biallelic inactivation of the *VHL* gene in clear cell RCC cells mirror those which result from VHL degradation in response to hypoxia. Expression of HIF targets such as VEGF, PDGF, and TGF- β are upregulated.

The *VHL* gene product, pVHL, is an E3 ubiquitin ligase that promotes the proteasomal degradation of HIF-1 α , -2 α and -3 α . Consequently, renal carcinomas with mutations in *VHL* have high steady-state levels of HIF expression. Functional studies show that HIF is sufficient for transformation caused by loss of *VHL*, thereby establishing HIF as the primary oncogenic driver in kidney cancers (Maranchie et al., 2002). mTOR increases the translation of HIF-1 and HIF-2 which in turn can drive the expression of angiogenic factors such as VEGF, PDGF- β , bFGF and TGF- α . Thus, much interest has recently focused on targeting one or both HIF factor signals for cancer therapy. EZN-2968 is an RNA antagonist that specifically binds and inhibits HIF-1 α mRNA *in vitro* and *in vivo* (Greenberger et al., 2008). In this study it proved to be a potent, selective, and durable antagonist of HIF-1 mRNA and protein expression resulting in reduced prostate and glioblastoma tumor cell growth. Its efficacy in RCC has not yet been investigated. In contrast, targeting heat shock protein 90 (HSP90) with 17-dimethylaminoethylamino-17-demethoxygeldanamycin (17-DMAG) which reduces levels of HIF-1 α in the setting of *VHL* loss has shown promising results in clinical trials including patients with RCC (Kummar et al., 2010; Ronnen et al., 2006). Furthermore, YC-1, 3-(5'-hydroxymethyl-2'-furyl)-1-benzylindazole (an agent originally developed for circulatory disorders) and YC-1 analogs, 1, 3-disubstituted selenolo[3,2-c]pyrazole derivatives have now been found to repress HIF-1 activity and inhibit renal cancer tumour growth (Chou et al., 2010). Lastly, PX-478 (S-2-amino-3-[4'-N,N-bis(2-chloroethyl)amino]phenyl propionic acid N-oxide dihydrochloride) an inhibitor of constitutive and hypoxia-induced HIF-1 α levels and thus HIF-1 activity has proven efficacy *in vitro* with different RCC cell lines (Koh et al., 2008).

8.1 HIF-2 α

HIF-2 α , also referred to as endothelial PAS domain protein 1 shares 48% homology with HIF-1 α . Current knowledge pertaining to the regulation of HIF-2 α is somewhat lacking when compared with HIF-1 α . However, the tumourigenic role of HIF-2 α has been studied most extensively in RCC. Both *in vitro* and *in vivo* studies with human kidney tumours suggest that HIF-2 α is more oncogenic than HIF-1 α (Maranchie et al., 2002; Raval et al., 2005). RCC tumours express either HIF-1 α and HIF-2 α or HIF-2 α alone, leaving HIF-2 α expression as a common point of *VHL* mutated cancers. Moreover, consistent with this data, HIF-1 α expression has been shown to decrease in advanced lesions as HIF-2 α expression increases (Mandriota et al., 2002). Resulting from these observations HIF-2 α is now being studied as the more important isoform for therapeutic intervention of RCC. Although several potentially important drugs targeting HIF-1 α have been described (as outlined above) reports of HIF-2 α are few. One potentially effective drug that needs further investigation is emetine, a protein synthesis inhibitor that blocks the translocation of peptidyl-tRNA from the acceptor site to the donor site on the ribosome. Emetine is not a novel drug (in fact it has been around for almost a century) but has been used for the treatment of bacterial, viral and amoeba *Entamoeba histolytica* infections as well as being used as an antiemetic (Zhou et al., 2005). It has been shown to induce HIF-2 α downregulation in the setting of *VHL* loss in RCC cell lines. Further analysis of this drug is necessary for its efficacy in the *in vivo* setting of RCC.

9. HIF targets-Ror2

Regulated receptor tyrosine kinase-like orphan receptor 2 (Ror2) is a member of a family of orphan RTKs. Ror2 is found heavily phosphorylated in the kidney of RCC patients and is

expressed highly in human RCC cell lines indicating a role for Ror2 in the pathology of RCC (Wright et al., 2009). In fact suppressed expression of Ror2 results in reduced expression of matrix metalloproteinase (MMP)-2, whose upregulation correlates with advanced stages of RCCs (Slaton et al., 2001). Thus, Ror2 represents a promising therapeutic target for patients with RCC. Although the direct target of Ror2 kinase activity has yet to be deciphered, it does appear to act as a mediator of Wnt signals in the further activation of tumour cell signalling events (Figure 2). There are currently no clinically available drugs targeting Ror2 for the treatment of RCC.

9.1 Carbonic anhydrase IX

Carbonic anhydrase IX (CAIX), a hypoxia-induced protein, is unique in that it is a cell surface protein that is present in human tumours but absent from normal tissue (Figure 2). It is found to be highly expressed in clear cell RCC and is associated with grade (Genega et al., 2010). Currently, CAIX is being pursued as a prognostic indicator, diagnostic tool and a future potential targeted therapy for the treatment of RCC. Presently, there exists a chimeric antibody (cG250) used for its localisation, but also for direct antibody-dependent cellular cytotoxicity (ADCC). Thus, it has progressed through phase 1 (Davis et al., 2007), phase 2 (Bleumer et al., 2004), and is presently undergoing a phase 3 trial (NCT00087022) in patients with RCC. In addition, cG250 accumulation in RCC lesions is extremely high and so is being investigated as a strategy to deliver tumour-sterilising radiation doses with cG250 as a carrier molecule (Divgi et al., 2004). Furthermore, preliminary research with dendritic cells loaded with CAIX-derived peptides have shown to activate the cellular and humoral immune system in patients with cytokine refractory RCC (Uemura et al., 2006). Large prospective trials, however, are required to establish dendritic cell vaccination with CAIX-derived peptides or indeed direct vaccination with these peptides.

9.2 Angiopoietins and Tie-2

Angiopoietin/Tie-2 signalling pathways are important together with VEGF/VEGFR in the process of vascular endothelial growth for angiogenesis (Figure 1). Due to the highly vascular nature of RCC identifying new anti-angiogenic agents is highly desirable in an effort to try and treat this largely refractory cancer. One such target is Tie-2, an endothelium-specific tyrosine kinase, which serves as a receptor for the family of angiopoietin ligands, angiopoietin-1 (Ang-1) and angiopoietin-2 (Ang-2), pro-angiogenic targets of HIF transcriptional activity. Binding of the former induces autophosphorylation of Tie-2, the latter antagonizes the actions of Ang-1 by competitively binding to Tie-2 without activating it. Ang-1 plays an important role in the assembly of newly formed vasculature and in the maintenance of vascular integrity. The role of Ang-2 in angiogenesis is highly dependent on the presence of other angiogenic factors, particularly VEGF. Tie-2 expression has been shown to correlate with angiopoietin-2 expression in RCC tumours (Liu et al., 2008).

Development of therapeutic drugs targeting the Angiopoietin/Tie-2 pathway differ somewhat. They may be direct inhibitors of the tyrosine kinase i.e. to target Tie-2, selective and non-selective traps to target Ang-1 or -2, or systemic delivery of angiopoietins to induce their anti-tumour effects (Huang et al., 2010). Tie-2 kinase inhibitors include CEP-11981 and CE-245677, the former is currently being evaluated in an open label phase 1 trial in patients with advanced solid tumours. The latter tested in a phase I trial has been discontinued owing to unacceptable side effects. There are currently two angiopoietin traps in clinical

development. AMG-386 is an anti-angiopoietin peptibody which inhibits the interaction between ligands Ang-1 and -2 with the Tie-2 receptor. It is currently undergoing phase II trials in combination with sorafenib and sunitinib for the treatment of RCC (Huang et al., 2010). The second compound PF-4856884 (also known as CVX-060) selectively targets Ang-2 and in a phase I study demonstrated a significant reduction in RCC tumour blood flow. The mild side effect profile of both of these drugs provides an attractive basis for their combination with other anti-angiogenic or chemotherapeutic agents.

9.3 Notch

Notch signalling controls a variety of processes, involving cell fate specification, differentiation, proliferation, and survival (Artavanis-Tsakonas et al., 1999). Mammals have four Notch proteins, namely Notch 1-4, that function as receptors for five Notch ligands – Jagged1 and 2, and the delta-like ligands (DLL)-1, -3 and -4. Ligand binding leads to at least three subsequent proteolytic cleavages that release the intracellular domain (ICD) of Notch. Notch ICD subsequently translocates into the nucleus, where it forms a complex with essential cofactors such as c-promoter binding factor 1 (CBF1), mastermind-like 1 (MAML1) and the transcription factor CSL. This complex mediates the transcription of target genes such as that encoding Deltex, genes in the hairy enhancer of split (HES) and HES-related families of basic helix-loop-helix transcription factors, and others (Figure 2). Aberrant signalling within this pathway has previously been reported in multiple malignancies (Miele et al., 2006) including RCC with elevated Notch 1, 3 and Jagged-1 mRNAs (Rae et al., 2000; Sjolund et al., 2008). Elevated expression of DLL-4 has also been reported in RCCs with reduction of such basal expression having considerable effects on endothelial function important in tumour angiogenesis (Patel et al., 2005). Interestingly, Notch signalling can lead to either tumour progression or suppression depending on the cellular context (Nicolas et al., 2003, Xia et al., 2001). However, in the context of RCC, Notch signalling inhibition has led to inhibition of RCC growth thus indicating a potential novel therapeutic pathway in RCC. Presently, there is strong evidence for signalling crosstalk between Notch and HIF-1 α . Cleaved Notch ICD and HIF-1 α appear to play an important point between the two signalling cascades (Gustafsson et al., 2005). Moreover, there is recent evidence to support Notch signalling linking AKT and hypoxia in melanomas (Bedogni et al., 2008). Whether this interaction is pertinent to RCC has yet to be investigated. Inhibition of Notch signalling as a strategy for cancer treatment has been proposed in numerous studies (Nickoloff et al., 2003). Two approaches have been identified; selective strategies involving antisense, mAbs and RNA interference; nonselective strategies involving soluble or cell-associated Notch decoys, γ -secretase inhibitors, intracellular MAML1 decoys and Ras signalling inhibitors (Miele et al., 2006). Currently it is too early to evaluate the true efficacy of these strategies and of the different drugs involved but what is known from present findings is that Notch inhibition in cancer deserves a thorough investigation including in patients with RCC.

9.4 Wnt/ β -catenin signalling

Wnts are a family of secreted glycoproteins that regulate a wide range of cellular functions such as growth, differentiation, migration and polarity (Moon et al., 2004). Wnt signalling is controlled by the transcriptional coactivator β -catenin, which is emerging as a key molecule in the pathogenesis of renal cancer. In normal quiescent cells, β -catenin is bound to casein kinase 1, glycogen synthase kinase 3 β (GSK3), adenomatosis polyposis coli protein and axin. This complex controls β -catenin phosphorylation targeting it for proteosomal degradation.

Wnt positively regulates β -catenin, preventing its phosphorylation, ubiquitination and degradation. Thus, upon Wnt pathway activation hypophosphorylated β -catenin translocates into the nucleus and forms a complex with the DNA binding protein T cell factor (TCF) (Figure 2). The β -catenin/TCF complex activates transcription of a wide range of genes including growth promoting genes such as VEGF (Easwaran et al., 2003) as well as the *MYC* oncogene which shows copy number amplification in RCC (Beroukhi et al., 2009). Wnt can also mediate its effect on cell growth and tumour promotion by activating the mTOR pathway (Inoki et al., 2006). TSC2 is phosphorylated by GSK3 for its activation and subsequent inhibition of mTOR. Wnt activates mTOR pathway by inhibiting GSK3. There are several papers outlining the involvement of Wnt signalling in RCC. Overexpression of β -catenin can induce renal tumours in mice (Sansom et al., 2005). In some RCC tumours the *APC* gene promoter is aberrantly hypermethylated providing a mechanism by which β -catenin is liberated (Battagli et al., 2003). β -catenin is also degraded by the E3-ubiquitin ligase activity of VHL and so loss of VHL in RCC has been shown to enable HGF-driven oncogenic β -catenin signalling (Peruzzi et al., 2006). In a recent article further evidence for the activation of Wnt signalling in RCC was outlined when a deletion of *CXXC4* a gene coding for Idax, an inhibitor of this pathway, was identified in aggressive RCC (Kojima et al., 2009). In addition, various Wnt antagonists such as secreted-Frizzled receptor proteins, Dickkopf 2 and Wnt inhibitory factor 1 were found to be hypermethylated and thus silenced in RCC (Awakura et al., 2008; Hirata et al., 2009; Kawakami et al., 2009). It is also possible that loss of *VHL* could lead to the combined de-repression of HIFs and β -catenin which could also lead to RCC (Linehan et al., 2009). Finally, Jade-1 (gene for apoptosis and differentiation in epithelia) has been identified as a *VHL*-interacting protein which brings about β -catenin degradation. Thus, Jade-1 is thought to function as a renal tumour suppressor (Chitalia et al., 2008). Loss of *VHL* can bring about a reduction in Jade-1 levels with subsequent increases in β -catenin levels, providing another caveat by which loss of *VHL* can promote renal tumourigenesis. In summary Wnt signalling has a dual role in the pathogenesis of RCC. It induces transcription through activation of β -catenin but also activates mTOR signalling driving cellular growth. Thus, Wnt signalling and β -catenin provide attractive targets for therapeutic intervention in RCC. At present there are no clinically available drugs targeting this pathway in RCC but may become available in the near future.

10. HGF/MET signalling

Kidney tissue is an abundant source of hepatocyte growth factor (HGF) a stromal cell-derived cytokine involved in cell proliferation, tissue regeneration, tumour growth and tumour invasion through the HGF/scatter factor (SF):c-MET pathway (Cantley et al., 1994). HGF binding to MET leads to its phosphorylation and subsequent recruitment of adapter proteins such as Gab1, Gab2, SHC, STAT3 and PI3K with downstream activation of Ras/MAPK and PI3K/AKT pathways (Figure 2) resulting in RCC growth and metastasis (Eder et al., 2009). Different studies have shown that HGF and its receptor c-MET are overexpressed in RCC and play a significant role in the progression of RCC (Horie et al., 1999; Natali et al., 1996). Moreover, *VHL*-negative RCC cells exhibit cell invasion and branching morphogenesis in response to HGF (Koochekpour et al., 1999). c-MET has also been shown to be constitutively phosphorylated in RCC and high levels of serum HGF/SF in RCC patients are associated with

reduced survival (Tanimoto et al., 2008). Presently, MET is being targeted in clinical trials for the treatment of RCC (Giubellino et al., 2009). Strategies involve preventing c-MET autophosphorylation; prevention of HGF binding to c-MET and lastly targeting the signalling cascade of activated c-MET (Toschi & Janne, 2008). One such investigational drug is AMG 102, a fully human mAb that blocks HGF/SF binding to c-MET and blocks signalling events driving tumour proliferation, migration, invasion and survival (Figure 2). Reports of a phase II trial with AMG 102 identified that although the drug brought about tumour burden reduction and long-term disease stability, it was unclear from the study whether this drug is capable of tumour growth inhibition in a histologically diverse population of patients with mRCC (Schoffski et al., 2010). Other drugs currently in development include foretinib (GSK1363089) an oral multi kinase inhibitor of MET and VEGFRs (Kataoka et al., 2011), ARQ 197, a selective non-ATP competitive inhibitor of MET (Adjei et al., 2011) and a range of orally available c-MET kinase inhibitors namely (R)-3-[1-(2,6-dichloro-3-fluoro-phenyl)-ethoxy]-5-(1-piperidin-4-yl-1H-pyrazol-4-yl)-pyridin-2-ylamine (PF02341066) and 2-[4-(3-quinolin-6-ylmethyl-3H-[1,2,3]triazolo[4,5-b]pyrazin-5-yl)-pyrazol-1-yl]-ethanol (PF04217903) (Yamazaki et al., 2011). The efficacy of these drugs have yet to be investigated in patients with RCC. Thus, further investigations of these potentially effective therapeutic drugs is warranted at this time.

11. Conclusions and future directions

RCC is similar to other cancer types in that it is asymptomatic initially with a lack of early warning signs. This results in a high percentage of patients presenting with metastasis at diagnosis or indeed relapse following nephrectomy. RCC is also known for its unpredictable clinical behaviour. Historically RCC and mRCC has been associated with treatment resistance and poor prognosis. However, with ever increasing knowledge of angiogenesis and aberrant signalling pathways in patients with RCC recent basic and clinical developments has exerted a substantial impact on outcomes for patients with mRCC.

Throughout the past fifteen years there has been an increased understanding of the tumour biology of RCC. There is now a myriad of treatment options available making the treatment of RCC and mRCC immensely complex. Sequential therapy with targeted agents is currently the standard of care while combination therapies are still under active investigation. Combination therapies can provide additive or synergistic effects resulting from more complete blockade of the many aberrant signalling cascades outlined above. This approach can also prevent or delay the development of resistance that would eventually arise with single-agent therapy owing to signalling pathway redundancy. Despite recent advancements, however, current chemotherapeutics can only increase the overall survival of patients from weeks to months and unfortunately cannot cure RCC. Combination regimes have many drawbacks and in many instances have not proven beneficial in terms of inferior efficacy and excessive toxicity. It is also clear from the multitude of described and ongoing clinical trials that patient response to targeted agents is not universal. Thus, we have reached the stage where there is compelling need to identify new combinations with the goal of providing maximal efficacy with manageable toxicity. Increased knowledge of mechanisms of disease, drug resistance, new targets and new targeted agents may eventually provide optimal strategies for patients with RCC and mRCC.

Another area of note to improve the treatment of patients with RCC and mRCC is the identification of genetic and epigenetic markers as promising biomarkers (Pal et al., 2010; Vickers & Heng 2010). This may indicate the suitability of a patient to treatment with one

agent above another and also the optimal sequential or combination of therapies. Many RCC biomarkers have been examined over the past decade and include *VHL* gene mutation, plasma VEGF, tissue and plasma VEGFRs, tissue HIF and tissue and serum CAIX as outlined already in this report. Others include B7-H1 a cell surface glycoprotein that acts as a negative regulator of anti-tumoural T cell-mediated immunity and whose high levels of expression in patients with RCC has been associated with shorter survival (Vickers & Heng, 2010). Another prognostic biomarker includes neutrophil gelatinase-associated lipocalin (NGAL). NGAL is elevated in a number of cancers and has been linked to MMP-9, which is involved in the degradation of the extracellular matrix and therefore invasion and metastasis. Thus, lower levels of NGAL is associated with longer PFS in RCC patients (Vickers & Heng, 2010). Despite growing research in this area, however, there are currently no biomarkers used in the clinical management of patients with RCC. Future studies such as the NIH funded Cancer Genome Atlas project may provide further insight into the genome, mRNA and micro RNA transcriptome and methylome of RCC revealing the pathways and networking that is aberrant in RCC and thus aid in the identification of new biomarkers and therapeutic agents. Furthermore, the use of increasingly sophisticated integrative multivariate models which incorporate both molecular and genetic information will ultimately aid in the development of curative, non-toxic personalised therapies. Thus, research is ongoing and newer improved technologies hold promise in the expansion of our knowledge of pathogenesis and determinants of outcome. In summary, in the future researchers and clinicians alike will have to unite and develop a workable cohesive strategy to optimise use of available agents as well as those undergoing clinical trials and identify optimal strategies for the successful treatment of patients with RCC.

12. References

- Adjei, A. A., Schwartz, B. & Garmey, E. (2011). Early Clinical Development of ARQ 197, a Selective, Non-ATP-Competitive Inhibitor Targeting MET Tyrosine Kinase for the Treatment of Advanced Cancers. *Oncologist*, ISSN 1549-490X (Electronic)
- Angevin, E., Grünwald, V., Ravaud, A., Castellano, D. E., Lin, C., Gschwend, J. E., Harzstark, A. L., Chang, J., Wang, Y., Shi, M. M., Escudier, B. J. (2011). A phase II study of dovitinib (TKI258), an FGFR- and VEGFR-inhibitor, in patients with advanced or metastatic renal cell cancer (mRCC). *J Clin Oncol*, Vol. 29, suppl; abstr 4551,
- Antoun, S., Birdsell, L., Sawyer, M. B., Venner, P., Escudier, B. & Baracos, V. E. (2010). Association of skeletal muscle wasting with treatment with sorafenib in patients with advanced renal cell carcinoma: results from a placebo-controlled study. *J Clin Oncol*, Vol. 28, No. 6, pp. 1054-1060, ISSN 1527-7755 (Electronic)
- Artavanis-Tsakonas, S., Rand, M. D. & Lake, R. J. (1999). Notch signaling: cell fate control and signal integration in development. *Science*, Vol. 284, No. 5415, pp. 770-776, ISSN 0036-8075 (Print)
- Awakura, Y., Nakamura, E., Ito, N., Kamoto, T. & Ogawa, O. (2008). Methylation-associated silencing of SFRP1 in renal cell carcinoma. *Oncol Rep*, Vol. 20, No. 5, pp. 1257-1263, ISSN 1021-335X (Print)

- Battagli, C., Uzzo, R. G., Dulaimi, E., Ibanez de Caceres, I., Krassenstein, R., Al-Saleem, T., Greenberg, R. E. & Cairns, P. (2003). Promoter hypermethylation of tumor suppressor genes in urine from kidney cancer patients. *Cancer Res*, Vol. 63, No. 24, pp. 8695-8699, ISSN 0008-5472 (Print)
- Bedogni, B., Warneke, J. A., Nickoloff, B. J., Giaccia, A. J. & Powell, M. B. (2008). Notch1 is an effector of Akt and hypoxia in melanoma development. *J Clin Invest*, Vol. 118, No. 11, pp. 3660-3670, ISSN 0021-9738 (Print)
- Beroukhi, R., Brunet, J. P., Di Napoli, A., Mertz, K. D., Seeley, A., Pires, M. M., Linhart, D., Worrell, R. A., Moch, H., Rubin, M. A., Sellers, W. R., Meyerson, M., Linehan, W. M., Kaelin, W. G., Jr. & Signoretti, S. (2009). Patterns of gene expression and copy-number alterations in von-hippel lindau disease-associated and sporadic clear cell carcinoma of the kidney. *Cancer Res*, Vol. 69, No. 11, pp. 4674-4681, ISSN 1538-7445 (Electronic)
- Bhargava, P., Esteves, B., Al-Adhami, M., Nosov, D., Lipatov, O. N., Lyulko, A. A., Anischenko, A. A., Chacko, R. T., Doval, D. & Slichenmyer, W. J. (2010). Activity of tivozanib (AV-951) in patients with renal cell carcinoma (RCC): Subgroup analysis from a phase II randomized discontinuation trial (RDT). *ASCO Meeting Abstracts*, Vol. 28, No. 15_suppl, pp. 4599
- Bhargava, P. & Robinson, M. O. (2011). Development of second-generation VEGFR tyrosine kinase inhibitors: current status. *Curr Oncol Rep*, Vol. 13, No. 2, pp. 103-111, ISSN 1534-6269 (Electronic)
- Bleumer, I., Knuth, A., Oosterwijk, E., Hofmann, R., Varga, Z., Lamers, C., Kruit, W., Melchior, S., Mala, C., Ullrich, S., De Mulder, P., Mulders, P. F. & Beck, J. (2004). A phase II trial of chimeric monoclonal antibody G250 for advanced renal cell carcinoma patients. *Br J Cancer*, Vol. 90, No. 5, pp. 985-990, ISSN 0007-0920 (Print)
- Bukowski, R. M., Kabbinavar, F. F., Figlin, R. A., Flaherty, K., Srinivas, S., Vaishampayan, U., Drabkin, H. A., Dutcher, J., Ryba, S., Xia, Q., Scappaticci, F. A. & McDermott, D. (2007). Randomized phase II study of erlotinib combined with bevacizumab compared with bevacizumab alone in metastatic renal cell cancer. *J Clin Oncol*, Vol. 25, No. 29, pp. 4536-4541, ISSN 1527-7755 (Electronic)
- Cantley, L. G., Barros, E. J., Gandhi, M., Rauchman, M. & Nigam, S. K. (1994). Regulation of mitogenesis, motogenesis, and tubulogenesis by hepatocyte growth factor in renal collecting duct cells. *Am J Physiol*, Vol. 267, No. 2 Pt 2, pp. F271-280, 0002-9513 (Print)
- Carracedo, A. & Pandolfi, P. P. (2008). The PTEN-PI3K pathway: of feedbacks and cross-talks. *Oncogene*, Vol. 27, No. 41, pp. 5527-5541, ISSN 1476-5594 (Electronic)
- Casanovas, O., Hicklin, D. J., Bergers, G. & Hanahan, D. (2005). Drug resistance by evasion of antiangiogenic targeting of VEGF signaling in late-stage pancreatic islet tumors. *Cancer Cell*, Vol. 8, No. 4, pp. 299-309, 1535-6108 (Print)
- Chitalia, V. C., Foy, R. L., Bachschmid, M. M., Zeng, L., Panchenko, M. V., Zhou, M. I., Bharti, A., Seldin, D. C., Lecker, S. H., Dominguez, I. & Cohen, H. T. (2008). Jade-1 inhibits Wnt signalling by ubiquitylating beta-catenin and mediates Wnt pathway inhibition by pVHL. *Nat Cell Biol*, Vol. 10, No. 10, pp. 1208-1216, ISSN 1476-4679 (Electronic)

- Chou, L. C., Huang, L. J., Hsu, M. H., Fang, M. C., Yang, J. S., Zhuang, S. H., Lin, H. Y., Lee, F. Y., Teng, C. M. & Kuo, S. C. (2010). Synthesis of 1-benzyl-3-(5-hydroxymethyl-2-furyl)selenolo[3,2-c]pyrazole derivatives as new anticancer agents. *Eur J Med Chem*, Vol. 45, No. 4, pp. 1395-1402, ISSN 1768-3254 (Electronic)
- Couillard, D. R. & deVere White, R. W. (1993). Surgery of renal cell carcinoma. *Urol Clin North Am*, Vol. 20, No. 2, pp. 263-275, ISSN 0094-0143 (Print)
- Dancey, J. E. (2004). Epidermal growth factor receptor and epidermal growth factor receptor therapies in renal cell carcinoma: do we need a better mouse trap? *J Clin Oncol*, Vol. 22, No. 15, pp. 2975-2977, ISSN 0732-183X (Print)
- Dancey, J. E. (2005). Inhibitors of the mammalian target of rapamycin. *Expert Opin Investig Drugs*, Vol. 14, No. 3, pp. 313-328, ISSN 1744-7658 (Electronic)
- Davis, I. D., Liu, Z., Saunders, W., Lee, F. T., Spirkoska, V., Hopkins, W., Smyth, F. E., Chong, G., Papenfuss, A. T., Chappell, B., Poon, A., Saunderson, T. H., Hoffman, E. W., Old, L. J. & Scott, A. M. (2007). A pilot study of monoclonal antibody cG250 and low dose subcutaneous IL-2 in patients with advanced renal cell carcinoma. *Cancer Immunol*, Vol. 7, No. 14, ISSN 1424-9634 (Electronic)
- de Reijke, T. M., Bellmunt, J., van Poppel, H., Marreaud, S. & Aapro, M. (2009). EORTC-GU group expert opinion on metastatic renal cell cancer. *Eur J Cancer*, Vol. 45, No. 5, pp. 765-773, ISSN 1879-0852 (Electronic)
- Del Bufalo, D., Ciuffreda, L., Trisciuoglio, D., Desideri, M., Cognetti, F., Zupi, G. & Milella, M. (2006). Antiangiogenic potential of the Mammalian target of rapamycin inhibitor temsirolimus. *Cancer Res*, Vol. 66, No. 11, pp. 5549-5554, ISSN 0008-5472 (Print)
- Deprimo, S. E., Bello, C. L., Smeraglia, J., Baum, C. M., Spinella, D., Rini, B. I., Michaelson, M. D. & Motzer, R. J. (2007). Circulating protein biomarkers of pharmacodynamic activity of sunitinib in patients with metastatic renal cell carcinoma: modulation of VEGF and VEGF-related proteins. *J Transl Med*, Vol. 5, No. 32, ISSN 1479-5876 (Electronic)
- Di Lorenzo, G., Carteni, G., Autorino, R., Bruni, G., Tudini, M., Rizzo, M., Aieta, M., Gonnella, A., Rescigno, P., Perdonà, S., Giannarini, G., Pignata, S., Longo, N., Palmieri, G., Imbimbo, C., De Laurentiis, M., Mirone, V., Ficorella, C. & De Placido, S. (2009). Phase II study of sorafenib in patients with sunitinib-refractory metastatic renal cell cancer. *J Clin Oncol*, Vol. 27, No. 27, pp. 4469-4474, ISSN 1527-7755 (Electronic)
- Divgi, C. R., O'Donoghue, J. A., Welt, S., O'Neel, J., Finn, R., Motzer, R. J., Jungbluth, A., Hoffman, E., Ritter, G., Larson, S. M. & Old, L. J. (2004). Phase I clinical trial with fractionated radioimmunotherapy using ¹³¹I-labeled chimeric G250 in metastatic renal cancer. *J Nucl Med*, Vol. 45, No. 8, pp. 1412-1421, ISSN 0161-5505 (Print)
- Dowling, R. J., Topisirovic, I., Fonseca, B. D. & Sonenberg, N. (2010). Dissecting the role of mTOR: lessons from mTOR inhibitors. *Biochim Biophys Acta*, Vol. 1804, No. 3, pp. 433-439, ISSN 0006-3002 (Print)
- Easwaran, V., Lee, S. H., Inge, L., Guo, L., Goldbeck, C., Garrett, E., Wiesmann, M., Garcia, P. D., Fuller, J. H., Chan, V., Randazzo, F., Gundel, R., Warren, R. S., Escobedo, J., Aukerman, S. L., Taylor, R. N. & Fantl, W. J. (2003). beta-Catenin regulates vascular

- endothelial growth factor expression in colon cancer. *Cancer Res*, Vol. 63, No. 12, pp. 3145-3153, ISSN 0008-5472 (Print)
- Eder, J. P., Vande Woude, G. F., Boerner, S. A. & LoRusso, P. M. (2009). Novel therapeutic inhibitors of the c-Met signaling pathway in cancer. *Clin Cancer Res*, Vol. 15, No. 7, pp. 2207-2214, ISSN 1078-0432 (Print)
- Eisen, T., Joensuu, H., Nathan, P., Harper, P., Wojtukiewicz, M., Nicholson, S., Bahl, A., Tomczak, P., Wagner, A. & Quinn, D. (2009). Phase II study of BAY 73-4506, a multikinase inhibitor, in previously untreated patients with metastatic or unresectable renal cell cancer. *ASCO Meeting Abstracts*, Vol. 27, No. 15S, pp. 5033
- Ellis, L. M. & Hicklin, D. J. (2008). VEGF-targeted therapy: mechanisms of anti-tumour activity. *Nat Rev Cancer*, Vol. 8, No. 8, pp. 579-591, ISSN 1474-1768 (Electronic)
- Emoto, N., Isozaki, O., Ohmura, E., Ito, F., Tsushima, T., Shizume, K., Demura, H. & Toma, H. (1994). Basic fibroblast growth factor (FGF-2) in renal cell carcinoma, which is indistinguishable from that in normal kidney, is involved in renal cell carcinoma growth. *J Urol*, Vol. 152, No. 5 Pt 1, pp. 1626-1631, ISSN 0022-5347 (Print)
- Escudier, B., Bellmunt, J., Negrier, S., Bajetta, E., Melichar, B., Bracarda, S., Ravaud, A., Golding, S., Jethwa, S. & Sneller, V. (2010). Phase III trial of bevacizumab plus interferon alfa-2a in patients with metastatic renal cell carcinoma (AVOREN): final analysis of overall survival. *J Clin Oncol*, Vol. 28, No. 13, pp. 2144-2150, ISSN 1527-7755 (Electronic)
- Escudier, B., Eisen, T., Stadler, W. M., Szczylik, C., Oudard, S., Siebels, M., Negrier, S., Chevreau, C., Solska, E., Desai, A. A., Rolland, F., Demkow, T., Hutson, T. E., Gore, M., Freeman, S., Schwartz, B., Shan, M., Simantov, R. & Bukowski, R. M. (2007b). Sorafenib in advanced clear-cell renal-cell carcinoma. *N Engl J Med*, Vol. 356, No. 2, pp. 125-134, ISSN 1533-4406 (Electronic)
- Escudier, B., Eisen, T., Stadler, W. M., Szczylik, C., Oudard, S., Staehler, M., Negrier, S., Chevreau, C., Desai, A. A., Rolland, F., Demkow, T., Hutson, T. E., Gore, M., Anderson, S., Hofilena, G., Shan, M., Pena, C., Lathia, C. & Bukowski, R. M. (2009). Sorafenib for treatment of renal cell carcinoma: Final efficacy and safety results of the phase III treatment approaches in renal cancer global evaluation trial. *J Clin Oncol*, Vol. 27, No. 20, pp. 3312-3318, ISSN 1527-7755 (Electronic)
- Escudier, B., Pluzanska, A., Koralewski, P., Ravaud, A., Bracarda, S., Szczylik, C., Chevreau, C., Filipek, M., Melichar, B., Bajetta, E., Gorbunova, V., Bay, J. O., Bodrogi, I., Jagiello-Gruszfeld, A. & Moore, N. (2007a). Bevacizumab plus interferon alfa-2a for treatment of metastatic renal cell carcinoma: a randomised, double-blind phase III trial. *Lancet*, Vol. 370, No. 9605, pp. 2103-2111, ISSN 1474-547X (Electronic)
- Faivre, S., Kroemer, G. & Raymond, E. (2006). Current development of mTOR inhibitors as anticancer agents. *Nat Rev Drug Discov*, Vol. 5, No. 8, pp. 671-688, ISSN 1474-1776 (Print)
- Fan, Q. W., Knight, Z. A., Goldenberg, D. D., Yu, W., Mostov, K. E., Stokoe, D., Shokat, K. M. & Weiss, W. A. (2006). A dual PI3 kinase/mTOR inhibitor reveals emergent efficacy in glioma. *Cancer Cell*, Vol. 9, No. 5, pp. 341-349, ISSN 1535-6108 (Print)
- Fernando, N. T., Koch, M., Rothrock, C., Gollogly, L. K., D'Amore, P. A., Ryeom, S. & Yoon, S. S. (2008). Tumor escape from endogenous, extracellular matrix-associated

- angiogenesis inhibitors by up-regulation of multiple proangiogenic factors. *Clin Cancer Res*, Vol. 14, No. 5, pp. 1529-1539, ISSN 1078-0432 (Print)
- Fishman, M. N., Srinivas, S., Hauke, R. J., Amato, R. J., Esteves, B., Dhillon, R., Cotreau, M., Al-Adhami, M., Bhargava, P. & Kabbinavar, F. F. (2009). Abstract B60: Combination of tivozanib (AV-951) and temsirolimus in patients with renal cell carcinoma (RCC): Preliminary results from a phase 1 trial. *Molecular Cancer Therapeutics*, Vol. 8, Supplement 1, pp. B60
- Flaherty, K. T. & Puzanov, I. (2010). Building on a foundation of VEGF and mTOR targeted agents in renal cell carcinoma. *Biochem Pharmacol*, Vol. 80, No. 5, pp. 638-646, ISSN 1873-2968 (Electronic)
- Genega, E. M., Ghebremichael, M., Najarian, R., Fu, Y., Wang, Y., Argani, P., Grisanzio, C. & Signoretti, S. (2010). Carbonic anhydrase IX expression in renal neoplasms: correlation with tumor type and grade. *Am J Clin Pathol*, Vol. 134, No. 6, pp. 873-879, ISSN 1943-7722 (Electronic)
- Gingras, A. C., Raught, B., Gygi, S. P., Niedzwiecka, A., Miron, M., Burley, S. K., Polakiewicz, R. D., Wyslouch-Cieszynska, A., Aebersold, R. & Sonenberg, N. (2001). Hierarchical phosphorylation of the translation inhibitor 4E-BP1. *Genes Dev*, Vol. 15, No. 21, pp. 2852-2864, ISSN 0890-9369 (Print)
- Giubellino, A., Linehan, W. M. & Bottaro, D. P. (2009). Targeting the Met signaling pathway in renal cancer. *Expert Rev Anticancer Ther*, Vol. 9, No. 6, pp. 785-793, ISSN 1744-8328 (Electronic)
- Gnarra, J. R., Tory, K., Weng, Y., Schmidt, L., Wei, M. H., Li, H., Latif, F., Liu, S., Chen, F., Duh, F. M. & et al. (1994). Mutations of the VHL tumour suppressor gene in renal carcinoma. *Nat Genet*, Vol. 7, No. 1, pp. 85-90, ISSN 1061-4036 (Print)
- Gomez-Rivera, F., Santillan-Gomez, A. A., Younes, M. N., Kim, S., Fooshee, D., Zhao, M., Jasser, S. A. & Myers, J. N. (2007). The tyrosine kinase inhibitor, AZD2171, inhibits vascular endothelial growth factor receptor signaling and growth of anaplastic thyroid cancer in an orthotopic nude mouse model. *Clin Cancer Res*, Vol. 13, No. 15 Pt 1, pp. 4519-4527, ISSN 1078-0432 (Print)
- Gordan, J. D., Lal, P., Dondeti, V. R., Letrero, R., Parekh, K. N., Oquendo, C. E., Greenberg, R. A., Flaherty, K. T., Rathmell, W. K., Keith, B., Simon, M. C. & Nathanson, K. L. (2008). HIF- α effects on c-Myc distinguish two subtypes of sporadic VHL-deficient clear cell renal carcinoma. *Cancer Cell*, Vol. 14, No. 6, pp. 435-446, ISSN 1878-3686 (Electronic)
- Greenberger, L. M., Horak, I. D., Filpula, D., Sapra, P., Westergaard, M., Frydenlund, H. F., Albaek, C., Schroder, H. & Orum, H. (2008). A RNA antagonist of hypoxia-inducible factor-1 α , EZN-2968, inhibits tumor cell growth. *Mol Cancer Ther*, Vol. 7, No. 11, pp. 3598-3608, ISSN 1535-7163 (Print)
- Guertin, D. A. & Sabatini, D. M. (2007). Defining the role of mTOR in cancer. *Cancer Cell*, Vol. 12, No. 1, pp. 9-22, ISSN 1535-6108 (Print)
- Guo, P., Hu, B., Gu, W., Xu, L., Wang, D., Huang, H. J., Cavenee, W. K. & Cheng, S. Y. (2003). Platelet-derived growth factor-B enhances glioma angiogenesis by stimulating vascular endothelial growth factor expression in tumor endothelia and

- by promoting pericyte recruitment. *Am J Pathol*, Vol. 162, No. 4, pp. 1083-1093, ISSN 0002-9440 (Print)
- Gustafsson, M. V., Zheng, X., Pereira, T., Gradin, K., Jin, S., Lundkvist, J., Ruas, J. L., Poellinger, L., Lendahl, U. & Bondesson, M. (2005). Hypoxia requires notch signaling to maintain the undifferentiated cell state. *Dev Cell*, Vol. 9, No. 5, pp. 617-628, ISSN 1534-5807 (Print)
- Hainsworth, J. D., Spigel, D. R., Burris, H. A., 3rd, Waterhouse, D., Clark, B. L. & Whorf, R. (2010). Phase II trial of bevacizumab and everolimus in patients with advanced renal cell carcinoma. *J Clin Oncol*, Vol. 28, No. 13, pp. 2131-2136, ISSN 1527-7755 (Electronic)
- Hara, S., Oya, M., Mizuno, R., Horiguchi, A., Marumo, K. & Murai, M. (2005). Akt activation in renal cell carcinoma: contribution of a decreased PTEN expression and the induction of apoptosis by an Akt inhibitor. *Ann Oncol*, Vol. 16, No. 6, pp. 928-933, ISSN 0923-7534 (Print)
- Hartford, C. M., Desai, A. A., Janisch, L., Karrison, T., Rivera, V. M., Berk, L., Loewy, J. W., Kindler, H., Stadler, W. M., Knowles, H. L., Bedrosian, C. & Ratain, M. J. (2009). A phase I trial to determine the safety, tolerability, and maximum tolerated dose of deforolimus in patients with advanced malignancies. *Clin Cancer Res*, Vol. 15, No. 4, pp. 1428-1434, ISSN 1078-0432 (Print)
- Harzstark, A. L., Small, E. J., Weinberg, V. K., Sun, J., Ryan, C. J., Lin, A. M., Fong, L., Brocks, D. R. & Rosenberg, J. E. (2011). A phase 1 study of everolimus and sorafenib for metastatic clear cell renal cell carcinoma. *Cancer*, ISSN 0008-543X (Print)
- Hay, N. & Sonenberg, N. (2004). Upstream and downstream of mTOR. *Genes Dev*, Vol. 18, No. 16, pp. 1926-1945, ISSN 0890-9369 (Print)
- He, Y., Rajantie, I., Pajusola, K., Jeltsch, M., Holopainen, T., Yla-Herttuala, S., Harding, T., Jooss, K., Takahashi, T. & Alitalo, K. (2005). Vascular endothelial cell growth factor receptor 3-mediated activation of lymphatic endothelium is crucial for tumor cell entry and spread via lymphatic vessels. *Cancer Res*, Vol. 65, No. 11, pp. 4739-4746, ISSN 0008-5472 (Print)
- Hirata, H., Hinoda, Y., Nakajima, K., Kawamoto, K., Kikuno, N., Kawakami, K., Yamamura, S., Ueno, K., Majid, S., Saini, S., Ishii, N. & Dahiya, R. (2009). Wnt antagonist gene DKK2 is epigenetically silenced and inhibits renal cancer progression through apoptotic and cell cycle pathways. *Clin Cancer Res*, Vol. 15, No. 18, pp. 5678-5687, ISSN 1078-0432 (Print)
- Horie, S., Aruga, S., Kawamata, H., Okui, N., Kakizoe, T. & Kitamura, T. (1999). Biological role of HGF/MET pathway in renal cell carcinoma. *J Urol*, Vol. 161, No. 3, pp. 990-997, ISSN 0022-5347 (Print)
- Hu-Lowe, D. D., Zou, H. Y., Grazzini, M. L., Hallin, M. E., Wickman, G. R., Amundson, K., Chen, J. H., Rewolinski, D. A., Yamazaki, S., Wu, E. Y., McTigue, M. A., Murray, B. W., Kania, R. S., O'Connor, P., Shalinsky, D. R. & Bender, S. L. (2008). Nonclinical antiangiogenesis and antitumor activities of axitinib (AG-013736), an oral, potent, and selective inhibitor of vascular endothelial growth factor receptor tyrosine

- kinases 1, 2, 3. *Clin Cancer Res*, Vol. 14, No. 22, pp. 7272-7283, ISSN 1078-0432 (Print)
- Huang, H., Bhat, A., Woodnutt, G. & Lappe, R. (2010). Targeting the ANGPT-TIE2 pathway in malignancy. *Nat Rev Cancer*, Vol. 10, No. 8, pp. 575-585, ISSN 1474-1768 (Electronic)
- Hudes, G., Carducci, M., Tomczak, P., Dutcher, J., Figlin, R., Kapoor, A., Staroslawska, E., Sosman, J., McDermott, D., Bodrogi, I., Kovacevic, Z., Lesovoy, V., Schmidt-Wolf, I. G., Barbarash, O., Gokmen, E., O'Toole, T., Lustgarten, S., Moore, L. & Motzer, R. J. (2007). Temsirolimus, interferon alfa, or both for advanced renal-cell carcinoma. *N Engl J Med*, Vol. 356, No. 22, pp. 2271-2281, ISSN 1533-4406 (Electronic)
- Hudes, G. R., Berkenblit, A., Feingold, J., Atkins, M. B., Rini, B. I. & Dutcher, J. (2009). Clinical trial experience with temsirolimus in patients with advanced renal cell carcinoma. *Semin Oncol*, Vol. 36 Suppl 3, No. pp. S26-36, ISSN 1532-8708 (Electronic)
- Inai, T., Mancuso, M., Hashizume, H., Baffert, F., Haskell, A., Baluk, P., Hu-Lowe, D. D., Shalinsky, D. R., Thurston, G., Yancopoulos, G. D. & McDonald, D. M. (2004). Inhibition of vascular endothelial growth factor (VEGF) signaling in cancer causes loss of endothelial fenestrations, regression of tumor vessels, and appearance of basement membrane ghosts. *Am J Pathol*, Vol. 165, No. 1, pp. 35-52, ISSN 0002-9440 (Print)
- Inoki, K., Corradetti, M. N. & Guan, K. L. (2005). Dysregulation of the TSC-mTOR pathway in human disease. *Nat Genet*, Vol. 37, No. 1, pp. 19-24, ISSN 1061-4036 (Print)
- Inoki, K., Ouyang, H., Zhu, T., Lindvall, C., Wang, Y., Zhang, X., Yang, Q., Bennett, C., Harada, Y., Stankunas, K., Wang, C. Y., He, X., MacDougald, O. A., You, M., Williams, B. O. & Guan, K. L. (2006). TSC2 integrates Wnt and energy signals via a coordinated phosphorylation by AMPK and GSK3 to regulate cell growth. *Cell*, Vol. 126, No. 5, pp. 955-968, ISSN 0092-8674 (Print)
- Jain, R. K. (2005). Normalization of tumor vasculature: an emerging concept in antiangiogenic therapy. *Science*, Vol. 307, No. 5706, pp. 58-62, ISSN 1095-9203 (Electronic)
- Jemal, A., Siegel, R., Ward, E., Hao, Y., Xu, J., Murray, T. & Thun, M. J. (2008). Cancer statistics, 2008. *CA Cancer J Clin*, Vol. 58, No. 2, pp. 71-96, ISSN 0007-9235 (Print)
- Kataoka, Y., Mukohara, T., Tomioka, H., Funakoshi, Y., Kiyota, N., Fujiwara, Y., Yashiro, M., Hirakawa, K., Hirai, M. & Minami, H. (2011). Foretinib (GSK1363089), a multi-kinase inhibitor of MET and VEGFRs, inhibits growth of gastric cancer cell lines by blocking inter-receptor tyrosine kinase networks. *Invest New Drugs*, ISSN 1573-0646 (Electronic)
- Kawakami, K., Hirata, H., Yamamura, S., Kikuno, N., Saini, S., Majid, S., Tanaka, Y., Kawamoto, K., Enokida, H., Nakagawa, M. & Dahiya, R. (2009). Functional significance of Wnt inhibitory factor-1 gene in kidney cancer. *Cancer Res*, Vol. 69, No. 22, pp. 8603-8610, ISSN 1538-7445 (Electronic)
- Kim, E. S., Serur, A., Huang, J., Manley, C. A., McCrudden, K. W., Frischer, J. S., Soffer, S. Z., Ring, L., New, T., Zabski, S., Rudge, J. S., Holash, J., Yancopoulos, G. D., Kandel, J. J. & Yamashiro, D. J. (2002). Potent VEGF blockade causes regression of coopted

- vessels in a model of neuroblastoma. *Proc Natl Acad Sci U S A*, Vol. 99, No. 17, pp. 11399-11404, ISSN 0027-8424 (Print)
- Klein, S. & Levitzki, A. (2009). Targeting the EGFR and the PKB pathway in cancer. *Curr Opin Cell Biol*, Vol. 21, No. 2, pp. 185-193, ISSN 1879-0410 (Electronic)
- Koh, M. Y., Spivak-Kroizman, T., Venturini, S., Welsh, S., Williams, R. R., Kirkpatrick, D. L. & Powis, G. (2008). Molecular mechanisms for the activity of PX-478, an antitumor inhibitor of the hypoxia-inducible factor-1alpha. *Mol Cancer Ther*, Vol. 7, No. 1, pp. 90-100, ISSN 1535-7163 (Print)
- Kojima, T., Shimazui, T., Hinotsu, S., Joraku, A., Oikawa, T., Kawai, K., Horie, R., Suzuki, H., Nagashima, R., Yoshikawa, K., Michiue, T., Asashima, M., Akaza, H. & Uchida, K. (2009). Decreased expression of CXXC4 promotes a malignant phenotype in renal cell carcinoma by activating Wnt signaling. *Oncogene*, Vol. 28, No. 2, pp. 297-305, ISSN 1476-5594 (Electronic)
- Koochekpour, S., Jeffers, M., Wang, P. H., Gong, C., Taylor, G. A., Roessler, L. M., Stearman, R., Vasselli, J. R., Stetler-Stevenson, W. G., Kaelin, W. G., Jr., Linehan, W. M., Klausner, R. D., Gnarr, J. R. & Vande Woude, G. F. (1999). The von Hippel-Lindau tumor suppressor gene inhibits hepatocyte growth factor/scatter factor-induced invasion and branching morphogenesis in renal carcinoma cells. *Mol Cell Biol*, Vol. 19, No. 9, pp. 5902-5912, ISSN 0270-7306 (Print)
- Kumar, R., Knick, V. B., Rudolph, S. K., Johnson, J. H., Crosby, R. M., Crouthamel, M. C., Hopper, T. M., Miller, C. G., Harrington, L. E., Onori, J. A., Mullin, R. J., Gilmer, T. M., Truesdale, A. T., Epperly, A. H., Bolor, A., Stafford, J. A., Luttrell, D. K. & Cheung, M. (2007). Pharmacokinetic-pharmacodynamic correlation from mouse to human with pazopanib, a multikinase angiogenesis inhibitor with potent antitumor and antiangiogenic activity. *Mol Cancer Ther*, Vol. 6, No. 7, pp. 2012-2021, ISSN 1535-7163 (Print)
- Kummar, S., Gutierrez, M. E., Gardner, E. R., Chen, X., Figg, W. D., Zajac-Kaye, M., Chen, M., Steinberg, S. M., Muir, C. A., Yancey, M. A., Horneffer, Y. R., Juwara, L., Melillo, G., Ivy, S. P., Merino, M., Neckers, L., Steeg, P. S., Conley, B. A., Giaccone, G., Doroshow, J. H. & Murgo, A. J. (2010). Phase I trial of 17-dimethylaminoethylamino-17-demethoxygeldanamycin (17-DMAG), a heat shock protein inhibitor, administered twice weekly in patients with advanced malignancies. *Eur J Cancer*, Vol. 46, No. 2, pp. 340-347, ISSN 1879-0852 (Electronic)
- Lang, J. M. & Harrison, M. R. (2010). Pazopanib for the treatment of patients with advanced renal cell carcinoma. *Clin Med Insights Oncol*, Vol. 4, No. pp. 95-105, ISSN 1179-5549 (Electronic)
- Le Tourneau, C., Faivre, S., Serova, M. & Raymond, E. (2008). mTORC1 inhibitors: is temsirolimus in renal cancer telling us how they really work? *Br J Cancer*, Vol. 99, No. 8, pp. 1197-1203, ISSN 1532-1827 (Electronic)
- Linehan, W. M., Rubin, J. S. & Bottaro, D. P. (2009). VHL loss of function and its impact on oncogenic signaling networks in clear cell renal cell carcinoma. *Int J Biochem Cell Biol*, Vol. 41, No. 4, pp. 753-756, ISSN 1878-5875 (Electronic)
- Liu, J., Lin, T. H., Cole, A. G., Wen, R., Zhao, L., Brescia, M. R., Jacob, B., Hussain, Z., Appell, K. C., Henderson, I. & Webb, M. L. (2008). Identification and characterization of

- small-molecule inhibitors of Tie2 kinase. *FEBS Lett*, Vol. 582, No. 5, pp. 785-791, ISSN 0014-5793 (Print)
- Mackenzie, M. J., Rini, B. I., Elson, P., Schwandt, A., Wood, L., Trinkhaus, M., Bjarnason, G. & Knox, J. (2011). Temsirolimus in VEGF-refractory metastatic renal cell carcinoma. *Ann Oncol*, Vol. 22, No. 1, pp. 145-148, ISSN 1569-8041 (Electronic)
- Maira, S. M., Stauffer, F., Brueggen, J., Furet, P., Schnell, C., Fritsch, C., Brachmann, S., Chene, P., De Pover, A., Schoemaker, K., Fabbro, D., Gabriel, D., Simonen, M., Murphy, L., Finan, P., Sellers, W. & Garcia-Echeverria, C. (2008). Identification and characterization of NVP-BEZ235, a new orally available dual phosphatidylinositol 3-kinase/mammalian target of rapamycin inhibitor with potent in vivo antitumor activity. *Mol Cancer Ther*, Vol. 7, No. 7, pp. 1851-1863, ISSN 1535-7163 (Print)
- Mamane, Y., Petroulakis, E., LeBacquer, O. & Sonenberg, N. (2006). mTOR, translation initiation and cancer. *Oncogene*, Vol. 25, No. 48, pp. 6416-6422, ISSN 0950-9232 (Print)
- Mandriota, S. J., Turner, K. J., Davies, D. R., Murray, P. G., Morgan, N. V., Sowter, H. M., Wykoff, C. C., Maher, E. R., Harris, A. L., Ratcliffe, P. J. & Maxwell, P. H. (2002). HIF activation identifies early lesions in VHL kidneys: evidence for site-specific tumor suppressor function in the nephron. *Cancer Cell*, Vol. 1, No. 5, pp. 459-468, ISSN 1535-6108 (Print)
- Maranchie, J. K., Vasselli, J. R., Riss, J., Bonifacino, J. S., Linehan, W. M. & Klausner, R. D. (2002). The contribution of VHL substrate binding and HIF1- α to the phenotype of VHL loss in renal cell carcinoma. *Cancer Cell*, Vol. 1, No. 3, pp. 247-255, ISSN 1535-6108 (Print)
- Merseburger, A. S., Hennenlotter, J., Kuehs, U., Simon, P., Kruck, S., Koch, E., Stenzl, A. & Kuczyk, M. A. (2008). Activation of PI3K is associated with reduced survival in renal cell carcinoma. *Urol Int*, Vol. 80, No. 4, pp. 372-377, ISSN 1423-0399 (Electronic)
- Miele, L., Golde, T. & Osborne, B. (2006). Notch signaling in cancer. *Curr Mol Med*, Vol. 6, No. 8, pp. 905-918, ISSN 1566-5240 (Print)
- Miele, L., Miao, H. & Nickoloff, B. J. (2006). NOTCH signaling as a novel cancer therapeutic target. *Curr Cancer Drug Targets*, Vol. 6, No. 4, pp. 313-323, ISSN 1568-0096 (Print)
- Moon, R. T., Kohn, A. D., De Ferrari, G. V. & Kaykas, A. (2004). WNT and beta-catenin signalling: diseases and therapies. *Nat Rev Genet*, Vol. 5, No. 9, pp. 691-701, ISSN 1471-0056 (Print)
- Motzer, R. J., Hudes, G. R., Curti, B. D., McDermott, D. F., Escudier, B. J., Negrier, S., Duclos, B., Moore, L., O'Toole, T., Boni, J. P. & Dutcher, J. P. (2007b). Phase I/II trial of temsirolimus combined with interferon alfa for advanced renal cell carcinoma. *J Clin Oncol*, Vol. 25, No. 25, pp. 3958-3964, ISSN 1527-7755 (Electronic)
- Motzer, R. J., Hutson, T. E., Tomczak, P., Michaelson, M. D., Bukowski, R. M., Oudard, S., Negrier, S., Szczylik, C., Pili, R., Bjarnason, G. A., Garcia-del-Muro, X., Sosman, J. A., Solska, E., Wilding, G., Thompson, J. A., Kim, S. T., Chen, L., Huang, X. & Figlin, R. A. (2009). Overall survival and updated results for sunitinib compared with interferon alfa in patients with metastatic renal cell carcinoma. *J Clin Oncol*, Vol. 27, No. 22, pp. 3584-3590, ISSN 1527-7755 (Electronic)

- Motzer, R. J., Hutson, T. E., Tomczak, P., Michaelson, M. D., Bukowski, R. M., Rixe, O., Oudard, S., Negrier, S., Szczylik, C., Kim, S. T., Chen, I., Bycott, P. W., Baum, C. M. & Figlin, R. A. (2007a). Sunitinib versus interferon alfa in metastatic renal-cell carcinoma. *N Engl J Med*, Vol. 356, No. 2, pp. 115-124, ISSN 1533-4406 (Electronic)
- Mulders, P. (2009). Vascular endothelial growth factor and mTOR pathways in renal cell carcinoma: differences and synergies of two targeted mechanisms. *BJU Int*, Vol. 104, No. 11, pp. 1585-1589, ISSN 1464-410X (Electronic)
- Najafov, A., Sommer, E. M., Axten, J. M., Deyoung, M. P. & Alessi, D. R. (2010). Characterization of GSK2334470, a novel and highly specific inhibitor of PDK1. *Biochem J*, Vol. 433, No. 2, pp. 357-369, ISSN 1470-8728 (Electronic)
- Nakamura, K., Taguchi, E., Miura, T., Yamamoto, A., Takahashi, K., Bichat, F., Guilbaud, N., Hasegawa, K., Kubo, K., Fujiwara, Y., Suzuki, R., Shibuya, M. & Isae, T. (2006). KRN951, a highly potent inhibitor of vascular endothelial growth factor receptor tyrosine kinases, has antitumor activities and affects functional vascular properties. *Cancer Res*, Vol. 66, No. 18, pp. 9134-9142, ISSN 0008-5472 (Print)
- Natali, P. G., Prat, M., Nicotra, M. R., Bigotti, A., Olivero, M., Comoglio, P. M. & Di Renzo, M. F. (1996). Overexpression of the met/HGF receptor in renal cell carcinomas. *Int J Cancer*, Vol. 69, No. 3, pp. 212-217, ISSN 0020-7136 (Print)
- Negrier, S., Gravis, G., Perol, D., Chevreau, C., Delva, R., Bay, J. O., Blanc, E., Ferlay, C., Geoffrois, L., Rolland, F., Legouffe, E., Sevin, E., Laguerre, B. & Escudier, B. (2011). Temsirolimus and bevacizumab, or sunitinib, or interferon alfa and bevacizumab for patients with advanced renal cell carcinoma (TORAVA): a randomised phase 2 trial. *Lancet Oncol*, ISSN 1474-5488 (Electronic)
- Nickerson, M. L., Jaeger, E., Shi, Y., Durocher, J. A., Mahurkar, S., Zaridze, D., Matveev, V., Janout, V., Kollarova, H., Bencko, V., Navratilova, M., Szeszenia-Dabrowska, N., Mates, D., Mukeria, A., Holcatova, I., Schmidt, L. S., Toro, J. R., Karami, S., Hung, R., Gerard, G. F., Linehan, W. M., Merino, M., Zbar, B., Boffetta, P., Brennan, P., Rothman, N., Chow, W. H., Waldman, F. M. & Moore, L. E. (2008). Improved identification of von Hippel-Lindau gene alterations in clear cell renal tumors. *Clin Cancer Res*, Vol. 14, No. 15, pp. 4726-4734, ISSN 1078-0432 (Print)
- Nickoloff, B. J., Osborne, B. A. & Miele, L. (2003). Notch signaling as a therapeutic target in cancer: a new approach to the development of cell fate modifying agents. *Oncogene*, Vol. 22, No. 42, pp. 6598-6608, ISSN 0950-9232 (Print)
- Nicolas, M., Wolfer, A., Raj, K., Kummer, J. A., Mill, P., van Noort, M., Hui, C. C., Clevers, H., Dotto, G. P. & Radtke, F. (2003). Notch1 functions as a tumor suppressor in mouse skin. *Nat Genet*, Vol. 33, No. 3, pp. 416-421, ISSN 1061-4036 (Print)
- O'Reilly, K. E., Rojo, F., She, Q. B., Solit, D., Mills, G. B., Smith, D., Lane, H., Hofmann, F., Hicklin, D. J., Ludwig, D. L., Baselga, J. & Rosen, N. (2006). mTOR inhibition induces upstream receptor tyrosine kinase signaling and activates Akt. *Cancer Res*, Vol. 66, No. 3, pp. 1500-1508, ISSN 0008-5472 (Print)
- Oshiro, N., Yoshino, K., Hidayat, S., Tokunaga, C., Hara, K., Eguchi, S., Avruch, J. & Yonezawa, K. (2004). Dissociation of raptor from mTOR is a mechanism of rapamycin-induced inhibition of mTOR function. *Genes Cells*, Vol. 9, No. 4, pp. 359-366, ISSN 1356-9597 (Print)

- Oudard, S., George, D., Medioni, J. & Motzer, R. (2007). Treatment options in renal cell carcinoma: past, present and future. *Ann Oncol*, Vol. 18 Suppl 10, pp. x25-31, ISSN 0923-7534 (Print)
- Pal, S. K. & Figlin, R. A. (2011). Future directions of mammalian target of rapamycin (mTOR) inhibitor therapy in renal cell carcinoma. *Target Oncol*, Vol. 6, No. 1, pp. 5-16, ISSN 1776-260X (Electronic)
- Pal, S. K., Kortylewski, M., Yu, H. & Figlin, R.A. (2010). Breaking through a plateau in renal cell carcinoma therapeutics: development and incorporation of biomarkers. *Mol Cancer Ther*, Vol. 9, No. 12, pp. 3115-25, ISSN 1538-8514 (Electronic)
- Pantuck, A. J., Seligson, D. B., Klatter, T., Yu, H., Leppert, J. T., Moore, L., O'Toole, T., Gibbons, J., Belldegrun, A. S. & Figlin, R. A. (2007). Prognostic relevance of the mTOR pathway in renal cell carcinoma: implications for molecular patient selection for targeted therapy. *Cancer*, Vol. 109, No. 11, pp. 2257-2267, ISSN 0008-543X (Print)
- Patel, N. S., Li, J. L., Generali, D., Poulson, R., Cranston, D. W. & Harris, A. L. (2005). Up-regulation of delta-like 4 ligand in human tumor vasculature and the role of basal expression in endothelial cell function. *Cancer Res*, Vol. 65, No. 19, pp. 8690-8697, ISSN 0008-5472 (Print)
- Patel, P. H., Senico, P. L., Curiel, R. E. & Motzer, R. J. (2009). Phase I study combining treatment with temsirolimus and sunitinib malate in patients with advanced renal cell carcinoma. *Clin Genitourin Cancer*, Vol. 7, No. 1, pp. 24-27, ISSN 1558-7673 (Print)
- Peruzzi, B., Athauda, G. & Bottaro, D. P. (2006). The von Hippel-Lindau tumor suppressor gene product represses oncogenic beta-catenin signaling in renal carcinoma cells. *Proc Natl Acad Sci U S A*, Vol. 103, No. 39, pp. 14531-14536, ISSN 0027-8424 (Print)
- Pietras, K., Sjoblom, T., Rubin, K., Heldin, C. H. & Ostman, A. (2003). PDGF receptors as cancer drug targets. *Cancer Cell*, Vol. 3, No. 5, pp. 439-443, ISSN 1535-6108 (Print)
- Presta, L. G., Chen, H., O'Connor, S. J., Chisholm, V., Meng, Y. G., Krummen, L., Winkler, M. & Ferrara, N. (1997). Humanization of an anti-vascular endothelial growth factor monoclonal antibody for the therapy of solid tumors and other disorders. *Cancer Res*, Vol. 57, No. 20, pp. 4593-4599, ISSN 0008-5472 (Print)
- Qian, C. N., Huang, D., Wondergem, B. & Teh, B. T. (2009). Complexity of tumor vasculature in clear cell renal cell carcinoma. *Cancer*, Vol. 115, No. 10 Suppl, pp. 2282-2289, ISSN 0008-543X (Print)
- Rae, F. K., Stephenson, S. A., Nicol, D. L. & Clements, J. A. (2000). Novel association of a diverse range of genes with renal cell carcinoma as identified by differential display. *Int J Cancer*, Vol. 88, No. 5, pp. 726-732, ISSN 0020-7136 (Print)
- Raval, R. R., Lau, K. W., Tran, M. G., Sowter, H. M., Mandriota, S. J., Li, J. L., Pugh, C. W., Maxwell, P. H., Harris, A. L. & Ratcliffe, P. J. (2005). Contrasting properties of hypoxia-inducible factor 1 (HIF-1) and HIF-2 in von Hippel-Lindau-associated renal cell carcinoma. *Mol Cell Biol*, Vol. 25, No. 13, pp. 5675-5686, ISSN 0270-7306 (Print)
- Rixe, O., Bukowski, R. M., Michaelson, M. D., Wilding, G., Hudes, G. R., Bolte, O., Motzer, R. J., Bycott, P., Liau, K. F., Freddo, J., Trask, P. C., Kim, S. & Rini, B. I. (2007).

- Axitinib treatment in patients with cytokine-refractory metastatic renal-cell cancer: a phase II study. *Lancet Oncol*, Vol. 8, No. 11, pp. 975-984, ISSN 1474-5488 (Electronic)
- Ronnen, E. A., Kondagunta, G. V., Ishill, N., Sweeney, S. M., Deluca, J. K., Schwartz, L., Bacik, J. & Motzer, R. J. (2006). A phase II trial of 17-(Allylamino)-17-demethoxygeldanamycin in patients with papillary and clear cell renal cell carcinoma. *Invest New Drugs*, Vol. 24, No. 6, pp. 543-546, ISSN 0167-6997 (Print)
- Ryan, C. W., Vuky, J., Chan, J. S., Chen, Z., Beer, T. M. & Nauman, D. (2011). A phase II study of everolimus in combination with imatinib for previously treated advanced renal carcinoma. *Invest New Drugs*, Vol. 29, No. 2, pp. 374-379, ISSN 1573-0646 (Electronic)
- Sabatini, D. M. (2006). mTOR and cancer: insights into a complex relationship. *Nat Rev Cancer*, Vol. 6, No. 9, pp. 729-734, ISSN 1474-175X (Print)
- Sansom, O. J., Griffiths, D. F., Reed, K. R., Winton, D. J. & Clarke, A. R. (2005). Apc deficiency predisposes to renal carcinoma in the mouse. *Oncogene*, Vol. 24, No. 55, pp. 8205-8210, ISSN 0950-9232 (Print)
- Sarbasov, D. D., Ali, S. M., Sengupta, S., Sheen, J. H., Hsu, P. P., Bagley, A. F., Markhard, A. L. & Sabatini, D. M. (2006). Prolonged rapamycin treatment inhibits mTORC2 assembly and Akt/PKB. *Mol Cell*, Vol. 22, No. 2, pp. 159-168, ISSN 1097-2765 (Print)
- Schmelzle, T. & Hall, M. N. (2000). TOR, a central controller of cell growth. *Cell*, Vol. 103, No. 2, pp. 253-262, ISSN 0092-8674 (Print)
- Schoffski, P., Garcia, J. A., Stadler, W. M., Gil, T., Jonasch, E., Tagawa, S. T., Smitt, M., Yang, X., Oliner, K. S., Anderson, A., Zhu, M. & Kabbinar, F. (2010). A phase II study of the efficacy and safety of AMG 102 in patients with metastatic renal cell carcinoma. *BJU Int*, ISSN 1464-410X (Electronic)
- Shaw, R. J., Bardeesy, N., Manning, B. D., Lopez, L., Kosmatka, M., DePinho, R. A. & Cantley, L. C. (2004). The LKB1 tumor suppressor negatively regulates mTOR signaling. *Cancer Cell*, Vol. 6, No. 1, pp. 91-99, ISSN 1535-6108 (Print)
- Sjolund, J., Johansson, M., Manna, S., Norin, C., Pietras, A., Beckman, S., Nilsson, E., Ljungberg, B. & Axelson, H. (2008). Suppression of renal cell carcinoma growth by inhibition of Notch signaling in vitro and in vivo. *J Clin Invest*, Vol. 118, No. 1, pp. 217-228, ISSN 0021-9738 (Print)
- Slaton, J. W., Inoue, K., Perrotte, P., El-Naggar, A. K., Swanson, D. A., Fidler, I. J. & Dinney, C. P. (2001). Expression levels of genes that regulate metastasis and angiogenesis correlate with advanced pathological stage of renal cell carcinoma. *Am J Pathol*, Vol. 158, No. 2, pp. 735-743, ISSN 0002-9440 (Print)
- Sosman, J. & Puzanov, I. (2009). Combination targeted therapy in advanced renal cell carcinoma. *Cancer*, Vol. 115, No. 10 Suppl, pp. 2368-2375, ISSN 0008-543X (Print)
- Sosman, J. A., Flaherty, K.T., Atkins, M.B., et al. (2008). Updated results of phase I trial of sorafenib (S) and bevacizumab (B) in patients with metastatic renal cell cancer (mRCC) [abstract]. *J Clin Oncol*, Vol. 26(May 20 suppl)
- Soulieres, D. (2009). Review of guidelines on the treatment of metastatic renal cell carcinoma. *Curr Oncol*, Vol. 16 Suppl 1, pp. S67-70, ISSN 1198-0052 (Print)

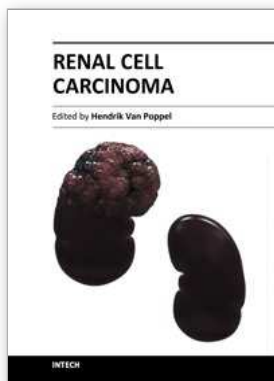
- Sourbier, C., Lindner, V., Lang, H., Agouni, A., Schordan, E., Danilin, S., Rothhut, S., Jacqmin, D., Helwig, J. J. & Massfelder, T. (2006). The phosphoinositide 3-kinase/Akt pathway: a new target in human renal cell carcinoma therapy. *Cancer Res*, Vol. 66, No. 10, pp. 5130-5142, ISSN 0008-5472 (Print)
- Stahler, M., Rohrmann, K., Haseke, N., Stief, C. G. & Siebels, M. (2005). Targeted agents for the treatment of advanced renal cell carcinoma. *Curr Drug Targets*, Vol. 6, No. 7, pp. 835-846, ISSN 1389-4501 (Print)
- Sternberg, C. (2010). Randomized, Double-Blind Phase III Study Of Pazopanib In Patients With Advanced/Metastatic Renal Cell Carcinoma (mRCC): Final Overall Survival (OS) Results. *Ann Oncol*, Vol. 21, Abstract LBA22
- Sternberg, C. N., Davis, I. D., Mardiak, J., Szczylik, C., Lee, E., Wagstaff, J., Barrios, C. H., Salman, P., Gladkov, O. A., Kavina, A., Zarba, J. J., Chen, M., McCann, L., Pandite, L., Roychowdhury, D. F. & Hawkins, R. E. (2010). Pazopanib in locally advanced or metastatic renal cell carcinoma: results of a randomized phase III trial. *J Clin Oncol*, Vol. 28, No. 6, pp. 1061-1068, ISSN 1527-7755 (Electronic)
- Sulzbacher, I., Birner, P., Traxler, M., Marberger, M. & Haitel, A. (2003). Expression of platelet-derived growth factor-alpha alpha receptor is associated with tumor progression in clear cell renal cell carcinoma. *Am J Clin Pathol*, Vol. 120, No. 1, pp. 107-112, ISSN 0002-9173 (Print)
- Takeda, M., Arao, T., Yokote, H., Komatsu, T., Yanagihara, K., Sasaki, H., Yamada, Y., Tamura, T., Fukuoka, K., Kimura, H., Saijo, N. & Nishio, K. (2007). AZD2171 shows potent antitumor activity against gastric cancer over-expressing fibroblast growth factor receptor 2/keratinocyte growth factor receptor. *Clin Cancer Res*, Vol. 13, No. 10, pp. 3051-3057, ISSN 1078-0432 (Print)
- Tanimoto, S., Fukumori, T., El-Moula, G., Shiirevnyamba, A., Kinouchi, S., Koizumi, T., Nakanishi, R., Yamamoto, Y., Taue, R., Yamaguchi, K., Nakatsuji, H., Kishimoto, T., Izaki, H., Oka, N., Takahashi, M. & Kanayama, H. O. (2008). Prognostic significance of serum hepatocyte growth factor in clear cell renal cell carcinoma: comparison with serum vascular endothelial growth factor. *J Med Invest*, Vol. 55, No. 1-2, pp. 106-111, ISSN 1343-1420 (Print)
- Thomas, G. V., Tran, C., Mellinghoff, I. K., Welsbie, D. S., Chan, E., Fueger, B., Czernin, J. & Sawyers, C. L. (2006). Hypoxia-inducible factor determines sensitivity to inhibitors of mTOR in kidney cancer. *Nat Med*, Vol. 12, No. 1, pp. 122-127, ISSN 1078-8956 (Print)
- Thoreen, C. C., Kang, S. A., Chang, J. W., Liu, Q., Zhang, J., Gao, Y., Reichling, L. J., Sim, T., Sabatini, D. M. & Gray, N. S. (2009). An ATP-competitive mammalian target of rapamycin inhibitor reveals rapamycin-resistant functions of mTORC1. *J Biol Chem*, Vol. 284, No. 12, pp. 8023-8032, ISSN 0021-9258 (Print)
- Toschi, L. & Janne, P. A. (2008). Single-agent and combination therapeutic strategies to inhibit hepatocyte growth factor/MET signaling in cancer. *Clin Cancer Res*, Vol. 14, No. 19, pp. 5941-5946, ISSN 1078-0432 (Print)
- Uemura, H., Fujimoto, K., Tanaka, M., Yoshikawa, M., Hirao, Y., Uejima, S., Yoshikawa, K. & Itoh, K. (2006). A phase I trial of vaccination of CA9-derived peptides for HLA-

- A24-positive patients with cytokine-refractory metastatic renal cell carcinoma. *Clin Cancer Res*, Vol. 12, No. 6, pp. 1768-1775, ISSN 1078-0432 (Print)
- Veronese, M. L., Mosenkis, A., Flaherty, K. T., Gallagher, M., Stevenson, J. P., Townsend, R. R. & O'Dwyer, P. J. (2006). Mechanisms of hypertension associated with BAY 43-9006. *J Clin Oncol*, Vol. 24, No. 9, pp. 1363-1369, ISSN 1527-7755 (Electronic)
- Vickers, M. M. & Heng, D.Y. (2010). Prognostic and predictive biomarkers in renal cell carcinoma. *Target Oncol*, Vol. 5, No. 2, pp. 85-94, ISSN 1776-260X (Electronic)
- Wilhelm, S. M., Adnane, L., Newell, P., Villanueva, A., Llovet, J. M. & Lynch, M. (2008). Preclinical overview of sorafenib, a multikinase inhibitor that targets both Raf and VEGF and PDGF receptor tyrosine kinase signaling. *Mol Cancer Ther*, Vol. 7, No. 10, pp. 3129-3140, ISSN 1535-7163 (Print)
- Wilhelm, S. M., Carter, C., Tang, L., Wilkie, D., McNabola, A., Rong, H., Chen, C., Zhang, X., Vincent, P., McHugh, M., Cao, Y., Shujath, J., Gawlak, S., Eveleigh, D., Rowley, B., Liu, L., Adnane, L., Lynch, M., Auclair, D., Taylor, I., Gedrich, R., Voznesensky, A., Riedl, B., Post, L. E., Bollag, G. & Trail, P. A. (2004). BAY 43-9006 exhibits broad spectrum oral antitumor activity and targets the RAF/MEK/ERK pathway and receptor tyrosine kinases involved in tumor progression and angiogenesis. *Cancer Res*, Vol. 64, No. 19, pp. 7099-7109, ISSN 0008-5472 (Print)
- Wright, T. M., Brannon, A. R., Gordan, J. D., Mikels, A. J., Mitchell, C., Chen, S., Espinosa, I., van de Rijn, M., Pruthi, R., Wallen, E., Edwards, L., Nusse, R. & Rathmell, W. K. (2009). Ror2, a developmentally regulated kinase, promotes tumor growth potential in renal cell carcinoma. *Oncogene*, Vol. 28, No. 27, pp. 2513-2523, ISSN 1476-5594 (Electronic)
- Wulff, C., Wilson, H., Wiegand, S. J., Rudge, J. S. & Fraser, H. M. (2002). Prevention of thecal angiogenesis, antral follicular growth, and ovulation in the primate by treatment with vascular endothelial growth factor Trap R1R2. *Endocrinology*, Vol. 143, No. 7, pp. 2797-2807, ISSN 0013-7227 (Print)
- Xia, X., Qian, S., Soriano, S., Wu, Y., Fletcher, A. M., Wang, X. J., Koo, E. H., Wu, X. & Zheng, H. (2001). Loss of presenilin 1 is associated with enhanced beta-catenin signaling and skin tumorigenesis. *Proc Natl Acad Sci U S A*, Vol. 98, No. 19, pp. 10863-10868, ISSN 0027-8424 (Print)
- Yamazaki, S., Skaptason, J., Romero, D., Vekich, S., Jones, H. M., Tan, W., Wilner, K. D. & Koudriakova, T. (2011). Prediction of oral pharmacokinetics of cMet kinase inhibitors in humans: physiologically based pharmacokinetic model versus traditional one-compartment model. *Drug Metab Dispos*, Vol. 39, No. 3, pp. 383-393, ISSN 1521-009X (Electronic)
- Yu, K., Shi, C., Toral-Barza, L., Lucas, J., Shor, B., Kim, J. E., Zhang, W. G., Mahoney, R., Gaydos, C., Tardio, L., Kim, S. K., Conant, R., Curran, K., Kaplan, J., Verheijen, J., Ayril-Kaloustian, S., Mansour, T. S., Abraham, R. T., Zask, A. & Gibbons, J. J. (2010). Beyond rapalog therapy: preclinical pharmacology and antitumor activity of WYE-125132, an ATP-competitive and specific inhibitor of mTORC1 and mTORC2. *Cancer Res*, Vol. 70, No. 2, pp. 621-631, ISSN 1538-7445 (Electronic)
- Zbar, B., Klausner, R. & Linehan, W. M. (2003). Studying cancer families to identify kidney cancer genes. *Annu Rev Med*, Vol. 54, No. pp. 217-233, ISSN 0066-4219 (Print)

Zhou, Y. D., Kim, Y. P., Mohammed, K. A., Jones, D. K., Muhammad, I., Dunbar, D. C. & Nagle, D. G. (2005). Terpenoid tetrahydroisoquinoline alkaloids emetine, klugine, and isocephaline inhibit the activation of hypoxia-inducible factor-1 in breast tumor cells. *J Nat Prod*, Vol. 68, No. 6, pp. 947-950, ISSN 0163-3864 (Print)

INTECH

INTECH



Renal Cell Carcinoma

Edited by Dr. Hendrik Van Poppel

ISBN 978-953-307-844-1

Hard cover, 144 pages

Publisher InTech

Published online 16, December, 2011

Published in print edition December, 2011

Surgical and medical oncologists have been unable to decrease renal cell carcinoma mortality for uncertain reasons, although a lot of progress has been made in diagnosis and imaging, recognition of different genetic and pathological entities, management of localized disease and in the research on new drug treatments for advanced stages of the disease, potentially combined with surgery. The purpose of this book, which tackles a number of separate interesting topics, is to provide further insight into the disease and the management of early and advanced renal cell carcinoma. The volume is divided into different parts; the first part covers the characterization of renal masses and the second part covers rare distinct pathological entity. In the management section, active surveillance, partial nephrectomy and radiofrequency ablation are presented. A separate chapter reviews the management of Von Hippel Lindau disease, and finally, conventional and aberrant signaling pathways are explored.

How to reference

In order to correctly reference this scholarly work, feel free to copy and paste the following:

Carol O'Callaghan and Orla Patricia Barry (2011). Exploitation of Aberrant Signalling Pathways as Useful Targets for Renal Clear Cell Carcinoma Therapy, *Renal Cell Carcinoma*, Dr. Hendrik Van Poppel (Ed.), ISBN: 978-953-307-844-1, InTech, Available from: <http://www.intechopen.com/books/renal-cell-carcinoma/exploitation-of-aberrant-signalling-pathways-as-useful-targets-for-renal-clear-cell-carcinoma-therap>

INTECH

open science | open minds

InTech Europe

University Campus STeP Ri
Slavka Krautzeka 83/A
51000 Rijeka, Croatia
Phone: +385 (51) 770 447
Fax: +385 (51) 686 166
www.intechopen.com

InTech China

Unit 405, Office Block, Hotel Equatorial Shanghai
No.65, Yan An Road (West), Shanghai, 200040, China
中国上海市延安西路65号上海国际贵都大饭店办公楼405单元
Phone: +86-21-62489820
Fax: +86-21-62489821